

Applications of Advanced Cementitious Materials in Infrastructure

Candidate

J. van Oosten
TU Delft and Heijmans

28-9-2015

Committee

Prof.dr.ir. D.A. Hordijk
Ir. A.D. Reitsema
Dr.ir. M. Ottelé
Dr.ir. C. van der Veen
Ir. L.J.M. Houben

TU Delft
TU Delft and Heijmans
TU Delft and Heijmans
TU Delft
TU Delft

Acknowledgement

This thesis is the result of the collaboration of the section Structural and Building Engineering at the faculty of Civil Engineering and Geoscience of Delft University of Technology and Heijmans NV.

From here, I would like to express my sincere gratitude to people who helped me to do this research. First I would like to thank the chairman of my graduate committee Prof.dr.ir. D.A. Hordijk. His guidance and advice helped me to take next steps. Further, the discussions we had gave me insights to go in a better direction. I am also very thankful for the intensive guidance of Ir. A.D. Reitsema. He helped me with a lot of different difficulties during the process. Further, his enthusiasm for my research was very infectious. Next, Dr.ir. M. Ottelé is thanked for his guidance during the literature study. His critical attitude helped to bring the research to the next level. At last, I would like to thank Dr.ir. C. van der Veen for guiding me to the right contacts at the beginning and his advices during the last stage of the research.

Next to the persons of my committee, I would like to thank the company Heijmans for facilitating me during my thesis. During my research, Heijmans created the right conditions for me to work in. These conditions were not only there during the weekdays from 9.00 to 17.00, but also in the evening and during weekends thanks to the security staff. Also, the access to knowledge of the company helped me a lot.

Jeroen van Oosten
Delft, 2015

Summary

As a contractor, Heijmans has the desire to be the best and to stay one step ahead of competitors. The application of innovative materials could be the key to success. Therefore, in this report research is done to the applications of Advanced Cementitious Materials (ACMs) in structures in infrastructure, to generate potential benefits. The objective of the research is to make an overview of combinations of new concrete materials and structures, which should be utilised to take advantage of potential benefits. The total research consists of three parts:

- Part 1 - Literature study
- Part 2 - Fields of applications
- Part 3 - SHCC Link Slab

For the case study an alternative approach is defined to research the potential of applying the SHCC link slab. The objective of the case study is to make an overview of points of attention of the SHCC link slab design that is expected to be utilised the most often. These points should be researched further in order to take the application of the link slab a step further towards realisation.

Part 1 - Literature study

In this part of the research nine ACMs and several infrastructural structures are analysed. The mechanical-, durability- and sustainability characteristics of these ACMs are compared to Normal Strength Concrete (NSC). The materials inside the scope of this research are listed below:

- Normal Strength Steel Fibre Reinforced Concrete (NSSFRC)
- High Performance Concrete (HPC)
- High Performance Steel Fibre Reinforced Concrete (HPSFRC)
- Ultra High Fibre Reinforced Performance Concrete (UHFRPC)
- Strain Hardening Cementitious Composite (SHCC)
- Self-Healing Cementitious Material
- Geopolymer concrete
- Self-cleaning nano concrete
- Self-sensing nano concrete

In the end, the best studied materials, NSC, NSFRC, HPC, HPFRC, UHPC and SHCC, are rated and compared on three themes; mechanical, durability and sustainability characteristics. The comparison shows that UHPC has the best mechanical and durable performance. Further, NSC has the best sustainability characteristics. After the three themes were compared and combined, the Ultra High Performance Concrete (UHPC) shows the best overall performance.

Part 2 – Field of Applications

In this part of the thesis, field of applications, combinations of ACMs and (part of) structures are made that potentially could be interesting to utilise in practice. The results of this study are based on the literature study. The three potentially most interesting applications are projected to be:

1. **Bridge joint made of SHCC**, because of durability advantages and the secondary positive effects of the durability of the joint.
1. **Bridge girders made of (U)HPC**, because longer span could be desirable. For example from a safety point of view, it could be desirable to leave an intermediate support out in a new situation.
2. **Deck of an underpass made of UHPC**, because of secondary benefits in the tunnel structure.

A complete overview of all fields of application can be seen in Table 1. The applications are grouped according to projected potential. Obviously, the very potential structures are the most interesting to research in more detail in order to apply them in practice.

Table 1 – Applications of ACMs and structures divided in three categories of potential

Very potential	Potential	Not or nearly potential
HPC bridge deck	UHPC bridge deck	NSSFRC/HPSFRC cross beam
(U)HPC bridge girder	UHPC joint	NSSFRC/HPSFRC culvert
(U)HPC sluice door	(U)HPC cross beam	NSSFRC/HPSFRC aqueduct
UHPC deck of underpass	NSC and UHPC sluice door	UHPC tunnel elements
	UHPC embankment	(U)HPC sewage
	UHPC retaining wall	(U)HPC foundation slab
	UHPC aqueduct	UHPC and NSC sewage
	UHPC and NSC aqueduct	Steel and UHPC sluice door
SHCC bridge deck	SHCC barrier	SHCC aqueduct joint
SHCC for repair (deck,tunnel,...)	SHCC embankment	NSC and SHCC in culverts
SHCC bridge joint	SHCC joint in tunnel	NSC and SHCC in tunnel
	NSC with SHCC bridge girders	NSC and SHCC aqueduct
	Self-healing concrete aqueduct	
	GPC sluice door	GPC foundation slab
		GPC embankment
		GPC culvert
		GPC sewage
		GPC foundation piles
		Steel and GPC sluice door
	Self-sensing foundation piles	Self-cleaning noise barrier

* colours in table: blue for NSSFRC, HP(SFR)C and UHPC; orange for SHCC; purple for self healing concrete; green for geopolymer concrete; yellow for nano concrete

Part 3 - Case study

The case study is done to the application of SHCC joints in order to generate additional of SHCC. The main advantages to apply the SHCC joints are:

- Horizontal deformation capacity
- Long expected service life, while probably low or no maintenance is required.
- Protection of the substructure, supports etc. under the link slab, because the link slab avoids that leakage water and chemicals can reach and attack these elements.

An SHCC joint is already applied in Michigan, USA over steel girders. This joint performs structurally the same as the NSC Flexible Joint (buigslappe voeg). So the joint takes care of traffic loads and has rotation- and vertical deformation capacity. But this joint can't deform horizontally.

More interesting to apply in practice seems the Thin SHCC Link Slab. At the moment, only the deformation capacity of this design is researched. Therefore this link slab is analysed in detail from a structural point of view. An analysis on the reaction of the link slab on external forces is done. In this analysis, vertical load, horizontal load and imposed deformations are considered.

From the analysis follows two main points of attention of the link slab from a structural point of view; execution of the debonding layer and vertical working load. The debonding layer has to do with the smoothness of the layer. If the layer could not be executed smooth enough, the joint can't deform horizontally in a proper way anymore. The vertical load can cause vertical peak stresses at the end of the substructure, what causes spalling at the end of the concrete substructure. Due to spalling, the reinforcement in the concrete is not covered and protected anymore. Subsequently, failure of the reinforcement could be expected, what may result in failure of the total bridge structure.

Spalling can be prevented by reducing the peak stress or increasing the resistance. Three options to reduce the risk of spalling, which are recommended to research in more detail are:

- **Chamfers at the end of the deck:** cheapest option but the effectiveness is a point of discussion
- **Very stiff vertical plate:** most effective option, but probably very expensive.
- **Very stiff horizontal plate:** option with additional advantages for the debonding layer.

Next to spalling, some other issues should be researched before the link slab can be applied. Interesting to analyse is the applications of a horizontal imposed deformation and a horizontal load working on the link slab. Also optimisations in the design are interesting to research in more detail.

Table 2 – From Flexible joint to Thin SHCC Link Slab by steps

		Structure	Advantage	Research
Flexible Joint	Pilot 1	Flexible joint made of SHCC	No adhesive strip Practical learning goal SHCC	SHCC material
	Pilot 2	Flexible joint made of SHCC with GFRP reinforcement	Durable reinforcement Practical learning goal GFRP Lower stiffness of the joint	GFRP
	Pilot 3	Flexible joint made of SHCC with a reduced amount of reinforcement	Less reinforcement Lower stiffness of the joint	Influence of PVA fibres
Thin Link Slab	Pilot 4	Thin SHCC link slab with GFRP rebars (intermediate supports only)	Horizontal deformation capacity Lower stiffness of the joint	Peak stresses Debonding zone
	Pilot 5	Thin SHCC link slab with GFRP rebars (all supports)	Horizontal deformation capacity in all joints	Influence on the abutment

Guide line

This main report consists of three parts. Every part is worked out in detail in the attached reports. The three parts are:

1. **Literature study** - research on the characteristics of Advanced Cementitious Materials
2. **Fields of Applications** - research on potential applications of materials in structures
3. **SHCC joint** - more detailed research on the potential of the SHCC link slab

Before these three main parts of the report are discussed in this main report, the approaches of the entire project and the case study are discussed in chapter 1 General introduction and chapter 4 Introduction to the case study: SHCC Link Slab respectively. Among other things, the research questions and objectives of the total research and case study are given in these chapters.

The first part of this research, the literature study, is given in chapter 2 Literature. The Advanced Cementitious Materials (ACMs) that are in the scope of this research are characterised in this part. The basis of the literature study are six tables that together characterise the ACMs. These six tables, which are given in paragraph 3.1 until 3.6, are:

- Paragraph 3.1. - Definition of the ACMs
- Paragraph 3.2. - The composition of the ACMs
- Paragraph 3.3. - The mechanical characteristics of the ACMs
- Paragraph 3.4. - The durability behaviour of the ACMs
- Paragraph 3.5. - The sustainability of the ACMs
- Paragraph 3.6. - Standards and recommendations

In paragraph 2.9 Multi Criteria Analysis of the ACMs, a MCA of the ACMs is given. In this analysis the ACMs are judged on three themes; mechanical characteristics, durability characteristics and sustainability characteristics. The best mechanical, most durable and most sustainable ACMs are determined according to this MCA.

The second part of the research, the field of applications of ACMs is described in chapter 3 Field of Applications. In this chapter an overview of combinations of ACMs and structures is given. Further, the applications are judged on their potential.

The third part of this research, which is about the case study to the SHCC link slab, is shown in chapter 5 Thin SHCC Link slab. A general design and the potential of the Thin SHCC Link Slab are given in the first paragraph of this chapter. The structural analysis to the Thin SHCC Link Slab results in two points of attention. Both points are described in paragraph 5.4 Structural analysis to the Thin SHCC Link Slab.

In the end, some conclusions of the research are made in chapter 6 Conclusion. Partly based on the conclusions, recommendations are given in chapter 7 Recommendations.

Table of Content

Acknowledgement.....	iii
Summary	iv
Guide line	vii
Table of Content	viii
1 General introduction.....	1
1.1 Problem definition.....	1
1.2 Research question	1
1.3 Objective.....	1
1.4 Methodology.....	1
2 Literature.....	3
2.1 Advanced Cementitious Materials	3
2.2 Compositions.....	4
2.3 Mechanical characteristics.....	4
2.4 Durability characteristics	7
2.5 Sustainability characteristics.....	9
2.6 Standards and recommendations	9
2.7 Researched applications and reference projects	10
2.8 Structures.....	10
2.9 Multi Criteria Analysis of the ACMs.....	11
3 Field of Applications.....	13
3.1 Design ideas	13
3.2 Constructions and ACMs.....	13
4 Introduction to the case study: SHCC Link Slab	16
4.1 Research question	16
4.2 Objective	16
4.3 Boundary conditions.....	16
5 Thin SHCC Link slab	17
5.1 Potential of the Thin SHCC Link Slab	17
5.2 Reference project: SHCC Deck Slab on steel girders (Michigan, USA).....	18
5.3 NSC flexible joint and SHCC link slab	19
5.4 Structural analysis to the Thin SHCC Link Slab	22
5.5 Variants to reduce the risk of spalling	24
5.6 SHCC Flexible Joint.....	25
6 Conclusion	27

6.1	Combinations of ACMs and structures	27
6.2	Thin SHCC Link Slab	27
7	Recommendations	29
7.1	Combinations of ACMs and structures	29
7.2	SHCC link slab	29
8	Bibliografie.....	31

1 General introduction

Concrete has been used for centuries to build all kind of structures. In the Roman Empire cementitious materials were already used for constructions. Nowadays, some of those structures are still there. The last decades, material development has led to concrete becoming increasingly stronger. By reducing the water binder ratio, nowadays a concrete compressive strength of 350 MPa can already be achieved. This much stronger concrete is known as Ultra High Performance Concrete (UHPC). Next to concretes with high compressive strengths, other innovative concretes have also been researched for the last years.

1.1 Problem definition

Although a lot of research is done on the topic of new concrete materials, which will be referred to as Advanced Cementitious Materials (ACM), ordinary normal strength concrete is still the most applied concrete in infrastructure. Not using these Advanced Cementitious Materials is undesirable as possibilities of enhancing infrastructures remain unexplored and already gathered research input remains unused. New materials have different characteristics compared to normal concrete. This new characteristics can lead to new design opportunities. Designs can, depending on the characteristics of the concrete material, for example be made cheaper, more slender or more durable. The problem is defined as:

A lot of research at developing Advanced Cementitious Materials is done, however infrastructure potential benefits are lost since utilisation is lacking

1.2 Research question

From the problem definition the research question of this research could be formulated. The answer to this question should be the solution of the problem defined above. The research question is:

Which combinations of Advanced Cementitious Materials and constructions should be utilised to generate benefits?

1.3 Objective

The objective of this thesis is to come up with infrastructural constructions where ACMs can be utilised to increase the benefits of a project. The main aim of this research is provide in:

An overview of combinations of Advanced Cementitious Materials and constructions, which can be utilised to generate potential benefits

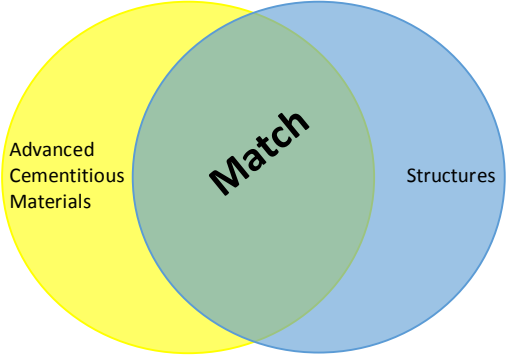
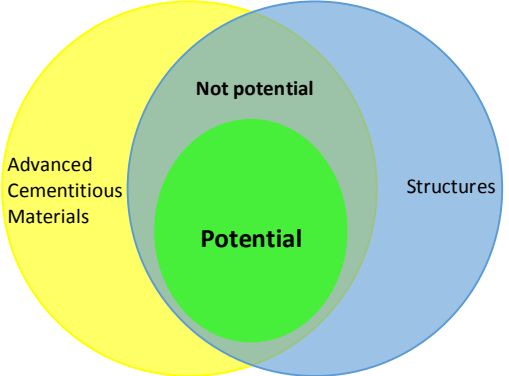
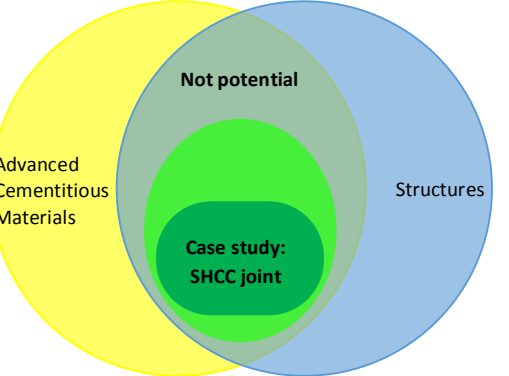
Potential benefits can be a number of things, for example higher durability or easier execution. A lot of benefits of the new concrete materials for constructions should still be explored. As soon as the benefits of the concrete materials are known, the benefits per material can be defined.

1.4 Methodology

This research is set up as wide as possible. In the beginning of this study many Advanced Cementitious Materials and structures are analysed. After that a list of potential applications is made. During the research, this list becomes shorter by steps, such that in the end only the best applications are left. First the list is shortened due to the outcome of the analysis to research applications and reference projects. Then the list is shortened by judging the potential of the applications. After this step, only the very potential applications remain. As a final step, the SHCC

joint, which is one of the potentially most interesting fields of applications, is researched in more detail in the case study. Point of attention of the design are researched and recommendations are given to improve these critical points. The steps taken to shorten the list are shown in Table 3.

Table 3 – Methodology of research to Advanced Cementitious Materials by step-by-step plan

 <p>Figure 1 - The schematically exhibition of the idea of linking the new concrete materials with infrastructure</p>	<table border="1"> <tbody> <tr> <td data-bbox="751 353 799 495">Step 1</td> <td data-bbox="799 353 1382 495"> <p>Literature research</p> <ul style="list-style-type: none"> - Material properties - Infrastructure structures </td> </tr> <tr> <td data-bbox="751 495 799 651">Step 2</td> <td data-bbox="799 495 1382 651"> <p>Researched applications</p> <p>Researches about potential applications of new concrete materials in single constructions.</p> </td> </tr> <tr> <td data-bbox="751 651 799 801">Step 3</td> <td data-bbox="799 651 1382 801"> <p>Reference projects</p> <p>Already realised projects where new concrete materials are applied</p> </td> </tr> <tr> <td data-bbox="751 801 799 1055">Step 4</td> <td data-bbox="799 801 1382 1055"> <p>Linking the right concrete to the right structure</p> <ul style="list-style-type: none"> - Which concrete has the best properties to apply in certain structures - Which structures do not have benefits by applying new concrete materials? - Table the possible fields of applications </td> </tr> </tbody> </table>	Step 1	<p>Literature research</p> <ul style="list-style-type: none"> - Material properties - Infrastructure structures 	Step 2	<p>Researched applications</p> <p>Researches about potential applications of new concrete materials in single constructions.</p>	Step 3	<p>Reference projects</p> <p>Already realised projects where new concrete materials are applied</p>	Step 4	<p>Linking the right concrete to the right structure</p> <ul style="list-style-type: none"> - Which concrete has the best properties to apply in certain structures - Which structures do not have benefits by applying new concrete materials? - Table the possible fields of applications
Step 1	<p>Literature research</p> <ul style="list-style-type: none"> - Material properties - Infrastructure structures 								
Step 2	<p>Researched applications</p> <p>Researches about potential applications of new concrete materials in single constructions.</p>								
Step 3	<p>Reference projects</p> <p>Already realised projects where new concrete materials are applied</p>								
Step 4	<p>Linking the right concrete to the right structure</p> <ul style="list-style-type: none"> - Which concrete has the best properties to apply in certain structures - Which structures do not have benefits by applying new concrete materials? - Table the possible fields of applications 								
 <p>Figure 2 - The schematically exhibition of potential fields of applications</p>	<table border="1"> <tbody> <tr> <td data-bbox="751 1055 799 1532">Step 5</td> <td data-bbox="799 1055 1382 1532"> <p>Judging the success of the matches</p> <ul style="list-style-type: none"> - Judging the applications to separate the wheat from the chaff - Separation between potential and not-potential applications - Arrangement of the applications that are potential <p><i>Note: the number of potential applications is not expected to be in proportion with the size of the green circle of Figure 2. Probably a low number of applications is potential.</i></p> </td> </tr> </tbody> </table>	Step 5	<p>Judging the success of the matches</p> <ul style="list-style-type: none"> - Judging the applications to separate the wheat from the chaff - Separation between potential and not-potential applications - Arrangement of the applications that are potential <p><i>Note: the number of potential applications is not expected to be in proportion with the size of the green circle of Figure 2. Probably a low number of applications is potential.</i></p>						
Step 5	<p>Judging the success of the matches</p> <ul style="list-style-type: none"> - Judging the applications to separate the wheat from the chaff - Separation between potential and not-potential applications - Arrangement of the applications that are potential <p><i>Note: the number of potential applications is not expected to be in proportion with the size of the green circle of Figure 2. Probably a low number of applications is potential.</i></p>								
 <p>Figure 3 - The schematically exhibition of the case study to SHCC link slab</p>	<table border="1"> <tbody> <tr> <td data-bbox="751 1532 799 1738">Step 6</td> <td data-bbox="799 1532 1382 1738"> <p>Case study: SHCC link slab</p> <ul style="list-style-type: none"> - Overview of point of attentions of the SHCC link slab design - Possibilities to improve the link slab design </td> </tr> <tr> <td data-bbox="751 1738 799 1998">Step 7</td> <td data-bbox="799 1738 1382 1998"> <p>Finish research</p> <ul style="list-style-type: none"> - Final conclusions and recommendations - Finish the definitive rapport and the presentation <p><i>Note: step 7 is not given in Figure 3</i></p> </td> </tr> </tbody> </table>	Step 6	<p>Case study: SHCC link slab</p> <ul style="list-style-type: none"> - Overview of point of attentions of the SHCC link slab design - Possibilities to improve the link slab design 	Step 7	<p>Finish research</p> <ul style="list-style-type: none"> - Final conclusions and recommendations - Finish the definitive rapport and the presentation <p><i>Note: step 7 is not given in Figure 3</i></p>				
Step 6	<p>Case study: SHCC link slab</p> <ul style="list-style-type: none"> - Overview of point of attentions of the SHCC link slab design - Possibilities to improve the link slab design 								
Step 7	<p>Finish research</p> <ul style="list-style-type: none"> - Final conclusions and recommendations - Finish the definitive rapport and the presentation <p><i>Note: step 7 is not given in Figure 3</i></p>								

2 Literature

In this chapter are shortly given the results of the literature study. The literature study starts with the definition of the Advanced Cementitious Materials (ACMs) that are included in the study. Then for every ACM is given a representative composition. Based on the composition of the ACMs the mechanical characteristics, durability and the sustainability of the ACMs are determined. After characterising the ACMs, some standards and recommendations that are specially made for certain ACMs are discussed. Then researched applications and reference projects are analysed, in order to prevent research to applications that have been researched or built already. Next, an analysis to structures is done. This literature study ends with a Multi Criteria Analysis of the ACMs. The results of the literature study are given in more detail in Appendix 1: Literature study.

2.1 Advanced Cementitious Materials

In this paragraph are given the Advanced Cementitious Materials (ACMs) that are in the scope of this research. The scope of ACMs is shown in Table 4. In Table 4 is also given the plain concrete where the ACMs are compared to, highlighted in grey. The plain concrete is a Normal Strength Concrete. The NSC and the ACMs are defined in more detail in the Appendix 1: Literature study. In this report are also discussed the cementitious materials that are not included in the scope of this research.

In order to make a quantitative comparison between the ACMs and plain NSC, for every type of ACM is defined a representative ACM and a representative NSC is defined. The representative mixtures should represent the characteristics of certain ACM type as good as possible, to make the comparison as good as possible. The representative ACMs and the representative NSC are defined in the Appendix 1: Literature study.

Table 4 – Overview of Advanced Cementitious Materials in the scope of the research, including the main characteristics and the themes the ACMs have mainly influence on

	Cementitious material	Main characteristic	Theme
Plain concrete	Normal Strength Concrete (NSC)		
ACM 1.	Normal Strength Steel Fibre Reinforced Concrete (NSSFRC)	Crack width control	Mechanical Durability
ACM 2.	High Performance Concrete (HPC)	Strength Compactness	Mechanical Durability
ACM 3.	High Performance Steel Fibre Reinforced Concrete (HPSFRC)	Strength Compactness Crack width control	Mechanical Durability
ACM 4.	Ultra High Fibre Reinforced Performance Concrete (UHFRPC)	Strength Compactness	Mechanical Durability
ACM 5.	Strain Hardening Cementitious Composite (SHCC)	Crack width control Strain hardening behaviour	Mechanical Durability
ACM 6.	Self-Healing Cementitious Material	Self-healing behaviour	Durability
ACM 7.	Geopolymer concrete	Low carbon footprint	Durability Sustainability
ACM 8.	Self-cleaning nano concrete	Unique mechanical, thermal and electrical properties	Durability
ACM 9.	Self-sensing nano concrete	Unique mechanical, thermal and electrical properties	Mechanical

* colours in table: blue for NSSFRC, HP(SF)RC and UHPC; orange for SHCC; purple for self healing concrete; green for geopolymer concrete; yellow for nano concrete

2.2 Compositions

In this paragraph are given the compositions of the representative ACM. In Table 5 is given the literature based overview of the compositions of the representative ACMs. The compositions in Table 5 are indicative values only, in order to make quantitative comparisons between the ACMs. In reality, a certain concrete could also be created with an alternative composition. For example, a C30/37 could also be created with CEM II instead of CEM I.

In Table 5 are shown some notable differences between the compositions of NSC and ACMs. A detailed description of the compositions is given in Appendix 1: Literature study. In short, the main differences are:

- In stronger concrete types (HPC and UHPC) is used more cement
- In stronger concrete types (HPC and UHPC) is used finer aggregate
- Self-healing concrete contains microcapsules, that give the self-healing behaviour
- Geopolymer concrete contains no Portland Cement
- Geopolymer concrete contains reactors to start the hardening reaction
- Self-cleaning concrete contains nano titanium oxide for the self-cleaning behaviour
- Self-sensing concrete contains nano iron oxide for the self-sensing behaviour

2.3 Mechanical characteristics

In this paragraph are given the mechanical characteristics of the representative ACMs. The mechanical characteristics are determined based on literature. In Table 6 is given the overview of the mechanical characteristics. Due to lack of knowledge, not all mechanical characteristics of all ACMs could be judged quantitatively. More details could be found in the Appendix 1: Literature study.

The representative ACMs show significant mechanical differences to each other, as shown in Table 6. The most important differences are listed here shortly. More details can be found in the Appendix 1: Literature study.

- More cement and finer aggregates in the composition result in a material with:
 - o Higher compressive strength
 - o Higher shear strength capacity
 - o Higher Young's modulus
- UHPC has a relative high tensile strain compared to NSC
- SHCC has a high shear strength compared to NSC
- SHCC has a relative low Young's modulus compared to NSC
- SHCC has a relative high maximum tensile strain compared to NSC
- SHCC shows very small cracks
- GPC has a relative low Young's modulus compared to NSC

Table 5 - Literature based overview of the compositions of the representative cementitious materials in this research

				Plain	ACM 1.	ACM 2.	ACM 3.	ACM 4.	ACM 5.	ACM 6.	ACM 7.	ACM 8.	ACM 9.
				NSC	NSSFRC	HPC	HPSFRC	UHPC	SHCC	Self-Healing	GPC	Self-cleaning	Self-Sensing
	Material	Grain diameter	Unit	C30/37 ^a	C30/37 ^b	C90/105 ^c	C90/105 ^b	C170/200 ^d	C40/50 ^e	C30/37 ^b	C30/37 ^f	C55/67 ^{i,b}	C30/37 ^g
Binders	CEM I	5 – 50 μm	[kg/m ³]	320	320	501	501	710	414	320			539
	CEM II	5 – 50 μm	[kg/m ³]									432	
	BFS	5 – 50 μm	[kg/m ³]						496		40		
Aggregate and additions	Aggregate	0 – 15 mm	[kg/m ³]										1148
	Coarse aggregate	4 – 32 mm	[kg/m ³]	1280	1280					1280	1209		
	Coarse aggregate	4 – 12.5 mm	[kg/m ³]			866	866					578	
	Fine aggregate	0 – 4 mm	[kg/m ³]	640	640	867	867			640		1003	
	Sand	0 – 2 mm	[kg/m ³]					1020			651		
	Fine sand	0 – 0.5 mm	[kg/m ³]										492
	Microcapsules	40 – 800 μm^h	[V%]							3			
	Crushed limestone	0 – 300 μm	[kg/m ³]										177
	Quartz powder	5 – 45 μm	[kg/m ³]					210					
	Limestone powder	5 – 20 μm	[kg/m ³]						827				
	Fly ash	0.2 – 40 μm	[kg/m ³]								360		
	Silica Fume	< 1 μm	[kg/m ³]					230					
	Nano titanium oxide	20 \pm 5 nm ⁱ	[kg/m ³]										18 ⁱ
	Nano iron oxide	15 \pm 3 nm ^g	[kg/m ³]										
Additives	Sodium hydroxide	–	[kg/m ³]								45.7		
	Sodium silicate	–	[kg/m ³]								114.3		
	Super-plasticizer	–	[kg/m ³]			8.5	8.5	13	7			2.5	
	Viscosity Modifying Agent (VMA)	–	[kg/m ³]									2	
Water	Water	–	[kg/m ³]	160	160	160	160	140	455	160		171	220
	Water/cement ratio	–	[–]	0.50	0.50	0.32	0.32	0.20	0.26	0.50		0.38	0.40
Fibres	PVA	$d = 40 \mu m, l = 8 mm$	[V%]						$\leq 2\%$ ^j				
	Steel Fibres (long)	$l = 60 mm^b$	[kg/m ³]		40-50 ^b								
	Steel Fibres (medium)	$l = 25 – 50 mm^b$	[kg/m ³]				70-85 ^b						
	Steel Fibres (short)	$l = 4 – 8 mm^b$	[kg/m ³]					100-160 ^b					

* colours in table: blue for NSSFRC, HP(SF)RC and UHPC; orange for SHCC; purple for self healing concrete; green for geopolymer concrete; yellow for nano concrete

- = unknown of N/A

^a (ENCI, 2008)

^b Assumptions and more details described in Appendix 1: Literature study

^c (Chen & Su, 2013)

^d (Paskvalin, 2015)

^e (Qian, et al., 2009)

^f (Deb, Nath, & Sarker, 2014)

^g (Nazari, Riahi, Riahi, Shamekhi, & Khademno, 2010)

^h (Pelletier, Brown, Shukla, & Bose, n.d.)

ⁱ (Jalal, Ramezaniapour, & Pool, 2013)

^j (Li, 2007)

Table 6 – Mechanical characteristics of the Advanced Cementitious Materials, based on Eurocode 2, Ultra High Performance Fibre-Reinforced Concretes Recommendations, Recommendations for Design and Construction of High Performance Fiber Reinforced Cement Composites with Multiple Fine Cracks (HPFRCC) and other literature.

			Plain	ACM 1.	ACM 2.	ACM 3.	ACM 4.	ACM 5.	ACM 6.	ACM 7.	ACM 8.	ACM 9.	
ACMs →			NSC	NSSFRC	HPC	HPSFRC	UHPC	SHCC	Self-Healing	GPC	Self-cleaning concrete	Self-sensing concrete	
Concrete characteristics ↓			C30/37 ^a	C30/37	C90/105 ^a	C90/105	C170/200 ^b	C40/50 ^c	C30/37	C30/37 ^d	C55/67 ^g	C30/37 ^g	
Strength	Characteristic compressive strength	f_{ck}	[MPa]	30	30	90	90	170	41	30	32	55	30.9
	Design value compressive strength	f_{cd}	[MPa]	20	20	60	60	96.3	26.8	20	21.3	37	20.6
	Mean axial tensile strength	f_{ctm}	[MPa]	2.9	2.9	5	5	12.9	5	2.9	2.1	4.9 ^e	1.7
	Characteristic axial tensile strength	$f_{ctk,0.05}$	[MPa]	2.0	2.0	3.5	3.5	9.0	-	2.0	1.5	3.4	1.2
	Design value axial tensile strength	f_{ctd}	[MPa]	1.4	1.4	2.3	2.3	6.0	3.4	1.4	1.0	2.3	0.8
	Characteristic elastic tensile strength	$f_{ctk,1}$	[MPa]	-	-	-	-	-	4.0	-	-	-	-
	Characteristic plastic tensile strength	$f_{ctk,2}$	[MPa]	-	-	-	-	-	4.4	-	-	-	-
	Fibre design tensile strength	f_{ctfd} or f_{vd}	[MPa]	-	-	-	-	6.9	3.4	-	-	-	-
Shear strength compared to NSC	V_{ACMx}/V_{NSC}	[-]	1.0	1.3-2.3 ^f	1.4	1.8-3.2 ^f	15	6	1.0	-	-	-	
Stiff	Mean Young's modulus	E_{cm}	[GPa]	33	33	44	44	50	18.5	33	23	+ ^g	-
	Effective Young's modulus	$E_{cd,eff}$	[GPa]	11	11	14.7	14.7	16.7	7.7	11	-	-	-
Strain	Maximum linear compressive strain	ϵ_{c3}	[%]	0.175	0.175	0.23	0.23	0.23	-	0.175	-	-	-
	Maximum compressive strain	ϵ_{cu3}	[%]	0.35	0.35	0.26	0.26	0.27	0.30	0.35	-	-	-
	Maximum mean compressive strain	ϵ_{cm}	[%]	-	-	-	-	-	-	-	0.24	-	-
	Maximum linear tensile strain	ϵ_{ct1}	[%]	0.01	0.01	0.01	0.01	0.014	0.178	0.01	-	-	-
	Maximum tensile softening strain	$\epsilon_{lim,soft}$	[%]	-	^g	-	^g	^g	-	-	-	-	-
	Maximum tensile hardening strain	$\epsilon_{lim,harden}$	[%]	-	-	-	-	≤0.25	1.73	-	-	-	-
	Crack pattern (tensile test)	-	-	One discrete crack*	< 2.5 mm if ϵ_{Fu} (ultimate tensile strain) = 1% ^h	One discrete crack*	< 2.5 mm if ϵ_{Fu} (ultimate tensile strain) = 1% ^h	0.039 mm at surface for $\epsilon_{sm,f} - \epsilon_{cm,f} = 0.36\%$	<0.1 mm for every strain ⁱ	One discrete crack*	One discrete crack*	-	-

colours in table: blue for NSSFRC, HP(SFR)C and UHPC; orange for SHCC; purple for self healing concrete; green for geopolymer concrete; yellow for nano concrete

- = unknown of N/A

* In general, NSC has a brittle crack behaviour if it is not reinforced. As soon as a crack arises, the crack becomes a through crack directly. For instance, if a small crack generates, the tensile force should be carried by a smaller cross section, so the stress increases a lot such that the total cross section fails. It is assumed that the influence of the microcapsules on the crack behaviour can be neglected. If concrete cracks the capsules should break open, so they should be quite brittle. Then the healing agent can be activated and the concrete can be healed. If the capsules would not fail brittle, the situation could be that the concrete cracks and the capsules remain uncracked. Geopolymer Concrete is like other cementitious composites brittle, with a low tensile strength and strain capacity (Ng, Htut, & Foster, 2010)

^a (Nederlands Normalisatie-instituut, 2011)

^b (AFGC's Scientific and Technical Committee, 2013)

^c (Qian, et al., 2009), (Japan Society of Civil Engineers, 2008)

^d (Shaikh, 2013), (Olivia & Nikraz, Properties of fly ash geopolymer concrete designed by Taguchi method, 2012), (Ryu, Lee, Koh, & Chung, 2013), (Hardjito, 2005), (Aldred, 2013)

^e (Jalal, Ramezaniapour, & Pool, 2013)

^f Depending on the fibres, more details described in Appendix 1: Literature study

^g Assumptions and more details described in Appendix 1: Literature study

^h (fib Bulletin 55, 2010)

ⁱ (Li, 2007)

2.4 Durability characteristics

In new contract types, maintenance of structures becomes a lot more important for the contractor. To estimate the maintenance during life time, the durability characteristics of materials are interesting to know. Therefore, in this paragraph are discussed the durability characteristics of the ACMs. These durability and the durability characteristics of the ACMs are described in detail in Appendix 1: Literature study.

Before the durability of the ACMs is determined, some research is done to the most important degradation mechanisms. The material characteristics that characterise the most important degradation mechanisms, so also the durability of concrete are:

- Water permeability
- Chloride diffusion coefficient
- Carbonation coefficient

The influence of a certain modification in the mixture on the three mechanisms is research in order to argue the durability of an ACM compared to the durability of NSC. For instance, UHPC has a low w/c ratio. A relative low w/c ratio results in a denser structure, what results in a lower permeability. An decreased permeability results in a higher durability of the concrete. Then, for example de-icing salts penetrate slower in the concrete. So if only the w/c ratio is taken into consideration, it could be concluded that UHPC is expected to be more durable than NSC, because the w/c ratio.

In Table 7 is given an overview of the above mentioned durability characteristics. In the upperpart of the table are given theoretical value of the water permeability, chloride diffusion and carbonation. In the lower part of the table are given some practical values to give a practical meaning to the theoretical characteristic. Some ACMs are only judged qualitatively, because they are not known well enough at the moment.

The most notable thing from Table 7 are:

- Denser types of concrete, HPC and UHPC, have a significant lower water permeability, chloride diffusion coefficient and carbonation rate.
- Geopolymer concrete can't carbonate or at least another mechanism takes place.

With the help of some models, the theoretical numbers can be turned in some practical graphs. The diffusion profile is determined according to Fick's second law, which is described in CUR Leidraad 1 (CUR bouw & infra, n.d.). The carbonation profile of the ACMs is determined according to the $k\sqrt{t}$ -formula. Both, the chloride profiles and the carbonation profiles of different ACMs are shown in Figure 4 and Figure 5. HPC and UHPC have both better chloride and carbonation resistance compared to NSC.

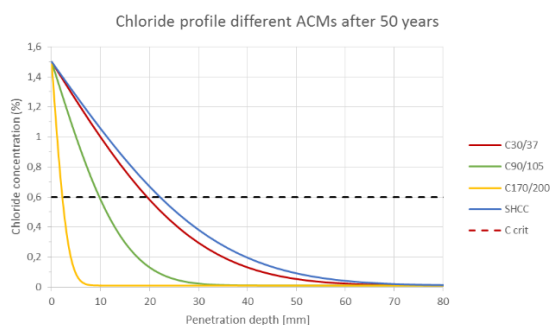


Figure 4 - Chloride profiles of ACMs exposed to 1.5% chloride concentration for 50 years (XD3, XS1)

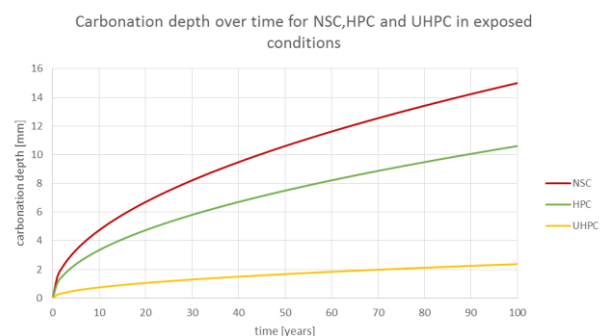


Figure 5 - Carbonation depth over time for NSC, HPC and UHPC according to the model $x = k\sqrt{t}$ in 'exposed' environment conditions

Table 7 - Durability characteristics per ACM at 28 days after casting

Concrete characteristic	Unit	Quantitative								Qualitative	
		Plain	ACM 1.	ACM 2.	ACM 3.	ACM 4.	ACM 5.	ACM 6.	ACM 7.	ACM 8.	ACM 9.
		NSC	NSSFRC	HPC	HPSFRC	UHPC	SHCC	Self-Healing	GPC	Self-cleaning concrete	Self-sensing concrete
Water permeability	[10^{-14} m/s]	100-10,000 ^a	100-10,000 ^a	10-100^b	10-100^b	0.4-0.5^c	5,000 ^d	100-10,000 ^e	40-5,000 ^{f,**}	+ ^{j,b}	+ ^g
Chloride diffusion coefficient	[$10^{-12} \text{ m}^2/\text{s}$]	>4 ^{k,*}	>4 ^{k,*}	<5 ^{b,k,*}	<5 ^{b,k,*}	<0.1 ^{k,*}	6.8 ^h	>4 ^{e,*}	<<1 ⁱ	+ ^{j,b}	+ ^b
Carbonation rate of passive reinforcement	[$\mu\text{m}/\text{year}$]	1.2 ^k	1.2 ^k	0.25^k	0.25^k	< 0.01 ^k	1.2^l	1.2 ^e	N/A	- ^b	unknown
Critical chloride depth after 50 years for above mentioned chloride diffusion coefficients (limit values)	[mm]	>14	>14	<16	<16	<2	22	>14			
Chloride diffusion coefficient for calculation	[$10^{-12} \text{ m}^2/\text{s}^2$]	8	8	2	2	0.1	6.8	8			
Critical chloride depth after 50 years by mean chloride diffusion coefficients	[mm]	19	19	10	10	2	22	19			
Carbonation depth after 50 years in an 'exposed' environment	[mm]	22.5	22.5			<3.8	22.5	22.5			

Bolded values are positive compared to NSC

colours in table: blue for NSSFRC, HP(SFR)C and UHPC; orange for SHCC; purple for self healing concrete; green for geopolymer concrete; yellow for nano concrete

* The chloride diffusion coefficients that are given in the table are indicative values that represent NSC, HPC and UHPC as good as possible. Probably, mixture could be made with a chloride diffusion coefficient that belong to the HPC group, but with compressive strength that belongs to the NSC group. However, the values of an ACM type are chosen such that they cover most for materials that belong to that ACM type based on mechanical characteristics. For example, most NSC mixtures will have a chloride diffusion coefficient higher than 4. The chloride diffusion coefficients of a group are just made quantitative to compare different type of ACMs to each other. The same is valid for HPC and UHPC. Probably, there are also mix design that have HPC or UHPC characteristics but a chloride diffusion coefficient higher than 5 or higher than 1 respectively.

** The water permeability of GPC is in quite a large range. There is not a lot of literature available according to the water permeability of GPC. The thing is that the water permeability is high in proportion to the better researched chloride diffusion coefficient. Earlier in this research is shown that the chloride diffusion coefficient depends, like the water permeability, for example on the permeability of the concrete. By combining both, reasons could be given that a lower water permeability could be expected.

Qualitative characteristics

- + positive influence on the durability, so a lower water permeability, chloride diffusion coefficient or carbonation depth compared to NSC
- +/- no positive or negative influence on the durability, so nearly no different water permeability, chloride diffusion coefficient or carbonation depth compared to NSC
- negative influence on the durability, so a higher water permeability, chloride diffusion coefficient or carbonation depth compared to NSC

^a (Tayeh, Bakar, Johari, & Voo, 2012), (Breyse & Gerard, 1997), (Liu, Chia, & Zhang, 2011), (Wang, Jansen, Shah, & Karr, 1997)

^b (Majorana, Salomoni, Mazzucco, & Khoury, 2010), (Gupta, et al., 2008)

^c (fib, 2009)

^d (Lepech & Li, 2005)

^e Assumptions done, further discussed in the rest of the chapter

^f (Olivia & Nikraz, Strength and water penetrability of fly ash geopolymer concrete, 2011), (Cheema, Lloyd, & Rangan, 2009)

^g Assumptions and more details described in Appendix 1: Literature study

^h (Li, 2007)

ⁱ (Yang, Yao, & Zhang, 2014), (Chindapasirt & Chalee, 2014), (Aldred, 2013)

^j (Jalal, Ramezaniapour, & Pool, 2013)

^k (AFGC's Scientific and Technical Committee, 2013)

^l (Japan Society of Civil Engineers, 2008)

2.5 Sustainability characteristics

In this paragraph is the sustainability of the ACMs characterised. The sustainability characteristics of the ACMs are determined with the computer software 'Rekentool Groen beton 3.0'. The program can calculate an environment costs index (MKI). The MKI includes eleven effects that the concrete has on the environment, like depletion of fossil energy, global warming and acidification. The MKI is a value that stands for the costs that should be made to compensate the effects that a certain volume of concrete has on the environment.

In Figure 6 are given the MKIs of the ACMs. Not all ACMs are known by the program yet. The MKI values that are given in Figure 6 are valid for one cubic concrete. The compositions of Table 5 are used as input to determine the MKIs. The MKIs of the representative mixture per ACM is compared to the MKI of C30/37, what is the representative mixture of NSC. In every column of the graph of Figure 6 is shown a number, the MKI-index. This index is a factor between the MKI of a representative ACM compared to the MKI of C30/37. As shown, most ACMs has 1.5 to 2 times worse effect on the environment (including eleven effect from the tool only) compared to NSC. More details could be found in the Appendix 1: Literature study.

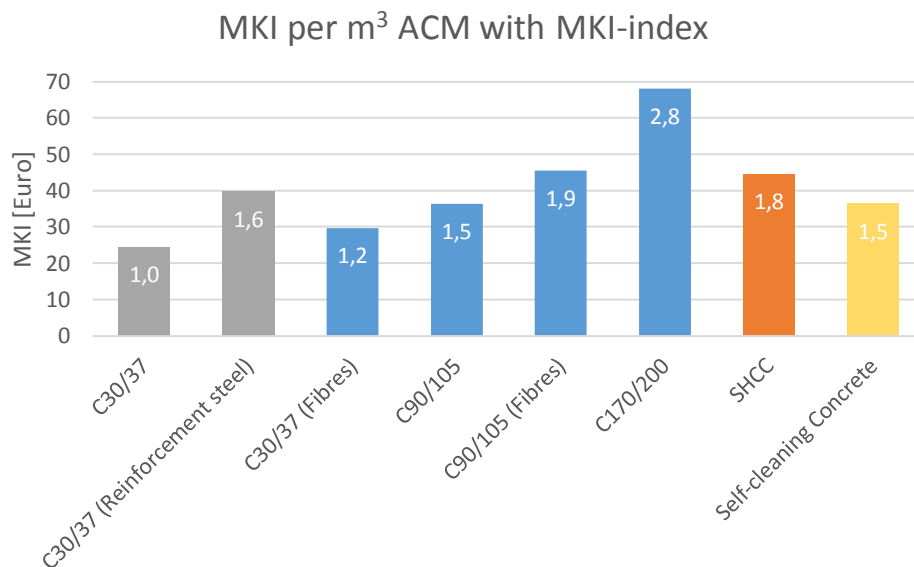


Figure 6 - MKI per cubic metre ACM with MKI-index

2.6 Standards and recommendations

The most ACMs are that innovative, that there are no general codes for them yet. In some countries, there are some standards or recommendations for certain ACMs. Some these standards are given in Table 8. More information of the standards and recommendations can be found in Appendix 1: Literature study. In this appendix are also given some calculation examples.

Table 8 – Standards and recommendations for Advanced Cementitious Materials

ACM	Standard/recommendation	Society	Country/Continent	Year of release
NSSFRC	Model Code 2010	FIB	Europe	2013
HPSFRC	Model Code 2010	FIB	Europe	2013
HPC	NEN-EN 1992-1-1+C2 (Eurocode 2)	NEN	Europe	2011
UHPC	Ultra High Performance Fibre-Reinforced Concretes - Recommendations	AFGC	France	2013

SHCC	Recommendations for Design and Construction of High Performance Fibre Reinforced Cement Composites with Multiple Fine Cracks (HPFRCC)	Japan Society of Civil Engineers	Japan	2008
GPC	CIA Z16-2011: Geopolymer Recommended Practice Handbook	Concrete Institute of Australia	Australia	2011

colours in table: blue for NSSFRCC, HP(SFR)C and UHPC; orange for SHCC; purple for self healing concrete; green for geopolymer concrete; yellow for nano concrete

2.7 Researched applications and reference projects

In this paragraph are discussed researched application and reference projects of ACMs. There is done a lot of research to applications of ACMs already. There are even applied in practice already. Both, researched and reference projects could be helpful to make combinations of constructions and ACMs. Ideas that are researched or construct already, are not researched again. However, these structures could be the inspiration for new applications. Some reasons to apply certain ACMs according to reference projects are shown in Table 9. All researched applications and reference projects that are analysed in this research can be found in Appendix 1: Literature study. In the appendix, for every project is given more information.

Table 9 - Reasons to apply certain ACMs according to reference projects

ACM	Reasons to apply
FRC	Complexity in reinforcement
HPC and UHPC	Durability and maintenance
	Aesthetics
SHCC	Durability
	Economical
GPC	Sustainability
	Durability
Self-cleaning concrete	Aesthetic

Some inspirational reference projects in this research are:

- UHPC bridge girders, because of the weight reduction and slenderness of a structure what is especially interesting if existing bridge girders must be replaced.
- HPC sluice doors, because of the durability of HPC what is especially interesting in sea locks.
- SHCC shotcrete, because of the reduced crack width, SHCC shotcrete is interesting to retrofit structures to increase the mechanical and durability characteristics of the structure.
- SHCC link slab, because SHCC seems an interesting material to make joints in bridges because of its strain capacity and limited crack width in SHCC.

2.8 Structures

In this paragraph are given the structures that are analysed in this research. Further, the analysis is explained shortly. A detailed analysis to the structures is given in Appendix 1: Literature study. Nine structure are included in the analysis. Before smart combinations with ACMs could be made, the constructions are analysed from a mechanical and durable point of view. The structures that are included in the research are shown below.

1. Foundation
2. Viaduct and girder bridge
3. Sluice
4. Embankment
5. Retaining wall
6. Noise barrier
7. Tunnels, culverts and sewage
8. Underpass
9. Aqueduct

In the analysis to the mechanics of the structures are determined the main mechanical requirements for the concrete material. For example, in many structures are requirements for the material in terms of the compressive strength and the stiffness of the material.

From durability reasons, for the main parts of the structures is determined the exposure class. In structures that are exposed to tough conditions, for example a sea lock, higher requirements for the material are expected. It is expected that in tough conditions a very durable ACM, could be interesting to apply.

2.9 Multi Criteria Analysis of the ACMs

In this paragraph, all mechanical, durability and sustainability characteristics of the ACMs are combined together in a Multi Criteria Analysis. For every of the three themes are given some typical characteristics, for example the compressive strength for the theme mechanics. The ACMs are judged on these characteristics.

The MCA is shown in Table 10. In the second column of the table are shown the material characteristics where the ACMs are judged on. In the third column is shown the weight factor per characteristic. The most important material properties have a weight factor 5, the least important characteristics have a weight factor of 1. The performance of the ACMs on the given characteristics are judged with a score between 1 and 5. If a material has a high compressive strength, the score on the compressive strength characteristic is 5. By multiplying the weight factor by the score per characteristic, a weighted score per characteristic is calculated. By adding the weighted values, a subtotal and weighted subtotal per theme can be determined. In the last two rows of the table, even a total and a weighted total of all the themes together is calculated per ACM. To end this chapter, under Table 10 are given some conclusions that follow from the Multi Criteria Analysis. More information about the analyses could be found in Appendix 1: Literature study.

Table 10 - Multi Criteria Analysis for plain concrete and the ACMs for mechanical, durability and sustainability characteristics including a general

		Quantitative analysed on mechanical, durability and sustainability characteristics											Partly not and/or partly qualitative analysed										
		plain		ACM 1		ACM 2		ACM 3		ACM 4		ACM 5		ACM 6		ACM 7		ACM 8		ACM 9			
		NSC		NSSFRC		HPC		HPSFRC		UHPC		SHCC		Self-healing concrete		GPC		Self-cleaning concrete		Self-sensing concrete			
		score	weighted	score	weighted	score	weighted	score	weighted	score	weighted	score	weighted	score	weighted	score	weighted	score	weighted	score	weighted		
	Weight factor																						
Mechanical	Compressive strength	5	1	5	1	5	3	15	3	15	5	25	1	5	1	5	1	5	2	10	1	5	
	Tensile strength	2	1	2	1	2	2	4	2	4	5	10	2	4	1	2	1	2	2	4	1	2	
	Shear resistance	3	1	3	2	6	1	3	2	6	5	15	3	9	1	3		0		0		0	
	Young's modulus	3	3	9	3	9	4	12	4	12	5	15	1	3	3	9	2	6		0		0	
	Linear compressive strain	1	1	1	1	1	2	2	2	2	2	2	1	1	1	1		0		0		0	
	Max compressive strain	2	3	6	3	6	1	2	1	2	1	2	2	4	3	6		0		0		0	
	Linear tensile strain	1	1	1	1	1	1	1	2	2	2	2	0	0	1	1		0		0		0	
	Max tensile strain	3	2	6	2	6	1	3	2	6	2	6	5	15	2	6		0		0		0	
	Subtotal mechanical			33		36		42		49		77		41		33		13		14		7	
	Weighted subtotal mechanics			3.3		3.6		4.2		4.9		7.7		4.1		3.3							
Durability	Permeability	2	1	2	1	2	3	6	3	6	5	10	2	4	1	2	2	4		+		+	
	Chloride penetration	4	1	4	1	4	3	12	3	12	5	20	2	8	1	4	4	16		+		+	
	Carbonation depth	3	1	3	1	3	3	9	3	9	5	15	3	9	1	3	5	15		-		?	
	Crack behaviour	5	1	5	3	15	1	5	3	15	4	20	5	25	1	5	1	5		?		?	
	Subtotal durability			14		24		32		42		65		46		14		40		+		+	
	Weighted subtotal durability			2.0		3.4		4.6		6.0		9.3		6.6		2.0		5.7					
Sustainability	MKI	4	5	20	5	20	4	16	3	12	1	4	3	12		0		0	4	16		0	
	Carbon dioxide emission	2	4	8	4	8	3	6	3	6	1	2	3	6		0	5	10	4	8		0	
	Subtotal sustainability			28		28		22		18		6		18		0		10		24		0	
	Weighted subtotal sustainability			9.3		9.3		7.3		6.0		2.0		6.0						8.0			
Total			70		73		91		94		128		80		42		58		38		7		
Weighted total			4.9		5.5		5.4		5.6		6.3		5.6										

colours in table: blue for NSSFRC, HP(SFR)C and UHPC; orange for SHCC; purple for self healing concrete; green for geopolymer concrete; yellow for nano concrete

Qualitative characteristics

1. Very bad or negative performance on characteristic. For example very low strength, very low permeability, very high MKI
2. Bad or negative performance on characteristic. For example low strength, low permeability, high MKI
3. Mean performance on characteristic. For example mean strength, mean permeability, mean MKI
4. Good or positive performance on characteristic. For example high strength, high permeability, low MKI
5. Very good or positive performance on characteristic. For example very high strength, very high permeability, very low MKI

Qualitative characteristics

- + Positive influence on the durability, so a lower water permeability, chloride diffusion coefficient or carbonation depth compared to NSC
- +/- No positive or negative influence on the durability, so nearly no different water permeability, chloride diffusion coefficient or carbonation depth compared to NSC
- Negative influence on the durability, so a higher water permeability, chloride diffusion coefficient or carbonation depth compared to NSC
- ? Unknown

Some conclusions from Table 10:

- The best weighted subtotal **mechanics** is for UHPC. This could be expected on forehand, since this concrete has an extremely high compressive strength and a high stiffness
- The worst weighted subtotal **mechanics** is for NSC. Most other types of concrete are stronger or have better strain capacities
- The best weighted subtotal **durability** is for UHPC. This could be expected on forehand, since this concrete is extremely dense compared to the other ACMs.
- The worst weighted subtotal **durability** is for NSC. Most other types of concrete are denser or have a better crack behaviour.
- The best weighted subtotal **sustainability** is for NSC. NSC has the lowest amount of cement, which has quite a large influence on the sustainability. GPC is probably more sustainable than NSC, but the sustainability of this type of concrete is hard to quantify at the moment.
- The worst weighted subtotal **sustainability** is for UHPC. Probably, the low sustainability is mainly caused by the very high cement content in UHPC.
- The weighted **total** of the three themes shows that UHPC performs the best on the given characteristics and NSC the worst, assuming that all the mechanical, durability and sustainability characteristics are even important.
- Most ACMs perform significant better on durability than NSC.
- Most ACMs perform significant worse on sustainability than NSC.

3 Field of Applications

In this chapter are given fields of applications of structure and ACMs. The applications are based on some problems from practice and on some design ideas. Problems from practice are mentioned in more detail in Appendix 2: applications study. The design ideas are mentioned here shortly. After that an overview of combinations is given. At last, the best applications are pick out and are discussed in some more detail.

3.1 Design ideas

Just before applications between ACMs and structures are made, in this paragraph some general design ideas are given. The design ideas are shown in Table 11. The ideas are divided by the three themes of this research; mechanics, durability, sustainability. Most of the ideas are based on costs. The ACMs are relative expansive compared to NSC, so they should be applied efficiently. Probably a combination of NSC with an ACM is smarter to apply than a structure fully made of one ACM.

Table 11 – Design ideas for ACMs from different themes

Theme	Design ideas
Mechanics	<ul style="list-style-type: none"> - Reduction of structure <i>height</i> by strong concrete - Reduction of the <i>self-weight</i> by strong concrete - Increase the <i>building speed</i> by applying a strong concrete (Ottelé, 2015) - Stiff concrete if <i>deformation</i> is the governing design parameter - Strong concrete at <i>highly loaded</i> parts of a structure - Fibre reinforced concrete in structures with <i>special shapes</i> if the reinforcement design become too complex
Durability	<ul style="list-style-type: none"> - Very <i>durable</i> concrete only at the outside of the concrete - Concrete with a very limited <i>crack width</i> only at the surface of the concrete - Concrete with a limited <i>cracks width</i> if the crack width is the governing design parameter - Self-cleaning concrete for structures with a high <i>aesthetic value</i>
Sustainability	<ul style="list-style-type: none"> - <i>Minimize the amount of ACMs</i> with a low sustainability - Self-sensing on <i>critical parts</i> of a structure (potential increase of service life) - Self-sensing on elements that are <i>hard to monitor</i> with current methods (potential increase of service life)

3.2 Constructions and ACMs

In this paragraph are given applications of ACMs in structures. Also the potential of the applications is judged. The applications are divided in three groups of potential. After that, from best potential group the top 3 most potential applications are determined. From the best three, one application is chosen to research in more detail in the case study. A detailed description of the applications is given in Appendix 2: Field of applications.

Taking the design ideas from chapter 3.1 Design ideas into consideration, combinations of structures and ACMs are made. An overview of all applications is given in Table 12. The applications of Table 12 are divided in three categories of potential;

- **Very potential:** Application that seem to be very potential in theory
- **Potential:** Application that are expected to be potential, but less potential the very potential applications or only in specific circumstances
- **Not or nearly potential:** application that should not be applied in practice, because these structures seem to have no or nearly no benefits

All the applications of Table 12 are discussed in more detail in Appendix 2: Field of applications

Table 12 – Overview of combinations of ACMs and structures divided in three categories of potential

Very potential	Potential	Not or nearly potential
HPC bridge deck	UHPC bridge deck	NSSFRC/HPSFRC cross beam
(U)HPC bridge girder	UHPC joint	NSSFRC/HPSFRC culvert
(U)HPC sluice door	(U)HPC cross beam	NSSFRC/HPSFRC aqueduct
UHPC deck of underpass	NSC and UHPC sluice door	UHPC tunnel elements
	UHPC embankment	(U)HPC sewage
	UHPC retaining wall	(U)HPC foundation slab
	UHPC aqueduct	UHPC and NSC sewage
	UHPC and NSC aqueduct	Steel and UHPC sluice door
SHCC bridge deck	SHCC barrier	SHCC aqueduct joint
SHCC for repair (deck,tunnel,...)	SHCC embankment	NSC and SHCC in culverts
SHCC bridge joint	SHCC joint in tunnel	NSC and SHCC in tunnel
	NSC with SHCC bridge girders	NSC and SHCC aqueduct
	Self-healing concrete aqueduct	
	GPC sluice door	GPC foundation slab
		GPC embankment
		GPC culvert
		GPC sewage
		GPC foundation piles
		Steel and GPC sluice door
	Self-sensing foundation piles	Self-cleaning noise barrier

colours in table: blue for NSSFRC, HP(SFR)C and UHPC; orange for SHCC; purple for self healing concrete; green for geopolymer concrete; yellow for nano concrete

Analysing the very potential applications in some more detail, these applications could be divided in two groups as shown below. The first one is the slenderness optimisation and the second one is an optimisation in terms of durability issues. Mainly, applications with HPC and UHPC are optimisation in terms of slenderness and applications with SHCC are optimizations in terms of durability.

Slenderness optimisation	Durability issues
- HPC bridge deck	- SHCC bridge deck
- (U)HPC bridge girder	- SHCC repair
- UHPC deck of underpass	- SHCC joint in bridge
	- (U)HPC sluice door

From the very potential combinations, the top 3 most potential applications of ACMs in structures is made by; UHPC bridge girder, UHPC deck of an underpass and SHCC joint in a bridge or viaduct. This three options are shortly described here. The description is given in a random order.

- **(U)HPC bridge girder:** there are a lot of old viaducts and bridges in the Netherlands. Probably a lot of them should be replaced in the next decades. In some cases it could be interesting to construct the new bridge of (U)HPC. For example, from a safety point of view, it could be desirable to left out an intermediate support in the new situation. Then the span length increases, so the concrete should be stronger.
- **UHPC deck of an underpass:** short calculations in Appendix 2: Combination study show that the deck of an underpass that is made of UHPC is probably interesting to apply in terms of money. The deck is more expensive, because it is made of UHPC instead of NSC. However, because the deck can be made more slender, the underpass structure is reduced. The

benefits of this secondary effect are in potential larger than the cost difference between the NSC deck and the UHPC deck.

- **SHCC joint in a bridge:** in the reference projects is described the idea of a bridge joint made of SHCC that is applied in the USA. From a durability point of view, this idea seems very interesting to apply in The Netherlands too. Further, the durability of the SHCC joint is expected to have some additional secondary advantages. Moreover, the SHCC link slab does have a certain deformation capacity.

In the end, the SHCC joint in a bridge is chosen as most interesting application to research in more detail in the case study. The main advantage of this idea is the durability of the structure, what results in a lot of secondary advantages. Reasons to expect that this application has a lot of potential are shown in the list below. This reasons are explained in more detail in chapter 5 Thin SHCC Link slab.

- Deformation capacity
- Road comfort
- Protection of the substructure because leakage water can hardly penetrate through the link slab.
- Protection of the substructure because chemicals, for example from de-icing salts, can hardly diffuse through the link slab.
- Low stresses in the link slab if the link slab is exposed to imposed deformation (assuming only tensile stresses are generated in the design)
- GFRP reinforcement can't corrode
- Probably less (or maybe even no) cost for maintenance required
- Increase service of the road because less maintenance is required
- Longer expected service life compared to most other types of connection

4 Introduction to the case study: SHCC Link Slab

The case study is an in depth research to the SHCC link slab. For this research is made a new framework, which is given in this chapter. In this chapter, the framework is given shortly only. More details could be found in Appendix 3: SHCC Link Slab In general, joints are vulnerable and complex parts of a construction that should be able to move without causing reaction stresses and it should be strong enough to resist the same loads as the rest of the structure. This is exactly the complexity of the joint, it should move freely and resist large loads. On forehand, it is expected that a link slab made of SHCC is able to do this job. Further, compared to a lot other joints, additional benefits are expected by utilising SHCC link slabs.

4.1 Research question

In the combination study is mentioned the idea of a joint that is made of SHCC. Compared to NSC, SHCC has a relative low stiffness, a fine cracking pattern, a high tensile strain and a comparable strength. Therefore, it is expected that SHCC could be a potential alternative material to make proper joints. The question is how SHCC should be applied in a joint to make a proper design. Therefore, the research question is:

How look the designs of SHCC joints?

4.2 Objective

As mentioned in the research question, SHCC seems a potential alternative material to construct proper joints. Therefore research should be done to different types of SHCC joints as mentioned in research question. Then the most interesting joint is analysed in more detail. It is assumed that from this analysis, some points of attention in the link slab design are found. These points should be researched before the joint could be applied in practice. Therefore to make take the next step in order to apply the link slab design, the objective in the case study is:

An overview of points of attention of different SHCC link slab designs

4.3 Boundary conditions

In this paragraph are given some boundary conditions that are set up to keep the research practical to do. Every condition is explained in some detail. The included boundary conditions are:

- **Interesting SHCC link slab design:** during the analysis, the most interesting SHCC link slab will be determined. This is probably the design that is expected to be applied frequently by Heijmans or the design that has the most potential benefits.
- **Joint parameters:** the joint that is taken into consideration is situated at a middle support of a bridge or viaduct.
- **Homogenous material:** from reasons of simplicity, SHCC is assumed to be a homogenous material. That means that if multiple link slabs are applied, for example all link slabs crack and fail at the same stress or imposed deformation.
- **Structural point of view:** the points of attention are considered from a structural point of view only.

5 Thin SHCC Link slab

In this chapter is discussed the case study to the SHCC link slab. After some literature research, which can be found in Appendix 3: SHCC Link Slab, the thin SHCC link slab design that is constructed on a concrete deck is chosen to research in more detail. In this chapter first the potential of the Thin SHCC link slab is discussed. After that, a reference project where SHCC is applied in the deck of steel bridge is shown. Then the SHCC link slab is compared to the NSC flexible joint, which is applied for decades already. From this comparison follows some potential advantages of the SHCC link slab compared to the conventional NSC flexible joint. Next, an analysis to the way loads and imposed deformations are carried by the link slab is presented. From this structural analysis, some points of attention are given. This points should be researched in more detail before the link slab can be utilised. In the end, one of these points is researched in some more detail.

5.1 Potential of the Thin SHCC Link Slab

In this paragraph is clarified the potential of the Thin SHCC Link Slab. However, before the potential of the Thin SHCC link slab is argued, the design is described shortly. According to the design, the potential of the link slab is analysed. A detailed description of the SHCC link slab could be found in Appendix 3: SHCC Link Slab. In Figure 7 is schematically shown the cross section of the SHCC link slab design. The link slab consists of three parts; two passive parts with an active part in between. The total link slab must be able to resist horizontal and vertical loads. The active part of the link slab must take care of imposed deformation. Under the active section is created a debonding layer, in order to prevent localisation of cracks as much as possible. In this manner, the crack width could be controlled till a minimum such that a durable connection is created. The passive parts of the link slab must create a proper connection between the active section and the concrete substructure. In the passive parts, no cracks should be formed.

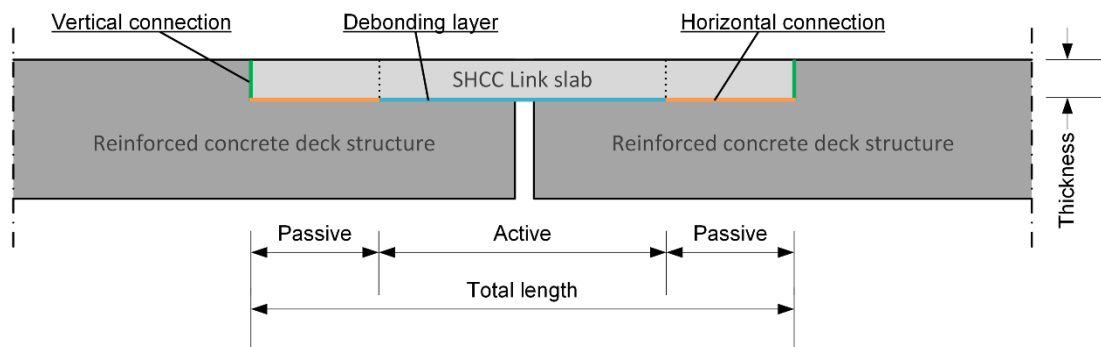


Figure 7 – Schematisation of the design of the Thin SHCC Link Slab

Now the potential of the SHCC link slab can be discussed according to the above described design. As concluded in the study to applications in chapter 3 Field of Applications, the SHCC link slab seems to be one of the most potential applications to utilise in practice. Below, the potential advantages of the SHCC link slab are listed shortly. The advantages are:

- The longitudinal deformation capacity of the joint is in the order of 1 % of the active length of the link slab. Maximum allowed strain depends on the design (Reyes & Robertson, 2011), (Lárusson, 2013).
- The road comfort is better compared to most other joint types because the deck surface is continuous.
- Until the maximum strain ($\epsilon \approx 1\%$), the permeability of cracked SHCC is about the same as the permeability of uncracked SHCC. That means that leakage water can hardly penetrate through the link slab, even if the SHCC is fully cracked. (Lárusson, 2013)

- Until the maximum strain ($\varepsilon \approx 1\%$), the chloride diffusion coefficient of cracked SHCC is about the same as the chloride diffusion coefficient of uncracked SHCC. That means that for example de-icing chemicals can hardly diffuse through the link slab, even if the SHCC is fully cracked. (Lárusson, 2013)
- GFRP reinforcement can't be damaged by chlorides or water.
- The SHCC Link Slab may lead to reduced maintenance.
- The durability of the design may result in a longer service life.
- If the maintenance is reduced and the service life increase, a higher service of the road could be expected.

5.2 Reference project: SHCC Deck Slab on steel girders (Michigan, USA)

In Michigan, USA, SHCC is applied in practice already to create a joint between two spans. However, this link slab does differ significant from the Thin SHCC Link Slab that is described in the previous paragraph. The main difference is that the horizontal deformation capacity of the SHCC Deck Slab could be neglected. This link slab is able to take care of rotation only. A detailed description of the SHCC Deck Slab is given in Appendix 3: SHCC Link Slab. The SHCC Deck Slab has some advantages compared to a link slab that is made of normal strength concrete. In short:

- Lower amount of reinforcement compared to the NSC Link Slab
- Lower stiffness of the link slab compared to the NSC Link Slab, such that the joint act more like a hinge.
- The crack width under cycling load are limited because the crack width under cycling load is independent of the reinforcement ratio.
- No cracks were observed at the interface between the SHCC Link Slab and the NSC Deck Slab

This structure is analysed in this paragraph shortly. The structure consists of steel girders, where a concrete deck is placed on. Between two spans, at the intermediate support, is the concrete deck replaced by an SHCC Deck Slab. The idea of the design is schematically given in Figure 8. The SHCC Deck Slab must carry vertical and horizontal stresses, same as in the NSC deck. Further, the SHCC Deck Slab has a rotation capacity, so the Deck Slab could take care of imposed curvatures. The SHCC Deck Slab can't take care of imposed horizontal deformations. So this joint type should be applied in combination with an expansion somewhere else in the bridge.

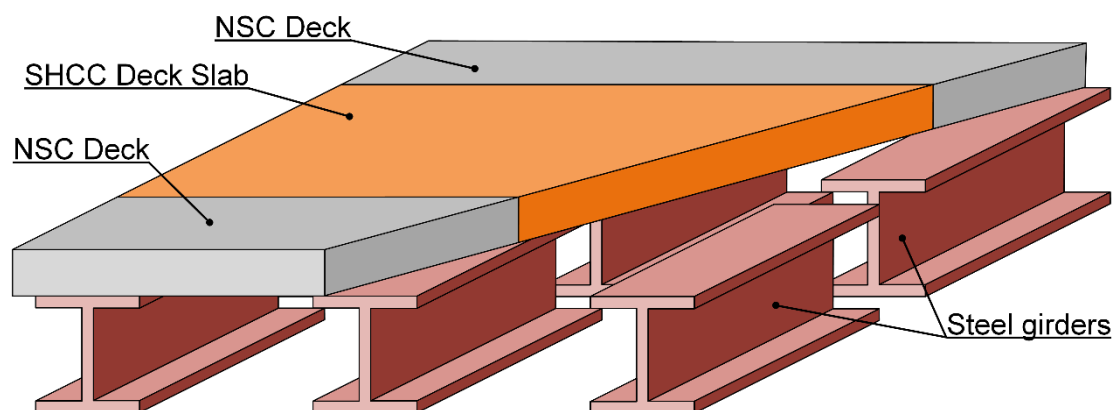


Figure 8 – Overview of the SHCC Deck Slab placed on steel girders

In Figure 9 is shown the Deck Link Slab design that is constructed in Michigan USA (Li, et al., 2003). The figure shows a cross section of the link slab. The drive direction is from the left to the right on the figure and the other way around. As shown in Figure 9, there is a gap of 25 mm (2") between the girders. Because of this gap, a vertical peak stress at the end of the steel girder could be expected, same as in case of the thin link slab.

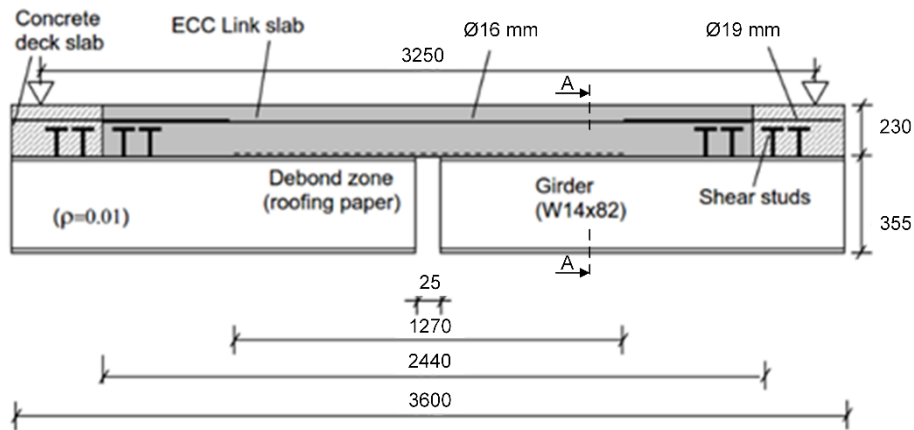


Figure 9 – Geometry of the link slab designs (Li, et al., 2003)

In Figure 10 is shown the cross section of the link slab that is analysed in Appendix 3: SHCC Link Slab in more detail. The place of the cross section is shown in Figure 9 (cross section AA). The steel girders could be supported as simple supports. In the active zone of the link slab, this support can only take care of vertical forces from the deck slab.

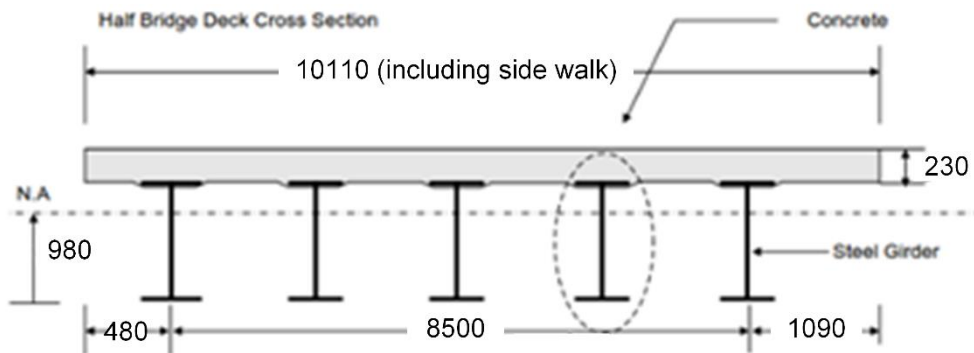


Figure 10 – Cross section AA of Figure 9, SHCC Deck Slab and steel girders at the active section of the link slab (Li, et al., 2003)

In short, the most important characteristics of the SHCC Deck Slab are listed below. From this characteristics could be concluded that in Michigan, USA, is made an alternative design of the NSC Flexible Joint that is applied in the Netherlands for years. The NSC Flexible joint is discussed in more detail in paragraph 5.3 NSC flexible joint and SHCC link slab. Both designs differ a lot, but are in essence the same. The most important characteristics of the SHCC Deck Slab that is applied in Michigan are:

- Horizontal load capacity
- Vertical load capacity
- Rotation capacity
- No horizontal deformation capacity

5.3 NSC flexible joint and SHCC link slab

Concrete joints are successfully applied for decades already, the so-called NSC flexible joints. In this paragraph, the SHCC link slab is compared to the NSC Flexible Joint in order to analyse the advantage of the SHCC link slab compared to the NSC flexible joint. Therefore, the main characteristics and behaviour of both joints are analysed, such that the difference between both could be made clear in a proper way. More details of both the NSC flexible joint and the SHCC link slab could be found in Appendix 3: SHCC Link Slab.

In Table 13 is given an overview of the main characteristics of the NSC flexible joint and the SHCC link slab. In the upper part of the table are shown the designs schematically. Per design is given a model to describe the mechanical scheme of the two different span connections. In the lower part of Table 13 are shown the main characteristics of the NSC flexible joint and the SHCC link slab. The most important characteristic differences between both systems are highlighted green. From the table the next conclusions for the structure behaviour of both types of joint could be made:

- The NSC flexible joint works as a small ‘bridge’ between the two spans, modelled as a clamped beam.
- Vertical loads that are working on the NSC flexible joint are carried by shear forces and bending moments.
- The NSC flexible joint has a negligible horizontal deformation capacity
- The SHCC link slab is in general only able to transfer vertical loads by compressive stresses.
- The SHCC link slab has a significant horizontal deformation capacity

From the above mentioned conclusion for the NSC flexible joint and the SHCC link slab, mechanical differences between the NSC flexible joint and the SHCC link slab could be determined. Both joints are able to resist the actions that work on the joint. The difference between both connections is that the SHCC link slab has a certain deformation capacity, while the deformation capacity NSC flexible joint is negligible.

Table 13 – Overview of characteristics of the flexible joint and the link slab according to Nosewicz & Jong (2009), Reyes & Robertson (2011) and Lárusson (2013)

	NSC flexible joint		SHCC link slab	
Design				
Variable	Flexible joint	Link slab		Unit
Concrete type	NSC	SHCC		[-]
Reinforcement	Steel	Glass Fibre Reinforced Polymer		[-]
Amount of fibres	No fibres	2.0		[V%]
		Reyes & Robertson	Lárusson	[-]
Type of fibre	No fibres	Polyethylene	PVA	[-]
Total length	0.8	2.4	2.0	[m]
Length debond zone	0.8	1.8	1.0	[m]
Length bonded zone	No debonded zone	0.3	0.5	[m]
Thickness	130	75		[mm]
Reinforcement ratio ρ (debond zone)	2.3	0.3-0.6		[%]

Bar diameter	12	6.4 or 9.5		[mm]
Casting method	Cast in situ	Prefab or cast in situ		[-]
Debonding layer	No connection (air)	Plexiglass	Roofing paper and plastic sheeting	[-]
Horizontal connection (passive zone)	Supporting system	Roughened NSC Steel anchor hooks or steel dowels Grouted		[-]
Vertical connection (passive zone)	Steel reinforcement	Grouted GFRP reinforcement		[-]
Horizontal joint deformation capacity	≈ 1.4	≈ 15		[mm]

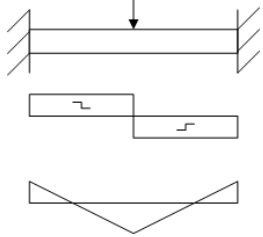
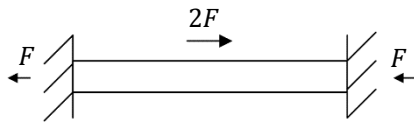
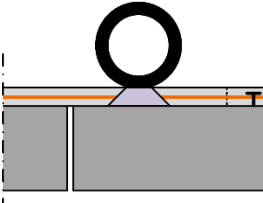
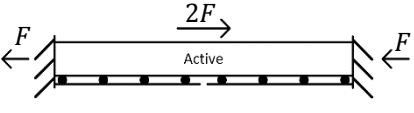
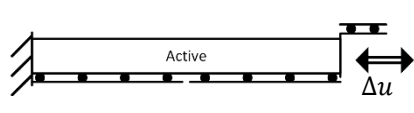
According to the information that is given in Table 13, the mechanical schemes of the NSC flexible joint and the SHCC link slab exposed to horizontal loads, vertical loads or imposed deformations can be determined. A detailed analysis to the reaction of the joints that are exposed to these actions is given in Appendix 3: SHCC Link Slab The actions that could work on the link slab and taken into account in the analyses are:

- **Vertical load**, for example because of vehicles
- **Horizontal loads**, for example because of braking vehicles
- **Imposed horizontal deformation**, for example because of shrinkage of concrete
- **Imposed rotation**, for example because of temperature gradient over the height of the concrete girders. However, imposed rotation from the span results in imposed horizontal deformation in the link slab.
- **Imposed vertical deformation**, for example because of different deformations in the support blocks. However, this deformation differences between blocks are assumed to be negligible.

As shown in Table 14, for both the NSC flexible joint and the SHCC link slab, models could be made to describe the reaction of the joints if they are exposed to one of the above defined actions. As shown in the table, the NSC flexible joint is able to transfer vertical and horizontal loads by bending moments, shear forces and normal forces working in the concrete joint. The horizontal imposed deformation capacity in the NSC flexible joint is neglected, so in fact, the flexible joint can't take up imposed horizontal deformation. The horizontal deformation capacity of the SHCC link slab is a significant advantage compared to the horizontal deformation capacity of the NSC flexible joint.

Also shown in Table 14, the vertical loads working on the SHCC link slab are transferred to the substructure by direct compressive stresses. The horizontal loads working on the link slab are transferred by normal stresses. In contradiction to the NSC flexible joint, the SHCC link slab is able to take up horizontal imposed deformations. Only tensile stresses are allowed to be generated in the link slab due to imposed horizontal deformations, because the tensile strength of SHCC is relative small. If imposed deformation generates compressive stresses in the link slab, damage of the connection could be expected, because compressive strength of SHCC is very high compared to tensile strength. So the design should prevent that compressive stresses can be generated by imposed horizontal deformation.

Table 14 – Reaction of flexible joint and SHCC link slab under vertical and horizontal load and horizontal imposed deformation

	Vertical load	Horizontal load	Horizontal imposed deformation
NSC flexible joint			Negligible horizontal deformation capacity
SHCC link slab			

5.4 Structural analysis to the Thin SHCC Link Slab

The Thin SHCC Link Slab and the potential of this joint is already described in paragraph 5.1 Potential of the Thin SHCC Link Slab. The Thin SHCC Link Slab looks like the SHCC Deck Slab that is described in paragraph 5.2 Reference project: SHCC Deck Slab on steel girders (Michigan, USA). However, the thin link slab is of course thinner and is reinforced by GFRP bars. This results in some different behaviour from the thick steel reinforced joint that is applied in Michigan, USA.

The Thin SHCC Link Slab is a joint that is placed in a concrete deck. In the Netherlands, there are a lot of bridges and viaducts with a concrete deck. So it seems that the Thin SHCC Link Slab could be applied in a lot bridge and viaducts. In Appendix 3: SHCC Link Slab, the Thin SHCC Link Slab is analysed from a structural point of view. From this analysis followed two points of attention, which are shortly described here. A more detailed analysed and description could be found in Appendix 3: SHCC Link Slab.

Before this analysis is described, three main advantages of the Thin SHCC Link Slab are given compared to the SHCC Deck Slab. These are also described in more detail in Appendix 3: SHCC Link Slab. In short, the three advantages are:

1. Horizontal deformation capacity (Reyes & Robertson, 2011), (Lárusson, 2013)
2. Lower stress required for deformations in the SHCC link slab (Reyes & Robertson, 2011)
3. Lower stiffness and tight crack width due to the application of GFRP bars instead of steel bars (Reyes & Robertson, 2011), (Lárusson, 2013)

However, there are some point of attentions in the design of the Thin SHCC Link Slab from a structural point of view. The analysis that is done to determine the points of attention is based on the way actions are carried by the thin SHCC link slab, as described in paragraph 5.3 NSC flexible joint and SHCC link slab. From the analyses, that is given in detail in Appendix 3: SHCC Link Slab, could be concluded that the main points of attention are the peak stress that works at the end of the concrete deck and the creation of the debonding zone in the active part of the link slab. Both point are discussed here in more detail.

The problem of spalling, that is caused by vertical stresses is shown in Figure 11. At the left of Figure 11 is shown the cross section of the SHCC link slab, which is loaded by a vertical wheel load near the end of the substructure. In the first detail in the middle of Figure 11 is shown the vertical stress

distribution that is expected over the length of the link slab. Assuming the dotted line is the maximum vertical stress that can be resisted by the substructure, then failure of the concrete is expected at the end of the substructure. In the second detail at the right on Figure 11 are some concrete particles that are exposed to a vertical peak stress. According to this detail, the failure mode can be determined. The vertical stress that works on the blue particle, creates reaction forces in the connections between the blue particle and other particles. The black arrows show two compressive reaction stresses. The red arrow shows tensile reaction stress. If the working tensile stress is higher than the tensile strength, failure is expected. Then both blue particles will spall, because of the vertical peak stress that work on it. Spalling could be expected until the reinforcement is not covered and protected by concrete any more as described in Appendix 3: SHCC Link Slab. So spalling can reduce the durability of the substructure significantly.

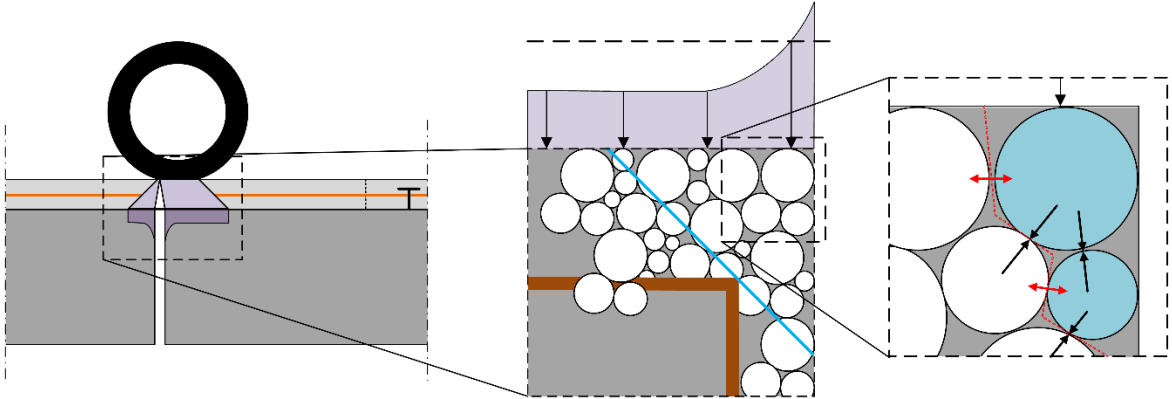


Figure 11 – Peak stresses working on the end of the substructure

Because the vertical peak stress that works on the substructure also works on the link slab itself, the link slab could also be damaged by the vertical peak stress. However, the risk of spalling in the substructure is assumed to be larger than failure of the SHCC link slab. The SHCC in the link slab is enclosed, while the NSC is not. So SHCC can carry the peak stress by compressive stresses. Further, in SHCC are put fibres, which could also be expected to reduce the risk of a lot of failure mechanisms.

In Figure 12 is shown the trouble that is expected in the debonding layer. In the detail of the figure is shown the connection between SHCC and concrete in the active zone of the link slab. Between SHCC and concrete is placed a layer of teflon (blue) to avoid shear stresses between both. However, as shown in the detail of Figure 12, due to limited smoothness of the surface of NSC and SHCC in practice, shear stresses could still be expected, even if teflon is applied. Due to shear stresses, the active zone does not function properly anymore. This problem could have a significant negative influence on the success of the SHCC link slab. The problem is explained in more detail in Appendix 3: SHCC Link Slab.

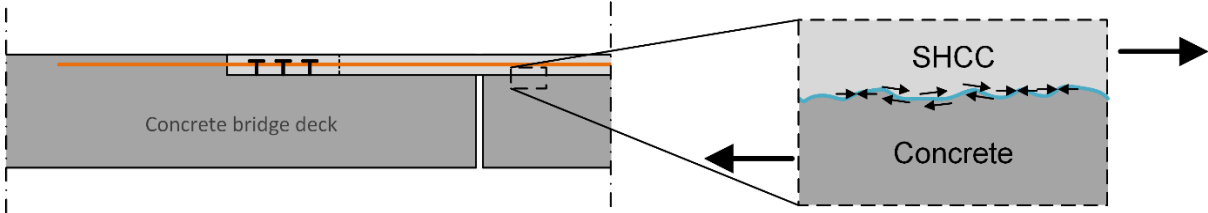


Figure 12 – Shear stresses working in active connection between the SHCC link slab and the concrete substructure

The vertical load is a problem in theory and practice. The debonding zone is a problem in practice only. In fact, in theory, the debonding zone does not result in any problems, but to execute the

debonding zone properly, problems could be expected. Therefore, the vertical load is chosen as the critical point of attention to researched in more detail in this case study.

However, design modifications to reduce the risk of spalling could also have a certain influence on the debonded zone, because the vertical peak stress works upon the debonded zone of the link slab. Therefore, trouble according to the debonding layer is also taken into account in the process, but as an additional advantage only.

In Table 15 is given an overview of the variables that are expected to have an influence on the two given points of attention in the link slab; the peak stress and the debonding layer. These variables are the basis of the suggested options to reduce the risk of spalling, which are given in paragraph 5.5 Variants to reduce the risk of spalling.

Table 15 – Variables that influence the main points of attention of the link slab, classified by different categories

Point of attention	Category	Variables
Peak stress at the end of the concrete deck	Resistance of the NSC deck	Tensile strength of NSC
		Reinforcement design
		Addition of fibres
	Decrease the working peak stress by design	Stiffness of NSC and SHCC
		Moment of inertia of link slab and substructure
		Length of the gap
Execution of the debonding layer	Material characteristic	Thickness of the link slab
		Stiffness of the debonding layer
	Execution	Vertical strength
		The smoothness of the deboning layer
		Thickness of the deboning layer

5.5 Variants to reduce the risk of spalling

In this paragraph are shown some design options to reduce the risk of spalling of the concrete of the substructure. All options are described shortly. According to the description, it is recommended which options should be research in more detail to solve the problem. More detailed descriptions of the designs and the recommended options are both given in Appendix 3: SHCC Link Slab.

In Figure 13 is given an overview of three options that could reduce the risk of spalling in the substructure. In the options is tried to increase the resistance against spalling or to decrease the vertical peak stress that causes spalling. The options are based on the analysis from Table 15, which is given in the previous paragraph. In short, the options are described in the list below.

1. **Chamfer:** due to the chamfer at the end of the substructure, the vertical peak stresses could be carried by compressive stresses in the concrete. The peak stress divided over a larger area, depending on the height of the chamfer. At the end of the chamfer, the vertical peak stress in the substructure causes tensile stresses again. However, because the vertical peak stress is decreased, the tensile stresses are also decreased, so the risk of spalling is reduced.
The chamfer variant is expected to be the **cheapest option**. Applying a chamfer requires only a small modification in the design, which is expected to be easy to execute. Only the formwork should be modified a bit. However, the effectiveness of this option should be researched in more detail to judge if this option is able to reduce the risk of spalling to a required minimum.
2. **Redistribution by stiff interlayer:** this plate should redistribute the vertical stresses over the length of the substructure, such that the peak stresses are reduced.

The very stiff vertical plate with prestressed anchors is expected to be the **most effective option**. However, this option is expected to be very expensive compared to the other options, mainly because of the prestressed anchors. Further, this solution requires some additional steps during execution, what increase the building time and the costs.

3. **Prestressed anchored plate:** this plate should create a horizontal compressive stress to compensate the horizontal tensile stresses at the end of the concrete substructure. If the tensile stresses are compensated, the risk on spalling is reduced.

The very stiff horizontal plate is the option where the **most additional advantages** are expected in, provided that the surface of the plate can be made very smooth easily. The smooth surface of the plate should prevent trouble in the debonding layer in the active section, assuming that a material like teflon is applied. However, if additional research shows that the smoothness of the concrete and SHCC surfaces does not result in bad function debonding layer, probably the other options are more interesting to apply. Also if the surface of the stiff material can't be made smooth easily, this option is not interesting to apply.

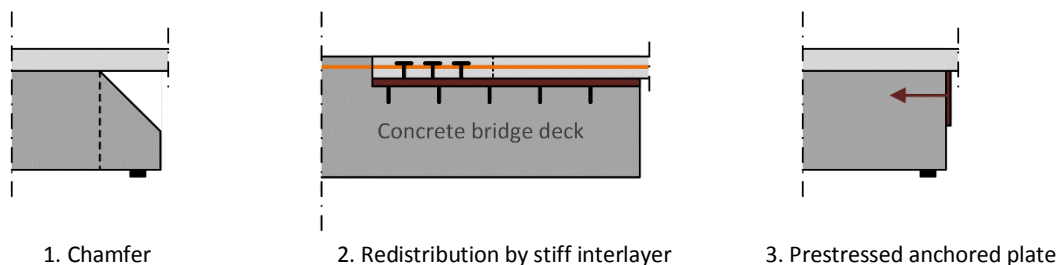


Figure 13 – Overview of options to prevent spalling

5.6 SHCC Flexible Joint

From the above sections, two conclusions could be made. First of all, a link slab with more or less the same characteristics as the NSC Flexible Joint could be made of SHCC. This is done in practice in Michigan, USA. As second, the Thin SHCC Link Slab shows that SHCC could also be used to create a joint with a certain horizontal deformation capacity.

Maybe, a flexible joint that is made of SHCC instead of NSC is a possible step towards the application of SHCC in practice in the Netherlands. Until now, SHCC in the Netherlands is only used in the lab. To have some practical experience with SHCC, it may be interesting to apply it in a structure that is applied successfully in practice for a long time already. The flexible joint seems a useful structure to get some experience with SHCC in practice. Then the idea of the SHCC Deck Slab that is constructed in Michigan, USA, is combined with the commonly applied NSC Flexible Joint.

Further, the SHCC Flexible Joint may have some interesting advantages compared to the NSC Flexible Joint. The SHCC Deck Slab in Michigan, USA, has some advantages compared to a concrete deck slab (Li, et al., 2003). Maybe, an SHCC Flexible Joint also has some advantages compared to the NSC Flexible joint. Therefore, in this paragraph are shortly analysed the expected advantages of an SHCC Flexible Joint compared to the NSC Flexible joint.

Before the SHCC Flexible Joint is analysed, the commonly applied situation is shortly described. In Figure 14 is shown a common situation of a precast concrete inverted T-girder with a cast in situ concrete deck to make a bridge construction (Consolis Spanbeton, n.d.). The bridge spans are connected by a flexible joint. The flexible joint is shown in the left picture of Figure 14, schematised as a block (light blue). As shown in the figure, the flexible joint creates a small bridge between both

bridge spans. This joint can't take care of horizontal imposed deformations. More details of the NSC Flex joint are given in Appendix 3: SHCC Link Slab. In practice, the NSC Flexible joint has:

- Vertical and horizontal load capacity
- Rotation capacity
- No horizontal deformation capacity

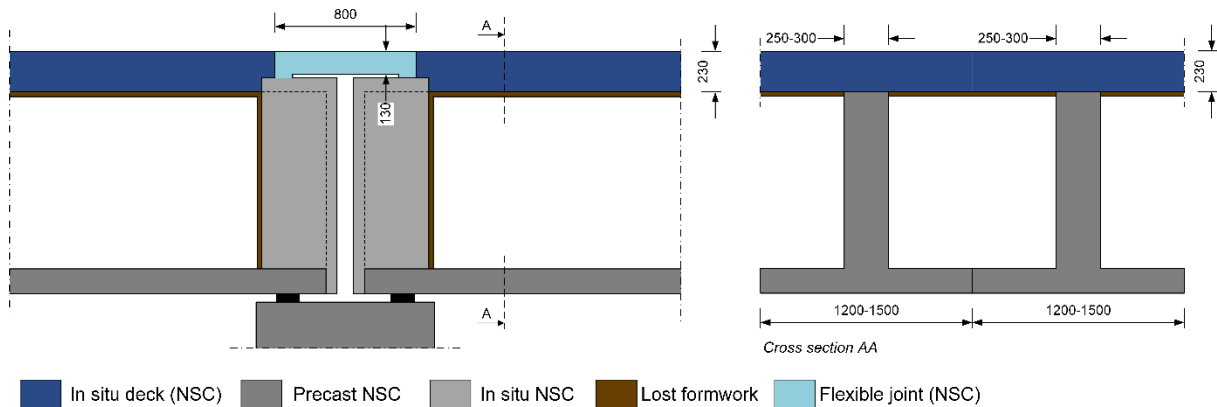


Figure 14 – Precast NSC inverted T-girder with in situ NSC deck and flexible joint according to (Consolis Spanbeton, n.d.)

It is assumed that the SHCC Flexible joint is also able to carry vertical and horizontal loads. In fact, the Deck Slab in Michigan, USA, already shows that SHCC could carry vertical and horizontal loads. However, maybe the dimensions of the SHCC Flexible Joint should differ a bit from the dimensions of the NSC Flexible joint.

The Deck Slab in Michigan, USA, have a certain rotation capacity. So probably, if the flexible joint is made of SHCC, the requirements according to the rotation capacity should still be met. Besides, the stiffness of SHCC is smaller than the stiffness of NSC. Further, probably less reinforcement is required in an SHCC Flexible Joint. This also increases the rotation capacity of the link slab.

In the end, it seems that SHCC is a proper material to construct a flexible joint. But, there are expected some advantages of the SHCC Flexible Joint compared to the NSC Flexible Joint. Most of these advantages are based on the results of the SHCC Deck Slab that is made in Michigan, USA. Next to the advantage of the SHCC Flexible Joint itself, an important goal of course is to have some practical experience with SHCC. Practical experience could be an important to take the next step to the Thin SHCC Link Slab. All the advantages in short are:

- Practical experience with SHCC
- Lower amount of reinforcement compared to the NSC Flexible Joint because of:
 - o The high tensile ductility of SHCC
 - o In SHCC, the crack width is independent of the reinforcement ratio.
- No adhesive strip
- Lower stiffness of the SHCC Flexible Joint compared to the NSC Flexible Joint, such that the joint act more like a hinge.
- The crack width under cycling load are limited

6 Conclusion

This conclusion consists of two parts. The first part of this conclusion is about the combinations of ACMs and structures. In the second part are given the conclusions about the SHCC link slab.

6.1 Fields of applications of ACMs

The three applications that are expected to be the most beneficial are:

1. Bridge joint made of SHCC, because of durability advantages, secondary effects of the durability of the joint and drive comfort in combination with horizontal deformation capacity of the joint.
2. Bridge girders made of (U)HPC, because of various reasons, for example leaving out an intermediate support. Then the span length increases.
3. Deck of an underpass made of UHPC, because of secondary benefits in the tunnel.

In Table 16 is given an overview of the applications of ACMs in structures. Of course the applications that should be utilize to take up the most potential benefits are in the column 'Very potential'. However, also the applications that are 'not or nearly potential' are interesting to know, because these applications should not be included in additional research. At last, the 'potential' applications could in some situations also be interesting to utilize, but the benefits are expected to be lower compared to the group 'very potential'.

Table 16 – Applications of ACMs in structures divided in three categories of potential

Very potential	Potential	Not or nearly potential
HPC bridge deck	UHPC bridge deck	NSSFRC/HPSFRC cross beam
(U)HPC bridge girder	UHPC joint	NSSFRC/HPSFRC culvert
(U)HPC sluice door	(U)HPC cross beam	NSSFRC/HPSFRC aqueduct
UHPC deck of underpass	NSC and UHPC sluice door	UHPC tunnel elements
	UHPC embankment	(U)HPC sewage
	UHPC retaining wall	(U)HPC foundation slab
	UHPC aqueduct	UHPC and NSC sewage
	UHPC and NSC aqueduct	Steel and UHPC sluice door
SHCC bridge deck	SHCC barrier	SHCC aqueduct joint
SHCC for repair (deck,tunnel,...)	SHCC embankment	NSC and SHCC in culverts
SHCC bridge joint	SHCC joint in tunnel	NSC and SHCC in tunnel
	NSC with SHCC bridge girders	NSC and SHCC aqueduct
	Self-healing concrete aqueduct	
	GPC sluice door	GPC foundation slab
		GPC embankment
		GPC culvert
		GPC sewage
		GPC foundation piles
		Steel and GPC sluice door
	Self-sensing foundation piles	Self-cleaning noise barrier

6.2 Thin SHCC Link Slab

The SHCC link slab is expected to be one of the most potential applications from the study to fields of applications. Here conclusions are given according to the Thin SHCC Link Slab about the potential, design, points of attention and a recommended step along the way to the Thin SHCC Link Slab in practice.

- The main reasons that the SHCC link slab is expected to be a potential alternative joint are:
 - o Horizontal deformation capacity
 - o Long expected service life, while low or no maintenance is expected
 - o Protection of the substructure, supports etc. under the link slab, because the link slab avoids that leakage water and chemicals can reach and attack these elements
- The Thin SHCC Link Slab (schematically shown in Figure 15), which is poured in one, consists of:
 1. An active part that should take care of imposed deformation and traffic loads.
 2. Two passive part at both ends of the active part to connect the active part to the concrete substructure. The part should also take care of traffic loads.

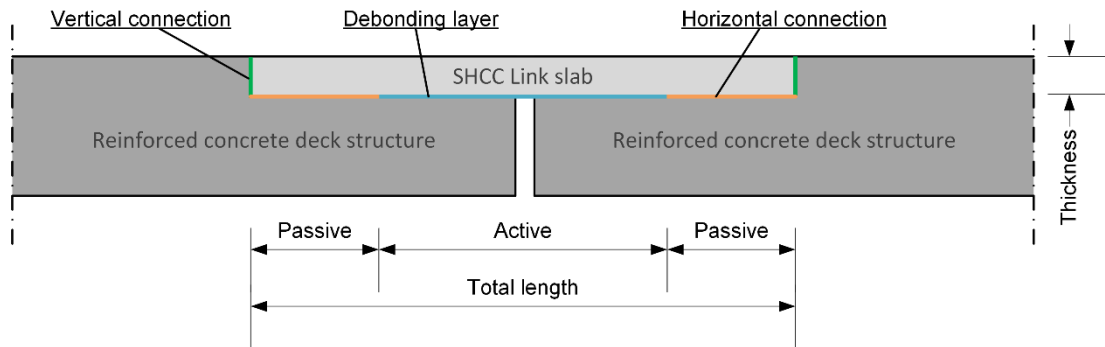


Figure 15 – Schematisation of the design of the Thin SHCC Link Slab

- To pick up potential benefits by utilising the Thin SHCC Link Slab, from a structure point of view two important points of attention to research is more detail are:
 1. Vertical peak stresses that could cause spalling of the concrete substructure
 2. Design of the debonding layer according to the execution
- There are suggested three options to reduce the risk on spalling of the concrete substructure:
 1. The cheapest way to reduce the risk on spalling is the application of chamfers at the ends of the deck. However, the effectiveness of the chamfers is a point of discussion, because chamfers also cause an increase of the peak stress.
 2. Probably the most effective way is a very stiff vertical plate at the end of the deck that is connected to prestressed anchors. However, this is probably a very expensive option.
 3. The option with the most additional advantages is the very stiff horizontal plate. Depending on the material, a properly working debonding layer could be created easier.
- The SHCC Flexible Joint seems a first practical step to applying the Thin SHCC Link Slab. The main advantages of this structure are:
 1. Practical experience with SHCC in a structure that is applied successfully for years
 2. Probably a lower amount of reinforcement is required and no adhesive strip is needed
 3. Low stiffness of the SHCC Flexible joint compared to the NSC Flexible joint

7 Recommendations

In this chapter are given some recommendations after the research that is done. There is made a separation between recommendations for the fields of applications of ACMs and recommendations for to the SHCC link slab. For both, the recommendations consist mainly of recommended additional research.

7.1 Fields of applications of ACMs

In this paragraph are given the recommendations according to the study to applications of ACMs in structures. The recommendation are:

- Application of ACMs in other structures, than the structures that are included in this research
- Additional research to the applications that are expected to be very potential
- The applications that are labelled as 'potential', are only recommended to research in more detail if additional benefits are generated by utilising them a specific project. Additional benefits could for example be created in a project due to specific conditions, which create additional benefits to apply a certain ACM.
- It is recommended not include the applications that are judge as not or nearly potential in additional research.
- It is interesting to observe that there are made more fields of applications for the best known ACMs. It seems that there is a relation between the number of applications of a certain ACM and the knowledge of that ACM. So if more knowledge of a certain ACM is available in the next years, probably more possible application in structure could be made. So after a few years from now, maybe more applications could be made with the same ACMs.
- Application of an ACM on higher level of detail. There could be done research to application of ACMs in smaller parts of a structure. Maybe more applications can be found then, because the structure is split up in more elements.

7.2 SHCC link slab

To end this chapter, in this paragraph are given recommendations for the SHCC link slab. There is suggested a plan of pilot projects to apply the Thin SHCC Link slab in practice. This plan is given in Table 17. The first three pilot projects are flexible joints, which are made a bit different from the 'classic' NSC Flexible Joint. The idea is mainly to have some experience with new materials, like SHCC and GRFP. The last two pilot projects are Thin SHCC Link slab.

Table 17 – From NSC Flexible Joint to Thin SHCC Link Slab by steps

		Structure	Advantage	Research
Flexible Joint	Pilot 1	Flexible joint made of SHCC	No adhesive strip Practical learning goal SHCC	SHCC material
	Pilot 2	Flexible joint made of SHCC with GFRP reinforcement	Durable reinforcement Practical learning goal GFRP Lower stiffness of the joint	GFRP
	Pilot 3	Flexible joint made of SHCC with a reduced amount of reinforcement	Less reinforcement Lower stiffness of the joint	Influence of PVA fibres
Thin Link Slab	Pilot 4	Thin SHCC link slab with GFRP rebars (intermediate supports only)	Horizontal deformation capacity Lower stiffness of the joint	Peak stresses Debonding zone
	Pilot 5	Thin SHCC link slab with GFRP rebars (all supports)	Horizontal deformation capacity in all joints	Influence on the abutment

However, from the research to the SHCC Link Slab are also some recommendations according to additional research to the Thin SHCC Link Slab itself. However, if the plan of Table 17 is carried, a lot of these recommendations should be researched before a pilot project is executed or analysed in practice during a pilot project. A more detailed description of the recommendations is given in Appendix 3: SHCC Link Slab. These recommendations are:

- The behaviour of the SHCC link slab if it is exposed to a combination of imposed horizontal deformation and a horizontal load.
- Additional research to check if the vertical imposed deformation could indeed be neglected. Researching should be done to the difference of the vertical stiffness of the support blocks due to imperfections during execution and influence of exposure conditions.
- Effect of the vertical peak stresses on the SHCC link slab.
- Additional research to the option to reduce the risk of spalling at the end of the substructure:
 1. Chamfers:
 - Effectiveness
 - Better determination of maximum length of the chamfer
 2. Very stiff vertical plate connected to prestressed anchors:
 - Choice of a material
 - Effect of the stiffness of a material on the effectiveness of this option
 - Costs
 3. Very stiff horizontal plate, because of potential additional benefits for the debonding layer
 - The consequences of the limited smoothness of SHCC and concrete on the functioning of the active zone
 - Effect of the stiffness of a certain material on the effectiveness of this option
 - Material of the plate
 - Smoothness of the surface of the plate
 - Effect of the peak stress at the other end of the plate

Some additional recommended research, mainly from a practical point of view:

- Imposed horizontal deformation should only result in tensile stresses in the link slab and no compressive stresses, in order to prevent large stresses in the link slab that could result in failure of the connection.
- Inhomogeneity of SHCC, what could result in bad collaboration of SHCC link slabs if multiple SHCC link slabs should work together. In the research, SHCC is assumed to be homogeneous.
- Stresses working in the transverse direction of the link slab
- Increase of the strain in SHCC, to increase the deformation capacity of the joint in order to create a more efficient joint.
- Optimisation of the vertical and horizontal connections at the boundaries of the passive zone with the concrete deck by alternative connection methods.
- Optimum length of the passive zone to reduce the amount of SHCC, while there is a proper connection between the active zone and the substructure
- Optimum thickness of the link slab, which is the optimum ratio between forces that are generated by imposed deformation and the strength that the link slab should have to resist working loads.
- The required smoothness of the SHCC and NSC surface in order to have a properly working debonding layer, assuming the debonding layer is created by a thin layer, like teflon.
- Debonding layer made of a relative thick layer of soft material, if the thin debonding layer is not possible due to execution issues

8 Bibliografie

- AFGC's Scientific and Technical Committee. (2013). *Ultra High Performance Fibre-Reinforced Concretes Recommendations*.
- Aldred, J. M. (2013). Engineering Properties of a Proprietary Premixed Geopolymer Concrete.
- Breyse, D., & Gerard, B. (1997). modelling of permeability in cement-based materials: part 1- uncracked medium. *Cement and Concrete Research*, Vol. 27. No. 5, 761-775.
- Cheema, D. S., Lloyd, N. A., & Rangan, V. B. (2009). Durability of geopolymer concrete box culverts - a green alternative. *34th Conference on our world in concrete & structures*. Singapore.
- Chen, H., & Su, R. (2013). Tension softening curves of plain concrete. *Construction and Building Materials* 44, 440-451.
- Chindapasirt, P., & Chalee, W. (2014). Effect of sodium hydroxide concentration on chloride penetration and steel corrosion of fly ash-based geopolymer concrete under marine site. *Construction and Building Materials* 63, 303-310.
- Consolis Spanbeton. (n.d.). *Railbalkoplossingen ZIP & ZIPXL*. Opgehaald van Spanbeton: http://www.spanbeton.nl/content/files/Files/Kennisportaal/Railbalk/ZIPZIPXL_A4_projectbladen_v6.pdf
- CUR bouw & infra. (n.d.). *Leidraad 1: Duurzaamheid van constructief beton met betrekking tot chloride-geïnitieerde wapeningscorrosie*.
- Deb, P. S., Nath, P., & Sarker, P. K. (2014). The effects of ground granulated blast-furnace slag blending with fly ash and activator content on the workability and strength properties of geopolymer concrete cured at ambient temperature. *Materials and Design* 62, 32-39.
- ENCI. (2008, April). Opgehaald van hout-en-bouwmaterialen.nl: <http://www.hout-en-bouwmaterialen.nl/downloads/enci-eenvoudig-betonwerk-algemene-en-technische-informatie.pdf>
- fib. (2009). *Structural Concrete: Textbook on behaviour, design and performance, second edition, Volume 1*. DCC Document Competence Center siegmar Kastl.
- fib Bulletin 55. (2010). *Model Code 2010, First complete draft – Volume 1*.
- Gupta, S., Aggarwal, P., Aggarwal, Y., Sehga, V., Siddique, R., & Kaushik, S. (2008). Permeability of high strength concrete. In M. C. Limbachiya, & H. Y. Kew, *Excellence in Concrete Construction through Innovation* (pp. 159-163). London: CRC Press.
- Hardjito, D. (2005). *Studies on Fly Ash-Based Geopolymer Concrete*. Ph. D. Curtin University of Technology, Dept. of Civil Engineering.
- Jalal, M., Ramezaniapour, A. A., & Pool, M. K. (2013). Split tensile strength of binary blended self compacting concrete containing low volume fly ash and TiO₂ nanoparticles. *Composites Part B: Engineering*, Volume 55, 324-337.
- Japan Society of Civil Engineers. (2008). *Recommendations for Design and Construction of High Performance Fiber Reinforced Cement Composites with Multiple Fine Cracks (HPFRCC)*.
- Lárusson, L. H. (2013). *Development of Flexible Link Slabs using Ductile Fiber Reinforced Concrete*. Lyngby.

- Lepech, M., & Li, V. (2005). Proceedings of Eleventh International Conference on Fracture. *Water permeability of cracked cementitious composites*, (pp. 20-25). Turin, Italy.
- Li, V. C. (2007). *Engineered Cementitious Composites (ECC) – Material, Structural, and Durability Performance*.
- Li, V. C., Fischer, G., Kim, Y., Lepech, M., Qian, S., Weimann, M., & Wang, S. (2003). *Durable Link Slabs for Jointless Bridge Decks Based on Strain-Hardening Cementitious Composites*.
- Li, V. C., Lepech, M., & Li, M. (2005). *Final Report On Field Demonstration of Durable Link Slabs for Jointless Bridge Decks Based on Strain-Hardening Cementitious Composites*. Michigan Department of Transportation.
- Liu, X., Chia, K. S., & Zhang, M.-H. (2011). Water absorption, permeability, and resistance to chloride-ion penetration of lightweight aggregate concrete. *Construction and Building Materials* 25, 335-343.
- Majorana, C., Salomoni, V., Mazzucco, G., & Khoury, G. (2010). An approach for modelling concrete spalling in finite strains. *Mathematics and Computers in Simulation* 80, 1694-1712.
- Nazari, A., Riahi, S., Riahi, S., Shamekhi, S. F., & Khademno, A. (2010). The effects of incorporation Fe₂O₃ nanoparticles on tensile and flexural strength of concrete. *Journal of American Science*, 90-93.
- Nederlands Normalisatie-instituut. (2011). *NEN-EN 1992-1-1+C2*. Delft.
- Ng, T., Htut, T., & Foster, S. J. (2010). Mode I and II fracture behaviour of steel fibre reinforced high strength geopolymer concrete: an experimental investigation. In e. a. B.H. Oh, *Fracture Mechanics of Concrete and Concrete Structures - High Performance, Fiber Reinforced Concrete, Special Loadings and Structural Applications*.
- Olivia, M., & Nikraz, H. (2012). Properties of fly ash geopolymer concrete designed by Taguchi method. *Materials and Design* 36, 191-198.
- Olivia, M., & Nikraz, H. R. (2011). Strength and water penetrability of fly ash geopolymer concrete. *ARPN Journal of Engineering and Applied Sciences*, Vol. 6, No.7.
- Ottel , M. (2015, May 1). Faalkosten. (J. v. Oosten, Interviewer)
- Paskvalin, A. (2015). *Application of Ultra High Performance Concrete in the new Leiden Bridge*. Delft.
- Pelletier, M. M., Brown, R., Shukla, A., & Bose, A. (n.d.). Self-healing concrete with a microencapsulated healing agent.
- Qian, S., Zhou, J., Rooij, M. d., Schlangen, E., Ye, G., & Breugel, K. v. (2009). Self-healing behavior of strain hardening cementitious composites incorporating local waste materials. *Cement & Concrete Composites* 31, 613-621.
- Reyes, J., & Robertson, I. (2011). *Precast link slabs for jointless bridge decks*.
- Ryu, G. S., Lee, Y. B., Koh, K. T., & Chung, Y. S. (2013). The mechanical properties of fly ash-based geopolymer concrete with alkaline activators. *Construction and Building Materials* 47, 409-418.
- Shaikh, F. U. (2013). Review of mechanical properties of short fibre reinforced geopolymer composites. *Construction and Building Materials* 43, 37-49.

- Tayeh, B. A., Bakar, B. A., Johari, M. M., & Voo, Y. L. (2012). Mechanical and permeability properties of the interface between normal concrete substrate and ultra high performance fiber concrete overlay. *Construction and Building Materials* 36, 538-548.
- Wang, K., Jansen, D. C., Shah, S. P., & Karr, A. F. (1997). Permeability study of cracked concrete. *Cement and Concrete Research*, Volume 27, Issue 3, 381-393.
- Yang, T., Yao, X., & Zhang, Z. (2014). Quantification of chloride diffusion in fly ash–slag-based geopolymers by X-ray fluorescence (XRF). *Construction and Building Materials* 69, 109-115.

Applications of Advanced Cementitious Materials in Infrastructure

Appendix 1: Literature Study

Candidate

J. van Oosten
TU Delft and Heijmans

28-9-2015

Committee

Prof.dr.ir. D.A. Hordijk
Ir. A.D. Reitsema
Dr.ir. M. Ottelé
Dr.ir. C. van der Veen
Ir. L.J.M. Houben

TU Delft
TU Delft and Heijmans
TU Delft and Heijmans
TU Delft
TU Delft

Summary

This report is the first part of the research to the applications of Advanced Cementitious Material in infrastructure, to take up potential benefits. The objective of the total research is to make an overview potential applications of new concrete materials in structures in the infrastructure, which can be utilised to take up potential benefits. The total research is made up of three parts:

- Part 1 - Literature study
- Part 2 - Field of applications
- Part 3 - SHCC Link Slab

In this part, the literature study, are nine ACMs research and is done an analysis to some constructions. The materials of the scope of this research are: Normal Strength Steel Fibre Reinforced Concrete (NSSFRC), High Performance Concrete (HPC), High Performance Steel Fibre Reinforced Concrete (HPSFRC), Ultra High Fibre Reinforced Performance Concrete (UHFRPC), Strain Hardening Cementitious Composite (SHCC), Self-Healing Cementitious Material, Geopolymer concrete, Self-cleaning nano concrete and Self-sensing nano concrete. The mechanical, durable and sustainable characteristics of these ACMs are compared to Normal Strength Concrete (NSC).

In general, the dens concretes HPC and UHPC have better mechanical and durable characteristics. The density of the concretes is due to the finer particles in the mixtures. Because a lot of cement is used in these ACMS sustainability is very low. The addition of steel fibres to NSC and HPC results in NSSFRC and HPSFRC with an alternative cracking pattern having smaller cracks.

Strain hardening cementitious composites have high tensile strain due to the strain hardening behaviour. They can absorb a lot of energy before it fails. The cracks in SHCC are very small, which results in better durability if it is cracked. Both characteristics are mainly caused by short plastic fibres. The sustainability of SHCC is worse than NSC, for instance due to increased amount of cement.

Self-healing cementitious material can heal due to the addition of healing agents. If the concrete is cracked, the mechanical and durable characteristics are positively influenced by healing the cracks. if the concrete is uncracked, the mechanical and durable characteristics are more or less the same as for NSC.

Geopolymer concrete contains an alternative binder instead of Portland cement. This results in unique durable and sustainable characteristics of this concrete. The mechanical characteristics seem to be similar to NSC.

Self-cleaning nano concrete is a concrete mixture where nano titanium oxide is added to. The titanium oxide makes that in combination with rain, the dirt will be removed from the surface. The addition of nano particles results also in some better durability due to a denser mixture. The sustainability is some worse.

Self-sensing concrete is concrete with nano iron oxide is added to. Due to iron oxide, the concrete has a certain electrical conductivity, which make that cracks in the concrete can be monitored by the concrete itself. Next to this unique characteristics, the durability of the self-sensing concrete is some better.

Of course for NSC and some HPC classes, Eurocode 2 is valid. For the some other type of concrete are other standard of recommendations abroad. Steel fibre reinforced NSC and HPC are included the Model Code 2010. In Japan, France and Australia are made recommendations for SHCC, UHPC and GPC respectively.

Reference projects show that the most applied ACMs are HPC and UHPC. Both are mainly applied in bridge constructions, especially for joints and beams. Less applied ACMs are SHCC, GPC and self-cleaning concrete. SHCC is mainly applied in Japan, because there are earthquake prone areas here.

With the analysis to the constructions are the mechanical and durable requirements to the concrete determined. Most of the construction elements are mainly loaded by compressive or bending moments. The exposure class depends mainly on the function and the place of the construction.

In the end, the mechanical, durable and sustainable characteristics are combined together in a MCA. The MCA includes NSC, NSFRC, HPC, HPFRC, UHPC and SHCC, because this are the only ACMs that can be judged quantitatively on all characteristics. The MCA shows that UHPC has the best mechanical and durable performance. NSC has the best sustainable characteristics. Combining all characteristics, UHPC performs the best.

Guide line

The basis of this literature study are six main tables about Advanced Cementitious Materials (ACMs). These six tables are:

1. Definition of the ACMs	Page 4	<i>Table 2</i>
2. The composition of the ACMs	Page 20	<i>Table 11</i>
3. The mechanical characteristics of the ACMs	Page 26	<i>Table 14</i>
4. The durability behaviour of the ACMs	Page 78	<i>Table 25</i>
5. The sustainability of the ACMs	Page 105	<i>Figure 51</i> and Page 105 <i>Figure 52</i>
6. Standards and recommendations	Page 106	<i>Table 37</i>

In the end, the 2nd, 3rd and 4th table about the mechanical, durable and sustainable characteristics are combined in a MCA in chapter 6 Multi Criteria Analysis of the ACMs. In the MCA the ACMs are judge on mechanical, durable and sustainable characteristics separately. At last, the categories are combined to give an overall rating.

The six main tables are described in chapter 2. Advanced Cementitious Materials in the paragraph 2.1 until paragraph 2.6. Every paragraph consists a table, which is explained in more detail in the remaining part of the paragraph. In Paragraph 2.4 Durability, an exception of this rules because the durability table is presented in paragraph 2.4.9. Chapter 2 ends with some design standards and recommendations and some information about the costs. According to the given design rules, some calculations are done.

After the description of the ACMs a summery is given of applications that are researched already and reference projects that are utilized in practice already, which can be found in chapter 3. Researched applications and chapter 4. Reference projects. These projects are described in more detail in Reference projects of this research.

The last part of the literature study is about constructions in the infrastructure. The constructions are split up until a certain level. For every element of the construction the mechanical and environmental requirements are given, which the building material should meet.

Table of content

Summary	ii
Guide line	iv
Table of content	v
1 General introduction	1
1.1 Problem definition.....	1
1.2 Research question	1
1.3 Objective	2
1.4 Methodology.....	2
2 Advanced Cementitious Materials.....	4
2.1 Scope of Advanced Cementitious Materials	4
2.1.1 Normal Strength Concrete	5
2.1.2 Normal Strength Steel Fibre Reinforced Concrete	8
2.1.3 High Performance Concrete and High Performance Steel Fibre Reinforced Concrete	9
2.1.4 Ultra High Performance Fibre Reinforced Concrete	9
2.1.5 Strain Hardening Cementitious Composite.....	10
2.1.6 Self-Healing Cementitious Materials	10
2.1.7 Geopolymer Concrete.....	14
2.1.8 NANO Concrete	16
2.2 Composition.....	19
2.3 Mechanical characteristics.....	25
2.3.1 Fibre Reinforced Concrete	27
2.3.2 UHPC, C170/200	29
2.3.3 GPC.....	30
2.3.4 Self-cleaning concrete.....	35
2.3.5 Self-sensing nano concrete	35
2.3.6 Shear resistance.....	36
2.3.7 Creep and shrinkage	50
2.4 Durability.....	58
2.4.1 Physical attack	58
2.4.2 Chemical attack	59
2.4.3 Corrosion of reinforcement bars	59
2.4.4 Summary of concrete attack	60
2.4.5 Ettringite.....	60
2.4.6 Penetration and diffusion	62

2.4.7	Pozzolan material	67
2.4.8	In depth analysis degradation processes	67
2.4.9	Durability of the Advanced Cementitious Materials.....	77
2.5	Sustainability.....	97
2.5.1	Sustainable and durable structures	97
2.5.2	Rekentool Groen beton 3.0	99
2.5.3	Results.....	104
2.6	Design standards and recommendations	106
2.7	Design calculations	106
2.7.1	NSC and HPC.....	106
2.7.2	SHCC.....	112
2.7.3	UHPC	117
2.8	Costs of ACMs	124
3	Researched applications.....	125
4	Reference projects	127
5	Constructions.....	128
5.1	Exposure classes	128
5.2	Types of constructions.....	129
5.2.1	Foundation	129
5.2.2	Viaduct and girder bridge.....	130
5.2.3	Other bridges.....	132
5.2.4	Sluice	133
5.2.5	Embankment	135
5.2.6	Retaining wall	136
5.2.7	Noise barrier.....	137
5.2.8	Tunnels, culverts and sewages	138
5.2.9	Underpass.....	139
5.2.10	Aqueduct.....	141
5.3	Mechanical models.....	143
5.4	Water tightness.....	143
5.5	Demand of constructions.....	144
5.5.1	Bridges.....	144
5.5.2	Sluices.....	145
6	Multi Criteria Analysis of the ACMs	147
7	Bibliography.....	149
Appendix A:	Reference projects.....	162

A.1.	Reference projects for FRC	162
A.1.1	Park Oceanographic, Valencia, Spain	162
A.2.	Reference projects for HPC and UHPC	163
A.2.1	Hodder Avenue Underpass: An Innovative Bridge Solution with Ultra-High Performance Fibre-Reinforced Concrete	164
A.2.2	Kampung Ula Geroh Bridge	165
A.2.3	Kampung Linsum Bridge.....	166
A.2.4	Cable-Stayed Footbridge with UHPC Segmental Deck in the Czech Republic.....	168
A.2.5	Jakway Park Bridge, Buchanan County, Iowa USA.....	169
A.2.6	Jean Bouin Stadium, Paris, France: Focus on Ductal® UHPC Roof and Façade Panels	170
A.2.7	Shawnessy Light Rail Transit Station, Calgary, Canada	170
A.2.8	Wapello County Mars Hill Bridge (2006).....	172
A.2.9	Sluis 0124, Amsterdam, The Netherlands	173
A.2.10	Summary of reasons to apply HPC or UHPC.....	174
A.3.	Reference projects for SHCC	174
A.3.1	ECC in high-rise buildings to increase the earthquake resistance of the structure: Glorio Rappongi High Rise, Tokyo, Japan and the Nabeaure Tower, Yokohama, Japan	174
A.3.2	Ellsworth Road Bridge over US-23.....	175
A.3.3	Grove Street Bridge Project, Michigan, US: ECC Link Slab in Bridge.....	176
A.3.4	Mihara Bridge, Hokkaido, Japan	178
A.3.5	Mitaka Dam near Hiroshima	179
A.3.6	Retaining wall in Japan.....	180
A.3.7	Summary of reasons to apply SHCC.....	181
A.4.	Reference projects for Geopolymer Concrete	182
A.4.1	Global Change Institute, multi-storey building, Australia, Brisbane.....	182
A.4.2	Water Tanks.....	182
A.4.3	Geopolymer Aircraft Pavements at Brisbane West Wellcamp Airport (BWWA), Australia	183
A.4.4	Rocky Point Boat Ramp, Bundaberg, Australia.....	183
A.4.5	Summary of reasons to apply GPC.....	184
A.5.	Reference projects for Self-cleaning Concrete.....	184
A.5.1	Jean Bleuzen street, Vanves, France	184
A.5.2	Dives in Misericordia Church, Rome, Italy	185
A.5.3	La Cité de la Musique et des Beaux-Arts, Chambéry, France	186
A.5.4	Hotel de Police, Bordeaux, France	186
A.5.5	Summary of reasons to apply Self-cleaning concrete.....	187

1 General introduction

Concrete is already used for centuries to build all kind of structures. In the Roman Empire cementitious materials are used already to construct. Some of those structures are nowadays still there. The last decades, material development have led to concrete that becomes stronger and stronger. One of the most important reasons is a reduced water binder ratio. This is schematically given in Figure 1. In the graph is shown that in 1950 the compressive strength of concrete was only 20 MPa with a w/c ratio of 0.65. Over the years the compressive strength increased with a decreasing water binder ratio. In the beginning of the 21st century, compressive strength of 350 MPa could already be reached. This much stronger concrete is well known as Ultra High Performance Concrete (UHPC). Nowadays research is still going on to make even stronger and better concrete materials.

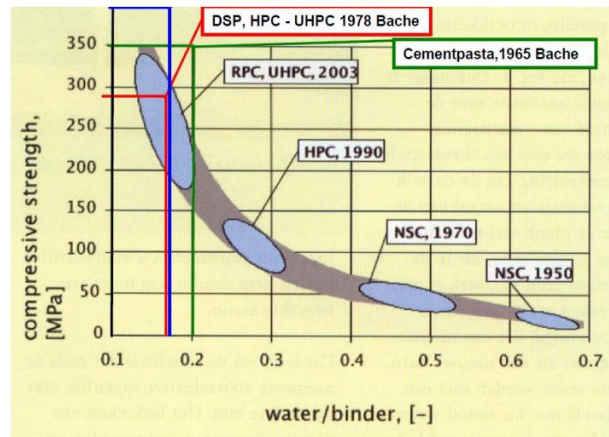


Figure 1 – Compressive strength of different concrete materials as a function of the water/binder ratio. Breugel and Schlangen (2014)

Besides concretes with high compressive strengths, other innovative concretes have been researched for the last years. These kinds of concretes have in comparison to ordinary concrete special properties. An example is the Strain Hardening Cementitious Composite (SHCC). This composite has a strain hardening effect which makes the material more ductile compared with normal strength concrete. (Naaman, 2008)

1.1 Problem definition

Although a lot of research is done to new concrete materials, ordinary normal strength concrete is still the most applied concrete in infrastructure. Not using these new concrete materials is undesirable for both the unexplored possibilities of enhancing infrastructure, as leaving the research input already delivered. New materials have different characteristics compared to normal concrete. This new characteristics can lead to new design opportunities. Designs can, depending on the characteristics of the concrete material, for example be made cheaper, more slender or more durable. Altogether, this could be defined as the problem that should be solved. The problem is defined as:

A lot of research at developing new concrete materials is done, however infrastructure potential benefits are lost since utilisation is lacking

1.2 Research question

From the problem definition the research question of this research could be formulated. The answer to this question should be the solution of the problem defined above. The research question is:

Which combinations of new concrete materials and constructions should be utilised to take up potential benefits?

1.3 Objective

The objective of this thesis is more or less to come up with some infrastructural constructions where new concrete materials can be utilised to increase the benefits of a project. The main aim of this research is provide in:

An overview of combinations of new concrete materials and constructions, which can be utilised to take up potential benefits

In the definition of the objective four keywords are explained in more detail to understand the objective better. The key words are:

- New concrete materials
- Constructions
- Utilise
- Potential benefits

In this thesis will be searched to as many applications as possible for new concrete materials in the infrastructure. The new concrete materials are only interesting if it could take up potential benefits for infrastructure.

'Advantageous for the constructions' is quite a broad concept, because materials can be beneficial in many ways. This is written consciously, because the benefits of the new concrete materials for constructions should still be explored. As soon as the benefits of the concrete materials are known, the benefits per material can be defined.

1.4 Methodology

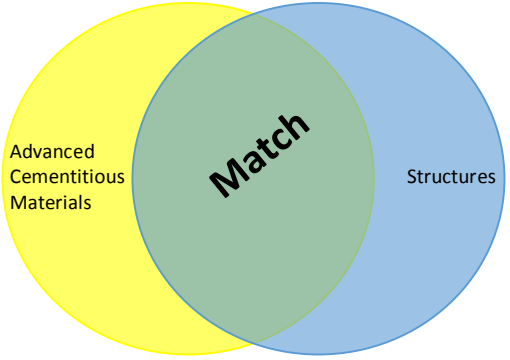
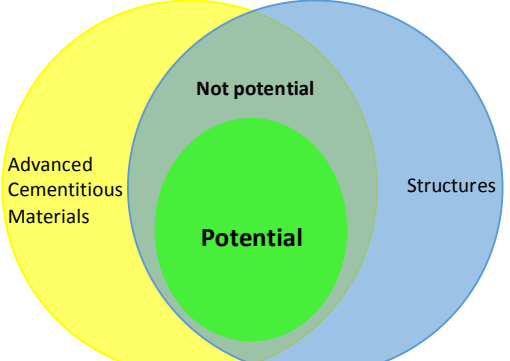
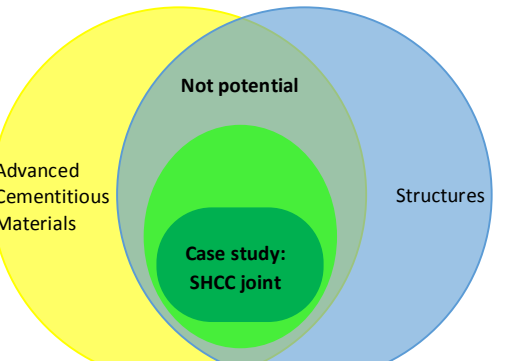
This research is set up as wide as possible. In the beginning of this study many new concrete materials and structures are analysed. Besides, researched applications and reference projects are analysed. After that a list of possible beneficial applications is made. This ends up in a big list of applications. During the research, this list becomes shorter by steps, such that in the end only the best combinations are left. The steps taken to shorten the list are shown in Table 1. Here the steps are explained briefly.

The first time that the list is shortened, is by the outcome of researched applications and reference projects. Some applications that are made in step 4 are probably already researched or even built. The results of these projects can strengthen or contradict some of the possible applications. If research from others is very negative about an application from the list, this application could be removed.

The second time that the list will be made shorter is when the potential of the combinations is judged. The potential applications are discussed with experts in the field of concrete structures. From the discussion, the best potential combination are chosen.

In the last step, one of the best potential combinations is researched in more detail in a case study. In the case study, literature is researched to make a list of points of attention of the SHCC link slab design. The critical issue of the design is researched in even more detail. In the end, some recommendations are given to improve the critical point of the design.

Table 1 – Methodology of research to Advanced Cementitious Materials by step-by-step plan

 <p>Figure 2 - The schematically exhibition of the idea of linking the new concrete materials with infrastructure</p>	<table border="1"> <tbody> <tr> <td data-bbox="758 280 813 414">Step 1</td> <td data-bbox="813 280 1402 414"> <p>Literature research</p> <ul style="list-style-type: none"> - Material properties - Infrastructure structures </td> </tr> <tr> <td data-bbox="758 414 813 548">Step 2</td> <td data-bbox="813 414 1402 548"> <p>Researched applications</p> <p>Researches about potential applications of new concrete materials in single constructions.</p> </td> </tr> <tr> <td data-bbox="758 548 813 694">Step 3</td> <td data-bbox="813 548 1402 694"> <p>Reference projects</p> <p>Already realised projects where new concrete materials are applied</p> </td> </tr> <tr> <td data-bbox="758 694 813 958">Step 4</td> <td data-bbox="813 694 1402 958"> <p>Linking the right concrete to the right structure</p> <ul style="list-style-type: none"> - Which concrete has the best properties to apply in certain structures - Which structures do not have benefits by applying new concrete materials? - Table the possible fields of applications </td> </tr> </tbody> </table>	Step 1	<p>Literature research</p> <ul style="list-style-type: none"> - Material properties - Infrastructure structures 	Step 2	<p>Researched applications</p> <p>Researches about potential applications of new concrete materials in single constructions.</p>	Step 3	<p>Reference projects</p> <p>Already realised projects where new concrete materials are applied</p>	Step 4	<p>Linking the right concrete to the right structure</p> <ul style="list-style-type: none"> - Which concrete has the best properties to apply in certain structures - Which structures do not have benefits by applying new concrete materials? - Table the possible fields of applications
Step 1	<p>Literature research</p> <ul style="list-style-type: none"> - Material properties - Infrastructure structures 								
Step 2	<p>Researched applications</p> <p>Researches about potential applications of new concrete materials in single constructions.</p>								
Step 3	<p>Reference projects</p> <p>Already realised projects where new concrete materials are applied</p>								
Step 4	<p>Linking the right concrete to the right structure</p> <ul style="list-style-type: none"> - Which concrete has the best properties to apply in certain structures - Which structures do not have benefits by applying new concrete materials? - Table the possible fields of applications 								
 <p>Figure 3 - The schematically exhibition of potential fields of applications</p>	<table border="1"> <tbody> <tr> <td data-bbox="758 958 813 1433">Step 5</td> <td data-bbox="813 958 1402 1433"> <p>Judging the success of the matches</p> <ul style="list-style-type: none"> - Judging the applications to separate the wheat from the chaff - Separation between potential and not-potential applications - Arrangement of the applications that are potential </td> </tr> </tbody> </table>	Step 5	<p>Judging the success of the matches</p> <ul style="list-style-type: none"> - Judging the applications to separate the wheat from the chaff - Separation between potential and not-potential applications - Arrangement of the applications that are potential 						
Step 5	<p>Judging the success of the matches</p> <ul style="list-style-type: none"> - Judging the applications to separate the wheat from the chaff - Separation between potential and not-potential applications - Arrangement of the applications that are potential 								
 <p>Figure 4 - The schematically exhibition of the case study to SHCC link slab</p>	<table border="1"> <tbody> <tr> <td data-bbox="758 1433 813 1635">Step 6</td> <td data-bbox="813 1433 1402 1635"> <p>Case study: SHCC link slab</p> <ul style="list-style-type: none"> - Overview of point of attentions of the SHCC link slab design - Possibilities to improve the link slab design </td> </tr> <tr> <td data-bbox="758 1635 813 1899">Step 7</td> <td data-bbox="813 1635 1402 1899"> <p>Finish research</p> <ul style="list-style-type: none"> - Final conclusions and recommendations - Finish the definitive rapport and the presentation </td> </tr> </tbody> </table>	Step 6	<p>Case study: SHCC link slab</p> <ul style="list-style-type: none"> - Overview of point of attentions of the SHCC link slab design - Possibilities to improve the link slab design 	Step 7	<p>Finish research</p> <ul style="list-style-type: none"> - Final conclusions and recommendations - Finish the definitive rapport and the presentation 				
Step 6	<p>Case study: SHCC link slab</p> <ul style="list-style-type: none"> - Overview of point of attentions of the SHCC link slab design - Possibilities to improve the link slab design 								
Step 7	<p>Finish research</p> <ul style="list-style-type: none"> - Final conclusions and recommendations - Finish the definitive rapport and the presentation 								

2 Advanced Cementitious Materials

In this chapter is done research to Advanced Cementitious Materials (ACMs). For the research is made use codes, standards, recommendations and literature. Before the research is done, the scope of ACMs is defined. For the ACMs of the scope then is given the composition. In the compositions are given the ingredients that are mixed together to make the ACMs. After that, the mechanical, durable and sustainable characteristics of the ACMs are given. Before the durability per ACM is given, an analysis to the durability of concrete is done. At last, some material costs, design standards and recommendations are given and are done some calculations according to these standards and recommendations.

2.1 Scope of Advanced Cementitious Materials

As mentioned before, a lot of research is done to quite a lot of new concrete materials. Not all of the advanced cementitious composites are researched in the same level of detail. Some materials are researched for a few years only, such that they are not researched well enough to apply already. For now, the materials where enough knowledge is present, applications can be found in a proper way. In this paragraph are the materials shown that seems to be researched well.

In Table 2 all the Advanced Cementitious Materials are shown within the scope of this research. In the third column of Table 2, a description of the main characteristics of the ACMs is given. For example ACM 5. Strain Hardening Cementitious Composite (SHCC), is specially characterized by its strain hardening behaviour and crack pattern. In the last column themes are given where the ACM has relations with. The three themes in this research are mechanical, durability and sustainability characteristics of the cementitious materials. For example the characteristics of strain hardening cementitious composite have strong relations with the mechanical and durable properties.

Table 2 – Overview of Advanced Cementitious Materials in the scope of the research, including the main characteristics and the themes the ACMs have mainly influence on

	Cementitious material	Main characteristic	Theme
Plain concrete	Normal Strength Concrete (NSC)		
ACM 1.	Normal Strength Steel Fibre Reinforced Concrete (NSSFRC)	Crack width control	Mechanical Durability
ACM 2.	High Performance Concrete (HPC)	Strength Compactness	Mechanical Durability
ACM 3.	High Performance Steel Fibre Reinforced Concrete (HPSFRC)	Strength Compactness Crack width control	Mechanical Durability
ACM 4.	Ultra High Fibre Reinforced Performance Concrete (UHFRPC)	Strength Compactness	Mechanical Durability
ACM 5.	Strain Hardening Cementitious Composite (SHCC)	Crack width control Strain hardening behaviour	Mechanical Durability
ACM 6.	Self-Healing Cementitious Material	Self-healing behaviour	Durability
ACM 7.	Geopolymer concrete	Low carbon footprint	Durability Sustainability
ACM 8.	Self-cleaning nano concrete	Unique mechanical, thermal and electrical properties	Durability
ACM 9.	Self-sensing nano concrete	Unique mechanical, thermal and electrical properties	Mechanical

There are a lot more cementitious materials, other than NSC, that could be interesting to apply in practice. In Table 3 some cementitious materials are given that are not in the scope of this research. In the second column of this table the main reason is given why the material is not included in this research. The most concretes that are left out are already relative long in practice or don not seem to have significant advantages.

Table 3 - Cementitious materials left out of the scope of this research

ACM	Reason	Source
Self-Compacting Concrete	Already applied successfully in practice for years. Moreover, Self-Compacting Concrete is included in Eurocode 2 as a NSC. Only the execution method differs.	
Very High Performance Concrete	Not included in any code. Not very interesting since the strength is just between UHPC and HPC.	
Hot Weather Concrete	Relative simple adjustment to the concrete mixture, production, placing or curing, which are done in practice already.	(Nayak & Jain, 2012)
Cold Weather Concrete	Relative simple adjustment to the concrete mixture, production, placing or curing, which are done in practice already.	(Nayak & Jain, 2012)
Pervious Concrete	Has been used in a wide range of applications already.	(Nayak & Jain, 2012)
Lightweight Concrete	Already applied successfully for about 100 years.	(Nayak & Jain, 2012)
High-Density Concrete	Just the application of heavy aggregate and a dense aggregate distribution. The weight of concrete is normally not too low.	(Nayak & Jain, 2012)
Underwater Concrete	A quite common execution method already. Optimisation could be there, but the idea itself is known well now.	
Roller Compacted Concrete	Not that practical to apply in constructions, due to the way it is compacted. Further, it is already applied for more than 25 years, so not very innovative any more.	(Nayak & Jain, 2012)
Foam Concrete	Already used for multiple uses all over the world since 1920.	(Nayak & Jain, 2012)
Acid Resistance Concrete	In fact a HPC, which is able to resist attack from acids well.	(Nayak & Jain, 2012)
Shotcrete	A quite common application.	
Limecrete	Very old technic, that seems to be some more popular nowadays. So it is not an innovative material.	(Jamal, 2014)
Concrete with reinforcement other than steel	Left out for reasons of simplicity. Only the concrete itself is researched.	

2.1.1 Normal Strength Concrete

Ordinary concrete in this research is the plain concrete where all the other cementitious materials are compared to. In this paragraph, normal strength concrete (NSC) is defined. Before the final definition

of NSC is given, some general information from standards and recommendations according to NSC is given. Further, the type of cement and the aggregate is described in some more detail.

2.1.1.1 General

Here, some general characteristics of NSC are given according to literature. General characteristics include the ratio of ingredients, the compressive strength and the weight of NSC.

- The 'Beton lexicon' describes that the cement to sand to gravel ratio for ordinary concrete is respectively 1 to 2 to 3. (BetonLexicon, n.d.)
- Betonpocket 2012 defines concrete with a cubic compressive strength between the 20 and 55 MPa as "ordinary concrete".
- Eurocode 2 part 1 includes the concrete class with a cubic concrete strength of 15 – 105 MPa.
- Eurocode 2 part 2 includes the concrete class with a cubic concrete strength of 37 – 85 MPa.
- NEN-EN 206-1 gives the next definition for the weight of ordinary concrete:

Ordinary concrete has an oven dry mass between 2000 kg/m³ and 2600 kg/m³

2.1.1.2 Type of cement

In chapter 5 of NEN-EN 206-1 Beton - Specificatie, eigenschappen, vervaardiging en conformiteit is literary written: 'Voor cement dat voldoet aan EN 197-1 is de geschiktheid in algemene zin aangetoond'. This means that every type of cement that is proved to meet the requirements of EN 197-1, could be applied in concrete. To judge if a type of cement is suitable for concrete, tests should be done as described in Aanbeveling 48 Geschiktheidsonderzoek van nieuwe cementen voor toepassing in beton.

In The Netherlands, Blast Furnace Cement, Ordinary Portland Cement and Portland Fly Ash Cement are the most commonly used types of cement (BetonLexicon, n.d.). The three types of cement give different characteristics to concrete. For example, concrete with blast furnace cement has in general a lower chloride diffusion coefficient, so a better durability. It is hard to find reliable facts about the types of cement used abroad. Some literature indicates that Ordinary Portland Cement seems to be the most frequently used cement in the world:

- Ordinary Portland Cement (OPC) is the most common cement used in general concrete construction when there is no exposure to sulphates in the soil or groundwater (Lafarge, 2015).
- Prior to 2007, Ordinary Portland Cement (OPC) was the most commonly used cement for general purpose applications (TCL, 2013)

Both BFC and OPC are used a lot in The Netherlands. The above shown citations suggest that abroad OPC is the most commonly used cement. Further is known that in The Netherlands relative a lot of BFC is used in concrete compared to other countries. To keep the possibility to use this research also for applications in other countries than The Netherlands, what is in the interest of Heijmans, OPC is chosen as the binder of NSC.

2.1.1.3 Aggregate

Normal Strength Concrete consists of a mixture of coarse and fine aggregate. In NEN-EN 206-1, NEN-EN 206:2014 (en) and NEN 5905:2005 are some definitions for aggregate. These definitions are used in this research to define the aggregate of NSC.

- NEN-EN 206:2014 (en) defines normal-weight aggregate as:
Aggregate in oven-dry condition with a particle density between 2,000 kg/m³ and 3,000 kg/m³, when determined according to EN 1097-6

- Coarse aggregate has a diameter $D > 4 \text{ mm}$ (Nederlands Normalisatie-instituut, 2014)
- Fine aggregate has a diameter $d > 0 \text{ mm}$ (Nederlands Normalisatie-instituut, 2014)
- The coarse aggregate ($4 \text{ mm} < d < 32 \text{ mm}$) for has a distribution according NEN 5905, chapter 4, table 2. The distribution is shown in Table 4.

Table 4 - Distribution of coarse aggregate with a grain diameter ($4 \text{ mm} < D < 32 \text{ mm}$) according to NEN 5905: chapter 4, table 2

Sieve size [mm]	63	45	31.5	22.4	16	11.2	8	5.6	4	2
Part falling through sieve [%]	100	98-100	90-99		25-70				0-15	0-5

2.1.1.4 Final definition

In Table 5 is given the final definition for the NSC in general and for the representative NSC C30/37. The representative NSC is used to make quantitative comparisons with the ACMs. This concrete class is chosen, because this is the most commonly used NSC in infrastructure that is applied by Heijmans. Under Table 5 is shortly reasoned the definition of NSC.

Table 5 – General definition of NCS and the representative NSC (C30/37) by different characteristics

Characteristics	General Definition NSC	Representative NSC (C30/37)
Strength	C12/15 until C50/60 $12 \leq f_{ck} < 53 \text{ MPa}^a$ $15 \leq f_{ck,cube} < 65 \text{ MPa}^a$	C30/37 ^b
Binder	Ordinary Portland Cement ^b	Ordinary Portland Cement ^b
Weight	2000 – 2600 kg/m^3 ^c	2300 kg/m^3 ^b
Composition (ratio cement : sand : gravel)	1 : 2 : 3 ^d	1 : 2 : 3 ^d
Water cement factor	Depending on strength	0.5 ^b
Fine aggregate	$d > 0 \text{ mm}^e$	$d > 0 \text{ mm}^e$
Coarse aggregate	$D > 4 \text{ mm}^e$	$D > 4 \text{ mm}^e$

In short, the reasons to define NSC as it is defined in Table 5 are:

- These concrete strengths are covered by the European design rules, Eurocode 2.
- NSC is less strong than HPC, which covers the concrete strength classes C53/65 until C100/115, as explained in chapter 2.1.3 High Performance Concrete and High Performance Steel Fibre Reinforced Concrete
- Aanbeveling 97 Hogesterktebeton (deel 1: NEN 6720 VBC 1995) defines HPC as concrete with a characteristic cubic compressive strength between ($65 \text{ MPa} < f_{ck,cube} < 105 \text{ MPa}$).
- OPC is one of the most common type of cement in The Netherlands and abroad.
- The self-weight of concrete is determined according to NEN-EN 206-1. For the representative NSC is assumed the mean self-weight of 2300 kg/m^3 .
- For the representative NSC: water cement ratio is assumed to be equal to 0.5 to get the desired strength.

^a (Nederlands Normalisatie-instituut, 2011), (Nederlands Normalisatie-instituut, 2004)

^b Assumptions done as described in 2.1.1 Normal Strength Concrete

^c (Nederlands Normalisatie-instituut, 2001)

^d (BetonLexicon, n.d.)

^e (Nederlands Normalisatie-instituut, 2014)

In this research, the durability characteristics of the concrete materials, as well as for NSC, are given in a range. The defined durability ranges used in this research for NSC are given in chapter 2.4.9 Durability of the Advanced Cementitious Materials.

2.1.2 Normal Strength Steel Fibre Reinforced Concrete

As the name already tells, fibre reinforced concrete is concrete containing fibres uniformly distributed and randomly oriented to reinforce the concrete. Fibres can be made out a lot different materials, like steel, PP, PVA or carbon. The fibres can control the cracks in the concrete and should take care of the brittle behaviour of the concrete itself.

In Dutch codes, Eurocode 2, are no rules for fibre reinforced concrete. Also in the Dutch national annex is nothing about fibres. In the Netherlands there are some CUR documents for fibre reinforced concrete:

- CUR 245: Staalvezelbeton: kennis en kennisleemten
- CUR 246: staalvezelbeton: inventarisatie van regelgeving
- CUR-Aanbeveling 96-9: Vezelversterkte kunststoffen in civiele draagconstructies
- CUR-Aanbeveling 36:2011 Ontwerpen van elastisch ondersteunde betonvloeren en – verhardingen
- CUR-Aanbeveling 42:2011 Bepaling van de invloed van polypropyleenvezels in beton op de vorming van plastische krimp scheuren
- CUR-Aanbeveling 111: Staalvezelbeton bedrijfspvloeren op palen – Dimensionering en uitvoering

Also in the first complete draft of the Model Code 2010 Fibre Reinforced Concrete (FRC) is included. The Model Code is valid for fibres made of steel, polymers, carbon, glass or natural material. Characterises of the FRC mention shortly in MC are (fib Bulletin 55, 2010):

- Post-cracking residual strength
- Early age crack-control
- Fire resistance
- Improving durability due to reduced crack spacing and crack width
- Partially or totally substitution of conventional reinforcement
- Elastic properties and compressive strength are not significantly affected by fibres, unless a high percentage of fibres is used.
- Hardening or softening behaviour of FRC, depending on their composition

From a mechanical point of view, FRC differs from NSC in cracking behaviour only. The crack pattern of both materials is different and the FRC has a certain hardening or softening behaviour. The alternative cracking pattern of FRC also causes better durability of concrete. In fact, the durability of uncracked concrete is similar to NSC, but if FRC is cracked, the improved crack pattern improves the durability compared to concrete without any fibres.

From the CUR-Aanbeveling documents, the knowledge of steel fibre concrete seems to be on a higher level compared to concretes containing other fibres. Further, steel fibres are relative cheap compared to other fibres (Ven, 2015). From reasons of simplicity, one type of fibres for FRC will be researched. From a practical and economical point of view, it seems to be the best to include steel fibres only. The next step for FRC could be the replacement of steel fibres by other fibres like polymers or glass.

2.1.3 High Performance Concrete and High Performance Steel Fibre Reinforced Concrete

High Performance Concrete (HPC) is developed around 1990. This concrete is characterised by its high compressive strength. The maximum strength for this type of concrete is limited from practical reasons. The strength of the aggregate particles does not allow a further increase of the bearing capacity of the concrete (Walraven, 2009). In fact HPC is strong through the durability of the concrete (Nayak and Jain, 2012), so it is more than just a concrete with a high strength. The properties of HPC differ from the lower strength materials, such that alternative models should be used than for NSC. Especially if creep and shrinkage is modelled, the models of the ordinary concretes do not fit any more. However, for reasons of simplicity, HPC is classified by its strength here. From literature, some definitions of the HPC by its strength are:

- Betonpocket 2012 defines HPC as concrete with a characteristic cubic compressive strength between 65 MPa and 115 MPa ($65\text{MPa} < f_{ck} < 115\text{MPa}$) (ENCI, Mebin en Sagrex, 2011).
- In NEN-EN 206-1:2001 High Performance Concrete is defined as concrete in compressive strength classes **higher than C50/60**. The maximum strength class taken into account in this document is C100/115.
- In Aanbeveling 97 Hogesterktebeton (deel 1: NEN 6720 VBC 1995) is a HPC defined as concrete with a characteristic cubic compressive strength between ($65\text{MPa} < f_{ck,cube} < 105\text{MPa}$). The upper limit is there because the rules of Eurocode are not valid any more for concrete higher concrete classes. In Eurocode are some concrete classes included that are in the range of HPC.

According to the above mentioned limits, the strength class of HPC in this research is defined C53/65 until C100/115.

HPC can also be applied in combination with fibres. The idea behind the application of fibres in HPC is more or less the same as for ordinary concrete. This idea is described in 2.1.2 Normal Strength Steel Fibre Reinforced Concrete. For the same reason as for FRC steel fibres will be applied for HPFRC, also mentioned in 2.1.2 Normal Strength Steel Fibre Reinforced Concrete

To compare the mechanical, durable and sustainable properties of HPC with NSC easily, one HPC class is chosen. The mean HPC class with the mean compressive strength, $f_{ck} = 90\text{MPa}$, would probably represent the most average characteristics of HPC. Moreover, this concrete class is the highest compressive strength Eurocode 2 is valid for. For a concrete stronger than C90/105 but still in the range of HPC (so $f_{ck} < 115\text{MPa}$) no accepted guidelines are present yet. So to do calculations for HPC, it is smart to use a concrete that is included in Eurocode 2. Further, a lower concrete class can't represent the high strength and durability properties of HPC in a proper way, because the difference between NSC and HPC for the lower HPC classes becomes relative small. Therefore, the C90/105 seems to be the best concrete class to use in the research as a HPC.

2.1.4 Ultra High Performance Fibre Reinforced Concrete

After researching HPC, developers tried to gain even a stronger concrete material. In the recent decades this is achieved by developing a new class of concrete: Ultra High Performance Concrete (Graybeal B. A., 2006). In the literature, different definitions for UHPC are given by the cubic concrete compressive strength, for example

- Higher than 180 MPa (Walraven, 2009).
- Betonpocket 2012: 150-200 MPa (indicative values)
- $150\text{MPa} < f_{ck} < 250\text{MPa}$ (AFGC's Scientific and Technical Committee, 2013)

In this rapport the definition of the AFGC will be used, because AFGC made recommendations for UHPC which can be used in research. To judge UHPC in a quantitative way, for example for the mechanical and durable characteristics, C170/200 is chosen. This concrete class has the average compressive strength in the range of UHPC, so this material should represent UHPC the best.

UPHC mostly contains fibres to ensure a ductile behaviour. Therefore, the UPHC is often named as Ultra High Performance-Fibre Reinforced Concrete (UHP-FRC), which is in its basics the same. The representative C170/200 contains fibres to ensure the ductile behaviour. To apply the French recommendations for UHPC steel fibres are added instead of fibres made of other materials, like plastic. If other types of fibres are added to UHPC, the French recommendations are not valid anymore, because of the different behaviour of different types of fibres.

2.1.5 Strain Hardening Cementitious Composite

Strain Hardening Cementitious Composite (SHCC) is a fibre reinforced concrete with strain hardening behaviour after elastic deformation when it is loaded in tension. The strain hardening behaviour makes the concrete very ductile compared with other concrete materials (Naaman, 2008). Due to this ductility a lot of energy can be taken by the concrete before it fails.

Strain hardening cementitious composite is in particular researched in Japan, because of the favourable properties of the SHCC for constructions subjected to earthquakes. In the Japanese standards already something about the design with SHCC is present. Next to this, some recommendations are written for SHCC. Expect some SHCC in constructions subjected to earthquakes, SHCC is nearly applied.

The representative SHCC for quantitative comparisons in this research is a mix from Qian, et al. (2009). In their research, they designed mix M4 that has almost the same compressive strength as C30/37. This mixture could be a good mixture to compare to C30/37. However, the tensile strain hardening behaviour of the slightly stronger SHCC mixture M3, was significant better compared to SHCC M4 mix. The main characteristic of SHCC is the strain hardening behaviour in tensile stress. For that reason the slightly stronger SHCC M4 mix with a larger tensile strain hardening behaviour will be used in this research.

Moreover, in the representative SHCC mix PVA fibres are added, where also other type of fibres could be applied. PVA fibres are the most utilized fibres in literature, but also other fibres are successfully applied. Li argues that the principle behind the design of SHCC does not depend on a particular fibre (Li V. C., Engineered Cementitious Composites (ECC) – Material, Structural, and Durability Performance, 2007). Since the chosen representative SHCC does have the unique SHCC characteristics, the utilisation of PVA fibres in the representative mix seems ok.

2.1.6 Self-Healing Cementitious Materials

Self-healing cementitious materials have a certain self-healing property, due to a built-in capability to repair structural damage autogenously or autonomously (Tang, Kardani, & Cui, 2015). Both types of self-healing will be discussed in some more detail.

Autogenous healing results from chemical and/or physical composition of the cementitious matrix. In principle, every cementitious material has a certain autogenous healing capacity. The maximum crack width healable by autogenous healing are reported to be between 200 – 300 μm (Tang, Kardani, & Cui, 2015). The process behind autogenous healing mainly relies on one or more of the following four mechanisms (also shown in Figure 5):

- a. Formation of calcium carbonate or calcium hydroxide;

- b. Settlement of the debris and loose cement particles in presence of water;
- c. Hydration of unhydrated cementitious particles;
- d. Further swelling of the hydrated cementitious matrix

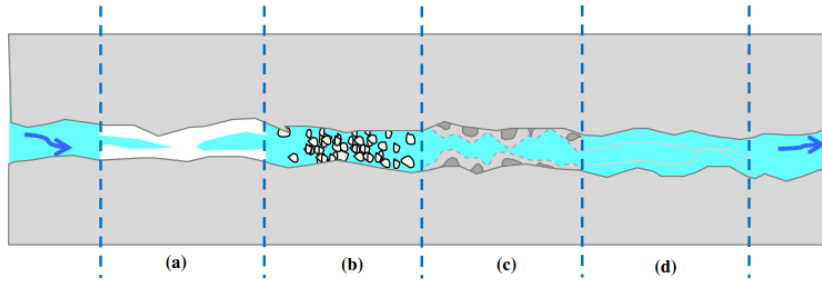


Figure 5 – Main mechanisms of autogenous healing: (a) formation of calcium carbonate from calcium hydroxide; (b) settlement of the debris and loose cement particles in presence of water; (c) hydration of unhydrated cementitious particles; (d) further swelling of the hydrated cementitious matrix (Tang, Kardani, & Cui, 2015)

Autonomous crack healing in concrete refers to self-healing mechanisms that are artificially triggered in the cementitious matrix mainly by presenting some chemical or biological agents into the cementitious matrix. The basic idea is that upon occurrence of cracks, the healing agent becomes active and heals the crack. Activating the agent can be done in different ways, for example by air or moisture. In literature, healable crack width of 500 – 970 μm are reported, which is about 2-3 times the heal capability of autogenous healing. The maximum healable crack width depends on the agent used (Tang, Kardani, & Cui, 2015).

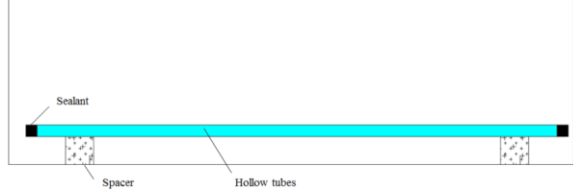
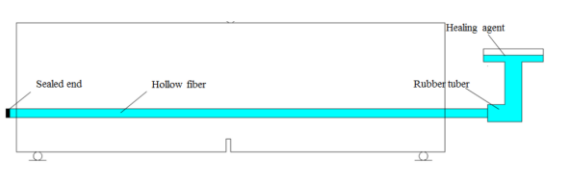
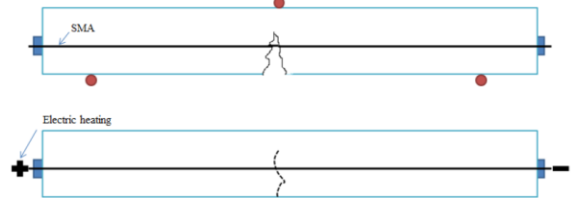
Autonomous healing property to concrete can be given in a few different ways. The main strategies to design a concrete with the self-healing characteristic are briefly shown in Table 6.

Table 6 – Different strategies of autonomous self-healing

Encapsulation and expansive agent	Bacteria
<p>When the crack ruptures embedded microcapsules, the healing agent is released into the crack plane through capillary action. Then the healing agent contacts the embedded catalyst, triggering polymerization that bonds the crack faces closed. Expansive agents encapsulated into (micro) capsules, could be an alternative. ^{f,g}</p>	<p>Bacteria on fresh crack surface become activated due to water ingression, start to multiply and precipitate minerals such as calcite, which eventually seal the crack and protect the steel reinforcement from further external chemical attack. ^{f,h}</p>
Hollow fibres: internal healing agent supply system	Hollow fibres: external healing agent supply system

^f (Xia Hua, 2010)

^g (Wu, Johannesson, & Geiker, 2012)

	
<p>Hollow fibres stores healing agents. When concrete cracks, under certain stimulus the healing agents flow out and heal the crack subsequently.^h</p>	<p>The idea is the same as for internal healing agent supply system, with the addition that the healing agent is supplied externally from the structure.^h</p>
Shape memory system	
	
<p>The change of electrical resistance of the SMA bars due to their elongation can be used to monitor the crack width in the concrete beam. The SMA cables can be electrically heated to return to its original shape to heal the crack.^{h,i}</p>	

In the scope of this research, a self-healing C30/37 is chosen as a representative concrete of the self-healing cementitious materials. In this way, a proper comparison between NSC and Self-healing concrete can be made. Because autonomous healing mechanisms can heal relative large cracks compared to autogenous healing mechanism, a C30/37 concrete with an autonomous healing behaviour is chosen. Besides, C30/37 does already has a certain autogenous healing character.

In Table 6 is shown that some additions should be present in the concrete to give the concrete the self-healing behaviour. The addition could be an agent, bacteria, hollow fibre or a shape memory system. In the first strategies, the concrete is healed by filling the crack. In the shape memory, the concrete heals due to closing the crack by bringing back the structure to its original shape. The representative concrete in this research depends on healing due to filling the crack, because most self-healing strategies depends on this. So the representative self-healing concrete here is a concrete with a self-healing agent.

It is assumed that the influence of self-healing additions (agents, bacteria or hollow fibres) on the mechanical behaviour of uncracked concrete can be neglected. The amount of additions for the self-healing property is normally in the order of magnitude of a few weight percent. Results of tests to the influence of the microcapsules on the concrete compressive strength are shown in Figure 5, Figure 6, Figure 7 and Table 8. In the figures and table, the compressive strength of concrete with microcapsules is compared to concrete without microcapsules. All results will be discussed here.

The test results given in Figure 6, show that the amount of microcapsules does not have a significant influence on the compressive strength. The amount of microcapsules in the matrix is shown in Table 7 (Sui, Mechanical behavior of FRP-confined self-healing concrete, 2014). The test is done for (fibre reinforced) normal strength concrete, with a mean strength in the order of 50 MPa (≈ 7 ksi) and 75 MPa (≈ 11 ksi) for NSC and FRC respectively

^h (Sui, Mechanical behavior of FRP-confined self-healing concrete , 2011)

ⁱ (Hassan, Mehrpouya, Emamian, & Sheikholeslam, 2013)

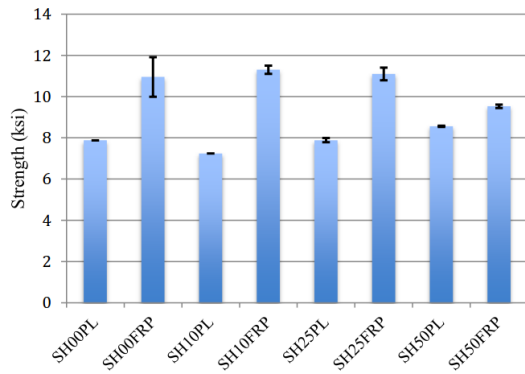


Figure 6 – Comparison of strength for concrete without microcapsules and with 0%; 1.0%; 2.5%; 5.0% of cement weight microcapsules (Sui, Mechanical behavior of FRP-confined self-healing concrete, 2014)

Table 7 – Amount of microcapsules (SS) by cement weight per concrete matrix (Sui, Mechanical behavior of FRP-confined self-healing concrete, 2014)

Test type	Specimen ID	SS content	Confinement type
Preliminary test	PR00PL	0.0%	Unconfined
	PR00FRP		FRP
Self-healing test	SH00PL	0.0%	Unconfined
	SH00FRP		FRP
Self-healing test	SH10PL	1.0%	Unconfined
	SH10FRP		FRP
Self-healing test	SH25PL	2.5%	Unconfined
	SH25FRP		FRP
Self-healing test	SH50PL	5.0%	Unconfined
	SH50FRP		FRP

In Figure 7 is the relative compressive strength shown as a function of the amount of microcapsules. As show in the figure, the addition of microcapsules results in a serious decreased strength if more than about 4% microcapsules are added. Lower additions do nearly influence the compressive strength.

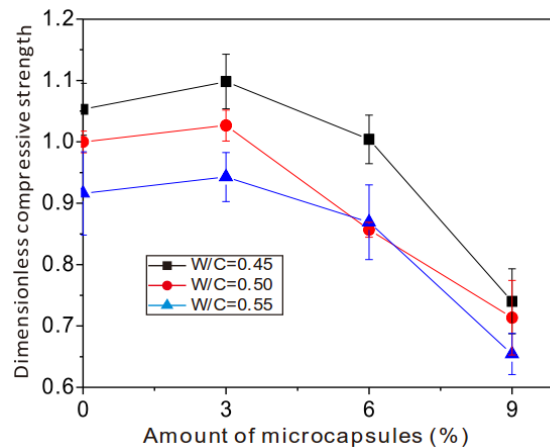


Figure 7 – The relative compressive strength as a function of the amount of microcapsules (x% to the cement mass) in mortar specimens (Wang, Xing, Zhang, Han, & Qian, Experimental Study on Cementitious Composites Embedded with Organic Microcapsules, 2013)

In Table 8 is shown that the addition of 2% by the volume of the concrete, microcapsules increases the compressive strength for all five samples. The average strength increase is about 10%.

Table 8 – Compressive strength of control samples and samples containing 2% vol. microcapsules (Pelletier, Brown, Shukla, & Bose, n.d.)

Sample	Control, strength (ksi)	With 2% vol. microcapsules (ksi)
1	2.279	2.253
2	2.283	2.307
3	2.247	2.875
4	2.244	2.579
5	2.276	2.718

From the above test results it can be concluded that microcapsules does not have a significant negative influence on the concrete compressive strength if:

- The addition of microcapsules is lower than 4% by the weight of the cement.
- The addition of microcapsules is 2% by the volume of the concrete.

In the literature study some research is done to the optimal dosage of microcapsules for the self-healing behaviour of the concrete. It is hard to give and general optimum because the healing behaviour of the concrete depends also on environmental conditions, for example the curing of the concrete (Li, Jiang, Yang, Zhao, & Yuan, 2013). From literature, some conclusions for the optimum dosage are:

- Between 2.5% and 3.5% by the volume of the concrete (Yuan & Chen, 2013)
- Depending on the curing conditions 1 – 2% by mass of the cement (Li, Jiang, Yang, Zhao, & Yuan, 2013)

Now the relation between the optimum dosage of microcapsules and the influence of the microcapsules on the mechanical characteristics can be made. The first optimum dosage of microcapsules is in the range where the capsules start to have a negative influence on the compressive strength. The second optimum is in the range where the influence of the capsules can be neglected. Therefore, the influence of the capsules will be neglected in this research. The dosage of microcapsules for the representative self-healing concrete is assumed to be 3% by the volume of the concrete.

2.1.7 Geopolymer Concrete

The term geopolymer was coined by Davidovits in 1978 to represent a broad range of materials characterized by chains or networks of inorganic molecules (U.S. Department of Transportation Federal Highway Administration, 2010). The unique thing about geopolymer concrete is that it does not contain any Portland cement, which significantly reduces the carbon footprint of this type of concrete. The aim of geopolymer cement is to create a cement that requires a minimum amount of natural materials and produces a minimum amount of industrial by-products during production.

A lot of research is done to compare the carbon footprint of geopolymer concrete to Portland concrete. One of the most positive researches concludes a CO_2 reduction of approximately 80% (Deventer, Provis, Duxson, & Brice, 2010). One of the most negative researches concludes a reduction of the carbon footprint of approximately 9% CO_2 -equivalent. This research claims that it includes the materials from sourcing raw materials to the manufacture and construction. It claims that other studies does mostly not include key factors as mining, treatment and transport of raw materials for manufacture of alkali activators. (Turner & Collins, 2013)

Since no Portland cement is included in geopolymer concrete, other binders should be in. Geopolymer concretes get it strength by combining:

- Source materials which are rich in silica and alumina such as fly ash (FA), ground granulated blast furnace slags (GGBFS) and metakaolin (Shaikh, 2013), (Ken, Ramli, & Ban, 2015)
- Source materials with strong alkali solutions such as sodium silicate (Na_2SiO_3) or potassium silicate (K_2SiO_3) and sodium hydroxide ($NaOH$) or potassium hydroxide (KOH) (Shaikh, 2013), (Ken, Ramli, & Ban, 2015)

In general, almost every compressive strength can be achieved using geopolymer concrete (Mackenzie & Welter, 2014). To make a fair comparison with ordinary concrete in terms of the sustainability, durability and mechanical behaviour, a geopolymer concrete with similar compressive strength ($f_{ck} = 30 MPa$) will be researched. So a geopolymer with a characteristic cubic compressive strength of 37

MPa will be used. In fact, a geopolymer concrete mix with the mechanical properties of a C30/37 and the unique geopolymer characteristics will be researched.

There are three main categories of geopolymer concrete, all three based on another silica and alumina rich material:

- Fly ash based geopolymer
- Metakaolin based geopolymer
- Blast furnace slag based polymer

In Table 9 the order of magnitude of aggregate, fly ash, metakaolin, blast furnace slag, sodium hydroxide and sodium silicate are given. The ingredients shown in the table are the main ingredients which are more or less the basic of a geopolymer concrete. Often, water or admixtures are also in the mix, but they are not required. For that reason, they are not included in Table 9.

Table 9 – Compositions of different types of geopolymer concretes

	Aggregate	Fly ash	Metakaolin	BFS	Sodium hydroxide	Sodium silicate
Fly ash based geopolymer	70 – 80%	10 – 30%			1 – 4%	5 – 10%
Metakaolin based geopolymer	55 – 65%		10 – 12%		1 – 4%	10 – 20%
GBFS based geopolymer	60 – 80%			5 – 15%	0 – 2%	0 – 5%

In Australia some structures are made of geopolymer concrete already (Geopolymer Institute, 2014). The geopolymer concrete applied a lot in these constructions is Earth Friendly Concrete (EFC) developed by Wagners CFT Manufacturing Pty Ltd (Wagners, 2015). EFC is based on BFS and fly-ash. The earth friendly material can be produced in all typical commercial compressive strength grades, as 32, 40 and 50 MPa (Glasby, Day, Kemp, & Aldred, Geopolymer concrete for durable linings, 2014). Next to this, EFC has unique durability characteristics as:

- High sulphate resistance
- High chloride ion ingress resistance
- High acid resistance
- Very low shrinkage
- Very low heat of reaction
- High early strength development (80% of 28 day strength achieved in 7 days for EFC)

Because the compressive strength of EFC could be the same as for C30/37 (NSC) and because EFC is applied in practice already, EFC should perfectly represent geopolymer concrete for quantitative comparisons with NSC. Not a lot of information about the composition of EFC can be found from economic issues. Therefore, a similar BFS-Fly-ash based geopolymer concrete from literature with a similar compressive strength will be used in the quantitative comparisons.

In literature a significant differences between slag based and fly ash based geopolymer concrete are shown in terms of durability. In the mixture of this research, the main binder is fly ash. Fly ash based concrete polymers seem to be better researched compared to concrete polymers based on the combination of both slag and fly ash. Because of this, fly ash based concrete will be used as

representative concrete in terms of durability if too little information is available about geopolymer concrete based on slag and fly ash.

2.1.8 NANO Concrete

In NANO concrete, nano-technology is applied in concrete. Unique properties can be achieved because of additives in the order of nanometres. These small particles influence the concrete matrix, which gives unique mechanical, thermal and electrical properties.

There are different kinds of nano particles that can be added to concrete, for example nano silica, nano-titanium oxide, nano-iron, nano alumina and nanoclay. A lot of work is done to invest the influence of nano-silica and nano-titanium oxide. The most important properties of concrete containing nanoparticles are (Sanchez & Sobolev, 2010):

- | | |
|---|--|
| <p>Nano-SiO₂</p> <ul style="list-style-type: none"> - Improve concrete workability - Improve strength - Increase resistance to water penetration - Control the leaching of calcium - Accelerate the hydration reactions - More efficient in enhancing strength than silica fume | <p>Nano-TiO₂</p> <ul style="list-style-type: none"> - Self-cleaning of concrete - Additional benefit of helping to clean the environment <p><i>Few studies have shown</i></p> <ul style="list-style-type: none"> - Accelerate the early-age hydration of Portland cement - Improve compressive strength - Improve flexural strengths - Enhance abrasion resistance |
| <p>Nano-Fe₂O₃</p> <ul style="list-style-type: none"> - Self-sensing capabilities - Improve compressive strength - Improve flexural strengths | <p>Nano-Al₂O₃</p> <ul style="list-style-type: none"> - Significantly increase the modulus of elasticity - Limited effect on the compressive strength |
| <p>Nanoclay</p> <ul style="list-style-type: none"> - enhancing the mechanical performance compression - enhancing resistance to chloride penetration - self-compacting properties - reducing permeability - reducing shrinkage | <p>nanotubes/nanofibers (reinforcement)</p> <ul style="list-style-type: none"> - extraordinary strength with moduli of elasticity on the order of TPa - tensile strength in the range of GPa - unique electronic properties - unique chemical properties |

Looking to the unique characteristics of the above-mentioned nano materials, four groups of nano-concrete could be made by the material properties. These groups are given in Table 10. In the first column are presented the unique properties. In the second are given the materials which have these material characteristics. Under Table 10, for every nano-group is briefly argued if it is interesting to include in this research.

Table 10 – Groups of nano-concretes separated by material characteristic

Material characteristic	Material
Self-cleaning	Nano-TiO ₂
Self-sensing	Nano-Fe ₂ O ₃
	nanotubes/nanofibers
Stiffness	Nano-Al ₂ O ₃ ,
	nanotubes/nanofibers

Densification	Nano-SiO ₂
	Nanoclay

Self-cleaning: nano-titanium oxide is the only nano-particle that gives concrete a self-cleaning character. Next to the self-cleaning character, nano-titanium has the additional benefit of cleaning the environment. These concrete properties are unique compared to other kinds of concretes. Constructions with self-cleaning concrete maintain their aesthetic appearance over time (Chen & Poon, 2009).

The amount of nano-titanium oxide has influence on the self-cleaning capability. An optimised mixture to create a concrete with the best self-cleaning property is not known yet. In literature, the amount of titanium oxide added to self-cleaning concrete is mostly in the range of 2.5 or 5% of the mass of cement (Diamanti, Lollini, Pedferri, & Bertolini, Mutual interactions between carbonation and titanium dioxide photoactivity in concrete, 2013). It is assumed here that the optimised amount of nano-titanium is in this range.

However, the roughness of the concrete surface also has an influence on the self-cleaning behaviour of nano-titanium concrete. A rough surface of concrete, could result in a bad or negligible self-cleaning behaviour because the residue of contaminants will smudge the surface of the concrete. They can't implement self-cleaning as the photo-catalytic glass yet. If the surface is smooth enough, the residue of contaminants will be washed away by the rain (Shen, et al., 2015)

Self-sensing: self-sensing properties can be given to the concrete through the addition of nano-iron particles or nanotubes/nanofibers. This character can probably increase the safety of the construction, because the conditions of concrete can be monitored better, even at spots where monitoring is normally hard to do. Due to the self-sensing capability, the lifetime may be increased too. Further it can be determined better if maintenance is needed or not.

Next to the improvements in maintenance, the information given by the self-sensing system can help to improve new design. Better monitoring could conclude that designs should be changed to for example optimise the construction in term of money.

As representative self-sensing concrete, a concrete with nano Fe₂O₃ is chosen. Nanotubes have in general more additional advantages compared to nano iron, but there are no concrete mixtures described in literature that can be used in this research. Most researches are done with mortars or cement or are not available to use.

In the representative self-sensing concrete is 2% nano iron by the mass of the cement assumed. This is the highest amount of nano iron where a mix composition and some mechanical characteristics are known for. Li, Xiao, & Ou (2004) show that the addition of 3% and 5% nano iron by the mass of the cement to mortar, results in a certain self-sensing capability (Li, Xiao, & Ou, A study on mechanical and pressure-sensitive properties of cement mortar with nanophase materials, 2004). It is assumed that the addition of 2% nano iron by the mass of the cement to concrete also results in a proper self-sensing capability. For the exact sensing capability of this mix composition, more research should be done.

Stiffness: the stiffness group is represented by the additives nano-aluminate and again nanotubes/nanofibers. A concrete with a high stiffness can for example be interesting if the deflection of a long beam becomes the governing design factor.

Nanotubes themselves are extremely stiff compared to steel fibres. Where steel has a Young's modulus around 20 GPa, nanotubes have a Young's modulus in the order of TPa. The modulus of elasticity of mortars with carbon nanotubes increases approximately by a factor 1.4 (Stynoski, Mondal, & Marsh,

2015), (Konsta-Gdoutos, Metaxa, & Shah, 2010). However, in literature are no available mixtures found with nanotubes. Probably the research to concrete with nanotubes is on quite a low level, such that there is no knowledge available about concrete mixtures containing nanotubes.

Another way to generate a very stiff concrete is to add nano Al_2O_3 . Li, Wang, He, Lu, & Wang (2006) show an increase of the Young's modulus of 143% after 28 days for a mixture of Portland cement with sand and nano-alumina (Li, Wang, He, Lu, & Wang, 2006). However, for concrete materials are no similar improvements of the stiffness found. Literature only shows improvement of the compressive strength and workability (Agarkar & Joshi, 2012), (Nazari & Riahi, Al_2O_3 nanoparticles in concrete and different curing media, 2011), improvement of splitting tensile strength, significant reduction of the water absorption (Nazari & Riahi, Al_2O_3 nanoparticles in concrete and different curing media, 2011) and a lower chloride permeability (Chen G. , 2012). In fact, this description of the improvement of strength and the reduced permeability is in line with the philosophy of HPC and UHPC. Since in literature is no further information found about the Young's modulus of concrete containing nano Al_2O_3 , concrete containing nano aluminium does not seem an interesting concrete to invest in this research, at the moment.

Densification: the last group of nano-particles is the group with nano-silicate and nanoclay that densify the concrete matrix which results in better strength and durability properties. In fact, this is also in line with the philosophy of HPC and UHPC; improvement of the durability and strength by densifying the matrix. Simply speaking, adding nano-silica or nanoclay to NSC, is just a method to create a HPC. If nano-silica is added to HPC, it may have the same properties as UHPC. If nano-silica is added to UHPC, it will probably result in a slightly stronger UHPC. Tests show an increase of 8% and 6.5% at 28 and 90 days respectively for UHPC with a mean 28 days compressive strength of 134 MPa (Ghafari, Costa, Júlio, Portugal, & Durães, 2014). Therefore, the most interesting research should be if nano-silica is added to UHPC to create maybe a next generation UHPC or at least a stronger UHPC. Because this group of nano concrete is not that special compared to UHPC, the densification group is left out of the scope.

Conclusion

In the end, concrete mixtures containing nano-titanium oxide and nano-iron seem to be the most interesting materials. These materials have unique **self-cleaning** or **self-sensing** capabilities. Further, these materials are researched relative good. Concrete containing nanotubes or nano aluminium are not researched well enough to include in this research. Concrete containing nano-silicate or nanoclay are not that innovative to include in this research.

2.2 Composition

In this chapter, compositions for all the ACMs are shown. The compositions shown are the most representative concrete mixtures for every ACM. The main objective of the table of compositions, Table 11, is to compare the different ACMs with each other in a quantitative way. For the application of an ACM in practice, the concrete mix will probably be a bit different from the compositions made here, such that the characteristics in practice could also be a bit different.

In the overview of compositions in Table 11, the first two rows give the general ACMs and the representative mix design per ACM. In the first column of the table all the ingredients to make the concrete mixtures are shown. Almost every ingredient is given in kg/m^3 , as shown in the third column. Further in the second column the average grain diameter are given. The ingredients, sort in different groups: binders, aggregate and additions, additives, water and fibres, are shown. Besides, the aggregate and additions are arranged from the coarsest to the finest particle. In the table is clearly shown that in stronger ACMs (HPC and UHPC) the maximum grain diameter is smaller.

After the table, the determination of the amount and kind of fibres is shown. From practical and ductility reasons, a maximum and minimum fibre content is determined. These limit values are also shown in Table 11.

Table 11 – Literature based overview of the compositions of the representative cementitious materials in this research

				Plain	ACM 1.	ACM 2.	ACM 3.	ACM 4.	ACM 5.	ACM 6.	ACM 7.	ACM 8.	ACM 9.
				NSC	NSSFRC	HPC	HPSFRC	UHPC	SHCC	Self-Healing	GPC	Self-cleaning	Self-Sensing
	Material	Grain diameter	Unit	C30/37 ⁱ	C30/37 ^k	C90/105 ^l	C90/105 ^k	C170/200 _m	C40/50 ⁿ	C30/37 ^k	C30/37 ^o	C55/67 ^{r,k}	C30/37 ^p
Binders	CEM I	5 – 50 μm	[kg/m ³]	320	320	501	501	710	414	320			539
	CEM II	5 – 50 μm	[kg/m ³]									432	
	BFS	5 – 50 μm	[kg/m ³]						496		40		
Aggregate and additions	Aggregate	0 – 15 mm	[kg/m ³]										1148
	Coarse aggregate	4 – 32 mm	[kg/m ³]	1280	1280					1280	1209		
	Coarse aggregate	4 – 12.5 mm	[kg/m ³]			866	866					578	
	Fine aggregate	0 – 4 mm	[kg/m ³]	640	640	867	867			640		1003	
	Sand	0 – 2 mm	[kg/m ³]					1020			651		
	Fine sand	0 – 0.5 mm	[kg/m ³]										492
	Microcapsules	40 – 800 μm^q	[V%]							3			
	Crushed limestone	0 – 300 μm	[kg/m ³]										177
	Quartz powder	5 – 45 μm	[kg/m ³]					210					
	Limestone powder	5 – 20 μm	[kg/m ³]						827				
	Fly ash	0.2 – 40 μm	[kg/m ³]								360		
	Silica Fume	< 1 μm	[kg/m ³]					230					
	Nano titanium oxide	20 \pm 5 nm ^r	[kg/m ³]										18 ^r
	Nano iron oxide	15 \pm 3 nm ^p	[kg/m ³]										
Additives	Sodium hydroxide	–	[kg/m ³]								45.7		
	Sodium silicate	–	[kg/m ³]								114.3		
	Super-plasticizer	–	[kg/m ³]			8.5	8.5	13	7			2.5	
	Viscosity Modifying Agent (VMA)	–	[kg/m ³]									2	
Water	Water	–	[kg/m ³]	160	160	160	160	140	455	160		171	220
	Water/cement ratio	–	[–]	0.50	0.50	0.32	0.32	0.20	0.50	0.50		0.38	0.40
Fibres	PVA	$d = 40 \mu m, l = 8 mm$	[V%]						$\leq 2\%$ ^s				
	Steel Fibres (long)	$l = 60 mm^k$	[kg/m ³]		40-50 ^k								
	Steel Fibres (medium)	$l = 25 – 50 mm^k$	[kg/m ³]				70-85 ^k						
	Steel Fibres (short)	$l = 4 – 8 mm^k$	[kg/m ³]					100-160 ^k					

ⁱ (ENCI, 2008)

^k Assumptions done or some more details described in rest of the paragraph

^l (Chen & Su, 2013)

^m (Paskvalin, 2015)

ⁿ (Qian, et al., 2009)

^o (Deb, Nath, & Sarker, 2014)

^p (Nazari, Riahi, Riahi, Shamekhi, & Khademno, The effects of incorporation Fe2O3 nanoparticles on tensile and flexural strength of concrete, 2010)

^q (Pelletier, Brown, Shukla, & Bose, n.d.)

^r (Jalal, Ramezaniapourl, & Pool, Split tensile strength of binary blended self compacting concrete containing low volume fly ash and TiO2 nanoparticles, 2013)

^s (Li V. C., Engineered Cementitious Composites (ECC) – Material, Structural, and Durability Performance, 2007)

Fibre reinforce concrete: practice and ductility

The compositions of fibre reinforce concrete are assumed to be the same as for concretes without fibres, but with the addition of fibres. The amount of fibres is determined from practical and ductility reasons. Practical reasons result in a maximum amount of fibres and ductility requires a minimum amount of fibres. Here is first estimated that no further tensile reinforcement is required to achieve the ductile behaviour of concrete. First the maximum amount of fibres will be determined and then the minimum amount.

Maximum amount of fibres

The maximum amount of fibres depends on the length and the diameter of the fibres. The length of the fibres depends on the diameter of the largest particle. Here, first the relation between the fibre length and the diameter of the largest particle is given. After that, the relation between the maximum amount of fibre and the ratio between the fibre length and the fibre diameter is shown, as a function of the maximum grain diameter.

Test results suggest that fibres which are shorter than the diameter of the maximum aggregate particles have little reinforcing effectiveness. Consequently, fibres in a concrete matrix are longer than fibres in a cement matrix (Johnston, 1996). This idea is schematically shown in Figure 8. Usually, the fibre length is 2-4 times the diameter of the maximum aggregate size (Grünewald, 2004). The minimum and maximum fibre lengths for mixtures with a certain maximum aggregate particle according to the rule of thumb from Grünewald (2004) are shown in Table 12.

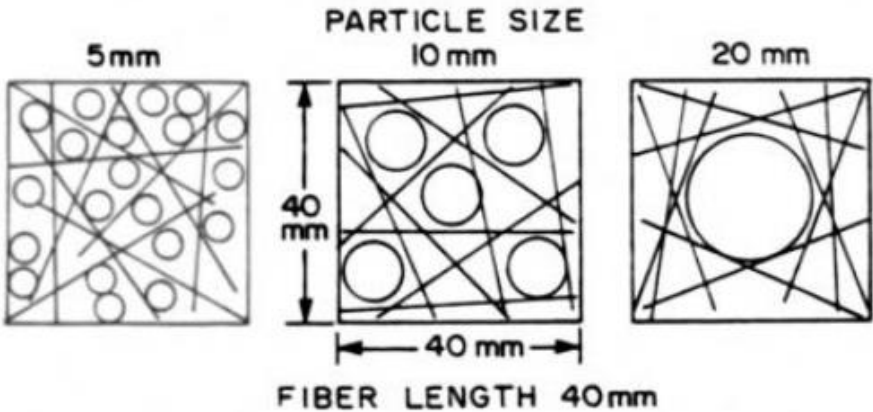


Figure 8 - Schematic of the effect of aggregate size on fibre arrangement in the concrete matrix (Johnston, 1996)

According to Table 12, the maximum fibre length is equal to 128 mm, assuming that the maximum grain diameter is equal to 64 mm. However, manufacturers make standard fibres with a maximum length of 60 mm only (ArcelorMittal Wire International , n.d.), (Chircu Prod - Impex Company SRL, 2009). It is assumed that the length of steel fibres is in the range of 4 – 60 mm for aggregate with a maximum particle in the range of 2 – 32 mm.

Table 12 - Minimum and maximum fibre length after Grünewald (2004)

Maximum aggregate particle [mm]	Minimum fibre length [mm]	Maximum fibre length [mm]
32	64	128
16	32	64
12,5	25	50
8	16	32
4	8	16

2	4	8
1	2	4

The other geometrical variable of fibres is the diameter. Depending on the ratio between the length and the diameter of the fibre, a certain maximum fibre content can be determined from reasons of workability. As shown in Table 13, for different length over diameter ratios and different maximum aggregate particles, the maximum fibre content is determined (Kooiman, 1996). These maximum contents are assumed to be the upper limit for the fibre content for fibre reinforced concrete. So for NSSFRC, where the maximum diameter of the aggregate is equal to 32 mm, the maximum amount of steel fibres is equal to 50 kg/m³ (orange rectangle in Table 13). To be on the safe site, the maximum amount of fibres in HPSFRC is 85 kg/m³, since the maximum particle size, which is 12 mm, is between 8 and 16 mm (blue rectangle in Table 13). The maximum amount of steel fibres for UHPC with a maximum particle diameter of 2 mm is not given in the table. As a first estimation, the maximum amount of fibres in UHPC is taken to be equal to 160 kg/m³, which is the maximum value for a mixture with maximum particles of 4 mm. Probably, the maximum fibre content for UHPC is even higher than 160 kg/m³. The minimum amount of fibres is taken as 100 kg/m³. This is the amount of fibres that is chosen in the mixture of Paskvalin (2015). Probably, the minimum amount of fibres can be taken some lower. For an optimised amount of fibres, further research should be done.

Table 13 - Maximum content of steel fibres in concrete (Grünewald (2004) after Kooiman (1996))

L_f/d_f	60	75	100
$d_{g,max}$	Normal (Pumping)	Normal (Pumping)	Normal (Pumping)
[mm]	[kg/m ³]	[kg/m ³]	[kg/m ³]
4	160 (120)	125 (95)	95 (70)
8	125 (95)	100 (75)	75 (55)
16	85 (65)	70 (55)	55 (40)
32	50 (40)	40 (30)	30 (25)

Minimum amount of fibres

To have a ductile concrete construction, the reinforcement steel should only yield if the concrete is cracked. So when a crack arise and the steel takes over the concrete tensile stress completely, the steel still has a certain deformation capacity before it fails. The concrete should be cracked before the steel yields, so the steel force during yielding should be larger than the concrete cracking force as shown in eq.(1). As an illustration, in Figure 9 a beam is shown with a reinforcement bar loaded in tension.

$$\begin{aligned}
 N_s &> N_{c,cr} \\
 A_s \cdot f_{yd} &> A_c \cdot f_{ctm} \\
 \frac{A_s}{A_c} &> \frac{f_{ctm}}{f_{yd}}
 \end{aligned}
 \tag{eq.(1)}$$

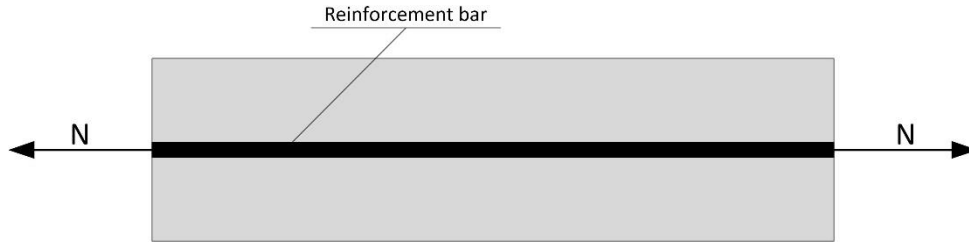


Figure 9 - Concrete beam with reinforcement bar loaded in tension on two sides

The same trick could be done for a beam reinforced with fibres only, as shown in Figure 10. Because the fibres are randomly distributed, the strength of the fibres should be divided by a factor K . This factor is used in the calculation according to AFGC's Scientific and Technical Committee (2013).

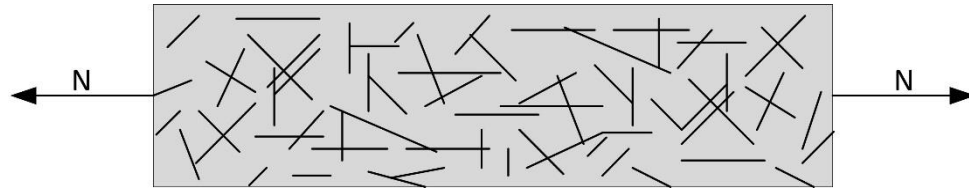


Figure 10 - Concrete beam with fibres bar loaded in tension on two sides

The equation that can be made here is:

$$N_{s,f} > N_c$$

$$\frac{1}{K} \cdot A_{s,f} \cdot f_{yd} > A_c \cdot f_{ctm} \rightarrow \frac{A_{s,f}}{A_c} > \frac{f_{ctm}}{f_{yd}} \cdot K \quad \text{eq.(2)}$$

Where, $K = 1.25$ (fibre orientation factor from the French recommendations for UHPC (AFGC's Scientific and Technical Committee, 2013))

Assuming a high strength steel type, S690, the minimum amount of steel fibres to achieve a ductile behaviour of the concrete is 41 kg/m^3 and 71 kg/m^3 for NSC and HPC respectively, as shown in eq. (3) and (4). In literature, similar steel strength classes are applied for steel fibres in concrete (Holschemacher & Müller, (n.d)).

$$\left. \begin{aligned} \left(\frac{A_{s,f}}{A_c}\right)_{NSC} &> \frac{f_{ctm}}{f_{yd}} \cdot K = \frac{2.9}{690} \cdot 1.25 = 0.53\% \\ \left(\frac{A_{s,f}}{A_c}\right)_{NSC} &= \frac{A_{s,f} \cdot b \cdot \rho_{steel}}{A_c \cdot b \cdot \rho_{steel}} = \frac{M_{steel}}{A_c \cdot b \cdot \rho_{steel}} = \frac{M_{steel}}{1 \cdot 1 \cdot 7800} \end{aligned} \right\} M_{steel} = 41 \text{ kg/m}^3 \quad \text{eq.(3)}$$

$$\left. \begin{aligned} \left(\frac{A_{s,f}}{A_c}\right)_{HPC} &> \frac{f_{ctm}}{f_{yd}} \cdot K = \frac{5.0}{690} \cdot 1.25 = 0.91\% \\ \left(\frac{A_{s,f}}{A_c}\right)_{HPC} &= \frac{A_{s,f} \cdot b \cdot \rho_{steel}}{A_c \cdot b \cdot \rho_{steel}} = \frac{M_{steel}}{A_c \cdot b \cdot \rho_{steel}} = \frac{M_{steel}}{1 \cdot 1 \cdot 7800} \end{aligned} \right\} M_{steel} = 71 \text{ kg/m}^3 \quad \text{eq.(4)}$$

In Eurocode are different classes given for the ductility of steel. These classes depends on the ratio between the tensile strength and yield strength. The three different classes are shown in eq.(5).

$$\frac{f_t}{f_y} \left\{ \begin{array}{ll} \geq 1.05 & \text{Class A} \\ \geq 1.08 & \text{Class B} \\ \geq 1.15 \text{ and } < 1.35 & \text{Class C} \end{array} \right. \quad \text{eq.(5)}$$

For S690, this ratio is equal to $\frac{770}{690} = 1.12$, so the fibres should be ductile according to class A and B. Here is estimated that the ductility formula from EC2 can also be applied for steel fibres.

Self-healing concrete

In chapter 2.1.6 Self-Healing Cementitious Materials is already shown the reasons to apply 3 V. %. Here is assumed that the self-healing agent could be added to NSC to give the self-healing character to concrete. In principle, a self-healing agent works in every composition. Depending on the crack-width, the self-healing agent has a certain effectiveness.

Self-cleaning concrete

As shown in Table 11, the representative self-cleaning concrete (C55/67) is much stronger than the one of NSC (C30/37). This is done because in literature no proper information is found about a self-cleaning concrete in the concrete class C30/37. The disadvantage of the higher strength class for self-cleaning concrete, is that it can not be compared to NSC in a proper way. This makes it hard to show the influence of the addition of nano titanium oxide properly. This is discussed in more detail in chapter 2.3 Mechanical characteristics

2.3 Mechanical characteristics

In this chapter the mechanical characteristics are given for the representative ACMs, as defined in chapter 2.1 Scope of Advanced Cementitious Materials and chapter 2.2 Composition. First an overview of the most important mechanical characteristics are given per ACM. After that some characteristics are explained in more detail. At last, also the creep and shrinkage behaviours per ACM is given. These are not included in the overview table, because not all ACMs can be determined quantitatively.

An overview of the most important mechanical characteristics is shown in Table 14. In the first two rows the representative ACMs are shown. The researched mechanical characteristics with the unity per characteristic are given in the first columns of the table. Under every ACM the values are given for the different material properties.

The mechanical properties of C30/37 (NSC) and C90/105 (HPC) are given in Eurocode 2. Most of the properties given in this chapter can be found in Eurocode 2 - table 3.1 (Nederlands Normalisatie-instituut, 2011). The mechanical characteristics of Self-Healing concrete are assumed to be equal to the mechanical characteristics of NSC according to Eurocode 2, as shown in the table below.

The mechanical characteristics of SHCC are already researched by (Qian, et al., 2009). His result will be used to describe the mechanical properties of SHCC. As mentioned in chapter 2.1.8 NANO Concrete, a self-cleaning concrete with the same mechanical characteristics is assumed as a representative self-cleaning concrete. The characteristics of the other cementitious materials are determined will be described in some more detail after the overview of Table 14.

In Table 14 are some value marked. These marked values are extreme values compared to C30/37. In green are the value which are significant larger, or for the cracking pattern more favourable, compared to C30/37. In orange are the values that are slightly lower compared to C30/37. In red are the values that are significant compared to C30/37.

Table 14 – Mechanical characteristic of the Advanced Cementitious Materials, based on Eurocode 2, Ultra High Performance Fibre-Reinforced Concretes Recommendations, Recommendations for Design and Construction of High Performance Fiber Reinforced Cement Composites with Multiple Fine Cracks (HPFRCC) and other literature.

			Plain	ACM 1.	ACM 2.	ACM 3.	ACM 4.	ACM 5.	ACM 6.	ACM 7.	ACM 8.	ACM 9.	
ACMs →			NSC	NSSFRC	HPC	HPSFRC	UHPC	SHCC	Self-Healing	GPC	Self-cleaning concrete	Self-sensing concrete	
Concrete characteristics ↓			C30/37 ^t	C30/37	C90/105 ^t	C90/105	C170/200 ^u	C40/50 ^v	C30/37	C30/37 ^w	C55/67 ^z	C30/37 ^z	
Strength	Characteristic compressive strength	f_{ck}	[MPa]	30	30	90	90	170	41	30	32	55	30.9
	Design value compressive strength	f_{cd}	[MPa]	20	20	60	60	96.3	26.8	20	21.3	37	20.6
	Mean axial tensile strength	f_{ctm}	[MPa]	2.9	2.9	5	5	12.9	5	2.9	2.1	4.9 ^x	1.7
	Characteristic axial tensile strength	$f_{ctk,0.05}$	[MPa]	2.0	2.0	3.5	3.5	9.0	-	2.0	1.5	3.4	1.2
	Design value axial tensile strength	f_{ctd}	[MPa]	1.4	1.4	2.3	2.3	6.0	3.4	1.4	1.0	2.3	0.8
	Characteristic elastic tensile strength	$f_{ctk,1}$	[MPa]	-	-	-	-	-	4.0	-	-	-	-
	Characteristic plastic tensile strength	$f_{ctk,2}$	[MPa]	-	-	-	-	-	4.4	-	-	-	-
	Fibre design tensile strength	f_{ctfd} or f_{vd}	[MPa]	-	-	-	-	6.9	3.4	-	-	-	-
Shear strength compared to NSC	V_{ACMx}/V_{NSC}	[-]	1.0	1.3-2.3 ^y	1.4	1.8-3.2 ^y	15	6	1.0	-	-	-	
Stiff	Mean Young's modulus	E_{cm}	[GPa]	33	33	44	44	50	18.5	33	23	+ ^z	-
	Effective Young's modulus	$E_{cd,eff}$	[GPa]	11	11	14.7	14.7	16.7	7.7	11	-	-	-
Strain	Maximum linear compressive strain	ϵ_{c3}	[%]	0.175	0.175	0.23	0.23	0.23	-	0.175	-	-	-
	Maximum compressive strain	ϵ_{cu3}	[%]	0.35	0.35	0.26	0.26	0.27	0.30	0.35	-	-	-
	Maximum mean compressive strain	ϵ_{cm}	[%]	-	-	-	-	-	-	-	0.24	-	-
	Maximum linear tensile strain	ϵ_{ct1}	[%]	0.01	0.01	0.01	0.01	0.014	0.178	0.01	-	-	-
	Maximum tensile softening strain	$\epsilon_{lim,soft}$	[%]	-	§	-	§	§	-	-	-	-	-
	Maximum tensile hardening strain	$\epsilon_{lim,harden}$	[%]	-	-	-	-	≤0.25	1.73	-	-	-	-
Crack pattern (tensile test)	-	-	One discrete crack*	< 2.5 mm if ϵ_{Fu} (ultimate tensile strain) = 1% ^{aa}	One discrete crack*	< 2.5 mm if ϵ_{Fu} (ultimate tensile strain) = 1% ^{aa}	0.039 mm at surface for $\epsilon_{sm,f} - \epsilon_{cm,f} = 0.36\text{‰}$	<0.1 mm for every strain ^{bb}	One discrete crack*	One discrete crack*	-	-	

- = unknown of N/A

§ No general known limit values. For example, the maximum tensile strain in softening behaviour for UHPC depends on the height of the construction and the fibre length (AFGC's Scientific and Technical Committee, 2013).

* In general, NSC has a brittle crack behaviour if it is not reinforced. As soon as a crack arises, the crack becomes a through crack directly. For instance, if a small crack generates, the tensile force should be carried by a smaller cross section, so the stress increases a lot such that the total cross section fails. It is assumed that the influence of the microcapsules on the crack behaviour can be neglected. If concrete cracks the capsules should break open, so they should be quite brittle. Then the healing agent can be activated and the concrete can be healed. If the capsules would not fail brittle, the situation could be that the concrete cracks and the capsules remain uncracked. Geopolymer Concrete is like other cementitious

composites brittle, with a low tensile strength and strain capacity (Ng, Htut, & Foster, 2010)

^t (Nederlands Normalisatie-instituut, 2011)

^u (AFGC's Scientific and Technical Committee, 2013)

^v (Qian, et al., 2009), (Japan Society of Civil Engineers, 2008)

^w (Shaikh, 2013), (Olivia & Nikraz, Properties of fly ash geopolymer concrete designed by Taguchi method, 2012), (Ryu, Lee, Koh, & Chung, 2013), (Hardjito, 2005), (Aldred J. M., 2013)

^x (Jalal, Ramezaniapour, & Pool, Split tensile strength of binary blended self compacting concrete containing low volume fly ash and TiO2 nanoparticles, 2013)

^y Depending on the fibres, further discussed in chapter 2.3.6.2 Shear resistance of fibre reinforced concrete

^z Assumptions done, further discussed in the rest of the chapter

^{aa} (fib Bulletin 55, 2010)

^{bb} (Li V. C., Engineered Cementitious Composites (ECC) – Material, Structural, and Durability Performance, 2007)

2.3.1 Fibre Reinforced Concrete

From a mechanical point of view, the FRC differs from NSC if it is cracked only. Therefore, the mechanical behaviour of NSFRC and HFRCPC are assumed to be similar to NSC and HPC respectively. Since the crack pattern and strain behaviour after cracking for both materials is different, the cracking behaviour of FRC will be described in some detail here. In Model Code 2010 are the next mechanical characteristic of FRC that are different from NSC (fib Bulletin 55, 2010):

- Post-cracking residual strength
- Crack spacing and crack width
- Tensile strain hardening or softening behaviour of FRC in the cracking stage, depending on their composition

The post-cracking residual strength and tensile strain hardening or softening behaviour in the cracking stage is shown in the graphs of Figure 11. In

Figure 11, at the left is shown the strain softening behaviour of FRC in tension. As shown in the graph, after the first crack, the concrete strength decreases if the deformation increases. However, where unreinforced NSC has no strength after the first crack, FRC has still a certain strength as shown in the graph. The right graph shows the hardening behaviour of FRC. Here the strength of the concrete still increases after the first crack is formed until a certain maximum. As soon as crack localization occurs, the strength of the FRC decreases with an increasing deformation.

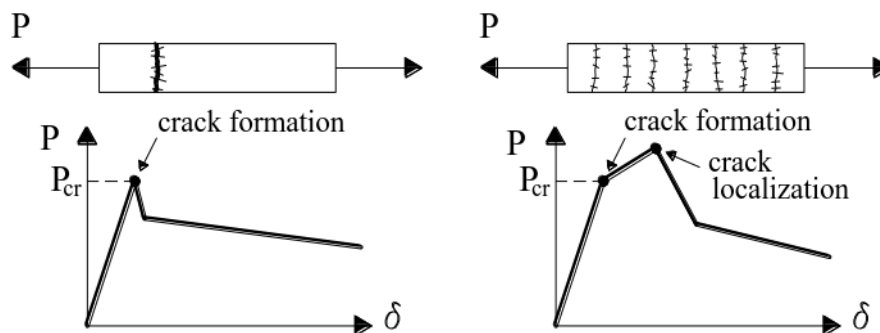


Figure 11 - Tensile softening (left) and hardening (right) behaviour of FRC (fib Bulletin 55, 2010)

The strain of FRC under tension is discussed in some more detail here. Some assumptions are done here to get an order of strain of FRC. The first tensile crack in FRC concrete will probably arise around the same strain as for NSC, $\varepsilon_{ct1} = 0.01\%$. In fact, fibres has no or at least a neglectable influence if the concrete is not cracked. According to the same thought as for NSFRC, the first crack in HPSFRC arise at the same strain as for HPC, $\varepsilon_{ct1} = 0.01\%$. So the maximum elastic strain for both fibre reinforced concretes is assumed to be $\varepsilon_{ct1} = 0.01\%$.

To make an assumption for the maximum tensile strain of FRC, a comparison with UHPC is made. The tensile strength of UHPC is higher than the tensile strength of HPC and NSC, while the elastic strains of these concretes have similar value. Assuming a similar softening behaviour of these three types of concrete, the ultimate tensile strain of UHPC will be larger than the ultimate tensile strain of HPSFRC and the ultimate tensile strain of HPSFRC will be larger than the ultimate tensile strain of NSFRC. This idea is shown in the graph of Figure 12. The ultimate tensile strain of UHPC can be determined by the fibre length and the construction height, as explained in chapter 2.3.2 UHPC, C170/200. As an indication, if the fibre length is equal to 6.0 mm and the construction height 500 mm , the ultimate strain in tension for UHPC with a softening behaviour is equal to $\varepsilon_{lim} = 0.45\%$. The same construction made of HPSFRC and NSFRC then will probably be in the order of 0.1% and 0.3% .

Stress-strain diagram for FRC with strain softening behaviour

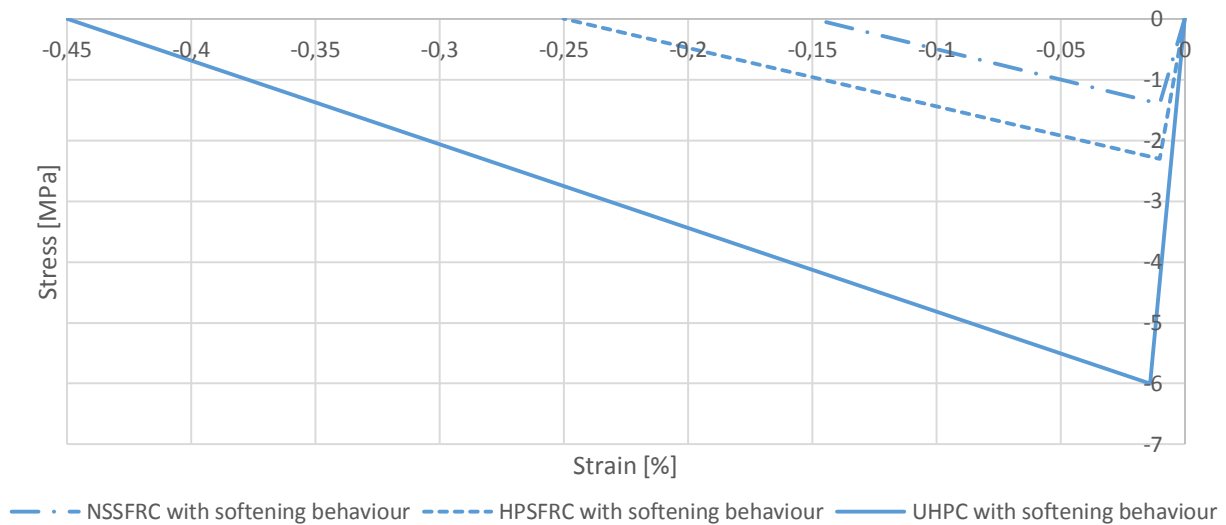


Figure 12 - Stress-strain diagram for FRC with strain softening behaviour

In a similar way, the maximum tensile strain in strain hardening behaviour could be determined. For UHPC, the limited tensile strain is assumed to be 0.25‰ if the concrete has a strain hardening behaviour as explained in chapter 2.3.2 UHPC, C170/200. The maximum tensile strain for NSSFRC and HPSFRC then will probably be in the order of 0.1% to 0.25%.

After the cracking, the fibres also influence the strain behaviour in compression, as shown in Figure 13 where the compressive strength of concrete is shown as a function of the strain. It is clearly shown that FRC (blue line) has a more ductile behaviour in compression compared to plain concrete (red line). Further, the dotted blue line shows that an increase of the fibre volume, increases the ductility of concrete.

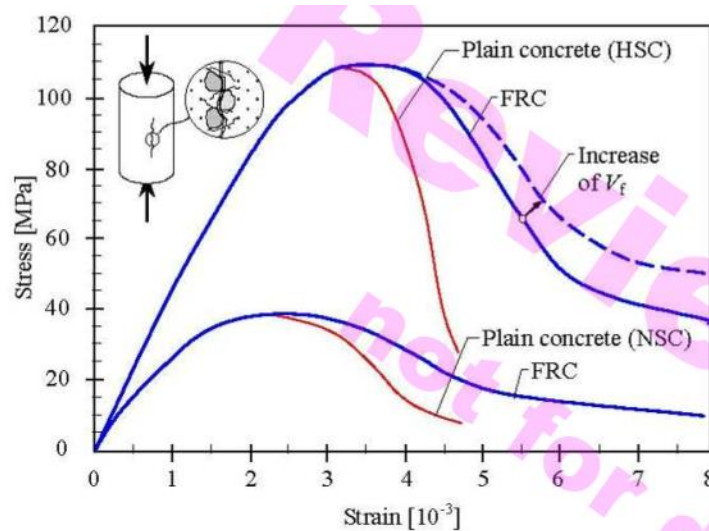


Figure 13 - Strain behaviour of FRC loaded in compression compared to plain concrete (fib Bulletin 55, 2010)

Since one of the most important parameter of FRC seems to be the crack width, some information about the crack width should be known. The Model Code gives some rules to calculate the ultimate crack width, as shown in eq.(6).

$$w_u = l_{cs} \cdot \varepsilon_{Fu} \quad \text{eq.(6)}$$

Where,

l_{cs} is the characteristic length = $\min\{s_{rm}, y\}$

Where,

- s_{rm} is the mean distance value between cracks
- y is the distance between neutral axis and tensile side of the cross section, evaluated in the elastic cracked phase assuming no tensile strength of the fibre reinforced concrete, and for a load configuration corresponding to the serviceability state of crack opening and crack spacing.

ε_{Fu} is the ultimate strain of the fibre

By assuming $\varepsilon_{Fu} = 2\%$ for variable strain distribution along the cross section and $\varepsilon_{Fu} = 1\%$ if only tensile strain is distributed along the cross section, the maximum crack width may not exceed 2.5 mm (fib Bulletin 55, 2010).

2.3.2 UHPC, C170/200

Some design rules for the mechanical behaviour of C170/200 are given in recommendations from the AFGC's Scientific and Technical Committee (2013). Interesting to explain in more detail is the stress-strain relation for UHPC, which will be done in this chapter.

In Figure 14 and Figure 15 are shown the stress-strain relations of UHPC in compression and tension respectively. Under the figures are given values for different strains. The stress-strain relation in compression (Figure 14) is given for SLS and ULS. These relations are quite similar to the compressive stress-strain relation that is in Eurocode 2.

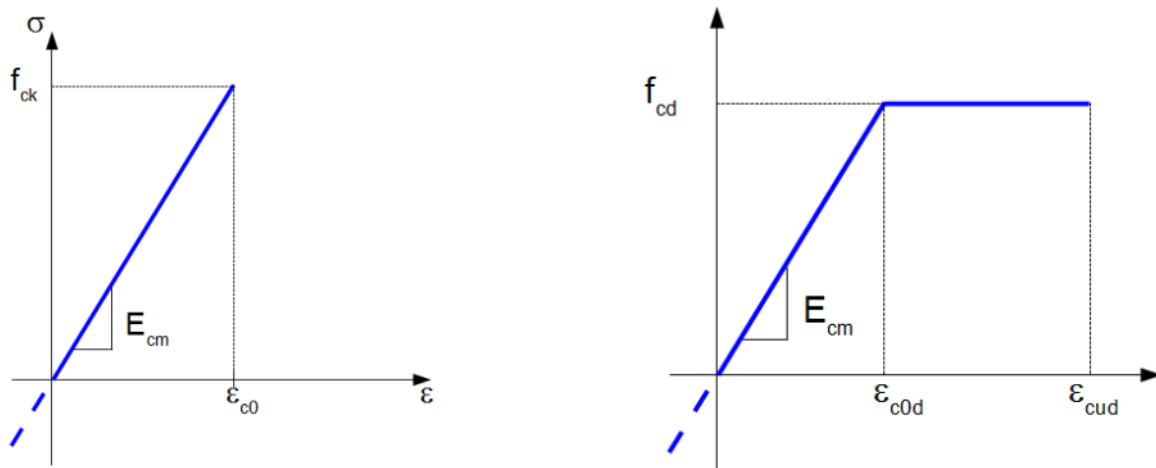


Figure 14 - Stress-strain relations for UHPC in SLS (left) and ULS (right)

SLS

$$\varepsilon_{c0} = \frac{f_{ck}}{E_{cm}} = \frac{170}{50000} = 3.4\text{‰}$$

ULS

$$\varepsilon_{c0d} = \frac{f_{cd}}{E_{cm}} = \frac{96.3}{50000} = 2.3\text{‰}$$

$$\varepsilon_{cud} = 2.7\text{‰} \text{ (recommended value (AFGC's Scientific and Technical Committee, 2013))}$$

In Figure 15 are shown the stress-strain relations for UHPC in tension with a tensile strain softening and hardening behaviour respectively. This behaviour mainly depends on the fibres in the concrete. Under both figures are shown the calculated values for the strains. These strains are calculated according to AFGC's Scientific and Technical Committee (2013). Some values depends on the dimensions of the construction. These dimensions are unknown, since this is just a general description.

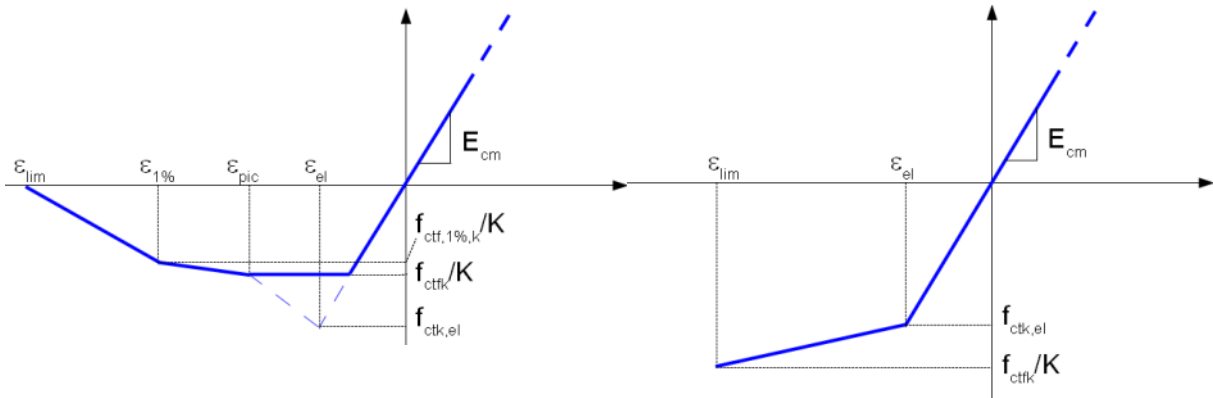


Figure 15 - Stress-strain relations for UHPC with strain softening (left) and strain hardening (right) behaviour with values in SLS

SLS

$$\varepsilon_{el} = \frac{f_{ctk,el}}{E_{cm}} = \frac{9}{50000} = 0.18\text{‰}$$

ULS

$$\varepsilon_{u,el} = \frac{f_{ctk,el}}{\gamma_{cf} E_{cm}} = \frac{9}{1.3 \cdot 50000} = 0.14\text{‰}$$

Strain softening behaviour

$$\varepsilon_{peak} = \frac{w_{peak}}{l_c} + \frac{f_{ctk,el}}{E_{c,eff}} \qquad \varepsilon_{u,peak} = \frac{w_{peak}}{l_c} + \frac{f_{ctk,el}}{\gamma_{cf} E_{c,eff}}$$

$$\varepsilon_{1\%} = \frac{w_{1\%}}{l_c} + \frac{f_{ctk,el}}{E_{c,eff}} = \frac{0.01H}{\frac{2}{3}h} + \frac{9}{16700} \qquad \varepsilon_{u,1\%} = \frac{w_{1\%}}{l_c} + \frac{f_{ctk,el}}{\gamma_{cf} E_{c,eff}} = \frac{0.01H}{\frac{2}{3}h} + \frac{9}{1.3 \cdot 16700}$$

Strain softening behaviour

$$\varepsilon_{lim} = \varepsilon_{u,lim} = \frac{l_f}{4l_c} = \frac{l_f}{4 \cdot \left(\frac{2}{3}h\right)}$$

So for example if assumed; $l_f = 6.0 \text{ mm}$; $h = 500 \text{ mm}$, then $\varepsilon_{lim} = 0.45\text{‰}$

Strain hardening behaviour

$$\varepsilon_{lim} = \varepsilon_{u,lim} \leq 2.5\text{‰}, \text{ except if characterisation was carried out using direct tensile tests}$$

2.3.3 GPC

Geopolymer concrete is a relative new concrete. In Europe no standards or recommendations for this kind of concrete are present. In Australia some recommendations are given (Geopolymer Alliance,

n.d.), however these are not open for access. Therefore the mechanical properties of GPC are determined according literature. The properties determined in this chapter are:

- Compressive strength
- Tensile strength
- Young's modulus
- Stress-strain relation in compression

Van Jaarsveld et al. (2003) shows that particle size, calcium content, alkali metal content, amorphous content as well as morphology and origin of the fly ash can greatly affect the properties that have impact on both the initial synthesis mix as well as the final product (Jaarsveld, Deventer, & Lukey, 2003). For this reason the mechanical characteristics for geopolymer concretes with the same compositions, can show different mechanical behaviour. Therefore, it seems hard to describe general properties for GPC. In practice, the fly ash should always be tested before it is applied, to determine the real properties of the mixture. This tests are also done for ordinary Portland concrete, but for fly ash based geopolymer concrete, the difference between different kinds of fly-ash seems to have more impact on the concrete than differences in Portland cement.

Compressive strength

In general, GPC exhibits higher compressive strength than OPC concrete (Shaikh, 2013). Other research compared the compressive strength of fly ash geopolymer concrete with ordinary Portland cement concrete over time. Results show that the Portland concrete has compared to geopolymer concrete a lower compressive strength after 7 days hydration, but a higher compressive strength after 91 days (Olivia & Nikraz, Properties of fly ash geopolymer concrete designed by Taguchi method, 2012).

In this research a composition is assumed where the mean compressive strength is equal to 40 MPa. Assuming that the standard deviation of GPC is similar to standard deviation of NSC. This makes the characteristic concrete compressive strength equal to $40 - 8 = 32 \text{ MPa}$. This compressive strength is slightly higher than the compressive strength of C30/37. From practical reasons this slightly stronger mixture is chosen for the composition of the mixture.

Tensile strength

The tensile strength of GPC can be expressed by a simple model. Numerous researchers have proposed empirical formula in the form of eq.(7) to express the relationship between the compressive strength and the splitting tensile strength (Ryu, Lee, Koh, & Chung, 2013).

$$f_{sp} = k(f'_c)^n \quad \text{eq.(7)}$$

Different constants for k and n are obtained by analysis of experimental data. Some of them are shown in Figure 16. As shown in the figure, most models overestimate the tensile strength of GPC. The red line is a model for GPC according to the formula of eq.(8), with $k = 0.17$ and $n = 3/4$. The total formula is shown in eq(8). The formula is based on experimental results from geopolymer concrete. (Ryu, Lee, Koh, & Chung, 2013).

$$\left. \begin{array}{l} f_{sp} = 0.17(f'_c)^{3/4} \quad [Ryu, Lee, Koh, \& Chung, 2013] \\ f_{ct} = 0.9f_{ct,sp} \quad [Eurocode 2] \end{array} \right\} \rightarrow f_{ct} = 0.159(f_{ck})^{3/4} \quad \text{eq.(8)}$$

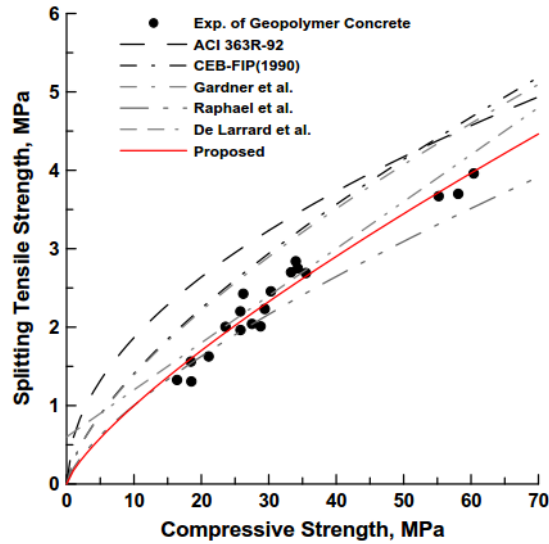


Figure 16 – Different models describing the relationship between splitting tensile strength and the compressive strength (Ryu, Lee, Koh, & Chung, 2013)

Assuming that this model is in general representative for GPC, the tensile strength of geopolymer concrete is some lower compared to NSC with the same compressive strength. For a character compressive strength of 32 MPa, the mean tensile strength can be expressed as shown in eq.(9)

$$f_{ctm} = 0.159(32)^{3/4} = 2.1 \text{ MPa} \quad \text{eq.(9)}$$

Assuming the geopolymer has a similar standard deviation, the characteristic tensile strength for geopolymer concrete can be calculated in the same ways as for NSC as described in Eurocode 2. Since both materials are made from natural resources, this assumption is probably good enough as a first estimation.

$$f_{ctk,0.05} = 0.7 \cdot f_{ctm} = 1.5 \text{ MPa} \quad \text{eq.(10)}$$

Other research shows a similar splitting tensile strength for both fly ash based GPC and OPC, for mixtures with similar compressive strengths. This was valid after 28 and 91 days (Olivia & Nikraz, Properties of fly ash geopolymer concrete designed by Taguchi method, 2012). Maybe the reduction of the concrete tensile strength is a bit conservative, but at least at the safe side.

Young's modulus

Olivia and Nikraz concluded in their research that the Young's modulus for fly ash geopolymer concrete is lower than for OPC (Olivia & Nikraz, Properties of fly ash geopolymer concrete designed by Taguchi method, 2012). This is in line with the test results of the Young's modulus of geopolymer concrete by Hardjito (2005). These test results are shown in the second column of Table 15. In the first column of the same table the strength of the different test specimens is shown. In the third column the values of the Young's modulus for the different concrete specimens, calculated by the equation of the Eurocode 2: 3.1.3 Tabel 3.1 are given. This formula is shown in eq.(11). In the fourth column is given the difference between the measured and the calculated values of the Young's modulus for different

strength classes. As shown in the table is the difference between both values about 30%, independent of the compressive strength.

$$E_{cm} = 22 \left[\frac{f_{cm}}{10} \right]^{0.3} \quad \text{eq.(11)}$$

Table 15 - Measured Young's modulus from tests compared to the calculated Young's modulus according to Eurocode 2

f_{cm}^{29}	E_c measured ²⁹	E_{cm} by EC2	Difference
89	30.8	42	27%
68	27.3	39	30%
55	26.1	37	29%
44	23.0	34	33%

As shown in the table, the equation used to calculate the modulus of elasticity for ordinary concrete does overestimate the measured values for the modulus of elasticity of geopolymer concrete for different strength classes. As shown in the fourth column, the real modulus of elasticity of geopolymer concrete is about 70% of the calculated modulus of elasticity according to EC2. As a first estimation, it is assumed that the modulus of elasticity for geopolymer concrete can be calculated by reducing the expression from Eurocode 2 by 70%, as shown in eq.(12).

$$E_{cm} = 15.4 \left[\frac{f_{cm}}{10} \right]^{0.3} \quad \text{eq.(12)}$$

Aldred did some research on ERC Grade 40 geopolymer concrete, which is used in floor panels in 2012. In his research he concluded that the modulus of elasticity is comparable to Portland cement based concretes, unlike some other geopolymer concrete (Aldred J. M., 2013). The composition of this concrete is unknown from economic reasons of the fabricant, so it is hard to explain the different conclusions.

In the end, the reduced, and maybe a bit conservative, modulus of elasticity is chosen as material characteristic for GPC. Probably a lot of geopolymer concretes have a Young's modulus equal or higher than this assumed Young's modulus. It should be noticed that as soon as the low Young's modulus is a problem in a practical case, some more research should be done to a GPC composition which has the desired modulus of elasticity. Also for some optimisation in the design, some more research could be desirable.

Strain in compression

Collins et al proposed in 1993 that the stress-strain relation of Portland concrete in compression can be predicted using the following formula (Hardjito, 2005):

$$\sigma_c = f_{cm} \frac{\varepsilon_c}{\varepsilon_{cm}} \frac{n}{n - 1 + \left(\frac{\varepsilon_c}{\varepsilon_{cm}} \right)^{nk}} \quad \text{eq.(13)}$$

Where,

$$f_{cm} = \text{peak stress}$$

²⁹ (Hardjito, 2005)

$\varepsilon_{cm} = \text{strain at peak stress}$

$$n = 0.8 + \frac{f_{cm}}{17}$$

$$k = \begin{cases} 0.67 + \frac{f_{cm}}{62} & \text{for } \frac{\varepsilon_c}{\varepsilon_{cm}} > 1 \\ 1 & \text{for } \frac{\varepsilon_c}{\varepsilon_{cm}} < 1 \end{cases}$$

Hardjito (2005) applied this expression to describe the stress-strain relation of geopolymer concrete and the formula seems to be valid for geopolymer concrete as well. In the same rapport Hardjito measured that the strain at the peak stress, ε_{c1} , for a similar geopolymer based on fly-ash is equal to 2.4‰. It is assumed that this peak strain is representative for this research, because it has a similar compressive strength as the representative GPC of this research. Knowing the mean compressive stress of the concrete, $f_{cm} = 40 \text{ MPa}$, the stress-strain relation can be determined according to eq.(13) as shown in the graph of Figure 17.

In the diagram of Figure 17 also the graphs are given for $\varepsilon_{c,max} = 2.2‰$ and $\varepsilon_{c,max} = 2.6‰$. As shown in the figure, the different peak strains do not make much difference in the stress-strain relation, especially in the elastic zone. So the assumed 2.4‰ peak strain probably results in a quite good representative stress-strain relation. The shape of the stress-strain curve shown in Figure 17 is comparable to the stress-strain relation of the researched ERF geopolymer (Aldred J. M., 2013).

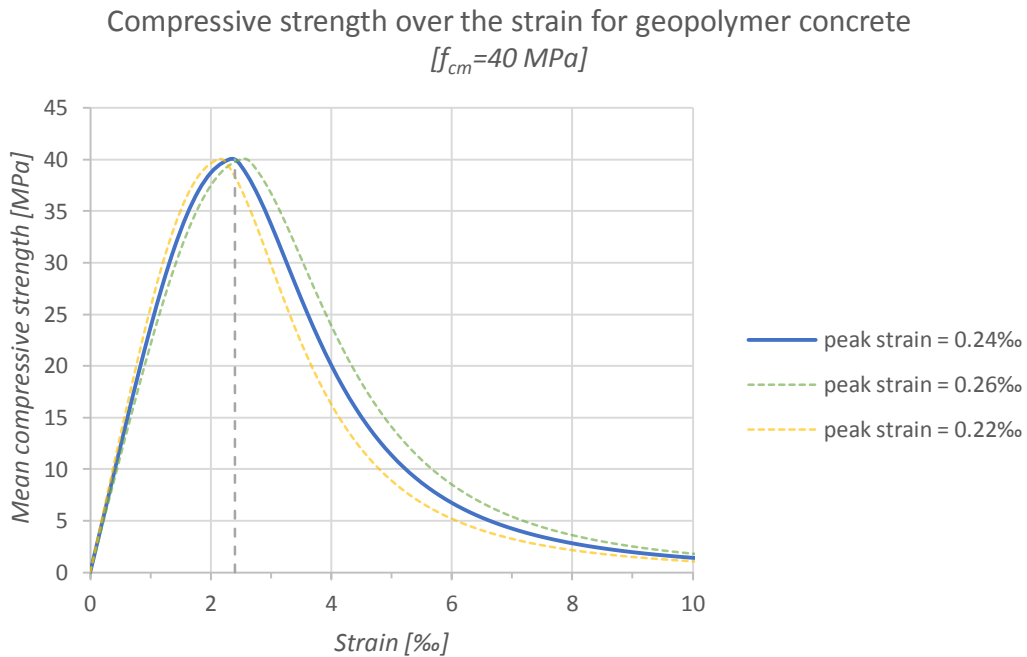


Figure 17 - Graph of the compression strength as a function of the strain for a geopolymer concrete $f_{cm} = 40 \text{ MPa}$, according to the expression from (Hardjito, 2005)

Crack pattern

The cracking pattern is described to be similar to the cracking pattern of Portland concrete. GPC will, since unreinforced Portland concrete normally does, shows one discrete crack if it is loaded under tension or bending.

2.3.4 Self-cleaning concrete

The best representative self-cleaning concrete found in literature is a Self-Compacting Concrete. The compressive and tensile strength after 28 days of this mixture is increased by 15-20% and 25-35% respectively compared with the same mixture without nano iron. After 90 days, the compressive and tensile strength was even increase by 20-25% and 35-45% respectively (Jalal, Ramezaniapourl, & Pool, Split tensile strength of binary blended self compacting concrete containing low volume fly ash and TiO₂ nanoparticles, 2013). As a conclusion, the nano-titanium oxide does have a significant positive influence on the strength properties of concrete. According to Jalal, Ramezaniapourl, & Pool (2013), the improved strength properties are probably due to the:

- Rapid consumption of crystalline Ca(OH)₂ as a result of the high reactivity of nano titanium oxide particles.
- Nano titanium oxide particles increase the particle packing density of the blended cement, indicating a reduced volume of larger pores in the cement paste.

The compressive strength from tests is about 63 MPa. It is assumed that same as for NSC, the characteristics compressive strength can be calculated from the mean compressive strength according to Eurocode 2, so the same standard deviation is assumed.

$$f_{ck} = f_{cm} - 8[MPa] = 55 MPa \quad \text{eq.(14)}$$

This makes the characteristic compressive strength equal to 55 MPa. It is assumed that the design strength can be determined according to Eurocode 2. This makes the design strength equal to 37 MPa as shown in eq.(15).

$$f_{cd} = \frac{f_{ck}}{1.5} = 37 MPa \quad \text{eq.(15)}$$

The mean splitting tensile strength from the test is 4.9 MPa. According to Eurocode 2, the mean splitting tensile strength can be calculated to the characteristic tensile strength by a factor 0.9, as shown in eq.(16). This makes the characteristic tensile strength equal to 3.1 MPa.

$$\begin{aligned} f_{ctm} &= 0.9f_{ctm,sp} \quad \text{eq.(16)} \\ f_{ctk,0.05} &= 0.7 \cdot 0.9f_{ctm,sp} \\ f_{ctk,0.05} &= 0.7 \cdot 0.9 \cdot 4.9 = 3.1 MPa \end{aligned}$$

The Young's modulus of self-cleaning concrete is probably some higher than for NSC. Since the concrete is stronger than NSC due to a denser matrix, the Young's modulus will probably some higher than for NSC, same as for HPC.

2.3.5 Self-sensing nano concrete

The right amount of nano iron in concrete could significantly increase the tensile strength and the flexural strength of concrete (Sanchez & Sobolev, 2010). However, no significant increase of the strength is found in other literature. Same as for self-cleaning concrete the characteristic and design values for the compressive and tensile strength are determined according to Eurocode 2. The result are shown below. The characteristic compressive strength and tensile strength are 30.9 MPa and 1.2 MPa respectively (Nazari, Riahi, Riahi, Shamekhi, & Khademno, The effects of incorporation Fe₂O₃

nanoparticles on tensile and flexural strength of concrete, 2010) and (Nazari, Riahi, Riahi, Shamekhi, & Khademno, Benefits of Fe2O3 nanoparticles in concrete mixing matrix, 2010).

Compressive strength

$$f_{cm} = 38.9 \text{ MPa}$$

$$f_{ck} = f_{cm} - 8[\text{MPa}] = 30.9 \text{ MPa}$$

$$f_{cd} = \frac{f_{ck}}{1.5} = 20.6 \text{ MPa}$$

Tensile strength

$$f_{ctm,sp} = 1.9 \text{ MPa}$$

$$f_{ctm} = 0.9f_{ctm,sp} = 1.7 \text{ MPa}$$

$$f_{ctk,0.05} = 0.7 \cdot 0.9f_{ctm,sp} = 1.2 \text{ MPa}$$

2.3.6 Shear resistance

The shear resistance for different ACMs is calculated according to different models. In Table 16, available design rules are given per cementitious material. Not all materials are in the table, because not for all ACMs are design rules yet or at least accessible design rules. Therefore, the shear capacity of GPC and nano-concrete is not calculated.

Table 16 - Standards and recommendations to determine the shear resistance for different ACMs

ACM	Standard or recommendation
NSC	Eurocode 2
HPC	Eurocode 2
NSSFRC	Model Code 2010
HPSFRC	Model Code 2010
UHPC	Ultra High Performance Fibre-Reinforced Concretes Recommendations
SHCC	Recommendations for Design and Construction of High Performance Fiber Reinforced Cement Composites with Multiple Fine Cracks (HPFRCC)

To compare the shear capacity of the ACMs with each other, a standard beam with a certain amount of reinforcement steel is used. A cross section of the beam is shown in Figure 18. The width and height of the beam is 1000 mm. In the beam, longitudinal reinforcement of 10 bars with a diameter of 25 mm is present at the bottom. Shear and practical reinforcement is not included in the beam. Fibres are not shown in the figure. However, for NSSFRC, HPSFRC, UHPC and SHCC are fibres included in the determination of the shear capacity.

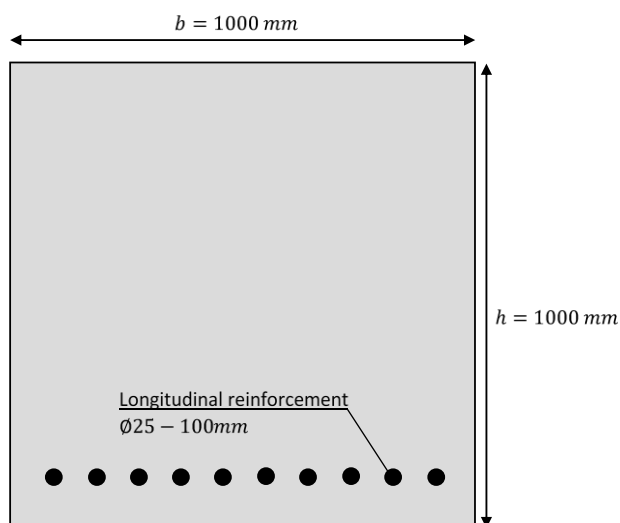


Figure 18 – Cross section of beam to determine the shear strength

The result of the shear capacity of the different ACMs is shown in the next paragraphs. The shear capacity per ACM is compared to the shear capacity of C30/37 by using a shear index. The index of C30/37 is defined as 1. If the shear capacity of an ACM is 3 times the shear capacity of C30/37, then the shear index of that ACM is equal 3. This can be written as a formula as shown in eq.(17).

$$shear\ index = \frac{V_{Rd,ACM}}{V_{Rd,C30/37}} \quad eq.(17)$$

The result of the calculation for the shear index are shown in Figure 19 and Figure 20. In Figure 19 is the comparison between NSC and NSSFRC with different maximum fibre stresses and HPSFRC with different maximum fibre stresses shown. In Figure 20 the comparison is given between NSC and all fibre reinforced materials as, NSSFRC, HPSFRC, UHPC and SHCC.

In Figure 19 is shown the influence of the fibres on the shear capacity clearly. Depending on the amount and the strength of fibres, fibres can double the shear capacity of a material. In the graph are shown three categories of ultimate residual tensile strengths, the strength after the first crack. In the first category, the residual strength is equal to the minimum required ultimate residual tensile strength for FRC as shown in the calculations in paragraph 2.3.6.2 Shear resistance of fibre reinforced concrete. The second category is for ultimate residual tensile strength for FRC equal to the characteristic tensile strength of the concrete. In the third category the ultimate residual tensile strength for FRC is chosen 1 MPa higher than the characteristic tensile strength of the concrete. In the third category, the material has a strain hardening behaviour.

In Figure 20 the shear indexes of UHPC and SHCC are compared to NSC. As an illustration, NSSFRC and HPSFRC with a strain hardening behaviour under tension are also shown in the figure. UHPC and SHCC both have an extreme high shear resistance compared to the other cementitious materials, with a shear index of 16 and 8 respectively. The calculation of the shear forces of both materials are presented in paragraph 2.3.6.3 Shear resistance of UHPC according to AFGC (2013 and paragraph 2.3.6.4 Shear resistance of SHCC according to the Japan Society of Civil Engineers.

Note: the given shear capacities here are just indicative values, according to the design rules. As mentioned before, the shear capacity is calculated for a cross section with a height and width of 1.0 m. In practice, the height of a beam for example is mainly smaller than 1.0 m. The height has an influence on the shear ratios between different ACMs. For example smaller height makes the differences between shear capacity of NSC and UHPC also smaller.

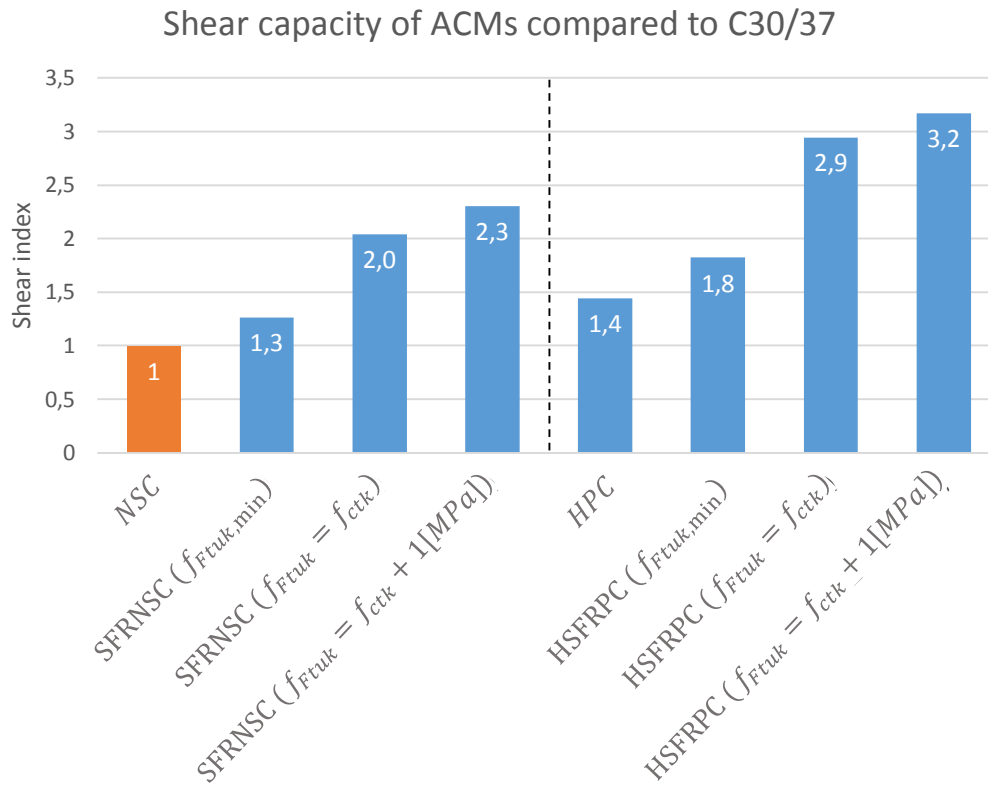


Figure 19 - Comparison of shear resistance between NSC, NSSFRC and HPSFRC with different ultimate residual tensile strengths

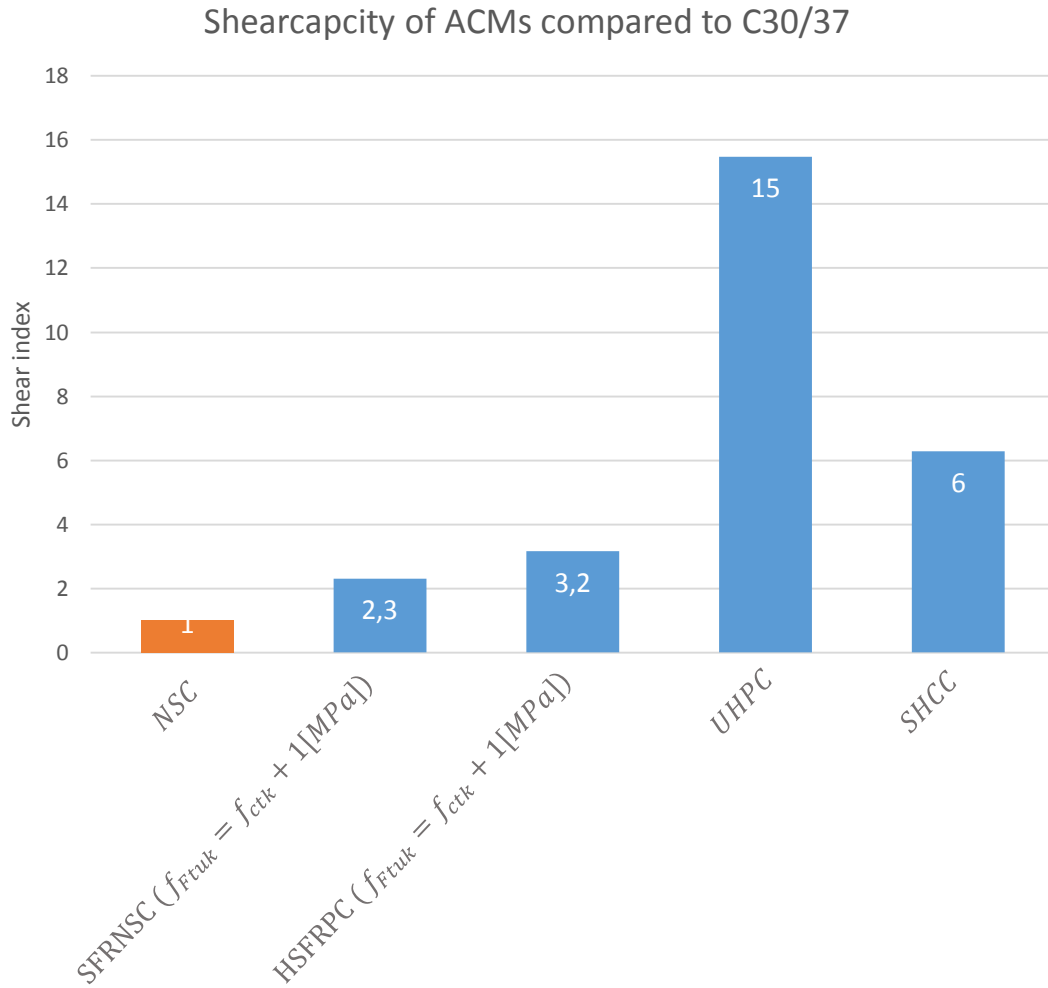


Figure 20 - Comparison of shear resistance between NSC, NSSFRC, HPSFRC, UHPC and SHCC

2.3.6.1 Shear resistance of NSC and HPC according to Eurocode 2

Eurocode 2 can be applied to determine the shear strength of a beam made out of NSC or HPC. According to the Eurocode, it is not allowed to include fibres in the calculation of the shear capacity. The shear capacity of a concrete beam can be calculated by Eurocode 2, equation 6.2.2 (1)(6.2a) as shown below. There is also a certain minimum value for the shear capacity of a beam in Eurocode 2 given by equation 6.2.2 (1)(6.2b), as shown in below.

$$V_{Rd,c} = \left[C_{Rd,c} \cdot k(100\rho_l \cdot f_{ck})^{\frac{1}{3}} + k_1\sigma_{cp} \right] b_w d \quad (\text{Eurocode 2, 6.2.2(1)(6.2.a)})$$

$$V_{Rd,c,min} = (v_{min} + k_1\sigma_{cp})b_w d \quad (\text{Eurocode 2, 6.2.2(1)(6.2.b)})$$

Where, $C_{Rd,c} = \frac{0.18}{\gamma_c} = \frac{0.18}{1.5} = 0.12$; $k = \min\left(1 + \sqrt{\frac{200}{d}}\right) = 1.47$; $d = 0.9h = 900 \text{ mm}$

$$\rho_l = \min\left(\frac{0.02}{\frac{A_s}{b_w d}}\right) = 0.55\%; k_1 = 0.15; v_{min,C30/37} = 0.035k^{\frac{3}{2}} \cdot f_{ck}^{\frac{1}{2}} = 0.34; v_{min,C90/105} = 0.59;$$

Filling in all variables, the design values for the shear capacity for both C30/37 and C90/105 are equal to:

$$V_{Rd,c} = \left[C_{Rd,c} \cdot k(100\rho_l \cdot f_{ck})^{\frac{1}{3}} \right] b_w d \quad \text{eq.(18)}$$

$$V_{Rd,c,C30/37} = 403 \text{ kN}$$

$$V_{Rd,c,C90/105} = 582 \text{ kN}$$

The minimum values for the shear capacity of both C30/37 and C90/105 are equal to:

$$V_{Rd,c,min} = (v_{min} + k_1 \sigma_{cp}) b_w d \quad \text{eq.(19)}$$

$$V_{Rd,c,min,C30/37} = 307 \text{ kN}$$

$$V_{Rd,c,min,C90/105} = 533 \text{ kN}$$

The design value for the shear value is equal to the maximum value of both formulæ from Eurocode 2, 6.2.2(1) as mentioned before. For C30/37 and C90/105 these values are equal to:

$$V_{Rd,C30/37} = \max\left(\begin{array}{l} V_{Rd,c,C30/37} = 403 \text{ kN} \\ V_{Rd,c,min,C30/37} = 307 \text{ kN} \end{array}\right) = 403 \text{ kN}$$

$$V_{Rd,C90/105} = \max\left(\begin{array}{l} V_{Rd,c,C90/105} = 432 \text{ kN} \\ V_{Rd,c,min,C90/105} = 533 \text{ kN} \end{array}\right) = 533 \text{ kN}$$

To have an idea of the shear strength of C30/37 and C90/105 for concrete cross sections with different heights, the shear strength as a function of the construction height is shown in Figure 21. In the figure is also UHPC (C170/200) included. This type of concrete is actually not included in Eurocode 2. For the graphs a reinforcement ratio of 2% is assumed in the tension zone, different from calculations above, and a width of 1.0 m. 2% reinforcement is, according to Eurocode 2, the maximum amount of longitudinal reinforcement to take into consideration in the shear calculation. In fact, the graph of Figure 21 shows the maximum shear capacity of NSC (C30/37), HPC (C90/105) and UHPC (C170/200) without shear reinforcement according to Eurocode 2.

Shear strength according to Eurocode 2

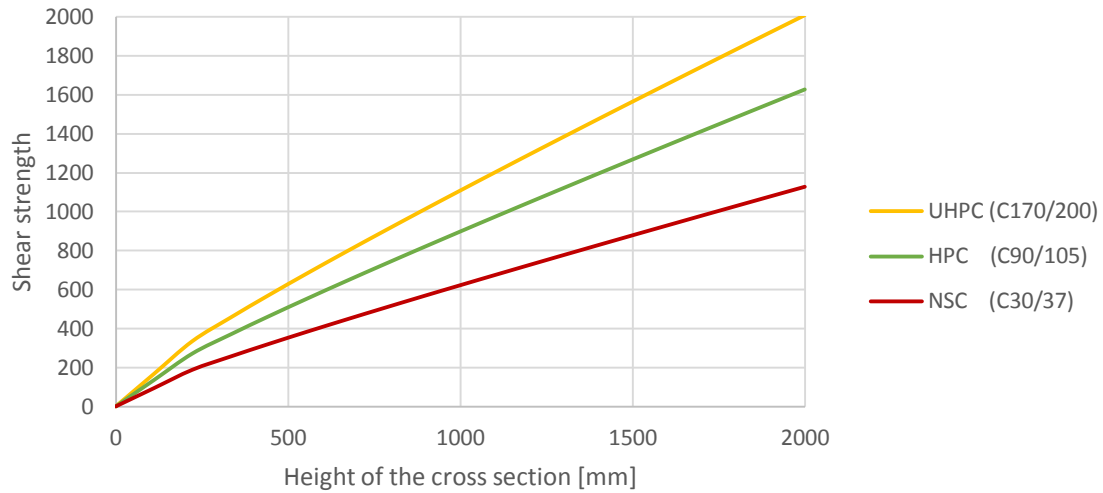


Figure 21 - Shear strength for NSC (C30/37), HPC (C90/105) and UHPC (C170/200) with 2% longitudinal reinforcement in the tension zone, ρ_l (ratio between area of longitudinal reinforcement and the effective concrete area) = 0.02, and a width $b_w = 1.0$ m.

2.3.6.2 Shear resistance of fibre reinforced concrete

The shear resistance of fibre reinforced concrete can be calculated according to the Model Code 2010. The use of this code is explained in a PowerPoint presentation of Vandewall and Plizzari (Vandewalle & Plizzari, 2010). Their method is worked out in this paragraph for NSSFRC and HPSFRC.

In the Model Code is given a formula to calculate the shear capacity of fibre reinforced concrete. This formula, shown in eq.(20) below, looks like the equations for the shear calculation from Eurocode 2. In fact, the equation is more or less the same as the shear capacity formula from Eurocode 2 with the addition of the in blue written term. The formula for the minimum value of the shear capacity is the same as in Eurocode 2, as shown in eq.(21).

$$V_{Rd,F} = \left[C_{Rd,c} \cdot k \left(100\rho_l \cdot \left(1 + 7.5 \cdot \frac{f_{Ftuk}}{f_{ctk}} \right) f_{ck} \right)^{\frac{1}{3}} + k_1 \sigma_{cp} \right] b_w d \quad \text{eq.(20)}$$

$$V_{Rd,Fmin} = (v_{min} + k_1 \sigma_{cp}) b_w d \quad \text{eq.(21)}$$

Where,

f_{Ftuk} is the characteristic value of the ultimate residual tensile strength for FRC in [MPa], by considering $w_u = 1.5$ mm

f_{ctk} is the characteristic value of the tensile strength for the concrete matrix in [MPa]

$$C_{Rd,c} = \frac{0.18}{\gamma_c} = \frac{0.18}{1.5} = 0.12; \quad k = \min \left(1 + \sqrt{\frac{200}{d}} \right) = 1.47; \quad d = 0.9h = 900 \text{ mm}$$

$$\rho_l = \min \left(\frac{0.02}{\frac{A_{sl}}{b_w d}} \right) = 0.55\%; \quad k_1 = 0.15; \quad v_{min} = 0.035 k^{\frac{3}{2}} \cdot f_{ck}^{\frac{1}{2}};$$

In the Model Code is given a formula for the minimum the characteristic value of the ultimate residual tensile strength for FRC, where no shear reinforcement is required any more. The use of shear reinforcement (stirrups) can be prevented if:

$$f_{Ftuk} \geq \frac{\sqrt{f_{ck}}}{20} \quad \text{eq.(22)}$$

To avoid shear stirrups, the minimum values for f_{Ftuk} for both $f_{ck} = 30 \text{ MPa}$ and $f_{ck} = 90 \text{ MPa}$ should be equal to:

$$f_{Ftuk,C30/37} \geq \frac{\sqrt{30}}{20} = 0.27 \text{ MPa}$$

$$f_{Ftuk,C90/105} \geq \frac{\sqrt{90}}{20} = 0.47 \text{ MPa}$$

Filling in these values for the characteristic value of the ultimate residual tensile strength for FRC in eq.(20) and eq.(21), the design value for the shear capacity for both C30/37 and C90/105 are equal to:

$$V_{Rd,c,C30/37} = 511 \text{ kN}$$

$$V_{Rd,c,C90/105} = 735 \text{ kN}$$

The same calculations could be done with other values of f_{Ftuk} . In the graph in Figure 22 the shear capacity of NSSFRC (C30/37) and HPSFRC (C90/105) as a function of f_{Ftuk} is given. As shown in the figure, a higher value of f_{Ftuk} results in a higher value for the shear capacity of the FRC.

Shear capacity of fibre reinforced concrete for different values of f_{Ftuk}

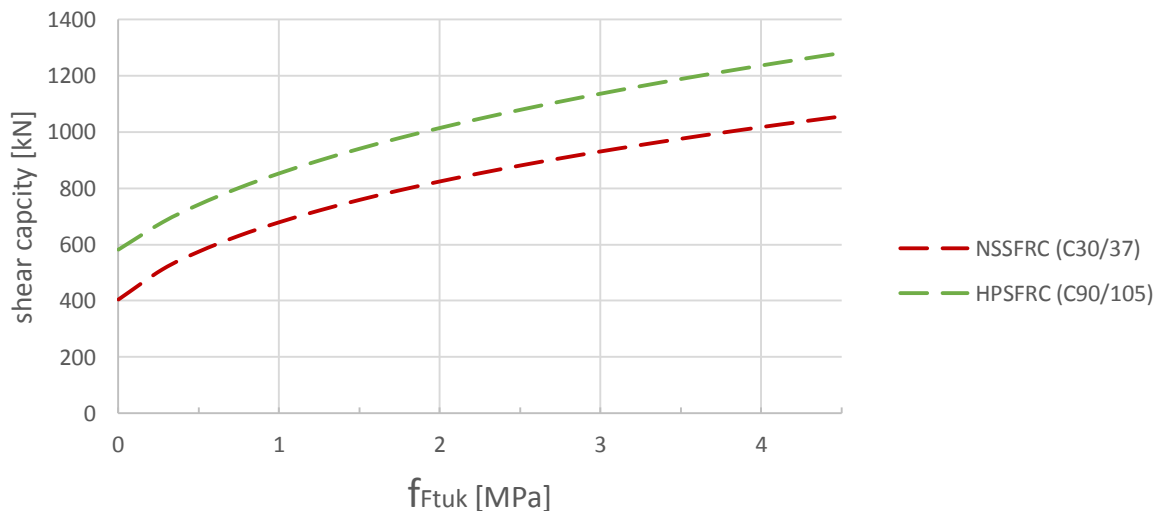


Figure 22 - Shear capacity of NSSFRC (C30/37) and HPSFRC (C90/105) without stirrups for different values of f_{Ftuk}

Next to the minimum value of f_{Ftuk} such that no stirrups are required, the value where $f_{Ftuk} = f_{ctk}$ and $f_{Ftuk} > f_{ctk}$ are points of interest. The point where $f_{Ftuk} = f_{ctk}$ is the border between both, a concrete with a strain softening behaviour and a strain hardening behaviour. If $f_{Ftuk} > f_{ctk}$, the concrete has a strain hardening behaviour when it is loaded in shear. As a point of interest in the strain hardening zone is chosen $f_{Ftuk} = f_{ctk} + 1[MPa]$. The values for these point of interest can be determined by Figure 22. The results are show in Table 17.

Table 17 - shear capacity of C30/37 and C90/105 for different interesting values of f_{Ftuk}

Concrete class	Point of interest	Ultimate residual tensile strength for FRC	Shear capacity
		[MPa]	[kN]
C30/37	no stirrups required	0.27	511
	$f_{Ftuk} = f_{ctk}$	2.00	823
	$f_{Ftuk} = f_{ctk} + 1[MPa]$	3.00	930
C90/105	no stirrups required	0.47	735
	$f_{Ftuk} = f_{ctk}$	3.50	1,187
	$f_{Ftuk} = f_{ctk} + 1[MPa]$	4.50	1,280

2.3.6.3 Shear resistance of UHPC according to AFGC (2013)

The shear resistance for UHPC can be calculated according to the recommendations of the AFGC from 2013. The shear capacity according to this recommendation is equal to the summation of the shear contribution of the concrete itself, the steel fibres and the shear reinforcement, as described eq.(23). All contributions are calculated here separately and in the end added together.

$$V_{Rd} = V_{Rd,c} + V_{Rd,f} + V_{Rd,s} \quad \text{eq.(23)}$$

Where,

$V_{Rd,c}$ = the contribution of the concrete

$V_{Rd,f}$ = the contribution of the steel fibres

$V_{Rd,s}$ = the contribution of shear reinforcement

According to AFGC's Scientific and Technical Committee (2013), the maximum value of the shear resistance is equal to:

$$V_{Rd,max} = 2 \cdot 1.14 \cdot \frac{\alpha_{cc}}{\gamma_c} b_w z \cdot f_{ck}^{\frac{2}{3}} \cdot \frac{1}{\cot\theta + \tan\theta}$$

Where, $\alpha_{cc} = 0.85$; $\gamma_c = 1.5$; $b_w = 1.0 \text{ m}$; $z = 787.5 \text{ mm}$; $f_{ck} = 170 \text{ MPa}$; $\theta = 30^\circ$

$$V_{Rd,max} = 75,897 \text{ kN}$$

Contribution of the concrete

The contribution of the concrete to the shear force capacity can be calculated by eq.(24).

$$V_{Rd,c} = \frac{0.21}{\gamma_{cf} \gamma_e} k \cdot (f_{ck})^{\frac{1}{2}} \cdot b_w \cdot 0,875h \quad \text{eq.(24)}$$

Where, assuming no prestressing force, $\gamma_{cf}\gamma_e = 1.5$; $k = 1 + \frac{3\sigma_{cp}}{f_{ck}} = 1$ ($\sigma_{cp} = 0$); $b_w = 1000mm$; $h = 1000mm$; $f_{ck} = 170 MPa$

Given these parameters, the shear capacity from the concrete is equal to:

$$V_{Rd,c} = \frac{0.21}{1.5} \cdot 1 \cdot (170)^{\frac{1}{2}} \cdot 1000 \cdot 0.875 \cdot 1000 = 1,597 kN \quad \text{eq.(25)}$$

Contribution of the fibres

According to the French recommendation again, the contribution of the fibers can be calculated as:

$$V_{Rd,f} = \frac{A_{fv} \cdot \sigma_{Rd,f}}{\tan\theta} \quad \text{eq.(26)}$$

Where,

$$A_{fv} = \text{area of fibre effect} = b_w \cdot z = b_w \cdot 0.9d = b_w \cdot 0.9 \cdot \frac{7}{8}h = 0.7875 \cdot 1000 \cdot 1000 = 787 \cdot 10^3 mm^2$$

θ = angle between principal compression stress and beam axis = 30° (recommended as minimum value by (AFGC's Scientific and Technical Committee, 2013))

$\sigma_{Rd,f}$ = residual tensile strength of the fibre-reinforced cross section.

The value of the residual tensile strength depends on the strain hardening or softening behaviour of the concrete in tension. Depending of this behaviour, the residual tensile strength of the fibre-reinforced cross section is equal to:

$$\sigma_{Rd,f} = \begin{cases} \frac{1}{K \cdot \gamma_{cf}} \cdot \frac{1}{w_{lim}} \int_0^{w_{lim}} \sigma_f(w) dw & \text{(Strain-softening or low strain hardening)} \\ \frac{1}{K \cdot \gamma_{cf}} \cdot \frac{1}{\varepsilon_{lim} - \varepsilon_{el}} \int_{\varepsilon_{el}}^{\varepsilon_{lim}} \sigma_f(\varepsilon) d\varepsilon & \text{(High strain-hardening)} \end{cases}$$

Strain softening or low strain hardening

The above given formula for the strain-softening behaviour could also be written as a function of the strain. The value of the integral given in the formula then is equal to the blue coloured area in Figure 23. Calculating the residual tensile strength like this is favourable, since no information of the stress as a function of the crack width is known. In the calculations the strain from the first crack, ε_{ct} , until the strain where $w = 0.3mm$, $\varepsilon_{ct,0.3}$ is taken into consideration. The upper limit for the crack width is chosen equal 0.3 mm according to AFGC's Scientific and Technical Committee (2013). The recommendations show that after a crack width of 0.3 mm, the tensile strength can be neglected. This makes that the formula for the residual tensile strength of the fibre-reinforced cross section can be rewritten as a function of the strain as:

$$\sigma_{Rd,f} = \frac{1}{K \cdot \gamma_{cf}} \cdot \frac{1}{w_{lim}} \int_0^{w_{lim}} \sigma_f(w) dw \quad \text{eq.(27)}$$

$$\sigma_{Rd,f} = \frac{1}{K \cdot \gamma_{cf}} \cdot \frac{1}{\varepsilon_{ct,0.3} - \varepsilon_{u,el}} \cdot \left[\frac{f_{ctk}}{K \cdot \gamma_{cf}} \cdot (\varepsilon_{ct,0.3} - \varepsilon_{u,el}) \right]$$

Where,

$$\varepsilon_{ct,0.3} = \varepsilon_{u,peak|w=0.3mm} = \frac{w_{0.3mm}}{l_c} + \frac{f_{ctk,el}}{\gamma_{cf} E_{c,eff}} = \frac{w_{0.3mm}}{\frac{2}{3}h} + \frac{f_{ctk,el}}{\gamma_{cf} E_{c,eff}}$$

$$\varepsilon_{ct,0.3} = \varepsilon_{u,peak|w=0.3mm} = \frac{0.3}{\frac{2}{3} \cdot 1000} + \frac{9}{1.3 \cdot 16700} = 0.86\text{‰}$$

$$\varepsilon_{u,el} = \frac{f_{ctk,el}}{\gamma_{cf}} \cdot \frac{1}{E_{cm}} = \frac{9}{1.3} \cdot \frac{1}{50000} = 0.4\text{‰} \text{ (Figure 23)}$$

$$K = 1.25; \gamma_{cf} = 1.3; f_{ctk} = 9.0 \text{ MPa}$$

This makes the residual tensile strength of the fibre-reinforced cross section equal to:

$$\sigma_{Rd,f} = \frac{1}{1.25 \cdot 1.3} \cdot \frac{1}{0.00086 - 0.0001} \cdot \left[\frac{9.0}{1.25 \cdot 1.3} \cdot (0.00086 - 0.0001) \right] = 3.41 \text{ MPa}$$

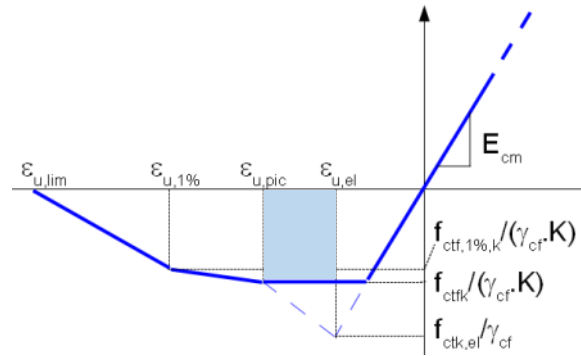


Figure 23 - Stress-strain diagram for UHPC in ULS with strain softening or low strain hardening behaviour (AFGC's Scientific and Technical Committee, 2013)

Strain hardening

The residual tensile strength for UHPC with a strain hardening behaviour, is calculated in a similar way as for UHPC with a strain softening behaviour. The integral for the fibre tensile strength, shown in eq.(28), is equal to the blue area in the stress-strain graph of Figure 24. The residual tensile fibre strength now can be expressed as:

$$\begin{aligned} \sigma_{Rd,f} &= \frac{1}{K \cdot \gamma_{cf}} \cdot \frac{1}{\varepsilon_{lim} - \varepsilon_{el}} \int_{\varepsilon_{el}}^{\varepsilon_{lim}} \sigma_f(\varepsilon) d\varepsilon \\ &= \frac{1}{K \cdot \gamma_{cf}} \cdot \frac{1}{\varepsilon_{u,lim} - \varepsilon_{u,el}} \cdot \left[(\varepsilon_{u,lim} - \varepsilon_{u,el}) \cdot \frac{f_{ctfk}}{K \cdot \gamma_{cf}} \right] = 3.41 \text{ MPa} \end{aligned} \quad \text{eq.(28)}$$

Where,

$$K = \text{fibre orientation} = K_{global} = 1.25$$

$$\gamma_{cf} = \text{Partial safety factor on fibres} = 1.3$$

$f_{ctfk} = 9 \text{ MPa}$, recommended in the French recommendation (AFGC's Scientific and Technical Committee, 2013)

$\varepsilon_{u,lim} = 2.5\text{‰}$, recommended in the French recommendation (AFGC's Scientific and Technical Committee, 2013)

$$\varepsilon_{u,el} = \frac{f_{ctk,el}}{\gamma_{cf}} \cdot \frac{1}{E_{cm}} = \frac{9}{1.3} \cdot \frac{1}{16700} = 0.4\text{‰}$$

Note: since the characteristic value of the concrete tensile strength is equal to the recommended value for the tensile fibre strength, there is actually no strain hardening effect in this case. In practice, to design an UHPC with a strain hardening behaviour in tension, the fibres strength should be larger than the concrete strength.

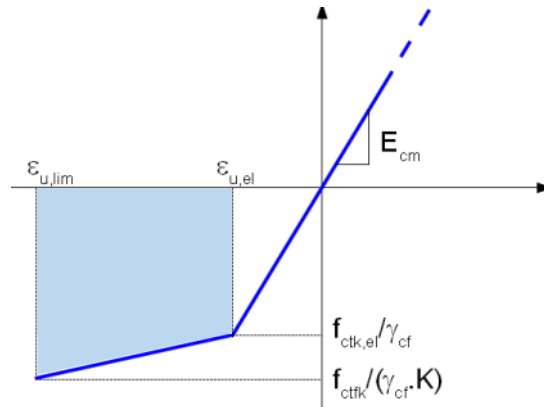


Figure 24 - Stress-strain diagram for UHPC in ULS with strain hardening behaviour (AFGC's Scientific and Technical Committee, 2013)

Since both strain hardening and strain softening behaviour concretes have the same value of the residual tensile strength of the fibre-reinforced cross section, both gives the same value of the shear capacity from the steel fibre. Filling in all variables, the contribution of the fibres to the shear capacity is equal to:

$$V_{Rd,f} = \frac{A_{fv} \cdot \sigma_{Rd,f}}{\tan\theta} = \frac{0.788 \cdot 1000 \cdot 1000 \cdot 3.41}{\tan(30)} = 4,649 \text{ kN} \quad \text{eq.(29)}$$

The total shear force becomes:

$$V_{Rd} = 1,597 + 4,649 = 6,246 \text{ kN} \quad \text{eq.(30)}$$

Doing the above shown calculations for different heights, the shear capacity of UHPC (C170/200) can be shown as a function of the height of the cross section as shown in Figure 25. In the figure is also shown the fibre and the concrete contribution to the total shear capacity. From the figure can be concluded that the fibre and the concrete contribution of the total shear capacity of the cross section of UHPC (C170/200) is 74% and 26% respectively. This values will probably be different for other types of UHPC, but the graph of Figure 25 at least gives an indication of shear strength and the contribution of both the fibres and the concrete.

Shear strength UHPC as a function of the height fibre and concrete contribution to the total shear capacity

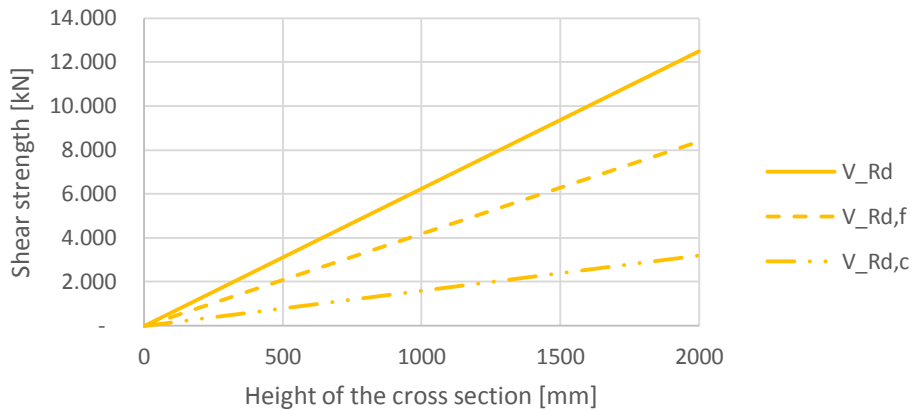


Figure 25 – Shear capacity of C170/200 (UHPC) as a function of the height with a width of 1.0m

2.3.6.4 Shear resistance of SHCC according to the Japan Society of Civil Engineers

The determination of shear resistance of SHCC is described in recommendations of the Japan Society of Civil Engineering. According to these recommendations, the total shear resistance is a summation of the four components as shown in the eq.(31).

$$V_{yd} = V_{cd} + V_{sd} + V_{fd} + V_{ped} = V_{Rd} \quad \text{eq.(31)}$$

Here the four different components are defined as:

V_{cd} = the design shear capacity of a linear concrete member without any shear reinforcing steel, excluding the strength exerted by reinforcing fibres.

V_{sd} = the design shear capacity of shear reinforcement, which is equal zero in this calculation, since no shear reinforcement is in.

V_{fd} = is the design value of the shear capacity accommodated by the reinforcing fibres.

V_{ped} = the component of effective tensile force in longitudinal prestressing steel parallel to the shear force, which is equal zero in this case since there is no prestressing steel in the beam.

Contribution of the concrete

The contribution of the concrete itself to the shear capacity of the total material can be calculated by eq.(32).

$$V_{cd} = \beta_d \cdot \beta_p \cdot \beta_n \cdot f_{ved} \cdot \frac{b_w \cdot d}{\gamma_b} \quad \text{eq.(32)}$$

Where,

$$f_{ved} = 0.7 \cdot 0.20^3 \sqrt{f'_{cd}} = 0.42 \text{ MPa}$$

$$\beta_d = \min\left(\frac{\sqrt[4]{1/d}}{1.5}\right) = 1.03$$

$$\beta_p = \min \left(\frac{\sqrt[3]{100A_s}}{\sqrt{b_w \cdot d}} \cdot 1.5, \beta_n = 2, \gamma_b = 1.3 \right) = 0.82$$

This makes the contribution of the concrete to the shear force resistance equal to:

$$V_{cd} = 1.03 \cdot 0.81 \cdot 2 \cdot 0.42 \cdot \frac{1000 \cdot 900}{1.3} = 487 \text{ kN} \quad \text{eq.(33)}$$

Contribution of the fibres

The fibre contribution to the shear capacity of the UHPC can be calculated by eq.(34)

$$V_{fd} = \frac{f_{vd}}{\tan(\beta_u)} \cdot \frac{b_w \cdot z}{\gamma_b} \quad \text{eq.(34)}$$

Where,

$$f_{vd}(\text{design tensile strength}) = 3.4 \text{ MPa}$$

$$\tan(\beta_u) = \tan(45^\circ) = 1 \text{ (recommended value (Japan Society of Civil Engineers, 2008))}$$

$$z = h \cdot \frac{0.9}{1.15} = 783 \text{ mm}$$

$$\gamma_b = 1.3$$

This makes the contribution of the fibres to the shear force resistance equal to:

$$V_{fd} = \frac{3.4}{1} \cdot \frac{1000 \cdot 783}{1.3} = 2047 \text{ kN}$$

Total shear strength capacity

The total shear capacity of the concrete beam made of SHCC is in this case the summation of both the contribution of the concrete and the fibres, since there is no prestressing steel and shear reinforcement in the cross section. The total shear strength capacity is equal to:

$$V_{Rd} = V_{yd} = V_{cd} + V_{fd} = 361 + 2047 = 2533 \text{ kN} \quad \text{eq.(35)}$$

The total shear strength of SHCC and contribution of fibres and concrete as a function of the height of the cross section are shown in the graph of Figure 26. As shown in the figure is, depending on the height, the contribution of the concrete around 25-35% and the contribution of the fibres 65-75%. These values will probably be different for other types of SHCC, but the graph of Figure 26 at least gives an indication of shear strength and the contribution of both the fibres and the concrete.

Shear strength SHCC as a function of the height, fibre and concrete contribution to the total shear capacity

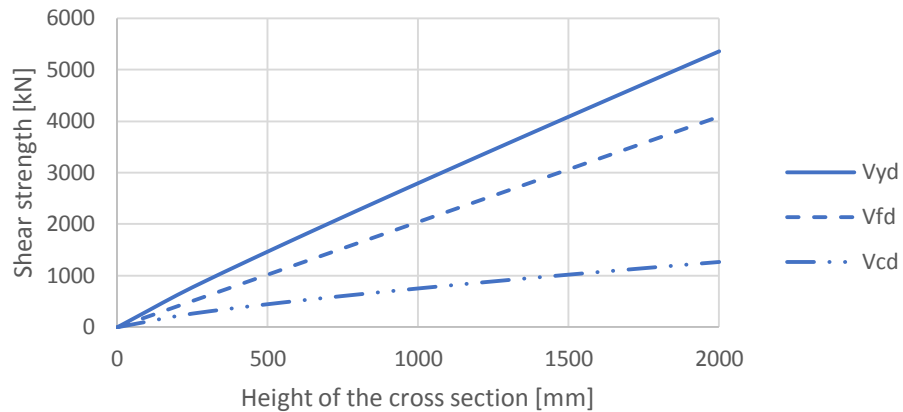


Figure 26 - Shear capacity of the representative SHCC of this research as a function of the height with a width of 1.0m

Another way to show the comparison of shear capacity of the different ACMs is shown in Figure 27. In this figure is shown the shear capacity of every ACM calculated above as a function of the height of the cross section. The calculations are done according to the design rules that are valid per ACM, as explained earlier. For the calculations almost the same assumptions are done as for the calculations above. The only difference is the amount of longitudinal reinforcement. For this comparison, a reinforcement ratio of $\rho_l = 2\%$ is applied for NSC, HPC, NSSFRC and HPSFRC. This is according to Eurocode 2 the highest amount of reinforcement steel that can be taken into consideration in the calculation to the shear capacity of a structure.

Shear strength for different ACMs according to their own design rules as a function of the height

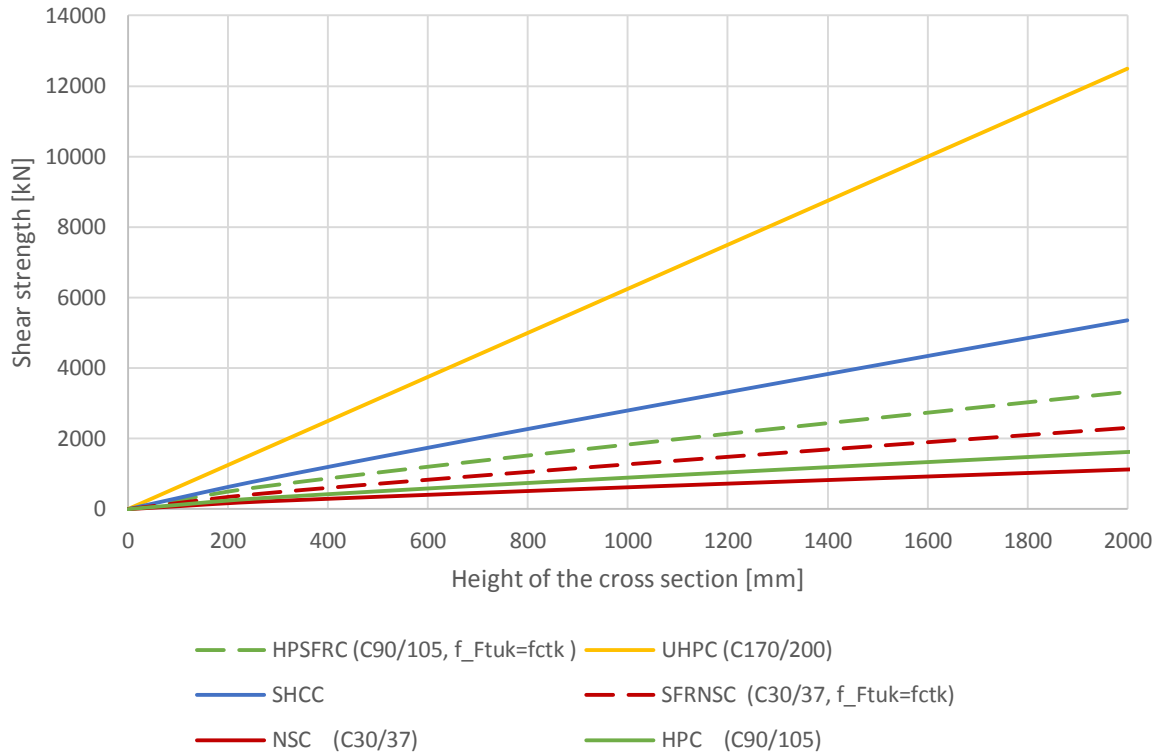


Figure 27 - Comparison of the shear capacity of different ACMs for different heights of the concrete cross section according to their own design rules as mentioned above

2.3.7 Creep and shrinkage

Creep and shrinkage both depend on the moisture content in the environment, design of concrete element and the composition of concrete (Nederlands Normalisatie-instituut, 2011). Both mechanisms will be discussed in some more detail here. To calculate the amount of creep and shrinkage, Eurocode 2, French recommendations and Japanese recommendations will be used, depending of the ACM. The amount of creep or shrinkage for ACMs that are not described in recommendations or standards is determined qualitatively.

An overview of the creep and shrinkage for the ACMs is given in Table 18. In the first column of the table are the different ACMs shown. In the second and the third column are given calculated the creep and shrinkage. The creep is calculated assuming a compressive stress equal to 10 MPa.

Table 18 - Creep and shrinkage per ACM. Creep calculated for a stress of 10 MPa

ACM	Creep [%]	Shrinkage [%]
NSC	0.48	0.15
HPC	0.18	0.35
UPHC untreated	0.18	0.55 ³⁰
UHPC treated type 1	0.09	
UHPC treated type 2	0.05	

³⁰ (AFGC's Scientific and Technical Committee, 2013)

SHCC	0.61	-
Self-healing concrete	+/-	+/-
GPC	++	++
Self-sensing concrete (tubes)	+	-
Self-cleaning and stiff concrete	+	+

Qualitative characteristics

- ++ very low creep or shrinkage compared to NSC
- + low creep or shrinkage compared to NSC
- +/- similar creep or shrinkage as NSC
- high creep or shrinkage compared to NSC
- very high creep or shrinkage compared to NSC

The quantitative creep values are calculated into a creep index. Here the index of NSC is defined equal 1. An ACM with a creep index equal 0.5 has a creep strain which is half of the creep strain of NSC. All creep indexes are shown in Figure 28. Notice that the stronger ACMs, HPC and UHPC, show less creep.

The detailed calculation methods and some more explanation of the creep and shrinkage behaviour of different ACMs are given in the next few paragraphs of this chapter.

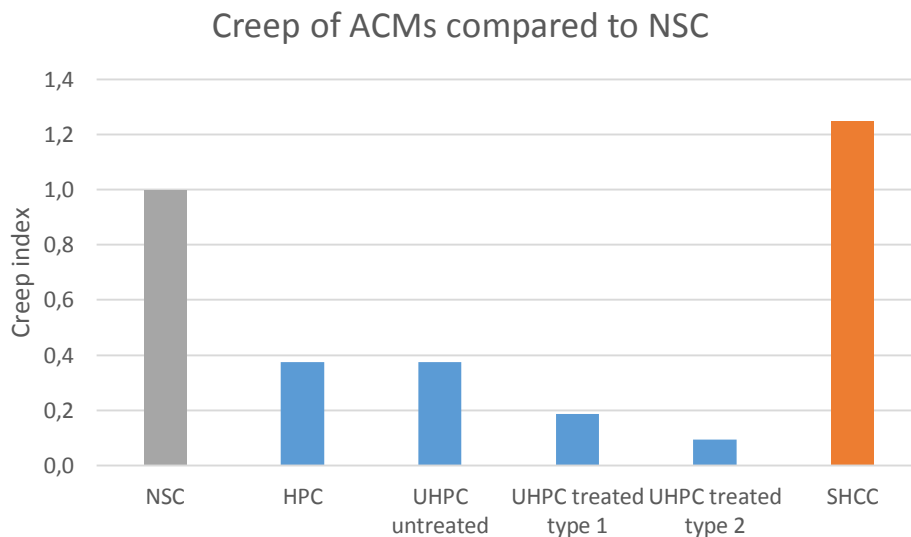


Figure 28 - Creep behaviour of different ACMs compared to NSC

2.3.7.1 Creep

Before the creep of the ACMs will be described according to standards and literature, the creep mechanism itself is explained in some more detail. Creep can be modelled by two mechanisms; short-time creep, which is caused by the redistribution of water in the capillary pores and long-time creep, which is caused by the changing of location of gel particles. In practice, the long-term creep is the most important one. The most important parameters for the magnitude of long-term creep are the changes in temperature, moisture and concentration.

For ordinary concrete, there are a few internal parameters which influence the creep behaviour of the concrete. Those parameters are:

- **Cement:** rapid hardening cement results in less creep.
- **W/C ratio:** a higher W/C ratio gives more creep.
- **Cement content:** more cement gives more creep in the concrete.

- **Kind of aggregate:** more creep if aggregate is less stiff.
- **Additives:** increase or decrease of the creep, depending on the kind of additive.
- **Degree of hydration:** more hydrated concrete results in less creep.
- **Moisture content:** a high moisture content results in more creep to the concrete.

2.3.7.1.1 Eurocode 2

Eurocode 2 makes a distinction between linear and non-linear creep. Non-linear creep should be applied if the concrete compressive strength is higher than $0.45 f_{ck}$, because then micro-crack are generated. Both linear and non-linear creep are calculated by the creep coefficient. This coefficient depends on:

- Time
- Relative humidity
- Construction height
- Cement class

In this creep coefficient, only the cement class is a material property. A higher cement class results in a lower creep coefficient, so a lower creep. The formulas for linear and non-linear creep according to Eurocode 2 are shown here.

<p>Linear creep</p> $\varepsilon_{cc}(\infty, t_0) = \varphi(\infty, t_0) \cdot \left(\frac{\sigma_c}{E_c}\right)$	<p>Non-linear creep</p> $\varepsilon_{cc}(\infty, t_0) = \varphi_{nl}(\infty, t_0) \cdot \left(\frac{\sigma_c}{E_c}\right)$ $\varphi_{nl}(\infty, t_0) = \varphi(\infty, t_0) e^{1.5(k_\sigma - 0.45)}$
--	---

Where,

$$k_\sigma = \frac{\sigma_c}{f_{ck}(t_0)}$$

$\varphi(\infty, t_0)$ = the linear creep coefficient

$\varphi_{nl}(\infty, t_0)$ = the non-linear creep coefficient

2.3.7.1.2 French Recommendations Ultra High Performance Fibre-Reinforced Concretes

The creep of UHPC can be calculated using the French recommendations. The recommendations describe that the creep of UHPFRC is similar to that of HPC if there is no treatment. It is assumed this is valid for the long term creep. Treatment can significantly reduce the long-term creep. If nothing is known during the preliminary design phase of the project, the following indicative values of the long-term creep ϕ are adopted:

- $\phi = 0.8$ if there is no treatment;
- $\phi = 0.4$ with treatment of the first type;
- $\phi = 0.2$ with treatment of the second type.

As a conclusion, the creep of UHPC is lower if the concrete is treated. If concrete is not treated, the creep of UHPC is similar to creep of HPC. So in the end, the creep of UHPC is equal or smaller than the creep of HPC, depending on the treatment. The first and second type of treatment then will give a creep that is half and quart of the creep of non-treated UHPC.

2.3.7.1.3 Japanese Recommendations for SHCC

The Japanese recommendations make a difference between tensile and compressive creep strain. The first one, tensile creep strain, must be determined on data or experiments. The compressive creep strain can be obtained by eq.(36).

$$\varepsilon'_{cc} = \frac{\varphi \sigma'_{cp}}{E_{ct}} \quad \text{eq.(36)}$$

Where,

φ = the creep coefficient

σ'_{cp} = the compressive stress at work

E_{ct} = the Young's modulus at the age when loading is applied

The recommendations show that the creep coefficient for SHCC is smaller than for ordinary concrete with the same compressive strength. The Young's modulus for SHCC is in general a factor 1/2 to 2/3 smaller compared to ordinary concrete. In the recommendations is not described how the Young's modulus of SHCC behaves over the time, compared to ordinary concrete. It is estimated both moduli of elasticity behave similar over time.

The smaller Young's modulus of SHCC gives 1.5 - 2.0 times more creep strain compared to NSC. The smaller creep coefficient compensate a bit, but as described by the Japanese, the total creep strain of SHCC is large compared to NSC.

2.3.7.1.4 Fibre Reinforced Concrete, Self-Healing Concrete, Geopolymer Concrete and NANO Concrete

The creep of FRC, self-healing concrete, GPC and nano concrete are not mentioned in code or standards. Therefore, in this paragraph these ACMs are described qualitatively by literature.

FRC shows lower basic creep compared to the same concrete mixture without any fibres (Chern & Young, 1989). Zhang J. (2003) shows that the total creep of a fibre reinforced cementitious composite has a similar relation with the fibre content. The higher the fibre content is, the lower the composite creep will be (Zhang J. , 2003).

For self-healing concrete is assumed that the creep behaviour is similar to the creep behaviour of NSC. Since the composition of both kinds of concretes is almost equal and the micro-capsules does not influence the mechanical characteristics that much, it seems a good estimation.

The creep behaviour of geopolymer concrete is very favourable compared to NSC. Researches to the creep behaviour shows the creep of GPC is very limited (Aldred J. M., 2013), (Wallah & Rangan, 2006).

Adding nano particles, densifies the concrete matrix. A denser matrix is less permeable. This means that it is harder for moisture to come in or go out of the concrete, which decrease the magnitude of creep (Reinhardt, 2000). So it could be assumed that the creep of nano concrete is a little lower compared to NSC.

2.3.7.1.5 Creep calculations ACMs

To compare the creep behaviour of different ACMs, some calculation describe above are made here. For the ACMs no calculations rules are written yet, a qualitative comparison is made. For the calculation a few assumption are made.

General assumptions

- Only linear creep is calculated, from reasons of simplicity. The given calculations are just an illustration.
- Concrete is situated outside, where the relative humidity is 80%
- $h_0 = 1500 \text{ mm}$

For NSC

- Cement class N

For HPC

- Cement class R

NSC and HPC

The creep strains for NSC and HPC are given in Table 19. In the first column is the creep calculation for C30/37, the representative NSC, given. In the second column are the creep calculations for C90/105, the representative HPC, given.

Table 19 - Linear creep behaviour of C30/37 and C90/105 according to Eurocode 2

C30/37 (NSC)	C90/105 (HPC)
$\varepsilon_{cc}(\infty, t_0) = \varphi(\infty, t_0) \cdot \left(\frac{\sigma_c}{E_c}\right)$	$\varepsilon_{cc}(\infty, t_0) = \varphi(\infty, t_0) \cdot \left(\frac{\sigma_c}{E_c}\right)$
$\varepsilon_{cc}(\infty, t_0) = 1.6 \cdot \left(\frac{10}{33,000}\right)$	$\varepsilon_{cc}(\infty, t_0) = 0.8 \cdot \left(\frac{10}{44,000}\right)$
$\varepsilon_{cc}(\infty, t_0) = 0.48\text{‰}$	$\varepsilon_{cc}(\infty, t_0) = 0.18\text{‰}$

UHPC

Untreated UHPC is assumed to have a similar creep behaviour as HPC, as mentioned earlier. The creep of C90/105 is according to Eurocode 2 equal to 0.18‰. In the France recommendations are two types of treatment described, both with another value for creep. The creep of UHPC with the first and second type of treatment is respectively equal to 0.09‰ and 0.05‰.

SHCC

In Figure 29 is a comparison given of the creep coefficient of a cylinder made of ordinary concrete and SHCC (HPFRCC). The shape of both graphs of the creep coefficient over time is more or less the same. After 100 day, the creep coefficient of SHCC is about 70% of the creep coefficient of ordinary concrete with the same compressive strength. Therefore the total creep of SHCC is estimated to be 70% of the NSC.

$$\varepsilon'_{cc} = \frac{\varphi \sigma'_{cp}}{E_{ct}} = \frac{0.7 \cdot \varphi_{C30/37} \cdot 10}{18500} = 0.61\text{‰}$$

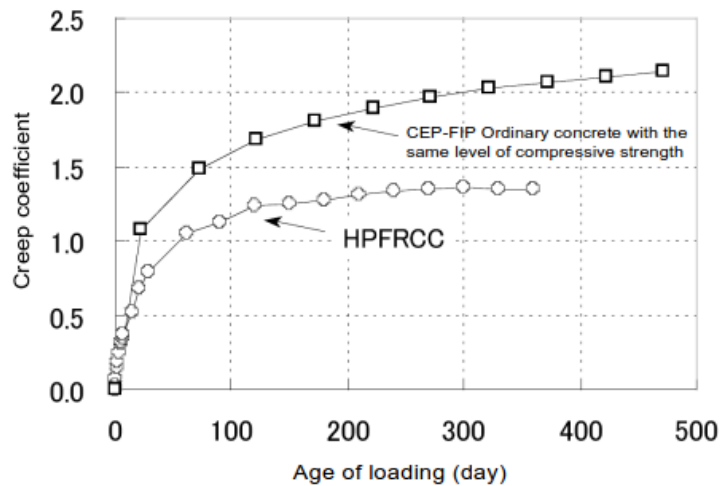


Figure 29 - Comparison between the creep coefficients of a cylinder 100mm in diameter and 200mm in height made of SHCC and ordinary concrete

2.3.7.2 Shrinkage

There are a few different mechanisms behind shrinkage. The six most important types of shrinkage in concrete are (Microlab TU Delft, 2014):

1. Plastic shrinkage
2. Chemical shrinkage
3. Autogenous shrinkage
4. Drying shrinkage
5. Carbonation shrinkage
6. Thermal shrinkage

The sum of the chemical shrinkage and autogenous shrinkage is called the hardening shrinkage.

2.3.7.2.1 Eurocode 2

The total creep according to Eurocode 2 is the summation of the drying shrinkage and autogenous shrinkage only. Both can be calculated using the equations shown below. For drying shrinkage, the only material characteristic is in the $\varepsilon_{cd,0}$ factor. This factor depends, next to the relative humidity, on the concrete compressive strength. The higher the strength, the lower the value of the $\varepsilon_{cd,0}$ factor.

The autogenous shrinkage depends, same as the drying shrinkage, on the concrete compressive strength as the only material factor. The autogenous shrinkage increases linearly by a stronger compressive strength.

Drying shrinkage

$$\varepsilon_{cd}(t) = \beta_{as}(t, t_s) \cdot k_h \cdot \varepsilon_{cd,0}$$

Autogenous shrinkage

$$\varepsilon_{ca}(t) = \beta_{as}(t) \varepsilon_{ca}(\infty)$$

$$\varepsilon_{ca}(\infty) = 2.5(f_{ck} - 10) \cdot 10^{-6}$$

2.3.7.2.2 French Recommendations Ultra High Performance Fibre-Reinforced Concretes

The French recommendations give some indicative values for shrinkage for the long term effects (AFGC's Scientific and Technical Committee, 2013). These indicators can be applied in the design phase if nothing is known yet. The indicators for shrinkage depends on the treatment. A separations is made

between no heat treatment and first and second type of heat treatment. The indicative shrinkage values according to AFGC's Scientific and Technical Committee (2013) are:

- **No heat treatment:** 550 $\mu\text{m}/\text{m}$ for endogenous (chemical) shrinkage and 150 $\mu\text{m}/\text{m}$ for drying shrinkage in an outdoor environment with an average relative humidity of about 50 to 70%.
- **Heat treatment of the first type:** 550 $\mu\text{m}/\text{m}$ total shrinkage, for an outdoor environment with a relative humidity of 50 to 70%.
- **Heat treatment of the second type:** total shrinkage of 550 $\mu\text{m}/\text{m}$ before the end of the heat treatment, after which the total shrinkage is nil.

In the appendix of French recommendations some conclusions for autogenous shrinkage are presented:

- After heat treatment there is no autogenous shrinkage
- Autogenous shrinkage increases with a decreasing W/B (water/binder ratio) in the range of very low W/B:
 - o W/B = 0.09 $\epsilon = 250 \mu\text{m}/\text{m}$
 - o W/B = 0.15 $\epsilon = 350 \mu\text{m}/\text{m}$
- Total shrinkage is 550 $\mu\text{m}/\text{m}$ for W/B = 0.17 – 0.20

2.3.7.2.3 Japanese Recommendations for SHCC

The Japanese recommendations show no formulas to determine the shrinkage of SHCC. They recommend to determine the shrinkage based on experimental results, because there are large variations depending on materials used and mix proportions. These experiments should be done according to the JIS (Japanese Industrial Standards). Because the unit water of SHCC tends to be greater than for NSC, larger shrinkage is expected.

2.3.7.2.4 Fibre Reinforced Concrete, Self-Healing Concrete, Geopolymer Concrete and NANO Concrete

For FRC, self-healing concrete, GPC and nano concrete are again no standards or recommendations available to calculate the shrinkage behaviour. The shrinkage of NSSFRC is, depending on the amount of fibres, smaller than the shrinkage of the same mixture without fibres (Chern & Young, 1989). The total shrinkage of HPSFRC is also lower than for HPC (Bywalski, Kaminski, Maszczak, & Balbus, 2015). So the shrinkage of FRC is assumed to be smaller than for the same concrete without any fibres. Again for self-healing concrete is assumed that the shrinkage behaviour is similar to the shrinkage behaviour of NSC, since both has a similar composition and similar mechanical characteristics.

The shrinkage in GPC seems to be very low compared to Portland Concrete. The applied GPC EFC shows after 56 days after casting a drying shrinkage which is almost half of the drying shrinkage of a typical Australian concrete mad with similar sands and aggregates and with the same strength grade. The tests were done according to the Australian Standards (Aldred & Day, 2012). Also other researchers show a low drying shrinkage of GPC. Wallah & Rangan (2006) shows that heat-cured fly ash-based geopolymer concrete undergoes very low drying shrinkage (Wallah & Rangan, 2006). The low drying shrinkage can be explained by the small amount of remaining water in the micro-pores of the hardened concrete. This low water in the pores induced that the drying shrinkage is also very low (Gupta S. , n.d.).

There is some literature about the shrinkage behaviour of nano-concrete. In general, finer pores will increase the shrinkage (Jalal, Fathi, & Farzad, Effects of fly ash and TiO₂ nanoparticles on rheological, mechanical, microstructural and thermal properties of high strength self compacting concrete, 2013).

In finer pores, the capillary stresses will be higher than in small pores, so the autogenous shrinkage will be higher. So the conclusion of Jalala, Fathi, & Farzad (2013) is quite logic. Research to the influence of nano titanium oxide to cement shows an increasing chemical shrinkage for increasing amount of TiO₂ in the cement (Jayapalan, Lee, & Kurtis, 2013).

Taking into consideration the above test results, probably concretes containing nano particles have a higher shrinkage behaviour.

2.3.7.2.5 Shrinkage calculations ACMs

Here the calculations for shrinkage according to Eurocode 2 are shown for concrete class C30/37 and C90/105. In the calculations is assumed that:

- Concrete is situated outside, where the relative humidity is 80%
- $h_0 = 1500 \text{ mm}$

The results of the calculations of C30/37 and C90/105 are shown in Table 20 and Table 21 respectively. In the first column of the tables, is the drying shrinkage calculated and in the second column are the calculation results of the autogenous shrinkage shown. In the last row, the total shrinkage is shown.

Table 20 - Drying and autogenous shrinkage for C30/37 according Eurocode 2

Drying shrinkage	Autogenous shrinkage
$\varepsilon_{cd}(t) = \beta_{ds}(t, t_s) \cdot k_h \cdot \varepsilon_{cd,0}$	$\varepsilon_{ca}(t) = \beta_{as}(t) \varepsilon_{ca}(\infty)$
$\varepsilon_{cd}(t) = \beta_{ds}(t, t_s) \cdot 0.70 \cdot 0.27$	$\varepsilon_{ca}(\infty) = 2.5(f_{ck} - 10) \cdot 10^{-6}$
Where, $\beta_{ds}(t, t_s) = \frac{t - t_s}{(t - t_s) + 0.04 \sqrt{h_0^3}}$	$\varepsilon_{ca}(\infty) = 2.5(30 - 10) \cdot 10^{-6}$
$\varepsilon_{cs} = \varepsilon_{cd} + \varepsilon_{ca}$ $\varepsilon_{cs} = 0.15 + 0.05 = 0.20\%$	

Table 21 - Drying and autogenous shrinkage for C90/105 according Eurocode 2

Drying shrinkage	Autogenous shrinkage
$\varepsilon_{cd}(t) = \beta_{ds}(t, t_s) \cdot k_h \cdot \varepsilon_{cd,0}$	$\varepsilon_{ca}(t) = \beta_{as}(t) \varepsilon_{ca}(\infty)$
$\varepsilon_{cd}(t) = \beta_{ds}(t, t_s) \cdot 0.70 \cdot 0.13$	$\varepsilon_{ca}(\infty) = 2.5(f_{ck} - 10) \cdot 10^{-6}$
Where, $\beta_{ds}(t, t_s) = \frac{t - t_s}{(t - t_s) + 0.04 \sqrt{h_0^3}}$	$\varepsilon_{ca}(\infty) = 2.5(90 - 10) \cdot 10^{-6}$
$\varepsilon_{cs} = \varepsilon_{cd} + \varepsilon_{ca}$ $\varepsilon_{cs} = 0.15 + 0.2 = 0.35\%$	

To determine the drying shrinkage, it is easier to use the method from Figure 30 than calculate the beta-factor from Eurocode since nothing is known about the curing time of concrete. From the figure, a drying shrinkage of 0.15‰ is estimated after 30 years for an environment outside.

The method to determine the drying shrinkage from Figure 30 gives an indication for the drying shrinkage. The method works quite well for the Dutch environment. C30/37 and C90/105 are around the limits of this method, so a relative large difference between the real drying shrinkage and the shrinkage from the method of Figure 30 could be expected.

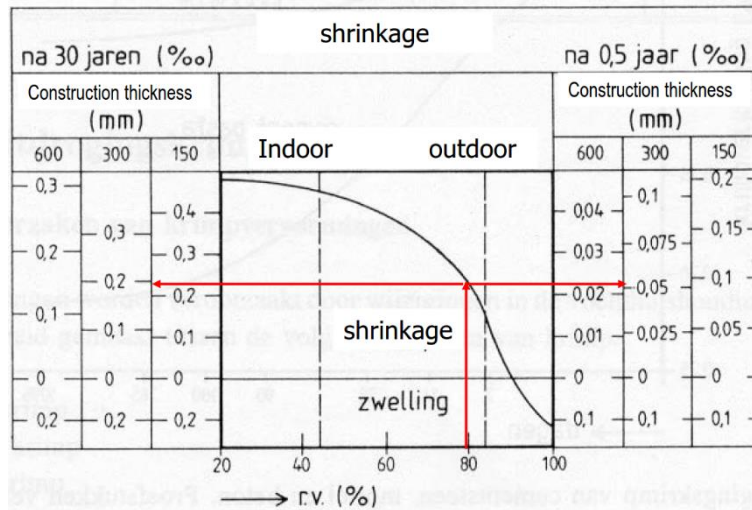


Figure 30 – Method to approximate the drying shrinkage of NSC (Microlab TU Delft, 2014)

2.4 Durability

In this chapter the durability of the chosen ACMs are discussed. The durability of a materials is more or less the service life of the material; the more durable a material is, the longer it could meet its functional requirements. This strongly depends on the resistance of a material against different attacks from the environment. In this chapter the most important attacks on concrete will be described. In this description a distinction will be made between physical attacks and chemical attacks on the concrete and corrosion of the reinforcement steel. In relation with HPC and UHPC expected problem due to the formation of ettringite will also be explained. From the description of these damage mechanisms the parameters will be defined which influence the durability of the material. These parameter will be discussed in some more detail. When the influence of the parameter on the durability of concrete is known, the durability behaviour of the different ACMs can be judged. Before that is done, the reaction of pozzolan additions is clarified.

2.4.1 Physical attack

There are three physical mechanisms included in the research. These mechanisms are abstraction, frost attack and de-icing salts attack. Damage due to de-icing salt or road salt is especially important for infrastructural constructions.

Abrasion

Abrasion is a type of erosion, where solid parts clash or scrape the surface of the concrete. Cement particles and fine and/or soft parts will erode due to solid parts clashing or scraping the concrete. This simple type of erosion depends mainly on the compressive strength of the concrete

Frost

Frost can attack concrete in a physical way by tensile stresses caused by the increase of the specific volume of water in the concrete pores. The volume of the frozen water is about 9% higher than the volume of liquid water with a temperature between 0°C and 8°C. If there is space enough in the concrete for the water to expand, there won't be any problems. But if there is no space in the concrete for water to expand, the frozen water will generate stresses in the concrete. So the main material factors that influence the frost damage of concrete are the porosity and pore diameters of the matrix.

De-icing salt

In the Netherlands as well as in many other countries, roads are de-iced by de-icing salts. These salts can damage the concrete material in a physical ways. The mechanism behind this attack is quite complex, but will be describe briefly in this paragraph.

Damage on concrete will occur if anti-frost salt is scattered over the surface of the concrete, while the water in the concrete is already frozen. The mechanisms which can damage the concrete by the de-icing salts are:

- Increase of water content: due to the hygroscopic characteristics of de-icing salt, a concrete surface with de-icing salt will be wetter than a concrete surface without any road salt.
- Freezing layer by layer; this can result in stress differences between different layers in the concrete.
- Temperature shock; in combination with another mechanism the concrete can be damaged.
- Reduction of the temperature, crystallization pressure and the osmotic pressure.

The exact processes happen in the concrete due to the de-icing in the concrete are not known yet (Reinhardt, 2000). There are some general measures to reduce the damage to concrete:

- Reduction of the diffusion and/or permeability of water.
- Water in the concrete should be free to expand.
- Higher strength of the concrete.

2.4.2 Chemical attack

The chemical attack on the concrete is generally driven by diffusion or permeability of the concrete. Chemical substances can come from the air, water or ground. The most common chemical attacks on concrete are caused by:

- Soft water: leaching of calcium hydrates of the cement.
- Acids: leaching out calcium hydrates or aluminate hydrates, because of the reaction with an acid. The speed of leaching depends on pH-value and refreshing. If there is no refreshing of the acids, the situation will run to a neutral steady state.
- Bases: stronger bases can react with silicates and aluminates by an exchange reaction. The reaction products will leach out.
- Salt can concrete damage in different ways, depending on the type of salt. In the case of concrete damage, the most important salts are:
 - o Chlorides (which can be in road salts): increase the probability of corrosion of the steel bars, more information in 2.4.3 *Corrosion of reinforcement bars*.
 - o Ammonium salt: exchange reaction with the calcium hydrates. The reaction products leach out of the concrete.
 - o Sulphate: reaction with the calcium hydrates which gives the expending reaction product ettringite.
 - o Nitrate: leaching out of calcium silicate hydrates by the reaction with nitrate.
- Alkali-Silica-Reaction (ASR): reaction between sodium oxide (Na_2O), water and silicon ($SiO_2 \cdot nH_2O$), which gives a reaction product ($Na_2SiO_3(n + 1)H_2O$) which doubles the total volume.

2.4.3 Corrosion of reinforcement bars

Corrosion of the reinforcement bars is mainly caused by the carbonation of the concrete or by a the ingress of chlorides into the concrete. Both processes are described briefly.

- Carbonation can be defined as the decrease of the pH-value due to diffusion of carbon dioxide, which reacts with the $\text{Ca}(\text{OH})_2$, $\text{K}(\text{OH})$ and $\text{Na}(\text{OH})$. The carbonation in concrete depends on:
 - o Partial pressure CO_2
 - o Permeability of the concrete
 - o Amount of substances which can carbonate.
- Chloride penetration: de-activation of the passive layer around the iron by chloride ions. This results in active iron, which can corrode easily.

2.4.4 Summary of concrete attack

In Table 22 is a summary given of the above mentioned ways concrete could be damaged during its life time. In the third column of the table are the concrete characteristic given which mainly affect the damage on the concrete from the attack called in the second column.

From the Table 22 can be concluded that the most important concrete characteristics for the durability of the concrete are the permeability and diffusion of the concrete. In the chapter 2.4.6 Penetration and diffusion, these characteristics will be discussed in more detail.

Because the permeability and the diffusion seems to be the main items for the durability of the concrete, the attacks for which permeability and diffusion is an important parameter will be researched in more detail. Damage from ASR will be out of the scope, because this degradation process can already be prevented nowadays by the mixture design. This makes that the degradation processes in the scope of this research includes:

- De-icing salts
- Soft water, acids, bases and salt
- Carbonation
- Chloride penetration

Table 22 - Summary of manners concrete could be damaged

Category	Attack	Concrete characteristic
Physical attack	Abrasion	Compressive strength
	Frost	Porosity
		Pore diameter
	De-icing salts	permeability
		Diffusion
		Compressive strength
Chemical attack	Soft water, acids, bases, salt	Permeability
		Diffusion
	ASR	Permeability
		Sensitivity of aggregate
		Availability of alkalis
	Corrosion	Carbonation
Diffusion		
Chloride		Permeability
		Diffusion

2.4.5 Ettringite

In concrete ettringite can be formed in two ways (Portland Cement Association, n.d.):

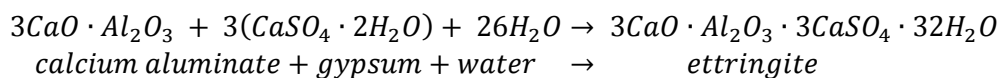
1. Due to the reaction between sulphate from outside the concrete and calcium aluminate from the cement
2. Due to the reaction between gypsum or other sulphate compounds and calcium aluminate from the cement (Delayed Ettringite Formation)

Both will be explained in more detail. First the reason why ettringite is in the concrete will be explained shortly. Then the formation of ettringite formed from sulphates from the environment of the concrete structure will be clarified. At last the formation of ettringite from components from the concrete itself in the hardened phase will be discussed.

General

The reaction between gypsum and cement takes place after some hours after the start of the hydration. This reaction controls the rapid stiffening in the cement. If higher amounts of gypsum react with the calcium aluminate, the early stiffness will be smaller.

The reaction between the calcium aluminate and the gypsum needs water. The reaction product is ettringite. Ettringite has a volume which is seven times the volume of the reaction products. If ettringite is formed when the concrete is hardened, the ettringite will introduce tensile stresses in the concrete matrix. This will probably cause cracks in the concrete. The total reaction of ettringite is:



If all the gypsum has been reacted with the tri-calcium aluminate, the tri-calcium aluminate will react with the previously formed ettringite into a compound called calcium mono-sulphoaluminate. This compound takes up less space than ettringite. Further this compound is stable unless additional sulphates from outside reacts with the mono-sulphoaluminate to reform ettringite again.

Sulphates from outside

As mentioned before, the monosulphoaluminate can retransform in ettringite again if sulphates penetrates into the concrete. Sulphates can penetrate the concrete depending on the diffusion coefficient and the permeability of the concrete. Of course if the concrete is cracked, sulphates can easily penetrate into the concrete. So the diffusion, permeability and crack behaviour of the concrete are the most important properties for the amount of sulphates that penetrate the concrete.

Delayed ettringite formation

It has been known for some time that concrete subjected to early-age temperatures high enough to destroy some or all of the ettringite originally formed can, in the presence of moisture, undergoes deterioration with the reformation of ettringite in the hardened paste system. So if water can penetrate the concrete, ettringite can be reformed again in the already hardened concrete. The term “**delayed ettringite formation**” (DEF) is commonly used to refer to the potentially deleterious reformation of ettringite in moist concrete, mortar or paste after destruction of primary ettringite by high temperature. Such early-age temperatures may result from heat treatment or in extreme cases, from internal heat of hydration.

The temperature conditions for deleterious expansion due to DEF have not been conclusively defined yet. This temperature is affected by factor such as:

- Moisture conditions during heat treatment
- Cement characteristics

- The concrete mix
- Interactive effects of other deterioration mechanisms, such as alkali-silica reactivity, and freezing and thawing.

Based on laboratory tests of mortars, Kelham identified characteristics of cement that show increased sensitivity to heat treatment [Kelham, 1997 and 1999]. When cured at temperatures above 90 °C the following characteristics of cement led to greater expansions in mortars subjected to extended periods (5 years) of moist curing:

- Higher fineness
- Higher amount C_3A
- Higher amount C_3S
- Higher amount alkali (Na_2O_{eq})
- Higher amount MgO

Other factors that have an impact on the DEF are:

- Aggregates; limestone aggregates show better paste-aggregate transition zone, which decrease the DEF.
- Air entrainment reduces expansions as compared to non-air-entrained mortars. It does not prevent DEF, but apparently permits ettringite formation in air voids rather than in confined past pore structure.
- Any deterioration of concrete by freeze-thaw action, alkali-silica reactivity (ASR), or other means, accelerates the rate at which ettringite leaves its original location in the paste to go into solution and recrystallize in larger spaces such as voids or cracks. This is because both, water and space must be present for the crystals to form.

2.4.6 Penetration and diffusion

Penetration and diffusion are both transport mechanism of gas or liquid, and also ions in case of diffusion, through concrete. Penetration of a liquid is driven by pressure differences. The concrete influences the penetration by its permeability. Diffusion is driven by concentration differences. In this case the influence of the concrete is included in the diffusion coefficient, which depends on the type of concrete. The diffusion coefficient has a strong relation with the permeability of the concrete. This means that both, the diffusion and the penetration of concrete depends on the permeability of the concrete. Bothe, the penetration and diffusion in concrete are explained in more detail in the next few paragraphs.

2.4.6.1 Penetration: permeability

The flow of a liquid through a concrete material can be expressed according Darcy's law. In the literature this expression from Darcy is expressed in a few different ways, according to (Reinhardt, 2000) and (Materials Science and Engineering, Division of Engineering, The University of Edinburgh, 2001. Retrieved 13 November 2012) Three different expressions applied a lot in literature will be mentioned here. The first one is the closest to the expression from Darcy:

$$u = k \cdot \frac{\Delta p}{L} \quad \text{eq.(37)}$$

Where,

$$u = (\text{scalar})\text{flow rate} \left[\frac{L}{T} \right]$$

$$k = \text{permeability} \left[\frac{L}{T} \right]$$

$\Delta p = \text{pressure differences over the length } L [L]$

The penetration can also be written as a function of the pressure potential $P = \frac{p}{\rho \cdot g}$, where $\rho = \text{liquid density}$. This pressure potential is equivalent to the hydrostatic head. The rewritten equation, the second way to express the penetration, is:

$$u = -K_s \nabla P \quad \text{eq.(38)}$$

Where,

$u = \text{vector flow rate } [T^{-1}]$

$K_s = \text{the conventional saturated permeability } \left[\frac{L}{T} \right]$

$P = \text{pressure potential } [L]$

The third way to express the permeability of the concrete is with the intrinsic permeability. The conventional saturated permeability and the intrinsic permeability have a linear relation with each other, expressed as:

$$k' = \frac{K_s \eta}{\rho g} \quad \text{eq.(39)}$$

Where,

$k' = \text{intrinsic permeability } [L^2]$

$\eta = \text{fluid viscosity } \left[\frac{M}{T \cdot L} \right]$

$\rho = \text{density of the fluid } \left[\frac{M}{L^3} \right]$

$g = \text{acceleration of gravity } \left[\frac{L}{T^2} \right]$

Depending on the temperature and the type of liquid, the linear relation between both expressions for the permeability can be expressed. For example for water of 25 degrees Celsius, the ratio between the intrinsic permeability and the saturated permeability is equal to: $\frac{k'}{K_s} = 9.103 \cdot 10^{-8} m$ (Materials Science and Engineering, Division of Engineering, The University of Edinburgh, 2001. Retrieved 13 November 2012).

In the above mentioned equations the amount of liquid or the speed of the water penetrating through the concrete, depends on the properties of the water and the properties of the concrete. The properties of the concrete for the penetration of liquid through the concrete are all included in, depending on the expression used, the permeability, conventional saturated permeability or the intrinsic permeability.

Permeability of concrete can experimentally be determined from the penetration of water through the concrete. Therefore, the porosity of the concrete should be known. Valenta expressed the relation between the permeability and the penetration as:

$$k = \frac{x^2 v}{2ht} \quad \text{eq.(40)}$$

Where,

$x = \text{penetration depth [m]}$

$v = \text{porosity of the concrete } \left[\frac{\text{m}^2}{\text{m}^3} \right]$

$h = \text{water column [m]}$

$t = \text{time [s]}$

2.4.6.2 Diffusion: diffusion coefficient

The diffusion in concrete includes the movement of liquid, ions or gas driven by a difference in concentration. The flow through concrete driven by diffusion can be expressed according to the first law of Fick (Reinhardt, 2000):

$$q = -DA \frac{\partial c}{\partial x} \quad \text{eq.(41)}$$

Where,

$D = \text{diffusion coefficient } \left[\frac{\text{L}^2}{\text{T}} \right]$

$A = \text{area the diffusion is working on } [\text{L}^2]$

$C = \text{concentration } \left[\frac{\text{M}}{\text{L}^3} \right]$

The diffusion coefficient includes all the characteristics of the concrete for the diffusion through the concrete. The other variables for the diffusion rate is the concentration difference and the area of diffusion, which are independent of the concrete mix.

Diffusion is one of the most important mechanisms for the transportation of ions through concrete. This transport mechanism is especially interesting for the penetration of chemicals, which can damage the concrete, such as Cl^- , SO_2^{4-} and Mg^{2+} . In the literature diffusion is normally expressed in the diffusion coefficient.

For gasses the diffusion can also be expressed as a function of the partial pressure, using the law of ideal gasses. This turn eq.(41) into eq.(42):

$$q_{gas} = -D \frac{M}{RT} A \frac{\partial p}{\partial x} \quad \text{eq.(42)}$$

Where,

$M = \text{molar mass } \left[\frac{\text{kg}}{\text{kmol}} \right]$

$R = \text{universal gas constant } \left[\frac{\text{J}}{\text{K} \cdot \text{mol}} \right] = \left[\frac{\text{kg} \cdot \text{m}^2}{\text{K} \cdot \text{mol} \cdot \text{s}^2} \right]$

$T = \text{temperature [K]}$

For gas, the term $D \frac{M}{RT}$ is called the permeability for gasses. This makes the dimension of the so called gas permeability equal to seconds [s].

The penetration of gasses into concrete depends, next to the permeability of the concrete, on the moisture content in the concrete. It should be clear that gas will penetrate deeper in a more permeable. Next to that, water in the pores can decrease the gas permeability of the concrete. Before

gas can penetrate the concrete, water should be driven out by the gas. In general, ordinary concrete has a gas permeability in the order of 10^{-12} s.

2.4.6.3 General relation between concrete mixture and permeability

In this paragraph the general relation between the concrete mixture and the permeability of the concrete are given. According to (Reinhardt, 2000), the concrete characteristics and parameters described here which influences the permeability of the mix are:

- w/c ratio
- degree of hydration
- compaction of the concrete
- curing
- type of cement
- aggregate
- connection between the aggregate and the cement

All are described briefly bellow. The most of them are explained in a qualitative way only.

Water-cement ratio and degree of hydration

As mentioned before, the permeability of a concrete mix mainly depends on the porosity of that mix. In Figure 31 is the permeability shown as a function of the porosity. As shown in the figure, the porosity is a function of the water-cement ratio and the degree of hydration. A larger w/c ratio results in a more permeable material. A higher degree of hydration results in a less permeable system.

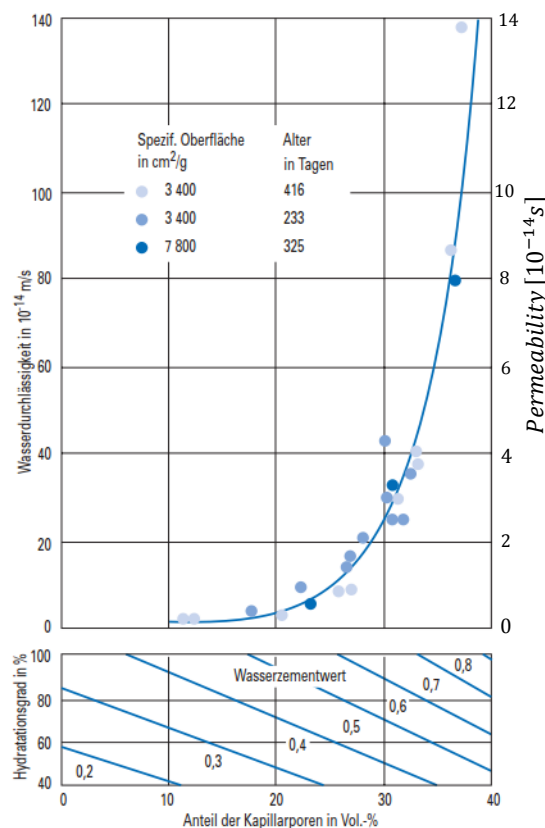


Figure 31 - Relation between the permeability and the porosity of cement (Verein Deutscher Zementwerke e.V., 2002)

Compaction of concrete

A concrete which is very compact, will have a lower permeability. For example the addition of silica fume to concrete, especially in combination with a super plasticiser, can significantly decrease the permeability of concrete (Reinhardt, 2000).

Curing

The curing of the concrete can have a significant influence on the permeability of the concrete. As shown in Table 23, if the concrete hydrates in a dry environment the permeability can be significant lower compared with environment with a high moisture.

Table 23 - permeability for air depending on the curing conditions (Reinhardt, 2000)

Curing	$k \left[10^{-12} \frac{m}{Ns} \right]$	$k \left[10^{-12} s \right]$
Hydrated 1 week at 105°C	1.95	2.40
Hydrated in a 57% moisture environment	0.43	0.53

Type of cement

The type of cement can have influence on the permeability of concrete. For example the chloride permeability of CEM III/A can be very effective to reduce the chloride permeability of concrete. (Guneysi, Gesoglu, Ozturan, & Ozbay, 2009)

Aggregate and the connection between the aggregate and the cement

The adjustment of aggregates to cement generally increases the permeability of the mix. This is caused by the relative weak interfacial zone between the cement and the aggregate. In Figure 32 is shown how an increasing amount of sand, increases the permeability of the mix.

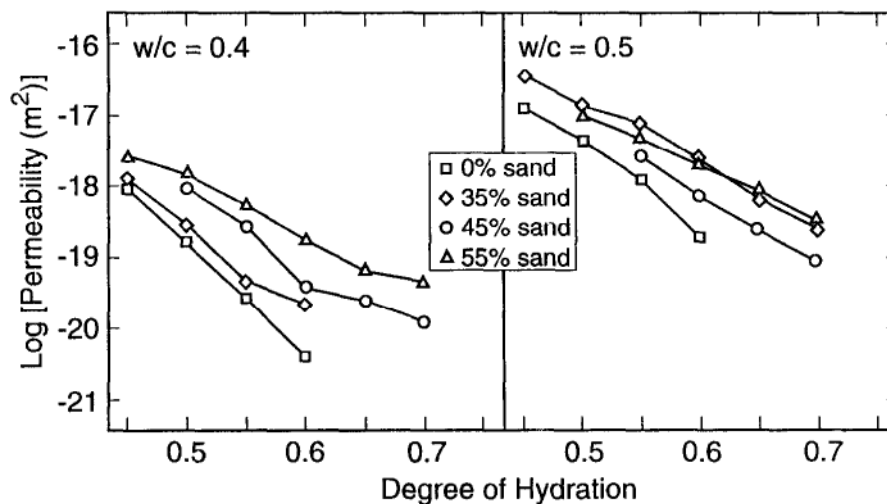


Figure 32 – The relation between the permeability and the amount of sand in concrete for different w/c ratios as a function of the degree of hydration (Halamickova & Detwiler, 1995)

It is obvious that the connection between the aggregate and the cement has influence on the permeability of the concrete. As known a light weight aggregate has a better connection with the cement than a normal weight aggregate, since the cement can penetrate a bit in the LWA. In the case of a LWA, the interfacial zone will probably be less permeable.

2.4.7 Pozzolan material

In the in-depth analysis to different degradation processes, a lot of pozzolan additions will be discussed. Therefore, a general description of the pozzolan working will be given here. Pozzolan additions to concrete can significantly influence the durability of the concrete in a positive way. Pozzolan material are responsible for two important mechanism during hardening:

- The reduction in the portlandite (CH) produced by cement hydration
- The densification of the microstructure of the hardened cement paste matrix

From a durable point of view, the reduction of portlandite is generally a negative effect and the densification of the microstructure is a positing effect. The reduction of portlandite is caused by the chemical reaction with the pozzolan material. In fact, this reaction is the reason that the microstructure of the matrix becomes denser. In the end, the positive effect of the denser structure is more effective than the reduction of portlandite. So in the end the addition of pozzolan material to the concrete generally has a positive effect on the durability of the concrete.

2.4.8 In depth analysis degradation processes

In this paragraph are the degradation processes of this research described in more detail. Every attack is explained and some models are given. For every process is also the influence given of certain additions, such as fly-ash or silica fume. Before the description of the degradation processes, an overview of the influences of different additions is given in Table 24. The degradation processes included in the scope of this research again are:

- De-icing salts
- Soft water, acids, bases, salt
- Carbonation
- Chloride

Table 24 – Influence of different concrete ingredients on the degradation processes of the scope of the research

		cement				aggregate		Additives								
		Decrease w/c ratio	Substitution of Portland by Blast Furnace Slag (CEM III)	CEM Type V	Aluminium cement	Increasing amount of C_3A	Increasing coarse aggregate	Increasing fine aggregate	Addition of Limestone	Addition of fly ash	Addition of glass powder	Addition of silica fume	Addition of natural zeolite	Addition of metakaolin	Air-entraining	Addition of PP fibres
De-icing salts															Slightly	
	permeability	Denser structure and pore distribution						Denser structure		Denser structure if aggregate is substituted		Densifying microstructure and ITZ	Improvements in pore volume and pore distribution			
	Diffusion															
	Compressive strength	Increase strength														Reduction strength
	Additional effects								Positive or negative effect, depending on type of cement			Low degree of saturation due to self-desiccation during hydration				Space for ice forming
Soft water, acids, bases, salt																
	Permeability	Denser structure and pore distribution	Denser structure						Reduction of permeability because limestone is finer than OPC			Denser structure	Improvements in pore volume and pore distribution	Reduction of pore size and improved ITZ binding		
	Diffusion	Denser structure and pore distribution	Pore structure													
	Additional effect			Low C_3A content		Direct reaction with sulphate			- increased capacity to consume more aggressive acid - substitution of OPC, reduction of portlandite	Reduction of C_3A and calcium hydroxide		Reduction of C_3A and calcium hydroxide		Reduction calcium hydroxide		
carbonation														After some time only	Depending on circumstances	
	Permeability	Improvements pore volume and distribution	Improvements pore volume and distribution				Longer and more tortuous path for CO_2	Probably decreases the tortuosity		Densifies microstructure		Reduction due to fineness of silica fume	Improvements pore volume and distribution	Lower porosity		
	Diffusion															
	Portlandite		Reduction of portlandite							Reduction of portlandite		Reduction of portlandite	Reduction of portlandite	Reduction of portlandite		
	Additional effects		More sensitive for curing													
Chloride																
	Permeability	Decrease of porosity	Binding of chlorides			Binding of chlorides			Can reduce permeability in combination with another addition	Binding of chlorides	Refinement		Decrease	Smaller average pore diameter and lower porosity		
	Diffusion		Binding of chlorides			Binding of chlorides				Binding of chlorides	Higher alkali	Decrease of chloride binding	Decrease			
Additional effects			More sensitive for curing										Long-term curing			
		Decrease w/c ratio	Substitution of Portland by Blast Furnace Slag (CEM III)	CEM Type V	Aluminium cement	Increasing amount of C_3A	Increasing coarse aggregate	Increasing fine aggregate	Limestone	Addition of fly ash	Addition of glass powder	Addition of silica fume	Addition of natural zeolite	Addition of metakaolin	Air-entraining	Addition of PP fibres

Green = positive effect on the durability. So reduction of the permeability, diffusion, ...

Red = negative effect on the durability. So increase of the permeability, diffusion, ...

Orange = positive and negative effect under certain circumstances on the durability

Blue = not enough data found to judge

2.4.8.1 De-icing salts

De-icing salts can damage the concrete in a physical way. The most important mechanisms caused by de-icing salts with damage as a consequence are;

- **Increase of water content:** due to the hygroscopic characteristics of de-icing salt, a concrete surface covered with de-icing salt will be wetter than a concrete surface without any road salt.
- **Freezing layer by layer:** due to de-icing agents, a stress differences between different layers in the concrete can be generated. The idea of freezing layer by layer is schematically shown in Figure 33
- **Temperature shock:** in combination with another mechanism the concrete could be damaged.
- **Reduction of the temperature, crystallization pressure and the osmotic pressure.**

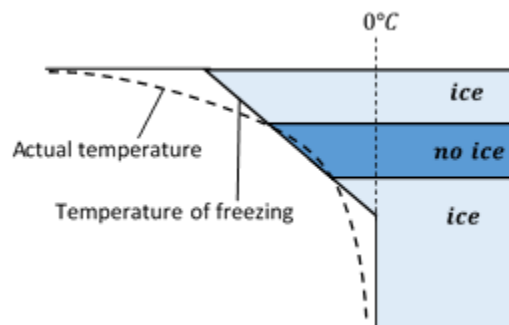


Figure 33 - Schematisation of freezing layer by layer

One of the most important material parameters according to damage caused by de-icing salt is the moisture content in the concrete. The moisture content in concrete mainly depends on the permeability of concrete. Freezing of the water in combination with de-icing salts can generate stresses that damage the concrete, due to the thermal expansion of the water. This is illustrated in Figure 34, where the thermal expansion is shown as a function of the temperature for different relative humidities. The solid line shows the thermal expansion during cooling and the dashed line the expansion during heating. During heating the expansion of water is larger than during freezing, what

can result in stresses that damage the concrete. In general, every measure that reduces the water penetration prevents the physical damage to concrete. (Reinhardt, 2000)

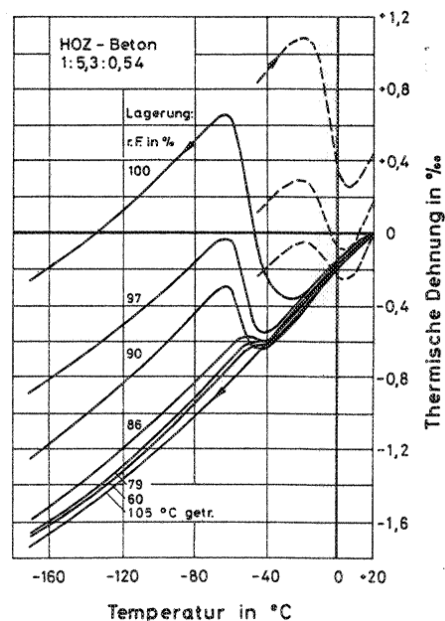


Figure 34 - Thermal expansion as a function of the temperature for different relative humidities (Wiedemann, 1982)

Now the mechanisms behind damage caused by de-icing salt are described in some more detail, the influence of different changes in the concrete mixture are illustrated. Some literature research is done to the most important changings of the concrete mix design according to minimize the physical damage caused by de-icing salts. Probably not all possibilities to minimise the damage are mentioned, but probably the most important additives are there.

W/C ratio: the water cement ratio has a direct influence on the pore spacing and the distribution of the pores, so this ratio influence the permeability. To have a low permeable concrete, the w/c ratio should be low as well. So a low w/c ratio can reduce the damage of concrete.

The addition of **BFS** decreases the resistance against de-icing salts. From research can be conclude that concrete containing both, PC and BFS, has a worse resistance against de-icing salts compared to concrete containing PC only (Vejmelková, et al., 2015)

Aggregate: the damage on the aggregate depends on the porosity of it, compared with the porosity of the cement. Smaller pores attract more water, so if pores in aggregate are smaller than in the cement, the aggregate will be damaged first, and the other way around. (Reinhardt, 2000)

Fine aggregate or additions: in general fine addition can increase the resistance against damage caused by de-icing salts, because it makes the concrete denser. In a denser concrete, it is harder for water to penetrate in. (Reinhardt, 2000)

Limestone aggregate can improve the resistance against de-icing salts. The resistance can be improvement in combination with CEM II/B-W. It worsens the resistance of blended cement CEM II/B-M(W-V) and CEM V/A(S-W). And at last it has no influence on scaling resistance of concrete made of CEM I. (Dabrowski & Glinicki, 2012)

Addition of **Fly ash** can successfully increase the resistance against de-icing agents. Other ingredient can be substituted by fly ash. The effect of fly ash depends on the ingredients that are substituted by fly ash (Mardani-Aghabaglou, Andiç-Çakir, & Ramyar, 2013). For example:

- Substitution of aggregate by fly ash increases the resistance to freezing and thawing action, most likely due to an improved impermeability, which is the result of a better compatibility.
- Substitution of Portland cement by fly ash decreases the resistance to freezing and thawing action.

Addition of **Silica Fume** can decrease the damage (Khana & Siddique, 2011):

- Silica fume thanks its excellent frost resistance performance to a low degree of saturation due to self-desiccation during hydration.
- Concretes made with 10% or 15% silica fume and a water–cementitious materials ratio of 0.45 had barely acceptable resistance to salt-scaling. Resistance to salt scaling correlated well with the water/cement ratio.
- Moderate additions of silica fume seems to densify the ITZ of the microstructure.

Zeolite can increase the resistance as well. The frost resistance and de-icing salt resistance of zeolite containing mixes with an up to 20% cement replacement level is better than the reference mix. Higher zeolite dosage appeared as quite unsatisfactory. This was an apparent consequence of the significant improvements in both total pore volume and pore distribution (Vejmelková, et al., 2015).

As last addition the effect of **metakaolin** on the concrete will be described. Metakaolin has a small influence on the resistance of concrete against de-icing salts. Vejmekova et al. described that the resistance against de-icing salts for concrete containing metakaolin is slightly worse (Vejmekova, et al., 2010).

Air-entraining can increase the resistance against de-icing salts. Relative large air bubbles will interrupt capillary suction, such that the concrete mix will have a high resistance against the action of de-icing agents (Reinhardt, 2000), (Deja, 2003).

Addition of **polypropylene fibres** highly effect the resistance against de-icing salt (Deja, 2003). The reason for this is probably the larger tensile strength of concrete due to the fibres.

2.4.8.2 Soft water, acids, bases and salt

The chemical attack of the concrete by soft water, acids, bases and salt can generally be described in the same paragraph, because of the similarities between them. In general, the concrete parameters that influence the damage on the concrete in a chemical way are (Reinhardt, 2000):

- Type of cement
- W/C factor
- Cement content
- Addition of pozzolan material in general
- Aluminium cement
- Addition of silica fume

The addition of **silica fume** (SF) or **blast furnace slag** (BFS), can increase the resistance to sodium sulphate attack (Al-Amoudi, 2002). Both materials, SF and BFS, have a pozzolan working during hardening of the concrete. This pozzolan mechanism is described in more detail in chapter 2.4.7 Pozzolan . In short, the two mechanisms during hardening caused by the pozzolan character are:

- The reduction in the portlandite (CH) produced by cement hydration
- The densification of the microstructure of the hardened cement paste matrix.

Next to the blended cement types with SF and BFS, **CEM V** contributes to a higher resistance against sulphate attack. The reason for this is the low amount of **C₃A** in CEM V compared to CEM I. In cements

with a relative high amount of C_3A , exposed to sodium sulphate environments, ettringite formations leading to expansion and cracking is the major form of concrete deterioration. (Al-Dulaijan, et al., 2003)

Limestone can also have a positive influence on the resistance against acids. Three important factors attributed to this better resistance are (Senhadji, Escadeillas, Mouli, Khelafi, & Benosman, 2014):

1. Limestone filler is much finer than OPC, such that it fills the micro-pores in cement mortar. The ability of mortar to resist nitric and sulphuric acids attack was improved due to the reduced permeability and porosity.
2. The presence of a high calcium carbonate ($CaCO_3$) content increased the capacity of limestone mortars to consume more aggressive acid.
3. The decreased proportion of cement reduces the portlandite (CH) content.

Metakaolin is also a pozzolan material that improves the durability by improving the micro-structure of concrete by (Asbridge, Jones, & Osborne, 1996):

- Reduction of the average pore size
- Reduction of the calcium hydroxide levels
- Improving the bonding between cement paste and aggregate

Also **natural pozzolan** has a pozzolanic character during hardening of the concrete. Again the permeability of the concrete and the amount of alkali present both decrease, what has a positive influence on for example the chemical resistance to nitric acid attack (Senhadji, Escadeillas, Mouli, Khelafi, & Benosman, 2014).

The fineness of natural pozzolan can significantly affect the expansion rate of mortars. Partial replacement of cement by a finer pozzolan can control or even eliminate the DEF expansion. This positive effect was explained by the higher pozzolanic activity of fine pozzolan particles. At the contrary, the substitution of cement with coarse pozzolan was not only ineffective but even accelerated the DEF expansion (Nguyen, Leklou, Aubert, & Mounanga, 2013).

Vejmelková et al. describe that the use of **zeolite** in the blended binders exhibit a clear positive effect on the resistance against Na_2SO_4 , $MgCl_2$ and NH_4Cl . This is an apparent consequence of the significant improvements in both total pore volume and pore distribution. (Vejmelková, et al., 2015)

2.4.8.3 Carbonation

Corrosion of the reinforcement bars is mainly caused by the carbonation process or by a combination of corrosion and chlorides. In practice, the carbonation depth can be expressed as a function of time. The depth is found to be linear with the square hood of the time, as shown in eq.(43)

$$X_c = k\sqrt{t} \quad \text{eq.(43)}$$

Where, $X_c = \text{carbonation depth [m] at } t = \text{time [s]}$;

In practice, the k-factor of a certain concrete is measured by experiences. Knowing the k-factor, the carbonation depth can be extrapolated over time. The k-factor can also be modelled as (Younsi, Turcry, Aït-Mokhtar, & Staquet, 2013):

$$k = \sqrt{\frac{2D_{CO_2}[CO_2]}{[CH]}}; \quad \text{eq.(44)}$$

Where,

D_{CO_2} = effective diffusion coefficient of carbon dioxide $\left[\frac{m^2}{s}\right]$;

$[CO_2]$ = molar concentration of carbon dioxide in gas phase in contact with concrete $\left[\frac{mol}{m^3}\right]$;

$[CH]$ = molar concentration of Portlandite in the concrete $\left[\frac{mol}{m^3}\right]$;

According to Younsi, Turcry, Ait-Mokhtar & Staquet (2013), the effective diffusion coefficient of carbon dioxide can be expressed as:

$$D_{CO_2}(\phi, S_1) = \phi(1 - S_1)\tau D_{Air,CO_2} \quad \text{eq.(45)}$$

Where,

D_{AIR,CO_2} = diffusion coefficient of CO_2 in the air;

ϕ = porosity;

S_1 = water saturation degree;

τ = parameter to model tortuosity;

As shown in the model, the coefficient k depends on some concrete characteristics and the environment. From the formula can be concluded that the speed of the carbonation can be influenced by the next concrete characteristics:

- Permeability of the concrete
- Diffusion coefficient
- Molar concentration of Portlandite

Substitutions or additions mostly influence the carbonation in more than just one way. For example the substitution of cement by fly-ash has consequences on the permeability of the concrete as well as for the molar concentration of Portlandite. The consequences of modifications on the concrete mixes for the carbonation are listed here and explained briefly.

Of course the **water-cement ratio** again affects the speed of the carbonation. A low water-cement factor will result in a low permeability, as long as the workability of the fresh concrete is above a certain minimum level.

Substitution of Portland cement by **fly-ash** or **blast furnace** will reduce the carbonation, due to their pozzolanic character. The addition of fly-ash or blast furnace has a few consequences (Younsi, Turcry, Ait-Mokhtar, & Staquet, 2013), (Müllauer, Beddoe, & Heinz, 2015):

- Substitution of Portland cement by fly-ash or BFS will reduce the permeability due to densifying the mortar.
- Substitution of Portland cement by fly-ash or BFS will reduce the amount of dissolvable alkalis (Portlandite) that can release.
- High substitutions, especially BFS substitutions, make the concrete more sensitive to water curing.

The carbonation depth decreases with an increasing **aggregate volume** fraction, probably because aggregate is more impermeable than cement. Further, more coarse aggregate proved a longer and more tortuous path for CO_2 distribution (Huang, Jiang, Zhang, Gu, & Dou, 2012)

Next to the volume of the aggregate, the carbonation depth is influenced by the **aggregate size**. The carbonation depth decreases with an increasing proportion of smaller aggregates. This could possibly

be because small aggregates have a larger surface area for an identical volume fraction, thus increases the tortuosity. (Huang, Jiang, Zhang, Gu, & Dou, 2012)

Silica fume can influence the carbonation of concrete due to its pozzolanic characteristic. The influence of silica fume depends on the amount of silica fume added to the mixture. Different amounts of silica fume result in different resistances against carbonation (Kulakowski, Pereira, & Molin, 2009):

- For concentrations of additions below 10%, silica fume increases the resistance to carbonation-induced corrosion even though it increases carbonation depth.
- In concrete preparations with 10% silica fume there is an increase in carbonation depth, but silica fume will not affect carbonation-induced corrosion.
- When the concentration of silica fume is above 10%, it not only increases carbonation depth but it also increases the variation in the intensity of carbonation-induced corrosion, particularly for higher w/b ratios.

Zeolite influences the carbonation resistance in a positive way. Vejmelková et al. describe that the carbonation resistance can increase for zeolite contents up to 20%. A zeolite content higher than 20% will slightly decrease the resistance (Vejmelková, et al., 2015).

Another research shows that the carbonation depth of mortars containing zeolite (clinoptilolite) is higher than in the control mortar at early ages. However, this negative effect disappeared at longer term ages depending on the pozzolanic reactions (Bilim, 2011).

Metakaolin influences the carbonation depth due to its pozzolanic reaction during hydration. In short the metakaolin is responsible for:

- A more permeable concrete
- Reduction of portlandite

Different researches have different conclusions according the exact influence of the metakaolin on the carbonation depth. Some conclusions are:

- Metakaolin reduces the carbonation depth (Bai, Wild, & Sabir, 2002)
- In alkali silicate-activated GBFS/MK mortars, the incorporation of MK leads to an increase of the carbonation (Bernal, Gutierrez, Provis, & Rose, 2010).
- Accelerated carbonation testing shows rather rapid carbonation accompanied by a loss in strength. This occurs faster at a higher metakaolin content, but the full interpretation of the test data also requires consideration of the evolution of the sample structures during the long duration of the tests (Bernal, Gutierrez, Provis, & Rose, 2010).

2.4.8.4 Chloride

Normally, steel reinforcement can't corrode due to the high pH value in concrete that forms a protecting layer around the steel. However, chlorides can passivate the protecting layer around the reinforcement steel, such that the reinforcement can corrode independent of the value of the pH. Chloride can be present in the concrete from casting or can penetrate the concrete by diffusion or penetration. Transport of chlorides by diffusion is quite a slow process.

To prevent corrosion by chlorides, the chloride content should be minimised. This can be done in three way.

1. No or at least a minimum amount of chlorides in the concrete composition
2. A concrete with an as low as possible permeability
3. A concrete with an as low as possible diffusion coefficient

Chlorides will always be present in the composition of concrete. There is often some chloride in water, aggregates or additives. As long as the amount of chloride in the concrete mix is minimized to a certain minimum, it probably won't give any problems.

A lower **w/c factor** increases the ingress of chlorides, because a lower w/c factor decreases the permeability of the concrete (Reinhardt, 2000).

The **w/b ratio** of concrete has small effect on the chloride binding capacity of concrete exposed to a marine environment (Cheewaket, Jaturapitakkul, & Chalee, 2010).

A higher **cement content** binds more chlorides, so a high cement content decreases the penetration of chlorides (Reinhardt, 2000). Research of Locher and Sprung (1970) proved that there is a negative linear relation between the logarithm of the penetration and the cement content over the porosity and the square hood of time (Locher & Sprung, 1970). The porosity of course has a strong relation with the permeability of the concrete. The relation from Locher and Sprung is shown in the graph of Figure 35.

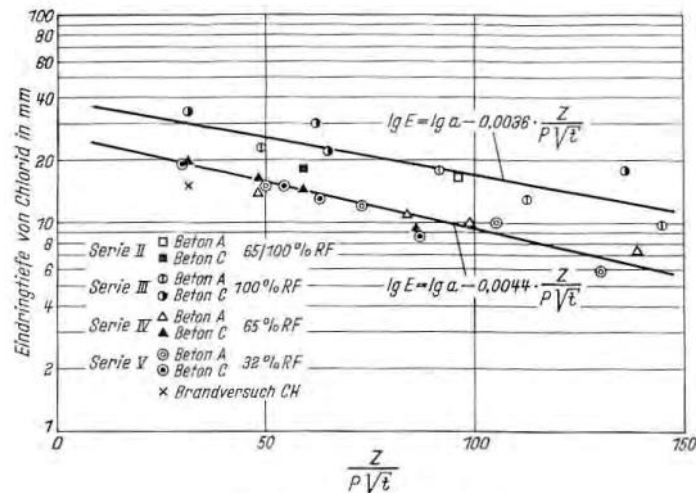


Figure 35 - penetration depth of chloride ions in concrete as a function of the cement content (Z), volume of the pores (P) and the time (t) (Locher & Sprung, 1970)

In general, concrete with **BFS** has a higher diffusion resistance compared to concrete with PC. So the ingress of chlorides in BFS concrete is normally lower. This is caused by the finer pores of the BFS concrete (Reinhardt, 2000). The replacement of cement by **ground granulated blast furnace slag (GGBFS)** increases the chloride binding capacity of cement-based materials (Orellan Herrera, Escadeillas, & Arliguie, 2006).

C₃A (tricalcium aluminate) plays the most important role in chloride binding. In a lesser extent, C₃S, C₂S and C₄AF contribute to chloride binding as well (Yuan, Shi, Geert, Audenaert, & Deng, 2009). A high binding capacity results in a higher concentration gradient and a smaller penetration depth (Reinhardt, 2000). The treatment efficiency seems to be unaffected or only slightly affected by C₃A content because the “physically” bound chloride can be released during treatment. (Orellan Herrera, Escadeillas, & Arliguie, 2006)

Limestone can influence the chlorides ingress positive or negative depending on the concrete mixture. Different researches show that:

- For w/b ratio of 0.6, the chloride ion permeability factor increases with an increasing amount of limestone filler. (Ghrici, Kenai, & Said-Mansour, 2007)

- The addition of limestone powder shows a similar 28-day RCP value as for plain concrete. (Hieu & Neithalath, 2010)
- The addition of limestone in combination with another addition, for example natural pozzolan or silica fume, can decrease the chloride permeability. (Hieu & Neithalath, 2010)

Fly ash as a pozzolan material, can increase the chloride resistance. The next description from the literature shows how fly ash increases the durability in terms of certain chemical attacks.

- The addition of fly ash or replacement of cement by fly ash increase the chloride binding capacity of cement-based materials (Orellan Herrera, Escadeillas, & Arliguie, 2006), (Cheewaket, Jaturapitakkul, & Chalee, 2010)
- RCP values are lower if fly ash is added to the concrete, due to refinement of the microstructure. (Jitendra & Neithalath, 2010)
- Unprocessed fly ash can increase the resistance to chloride ingress by a factor 2 to 4 (Dhir & Jones, 1999)
- Processed fly ash can increase the chloride ingress resistance by a factor 5. (Dhir & Jones, 1999)

Fly ash could also be combined with another additions. Dhir and Jones report that:

- The addition of a **combination of fly ash and silica fume** can reduce the chloride ingress by a factor 6. (Dhir & Jones, 1999)
- The addition of a **combination of fly ash and metakaolin** can reduce the chloride ingress by a factor 7. (Dhir & Jones, 1999)

The presence of a higher alkali content in **glass powder** and refinement of the microstructure, the glass powder modified concretes demonstrated similar or lower RCP values as compared to fly ash modified concretes of the same replacement level (Jitendra & Neithalath, 2010).

Silica fume decreases the chloride binding (Orellan Herrera, Escadeillas, & Arliguie, 2006). It was found that the use of silica fume markedly enhances the resistance of concrete mixtures against chloride diffusion (Dousti, Rashednia, Ahmadi, & Shekarchi, 2013)

It was found that the utilisation of **natural zeolite** markedly enhances the resistance of concrete mixtures against chloride diffusion (Dousti, Rashednia, Ahmadi, & Shekarchi, 2013).

The addition of **metakaolin** (MK) can have a significant positive influence on the durability of concrete according to the chloride penetration. This effect is probably caused by the smaller average pore diameters and the lower porosity (Poon, Kou, & Lam, 2006). Some other results from literature are:

- Reduction of the non-steady state chloride migration coefficient and an enhancement of the chloride penetration resistance by more than two classes. (Badogiannis, Sfikas, Voukia, Trezos, & Tsivilis, 2015)
- The MK replacement has the most significant effect on the chloride permeability. (Abouhussien & Hassan, 2015)
- Comparing the optimum Self Compacting Concrete mixture containing MK to Normal Concrete mixtures and mixtures containing Fly Ash, Silica Fume or Slag show that the 20% MK mixture exhibited the lowest chloride permeability. (Abouhussien & Hassan, 2015)

Due to **carbonation** of concrete, the chloride binding capacity of concrete decreases until zero. So due to carbonation all the chloride in the concrete can be dangerous for corrosion. (Reinhardt, 2000)

2.4.9 Durability of the Advanced Cementitious Materials

After determining the most important degradation mechanisms and the influence of different ingredient on the durability of a mixture, the durability of the ACMs can be determined. To quantify the durability of the ACMs, the water permeability, chloride diffusion coefficient and the carbonation depth is determined with the knowledge from literature. The conclusions of this study are shown in Table 25, where the durability characteristics of the ACMs are shown. The durability characteristics of nano concrete is determined qualitatively, because there is not enough knowledge available to describe nano concrete in a quantitative way. In the rest of this paragraph, the table is discussed in detail.

Table 25 is horizontally split up in two parts, the upper part contains the three durability characteristics (water permeability, chloride diffusion coefficient and the carbonation rate of passive reinforcement) and a lower part where some practical usage for the chloride penetration and the carbonation of the different ACMs are given. These practical usage are calculated in the next paragraphs.

In Table 25 are again some values marked. The bolded values are values that are significant more favourable than the values of NSC.

Some advanced concrete materials are explain is more detail. GPC has quite unique durability characteristics, so this material is explained in more detail. Also the durability characteristics of SHCC are explain in more detail, because of its unique durability character when it is deformed. Both nano concretes are described in more detail because they are judged in a qualitative way.

In durability of the ACMs is determined for the situations that the ACMs are uncracked. As mentioned before, the durability of uncracked FRC is assumed to be similar to uncracked concrete without any fibres. So the durability characteristics of NSC and HPC are also valid for uncracked NSSFRC and HPSFRC. Since the crack width is reduced compared to concrete without fibres, the durability of cracked FRC will also be better than for cracked concrete without fibres. In paragraph 2.4.9.6 Cracked concrete is the relation between the crack width and the permeability shown.

The same thing is valid for SHCC. As shown in Table 25, the durability of SHCC seems similar to the durability of NSC. However, the crack width of SHCC is very limited, so in practice, the durability of SHCC could be expected a lot higher than the durability of NSC. This is discussed further in paragraph 2.4.9.1 SHCC.

In literature nearly nothing is reported about the durability of self-healing concrete when it is uncracked. Since the mechanical characteristics of self-healing concrete are almost the same as for NSC, it is assumed that the durability of uncracked self-healing concrete is also comparable to NSC. If self-healing concrete cracks heal. The durability characteristics of healed concrete could almost recover to the durability characteristics of uncracked concrete. This will be explained further in chapter 2.4.9.2 Self-healing concrete.

Table 25 - Durability characteristics per ACM at 28 days after casting

Concrete characteristic	Unit	Quantitative							Qualitative		
		Plain	ACM 1.	ACM 2.	ACM 3.	ACM 4.	ACM 5.	ACM 6.	ACM 7.	ACM 8.	ACM 9.
		NSC	NSSFRC	HPC	HPSFRC	UHPC	SHCC	Self-Healing	GPC	Self-cleaning concrete	Self-sensing concrete
Water permeability	[10 ⁻¹⁴ m/s]	100-10,000 ^a	100-10,000 ^a	10-100^b	10-100^b	0.4-0.5^c	5,000 ^d	100-10,000 ^e	40-5,000 ^{f,**}	+ ^{j,k}	+ ^g
Chloride diffusion coefficient	[10 ⁻¹² m ² /s]	>4 ^{k,*}	>4 ^{k,*}	<5 ^{b,k,*}	<5 ^{b,k,*}	<0.1 ^{k,*}	6.8 ^h	>4 ^{e,*}	<<1 ^l	+ ^{j,k}	+ ^k
Carbonation rate of passive reinforcement	[μm/year]	1.2 ^k	1.2 ^k	0.25^k	0.25^k	< 0.01 ^k	1.2^l	1.2 ^e	N/A	- ^k	unknown
Critical chloride depth after 50 years for above mentioned chloride diffusion coefficients (limit values)	[mm]	>14	>14	<16	<16	<2	22	>14			
Chloride diffusion coefficient for calculation	[10 ⁻¹² m/s ²]	8	8	2	2	0.1	6.8	8			
Critical chloride depth after 50 years by mean chloride diffusion coefficients	[mm]	19	19	10	10	2	22	19			
Carbonation depth after 50 years in an 'exposed' environment	[mm]	22.5	22.5			<3.8	22.5	22.5			
Bolded values are positive compared to NSC											

- * The chloride diffusion coefficients that are given in the table are indicative values that represent NSC, HPC and UHPC as good as possible. Probably, mixture could be made with a chloride diffusion coefficient that belong to the HPC group, but with compressive strength that belongs to the NSC group. However, the values of an ACM type are chosen such that they cover most for materials that belong to that ACM type based on mechanical characteristics. For example, most NSC mixtures will have a chloride diffusion coefficient higher than 4. The chloride diffusion coefficients of a group are just made quantitative to compare different type of ACMs to each other. The same is valid for HPC and UHPC. Probably, there are also mix design that have HPC or UHPC characteristics but a chloride diffusion coefficient higher than 5 or higher than 1 respectively.
- ** The water permeability of GPC is in quite a large range. There is not a lot of literature available according to the water permeability of GPC. The thing is that the water permeability is high in proportion to the better researched chloride diffusion coefficient. Earlier in this research is shown that the chloride diffusion coefficient depends, like the water permeability, for example on the permeability of the concrete. By combining both, reasons could be given that a lower water permeability could be expected.

Qualitative characteristics

- + positive influence on the durability, so a lower water permeability, chloride diffusion coefficient or carbonation depth compared to NSC
- +/- no positive or negative influence on the durability, so nearly no different water permeability, chloride diffusion coefficient or carbonation depth compared to NSC
- negative influence on the durability, so a higher water permeability, chloride diffusion coefficient or carbonation depth compared to NSC

In Table 26, a comparison is given between the critical chloride penetration depth after 50 years and the carbonation depth after 50 years, assuming different chloride diffusion coefficients for different types of concrete. The assumed diffusion coefficients are done within the limits of Table 25. The carbonation depth of NSC is calculated by k-value according to Lagerblad (2006), explain in more detail in chapter 2.4.9.8 Carbonation profiles. The comparison shows that for concrete in sheltered or indoor conditions, the carbonation depth is governing for every type of concrete. However, according to (Ottel , 2015) the chloride penetration is assumed to be critical over the carbonation depth.

Table 26 – Comparison between chloride penetration and carbonation depth

	Assumed chloride diffusion coefficient 10 ⁻¹³ [m/s ²]	Critical chloride penetration 50 years [mm]	Carbonation depth after 50 years [mm]				
			wet	Buried	exposed	Sheltered	Indoors
NSC (C30/37)	80	19	5.3	7.1	10.6	28.3	42.4
HPC (C90/105)	20	10	3.75 ^e	5 ^e	7.5 ^e	20 ^e	30 ^e
UHPC (C170/200)	1	2	0.8 ^e	1.1 ^e	1.7 ^e	4.5 ^e	6.7 ^e
SHCC	68	22					

^a (Tayeh, Bakar, Johari, & Voo, 2012), (Breyse & Gerard, 1997), (Liu, Chia, & Zhang, 2011), (Wang, Jansen, Shah, & Karr, 1997)
^b (Majorana, Salomoni, Mazzucco, & Khoury, 2010), (Gupta, et al., 2008)
^c (fib, 2009)
^d (Lepech & Li, 2005)
^e Assumptions done, further discussed in the rest of the chapter
^f (Olivia & Nikraz, Strength and water penetrability of fly ash geopolymer concrete, 2011), (Cheema, Lloyd, & Rangan, 2009)
^g Assumptions done, further discussed in the rest of the chapter

^h (Li V. C., Engineered Cementitious Composites (ECC) – Material, Structural, and Durability Performance, 2007)
ⁱ (Yang, Yao, & Zhang, 2014), (Chindaprasirt & Chalee, 2014), (Aldred J. M., 2013)
^j (Jalal, Ramezani-pour, & Pool, Split tensile strength of binary blended self compacting concrete containing low volume fly ash and TiO₂ nanoparticles, 2013)
^k (AFGC's Scientific and Technical Committee, 2013)
^l (Japan Society of Civil Engineers, 2008)

2.4.9.1 SHCC

As shown in Table 25, the value of the chloride diffusion coefficient and water permeability of SHCC is comparable with NSC. Taking into account the knowledge from Table 24 and the composition of SHCC from Table 11, one could expect that:

- Due to the low W/B ratio, the water permeability and chloride diffusion coefficient decrease
- Due to the substitution of Portland cement by Blast Furnace Slag decrease, the water permeability and chloride diffusion coefficient decrease

With this knowledge, a chloride diffusion coefficient and water permeability nearly the same as HPC could be expected, since the w/c ratio of SHCC and HPC is nearly the same. However, in literature the chloride diffusion coefficient after 28 days is just slightly lower compared to NSC (Li V. C., Engineered Cementitious Composites (ECC) – Material, Structural, and Durability Performance, 2007).

However, the unique cracking pattern of SHCC does result in unique durability properties if SHCC is cracked. As shown in Figure 36, the water permeability and the chloride diffusion coefficient for cracked SHCC is almost the same as for uncracked SHCC.

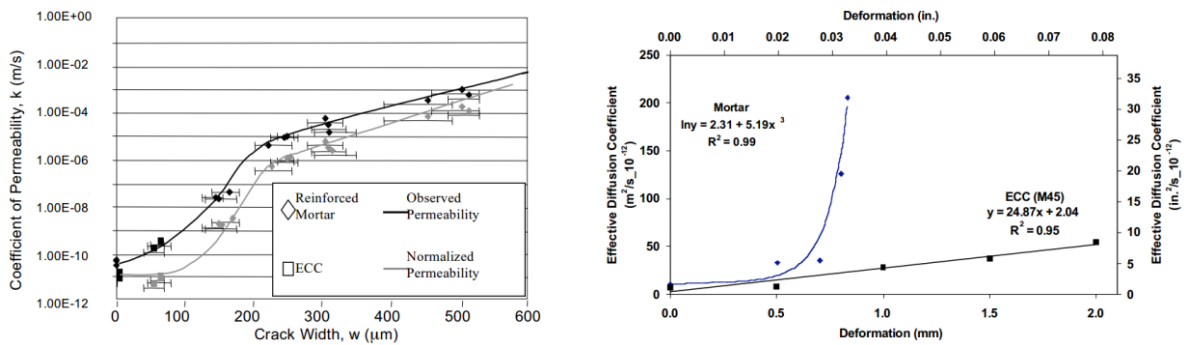


Figure 36 – Water permeability (left) and chloride diffusion coefficient (right) as a function of the crack width and deformation respectively (Li V. C., Engineered Cementitious Composites (ECC) – Material, Structural, and Durability Performance, 2007)

Next to the chloride diffusion coefficient, the carbonation should be discussed in some more detail. As shown in Table 25, the carbonation of SHCC is similar to the carbonation of NSC. In chapter 8.2 of the Japanese recommendations for HPFRCC is described that ‘it has been confirmed that HPFRCC’s carbonation rate is almost the same as that of the normal concrete with the same water-cement ration’ (Japan Society of Civil Engineers, 2008). In Table 11 is shown that the water-cement ratio of both the representative SHCC and NSC compositions are 0.5. Therefore, the resistance against carbonation is expected to be the same.

However, taking a closer look to the composition of SHCC and taking into account the knowledge of Table 24, according to the carbonation resistance of SHCC it could be expected that:

- Substitution of CEM I by CEM III increase the resistance against carbonation
- Finer aggregates decrease the resistance against carbonation

Compared to NSC, the amount of CEM I in SHCC is only half of the amount of CEM I included in NSC, because of the substitution of CEM I by CEM III in SHCC. The carbonation resistance could be expected to be increased due to this substitution.

The diameter of the largest aggregate particle of NSC is a lot larger than largest aggregate particle in SHCC. The largest particle in NSC is 32 mm. The largest particle in SHCC is 50 µm only. The tortuosity

in NSC therefore could be expected to be a lot higher than in SHCC, what decreases the carbonation resistance.

Apparently, the increase of the carbonation resistance due to the substitution of CEM I by CEM III is similar to the decrease of the carbonation resistance due to the finer aggregate in SHCC.

2.4.9.2 Self-healing concrete

Uncracked self-healing concrete is assumed to have similar durability characteristics as NSC, since the composition and the mechanical characteristics of both concrete materials are more or less the same. However, self-healing concrete has a unique self-healing capability. If self-healing concrete cracks, a better durability behaviour could be expected compared to the durability of NSC.

If the concrete heals, the matrix becomes denser again, so it should be logic that the water permeability, chloride diffusion coefficient and carbonation depth will decrease. Wang, Soens, Verstraete, & Belie (2014) show that the water permeability of cracked mortar with micro-captures is a factor 10 smaller compared to mortars without any micro-captures. This reduction of the water permeability was achieved in 8 weeks after cracking.

Also the chloride diffusion coefficient of cracked mortars with micro-captures is lower compared to mortars without micro-captures. After cracking, the chloride diffusion coefficient of mortars without captures is about 80% of the original value. For mortars with micro-captures the chloride diffusion coefficient can recover to 90 to 100% of the original coefficient (Wang, Xing, Zhang, Han, & Qian, Experimental Study on Cementitious Composites Embedded with Organic Microcapsules, 2013).

It is not found in literature, but it should be logic that the carbonation of cracked self-healing concrete also decreases because the permeability of the concrete increases. In Table 24 of chapter 2.4.8 In depth analysis degradation processes is shown that a decrease of the permeability lowers the carbonation depth. Further, by applying of certain healing agents, calcium carbonate is formed in the crack (Sisomphona, Copuroglu, & Koenders, 2012). Carbonation of concrete is the reaction with calcium carbonation, so the formation of calcium carbonation will probably reduce the carbonation depth or at least locally.

2.4.9.3 Geopolymer concrete

The durability characteristics of geopolymer concrete are quite different from the durability of ordinary concrete. For this reason, the behaviour of GPC attacked by chemical attack, ingress of chlorides, carbonation of the concrete and corrosion of the reinforcement steel is described in more detail.

The durability of geopolymer concretes is not well researched yet, so there is not a lot knowledge about the durability of this new concrete (Ahmed, 2014). This of course has a negative influence on the reliability of the below made conclusions.

Chemical attack

To define the resistance of GPC against chemical attack, some conclusions from the literature are reviewed. A few conclusions from research to acids are:

- In general, GPC has a **better acid resistance** compared to OPC. This can probably be explained by the absence of lime (CaO) in geopolymer concrete, which means that theoretically geopolymer concrete can't dissolve in acidic solutions (Zhang, et al., 2008).
- SFRGC (short fibre reinforced fly ash-geopolymer composites) has an **excellent resistance to strong acid attack**. After 1 month of pH = 1 sulphuric acid solution attack, no obvious

decrease of the impact strength and stiffness is observed for various SFRGC. In some cases even some increase is observed (Zhang, et al., 2008).

- The **better performance** of the geopolymer mortars in the **sulphate and sulphuric solutions** are due to the more stable cross-linked aluminosilicate polymer structure as compared to the Portland cement hydration structure (Sata, Sathonsaowaphak, & Chindaprasirt, 2012).
- The **best performance in different sulphate solutions** was observed in the geopolymer concrete prepared with sodium hydroxide and cured at elevated temperature. The strength of specimens increases 4–12% when they are immersed into sulphate solutions. Good performance was attributed to a more stable cross-linked aluminosilicate polymer structure (Bakharev, 2005).
- The **sulfuric acid** resistance of heat-cured geopolymer concrete is significantly better than for Portland cement concrete, as reported in earlier studies (Wallah & Rangan, 2006).
- Tests on heat-cured geopolymer mortar specimens indicate that the decrease of the compressive strength due to **sulfuric acid** attack is mainly caused by the degradation of the geopolymer matrix rather than the aggregates. (Wallah & Rangan, 2006)
- Wallah and Rangan reported an excellent resistance of GPC to **sulphate attack**. After one year exposure, the test results are (Wallah & Rangan, 2006):
 - a. No visual damage
 - b. 0.15 ‰ length change, where Portland cement concrete ($W/B = 0.4 - 0.5$) has a length change of 0.35 – 1.0 ‰
 - c. No reduction in mass:
 - i. Increase in mass of 1.5 for soaked in sodium sulphate solution
 - ii. Increase in mass of 1.8 for soaked in tap water
 - d. No effect on compressive strength
- ERC, the GPC already applied by the Australian company Wagners, has an **excellence performance** against acids as shown in the graph of Figure 37. Where Portland based concrete with a comparable binder content (400 kg/m^3) and a w/cm ratio of 0.4, shows a mass loss in the order of 1.5% till 6.5% after a year, is the ERC not affected at all (Aldred J. M., 2013).

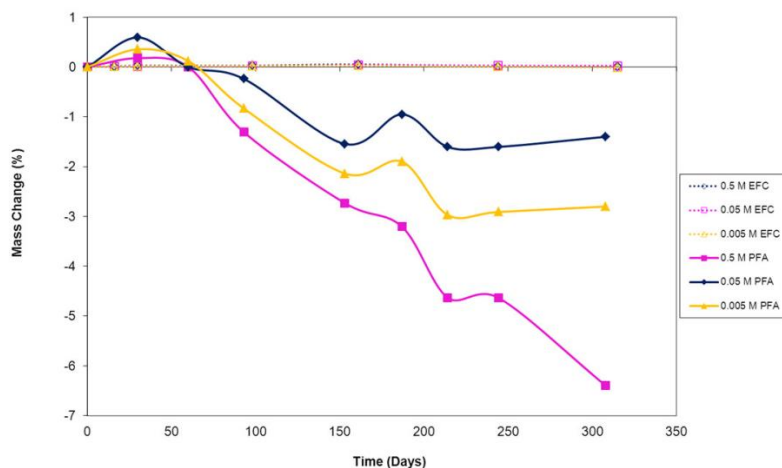


Figure 37 - Mass change due to immersion in sulphuric acid solutions for fly ash and geopolymer concrete (Aldred J. M., 2013)

As a conclusion, GPC has at least a better resistance against chemical attack. Some researchs even show that chemical attack does not influence GPC at all. The performance of GPC against chemical attack probably depends strongly on the source of the materials and the mixture.

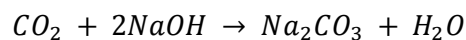
Carbonation

Not a lot research is done to the carbonation resistance of geopolymer concrete. Badar et al. did research to the corrosion of steel bars induced by carbonation. They especially researched the influence of the amount of calcium in fly ash based geopolymer concrete. For Ordinary Portland Concrete, the corrosion can be determined by the pH, the strength and the porosity of the material. These tests were also carried out for the geopolymer concrete. The result of the tests are (Badar, Kupwade-Patil, Bernal, Provis, & Allouche, 2014);

- A lower calcium fly ash based geopolymer concrete leads to a lower porosity, even after carbonation.
- Low calcium fly ash based geopolymer concrete has still a high pH-value, which results in an unchanged passive layer on the steel.
- All geopolymer concretes show a reduction in strength. Higher calcium fly ash geopolymer concrete show a slightly lower strength compared to low calcium fly ash.

The results from Badar, Kupwade-Patil, Bernal, Provis, & Allouche (2014) suggest that a lower calcium fly ash based geopolymer concrete has a denser structure at the rebar/concrete interface, which prevents the ingress of CO_2 . This helps to mitigate the pH reduction induced by carbonation and consequently helps to maintain alkalinity conditions required to promote the formation of a protective passivating layer on the steel bars.

Similar test results are found by Adam (2009). To understand the carbonation behaviour of geopolymer concrete, one should know that fly ash based geopolymer concrete does not contain both $Ca(OH)_2$ and C-S-H. This means that only NaOH can carbonate. The carbonation reaction of NaOH, according to Adam (2009), is shown below.



From experimental results, it seems that the carbonation of NaOH is a partial carbonation, where the carbonation of Portland concrete is a full carbonation, with an advanced front if the CO_2 penetrates the concrete. The pH of the pore solution of geopolymer concrete was not significantly affected by the CO_2 ingress. The pH of carbonated geopolymer concrete had a minimum value of 10-10.5 (Adam, 2009). This pH values in the range that a passive layer of oxide (Fe_2O_3 and Fe_4O_3) is on reinforcement steel, such that the steel won't corrode due to carbonation (Reinhardt, 2000). The pH of calcium carbonated Portland concrete can be lower than 9, such that the reinforcement steel can carbonate. (Adam, 2009)

The results of both researches, Badar, Kupwade-Patil, Bernal, Provis, & Allouche (2014) and Adam (2009), suggest that carbonation of GPC has no negative consequences for the reinforcement steel, because the pH value remains higher than nine. The high value of the pH passivates the corrosion of the reinforcement steel as explain in more detail in chapter 2.4.8.3 Carbonation.

Chloride diffusion coefficient

To get an idea of the chloride diffusion coefficient of geopolymer concrete, some result from literature are analysed. Here three researched are shown about the chloride diffusion coefficient of GPC. In the end, a conclusion of the chloride permeability of GPC is made.

The first research here finds that incorporation of slag as a secondary precursor in fly ash-based geopolymer concretes contributes to the refinement of the pore structure and restricts the transportation of chloride ions in the paste. In Figure 38 is shown that fly ash geopolymer concrete

(0G) has a worse chloride resistance compared to Portland Concrete (PC in Figure 38). The addition of slag until 50% can improve the chloride resistance above the chloride resistance of Portland Concrete. (Yang, Yao, & Zhang, 2014).

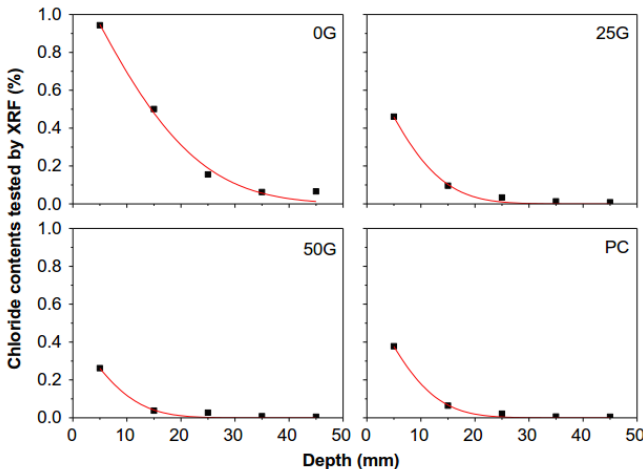


Figure 38 - Chloride ingress over the concrete depth for fly ash based geopolymer with 0, 25 and 50% slag and for PC. The results from Figure 38 are used to determine the chloride diffusion coefficient. These are shown in Table 27. The geopolymer concrete has a better chloride diffusion coefficient than PC if 50 % slag is added to the mix.

Table 27 - Chloride diffusion coefficient for fly ash based geopolymer concrete with 0, 25 or 50 % slag and for PC

Mix	D_a [$10^{-12}m^2/s$]	R
0G	15.43	0.9896
25G	5.14	0.9926
50G	3.93	0.9792
PC	4.29	0.9950

Chindaprasirt and Chalee did research to the influence of the NaOH concentration on the diffusion coefficient of fly ash-based geopolymer concrete. The results of this research in is shown in Figure 39. The figure suggests that the diffusion coefficient for different amount of NaOH is in the range of $3.0 \cdot 10^{-12}m^2/s$ to $6.0 \cdot 10^{-12}m^2/s$. (Chindaprasirt & Chalee, 2014)

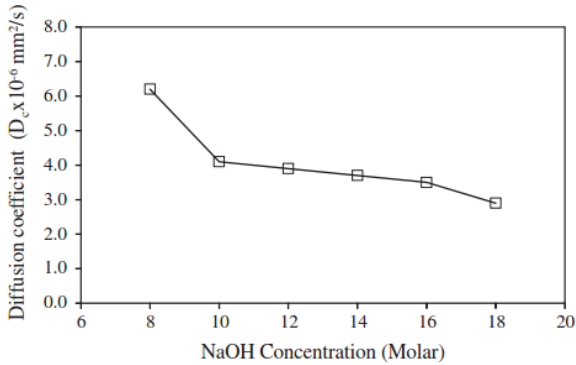


Figure 39 - The effect of sodium hydroxide (Na(OH)) concentrations on chloride diffusion coefficient of fly ash-based geopolymer concrete

Research to the commercial geopolymer Earth Friendly Concrete shows that the chloride penetrability of GPC appears to be extremely low. Tests according to ASTM C1202 results in a value of 229 coulombs, which is in the chloride diffusion class “very low”. In general, Portland cement concrete with a low w/c

ratio (< 0.4) are in the class “low”, which is one class higher than “very low”, what means a more chloride permeable concrete. In the same research is described that after 90 days ponding according to the AASHTO T259, effectively no chloride penetration was observed. A significantly lower chloride diffusion coefficient than $1 \cdot 10^{-12}$ is suggested (Aldred J. M., 2013), (Glasby, Day, Kemp, & Aldred, Earth Friendly Concrete – A sustainable option for tunnels requiring high durability, 2013).

In the end, the results of first two researches suggests a chloride diffusion coefficient is in the order of $10^{-12} m^2/s$. The research to the commercial EFC suggests a significantly lower chloride diffusion coefficient. Quantitative values of the chloride diffusion coefficient of EFC are not given. Because EFC is applied in practice, this mixture will probably give the most reliable results for practical applications. However, this value differs significantly from other values given in literature. One could doubt about the representativity of this value.

Corrosion

Due to the special material properties of GPC, the corrosion of the reinforcement steel is quite low. Here some scientific conclusions are mentioned that confirm the favourable behaviour of GPC with regards to the corrosion of the reinforcement steel.

- Accelerated corrosion tests showed that the geopolymer concretes exhibited considerably lower corrosion at 20 days than the control concrete (OPC) did. Time to failure for the geopolymer mixtures was 3.86–5.70 times longer than for Portland concrete. (Olivia & Nikraz, Properties of fly ash geopolymer concrete designed by Taguchi method, 2012).
- Also Aldred suggests, according to data of the Grade 40 geopolymer precast floor panels for the global Change Institute, that the corrosion in GPC is very low (Aldred J. M., 2013).
- Generally, the corrosion of steel in cement based concrete in seawater has deteriorated due to the incompatibility of the mix constituents. Both physical characteristics (i.e. pore distribution, pore size, connectivity of pores, shrinkage and movement cracks) and chemical characteristics (i.e. chloride binding capacity, alkalinity) of the cement paste significantly affect the corrosion rates of steel in concrete. (Chindaprasirt & Chalee, 2014)

2.4.9.4 Self-cleaning nano concrete

Because to less knowledge is available to determine quantitative values for the water permeability, chloride diffusion and carbonation depth of self-cleaning nano concrete, these will be described qualitatively. Because of the lack of knowledge in literature, only some indications for the durability variables are given here.

Water permeability

The water permeability of self-cleaning nano concrete is researched, as by some other, by Nazari and Riahi. They determined the water absorption of self-compacting concrete and ground granulated blast furnace concrete. For both concretes, the water absorption decreased on average from 3.9% to 1.5% and from 2.9% to 1.1% respectively (Nazari & Riahi, The effect of TiO₂ nanoparticles on water permeability and thermal and mechanical properties of high strength self-compacting concrete, 2010) and (Nazari & Riahi, TiO₂ nanoparticles effects on physical, thermal and mechanical properties of self compacting concrete with ground granulated blast furnace slag as binder, 2011). So nano titanium oxide seems to have a positive influence on the water permeability of concrete.

Chloride diffusion

The addition of nano titanium oxide to concrete seems to have a positive effect on the chloride diffusion coefficient. In literature a decrease of 26% (concrete containing 1.0% nano TiO₂ by the

weight of the cement) and 30% (mortar containing 1.0% nano TiO_2 by the weight of the cement) compared to Portland concrete is reported (Li H. , Xiao, Guan, Wang, & Yu, 2014) and (He & Shi, 2008).

Carbonation

The carbonation of concrete containing nano-titanium seems to be greater than for Portland concrete. An increase of carbonation depth by 25 % for concrete containing 5% TiO_2 by the weight of the cement after 70 days is reported (Diamanti, Lollini, Pedefferri, & Bertolini, Mutual interactions between carbonation and titanium dioxide photoactivity in concrete, 2013). Also Karatasios et al. concludes an increased carbonation depth due to the addition of nano-titanium oxide (Karatasios, et al., 2010).

The rate of carbonation in self-cleaning nano concrete is not only important for the reinforcement steel, but also for the self-cleaning capacity of the material. Lackhoffa et al. describe that the carbonation of the TiO_2 -modified cements leads to a very pronounced loss in catalytic efficiency, so the self-cleaning efficiency, over several months. This conclusion is the result from forced carbonation, which could be different from natural carbonation of cement in practice. Further research is recommended to determine the effect of the carbonation on the self-cleaning efficiency of concrete. (Lackhoffa, Prieto, Nestle, Dehn, & Niessner, 2003)

2.4.9.5 Self-sensing nano concrete

The durability behaviour of concrete containing nano Fe_2O_3 is researched on a very low level of detail. There is some information about the water permeability and chloride diffusion of mortars, which are used here to make some qualitative conclusions. For the carbonation of self-sensing concrete is actually to less knowledge available to run into conclusions.

Water permeability

In literature is shown that the water absorption for concrete containing 1 – 5% nano iron by the weight of the cement, can be 2-3 times lower compared to concrete without any nano iron particles. This is probably caused by the pozzolanic action and filler effect of the nano particles. The interfacial transition zone is also improved (Khoshakhlagh, Nazari, & Khalaj, 2010).

Chloride diffusion

Some research to the chloride diffusion of mortars containing nano iron is done. Madandoust, Mohseni, Mousavi, & Namnevis (2015) show that the addition of 2 wt% nano iron to mortar decreases the chloride permeability by 44% compared to a mortar without nano iron. The formation of the denser microstructure, decreasing of the pores and interruption of the pores, consequently reduced the chloride permeability (Madandoust, Mohseni, Mousavi, & Namnevis, 2015).

Carbonation

In literature no available information is found of the carbonation of concrete with nano iron. However, nano Fe_2O_3 also works as a filler, what decrease the permeability of the concrete. It could be argued that the lower permeability increases the carbonation as shown in Table 24. So probably the carbonation of concrete with nano Fe_2O_3 is lower than for concrete without nano iron.

2.4.9.6 Cracked concrete

The cracking behaviour of concrete does have a strong relation with the durability of concrete when it is cracked. This relation is shown in Figure 40, where the permeability coefficient of concrete is shown as a function of the crack opening. The permeability is given for the specimen loaded under the splitting tensile test and after unloading. As shown, the permeability of the loaded specimens is smaller than for unloaded specimens under the same crack opening displacement.

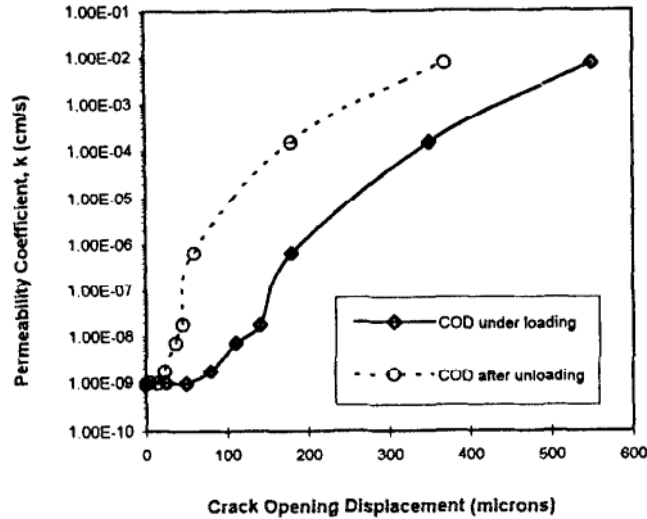


Figure 40 - Water permeability of concrete as a function of the crack width (Wang, Jansen, Shah, & Karr, 1997)

From the results of Figure 40 can be concluded that when the crack opening displacement is less than 50 microns under loading, the crack opening has little effect on the permeability. Between 50 and 200 microns, the water permeability increases rapidly (Wang, Jansen, Shah, & Karr, 1997). From the figure can be concluded that concrete with a better controlled crack pattern, like FRC or SHCC, does have a better durability behaviour.

2.4.9.7 Chloride profiles

The chloride diffusion coefficient of the ACMs is researched. Now according to Fick's second law, some chloride profiles can be made. In this paragraph, the model is explained first. After that, the chloride profiles are shown as a function of time and as a function of penetration depth.

Model CUR Leidraad 1

Chloride profiles per ACM can be calculated according to the CUR Leidraad 1. The CUR Leidraad 1 describes how the chloride concentration in the concrete can be determined according to Fick's second law (CUR bouw & infra, n.d.). The formula to calculate the chloride profiles is shown in eq.(46) This expression for the chloride concentration as a function of the depth and time, is valid for concrete structures that are included in Eurocode 2, so until strength class C90/105. In this research, the expression from the CUR Leidraad 1 is also applied for C170/200 (UHPC) and SHCC. UHPC could be behind the limits of the expression, because the strength of UHPC is significant higher compared to NSC and HPC. Also SHCC could be behind the limits of this expressions, since the composition is quite different from concrete types included in Eurocode 2. However, the expression is applied for both UHPC and SHCC. Maybe the results are not that accurate, but it the expression will at least give an indication.

$$C(x, t) = C_s - (C_s - C_i) \operatorname{erf} \left(\frac{x}{2 \sqrt{K_{tot} \cdot D_0 t \left(\frac{t_0}{t} \right)^{n_{cl}}}} \right) \quad \text{eq.(46)}$$

$C(x, t)$ is the chloride concentration in the concrete on a certain depth (x) at a certain time (t)

x is the depth from the concrete surface

C_s is the chloride concentration at the surface.

For bridges and environment near the sea the chloride concentration at the surface is equal to, $C_s = 1.5\%$ of the mass of the cement according to CUR Leidraad 1 (XD3, XS1). For constructions that are exposed in the splash or tidal zone of a marine environment the chloride concentration at the surface is equal to, $C_s = 3.0\%$ of the mass of the cement according to CUR Leidraad 1 (XS3). The chloride concentration at the surface for concrete that is sensitive for chloride penetration, like joints and places de-icing salts can accumulate, the concentration can be taken the same as for a marine environment, so $C_s = 3.0\%$. In the calculations below, a chloride concentration at the surface of 1.5% is assumed, because probably most structures are exposed in environments where the chloride concentration is in this range. To complete the story, a comparison with the marine environment ($C_s = 3.0\%$) will be made after the calculations

C_i is the initial chloride concentration in the concrete. $C_i = 0.01\%$ of the mass of the cement as a safe upper boundary according to CUR Leidraad 1

$$K_{tot} = k_e \cdot k_c$$

k_e is a coefficient to includes the environment impact. Recommended values according to CUR Leidraad 1 are:

<u>XD1, XD2, XD3, XS1</u>	<u>XS3</u>
- $k_e = 0.68$ for CEM I	- $k_e = 0.27$ for CEM I
- $k_e = 1.97$ for CEM III	- $k_e = 0.78$ for CEM III

k_c is a coefficient to includes curing. According to CUR Leidraad 1:

- For constructions on land, 3 days curing is recommended, such that $k_c = 1.50$
- For constructions at the sea, 7 days curing is recommended, such that $k_c = 1.00$

D_0 is the chloride diffusion coefficient at $t = t_0$. For the calculations below, $t = 28 \text{ days}$ is assumed.

n_{cl} is an exponent to include the age of the concrete. Probably the most important factors that influence n_{cl} are the type of binder and the w/b-ratio. In practice, values are given for different types of binders and exposure classes. The chosen for the age exponent for the calculations below are:

<u>XD1, XD3, XS1</u>	<u>XD2, XS3</u>
- $n_{cl} = 0.60$ for CEM I	- $n_{cl} = 0.40$ for CEM I
- $n_{cl} = 0.70$ for CEM III	- $n_{cl} = 0.50$ for CEM III

The chloride profiles are compared to the critical chloride concentration. In theory, if the chloride concentration is above the critical chloride concentration, the reinforcement steel will corrode. To understand the critical chloride concentration better, some information about the probabilistic design should be known. The failure of the system is calculated by probabilistic calculations. The limit state function, Z , should be smaller than zero, where the limit state function is the difference between the resistance of the concrete, R , and the load from the environment, S . These rules are mathematically written in the equations below. The sigma in the equations is for the deviation in the model (CUR bouw & infra, n.d.).

$$P_f = \{Z < 0\}$$

$$Z = R(\sigma) - S(\sigma)$$

In CUR Leidraad 1, a mean critical chloride concentration of 0.5% of the cement mass, with a standard deviation equal 0.1% is recommended. This makes the critical chloride concentration equal to $C_{crit} = 0.6\%$ of the cement mass. This value is the maximum chloride concentration in the concrete such that there is no corrosion in the of reinforcement steel in the concrete.

Chloride profiles

Filling in all constants mentioned above, the chloride profiles can be drawn and compared to the critical chloride concentration. The variables are time and penetration depth perpendicular to the surface.

The critical chloride penetration depths for NSC, HPC, UHPC and SHCC at 5, 50 and 100 years is calculated for the limit values of the chloride diffusion coefficient from Table 25 and for assumed representative values for the chloride diffusion coefficient as shown in Table 28 and Table 29 respectively. The assumed chloride values are applied to come to an average value per type of concrete, to compare the different types as good as possible. The critical chloride penetration according to the representative assumed chloride diffusion coefficients at 5, 50 and 100 year are also shown in the graphs of Figure 41, Figure 42 and Figure 43 respectively.

From the table and the figures can be concluded that UHPC has an extremely low chloride permeability. This could of course be due to the limits of the applied expression. On the other hand, the chloride penetration of HPC is very low as well. Since the diffusion coefficient of UHPC is significant lower than the diffusion coefficient of HPC, a lower chloride penetration depth could be expected.

Table 28 - Depth of the critical chloride concentration at 5, 50 and 100 years for the limit values of the chloride diffusion coefficient per ACM

	Limit values of chloride diffusion coefficient $10^{-13} [m/s^2]$	Critical chloride penetration [mm]		
		5 years	50 years	100 years
NSC (C30/37)	>40	>9	>14	>16
HPC (C90/105)	<50	<10	<16	<18
UHPC (C170/200)	<1	<1,5	<2	<3
SHCC	68	15	22	24

Table 29 – Depth of the critical chloride concentration at 5, 50 and 100 years for assumed values of the chloride diffusion coefficient per ACM

	Assumed chloride diffusion coefficient $10^{-13} [m/s^2]$	Critical chloride penetration [mm]		
		5 years	50 years	100 years
NSC (C30/37)	80	12	19	22
HPC (C90/105)	20	6	10	11
UHPC (C170/200)	1	1	2	3
SHCC	68	15	22	24

Chloride profile different ACMs after 5 years

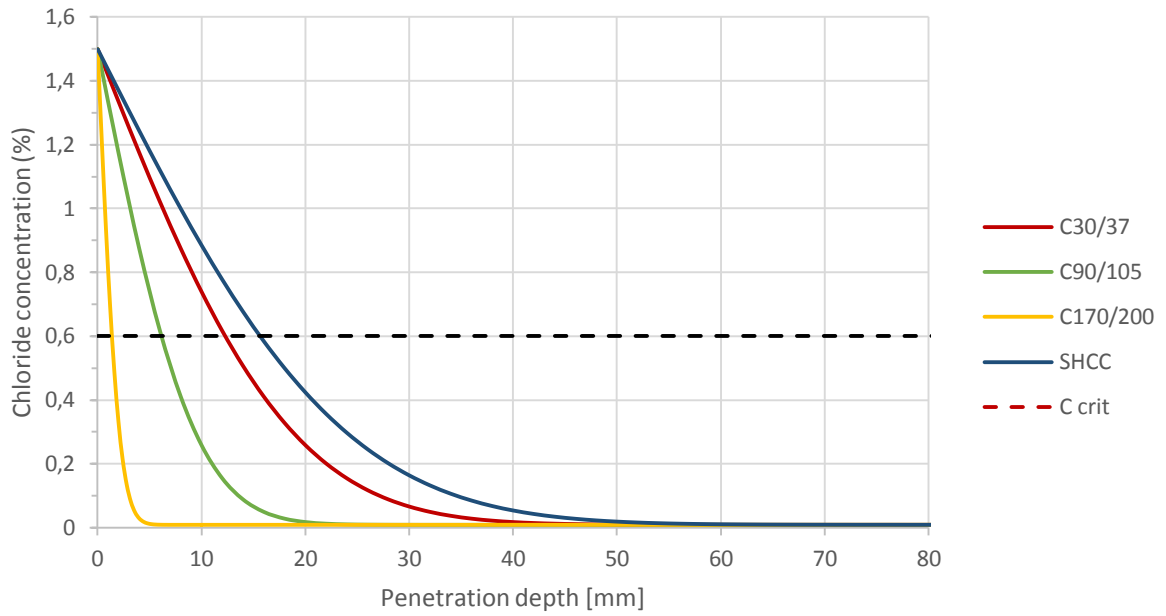


Figure 41 - Chloride profiles after 5 years life time for ACMs exposed to 1.5% chloride concentration outside (XD3, XS1)

Chloride profile different ACMs after 50 years

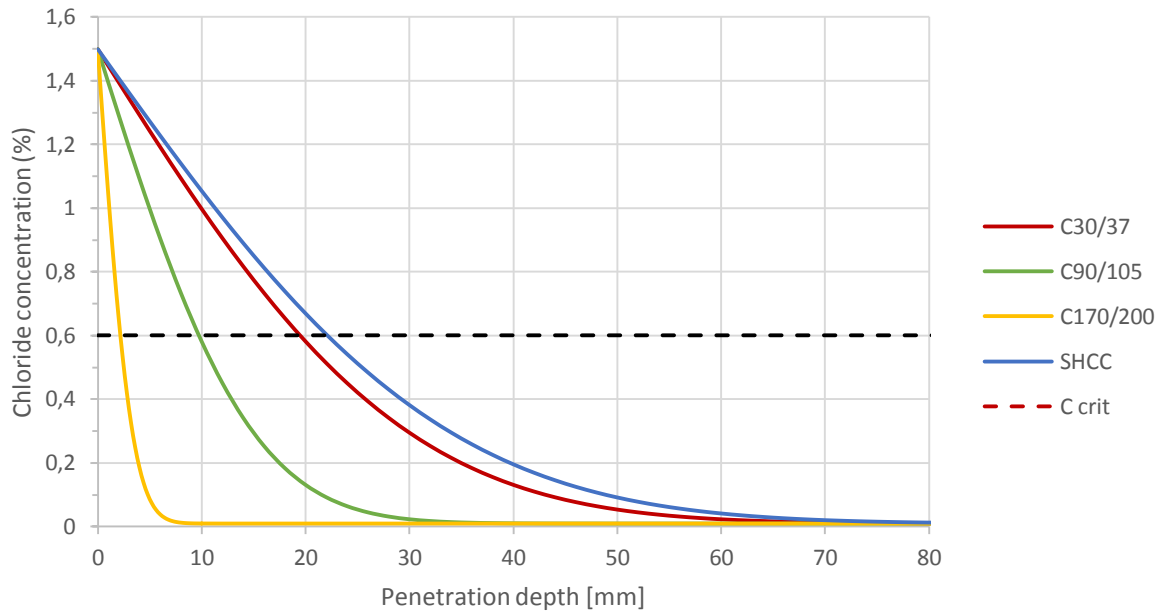


Figure 42 - Chloride profiles after 50 years life time for ACMs exposed to 1.5% chloride concentration outside (XD3, XS1)

Chloride profile different ACMs after 100 years

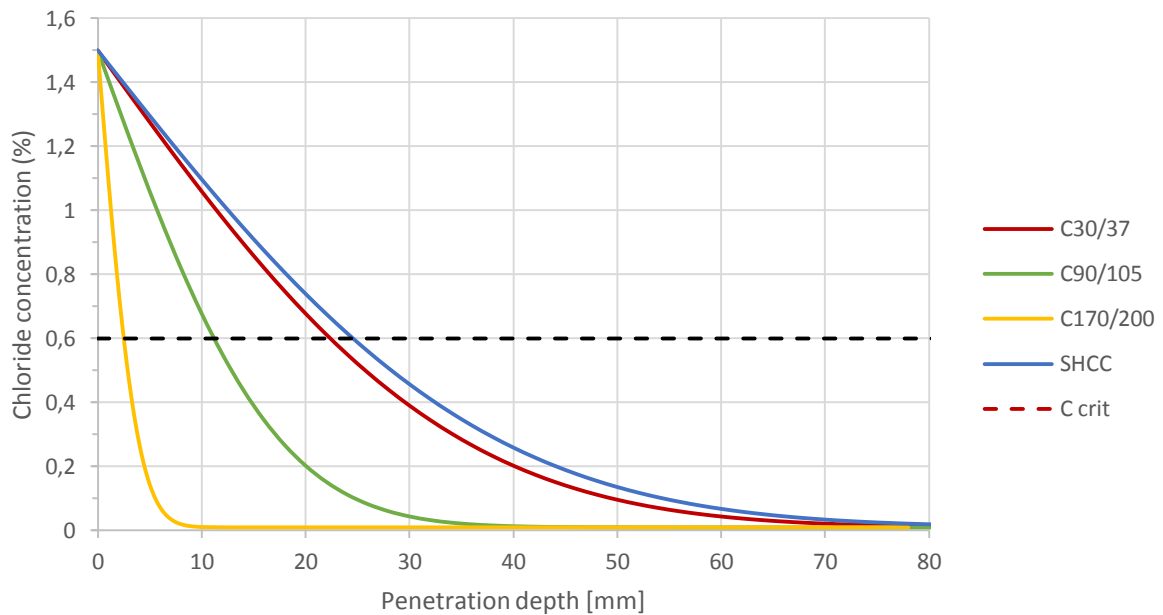


Figure 43 - Chloride profiles after 100 years life time for ACMs exposed to 1.5% chloride concentration outside (XD3, XS1)

The other way around, the chloride concentration could also be shown at a certain depth from the surface as a function of time. This is done in Figure 44, Figure 45 and Figure 46. In Table 30, the needed time to reach the critical chloride concentration at a certain depth is given assuming the representative chloride diffusion coefficients.

In Figure 44 is the chloride concentration at 20 mm depth shown from 0 to 100 years. In the figure is shown that the critical chloride concentration at 20 mm depth for C30/37 and SHCC are reached after

57 and 26 years respectively. The two stronger types of concrete are not even close to the critical chloride concentration after 100 years.

In Figure 45 is again the chloride concentration shown as a function of time for the four type of concrete, but now at a depth of 10 mm. At this distance from the surface, the high performance C90/105 reach the critical chloride concentration after 57 years. Again, C170/200 is not even close to the critical concentration.

In Figure 46 is the chloride penetration at 2 mm from the surface shown for UHPC only. At this distance, the critical chloride concentration is reached after 33 years. Again from these three figures is shown that the resistance against chloride penetration for UHPC (C170/200) is superior and for HPC (C90/105) it is very good. The resistance of SHCC is some worse than the chloride resistance of C30/37.

Table 30 – Needed of time before the critical chloride concentration is reached at 20, 10 and 2 mm

	Assumed chloride diffusion coefficient $10^{-13} [m/s^2]$	Time at critical chloride depth [years]		
		20 mm	10 mm	2 mm
NSC (C30/37)	80	57	2	<<1
HPC (C90/105)	20	>>100	57	<1
UHPC (C170/200)	1	>>100	>>100	33
SHCC	68	26	1	<<1

Chloride concentration as a function of time at 20 mm from the concrete surface

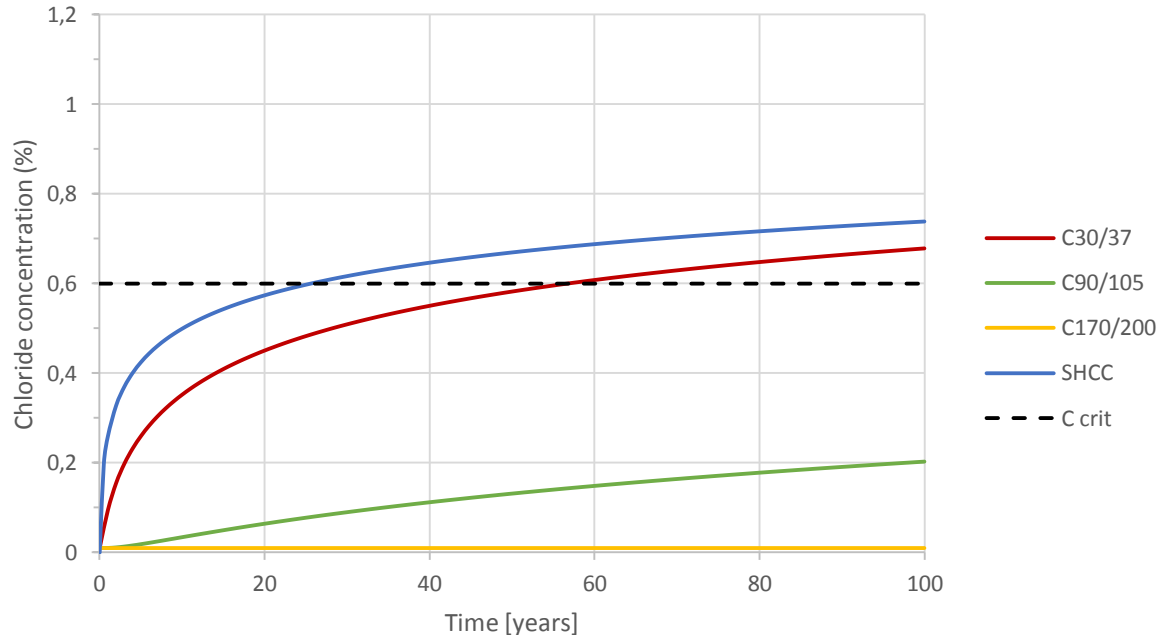


Figure 44 - Chloride concentration at 20 mm depth for ACMs exposed to 1.5% chloride concentration outside (XD3, XS1)

Chloride concentration as a function of time at 10mm from the concrete surface

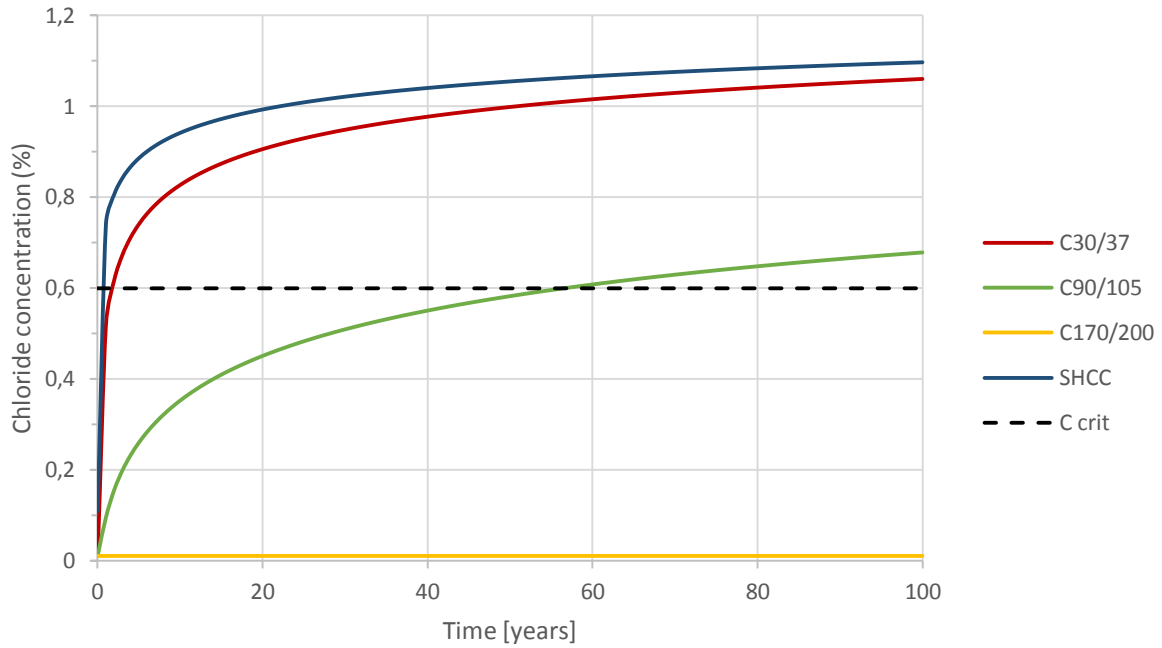


Figure 45 - Chloride concentration at 10 mm depth for ACMs exposed to 1.5% chloride concentration outside (XD3, XS1)

Chloride concentration as a function of time at 2 mm from the concrete surface

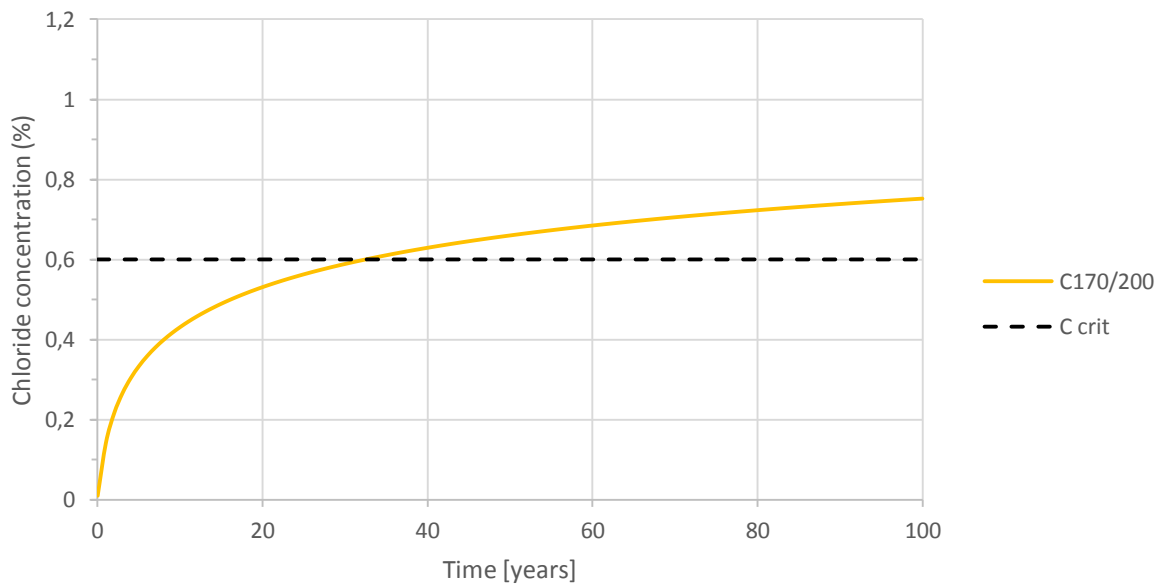


Figure 46 - Chloride concentration at 2 mm depth for C170/200 exposed to 1.5% chloride concentration outside (XD3, XS1)

At last, it is interesting to compare the chloride penetration of the two different environments with a chloride surface concentration of 1.5% and 3.0% with each other. In fact, this is the comparison between the exposure classes XD3, XS1 and XS3. As mentioned above, the other parameters for the calculation in XS3 are:

- $k_e = 0.27$ for CEM I and $k_e = 0.78$ for CEM III
- $k_c = 1.00$
- $n_{cl} = 0.40$ for CEM I and $n_{cl} = 0.50$ for CEM III

The comparison is made for ACMs exposed for 50 years, as shown in Figure 47. As shown, the critical chloride concentration for ACMs exposed to a maritime environment is deeper in the concrete compared to a land environment. The exact differences between both environments are given in Table 31. The comparison is done with the earlier mentioned assumed chloride diffusion coefficients. In the last column of Table 31, the increase of the critical chloride penetration depth between both environments is given. As shown in the table, the doubled surface concentration results in an increase of the critical chloride penetration depth of almost 50%.

Chloride profile different ACMs after 50 years

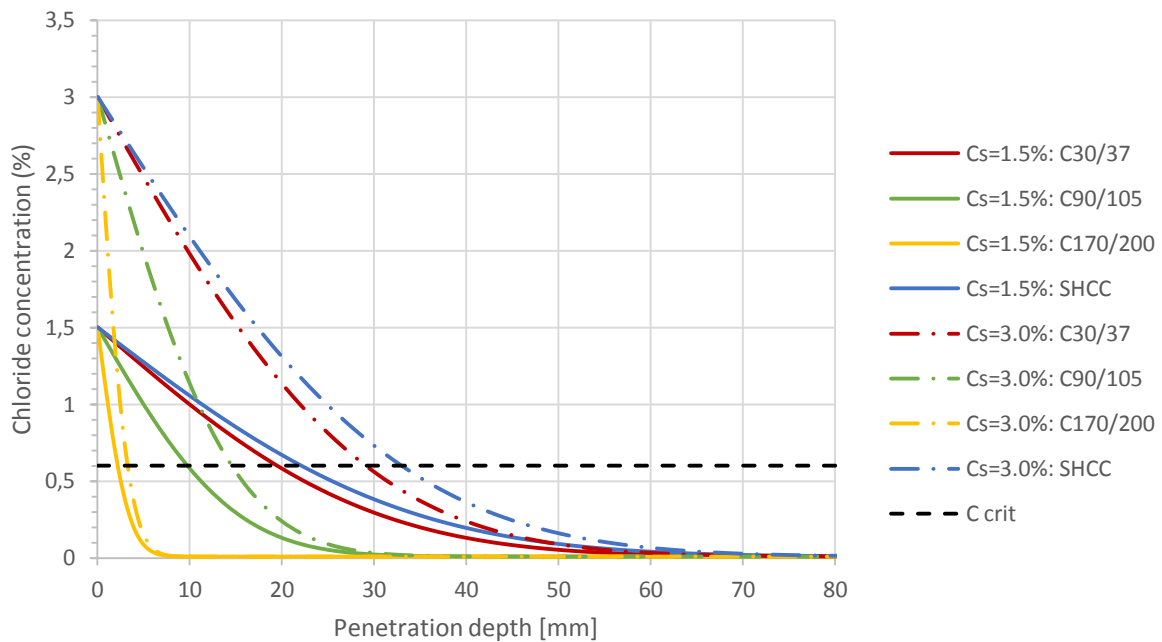


Figure 47 - Chloride profile for different ACMs after 50 years for chloride surface concentration of 1.5% (XD3, XS1) and 3.0% (XS3)

Table 31 - Depth of the critical chloride concentration at 50 years for assumed values of the chloride diffusion coefficient per ACM for a surface chloride concentration of 1.5% (XD3, XS1) and 3.0% (XS3)

	Assumed chloride diffusion coefficient $10^{-13} [m/s^2]$	Critical chloride penetration after 50 years [mm]		Increase of critical depth [%]
		$C_s = 1.5\%$ (XD3, XS1)	$C_s = 3.0\%$ (XS3)	
NSC (C30/37)	80	19	29	53
HPC (C90/105)	20	10	14	40
UHPC (C170/200)	1	2	3	50
SHCC	68	22	33	50

2.4.9.8 Carbonation profiles

The French recommendations for UHPC recommend a carbonation rate of passive reinforcement smaller than $0.01 \mu\text{m}/\text{year}$ for UHPC and $0.25 \mu\text{m}/\text{year}$ for HPC. Research, where is referred to in the

same recommendations, is stated that there is no corrosion risk in concrete if the carbonation rate of passive reinforcement is smaller than 1 $\mu\text{m}/\text{year}$ (Roux, Andrade, & Sanjuan, 1996).

NSC (C30/37) has a carbonation rate of passive reinforcement above 1 $\mu\text{m}/\text{year}$ (Roux, Andrade, & Sanjuan, 1996). As shown in Table 25, the carbonation of SHCC is comparable to the carbonation of NSC, because the W/C ratios are the same. The carbonations profile of concrete can be determined according to the formula $x = k\sqrt{t}$, as mentioned in chapter 2.4.8.3 Carbonation. This formula is here applied to determine the carbonation depth of C30/37. Only the value for k should be determined now.

Lagerblad (2006) has suggested some k-values for concrete with a cylinder compressive strength between 25 and 35 MPa for the Nordic climate. These suggested values are shown in the second column of Table 32. It is described that the k-value should be assumed higher in warmer environments (Lagerblad, 2006). In the Netherlands, the temperature is in average some higher compared to the Nordic climate, so the k-values should also be some higher too. On the other hand, the climate in the south of Scandinavia is comparable to the climate in the Netherlands. Next to that, there is quite a large scatter in the data (Lagerblad, 2006). However, these k-values will at least give an indication of the carbonation of concrete exposed to different conditions. For the exact k-value of a certain concrete mixture, experiments should be done.

Table 32 - K-value for Nordic environment for different exposure conditions (Lagerblad, 2006)

Exposure conditions	k-value [mm/year]
Wet/submerged	0.75
Buried	1.0
Exposed	1.5
Sheltered	4
Indoors	6

Carbonation depth

The values from Table 32 can be used in the model explained earlier in chapter 2.4.8.3 Carbonation to describe the carbonation depth as a function of time. The carbonation curve for C30/37 under different exposure conditions are shown in Figure 48. As shown in the figure, the carbonation depth after 100 years for sheltered and indoor concrete is much higher than for the other exposure classes, respectively 60 mm and 40 mm where the other carbonation depths are equal to 15, 10 and 7.5 mm for 'exposed', 'buried' and 'wet/submerged' exposure conditions respectively.

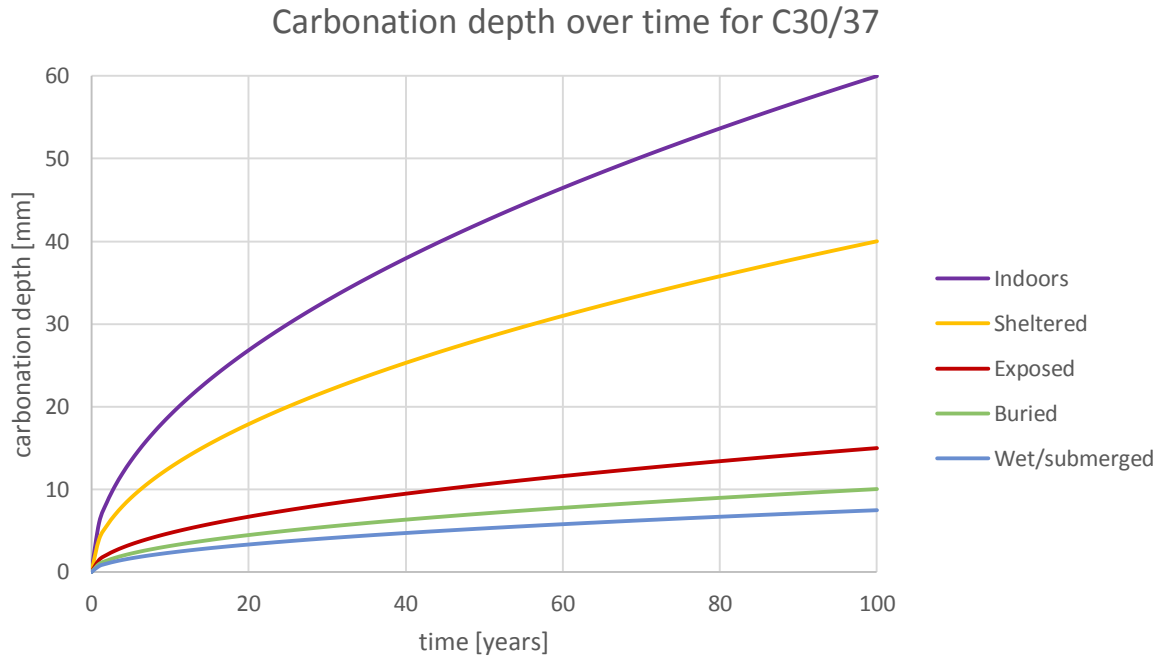


Figure 48 – Carbonation depth over time for C30/37 according to the model $x = k\sqrt{t}$ in different environment classes

According to Roux, Andrade, & Sanjuan (1996), there is no risk for carbonation for HPC and UHPC. However, with the k-value of C30/37, the k-values for C90/105 and C170/200 could be approached with eq.(47), where theoretical formula is given for the k-value (Younsi, Turcry, Aït-Mokhtar, & Staquet, 2013). This model is explained earlier in chapter 2.4.8.3 Carbonation. The formula shows that the material characteristics of the k-value are the diffusion coefficient (D_{CO_2}) and the concentration Portlandite ($[CH]$).

As shown above, the diffusion coefficient for HPC and UHPC are lower than for NSC. So for HPC and UHPC the k-value can be expected to be smaller than for NSC, taking into consideration the diffusion coefficient only.

Next to the diffusion coefficient, the amount of portlandite has a strong relation with the cement content and the content of pozzolan materials. In the compositions in this research are no ACMs with pozzolan materials. HPC and UHPC contain significant more cement than NSC. Therefore, significant higher concentration of Portlandite could be expected in these materials. However, the relation between the amount of cement and the concentration Portlandite is not linear. In the ACMs with higher amounts of cement, the water-cement ratio is normally lower ($W/C < 0.4$ à 0.3). That means that not all cement can react to form CSH and CH. This means that two times more cement does not result in two times more Portlandite in the concrete.

$$k = \sqrt{\frac{2D_{CO_2}[CO_2]}{[CH]}}; \quad \text{eq.(47)}$$

Where,

D_{CO_2} = effective diffusion coefficient of carbon dioxide $\left[\frac{m^2}{s}\right]$;

$[CO_2]$ = molar concentration of carbon dioxide in gas phase in contact with concrete $\left[\frac{mol}{m^3}\right]$;

$[CH]$ = molar concentration of Portlandite in the concrete $\left[\frac{mol}{m^3}\right]$;

As a conclusion, the materials HPC and UHPC definitely have smaller k-values so a lower carbonation depth than NSC. The carbonation depth of SHCC is similar to the carbonation depth of NSC. Both have the same W/C ratio, which results in a similar carbonation depth (Li V. C., Engineered Cementitious Composites (ECC) – Material, Structural, and Durability Performance, 2007).

In Figure 49 an indicative comparison is made between NSC, HPC and UHPC. The assumption done for this comparison are:

- NSC has the k-value of C30/37.
- According to the values of Table 25, the k-value of diffusion coefficient of HPC and UHPC are assumed to be 2 and 40 times smaller than for NSC. In average, the diffusion coefficient of HPC and UHPC are probably even lower.
- The different Portlandite concentrations for the different types of concrete is neglected, what probably gives conservative values for HPC and UHPC.
 - ➔ In the end, this makes the k-value for HPC and UHPC is 71% and 16% of the k-value of NSC.

Since a lot of uncertainties are in the calculation of the carbonation depth of HPC and UHPC, the results are just indicative ones. For the real carbonation depth, further research should be done.

Carbonation depth over time for NSC, HPC and UHPC in exposed conditions

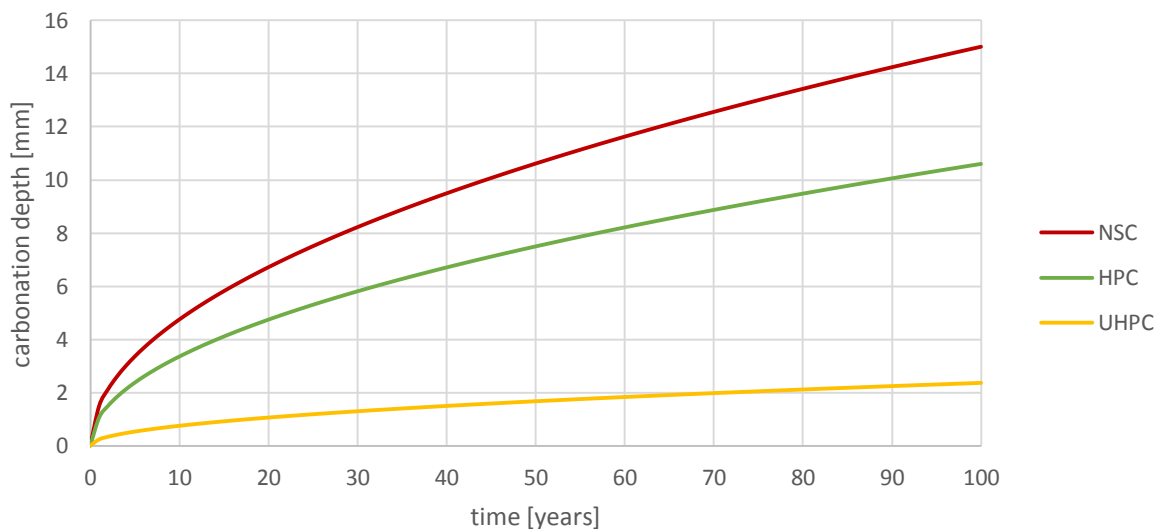


Figure 49 - Carbonation depth over time for NSC, HPC and UHPC according to the model $x = k\sqrt{t}$ in expose environment conditions

Note: to determine the diffusion coefficient of HPC and UHPC, it is assumed that the C30/37 has a diffusion coefficient near the lower limit of the range mentioned in Table 25. The diffusion coefficient of HPC is assumed to be the upper limit of HPC and the upper limit of UHPC. The diffusions coefficient is assumed to be the upper limit of UHPC. This is a quite conservative estimation.

In practice the chloride penetration depth in infrastructure structures is in general the governing parameter for the thickness of the cover (Ottel , 2015). This conclusion is more or less in line with the conclusions from the above mentioned calculations. Only for sheltered and indoor conditions,

carbonation is governing over the chloride penetration. However, infrastructure is mainly not placed indoor. So only in sheltered conditions, carbonation should be governing. Because of the large scatter from the k -value, the uncertainties in the calculations and the conservative assumption, the chloride penetration is assumed to be governing over the carbonation depth according to the advice of Ottelé (2015).

2.5 Sustainability

Nowadays the sustainability of building materials and constructions has become more and more important. Especially the CO_2 emission, which has a large impact on the global warming, is a hot item in a lot of building projects. For the fabrication of cement a lot of carbon dioxide is emitted. Some estimates suggest that the amount of carbon dioxide from the worldwide production of OPC may be as high as 7% of the total global CO_2 emissions (Yang, Jung, Cho, & Tae, 2014). But also energy consumption and the use of finite sources seem to be more and more important.

In this chapter is first an overview of design options to make a more sustainable and durable construction according to Stutech/Stufib studiecel 61/19 (2012) is given. In this overview are also some ACMs linked to the options. After that the most ACMs are judged on the sustainability by ReKentool Groen beton 3.0.

2.5.1 Sustainable and durable structures

Stutech/Stufib studiecel 61/19 (2012) did research to the durability and sustainability of constructions made of concrete. The main objective of this study was to judge possibilities and make recommendations to reduce the impact of concrete on the environment in the whole life-time, especially for CO_2 emission, such that durability and sustainability can be included in the design process. In the end, some practical basic options are given to design a more durable and sustainable construction (Stutech/Stufib studiecel 61/19, 2012).

The options for a more sustainable and durable concrete construction are divided over five phases in the life-time of a construction. These phases are:

1. Initial phase
2. Design phase
3. Execution phase
4. Service phase
5. Recycling phase

These phases are also shown in Figure 50. In every phase are option to make a construction more durable and sustainable. These options are shown in Table 33. In total, there are 16 options divided over the 5 phases to improve the durability and sustainability, as shown in the first two columns of the table. In the second column are the numbers of the option given, which are described shortly in the third column. A more detailed description can be found in the rapport of Stutech/Stufib studiecel 61/19 (2012).

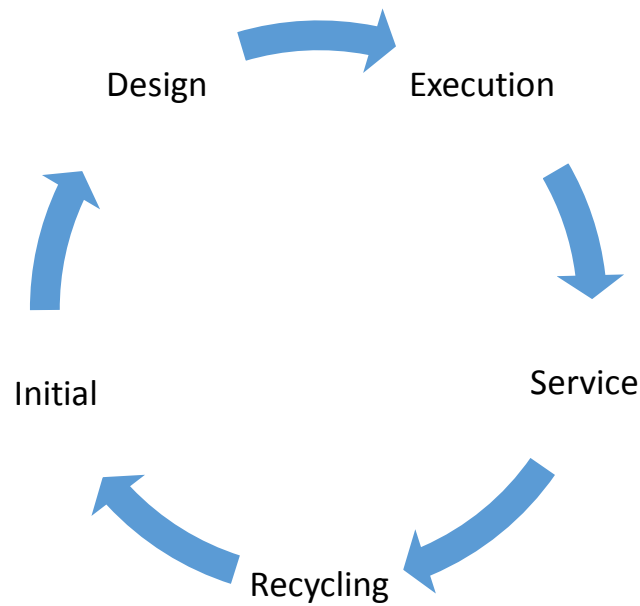


Figure 50 - Phases of a construction

Table 33 – Option to improve the durability and sustainability of a concrete structure classed by different phases (Stutech/Stufib studiecel 61/19, 2012)

Phase	Options	Description of the options
Initial phase	Option 1.	Increase of service life of the structure by keeping the same function
	Option 2.	Increase of service life of the structure by having another function
Design phase	Option 3.	Cast in situ vs. prefabrication
	Option 4.	Application of more slender columns
	Option 5.	Smart configuration of beams and slabs to improve the durability and sustainability
	Option 6.	Reduce the span
	Option 7.	Replace reinforced concrete by prestressed concrete
	Option 8.	Increase the concrete strength
	Execution phase	Option 9.
Option 10.		Reduce the binder content
Option 11.		Replace the aggregate by recycled aggregate
Option 12.		Optimisation in the curing period
Option 13.		Increase the time before the formwork is uninstalled
Option 14.		Apply the 56 or 91 days concrete strength as design value
Service phase	Option 15.	Application of concrete core activation
Recycling phase	Option 16.	Improve the recycling and reuse after demolition

Now it is interesting to link the options from Table 33 to the ACMs of this research. This is done in Table 34. Four of the options from Table 33 have direct relations with the composition of the concrete. These four are shown in the second column of Table 34 and are shortly described in the third column. In the fourth column of the table are the ACMs that have a negative (red) or positive (green) influence on the option compared to the influence of NSC. For example, HPC has a positive influence on option 8, because the concrete strength of HPC is higher than the concrete strength of NSC. Because no single ACM contains recycled aggregate, none of the ACMs is compared to NSC on option 11.

Table 34 - Options to improve the durability and sustainability of a concrete structure linked to the ACMs of this research

Phase	Options	Description of the options	ACM
Design phase	Option 8.	Increase the concrete strength	HPC
			UHPC
			Self-cleaning concrete
Execution phase	Option 9.	Adjust the binder composition	GPC
			SHCC
	Option 10.	Reduce the binder content	HPC
			UHPC
Option 11.	Replace the aggregate by recycled aggregate		

Positive influence on option compared to NSC

Negative influence on option compared to NSC

2.5.2 Rekentool Groen beton 3.0

To judge the sustainability of the cementitious composites themselves, the Excel-tool “Rekentool Groen Beton 3.0” is used. In this tool, the concrete is judged on eleven effects the concrete can have on the environment. A detailed description of the tool can be found in (Hofstra, 2013). The eleven effects of the tool are:

1. Depletion of abiotic sources
2. Depletion of fossil energy
3. Global warming
4. Ozone depletion
5. Photochemical oxidant formation
6. Acidification
7. Eutrophication
8. Human toxicological effects
9. Ecotoxicological, freshwater
10. Ecotoxicological, sea water
11. Ecotoxicological, soil

The program can combine all these effects to one value; MKI (environmental costs indicator). This value is expressed in terms of money. It presents the amount of money that should be spent to compensate the damage on the environment due to the fabrication of concrete. Since the indicator includes all effects in one value, the MKI makes it easy to make a total comparison between the different materials.

2.5.2.1 Assumptions

Before the results are shown, first some assumptions that are done should be mentioned. The assumptions done are split up in assumptions for the concrete mixture itself and assumption during execution. The assumption are put in Rekentool in the same order.

Concrete mixture

The assumptions done for the concrete mixtures are;

- In the program is a concrete cube with a width, height and depth of 1 metre inserted.
- For coarse aggregate, SBK Gravel from the river is assumed. It is assumed that coarse aggregate in the program is defined the same as in NEN-EN 206:2014, since the program is Dutch.

- For fine aggregate, SBK Betonzand (Nederland) is assumed because the most project of Heijmans are in The Netherlands. It is assumed that fine aggregate in the program is defined the same as in NEN-EN 206:2014, since the program is Dutch.
- The type of water in the ACMs is assumed surface water. For some ACMs, surface water may be too dirty to apply. For those ACMs the results are a bit too progressive.
- Energy usage is not included. The energy should be inserted per cubic concrete production. For concrete materials that are nearly applied it is quite hard to come with a realistic value for the energy usage. There is a default energy option in the program, but this value is probably not realistic for innovative cementitious materials. Besides, if for all the mixtures default energy usage is used, the energy consumption probably won't nearly influence the sustainability of the concrete at all.

Execution

The assumptions done for the execution of concrete are;

- Formwork is not included. In the comparison between different concrete materials for the same block, the amount of formwork will be the same.
- Concrete is assumed to be cast in situ.
- Transport of the concrete between the fabric and the building side is not included. Since every concrete block has the same dimensions, the transport emissions for all blocks is probably more or less the same.
- Reinforcement steel and fibres are included.
- Additional materials like mortars are not included.
- Additional processes in the building pit, for example curing, are not included.
- The transport of ingredients for the concrete mix to the fabric and the energy to produce the concrete are assumed to be equal to the default settings of the program "Rekentool Groen beton 3.0". The values for the transport and the energy are in Table 36.
- Waste during production is not taken into account. There is not enough knowledge about the waste of most ACMs since most of them are nearly applied in practice at the moment.
- Transport at the building pit is not taken into consideration. For the same blocks probably more or less the same transport is needed on the building pit.

2.5.2.2 Limitations

In this research is worked with innovative material. Because of this, some ingredients of ACMs are not in the program. Ingredients that are in the composition of ACMs but are not in the program are:

- Quarts (UHPC)
- Nano iron oxide (Self-sensing concrete)
- Healing agents (Self-healing concrete)
- Geopolymer concrete can't be inserted in the Rekentool Groen Beton 3.0

Self-sensing concrete, Self-healing concrete and Geopolymer concrete are not judged by Rekentool Groen beton 3.0. UHPC is judged by the Rekentool by a small trick, described in the next paragraphs.

2.5.2.3 Input

In this paragraph is exactly shown the input data that are inserted in the Rekentool program. In Table 35 is given the input for the mixtures for the different ACMs. As mentioned before, not all ACMs are taken into consideration. In Table 36 are the default settings given for the transport of the materials from the source to the fabric. These default settings are applied as input data.

As shown in Table 36, reinforced NSC is included in the comparison. Nowadays, most concrete applications are reinforced by steel. To have an idea of the difference in sustainability between one cubic metre unreinforced concrete, steel reinforced concrete and steel fibre reinforced concrete, these concrete are all included in the comparison. The amount of reinforcement is chosen equal 2.0 V. %, which is, as shown in Table 36, the same as $0.02 \cdot 7800 = 156 \text{ kg/m}^3$.

Table 35 - Input in "Rekentool Groen beton" for the compositions of the ACMs

			Plain concrete		ACM 1.	ACM 2.	ACM 3.	ACM 4.	ACM 5.	ACM 8.
			NSC		NSSFRC	HPC	HPSFRC	UHPC	SHCC	Self-cleaning
	Material	Unit	C30/37	C30/37 (reinforced)	C30/37 (fibres)	C90/105	C90/105 (fibres)	C170/200	-	-
Binder	SBK CEM-I NL c2	[kg/m ³]	320	320	320	501	501	710		320
	CEM III-A NL gem	[kg/m ³]							910	
Aggregate and additions	SBK Gravel, river	[kg/m ³]	1280	1280	1280	866	866			1280
	SBK Betonzand (Nederland)	[kg/m ³]	640	640	640	867	867	1020		640
	Lime stone	[kg/m ³]							827	
	Silica fume							230		
	Titanium oxide	[kg/m ³]								21.5
Additives	Superplasticiser	[kg/m ³]				8.5	8.5	13	7	
Water	Surface water	[kg/m ³]	160	160	160	160	160	140	455	160
	Water binder ratio		0.5	0.5	0.5	0.32	0.32	0.20	0.26	0.5
Fibres	Reinforcement steel	[kg/m ³]		156 ($\rho = 2.0\%$)						
	SBK plastic fibres	[kg/m ³]							28.6(= 2.0V.%)	
	Steel fibres	[kg/m ³]			40		70	100		
Total weight		[kg/m ³]	2400	2556	2440	2403	2473	2213	2228	2422

Table 36 – Transport properties for different concrete ingredients (default settings)

Ingredient	Transport to concrete fabric [km]		
	Truck	Inland vessel	Seagoing ship
First cement binder	186	0	0
Next cement binder	96	0	0
Gravel (river and sea)	10	239	51
Crushed stone	10	239	51
Lime stone	10	239	51
First sand aggregate	4	159	38
Second sand aggregate	0	200	0
Granulate	30	0	0
First filler: BFS, lime stone powder, fly ash, silica fume	150	0	0
Next: BFS, lime stone powder, fly ash, silica fume	50	300	0
(Super)plasticiser	150	0	0
Titanium oxide	150	0	0
Steel	150	0	0

2.5.2.4 Remarks

In the program are cubes of concrete inserted with a height, width and depth of 1 metre. As shown in Table 35, strong concrete such as HPC or UHPC contains a lot of cement per cub concrete. So a cubic HPC or UHPC is always less sustainable than NSC. The same is valid for FRC. If fibres are added to a cubic concrete, no matter if it is added to NSC or HPC, the concrete will be less sustainable. From a sustainable point of view, a NSC without any fibres seems to be the most sustainable concrete in every case.

However, a construction can be more sustainable by applying a concrete which is less sustainable per cubic. For the same structure, the application of a stronger concrete could result in a more sustainable construction, because a strong ACM can significantly reduce the amount of material needed for a construction. In the end, this reduction could result in a more sustainable structure.

Further, the life time of concrete is not include in the program to calculate the sustainability. A very durable material, like GPC or UHPC, could have a longer life time than NSC. A long service life increases the sustainability of the structure as well. So the durability and the sustainability of a structure have strong relations with each other.

Some remarks especially for some ACMs:

- **SHCC:** In the composition of SHCC is CEM I 42.5 N and BFS. BFS is not in the program. In the program CEM III is chosen, which has approximately the same amount of PC (44%) and BFS (56%). In the real composition of SHCC is 45% PC and 55% BFS. This difference between the program and the real composition is neglected here.
- **UHPC:** In the composition of UHPC is quarts, but in the Rekenool quarts can't be inserted. Therefore, UHPC is inserted in the Rekenool without any quarts. The weight of the inserted UHPC is less than the weight of the composition defined in Table 11. The inserted weight is 2213 kg/m^3 , where the weight should be 2423 kg/m^3 . Therefore, the results from the Rekenool are multiplied by $\frac{2423}{2213} = 1.10$. So the sustainability of quarts is taken as the average sustainability of UHPC without quarts. In reality, the sustainability of UHPC probably differs from the sustainability calculated with this assumption.

- **Self-cleaning concrete:** In the composition of Self-cleaning concrete is nano titanium oxide added. In Rekentool is titanium oxide included as a pigment to make white concrete. The titanium oxide particles in the program are probably not on nano level. To make nano titanium oxide particles, probably more energy is needed compared to the fabrication of titanium oxide from the Rekentool. Probably, the MKI and global warming impact are in reality higher.

2.5.3 Results

The best way to compare the sustainability of the different cementitious materials to each other is by using the MKI, as mentioned before. This factor includes eleven effects the concrete can have on the environment. The MKI is expressed in term of money; the money that is needed to compensate the damage to the environment. The results of the MKI per concrete is given in Figure 51.

The MKI also includes the effects on global warming. Since global warming is a hot item the last years, the influence of the concrete materials on global warming only is showed in Figure 52.

The results of Figure 51 and Figure 52 give an indication of the sustainability of the material. In practice, the composition or the amount of reinforcement steel of an ACM probably differs from the composition and reinforcement of the ACMs applied here. So the exact sustainability of a structure in practice is probably different from the value shown here.

To give an indication of the sustainability differences between reinforced, unreinforced and fibre reinforced concrete, also reinforced concrete is included in the results. Results show that the MKI of reinforced C30/37 is 1.6 times the MKI of unreinforced C30/37. Moreover, if the same amount of steel fibres would be added instead of 'classic' reinforcement, the MKI is 1.8 times the MKI of plain C30/37. So compared to reinforced concrete The MKI is increased by 20%.

As shown in Figure 51, the ACM with the by far highest MKI is UHPC, which is quite logic since it contains a lot of cement. For the same reason UHPC has also the largest influence on global warming, as shown in Figure 52. Most of the other MKI's are between 1.5 and 2.0 times the MKI of NSC. For the global warming most ACMs emit 1.3 to 1.8 times more CO₂ compared to NSC (C30/37).

The sustainability of GPC can't be calculated by Rekentool program yet. At this moment, the designers of the program have already made an updated version of the program where GPC is included, but that version can only be used for their own research. Therefore, the sustainability of GPC will be determined by literature. Some conclusions on the sustainability of GPC are listed below. The conclusions for sustainability are mainly focussed on the carbon dioxide emission of GPC compared to OPC concrete.

- A carbon emission life cycle assessment of this geopolymer concrete/binder compared with slag/GP blended cement concrete/binder estimated a reduction of more than **60%** of the emissions associated with a reference blended cement concrete (Aldred J. M., 2013).
- The CO₂ footprint of geopolymer concrete (binder: fly-ash, sodium silicate and sodium hydroxide) was approximately **9%** less than comparable concrete containing 100% OPC binder (Turner & Collins, 2013).
- The production of CO₂ decreases by **60%** comparing OPC based concrete with Fly Ash Based Geopolymer Concrete (Habert, Lacaillerie, Lanta, & Roussel, 2010).
- For the proposed "typical" Australian geopolymer product, there is an estimated **44-64%** improvement in greenhouse gas emissions over OPC (McLellan, Williams, Lay, Riessen, & Corder, 2011).

From the above mentioned conclusions can at least be concluded that GPC probably has lower carbon dioxide emission than OPC concrete and that it is not exactly known how much. Three of the

conclusions shows a reduction of 60%, where for one research 60 % is an upper boundary. The conclusion of 9% reduction deviates significantly from the others. However, given that the impact of location on overall sustainability is one of the determining factors, each application for GPC should be assessed for its specific location. The broad range of potential feedstock sources leads to a very wide range of potential impacts: compared with emissions from OPC concrete, emissions from geopolymer concrete can be 97% lower up to 14% higher (McLellan, Williams, Lay, Riessen, & Corder, 2011). From the above mentioned conclusions, the reduction is assumed to be about 40% compared to OPC concrete with quite a large deviation.

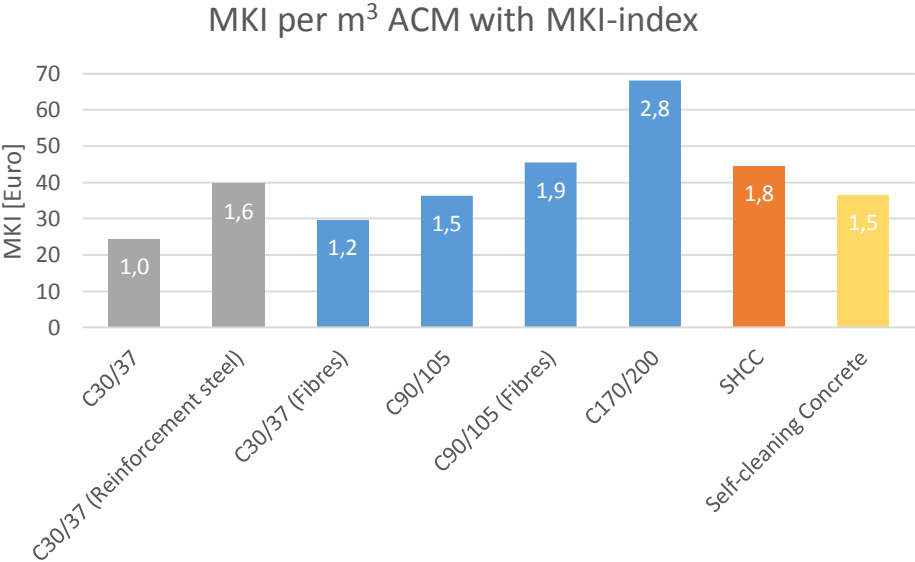


Figure 51 - MKI per cubic metre ACM with MKI-index

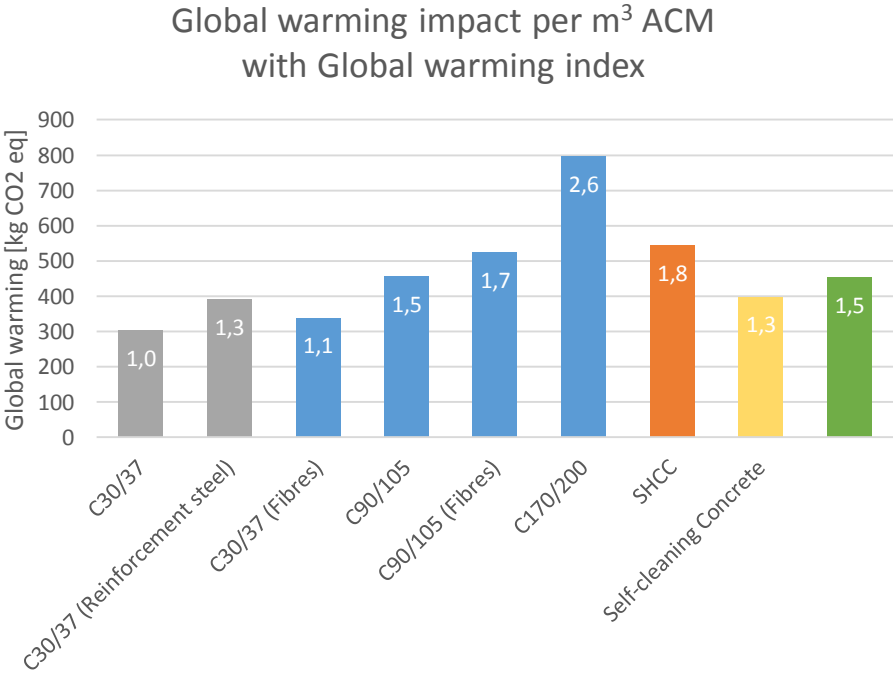


Figure 52 - Global warming impact per m3 ACM with Global warming index

2.6 Design standards and recommendations

To apply Advanced Cementitious Materials in practice, design standards and recommendations should be there. In certain countries are already design standards or recommendations for certain ACMs. For example, in Japan is already some rules in the codes about SHCC and in Australia are rules for GPC in the standards already. An overview of the standard and recommendations are given in Table 37. In the table are the ACMs summed. For every ACM is given what code or recommendation includes rules for that specific ACM. Not for all ACM are recommendation or standards written yet.

Table 37 - Standards and recommendations for Advanced Cementitious Materials

ACM	Standard/recommendation	Society	Country/ Continent	Year of release
NSSFRC	Model Code 2010	FIB	Europe	2013
HPSFRC	Model Code 2010	FIB	Europe	2013
HPC	NEN-EN 1992-1-1+C2 (Eurocode 2)	NEN	Europe	2011
UHPC	Ultra High Performance Fibre-Reinforced Concretes - Recommendations	AFGC	France	2013
SHCC	Recommendations for Design and Construction of High Performance Fibre Reinforced Cement Composites with Multiple Fine Cracks (HPRCC)	Japan Society of Civil Engineers	Japan	2008
	Durability of Strain-Hardening Fibre-Reinforced Cement-Based Composites (SHCC) – State-of-the-art	RILEM TC 208-HFC, SC 2	-	2010
	Strain Hardening Cement Composites: Structural Design and Performance	RILEM TC 208-HFC SC3	-	2013
	Mechanical Characterization and Testing of Strain-Hardening Fiber-Reinforced Cement-Based Composites (SHCC) - draft	RILEM Technical Committee 208-HFC	-	2011
GPC	CIA Z16-2011: Geopolymer Recommended Practice Handbook	Concrete Institute of Australia	Australia	2011
	Geopolymer Recommended Practice - Peer Review	Concrete Institute of Australia	Australia	2011

2.7 Design calculations

For NSC, HPC, UHPC, SHCC are rules written in standards and recommendations to make calculations. For GPC is probably something similar written by CIA, as mentioned in Table 37, but these rules are not available to use. For NSC and HPC, a simple supported beam will be calculated according Eurocode 2. For UHPC is done the same, but according to the Ultra High Performance Fibre-Reinforced Concretes – Recommendations. At last, a simply supported beam made of SHCC will be reviewed.

2.7.1 NSC and HPC

In this paragraph a simply supported concrete beam is made of NSC or HPC calculated. The calculations are done according to Eurocode 2. First the applied model will be explain in more detail, with some assumptions made. Then the calculations will be done for C30/37. The calculations for C90/105 are the same, but with some other parameter values.

2.7.1.1 Mechanical scheme and working load

The model of the simply supported beam is shown in Figure 53. In the figure, also the working loads are given.

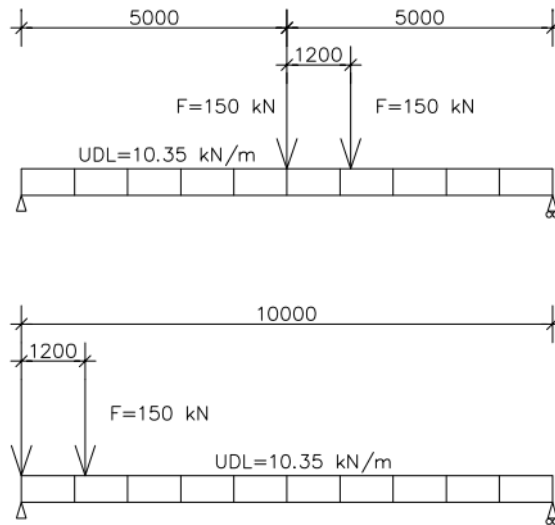


Figure 53 – Left: cross section of loaded beam. Right: loading schema of simply supported beam; above max bending moment, below max shear force (Leenders, 2014)

For the calculation, the self-weight of NSC is assumed to be equal to $\gamma_c = 25 \text{ kN/m}^3$ for the bending moment and shear force calculations. According to Eurocode 2 three load combinations are made; two in ULS and one SLS. The results of the working bending moment and shear force in the three load cases are shown in Table 38.

Table 38 - Three load cases for model shown in Figure 53 (Leenders, 2014)

	ULS 1	ULS 2	SLS
Bending moment [kNm]	1385	1575	1102
Shear force [kN]	576	657	

Next to the strength, the requirements according to the elastic deformation of the beam should be met. The ROK1.2 prescribes with respect to the elastic deflections the following:

$$u_{el} \leq L/1000 \text{ for } L \leq 3 \text{ m}$$

$$u_{el} \leq L/300 \text{ for } L > 10 \text{ m}$$

For spans $3 \text{ m} < L \leq 10 \text{ m}$ a linear interpolation needs to be done. The maximum allowed deflections are presented in Table 39.

Table 39 - Maximum allowed deflections for different span lengths according to ROK1.2

Span length [m]	Deflection [mm]
3	3.0
5	8.3
7.5	18.8
10	33.3
12.5	41.7
15	50.0
17.5	58.3

20	66.7
25	83.3
30	100.0
35	116.7

2.7.1.2 Resistance

Here the resistance calculations are presented for C30/37 according to Eurocode 2. The concrete cross section used for the calculations here, is shown in Figure 54. Characteristics of the reinforcement design is also given in Table 40. In this table also the results of the calculations are given. The calculations are worked out in more detail under Table 40.

Because the calculation methods for C90/105 are the same as for C30/37, for C90/105 are only the results given, as shown in Table 40. For this calculation, the same cross section is assumed. Only the concrete strength of C90/105 differs from the strength of C30/37.

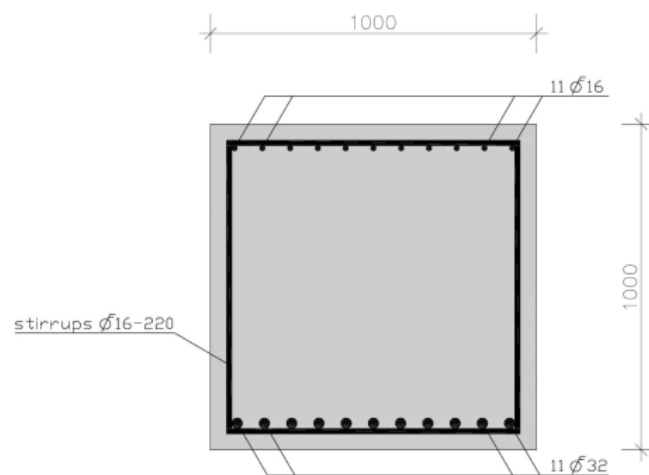


Figure 54 – Cross section of the simply supported beam (Leenders, 2014)

Table 40 - Reinforcement design of the simply supported beam and the results from the calculations according to Eurocode 2

	Variable	NSC	HPC	Unit
Reinforcement design	Number of bars (tension zone)	11	11	[mm]
	Diameters bars	32	32	[mm]
	Diameter stirrups	16	16	[mm]
	C.t.c. distance stirrups	220	220	[mm]
	Cover	50	50	[mm]
Calculation results	M_{Rd}	2890	3179	[kNm]
	M_{Ed}	1575	1575	[kNm]
	M_{Ed}/M_{Rd}	0.55	0.50	[-]
	rotation capacity ($X_u/d < 0.3$)	0.25	0.09	[-]
	M_{cr}	633	633	[kNm]
	$V_{Rd,c}$	496	715	
	$V_{Ed}/V_{Rd,c}$	1.3	0.92	
	V_{Rd}	821	821	[kN]
	V_{Ed}/V_{Rd}	0.8	0.8	[-]
	w_k	0.20	0.14	[mm]
	u	8.43	6.32	[mm]

Moment capacity

Here the moment capacity of the concrete section made of C30/37 is calculated. The forces working over the cross section, from the concrete (N_c) and the steel (N_s), are shown in Figure 55. In the figure are also some length given. These lengths are quantified in Table 41.

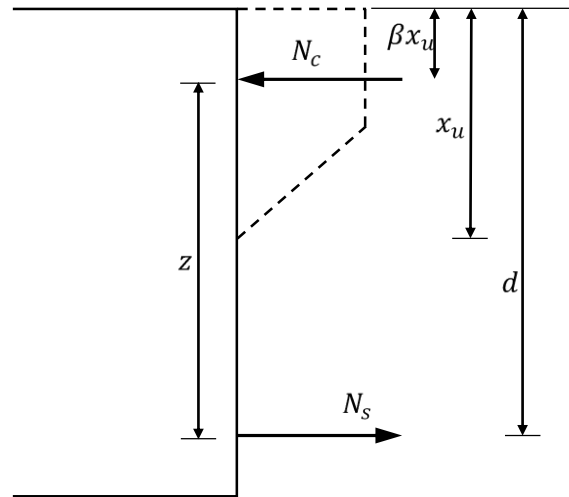


Figure 55 - Forces working over the height of the simply supported beam

Table 41 - Lengths shown in Figure 55

Length	Definition		
d	$1000 - cover - \phi_{stirrup} - 0.5 \cdot \phi_{longitudinal}$	918	mm
z_{guess}	$0.9d$	826	mm
z_{check}	$d = 0.38X_u$	829	mm
Δz		0.38	%

Knowing the working forces in the cross section, equations for horizontal and moment equilibrium could be created. The horizontal and moment equilibrium are expressed in eq.(48) and eq.(49) respectively.

$$\sum F_{hor} = 0 \quad \text{eq.(48)}$$

$$N_c + N_s = 0 \quad \text{eq.(48a)}$$

$$N_s = A_s \cdot f_{yd} = 11 \cdot \frac{1}{4} \cdot \pi \cdot 32^2 \cdot 435 = 3,848 \text{ kN} = N_c \quad \text{eq.(48b)}$$

$$X_u = \frac{N_c}{0.75 \cdot b \cdot f_{cd}} = \frac{3,848}{0.75 \cdot 1000 \cdot 20} = 257 \text{ mm} \quad \text{eq.(48c)}$$

$$\sum M = 0 \quad \text{eq.(49)}$$

$$N_c \cdot z = M_{Rd} (\geq M_{Ed}) \quad \text{eq.(49a)}$$

$$M_{Rd} = 3,848 \cdot 826 = 3179 \text{ kNm} \quad \text{eq.(49b)}$$

The unity check for the moment capacity is shown in eq.(50), The moment capacity of the beam is high enough.

$$\frac{M_{Ed}}{M_{Rd}} = 0.50 \quad \text{eq.(50)}$$

Rotation capacity

To prevent failure in the compression zone the rotation capacity is limited. The rotation capacity is described by the NEN-EN 1992-1-1 and the ROK1.2, as shown in eq.(51). The check shows that the rotation capacity is high enough.

$$\frac{X_u}{d} < 0.3 \quad \text{eq.(51)}$$

$$\frac{257}{918} = 0.28 < 0.3 \rightarrow OK$$

Cracking moment

The cracking moment can be determined by multiplying the cracking strength by the section modulus, as shown in eq.(52). The cracking moment should be smaller than the maximum design moment, such that the structure cracks before it fail. This mechanism gives a certain warning before the structure fails. The cracking strength is determined according to Eurocode 2: chapter 3.1.8 (3.23), as shown in eq.(52)

$$M_{cr} = \sigma_{cr} W \quad \text{eq.(52)}$$

Where,

$$\sigma_{cr} = \max \left\{ \left(1.6 - \frac{h}{1000} \right) f_{ctm}, f_{ctm} \right\} = 2.9 \text{ MPa} \quad \text{eq.(52a)}$$

$$W = \frac{1}{6} b h^2 = 1.67 \cdot 10^8 \text{ mm}^3 \quad \text{eq.(52b)}$$

$$M_{cr} = 483 \text{ kNm} \leq M_{Ed} \quad \text{eq.(53)}$$

Shear forces

The calculation of the shear force according to Eurocode 2 is already explained in chapter 2.3 Mechanical characteristics. Here the calculations will be done again for the simply supported beam. The calculations are not described in the same level of detail again.

$$V_{Rd,c} = \left[C_{Rd,c} \cdot k(100\rho_l \cdot f_{ck})^{\frac{1}{3}} + k_1 \sigma_{cp} \right] b_w d \quad (\text{Eurocode 2, 6.2.2(1)})$$

$$V_{Rd,c,min} = (v_{min} + k_1 \sigma_{cp}) b_w d \quad (\text{Eurocode 2, 6.2.2(1)})$$

Where, $C_{Rd,c} = \frac{0.18}{\gamma_c} = \frac{0.18}{1.5} = 0.12$; $k = \min\left(1 + \sqrt{\frac{200}{d}}\right) = 1.47$; $\sigma_{cp} = 0$ (no prestressing steel)

$$\rho_l = \min\left(\frac{0.02}{\frac{A_s}{b_w d}}\right) = 0.00964; k_1 = 0.15; v_{min} = 0.035k^{\frac{3}{2}} \cdot f_{ck}^{\frac{1}{2}} = 0.341$$

$$V_{Rd,c} = 496 \text{ kN} \quad \text{eq.(54)}$$

$$V_{Rd,c,min} = 313 \text{ kN} \quad \text{eq.(55)}$$

$$\text{Unity check: } \frac{V_{Ed}}{V_{Rd}} = 1.3 \rightarrow \text{not OK} \quad \text{eq.(56)}$$

Because the shear capacity of the concrete is not high enough ($\frac{V_{Ed}}{V_{Rd}} > 1.3$), shear reinforcement should be inserted. The shear capacity from shear reinforcement can be calculated according to formula (6.8) from Eurocode 2, as shown in eq.(57)

$$V_{Rd,s} = \frac{A_{sw}}{s} z \cdot f_{ywd} \cot\theta \quad \text{eq.(57)}$$

The shear reinforcement is chosen $\emptyset 16 - 220$, as shown in Table 40. According to Eurocode 2, angle theta is chosen equal to $\cot\theta = 2.5$. The yield force of the steel is equal to $f_{ywd} = 435 \text{ MPa}$. This makes the shear resistance equal to:

$$V_{Rd,s} = V_{Rd} = 821 \text{ kN}$$

$$\text{Unity check: } \frac{V_{Ed}}{V_{Rd}} = 0.80 \rightarrow \text{OK} \quad \text{eq.(58)}$$

Crack width

Eurocode 2, chapter 7.3.4, formula (7.8) describes the crack width calculation of NSC and HPC. The steps to calculate the crack width are briefly described here. As shown in eq.(59) the crack width is a function of the maximum space between cracks and the strain difference between steel and concrete. The maximum space between cracks and strain difference can be calculated as described in eq.(59).

$$w_k = s_{r,max}(\varepsilon_{sm} - \varepsilon_{cm}) \quad \text{eq.(59)}$$

Where,

$$s_{r,max} = k_3 c + \frac{k_1 k_2 k_4 \emptyset}{\rho_{p,eff}} \quad \text{eq.(59a)}$$

$$\varepsilon_{sm} - \varepsilon_{cm} = \frac{\sigma_s - k_t \cdot \frac{f_{ct,eff}}{\rho_{p,eff}} (1 + \alpha_e \cdot \rho_{p,eff})}{E_s} \geq 0,6 \cdot \frac{\sigma_s}{E_s} \quad \text{eq.(59b)}$$

Where,

$$\sigma_s = \frac{M_{sls}}{A_s \cdot z} = \frac{1102}{8847(0.9 \cdot 918)} = 150.8 \text{ MPa}$$

$$k_t = 0.4 \text{ (Long-term loading)}$$

$$A_{c,eff} = \min \left\{ \begin{array}{l} 2.5(h-d) \\ (h-X_u)/3 \\ h/2 \end{array} \right\} \cdot b = 205,000 \text{ mm}^2$$

$$k_1 = 0.8 \text{ (High bond value between the reinforcement and the concrete)}$$

$$k_2 = 0.5 \text{ (beam in bending)}$$

$$k_3 = 3.4; k_4 = 0.425 \text{ (recommended values from Eurocode 2)}$$

$$f_{ct,eff} = f_{ctm} = 2.9 \text{ MPa}$$

$$\rho_{p,eff} = \frac{A_s}{A_{c,eff}} = \frac{8,847}{205,000} = 0.043$$

$$\alpha_e = \frac{E_s}{E_{cm}} = \frac{200,000}{33,000} = 6.06$$

All together the crack width becomes equal to:

$$w_k = 0.17 \text{ mm} \quad \text{eq.(60)}$$

Deflection

According to ROK1.2 the maximum deflection of a beam with a span larger than 10 m is $l/300$. In this case, the span is 10 m, so the maximum deflection is equal to 33 mm. The deflection in the beam caused by a distributed load or a point load can be calculated by eq.(61) and eq.(62) respectively.

$$u_q = \frac{5}{384} \cdot \frac{qL^4}{EI} \quad \text{eq.(61)}$$

$$u_f = \frac{1}{48} \cdot \frac{FL^3}{EI} \quad \text{eq.(62)}$$

Where

$$I_c = \frac{1}{12} \cdot 1000 \cdot 1000^3 = 8.333 \cdot 10^{10} \text{ mm}^4 \quad \text{eq.(63)}$$

The total deflection of the beam is the summation of both deflections as shown in eq.(64)

$$u_{tot} = u_q + u_f = 5.02 + 3.41 = 8.43 \text{ mm} \quad \text{eq.(64)}$$

2.7.2 SHCC

In this paragraph is a simply supported concrete beam calculated for SHCC. The calculations are done according to Japan Society of Civil Engineers (2008). The model applied is the same as for NSC and HPC, as shown in the next paragraph. After the presentation of the model, the calculations are shown.

2.7.2.1 Mechanical scheme and working loads

Here the mechanical scheme and the working loads on the scheme are shown. The same scheme of a simply supported beam is used as for NSC, as shown in Figure 55.

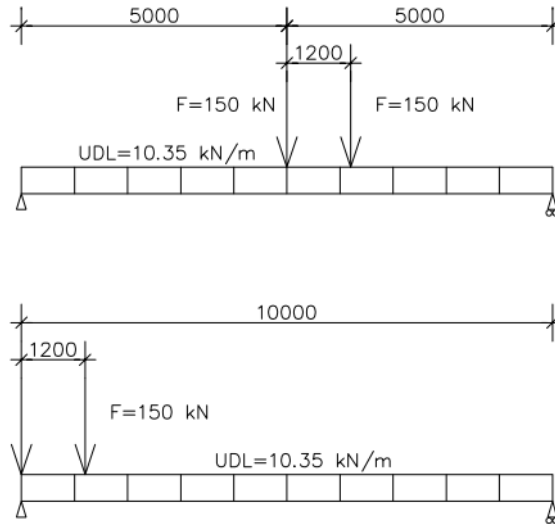


Figure 56 – Left: cross section of loaded beam. Right: loading schema of simply supported beam; above max bending moment, below max shear force (Leenders, 2014)

For the calculation, the self-weight of SHCC is assumed to be 25 kN/m^3 for the bending moment and shear force calculations. According to Eurocode 2 again the three load combinations are calculated, as shown in Table 38.

Table 42 - Three load cases for model shown in Figure 53 (Leenders, 2014)

	ULS 1	ULS 2	SLS
Bending moment [kNm]	1385	1575	1102
Shear force [kN]	576	657	

According to ROK1.2, the deflection again with respect to the elastic deflections is:

$$u_{el} \leq L/1000 \text{ for } L \leq 3 \text{ m}$$

$$u_{el} \leq L/300 \text{ for } L > 10 \text{ m}$$

The maximum allowed deflections for spans with a length between $3\text{m} < L \leq 10\text{m}$ are presented in Table 47

Table 43 - Maximum allowed deflections for different span lengths according to ROK1.2

Span length [m]	Deflection [mm]
3	3.0
5	8.3
7.5	18.8
10	33.3
12.5	41.7
15	50.0
17.5	58.3
20	66.7
25	83.3
30	100.0
35	116.7

2.7.2.2 Resistance

SHCC has a different stress-strain relation compared to NSC. In Figure 54 is shown the compressive stress as function of the strain (left) and the tensile stress as a function of the strain (right). The parabolic shape in the compressive elastic zone, is also in the cross section as shown in Figure 58. In Figure 58 are also shown the tensile stresses in the cross section. The working tensile stresses are caused by the fibres and reinforcement steel. In short, the three different working stresses cause three resultant forces:

- Compressive stresses from the concrete itself cause a resultant compressive force N_{cu}
- Tensile stresses from the fibres cause a resultant tensile force N_{cut}
- Tensile stresses from the reinforcement steel cause a resultant tensile force N_{su}

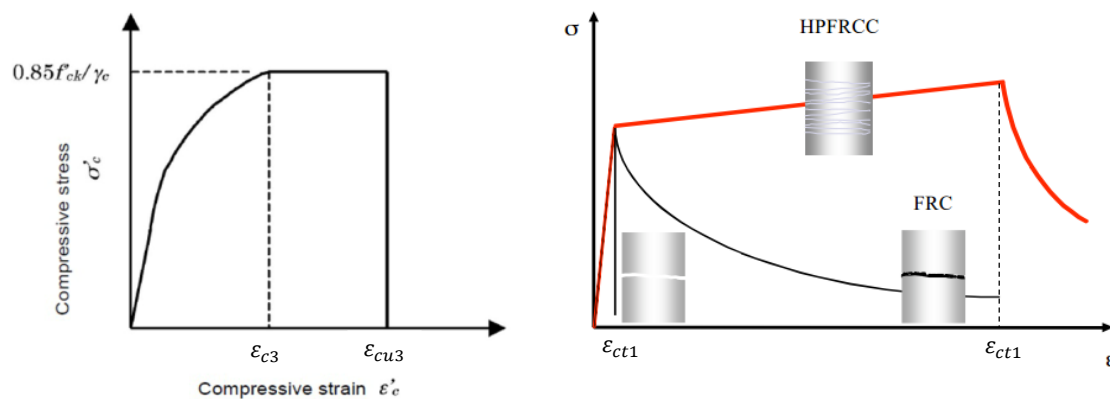


Figure 57 – Stress strain curve for SHCC in compression (left) and tension (right) (Leenders, 2014)

The calculation results for the simply supported beam in SHCC are shown in Table 44. The calculations are explained in detail after Table 44.

Table 44 - Reinforcement design of the simply supported beam and the results from the calculations (Leenders, 2014)

	Variable	SHCC	Unit
Reinforcement design	Beam height	1000	[mm]
	Number of bars	11	[mm]
	Diameters bars	32	[mm]
	Diameter stirrups	16	[mm]
	C.t.c. distance stirrups	220	[mm]
	Cover	50	[mm]
Calculation results	M_{Rd}	4,308	[kNm]
	M_{Ed}	1,575	[kNm]
	M_{Ed}/M_{Rd}	0.37	[-]
	M_{cr}	667	[kNm]
	V_{Rd}	3,217	[kN]
	V_{Ed}	657	[kN]
	V_{Ed}/V_{Rd}	0.20	[-]
	w_{max}	< 0.1 ⁴³	[mm]
	u_{max}	33	[mm]

⁴³ (Li V. C., Engineered Cementitious Composites (ECC) – Material, Structural, and Durability Performance, 2007)

u	16.9	[mm]
$u/u_{max} < 1$	0.51	[-]

Moment capacity

From Figure 58, equations for horizontal and moment equilibrium can be create. These equations are shown in eq.(65) and eq.(66). The variables in the equations are the material characteristics, which are given in chapter 2.3 Mechanical characteristics, and the dimensions of the beam, given in the model description of the previous paragraph and Figure 58.

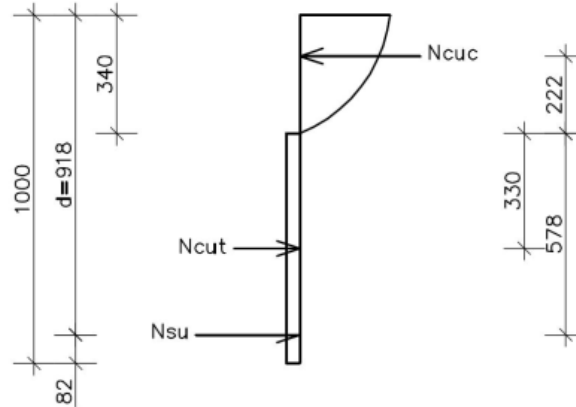


Figure 58 - Stress diagram of SHCC over the height of the cross section (Leenders, 2014)

Horizontal equilibrium is the summation of the concrete, steel and fibre forces that should be equal to zero, as shown in eq.(65).

$$\sum F_{hor} = 0 \quad \text{eq.(65)}$$

$$N_{su} + N_{cut} - N_{cuc} = 0 \quad \text{eq.(65a)}$$

Where,

$$N_{su} = A_s \cdot f_{yd} = 3,842 \text{ kN}$$

$$N_{cut} = f_{ctd}b(h - X_u) = 3,400(1000 - X_u)$$

$$N_{cuc} = \frac{2}{3}f_{cd}b \cdot X_u = 17,867X_u$$

This makes the compressive zone X_u equal to:

$$X_u = 340 \text{ mm}$$

Filling in the compressive zone in the formulas for the resistance forces, the different components equal to:

$$N_{su} = A_s \cdot f_{yd} = 3,842 \text{ kN}$$

$$N_{cut} = f_{ctd}b(h - X_u) = 2,229 \text{ kN}$$

$$N_{cuc} = \frac{2}{3}f_{cd}b \cdot X_u = 6,078 \text{ kN}$$

Moment equilibrium is taken in the point 340 mm under the top of the beam.

$$\sum M = 0 \quad \text{eq.(66)}$$

$$N_{su}a_{st} + N_{cut}a_{ct} + N_{cuc}a_{cc} - M_{Rd} = 0 \quad \text{eq.(66a)}$$

Where,

$$a_{cc} = 222 \text{ mm}$$

$$a_{ct} = 330 \text{ mm}$$

$$a_{st} = 578 \text{ mm}$$

This value are also given in Figure 58. Filling in all variables, the resistance bending moment of the beam of SHCC is equal to:

$$M_{Rd} = 4,309 \text{ kNm}$$

Cracking moment

The cracking moment of a beam in SHCC can be calculated the same way as for NSC, as shown in eq.(67)

$$M_{cr} = f_{ct1} \cdot W = 4.0 \cdot \frac{1}{6} \cdot 1000 \cdot 1000^2 = 667 \text{ kNm} < M_{Ed} \quad \text{eq.(67)}$$

Shear force

In short, the shear resistance can be calculated by adding four components as shown in eq.(68).

$$V_{yd} = V_{cd} + V_{sd} + V_{fd} + V_{ped} = V_{Rd} \quad \text{eq.(68)}$$

Here the different components are defined as:

V_{cd} is the design shear capacity of a linear member without any shear reinforcing steel, excluding the strength exerted by reinforcing fibres.

V_{sd} is the design shear capacity of shear reinforcement

V_{fd} is the design value of the shear capacity accommodated by the reinforcing fibres

V_{ped} is the component of effective tensile force in longitudinal prestressing steel parallel to the shear force.

The shear force capacity of SHCC is already calculated in detail in chapter 2.3.6 Shear resistance. Therefore, only some calculations results for the given variables are given here.

$$V_{cd} = \beta_d \cdot \beta_p \cdot \beta_n \cdot f_{ved} \cdot \frac{b_w \cdot d}{\gamma_b} \quad \text{eq.(69)}$$

$$V_{cd} = 1.02 \cdot 0.988 \cdot 2 \cdot 0.42 \cdot \frac{1000 \cdot 918}{1.3} = 598 \text{ kN}$$

$$V_{fd} = \frac{f_{vd}}{\tan(\beta_u)} \cdot \frac{b_w \cdot z}{\gamma_b} \quad \text{eq.(70)}$$

$$V_{fd} = \frac{3.4}{1} \cdot \frac{1000 \cdot \frac{918}{1.15}}{1.3} = 2,088 \text{ kN}$$

Assuming no shear reinforcement the total shear resistance is equal to:

$$V_{Rd} = V_{yd} = V_{cd} + V_{fd} = 598 + 2,088 = 2,686 \text{ kN} \quad \text{eq.(71)}$$

This resisting value is already higher than the working shear force. However, shear reinforcement is added in the cross section, so this component should also added up to the total shear resistance.

$$V_s = \left[\frac{A_w f_{wyd} (\sin \alpha_s + \cos \alpha_s)}{s_s} \right] \frac{z}{\gamma_b} \quad \text{eq.(72)}$$

$$V_s = \left[\frac{2 \cdot \frac{1}{4} \cdot \pi \cdot 16^2 \cdot 400 \cdot (\sin 90^\circ + \cos 90^\circ)}{220} \right] \frac{918/1.15}{1.10} = 531 \text{ kN}$$

With the component of the shear reinforcement, the total shear capacity of the cross section becomes equal to:

$$V_{Rd} = V_{yd} = V_{cd} + V_{fd} + V_s = 598 + 2,088 + 531 = 3,217 \text{ kN} \quad \text{eq.(73)}$$

Deflection

The calculation of the deflection of a beam made of SHCC is more or less the same as for NSC. Because the Young's modulus of SHCC is significantly lower than for NSC, the deflection of a SHCC beam is larger for the same loads. The calculation of the vertical deflection is shown in eq.(74).

$$u_{tot} = \frac{5}{384} \cdot \frac{qL^4}{EI} + \frac{1}{48} \cdot \frac{FL^3}{EI} \quad \text{eq.(74)}$$

Where

$$I_c = \frac{1}{12} \cdot 1000 \cdot 1000^3 = 8.333 \cdot 10^{10} \text{ mm}^4 \quad \text{eq.(74a)}$$

$$u_{tot} = \frac{5}{384} \cdot \frac{(25 + 10.35) \cdot 10,000^4}{7.7 \cdot 10^3 \cdot 8.333 \cdot 10^{10}} + \frac{1}{48} \cdot \frac{150,000 \cdot 10,000^3 \cdot 2}{7.7 \cdot 10^3 \cdot 8.333 \cdot 10^{10}} = 16.9 \text{ mm} \quad \text{eq.(74b)}$$

2.7.3 UHPC

The calculations of a simply supported beam in UHPC are done according to the recommendations from AFGC's Scientific and Technical Committee (2013). In this chapter the mechanical schema with working loads are firstly presented. After that, the resistance of the cross section is calculated.

2.7.3.1 Mechanical scheme and working loads

In this paragraph the mechanical scheme and the working loads on the scheme are shown. The beam and the cross section of the beam are shown in Figure 56.

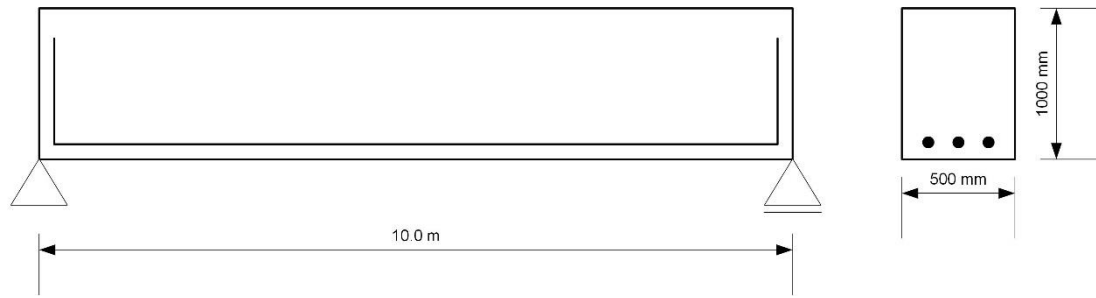


Figure 59 – Mechanical scheme and cross section of the UHPC beam

For the calculation, the self-weight of UHPC without reinforcement is assumed to be 25 kN/m^3 for the bending moment and shear force calculations. According to Eurocode 2 again the three load combinations are calculated, as shown in Table 38.

Table 45 - Three load cases for model shown in Figure 53 (Leenders, 2014)

	ULS 1	ULS 2	SLS
Bending moment [kNm]	1385	1575	1102
Shear force [kN]	576	657	

According to ROK1.2, the deflection again with respect to the elastic deflections is:

$$u_{el} \leq L/1000 \text{ for } L \leq 3 \text{ m}$$

$$u_{el} \leq L/300 \text{ for } L > 10 \text{ m}$$

The maximum allowed deflections for spans with a length between $3\text{ m} < L \leq 10\text{ m}$ are presented in Table 47

Table 46 - Maximum allowed deflections for different span lengths according to ROK1.2

Span length [m]	Deflection [mm]
3	3.0
5	8.3
7.5	18.8
10	33.3
12.5	41.7
15	50.0
17.5	58.3
20	66.7
25	83.3
30	100.0
35	116.7

2.7.3.2 Resistance

The calculations are done for a simply supported beam with a length of 10 metres, a height of 1,000 mm and a width of 500 mm, as shown in Table 47. In this table are also the result from the calculations shown. The detailed clarification of the calculations is shown under the table.

Table 47 – Design of the simply supported beam and the results from the calculations

	UHPC	Unit
Beam span	10,000	[mm]

Beam height	1,000	[mm]
Beam width	500	[mm]
Reinforcement steel	B500	
A_s	1,000	[mm ²]
E_s	210,000	[MPa]
M_{Rd}	1029	[kNm]
M_{Ed}	562.5	[kNm]
M_{Ed}/M_{Rd}	0.55	[-]
rotation capacity ($X_u/d < 0.3$)	0.10	[-]
M_{cr}	1029	[kNm]
V_{Ed}	225	[kN]
V_{Rd} (without shear reinforcement)	3480	[kN]
V_{Ed}/V_{Rd}	0.07	[-]
w_s (crack width at depth of passive steel)	0.035	[mm]
$w_t = w_{max}$ (crack width on most tensile zone)	0.039	[mm]
u_{max}	33	[mm]
u	15.6	[mm]
$u/u_{max} < 1$	0.47	[-]

For the calculations is the simplified stress-strain diagram for UHPC applied. This diagram is shown in Figure 60. The figure is a schematic view and not on scale.

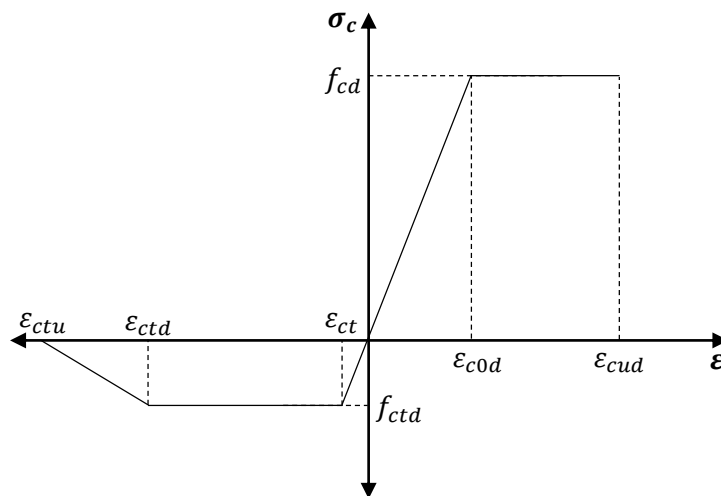


Figure 60 - Simplified stress-strain diagram for UHPC according to AFGC's Scientific and Technical Committee (2013)

For the calculation of the simply supported beam made of UHPC, the stresses and strains in the beam should be known. In Figure 61 are the stresses and the strains over the height of the beam shown. In the figure also a few lengths are shown. The stresses in the beam to resist the bending moment are the stresses from the concrete, the fibres and the reinforcement steel.

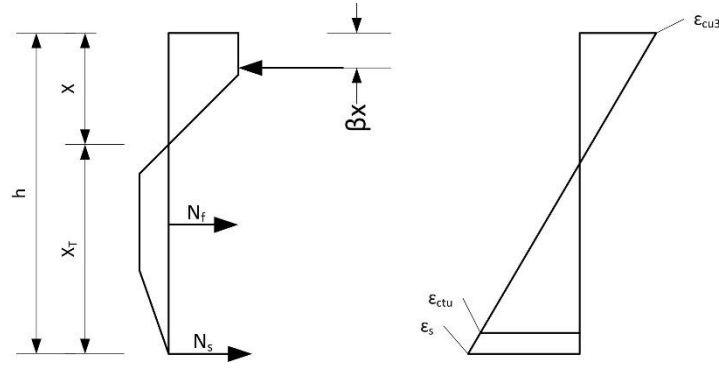


Figure 61 - Working stresses and strains over the height of the cross section according to (Paskvalin, 2015)

The tensile strength capacity of UHPC is high compared to NSC. Therefore, the tensile capacity of UHPC has to be taken into account in the calculation of the resisting bending moment. The tensile stress over the height of the cross section is shown in Figure 61, N_f . Now horizontal equilibrium should be there as shown in eq.(75).

$$\sum F_{hor} = 0 \quad \text{eq.(75)}$$

$$N_c - N_s - N_f = 0 \quad \text{eq.(75a)}$$

$$N_c = \alpha \cdot f_{cd} \cdot b \cdot X_u$$

Where, $\alpha = 0.56$;

$$N_s = A_s \cdot f_{yd}$$

$$N_f = 0.5 \cdot \frac{1}{\epsilon_{cu3}} \cdot X_u \cdot f_{ctd} \cdot b \cdot (\epsilon_{ctu} + \epsilon_{ctd} - \epsilon_{ct}) \quad \text{(Paskvalin, 2015)}$$

Where, $\epsilon_{cu3} = 2.6\text{‰}$; $\epsilon_{ctu} = 22.5\text{‰}$; $\epsilon_{ctd} = 15.1\text{‰}$; $\epsilon_{ct} = 0.12\text{‰}$ (Paskvalin, 2015)

Filling in all parameters, the height of the concrete compressive zone can be calculated. As shown in eq.(76)

$$X_u = \frac{A_s \cdot f_{yd}}{b \cdot (\alpha \cdot f_{cd} - \frac{1}{\epsilon_{cu3}} \cdot f_{ctd} \cdot (\epsilon_{ctu} + \epsilon_{ctd} - \epsilon_{ct}))} = 81.5 \text{ mm} \quad \text{eq.(76)}$$

$$X_t = \epsilon_{ctu} \cdot \frac{X_u}{\epsilon_{cu3}} = 705 \text{ mm}$$

Next to horizontal equilibrium, there should be moment equilibrium in the cross section. The moment equilibrium is taken at the point where the tensile and compressive stresses are equal zero. By moment equilibrium, the bending moment resistance can be calculated as shown in eq.(77)

$$\sum M = 0 \quad \text{eq.(77)}$$

$$N_c \cdot X_u \cdot (1 - \beta) + N_f \cdot a + N_s \cdot (0.9h - X_u) = M_{Rd} (\geq M_{Ed}) \quad \text{(Paskvalin, 2015)}$$

where, $\beta = 0.34$; $a = 306 \text{ mm}$;

(Paskvalin, 2015)

$$M_{Rd} = 1,029 \text{ kNm}$$

Knowing the bending moment resistance and the actual working design bending moment, the unity check calculated as shown in eq.(78).

$$\text{Unity check: } \frac{M_{Ed}}{M_{Rd}} = \frac{563}{1029} = 0.55 \quad \text{eq.(78)}$$

Rotation capacity

To prevent failure in the compression zone for a beam, the rotation capacity is limited. The rotation capacity for NSC is described by the NEN-EN 1992-1-1 and the ROK1.2. It is assumed that UHPC should have a similar rotation capacity. The rotation capacity for UHPC then can be expressed as shown in eq.(79). This check shows that the rotation capacity of an UHPC beam is large enough according to the rules for NSC.

$$\frac{X_u}{d} = \frac{X_u}{X_u + X_T} = \frac{83.21}{83.21 + 720.11} = 0.10 < 0.3 \quad \text{eq.(79)}$$

Shear

The calculation of the shear capacity of the UHPFRC is the summation the shear capacity of the concrete, the fibres and the shear reinforcement steel. The calculations for shear are already done in detail in chapter 2.3.6.3 Shear resistance of UHPC according to AFGC (2013). Here only the expression of the total shear capacity of UHPC is given where all the components of the concrete are mentioned separately as shown in eq.(80) more details of the calculation can be found in Paskvalin (2015).

$$V_{Rd} = V_{Rd,c} + V_{Rd,f} + V_{Rd,s} \quad \text{eq.(80)}$$

Where,

$V_{Rd,c}$ = the contribution of the concrete

$V_{Rd,f}$ = the contribution of the steel fibres

$V_{Rd,s}$ = the contribution of shear reinforcement

Crack width

Same as for the crack width calculation in Eurocode 2, the crack opening of UHPC is a function of maximum the space between the cracks and the difference between the main strain in the steel reinforcement combined with fibres and the mean strain in concrete between the cracks. The calculations for the crack width of the simply supported beam in UHPC will be explained in detail here, according to AFGC's Scientific and Technical Committee (2013). Beginning with the crack width at the level of the reinforcement, which can be expressed as shown in eq.(81)

$$w_s = s_{r,max,f} (\varepsilon_{sm,f} - \varepsilon_{cm,f}) \quad \text{eq.(81)}$$

With this crack width, the crack width of the chord under highest tension can be calculated according to eq.(82)

$$w_t = w_s \left(\frac{h - x - x'}{d - x - x'} \right) \quad \text{eq.(82)}$$

The verification check for the crack width under the highest tension according to the French recommendation is shown in eq.(83)

$$w_t \leq w_{max} \quad \text{eq.(83)}$$

In the above mentioned equations are a lot of variables. These variables are clarified here in detail. Beginning with the clarification of the second term of the equation to calculate the crack width at the level of reinforcement. The calculation of this term is shown in eq.(84)

$$\varepsilon_{sm,f} - \varepsilon_{cm,f} = \left[\frac{\sigma_s}{E_s} - \frac{f_{ctfm}}{E_s} - \left[k_t (f_{ctm,el} - f_{ctfm}) \left(\frac{1}{\rho_{eff}} + \frac{E_s}{E_{cm}} \right) \right] \right] \cdot \frac{1}{E_s} \quad \text{eq.(84)}$$

Where,

$$\rho_{eff} = \frac{A_s}{A_{c,eff}}, \text{ assuming that there is no prestressing steel}$$

$$A_{c,eff} = h_{c,eff} \cdot b$$

$$h_{c,eff} = \min \left(\frac{2.5(h - d)}{h/2} \right)$$

k_t time factor

The assumed values to calculate the second term are given in Table 48. Filling in these values in eq.(85), the strain part of the total equation becomes equal to

$$\varepsilon_{sm,f} - \varepsilon_{cm,f} = 0.000364 \quad \text{eq.(85)}$$

Table 48 – Assumed values to calculate the second term of the crack width expression

Variable	Chosen value	Explanation
Steel stress	$\sigma_s = 300 \text{ MPa}$	Assumed value
Mean maximal post-cracking stress	$f_{ctfm} = 9 \text{ MPa}$	Recommended value (AFGC's Scientific and Technical Committee, 2013)
Term for loading time	$k_t = 0.4$	Assuming long term loading
Mean limit of elasticity under tension	$f_{ctm,el} = 12.9 \text{ MPa}$	Recommended value (AFGC's Scientific and Technical Committee, 2013)
Distance between reinforcement and outer compressive fibre	$d = 0.9h = 900 \text{ mm}$	Assumed value

The first term of the calculations of the crack width at a level of reinforcement can be calculated as shown in eq.(86). The values of the unknown variable of eq.(86) are shown in Table 49.

$$s_{r,max,f} = 2.55(l_0 + l_t) = 2.55(34.5 + 3) = 95.7 \text{ mm} \quad \text{eq.(86)}$$

Where,

$$l_0 = 1.33 \cdot \frac{c}{\delta}$$

$$l_t = \left[0.3k_2 \left(1 - \frac{f_{ctfm}}{f_{ctm,el}} \right) \cdot \frac{1}{\delta \cdot \eta} \right] \geq \frac{l_f}{2}$$

$$\delta = 1 + 0.5 \left(\frac{f_{ctf,m}}{f_{ctm,el}} \right)$$

Table 49 - Assumed values to calculate the first term of the crack width expression

Variable	Chosen value	Explanation
Concrete cover	$c = 35 \text{ mm}$	Assumed value
Mean maximal post-cracking stress	$f_{ctfm} = 9 \text{ MPa}$	Recommended value (AFGC's Scientific and Technical Committee, 2013)
Mean limit of elasticity under tension	$f_{ctm,el} = 12.9 \text{ MPa}$	Recommended value (AFGC's Scientific and Technical Committee, 2013)
Type of loading	$k_2 = 0.5$	Loaded in bending (AFGC's Scientific and Technical Committee, 2013)
Fibres length	$l_f = 4 - 8 \text{ mm}$	Defined in chapter 2.2 Composition
Type of reinforcement	$\eta = 2.25$	Assumed ribbed bars (Table 7.2, (AFGC's Scientific and Technical Committee, 2013))
Mean maximal post-cracking stress	$f_{ctf,m} = 9 \text{ MPa}$	Recommended value (AFGC's Scientific and Technical Committee, 2013)

Knowing both terms of the crack width equation, the crack width at the reinforcement and at the chord under the highest tensions can be calculated as shown in eq.(87) and eq.(88).

$$w_s = 0.035 \text{ mm} \quad \text{eq.(87)}$$

$$w_t = w_s \left(\frac{h - x - x'}{d - x - x'} \right) = 0.035 \left(\frac{1000 - 81.5 - 3.76}{900 - 81.5 - 3.76} \right) = 0.039 \text{ mm} \quad \text{eq.(88)}$$

Where, $x' = x_t \cdot \frac{\varepsilon_{ct}}{\varepsilon_{ctu}} = 3.76 \text{ mm}$ (Paskvalin, 2015)

Deflection

The calculation of the vertical deflection of a beam made of UHPC is shown in eq.(89). Because the high Young's modulus of UHPC, the deflection of a UHPC beam is very small compared to NSC.

$$u_{tot} = \frac{5}{384} \cdot \frac{qL^4}{EI} + \frac{1}{48} \cdot \frac{FL^3}{EI} \quad \text{eq.(89)}$$

Where

$$I_c = \frac{1}{12} \cdot 500 \cdot 1000^3 = 8.333 \cdot 10^{10} \text{ mm}^4 \quad \text{eq.(89a)}$$

$$u_{tot} = \frac{5}{384} \cdot \frac{(25 + 10.35) \cdot 10,000^4}{16.7 \cdot 10^3 \cdot 8.333 \cdot 10^{10}} + \frac{1}{48} \cdot \frac{150,000 \cdot 10,000^3 \cdot 2}{16.7 \cdot 10^3 \cdot 8.333 \cdot 10^{10}} \quad \text{eq.(89b)}$$

$$u_{tot} = 15.6 \text{ mm}$$

2.8 Costs of ACMs

For the application of ACMs, the costs are probably the most important factors. In this paragraph is made a rough cost estimation for the materials in the scope of this research. Some ACMs are not researched well enough to give a practical estimation of the costs. Therefore, not all ACMs are included in the estimation of the production costs. However, probably most ACMs are more expensive than NSC.

An overview of the estimated production costs is shown in Table 50. In the upper part of this table are the costs of the ACMs mentioned. In the lower part are the costs of additional steel to the concrete mentioned. As shown in the table, is NSC by far the cheapest cementitious material. UHPC is by far the most expensive one. Between the production costs of NSC and UHPC is almost a factor 10. Also shown in the table, there is a relative large difference between the costs of steel reinforcement and steel fibres. The reduction is mainly caused by the labour reduction, because the execution of reinforcement steel is far more labour intensive.

Table 50 - Production costs of some ACMs per unit

Material	Price	Unit	Sources
NSC	75 – 100	Euro/m ³	(Leenders, 2014), (Paskvalin, 2015)
NSSFRC (40 kg/m ³)	90 – 115	Euro/m ³	Cost NSC + cost steel fibres
HPC (no fibres)	300	Euro/m ³	(Paskvalin, 2015)
HPSFRC (70 kg/m ³)	330	Euro/m ³	Cost HPC + cost steel fibres
UHPC (including fibres)	1000	Euro/m ³	(Paskvalin, 2015)
SHCC	150 – 300	Euro/m ³	(Leenders, 2014)
Steel reinforcement (incl. placing)	0.80 – 1.00	Euro/kg	(Leenders, 2014), (Paskvalin, 2015)
Steel fibres	0.40	Euro/kg	40% cost reduction compared to steel reinforcement, incl. placing (Mebin, 2012)
Prestressing steel	3	Euro/kg	(Paskvalin, 2015)

3 Researched applications

In this paragraph some researched applications of ACM are describe. The reason to do so is to learn from done research: avoid doing the same research twice and the researched applications indicate where ACMs are probably smart to apply.

The researched applications are shown in Table 51. The table is sort by the concrete materials. As shown in the table, research is mainly done to UHPC and SHCC. In the second column the applications given per ACM are given. In this column is also given the source of the research rapport or article. In the last column is the conclusion of the research given shortly.

Table 51 – Some researched applications of ACM

ACM	Application	Conclusion
UHPC	Retaining wall (López, Serna, & Camacho, n.d.)	<ul style="list-style-type: none"> - reliable mechanical behaviour - very ductile behaviour - reduction of the final costs
UHPC	Large span shell structure (Maten, 2011)	<ul style="list-style-type: none"> - material savings - higher expected lifespan
UHPC	AASHTO Type II Girder (Graybeal B. , 2008)	<ul style="list-style-type: none"> - Larger flexural capacity - UHPC carries tensile load after cracking - The crack spacing in the tension flange of a UHPC I-girder is inversely proportional to the maximum tensile strain observed in said cracked region
UHPC	Bolted joints (Camacho, Serna, & López, n.d.)	<ul style="list-style-type: none"> - Some verifying for the test method should be done. - Weakest failure: cleavage and net tension - Bearing failure was ductile
SHCC	Bridge decks without joints (Michigan Department of Transportation's Construction and Technology Division, 2005)	<ul style="list-style-type: none"> - Cost reduction - Reduction of CO₂ emission - Reduction of energy - Longer service life - Comfort during driving the bridge - Reduction bridge closings for routine maintenance
SHCC	Reinforced concrete beam strengthened with SHCC (flexural performance) (Kim, et al., 2014)	<ul style="list-style-type: none"> - Crack width of a beam can be controlled by applying the SHCC - The load-bearing capacity of beams can be improved by applying the SHCC and HSRS bars - A model for the nonlinear flexural analysis showed more significant strengthening effects of SHCC and in terms of load bearing capacity compared to behaviour the experiments
SHCC	Reinforced concrete beam strengthened with steel reinforced and unreinforced SHCC (Hussein, Kunieda, & Nakamura, 2012)	<ul style="list-style-type: none"> - The combination of the proposed steel reinforcement and UHP-SHCC, used to strengthen beam B-U- 2, was able to increase its load-carrying capacity to 100 kN, which is twice that of the control beam B-C. Moreover, it fulfilled the ductility criterion recommended by CEB-FIB (1990). - The role of the small amount of steel reinforcement is to reduce the stiffness degradation of the UHP-SHCC strengthening layer caused by cracking.
SHCC	Retrofitting unreinforced masonry walls with SHCC (Maalej, Lin, Nguyen, & Quek, 2010)	<ul style="list-style-type: none"> - Increase wall impact resistance - Preventing sudden and catastrophic failure - Contribute to damage mitigation in event of blast or explosion
SHCC	Corrosion resistant reinforced beams by replacing the concrete surround the main flexural reinforcement by SHCC (Maalej, et al., 2012)	<ul style="list-style-type: none"> - Mitigation of aggressive substances, therefore, preventing reinforcement corrosion - In the extreme case when corrosion initiates, accelerated corrosion due to longitudinal cracks would be reduced (if not eliminated), and spalling and delamination problems would be prevented.

4 Reference projects

Some ACMs are already applied in practice. To learn from practice, some reference projects are called in this research. In Table 52 is an overview given of reasons why certain ACMs could be applied in practice. A more detailed analysis of reference projects is done in Appendix A: Reference projects.

Table 52 - Main reasons to apply certain ACMs

ACM	Reasons to apply
FRC	Complexity in reinforcement
HPC and UHPC	Durability and maintenance
	Aesthetics
SHCC	Durability
	Economical
GPC	Sustainability
	Durability
Self-cleaning concrete	Aesthetic

5 Constructions

In this chapter are some concrete structures described. Mainly structures for infrastructure are described. Every construction is analysed on an element level. For instance, a viaduct is split up in elements; columns, beam, etc. For each element are the mechanical requirements for the concrete set up. For example, a column requires a certain compressive strength of the concrete. Further is for every element the exposure class determined. Before the constructions are analysed, the exposure classes are explain in some detail. After the construction analysis, some mechanical models are shown. According to these models, the most elements can be modelled as a beam on two supports. At last, the water tightness of concrete and the demand of concrete structures in the next decades are reviewed shortly.

5.1 Exposure classes

In Eurocode 2 are exposure classes defined for the durability of a concrete structure. Depending on the environment, a construction should meet the requirement of a certain exposure class. A construction exposed to a tough environment should meet higher requirements than construction placed in a 'concrete-friendly' environment. For example, a construction near the sea is in a higher exposure class than a construction in the midland. All exposure classes are mention in Tabel 4.1 of the Dutch standard (Nederlands Normalisatie-instituut , 2011).

An indication of exposure classes in buildings is shown in Figure 62 and Figure 63. As shown in the figures, the exposure class of a structure depends mainly on:

- Wet or dry environment, as well as cyclic wet and dry.
- Chlorides in the environment
- Construction in or above the ground
- Chemical components in the environment

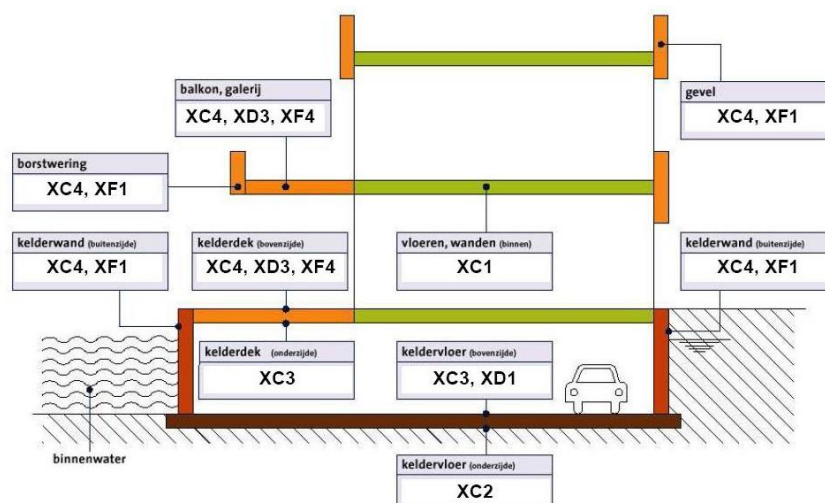


Figure 62 - Exposure classes of different parts of a building with a basement (Joostdevree.nl , n.d.)

In Figure 62 a general indication is given for the exposure classes of a building. In Figure 63 is made a distinction between a construction at the coast and a construction at the inlands, for a more detailed

indication of the related exposure class. Because of the relative high chloride concentration near the coast, a construction near the coast normally falls within a higher exposure class.

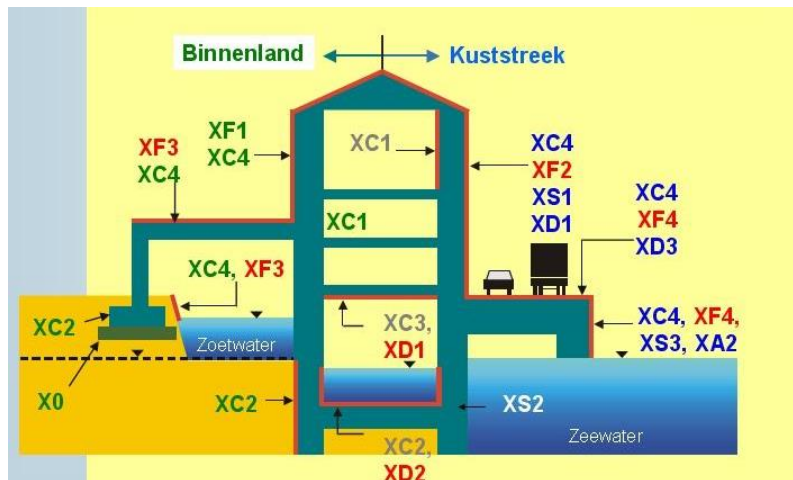


Figure 63 - Exposure classes of different parts of a building with the comparison between a construction at coast and a construction at inland (Joostdevree.nl , n.d.)

5.2 Types of constructions

In this paragraph are nine different constructions analysed. Before the constructions are analysed, a general analysis to foundations is done. It is assumed that the analysis of the foundation can be fitted in all structures. In the analysis to the foundation and the structures are the working loads and the exposure classes for every element of the construction included. The structures analysed in this chapter, including the foundations in general, are shown in the list below.

- Foundation
- Viaduct and girder bridge
- Sluice
- Embankment
- Retaining wall
- Noise barrier
- Tunnels, culverts and sewage
- Underpass
- Aqueduct

5.2.1 Foundation

Foundations are applied in every structure. In this research foundations are reviewed in a general way. As shown in Figure 64, the foundation is assumed to be a pile or shallow foundation. It is assumed that a shallow foundation is made by a foundation slab. The pile foundations are subdivided into driven and drilled piles.

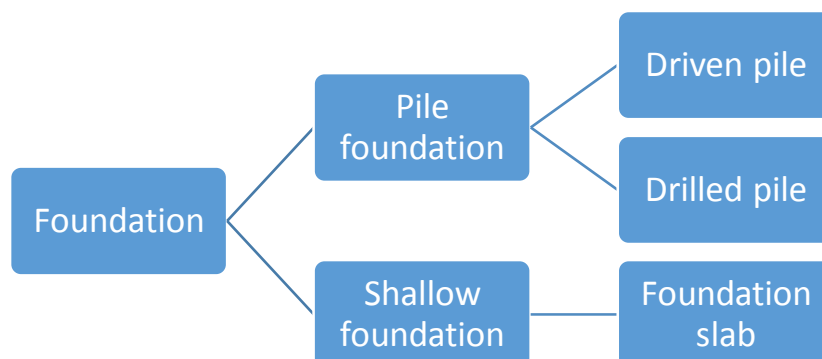


Figure 64 - Elements of a foundation

In Table 53, the main mechanical requirements and the exposure classes for foundation piles and foundations slabs are given. As shown in the last column of the table, foundations are generally exposed to a XC2 environment. The most important mechanical requirement is the compressive strength, because most foundations are mainly loaded in compression by the weight and other loads of the structure. As an exception, tensile piles are of course mainly loaded in tension.

Table 53 - Mechanical requirements and exposure classes for elements of a foundation during execution and service life

Construction part	Element	Main mechanical requirements	Exposure class
Foundation	Piles	<ul style="list-style-type: none"> - Compression strength - Tensile strength (if tension piles or/and during execution) - Stiffness 	<ul style="list-style-type: none"> - XC2 - XA2
	Foundation slab	<ul style="list-style-type: none"> - Compressive strength - Bending moment resistance - Shear resistance - Mass 	<ul style="list-style-type: none"> - XC2 - XA1

5.2.2 Viaduct and girder bridge

In the Netherlands, there are a lot of viaducts and girder bridges in the infrastructure. These structures are mainly loaded by traffic. The governing traffic loads of course are cars and trucks. The main loads from the traffic on the deck of the viaduct are:

- **Vertical loads:** weight of traffic
- **Horizontal loads:** braking and accelerating traffic

The loads from the deck are guided to the substructure construction under the deck. The substructure is made consists of beams which are supported on abutments and/or crossbeams that are mostly supported on columns. The abutments and columns are connected to the foundation of the construction. Depending on the conditions, the construction is on a shallow foundation or founded on piles. It is assumed that from a mechanical point of view, both the viaduct and the girder bridge are more or less the same. In Figure 65 is a viaduct or girder bridge construction split up in different construction components, until element level. The elements are also mentioned in Table 54, where the main loads per element are shown. It is assumed that horizontal loads are carried by the abutment or the columns. The table gives also an indication of the environment class mentioned. The foundation piles and foundations slab is not included in the table, because they are analysed in chapter 5.2.1 Foundation already. An overview of the exposure classes per element is also shown in Figure 66.

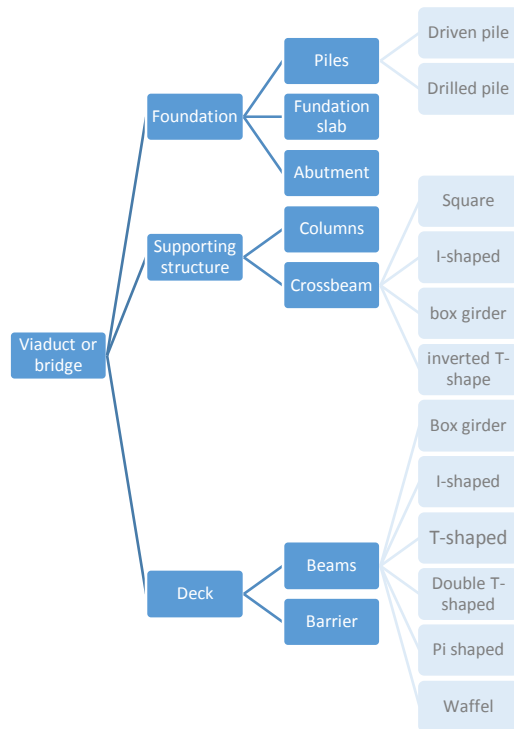


Figure 65 - Elements of a viaduct

Table 54 – Mechanical requirements and exposure classes for elements of a viaduct or bridge during execution and service life

Construction part	Element	Main mechanical requirements	Exposure class
Foundations	Abutment	<ul style="list-style-type: none"> - Compression strength - Bending moment resistance - Shear resistance - Mass 	<ul style="list-style-type: none"> - XC2 - XF2
Supporting structure	Columns	<ul style="list-style-type: none"> - Compression strength - Stiffness - Certain tensile strength during execution if precast column 	<ul style="list-style-type: none"> - XC3 - XF2 - XS1 (at coast) - XS3 and XC2 (if bridge over water)
	Crossbeam	<ul style="list-style-type: none"> - Bending moment resistance - Shear resistance - Stiffness - Certain tensile strength during execution if precast column 	<ul style="list-style-type: none"> - XC3 - XF2 - XS1 (at coast)
Deck	Beams	<ul style="list-style-type: none"> - Bending moment resistance - Torsional moment resistance - Shear resistance 	<ul style="list-style-type: none"> - XC3 - XD3 - XF2
	Barrier	<ul style="list-style-type: none"> - Compressive strength - Bending moment resistance - Energy capacity 	<ul style="list-style-type: none"> - XC4 - XD3 - XF2

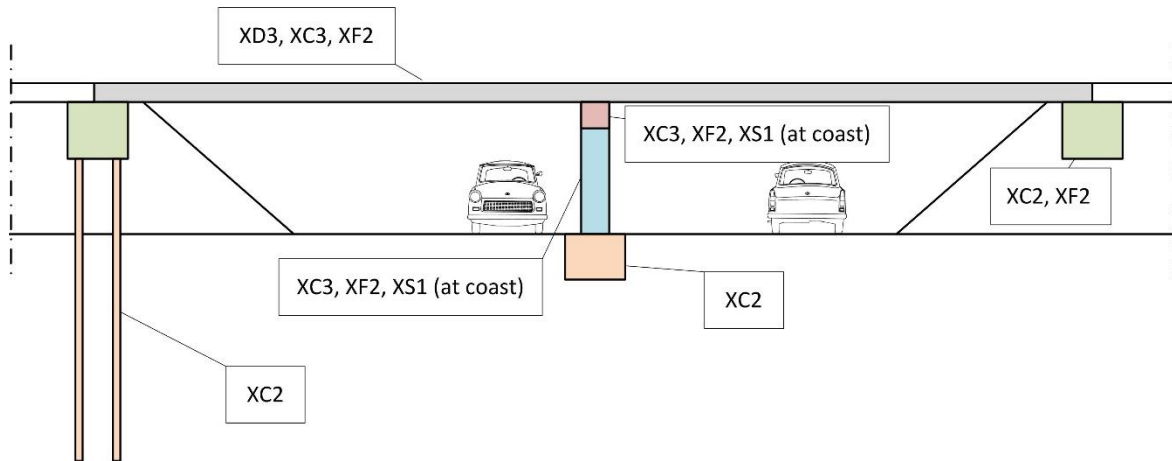


Figure 66 - Cross section of a viaduct with exposure classes

5.2.3 Other bridges

Next to viaducts and girder bridges, there are some other kind of bridges which are explained here briefly. The exposure classes for these bridges are assumed to be the same as for viaducts. The foundations of the bridges is also assumed to have similar mechanical requirements as for viaducts. So in this paragraph only the superstructures of the bridges are discussed. The bridges discussed below are:

- Arch bridge
- Cable-stayed bridge
- Suspension bridge
- Truss bridge
- Cantilever bridge

The main mechanical requirements for the concrete per element of the bridges are shown in Table 55. In the first column are shown the bridge types. In the second column are shown the elements of the constructions and in the last column are given the main mechanical requirements per element.

Table 55 - Mechanical requirements and exposure classes for elements of some bridges during execution

Construction	Element	Main mechanical requirements
Arch bridge	Arch	- Compression strength - Tensile strength (if precast) - Small bending - Torsional moment resistance - Stiffness
	Deck	- Compressive strength - Bending moment resistance - Torsional moment resistance - Shear resistance
	Posts between arch and deck	- Compression strength - Certain bending moment resistance
Cable-stayed bridge	Columns	- Compression strength - Bending moment resistance - Stiffness - Certain tensile strength (if precast)
	Deck (including beams)	- Bending moment resistance

		<ul style="list-style-type: none"> - Torsional moment resistance - Shear resistance - Stiffness
	Cables	<ul style="list-style-type: none"> - Tensile strength
Suspension bridge	Suspension structure	<ul style="list-style-type: none"> - Tensile strength
	Deck (including beams)	<ul style="list-style-type: none"> - Bending moment resistance - Torsional moment resistance - Shear resistance - Stiffness
Truss bridge	Pendulum rods	<ul style="list-style-type: none"> - Compressive strength - Tensile strength
	Deck (including beams)	<ul style="list-style-type: none"> - Bending moment resistance - Torsional moment resistance - Shear resistance - Stiffness
Cantilever bridge	Column	<ul style="list-style-type: none"> - Compression strength - Bending moment resistance - Stiffness - Certain tensile strength (if precast)
	Deck	<ul style="list-style-type: none"> - Bending moment resistance - Torsional moment resistance - Shear resistance - Stiffness

5.2.4 Sluice

In this paragraph is the analysis to sluice constructions shown. The sluice construction here is simplified to a concrete construction with a bottom and two walls connected to each other, where the water is into as shown in Figure 67. The lock can be closed by gates. The walls and bottom are mainly loaded by water and ground as shown in the figure. The gates are mainly loaded by water.

In Figure 67 also the ground and water loads are given that work on the sluice structure. As shown in the figure, the water loads working on the structure differ with the height of the water level in the sluice. The blue lines in Figure 67 shows the water loads in the lock for the highest water level. For the lowest water level, the same is done in orange. Of course the water level in the sluice varies a few times per day, depending on the number of ships that should cross the lock.

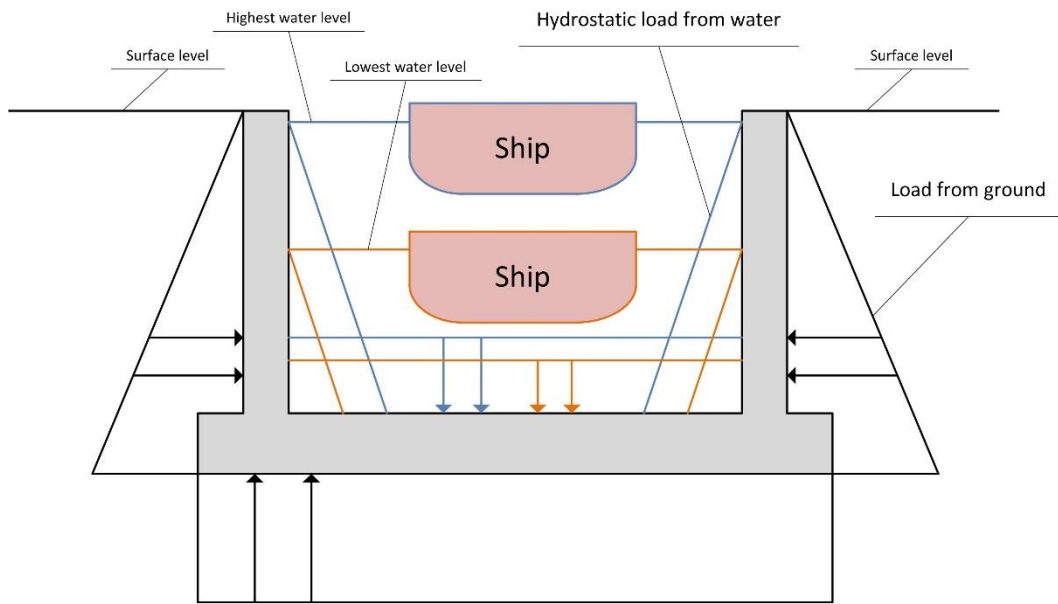


Figure 67 - Cross section of sluice with working loads on the construction

So the simple sluice construction here is split up in four elements; walls, bottom, foundation and doors, as shown in Figure 68. There are a few types of doors to close a sluice. The most common doors are as shown in the figure; horizontal moving gate, vertical rising gate, radial gate, two vertical flapping gates and sliding gate. Most doors are slightly different loaded due to their shape and supporting system, so they should be analysed separately as well.

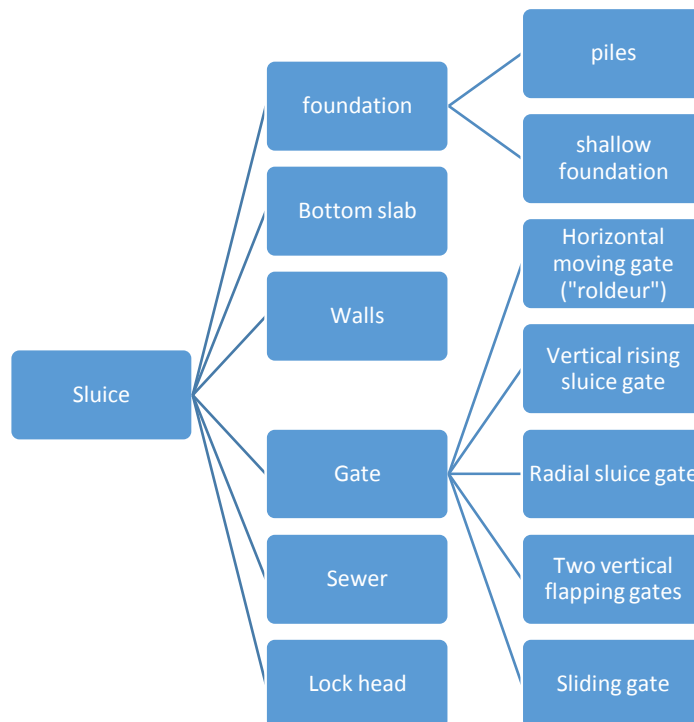


Figure 68 - Elements of a sluice

The mechanical and exposure analysis for the element from Figure 68 is done in Table 56. Again for each element are given the main mechanical requirements and the exposure class for the concrete. According to engineers of Heijmans, durability, especially for sea locks, is a governing issue.

Table 56 – Mechanical requirements and exposure classes for elements of a sluice during execution and service life

Construction part	Element	Main mechanical requirements	Exposure class
Lock chamber	Piles	<ul style="list-style-type: none"> - Compression strength - Tensile strength (especially during execution) - Stiffness 	- XC2
	Bottom	<ul style="list-style-type: none"> - Compression strength - Bending moment resistance - Shear resistance 	<ul style="list-style-type: none"> - XC2 - XF3 - XS2 (at coast)
	Walls	<ul style="list-style-type: none"> - Compression strength (self-weight) - Bending moment resistance - Shear resistance - Stiffness 	<ul style="list-style-type: none"> - XC4 - XF3 - XS3 (at coast) - XF4 (at coast)
Gate	Horizontal moving	<ul style="list-style-type: none"> - Compression strength - Tensile strength (during execution only) - Bending moment resistance - Shear resistance 	<ul style="list-style-type: none"> - XC4 - XF3 - XS2 (at coast) - XF4 (at coast)
	Vertical rising	<ul style="list-style-type: none"> - Compression strength - Tensile strength - Bending moment resistance - Shear resistance 	<ul style="list-style-type: none"> - XC4 - XF3 - XS2 (at coast) - XF4 (at coast)
	Radial gate	<ul style="list-style-type: none"> - Compression strength - Tensile strength (during execution only) - Bending moment resistance - Shear resistance 	<ul style="list-style-type: none"> - XC4 - XF3 - XS2 (at coast) - XF4 (at coast)
	Two vertical flapping gates	<ul style="list-style-type: none"> - Compression strength - Tensile strength (during execution only) - Bending moment resistance - Shear resistance 	<ul style="list-style-type: none"> - XC4 - XF3 - XS2 (at coast) - XF4 (at coast)

5.2.5 Embankment

An embankment itself is quite a simple construction; a wall holding the ground. The foundation of the embankment won't be explained here. The loads on the foundation and the exposure class of the foundation of the embankment are not analysed here. The general analysis in chapter 5.2.1 Foundation is assumed to be well enough for the description of the foundation of the embankment.

In this paragraph, two type of embankments are analysed here as shown Figure 69. The first type, Figure 69 (left), is a wall placed relative deep in the ground, to generate a contra (resisting) bending moment. The second type, Figure 69 (right), is a L-shaped wall where the weight of the ground above the horizontal part generate a contra (resisting) bending moment. Especially for large embankment, ground anchors helps to stabilize the structure, as shown on the left embankment of Figure 69

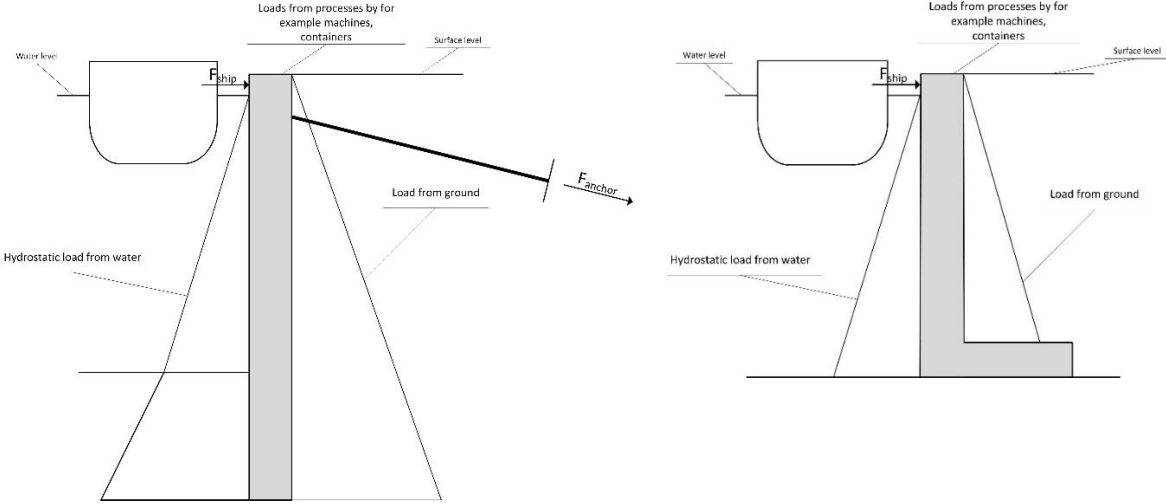


Figure 69 - Cross section of two type of embankments with working loads on the construction

Because an embankment is quite a simple construction in itself, it is not split up in different elements. The main mechanical requirements and exposure classes for the concrete are shown in Table 57.

Table 57 – Mechanical requirements and exposure classes for elements of an embankment during execution and service life

Construction part	Main mechanical requirements	Exposure class
Embankment	<ul style="list-style-type: none"> - Compression strength - Tensile strength (during execution only) - Bending moment resistance - Shear resistance - Resistance against impact load if the embankment is not protected against impact of a ship 	<ul style="list-style-type: none"> - XC4 - XF3 - XS3 (at sea) - XF4 (at coast)

5.2.6 Retaining wall

In this research are two types of retaining walls included. Both systems are shown in Figure 70. Same as for the embankments, in the first retaining wall type a contra (resistance) bending moment is generated by placing the wall a few meters in the ground. For the second type, the wall remains stable by the weight of the ground that generate a contra (resistance) bending moment against the ground. Also ground anchors can be applied to increase the bending moment resistance, as shown in Figure 70.

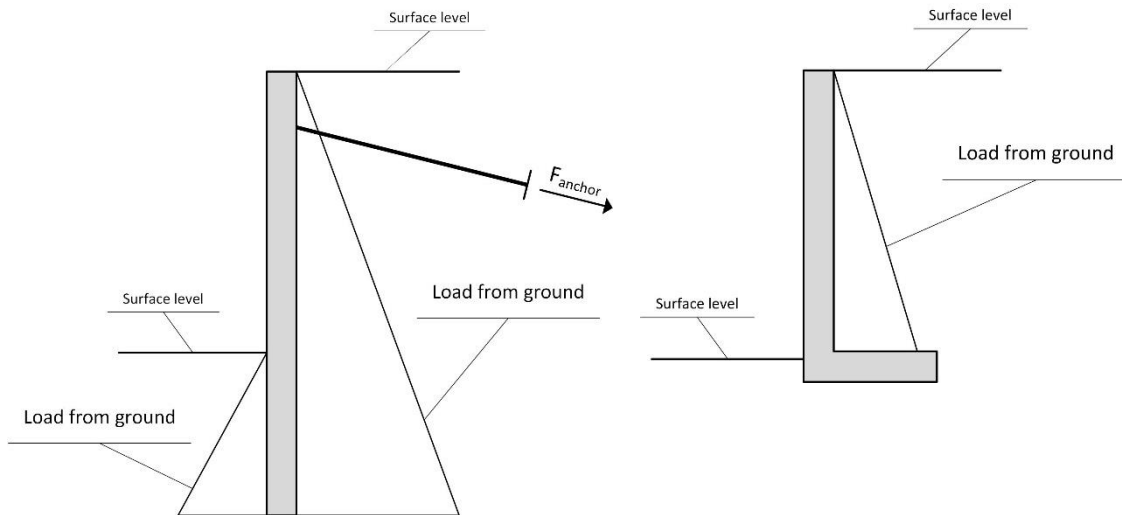


Figure 70 - Retaining walls with working loads. Left: retaining wall type 1. Right: retaining wall type 2

The working loads on the retaining wall are more or less the same as for the embankment. However, one side of the retaining wall is unloaded and the other side is loaded by the retaining ground. The requirements the concrete should meet from a mechanical point of view are shown in Table 58. Also the exposure classes of the wall are shown in this table. Possible foundation piles are not included here. The analysis of the foundations from chapter 5.2.1 Foundation is assumed to be a good description of the foundation of retaining walls.

Table 58 – Mechanical requirements and exposure classes for elements of a retaining wall during execution and service life

Construction part	Main mechanical requirements	Exposure class
Retaining wall	<ul style="list-style-type: none"> - Compression strength - Tensile strength (during execution only) - Bending moment resistance - Shear resistance - Possible resistance against impact load, for example near roads 	<ul style="list-style-type: none"> - XC2 - XC4 - XF2 (near roads) - XS1 (at coast) - XD1

5.2.7 Noise barrier

A noise barrier should absorb the noise as much as possible. From a mechanical point of view is a noise barrier not more than a wall that is load by its own weight and the wind. The wind and the possible eccentricity of the wall can generate some bending moments in the wall. The foundation of the wall is not described here. For the analysis of the foundations of the noise barrier is referred to the general description given in chapter 5.2.1 Foundation. The mechanical requirements to the concrete and the exposure class of the concrete are shown in Table 59.

Table 59 – Mechanical requirements and exposure classes for elements of a noise barrier during execution and service life

Construction part	Main mechanical requirements	Exposure class
Noise barrier	<ul style="list-style-type: none"> - Compression strength (self-weight) - Tensile strength (during execution only) - Bending moment resistance (wind load and eccentricity) - Shear resistance (wind load) 	<ul style="list-style-type: none"> - XF1 - XF2 (near roads or coast) - XS1 (at coast) - XD1

5.2.8 Tunnels, culverts and sewages

Tunnels, culverts and sewages are all constructions that serve under the ground surface. Because these three structures have a lot of similarities, they are discussed together. As a starting point, tunnels are clarified in detail. After that, some specialties for culverts and sewages are discussed.

Tunnels

There are two type of tunnels analysed in this research. The first type is a rectangular shaped tunnel and the second type is a circular shaped tunnel. Both types are shown in Figure 71 and Figure 72 respectively. An important functional requirement of tunnels is to resist the buoyancy loads, such that the tunnel remains stable in place. This can be achieved by the self-weight of the construction or with some modification in the cross section of the tunnel as shown in Figure 71 by the dotted rectangles. These modifications make that the weight of the ground above the toes help to stabilize the tunnel.

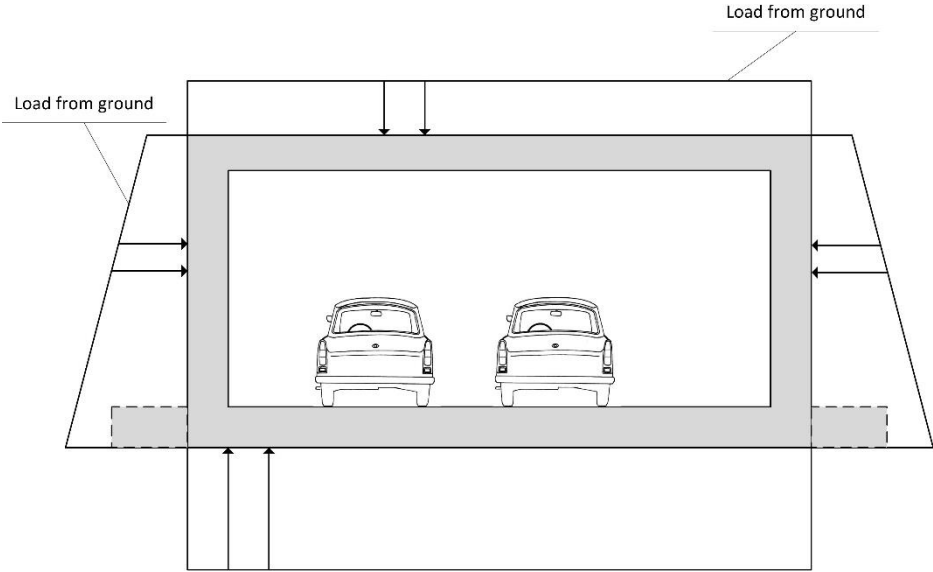


Figure 71 - Rectangular tunnel type with working loads from the ground

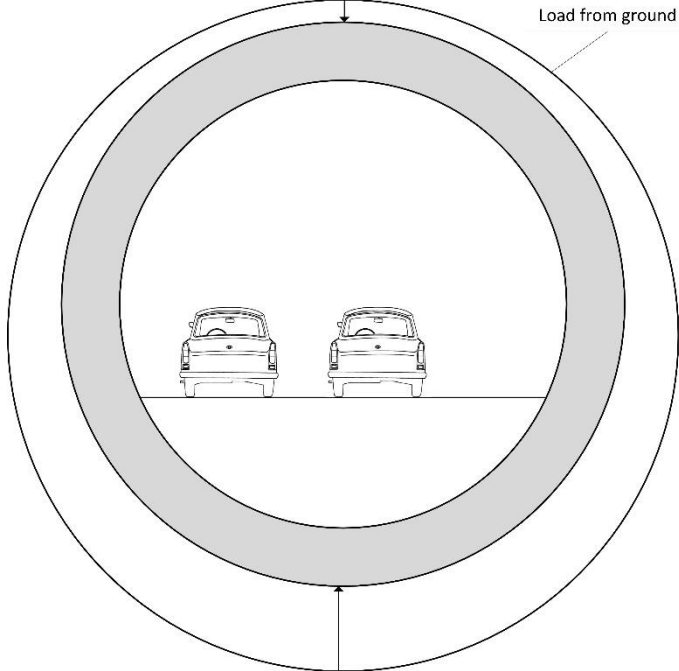


Figure 72 - Circular tunnel type with working loads from the ground

The main mechanical requirements and exposure classes for the concrete are both shown in Table 60. For the exposure class is XC2 chosen. Inside the tunnel, the exposure class is probably lower, because the tunnel is assumed to be dry inside.

Table 60 - Mechanical requirements and exposure classes for elements of a tunnel during execution and service life

Construction part	Main mechanical requirements	Exposure class
Tunnel	<ul style="list-style-type: none"> - Compression strength - Bending moment resistance - Shear resistance 	<ul style="list-style-type: none"> - XC2 - XF2 (road salt)

Culverts

Culverts have more or less the same shape as tunnels, circular or rectangular, but have probably some smaller dimensions. The exposure class from outside is also the same, since both are located into the ground. The big difference is that at the inside, culverts are loaded by water pressure and are exposed to water. In fact this means that, depending on the water level, inside the culverts is a certain contra pressure against the pressure from outside.

The exposure class inside culverts depends mainly on the water; water level and freshwater/sea water. This is shown in Table 61, where the exposure classes for fully or not fully water filled culverts with freshwater or sea water.

Table 61 - Exposure classes in culverts depending on the water level for freshwater and sea water

Water level	Freshwater	Sea water
Culvert fully filled with water	XC1	XS2
Culvert not fully filled with water	XC2 or XC4	XS3

Sewage

Also sewage are assumed to have the same shape as tunnels, mainly with some smaller dimensions. From the outside, sewages are exposed the same as tunnels and culverts (XC2). From the inside, sewage are exposed by dirty water. It is assumed that the sewage are not fully filled with water. The mechanical loads on the sewage are more or less the same as for tunnels, with the difference that sewage are loaded by hydrostatic pressure of the water from the inside of the sewage. However, the water pressure from inside is small, so could probably be neglected.

The concrete in sewages is at the inside exposed to the dirty water. It is assumed that sewage is exposed the classes XC4 and XA3 (Betoncentral Twenthe BV, Betoncentrale Rijnmond BV and Betoncentrale Diamant BV, n.d.).

5.2.9 Underpass

In the Netherlands are quite lot of railways and a lot of bike lanes, which crosses each other. A more and more applied solution for slow traffic to cross the railways, is a tunnel under the railway as shown in the side cross section of Figure 73. The cross section of the tunnel is shown in Figure 74. A similar construction of course can be made for cars to cross the railway or for car or slow traffic crossing a road.

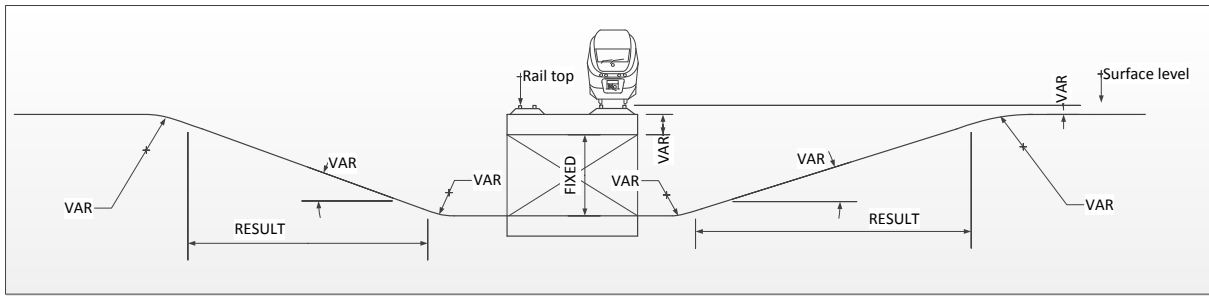


Figure 73 - Schematically cross section of a tunnel under railway including ramps (Bracht, 2015)

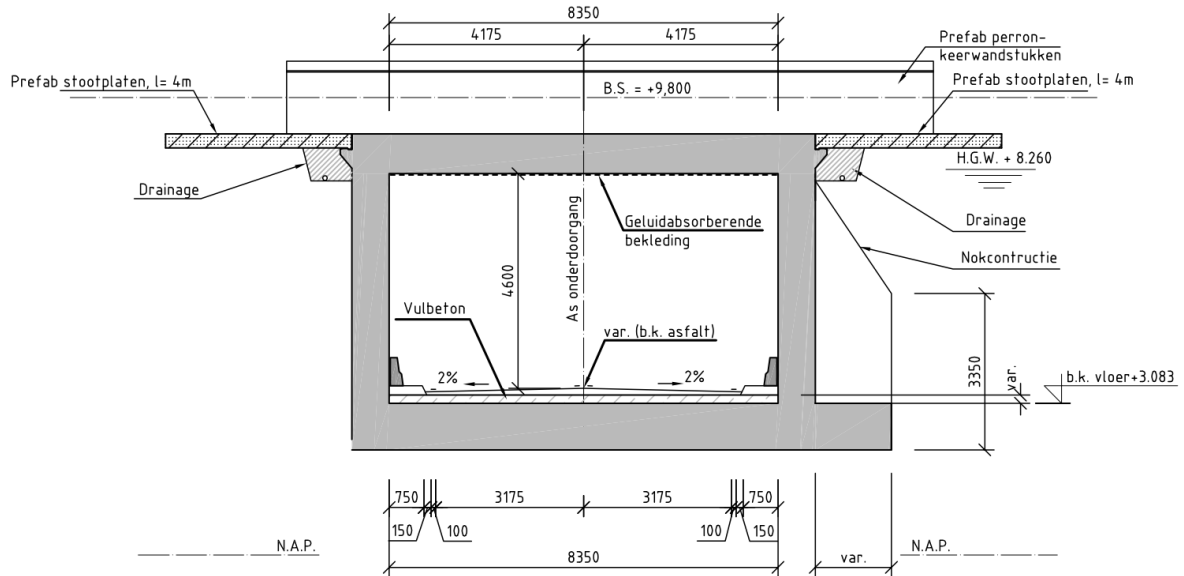


Figure 74 – Cross section of a tunnel under the railway (Heijmans Civiel B.V. Projecten, 2014)

The different elements from Figure 73 and Figure 74 are shown in Figure 75. For every element are given the main mechanical requirements and the exposure classes in Table 62. The foundation is not mentioned in the table. For the foundation in referred to the general analysis to foundations in chapter 5.2.1 Foundation.

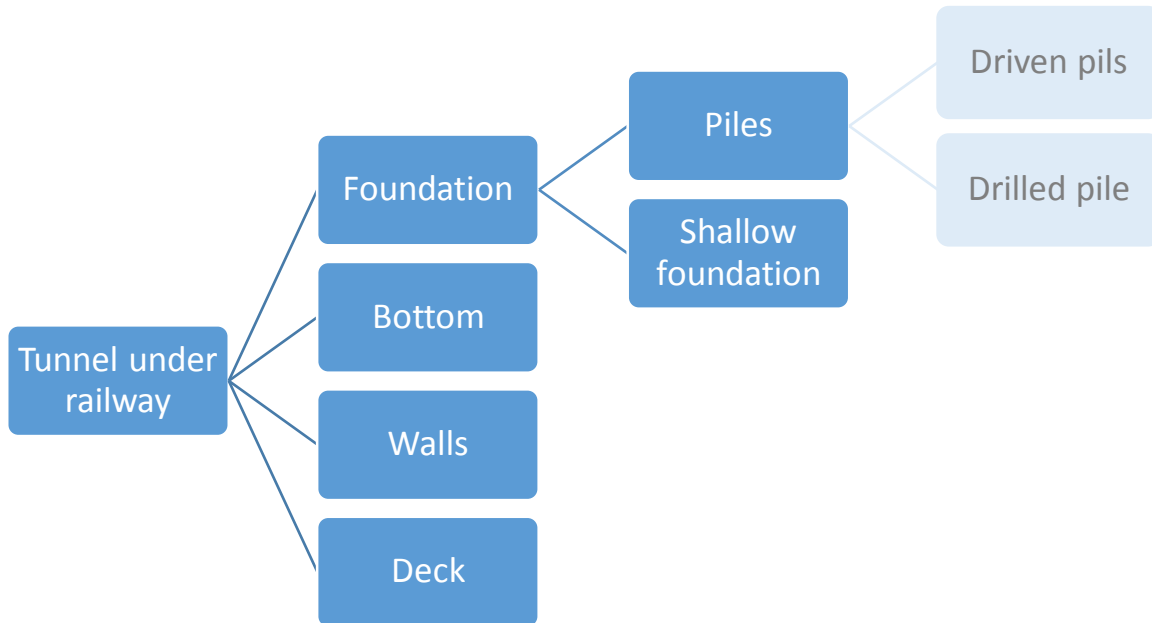


Figure 75 - Elements of a tunnel under the railway

Table 62 – Mechanical requirements and exposure classes for elements of a tunnel under a railway during execution and service life

Construction part	Element	Main mechanical requirements	Exposure class
Tunnel construction	Bottom	<ul style="list-style-type: none"> - Compression strength - Bending moment resistance - Shear resistance 	<ul style="list-style-type: none"> - XC2 - XD1 - XF2
	Walls	<ul style="list-style-type: none"> - Compression strength - Bending moment resistance - Shear resistance - Stiffness 	<ul style="list-style-type: none"> - XC2 - XF1 - XS1 (at coast) - XD1
	Deck	<ul style="list-style-type: none"> - Compressive strength - Bending moment resistance - Torsional moment resistance - Shear resistance - Stiffness 	<ul style="list-style-type: none"> - XF1 - XF4 (if road instead of rail) - XC4 - XD3

5.2.10 Aqueduct

An aqueduct is simple said a bridge for waterways to cross, for example a motorway. This is schematically shown in Figure 76. In the figure also the hydrostatic pressure from the water is shown. In Figure 77 a side view of the aqueduct is shown for the complete picture of the structure. With both figures, the mechanical requirements and the exposure classes are determined as shown in Table 63. Next to these requirements, the water tightness of the concrete of course is one of the most important requirements of the structure.

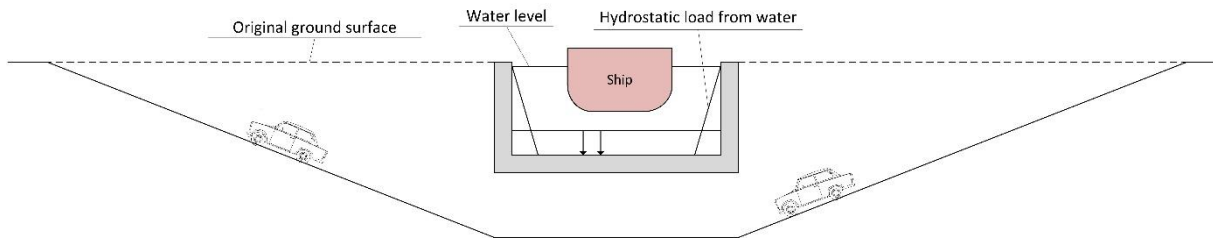


Figure 76 - Cross section of an aqueduct with a motorway

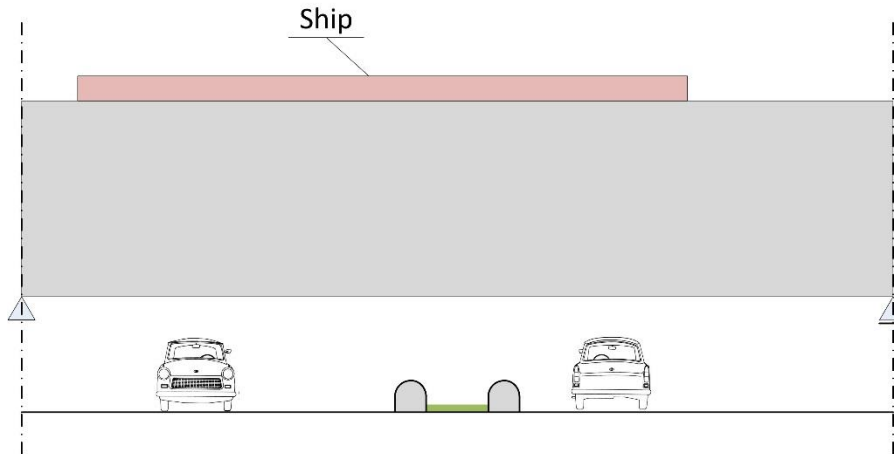


Figure 77 - Side view of an aqueduct

Special for aqueducts is that the exposure classes for the concrete in the aqueduct differs from the exposure classes of the outside, because inside the aqueduct is filled with water where the outside is surrounded by air. So concrete should meet the highest requirements of both environment classes. Further, the exposure classes inside the aqueduct depends on the kind of water in the aqueduct; freshwater or sea water. Therefore, in Table 63 the exposure classes are given at the inside and the outside of the construction and is given the exposure class inside if sea water is in the aqueduct instead of freshwater. To determine the exposure classes outside the construction, it is assumed that a road is located under the aqueduct.

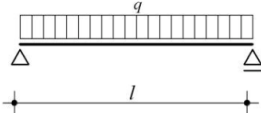
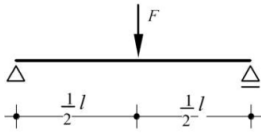
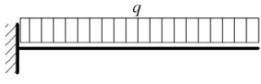
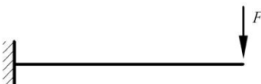
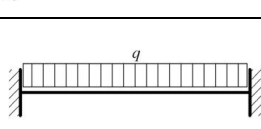
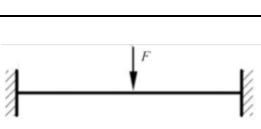
Table 63 - Mechanical requirements and exposure classes for an aqueduct during execution and service life

Construction part	Element	Main mechanical requirements	Exposure class (inside)	Exposure class (outside)
Aqueduct	Bottom	<ul style="list-style-type: none"> - Compression strength - Tension strength - Bending moment resistance - Shear resistance 	<ul style="list-style-type: none"> - XC2 - XD2 - XS2 (sea water) 	<ul style="list-style-type: none"> - XC3 - XD1 - XS1 (at coast) - XF2 (if road underneath)
	Walls	<ul style="list-style-type: none"> - Compression strength - Tension strength - Bending moment resistance - Shear resistance - Stiffness 	<ul style="list-style-type: none"> - XC2 - XC4 (splash zone) - XD2 - XS2 (sea water) - XS3 (splash zone sea water) 	<ul style="list-style-type: none"> - XC3 - XD1 - XS1 (at coast) - XF2 (if road underneath)

5.3 Mechanical models

Most of the above mentioned constructions can be modelled by three types of beams. These three beams are shown in Table 64. The beams are loaded by a distributed load or a point load. For every model is the maximum bending moment, shear force and vertical deflection given.

Table 64 - Some mechanical schematisations with the maximum moment, shear and deflection per schematisation (Beek, n.d.), (MCB Nederland, n.d.)

Model	Loading scheme	Schematisation	Maximum moment	Maximum shear	Maximum deflection
Simply supported beam	Distributed load		$\frac{1}{8}qL^2$	$\frac{1}{2}qL$	$\frac{5}{384} \frac{qL^4}{EI}$
	Point load		$\frac{1}{4}FL$	$\frac{1}{2}F$	$\frac{1}{48} \frac{FL^3}{EI}$
Cantilevered beam	Distributed load		$\frac{1}{2}qL^2$	qL	$\frac{1}{8} \frac{qL^4}{EI}$
	Point load		FL	F	$\frac{1}{3} \frac{FL^3}{EI}$
Double clamped beam	Distributed load		$M_{sup} = \frac{1}{12}qL^2$ $M_{mid} = \frac{1}{24}qL^2$	$\frac{1}{2}qL$	$\frac{1}{384} \frac{qL^4}{EI}$
	Point load		$M_{sup} = \frac{1}{8}FL$ $M_{mid} = \frac{1}{8}FL$	$\frac{1}{2}F$	$\frac{1}{192} \frac{FL^3}{EI}$

Analysing the expression from Table 64, it can be concluded that the vertical deflection has a linear relation with the stiffness of the concrete in every model. This is the only material characteristic that is directly in the models.

Another material characteristic that is in the models in a more indirect way is the self-weight of the beam. The self-weight of the beam can be written as a distributed load, which has in all models a linear relation with the maximum bending moment, maximum shear force and maximum deflection of the beam. The self-weight of the beam could also be reduced by the application of a very strong concrete. For a high strength concrete beam, less material is needed to achieve the desired strength in the beam, what decreases the self-weight of the structure. So for constructions where the vertical deflection is governing, for example a bridge with a long span, a very stiff concrete with a low self-weight or has a large strength is favourable.

5.4 Water tightness

The water tightness for NSC can be determined by the graph of Lohmeyer. This graph is shown in Figure 78. In the graph are also two other models shown. In practice, the model from Lohmeyer is the most practical one. The model works with the ratio between the liquid height and the width of the concrete construction, which is shown on the horizontal axis. The critical crack width, defined as the maximum width where the crack in the concrete is most probably able to heal itself, is shown on the vertical axis. As shown in the graph, as long as the ratio between the liquid height and the wall width is smaller than

approximately three, the critical crack width is 0.20 mm. Larger cracks are not able to heal themselves anymore. Therefore, only concrete with cracks smaller than the critical crack width is estimated to be water tight. For ratios between the liquid head and the width of the wall that are larger than three, the critical crack width decreases.

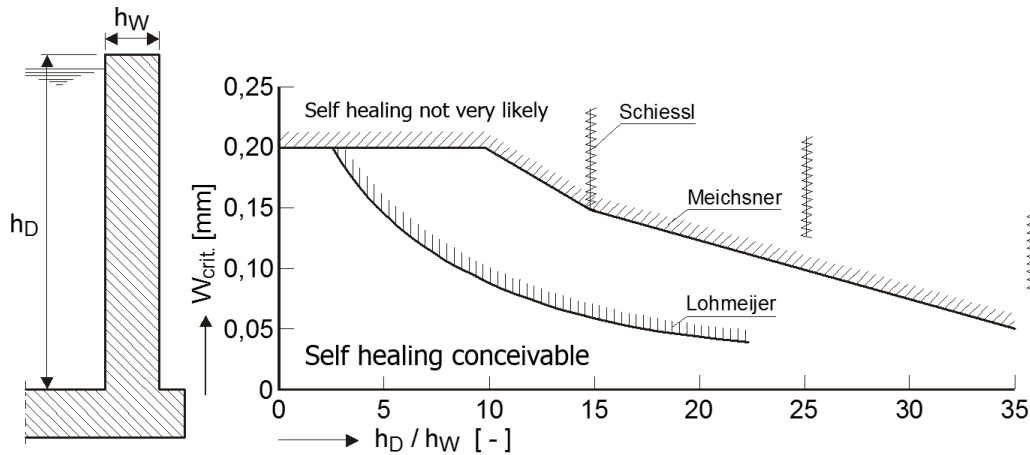


Figure 78 - Relation between critical crack width and ratio between liquid head and wall thickness (Breugel, 2014)

The relation of Lohmeyer is valid for NSC. The self-healing of the cracks is based on autogenous self-healing capacity of concrete which is described in chapter 2.1.6 Self-Healing Cementitious Materials. In this chapter four ways of autogenous self-healing of concrete are described. All four are briefly mentioned below.

1. Formation of calcium carbonate or calcium hydroxide;
2. Settlement of the debris and loose cement particles in presence of water;
3. Hydration of unhydrated cementitious particles;
4. Further swelling of the hydrated cementitious matrix

From these description of self-healing, concretes with a lot of cement, for example SHCC or UHPC, could have a higher autogenous self-healing capacity compared to NSC. Therefore, the relation found by Loymeyer may be a bit conservative for those ACMs. For GPC, which contains no cement, Lohmeyers relations is probably not valid as well. However, GPC seems to have an autogenous healing behaviour as well as suggested by Glasby, Day, Kemp, & Aldred, Earth Friendly Concrete – A sustainable option for tunnels requiring high durability (2013). From reasons of simplicity, Loymeyers relation is assumed to be valid for all ACMs if the maximum crack width should be determined. Beside, for most ACMs are not even relations like Loymeyers relation for NSC.

5.5 Demand of constructions

In this research are constructions from the infrastructure analysed where ACMs could be applied. To prevent designs with ACMs of constructions that are not or nearly expected to be built in the next years, an analysis of expected building projects is made here. Not for every construction mentioned above is the demand known. The construction where information is known about, are explained here.

5.5.1 Bridges

In Figure 79 the years of construction of bridges in The Netherlands are shown. The figure shows that a lot of bridges are made in the period between 1950 and 1979. Assuming a service life of 50 to 100

years, a lot of bridges should be retrofitted or replaced in the next years. So from an economical point of view, research to the combination of ACM and bridges could be interesting.

Figure 79 includes all bridges in The Netherlands, so all types of bridges. The most frequent bridges that are included in the figure are according to the NBS:

- Bascule bridge
- Arch bridge
- Swinging bridge
- Lift bridge
- Drawbridge
- Masonry bridge
- Box bridge
- Girder bridge
- Slab bridge
- Cable-stayed bridge
- Truss bridge



Figure 79 – Year of construction of bridges in The Netherlands (Heijmans, 2014)

5.5.2 Sluices

In Figure 80 is shown a similar research for sluices. In the figure are shown the expected number of sluices (inland sluice gates as well as sea locks) in The Netherlands that should be replaced every decade. As shown in the figure, in the period of 2030-2040 and 2060-2070 a lot of sluices should be replaced (25 in 10 years). It should be great if ACMs could already be applied in the first period, 2030-2040, to make more beneficial sluices. Until then, about 10 years more research to the application of an ACM to sluices could be done.

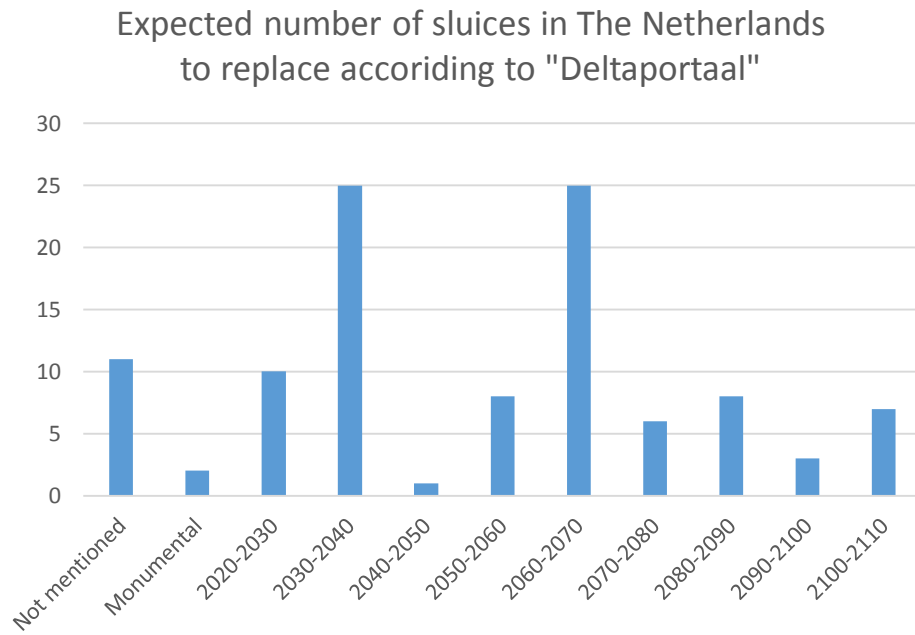


Figure 80 – Expected number of sluices in The Netherlands to replace according to “Deltaportaal” (Heijmans, n.d.)

6 Multi Criteria Analysis of the ACMs

In this chapter a Multi Criteria Analysis is presented for the ACMs. The MCA is made according to the knowledge of this literature research. The basic of the MCA are *Table 14*, *Table 25*, *Figure 51* and *Figure 52*.

In *Table 65*, the Multi Criteria Analysis to mechanical, durable and sustainable characteristics is shown for all the ACMs. The first five ACMs are totally judged in a quantitative way. The other ACMs, ACM 6 until ACM 9 are judged partly quantitatively, partly qualitatively. As mentioned in this research, not enough knowledge is there to judge them totally quantitatively.

In the second column of *Table 65* are shown the material characteristics where the materials are judge on. These characteristics are divided over the three themes; mechanics, durability and sustainability. For every characteristic is a weight factor determined as shown in the third column. The weight factor makes that the most important characteristics, for example the compressive strength, weights more in the total score compared to less important characteristics, for example the compressive strain.

Now for every ACM, including the plain concrete, is given a score and a weighted score per characteristic. The weighted score is the product of the weight factor and the score. These weighted scores can be summed up, to get a subtotal score per theme and a total score of all the themes together. The total score of all themes together is shown in the last row after one.

The subtotal score per theme is also calculated to a weighted subtotal. This subtotal is calculated by dividing the subtotal score per theme over the total available points and multiply by 10. This can be written as a formula as shown in eq.(90)

$$\text{Weighted subtotal} = \frac{\text{subtotal score}}{5 \cdot \sum(\text{weight factor})_i} \cdot 10 \quad \text{eq.(90)}$$

This way of calculating the weighted subtotals results values in the range from 2 to 10. Here a weighted subtotal of 10 is the best and of 2 is the worst. In the last row is the weighted total shown, where the mean values of the three weighted subtotals for mechanical, durable and sustainable characteristic are calculated.

One can imagine that for a certain project, for example durability is more important than the other two themes. In this case, the weight factor for durability should be increased in the calculation of the weighted total. In *Table 65* is assumed that all three themes are even important.

Table 65 - Multi Criteria Analysis for plain concrete and the ACMs for mechanical, durable and sustainable characteristics including a general

		Weight factor	Quantitative analysed on mechanical, durable and sustainable characteristics												Partly not and/or partly qualitative analysed							
			plain		ACM 1		ACM 2		ACM 3		ACM 4		ACM 5		ACM 6		ACM 7		ACM 8		ACM 9	
			NSC		NSSFRC		HPC		HPSFRC		UHPC		SHCC		Self-healing concrete		GPC		Self-cleaning concrete		Self-sensing concrete	
			score	weighted	score	weighted	score	weighted	score	weighted	score	weighted	score	weighted	score	weighted	score	weighted	score	weighted	score	weighted
Mechanical	Compressive strength	5	1	5	1	5	3	15	3	15	5	25	1	5	1	5	1	5	2	10	1	5
	Tensile strength	2	1	2	1	2	2	4	2	4	5	10	2	4	1	2	1	2	2	4	1	2
	Shear resistance	3	1	3	2	6	1	3	2	6	5	15	3	9	1	3		0		0		0
	Young's modulus	3	3	9	3	9	4	12	4	12	5	15	1	3	3	9	2	6		0		0
	Linear compressive strain	1	1	1	1	1	2	2	2	2	2	2	1	1	1	1		0		0		0
	Max compressive strain	2	3	6	3	6	1	2	1	2	1	2	2	4	3	6		0		0		0
	Linear tensile strain	1	1	1	1	1	1	1	2	2	2	2	0	0	1	1		0		0		0
	Max tensile strain	3	2	6	2	6	1	3	2	6	2	6	5	15	2	6		0		0		0
	Subtotal mechanical			33		36		42		49		77		41		33		13		14		7
	Weighted subtotal mechanics			3.3		3.6		4.2		4.9		7.7		4.1		3.3						
Durability	Permeability	2	1	2	1	2	3	6	3	6	5	10	2	4	1	2	2	4		+		+
	Chloride penetration	4	1	4	1	4	3	12	3	12	5	20	2	8	1	4	4	16		+		+
	Carbonation depth	3	1	3	1	3	3	9	3	9	5	15	3	9	1	3	5	15		-		?
	Crack behaviour	5	1	5	3	15	1	5	3	15	4	20	5	25	1	5	1	5		?		?
	Subtotal durability			14		24		32		42		65		46		14		40		+		+
Weighted subtotal durability			2.0		3.4		4.6		6.0		9.3		6.6		2.0		5.7					
Sustainability	MKI	4	5	20	5	20	4	16	3	12	1	4	3	12		0		0	4	16		0
	Carbon dioxide emission	2	4	8	4	8	3	6	3	6	1	2	3	6		0	5	10	4	8		0
	Subtotal sustainability			28		28		22		18		6		18		0		10		24		0
	Weighted subtotal sustainability			9.3		9.3		7.3		6.0		2.0		6.0						8.0		
Total			70		73		91		94		128		80		42		58		38		7	
Weighted total			4.9		5.5		5.4		5.6		6.3		5.6									

Qualitative characteristics

1. Very bad or negative performance on characteristic. For example very low strength, very low permeability, very high MKI
2. Bad or negative performance on characteristic. For example low strength, low permeability, high MKI
3. Mean performance on characteristic. For example mean strength, mean permeability, mean MKI
4. Good or positive performance on characteristic. For example high strength, high permeability, low MKI
5. Very good or positive performance on characteristic. For example very high strength, very high permeability, very low MKI

Qualitative characteristics

- + Positive influence on the durability, so a lower water permeability, chloride diffusion coefficient or carbonation depth compared to NSC
- +/- No positive or negative influence on the durability, so nearly no different water permeability, chloride diffusion coefficient or carbonation depth compared to NSC
- Negative influence on the durability, so a higher water permeability, chloride diffusion coefficient or carbonation depth compared to NSC
- ? Unknown

Some conclusions from Table 65:

- The best weighted subtotal **mechanics** is for UHPC. This could be expected on forehand, since this concrete is extremely strong and stiff
- The worst weighted subtotal **mechanics** is for NSC. Most other types of concrete are stronger or have better strain capacities
- The best weighted subtotal **durability** is for UHPC. This could be expected on forehand, since this concrete is extremely dense compared to the other ACMs.
- The worst weighted subtotal **durability** is for NSC. Most other types of concrete are denser or have a better crack behaviour.
- The best weighted subtotal **sustainability** is for NSC. NSC has the lowest amount of cement, which has quite a large influence on the sustainability. GPC is probably even more sustainable, but the sustainability of this type of concrete is hard to quantify.
- The worst weighted subtotal **sustainability** is for UHPC. This ACM has a very high cement content, which results in a low sustainability.
- The weighted **total** of the three themes shows that UHPC is the best and NSC the worst characteristics, assuming that the mechanical, durable and sustainable characteristics are all even important. The other four ACMs; NSSFRC, HPC, HPSFRC and SHCC, are all around 5.5.
- Most ACMs perform significant better on durability compared to NSC.
- Most ACMs perform significant worse on sustainability compared to NSC.

7 Bibliography

- Abouhussien, A. A., & Hassan, A. A. (2015). Optimizing the durability and service life of self-consolidating concrete containing metakaolin using statistical analysis. *Construction and Building Materials* 76, 297-306.
- ACE-MRL. (n.d.). *Durable Link Slab for Jointless Bridge Decks Based on Strain-Hardening Cementitious Composites Construction Timeline*. Retrieved from [www.umich.edu: http://www.umich.edu/~acemrl/NewFiles/projects/linkslab_timeline.html](http://www.umich.edu/~acemrl/NewFiles/projects/linkslab_timeline.html)
- Adam, A. A. (2009). *Strength and Durability Properties of Alkali Activated Slag and Fly Ash-Based Geopolymer Concrete*. Melbourne, Australia: School of Civil, Environmental and Chemical Engineering: RMIT University .
- AFGC's Scientific and Technical Committee. (2013). *Ultra High Performance Fibre-Reinforced Concretes Recommendations*.
- Agarkar, S. V., & Joshi, M. M. (2012). Study of effect of Al₂O₃ nanoparticles on the compressive strength and workability of blended concrete. *International Journal of Current Research, Vol. 4, Issue, 12*, 382-384.
- Ahmed, S. (2014). Fibre-reinforced geopolymer composites (FRGCs) for structural applications .
- Al-Amoudi, O. S. (2002). Attack on plain and blended cements exposed to aggressive sulfate environments. *Cement & Concrete Composites* 24, 305-316.
- Aldred, J. M. (2013). Engineering Properties of a Proprietary Premixed Geopolymer Concrete.
- Aldred, J., & Day, J. (2012). 37th Conference on Our World in Concrete & Structures . *Is geopolymer concrete a suitable alternative to traditional concrete?* , (p. 14). Singapore.
- Al-Dulaijan, S., Maslehuddin, M., Al-Zahrani, M., Sharif, A., Shameem, M., & Ibrahim, M. (2003). Sulfate resistance of plain and blended cements exposed to varying concentrations of sodium sulfate. *Cement & Concrete Composites* 25, 429-437.
- ArcelorMittal Wire International . (n.d.). *HE - Steel fibre - ArcelorMittal Distribution*. Retrieved from [ArcelorMittal : http://ds.arcelormittal.com/wiresolutions/steelfibres/products/hooked_end_fibres_he/language/EN](http://ds.arcelormittal.com/wiresolutions/steelfibres/products/hooked_end_fibres_he/language/EN)
- Asbridge, A., Jones, T., & Osborne, G. (1996). High Performance Metakaolin Concrete: results of large scale trials in aggressive environments. *Radical Concrete Technology*.
- Aspire. (2010). *FHWA, Iowa Optimize Pi Girder*. Retrieved from [www.aspirebridge.com: http://aspirebridge.com/magazine/2010Winter/jakway_win10.pdf](http://aspirebridge.com/magazine/2010Winter/jakway_win10.pdf)
- Badar, M. S., Kupwade-Patil, K., Bernal, S. A., Provis, J. L., & Allouche, E. N. (2014). Corrosion of steel bars induced by accelerated carbonation in low and high calcium fly ash geopolymer concretes. *Construction and Building Materials* 61, 79-89.
- Badogiannis, E. G., Sfikas, I. P., Voukia, D. V., Trezos, K. G., & Tsivilis, S. G. (2015). Durability of metakaolin Self-Compacting Concrete. *Construction and Building Materials* 82, 133-141.

- Bai, J., Wild, S., & Sabir, B. (2002). Sorptivity and strength of air-cured and water-cured PC–PFA–MK concrete and the influence of binder composition on carbonation depth. *Cement and Concrete Research* 32, 1813-1821.
- Bakharev, T. (2005). Durability of geopolymer materials in sodium and magnesium sulfate solutions. *Cement and Concrete Research* 35, 1233-1246.
- Beek, A. v. (n.d.). *werktuigbouw.nl*. Retrieved from www.werktuigbouw.nl: http://www.werktuigbouw.nl/calculators/image/vergeetmenietjes.jpg
- Bernal, S. A., Gutierrez, R. M., Provis, J. L., & Rose, V. (2010). Effect of silicate modulus and metakaolin incorporation on the carbonation of alkali silicate-activated slags. *Cement and Concrete Research* 40, 898-907.
- Betoncentral Twenthe BV, Betoncentrale Rijnmond BV and Betoncentrale Diamant BV. (n.d.). *Beton volgens NEN EN 206-1/NEN 8005: Hulpmiddel om eenvoudig - in zeven stappen - betonmortel te bestellen*. Retrieved from [betoncentrale.nl: http://www.betoncentrale.nl/media/bestanden/betonnormen1.pdf](http://www.betoncentrale.nl: http://www.betoncentrale.nl/media/bestanden/betonnormen1.pdf)
- BetonLexicon. (n.d.). *Cement*. Retrieved from Beton lexicon: <http://betonlexicon.nl/C/Cement/>
- BetonLexicon. (n.d.). *Samenstelling van beton*. Retrieved from Beton lexicon: <http://betonlexicon.nl/S/Samenstelling%20van%20beton/>
- Bilim, C. (2011). Properties of cement mortars containing clinoptilolite as a supplementary cementitious material. *Construction and Building Materials* 25, 3175-3180.
- Bouwinfonet . (n.d.). *Betonprijs 2011 Sluis 0124* . Retrieved from [bouwinfoNet.nl: http://www.bouwinfonet.nl/project_detail.php?pid=321](http://www.bouwinfonet.nl: http://www.bouwinfonet.nl/project_detail.php?pid=321)
- Bracht, H. v. (2015).
- Brain, P., & P.E., K. (2009, April 1). Use of UHPC in Iowa Structural Design/Construction Quality Workshop. Ames, Iowa, USA.
- Breugel, K. v. (2014, 11 27). Concrete Structures – Capita Selecta: tightness .
- Breysse, D., & Gerard, B. (1997). modelling of permeability in cement-based materials: part 1- uncracked medium. *Cement and Concrete Research, Vol. 27. No. 5*, 761-775.
- Bywalski, C., Kaminski, M., Maszczak, M., & Balbus, L. (2015). Influence of steel fibres addition on mechanical and selected rheological properties of steel fibre high-strength reinforced concrete. *Archives of Civil and Mechanical Engineering, Volume 15, Issue 3*, 742-750.
- Camacho, E., Serna, P., & López, J. (n.d.). UHPFRC bolted joints: failure modes of a new simple connection system.
- Cheema, D. S., Lloyd, N. A., & Rangan, V. B. (2009). 34th Conference on our world in concrete & structures. *Durability of geopolymer concrete box culverts - a green alternative*. Singapore.
- Cheewaket, T., Jaturapitakkul, C., & Chalee, W. (2010). Long term performance of chloride binding capacity in fly ash concrete in a marine environment. *Construction and Building Materials* 24, 1352-1357.
- Chen, G. (2012). *Concrete Surface with Nano-Particle Additives for Improved Wearing Resistance to Increasing Truck Traffic*.

- Chen, H., & Su, R. (2013). Tension softening curves of plain concrete. *Construction and Building Materials* 44, 440-451.
- Chen, J., & Poon, C.-s. (2009). Photocatalytic construction and building materials: From fundamentals to applications. *Building and Environment* 44, 1899-1906.
- Chern, J.-C., & Young, C.-H. (1989). Compressive creep and shrinkage of steel fibre reinforced concrete. *The International Journal of Cement Composites and Lightweight Concrete, Volume 11, Number 4*.
- Chindapasirt, P., & Chalee, W. (2014). Effect of sodium hydroxide concentration on chloride penetration and steel corrosion of fly ash-based geopolymer concrete under marine site. *Construction and Building Materials* 63, 303-310.
- Chircu Prod - Impex Company SRL. (2009). *Steel fibers for concrete reinforcement*. Retrieved from chircuprodimpex: <http://www.chircuprodimpex.com/products/steel-fibers-for-concrete-reinforcement/steel-fibers-for-concrete-reinforcement.htm>
- CUR bouw & infra. (n.d.). *Leidraad 1: Duurzaamheid van constructief beton met betrekking tot chloride-geïnitieerde wapeningscorrosie*.
- Dabrowski, M., & Glinicki, M. A. (2012). Influence of aggregate type on the durability of concrete made of blended cements with calcereous fly ash.
- De Boer & De Groot . (n.d.). *Nieuwbouw sluis 0124 te IJburg (2)*. Retrieved from De Boer & De Groot - Civiele werken: <http://www.deboerendegroot.nl/projecten/nieuwbouw-sluis-0124-te-ijburg-2>
- Deb, P. S., Nath, P., & Sarker, P. K. (2014). The effects of ground granulated blast-furnace slag blending with fly ash and activator content on the workability and strength properties of geopolymer concrete cured at ambient temperature. *Materials and Design* 62, 32-39.
- Deja, J. (2003). Freezing and de-icing salt resistance of blast furnace slag concretes. *Cement & Concrete Composites* 25, 357-361.
- Deventer, J. v., Provis, J., Duxson, P., & Brice, D. (2010). Chemical Research and Climate Change as Drivers in the Commercial Adoption of Alkali Activated Materials. *Waste Biomass Valor*, 145-155.
- Dhir, R., & Jones, M. (1999). Development of chloride-resisting concrete using fly ash. *Fuel* 78, 137-142.
- Diamanti, M., Lollini, F., Pedferri, M., & Bertolini, L. (2013). Mutual interactions between carbonation and titanium dioxide photoactivity in concrete. *Building and Environment* 62, 174-181.
- Diamanti, M., Lollini, F., Pedferri, M., & Bertolini, L. (2013). Mutual interactions between carbonation and titanium dioxide photoactivity in concrete. *Building and Environment* 62, 174-181.
- Dousti, A., Rashednia, R., Ahmadi, B., & Shekarchi, M. (2013). Influence of exposure temperature on chloride diffusion in concretes incorporating silica fume or natural zeolite. *Construction and Building Materials* 49, 393-399.
- Ductal. (n.d.). *Jean Bouin Stadium (France): Focus on Ductal® UHPC Roof and Façade Panels*. Retrieved from ductal: http://www.ductal.com/wps/portal/ductal/3_6_1-

Detail?WCM_GLOBAL_CONTEXT=/wps/wcm/connectlib_ductal/Site_ductal/AllKeyProject/KeyProjectDuctal+Page_1385395657489/Content+KeyProjectDuctal

- Ductal®. (n.d.). *Joint Fill - Road Bridges & Joint Fill*. Retrieved from Ductal: http://www.ductal.com/wps/portal/ductal/2_2_2-JoinFills
- ENCI. (2008, April). Retrieved from hout-en-bouwmaterialen.nl: <http://www.hout-en-bouwmaterialen.nl/downloads/enci-eenvoudig-betonwerk-algemene-en-technische-informatie.pdf>
- ENCI, Mebin en Sagrex. (2011). *Betonpocket 2012*. 's-Hertogenbosch: Bowprint, Haghorst.
- Endicott, W. (2007). A whole new cast.
- Europese prijs voor De Boer&De Groot*. (2012, 11 14). Retrieved from "Workum.nl": <http://www.workum.nl/de/home/nieuws/1842>
- fib. (2009). *Structural Concrete: Textbook on behaviour, design and performance, second edition, Volume 1*. DCC Document Competence Center siegmar Kastl.
- fib Bulletin 55. (2010). *Model Code 2010, First complete draft – Volume 1*.
- Geopolymer Alliance. (n.d.). *welcome*. Retrieved from geopolymer alliance: <http://www.geopolymers.com.au/>
- Geopolymer Institute. (2013, 12 10). *World's first public building with structural Geopolymer Concrete*. Retrieved from Geopolymer Institute - Promoting the Geopolymer science since 1979: <http://www.geopolymer.org/news/worlds-first-public-building-with-structural-geopolymer-concrete>
- Geopolymer Institute. (2014). *Construction - Geopolymer Institute*. Retrieved from Geopolymer: <http://www.geopolymer.org/tag/construction>
- Ghafari, E., Costa, H., Júlio, E., Portugal, A., & Durães, L. (2014). The effect of nanosilica addition on flowability, strength and transport properties of ultra high performance concrete. *Materials and Design* 59, 1-9.
- Ghrichi, M., Kenai, S., & Said-Mansour, M. (2007). Mechanical properties and durability of mortar and concrete containing natural pozzolana and limestone blended cements. *Cement & Concrete Composites* 29, 542-549.
- Glasby, T., Day, J., Kemp, M., & Aldred, J. (2013). Earth Friendly Concrete – A sustainable option for tunnels requiring high durability. *Arabian Tunnelling Conference & Exhibition*, (p. 11). Dubai, United Arab Emirates.
- Glasby, T., Day, J., Kemp, M., & Aldred, J. (2014, January). *Geopolymer concrete for durable linings*. Retrieved from Tunneltalk: <http://www.tunneltalk.com/TunnelTECH-Jan2014-Sustainable-Earth-Friendly-Concrete-for-high-durability-tunnels.php>
- Graybeal, B. (2008). Flexural Behavior of an Ultrahigh-Performance Concrete I-Girder. *Journal of bridge engineering*.
- Graybeal, B. (2009). Structural Behavior of a 2nd Generation UHPC Pi-Girder.
- Graybeal, B. A. (2006). *Material Property Characterization of Ultra-High Performance Concrete*.

- Grünewald, S. (2004). *Performance-based design of self-compacting fibre reinforced concrete*. Delft.
- Guneyisi, E., Gesoglu, M., Ozturan, T., & Ozbay, E. (2009). Estimation of chloride permeability of concretes by empirical modeling: Considering effects of cement type, curing condition and age. *Construction and Building Materials* 23, 469-481.
- Gupta, S. (n.d.). Durability of Flyash Based Geopolymer Concrete. Retrieved from <http://www.engineeringcivil.com/durability-of-flyash-based-geopolymer-concrete.html>
- Gupta, S., Aggarwal, P., Aggarwal, Y., Sehga, V., Siddique, R., & Kaushik, S. (2008). Permeability of high strength concrete. In M. C. Limbachiya, & H. Y. Kew, *Excellence in Concrete Construction through Innovation* (pp. 159-163). London: CRC Press.
- Habert, G., Lacaillerie, J. D., Lanta, E., & Roussel, N. (2010). Environmental Evaluation for Cement Substitution with Geopolymers. Retrieved from <http://www.claissse.info/Proceedings.htm>
- Haitsma . (2011, 11 18). *Betonprijs 2011 voor innovatieve sluisdeuren van Haitsma Beton*. Retrieved from haitsma beton: <http://www.haitsma.nl/>
- Halamickova, P., & Detwiler, R. (1995). WATER PERMEABILITY AND CHLORIDE ION DIFFUSION IN PORTLAND CEMENT MORTARS: RELATIONSHIP TO SAND CONTENT AND CRITICAL PORE DIAMETER . *Cement and Concrete Research*, Vol. 25. No. 4, 790-802.
- Hardjito, D. (2005). *Studies on Fly Ash-Based Geopolymer Concrete* . Ph. D. Curtin University of Technology, Dept. of Civil Engineering.
- Hassan, M., Mehrpouya, M., Emamian, S., & Sheikholeslam, M. (2013). Review of Self-Healing Effect on Shape Memory Alloy (SMA) Structures. *Advanced Materials Research* Vol. 701, 87-92.
- He, X., & Shi, X. (2008). Chloride Permeability and Microstructure of Portland Cement Mortars Incorporating Nanomaterials. *Transportation Research Record: Journal of the Transportation Research Board*, 13-21.
- Heijmans. (2014). Inventarisatie bruggen in NL 25-09-2014.
- Heijmans Civiel B.V. Projecten. (2014, 09 22). Onderdoorgang Elst, Aanbiedingsontwerp, Snelverkeerstunnel (SVT).
- Heijmans. (n.d.). Sluizen overzicht.
- Hieu, T. C., & Neithalath, N. (2010). Moisture and ionic transport in concretes containing coarse limestone powder. *Cement & Concrete Composites* 32, 486-496.
- Hofstra, U. (2013). *Handleiding CUR-Rekentool Groen beton: handleiding en verantwoording van de data* .
- Holschemacher, K., & Müller, T. ((n.d)). Influence of fibre type on hardened properties of steel fibre reinforced concrete.
- Huang, Q., Jiang, Z., Zhang, W., Gu, X., & Dou, X. (2012). Numerical analysis of the effect of coarse aggregate distribution on concrete carbonation. *Construction and Building Materials* 37, 27-35.
- Hussein, M., Kunieda, M., & Nakamura, H. (2012). Strength and ductility of RC beams strengthened with steel-reinforced strain hardening cementitious composites. *Cement & Concrete Composites* 34, 1061-1066.

- Italcementi. (2009). *TX Active - The Photocatalytic Active Principle*.
- Jaarsveld, J. v., Deventer, J. v., & Lukey, G. (2003). The characterisation of source materials in fly ash-based geopolymers. *Materials Letters* 57, 1272-1280.
- Jalal, M., Fathi, M., & Farzad, M. (2013). Effects of fly ash and TiO₂ nanoparticles on rheological, mechanical, microstructural and thermal properties of high strength self compacting concrete. *Mechanics of Materials, Volume 61*, 11-27.
- Jalal, M., Ramezani-pour, A. A., & Pool, M. K. (2013). Split tensile strength of binary blended self compacting concrete containing low volume fly ash and TiO₂ nanoparticles. *Composites Part B: Engineering, Volume 55*, 324-337.
- Jamal, H. (2014). *Lime Concrete - Definition and Manufacturing*. Retrieved from aboutcivil.org: <http://www.aboutcivil.org/lime-concrete-definition-manufacturing.html>
- Japan Society of Civil Engineers. (2008). *Recommendations for Design and Construction of High Performance Fiber Reinforced Cement Composites with Multiple Fine Cracks (HPFRCC)*.
- Jayapalan, A. R., Lee, B. Y., & Kurtis, K. E. (2013). Can nanotechnology be 'green'? Comparing efficacy of nano and microparticles in cementitious materials. *Cement & Concrete Composites* 36, 16-24.
- Jimwich. (2005, January). *J I M W I C H*. Retrieved from JAN 2005 Archive : http://www.anigami.com/jimwich/jimwich_archives/jimwich_1_2005.html
- Jitendra, J., & Neithalath, N. (2010). Chloride transport in fly ash and glass powder modified concretes – Influence of test methods on microstructure. *Cement & Concrete Composites* 32, 148-156.
- Johnston, C. (1996). Proportioning, mixing and placement of fibre-reinforced cements and concretes, Production Methods and Workability of Concrete. *Production Methods and Workability of Concrete*.
- Joostdevree.nl . (n.d.). *milieuklasse*. Retrieved from Joostdevree: <http://www.joostdevree.nl/shtmls/milieuklasse.shtml>
- Karatasios, I., Katsiotis, M. S., Likodimos, V., Kontos, A. I., Papavassiliou, G., Falaras, P., & Kilikoglou, V. (2010). Photo-induced carbonation of lime-TiO₂ mortars. *Applied Catalysis B: Environmental* 95, 78-86.
- Ken, P. W., Ramli, M., & Ban, C. C. (2015). An overview on the influence of various factors on the properties of geopolymer concrete derived from industrial by-products. *Construction and Building Materials* 77, 370-395.
- Khana, M. I., & Siddique, R. (2011). Utilization of silica fume in concrete: Review of durability properties. *Resources, Conservation and Recycling* 57, 30-35.
- Khoshakhlagh, A., Nazari, A., & Khalaj, G. (2010). Effects of Fe₂O₃ Nanoparticles on Water Permeability and Strength Assessments of High Strength Self-Compacting Concrete. *Sci. Technol.*, 2012, 28, 73-82.
- Kim, Y. J. (2014). *Advanced Composites in Bridge Construction and Repair*. Woodhead Publishing.

- Kim, Y. Y., Lee, B. Y., Bang, J.-W., Han, B.-C., Feo, L., & Cho, C.-G. (2014). Flexural performance of reinforced concrete beams strengthened with strain-hardening cementitious composite and high strength reinforcing steel bar. *Composites: Part B* 56, 512-519.
- Konsta-Gdoutos, M. S., Metaxa, Z. S., & Shah, S. P. (2010). Highly dispersed carbon nanotube reinforced cement based materials. *Cement and Concrete Research* 40, 1052-1059.
- Kooiman, A. (1996). *Staalvezelbeton in de linings van boortunnels, een state-of-the-art*.
- Kulakowski, M. P., Pereira, F. M., & Molin, D. C. (2009). Carbonation-induced reinforcement corrosion in silica fume concrete. *Construction and Building Materials* 23, 1189-1195.
- Kunieda, M., & Rokugo, K. (2006). Recent Progress on HPRCC in Japan: Required Performance and Applications. *Journal of Advanced Concrete Technology* Vol. 4, No. 1, 19-33.
- Lackhoffa, M., Prieto, X., Nestle, N., Dehn, F., & Niessner, R. (2003). Photocatalytic activity of semiconductor-modified cement—influence of semiconductor type and cement ageing. *Applied Catalysis B: Environmental* 43, 205-216.
- Lafarge. (2015). *Ordinary Portland Cement (OPC)*. Retrieved from Lafarge in Malaysia - Cement, concrete, aggregates: http://www.lafarge.com.my/wps/portal/my/2_3_B_1-Detail?WCM_GLOBAL_CONTEXT=/wps/wcm/connect/lib_my/Site_my/AllProductDataSheet/ProductDatashet+Exemple_1269347940892/ProductDatashet+EN
- Lagerblad, B. (2006). *Carbon dioxide uptake during concrete life cycle – State of the art*.
- Leenders, F. (2014). *Integral Abutment Bridge and Strain-Hardening Cementitious Composites*. Delft.
- Lepech, M., & Li, V. (2005). Proceedings of Eleventh International Conference on Fracture. *Water permeability of cracked cementitious composites*, (pp. 20-25). Turin, Italy.
- Li, H., Xiao, H., Guan, X., Wang, Z., & Yu, L. (2014). Chloride diffusion in concrete containing nano-TiO₂ under coupled effect of scouring. *Composites: Part B* 56, 698-704.
- Li, H., Xiao, H.-g., & Ou, J.-p. (2004). A study on mechanical and pressure-sensitive properties of cement mortar with nanophase materials. *Cement and Concrete Research* 34, 435–438.
- Li, M. (2009). *Multi-Scale Design for Durable Repair of Concrete Structures*. Michigan.
- Li, V. C. (2006). Bendable Composites: Ductile Concrete for Structures. *STRUCTURE magazine*, 45-48.
- Li, V. C. (2007). *Engineered Cementitious Composites (ECC) – Material, Structural, and Durability Performance*.
- Li, V. C. (n.d.). *Michigan's Experience with Ductile ECC for Bridge Decks*. Retrieved from [www.concretebridgeviews.com](http://www.concretebridgeviews.com/i77/Article2.php): <http://www.concretebridgeviews.com/i77/Article2.php>
- Li, V. C., Lepech, M., & Li, M. (2005). *Final Report On Field Demonstration of Durable Link Slabs for Jointless Bridge Decks Based on Strain-Hardening Cementitious Composites*. Michigan Department of Transportation.
- Li, W., Jiang, Z., Yang, Z., Zhao, N., & Yuan, W. (2013). Self-Healing Efficiency of Cementitious Materials Containing Microcapsules Filled with Healing Adhesive: Mechanical Restoration and Healing Process Monitored by Water Absorption. *PLoS ONE* 8(11): e81616. doi:10.1371/journal.pone.0081616.

- Li, Y. E., Guo, L., Rajlic, B., & Murray, P. (n.d.). Hodder Avenue Underpass: An Innovative Bridge Solution with Ultra-High Performance Fibre-Reinforced Concrete.
- Li, Z., Wang, H., He, S., Lu, Y., & Wang, M. (2006). Investigations on the preparation and mechanical properties of the nano-alumina reinforced cement composite. *Materials Letters* 60, 356–359.
- Liu, X., Chia, K. S., & Zhang, M.-H. (2011). Water absorption, permeability, and resistance to chloride-ion penetration of lightweight aggregate concrete. *Construction and Building Materials* 25, 335-343.
- Locher, F. W., & Sprung, S. (1970). Einwirkung von salzsäurehaltigen PVC-Brandgasen auf Beton. *Betontechn. Berichte* 11, 33-55.
- López, J., Serna, P., & Camacho, E. (n.d.). Structural design and previous tests for a retaining wall made with precast elements of UHPFRC.
- Maalej, M., Lin, V., Nguyen, M., & Quek, S. (2010). Engineered cementitious composites for effective strengthening of unreinforced masonry walls. *Engineering Structures* 32, 2432-2439.
- Maalej, M., Quek, S., Ahmed, S., Zhang, J., Lin, V., & Leong, K. (2012). Review of potential structural applications of hybrid fiber Engineered Cementitious Composites. *Construction and Building Materials - Volume 36*, 216-227.
- Mackenzie, K., & Welter, M. (2014). Geopolymer (aluminosilicate) composites: synthesis, properties and applications .
- Madandoust, R., Mohseni, E., Mousavi, S. Y., & Namnevis, M. (2015). An experimental investigation on the durability of self-compacting mortar containing nano-SiO₂, nano-Fe₂O₃ and nano-CuO. *Construction and Building Materials* 86, 44–50.
- Majorana, C., Salomoni, V., Mazzucco, G., & Khoury, G. (2010). An approach for modelling concrete spalling in finite strains. *Mathematics and Computers in Simulation* 80, 1694-1712.
- Mardani-Aghabaglou, A., Andiç-Çakir, Ö., & Ramyar, K. (2013). Freeze–thaw resistance and transport properties of high-volume fly ash roller compacted concrete designed by maximum density method. *Cement & Concrete Composites* 37, 259-266.
- Maten, R. t. (2011). *Ultra High Performance Concrete in Large Span Shell Structures*. Rotterdam.
- Materials Science and Engineering, Division of Engineering, The University of Edinburgh. (2001. Retrieved 13 November 2012). Porous materials: Permeability. *Module Descriptor, Material Science, Materials* 3, p. p.3.
- MCB Nederland. (n.d.). *mcbboek.nl*. Retrieved from MCB_BookTOC: http://www.mcbboek.nl/MCB_h14/images/afb429.png
- McLellan, B. C., Williams, R. P., Lay, J., Riessen, A. v., & Corder, G. D. (2011). Costs and carbon emissions for geopolymer pastes in comparison to ordinary portland cement. *Journal of Cleaner Production* 19, 1080-1090.
- Mebin. (2012). *Hoe ver kun je gaan in kant-en-klare wapening?*
- Michigan Department of Transportation's Construction and Technology Division. (2005). Bridge Decks Going Jointless. *C&T Research Record*.

- Michigan Technological University. (2007, August). Bendable Concrete Provides Insight into Sustainable Material Development Process. *MDOT Office of Research and National Best Practice*, pp. 1-4.
- Microlab TU Delft. (2014, September 25). Concrete science and technology - Lecture 26.09.2014: Volume changes; Shrinkage and swelling.
- Milan, K., Vaclav, K., Jan, K., L., V. J., Robert, B., & Petr, K. (n.d.). Cable-Stayed Footbridge with UHPC Segmental Deck.
- Müllauer, W., Beddoe, R. E., & Heinz, D. (2015). Leaching behaviour of major and trace elements from concrete: effect of fly ash and ggbs. *Cement and Concrete Composites*.
- Nayak, N., & Jain, A. (2012). *Handbook on Advanced Concrete Technology*. Narosa Publishing House Pvt. Ltd.
- Nazari, A., & Riahi, S. (2010). The effect of TiO₂ nanoparticles on water permeability and thermal and mechanical properties of high strength self-compacting concrete. *Materials Science and Engineering A* 528, 756-763.
- Nazari, A., & Riahi, S. (2011). Al₂O₃ nanoparticles in concrete and different curing media. *Energy and Buildings, Volume 43, Issue 6*, 1480-1488.
- Nazari, A., & Riahi, S. (2011). TiO₂ nanoparticles effects on physical, thermal and mechanical properties of self compacting concrete with ground granulated blast furnace slag as binder. *Energy and Buildings* 43, 995-1002.
- Nazari, A., Riahi, S., Riahi, S., Shamekhi, S. F., & Khademno, A. (2010). Benefits of Fe₂O₃ nanoparticles in concrete mixing matrix. *Journal of American Science*, 102-106.
- Nazari, A., Riahi, S., Riahi, S., Shamekhi, S. F., & Khademno, A. (2010). The effects of incorporation Fe₂O₃ nanoparticles on tensile and flexural strength of concrete. *Journal of American Science*, 90-93.
- Nederlands Normalisatie-instituut . (2001). *NEN-EN 206-1:2001: Beton - Deel 1: Specificatie, eigenschappen, vervaardiging en conformiteit*.
- Nederlands Normalisatie-instituut . (2004). *Aanbeveling 97: Hogesterktebeton - DEEL I NEN 6720 (VBC 1995)*.
- Nederlands Normalisatie-instituut . (2011). *NEN-EN 1992-1-1+C2*. Delft.
- Nederlands Normalisatie-instituut. (2014). *NEN-EN 206:2014 (en): Beton - Specificatie, eigenschappen, vervaardiging en conformiteit*.
- Ng, T., Htut, T., & Foster, S. J. (2010). Mode I and II fracture behaviour of steel fibre reinforced high strength geopolymer concrete: an experimental investigation. In e. a. B.H. Oh, *Fracture Mechanics of Concrete and Concrete Structures - High Performance, Fiber Reinforced Concrete, Special Loadings and Structural Applications*.
- Nguyen, V.-H., Leklou, N., Aubert, J.-E., & Mounanga, P. (2013). The effect of natural pozzolan on delayed ettringite formation of the heat-cured mortars. *Construction and Building Materials* 48, 479-484.
- NV Bekaert SA. (2008). Park Oceanographic .

- Olivia, M., & Nikraz, H. (2012). Properties of fly ash geopolymer concrete designed by Taguchi method. *Materials and Design* 36, 191-198.
- Olivia, M., & Nikraz, H. R. (2011). Strength and water penetrability of fly ash geopolymer concrete. *ARPN Journal of Engineering and Applied Sciences, Vol. 6, No.7.*
- Orellan Herrera, J., Escadeillas, G., & Arliguie, G. (2006). Electro-chemical chloride extraction: Influence of C3A of the cement on treatment efficiency. *Cement and Concrete Research* 36, 1936-1946.
- Ottelé, M. (2015, May 1). Faalkosten. (J. v. Oosten, Interviewer)
- Paskvalin, A. (2015). *Application of Ultra High Performance Concrete in the new Leiden Bridge*. Delft.
- Pelletier, M. M., Brown, R., Shukla, A., & Bose, A. (n.d.). Self-healing concrete with a microencapsulated healing agent.
- Perry, V. H., & Zakariasen, D. (2004, August). First Use of Ultra-High Performance Concrete for an Innovative Train Station Canopy. *Concrete Technology today Vol. 25, No.2.*
- Perry, V., Scalzo, P., & Gary Weiss, P. (2007). Innovative Field Cast UHPC Joints for Precast Deck Panel Bridge Superstructures - CN Overhead Bridge at Rainy Lake, Ontario. *Concrete Bridge Conference.*
- Poon, C., Kou, S., & Lam, L. (2006). Compressive strength, chloride diffusivity and pore structure of high performance metakaolin and silica fume concrete. *Construction and Building Materials* 20, 858-865.
- Portland Cement Association. (n.d.). Ettringite Formation and the Performance of Concrete.
- Qian, S., Zhou, J., Rooij, M. d., Schlangen, E., Ye, G., & Breugel, K. v. (2009). Self-healing behavior of strain hardening cementitious composites incorporating local waste materials. *Cement & Concrete Composites* 31, 613-621.
- Reinhardt, H. (2000). *Beton als constructiemateriaal: eigenschappen en duurzaamheid*. Delft.
- Roux, N., Andrade, C., & Sanjuan, M. A. (1996, February). Experimental Study of Durability of Ractive Powder Concretes. *Journal of materials in civil engineering.*
- Ryu, G. S., Lee, Y. B., Koh, K. T., & Chung, Y. S. (2013). The mechanical properties of fly ash-based geopolymer concrete with alkaline activators. *Construction and Building Materials* 47, 409-418.
- Sadev. (n.d.). *Jean Bouin stadium get a new look!* Retrieved from SADEV architectural glass systems: <http://www.sadev.com/blog/le-stade-jean-bouin-fait-peau-neuve/?lang=en>
- Sanchez, F., & Sobolev, K. (2010). Nanotechnology in concrete – A review. *Construction and Building Materials* 24, 2060-2071.
- Sata, V., Sathonsaowaphak, A., & Chindaprasirt, P. (2012). Resistance of lignite bottom ash geopolymer mortar to sulfate and sulfuric acid attack. *Cement & Concrete Composites* 34, 700-708.
- Senhadji, Y., Escadeillas, G., Mouli, M., Khelafi, H., & Benosman. (2014). Results of loss in weight after acidic attacks indicate generally superior acid resistance and microstructure of mortar. *Powder Technology* 254, 314-323.

- Shaikh, F. U. (2013). Review of mechanical properties of short fibre reinforced geopolymer composites . *Construction and Building Materials* 43, 37-49.
- Shawnessy Lightrail station Calgary in vvUHSB. (n.d.). Retrieved from Ultra Hoge Sterkte Beton: <http://www.uhsb.nl/?p=189#>
- Shen, W., Zhang, C., Li, Q., Zhang, W., Cao, L., & Ye, J. (2015). Preparation of titanium dioxide nano particle modified photocatalytic self-cleaning concrete . *Journal of Cleaner Production, Volume 87*, 762–765.
- Sisomphona, K., Copuroglu, O., & Koenders, E. (2012). Self-healing of surface cracks in mortars with expansive additive and crystalline additive crystalline additive. *Cement and Concrete Composites, Volume 34, Issue 4*, 566-574.
- Stutech/Stufib studiecel 61/19. (2012). *Duurzaamheid als ontwerpcriterium voor beton - toegespitst op CO2*. Delft.
- Stynoski, P., Mondal, P., & Marsh, C. (2015). Effects of silica additives on fracture properties of carbon nanotube and carbon fiber reinforced Portland cement mortar. *Cement & Concrete Composites* 55, 232-240.
- Sui, Y. (2011). *Mechanical behavior of FRP-confined self-healing concrete* . Xiamen University.
- Sui, Y. (2014). *Mechanical behavior of FRP-confined self-healing concrete*.
- Tang, W., Kardani, O., & Cui, H. (2015). Robust evaluation of self-healing efficiency in cementitious materials – A review. *Construction and Building Materials* 81, 233-247.
- Tayeh, B. A., Bakar, B. A., Johari, M. M., & Voo, Y. L. (2012). Mechanical and permeability properties of the interface between normal concrete substrate and ultra high performance fiber concrete overlay. *Construction and Building Materials* 36, 538-548.
- TCL. (2013). *Ordinary Portland Cement*. Retrieved from Trinidad Cement Limited: <http://www.tcl.co.tt/products-services/products/ordinary-portland-cement>
- Turner, L. K., & Collins, F. G. (2013). Carbon dioxide equivalent (CO₂-e) emissions: A comparison between geopolymer and OPC cement concrete. *Construction and Building Materials* 43, 125-130.
- U.S. Department of Transportation. (2013). *Ultra-High Performance Concrete: A State-of-the-Art Report for the Bridge Community*.
- U.S. Department of Transportation Federal Highway Administration. (2010, March). Retrieved from www.fhwa.dot.gov: <http://www.fhwa.dot.gov/pavement/concrete/pubs/hif10014/hif10014.pdf>
- Vandewalle, L., & Plizzari, M. d. (2010). MC2010: Overview on the shear provisions for FRC. Retrieved from <http://dicata.ing.unibs.it/shearworkshop2010/files/01%20VANDEWALLE.pdf>
- Vejmelková, E., Konáková, D., Kulovaná, T., Keppert, M., Zumár, J., Rovnaníková, P., . . . Cerny, R. (2015). Engineering properties of concrete containing natural zeolite as supplementary cementitious material: Strength, toughness, durability, and hygrothermal performance. *Cement & Concrete Composites* 55, 259-267.

- Vejmelkova, E., Pavlikova, M., Keppert, M., Kersner, Z., Rovnanikova, P., Ondracek, M., . . . Cerny, R. (2010). High performance concrete with Czech metakaolin: Experimental analysis of strength, toughness and durability characteristics. *Construction and Building Materials* 24, 1404-1411.
- Ven, J. v. (2015, April 29). Faalkosten. (J. v. Oosten, Interviewer) Rosmalen.
- Verein Deutscher Zementwerke e.V. (2002). *Zement-Taschenbuch 2002*. Düsseldorf: B.o.s.s Druck und Medien, Kleve.
- Voo, Y. L., Nematollahi, B., Said, A. B., Gopal, B. A., & Yee, T. S. (2012). Application of Ultra High Performances Fiber Reinforced Concrete - The Malaysia perspective. *International Journal of Sustainable Construction Engineering & Technology, Vol 3, Issue 1*.
- Wagners. (2015). *Earth Friendly Concrete*. Retrieved from Wagner: <http://www.wagner.com.au/capabilities/efc/>
- Wagners and Brisbane West Wellcamp Airport. (n.d.). EFC Geopolymer Aircraft Pavements at Brisbane West Wellcamp Airport (BWWA).
- Wagners. (n.d.). *Rocky Point Boat Ramp*. Retrieved April 8, 2015, from wagners: <http://www.wagner.com.au/projects/rocky-point-boat-ramp/>
- Wallah, S. E., & Rangan, B. V. (2006). *Low-calcium fly ash-based geopolymer concrete: long-term properties*. Perth, Australia : Faculty of Engineering Curtin University of Technology.
- Wang, K., Jansen, D. C., Shah, S. P., & Karr, A. F. (1997). Permeability study of cracked concrete. *Cement and Concrete Research, Volume 27, Issue 3*, 381-393.
- Wang, X., Xing, F., Zhang, M., Han, N., & Qian, Z. (2013). Experimental Study on Cementitious Composites Embedded with Organic Microcapsules. *Materials* 2013, 6, 4064-4081. doi:10.3390/ma6094064
- Wang, X., Xing, F., Zhang, M., Han, N., & Qian, Z. (2013). Experimental Study on Cementitious Composites Embedded with Organic Microcapsules. *Materials*, 4064-4081. doi:10.3390/ma6094064
- Wiedemann, G. (1982). Zum einfluss tiefer temperaturen auf festigkeit und verformung von beton.
- Wu, M., Johannesson, B., & Geiker, M. (2012). A review: Self-healing in cementitious materials and engineered cementitious composite as a self-healing material. *Construction and Building Materials* 28, 571-583.
- Xia Hua. (2010). *Self-healing of Engineered Cementitious Composites (ECC) in Concrete Repair System*. Delft.
- Yang, K.-H., Jung, Y.-B., Cho, M.-S., & Tae, S.-H. (2014). Effect of supplementary cementitious materials on reduction of CO2 emissions from concrete. *Journal of Cleaner Production*.
- Yang, T., Yao, X., & Zhang, Z. (2014). Quantification of chloride diffusion in fly ash–slag-based geopolymers by X-ray fluorescence (XRF). *Construction and Building Materials* 69, 109-115.
- Younsi, A., Turcry, P., Aït-Mokhtar, A., & Staquet, S. (2013). Accelerated carbonation of concrete with high content of mineral additions: Effect of interactions between hydration and drying. *Cement and Concrete Research, Volume 43*, 25-33.

- Yuan, H., & Chen, H. (2013). Quantitative solution of size and dosage of capsules for self-healing of cracks in cementitious composites . *Computers and Concrete, Vol. 11, No. 3*, 223-236.
- Yuan, Q., Shi, C., Geert, D. S., Audenaert, K., & Deng, D. (2009). Chloride binding of cement-based materials subjected to external chloride environment – A review. *Construction and Building Materials 23*, 1-13.
- Zhang, J. (2003). Modeling of the influence of fibers on creep of fiber reinforced cementitious composite. *Composites Science and Technology, Volume 63, Issue 13*, 1877-1884.
- Zhang, Y., Sun, W., Li, Z., Zhou, X., Eddie, & Chau, C. (2008). Impact properties of geopolymer based extrudates incorporated with fly ash and PVA short fiber. *Construction and Building Materials 22*, 370-383.

Appendix A: Reference projects

In this chapter are reference projects discussed for the advance cementitious materials in the scope of this research. Not all ACMs are applied in practice yet, so not all ACMs will be mentioned in this chapter. The ACMs which are already utilised in practice are: HPC and UHPC, which will be mention in the same chapter, SHCC, GPC and Self-cleaning nano concrete. There are no reference projects found for Self-healing cementitious material and self-sensing and stiff nano concrete

Reading about the reference project, probably it seems all the projects are successfully. But, where new materials are applied in practice, thing must go wrong; there should always be unexpected issues in practice. This is mostly not reported, which is quite logic of course. Besides, most ACMs are utilised for a few years only. Nowadays the ACMs can be a success, but it is still not exactly known how the ACMs will behave when it get aged, for example after 75 service years. Scientific predictions of course are made, but it ACMs could react worse than predicted.

A.1. Reference projects for FRC

- Tunnel linings
- Manholes,
- Risers,
- Burial Vaults,
- Septic Tanks,
- Curbs,
- Pipes,
- Covers,
- Sleepers

A.1.1 Park Oceanographic, Valencia, Spain

The roof of the park Oceanographic in Valencia, Spain, is a thin shell structure with combined reinforcement, as shown in Figure A.1. For the reinforcement, 50kg/m³ Dramix® RC-80/35-BN (end-hooked, length 35mm, diameter 0,45mm) and a single mesh Ø8-15cm were applied. Due to the curvature and the limited shell thickness of 6 cm to 12 cm it would have been very difficult to install a complicated traditional reinforcement in an accurate and safe way (NV Bekaert SA, 2008).



Figure A.1 – Overview of Park Oceanographic, Valencia, Spain

A.2. Reference projects for HPC and UHPC

In this chapter are project described where UHPC or HPC is used. Both, HPC and UHPC are discussed in the same chapter, because both are quite similar to each other. In fact, HPC could be considered as the 'little brother' of UHPC. Further, in practice HPC and UHPC are both defined by different strength limits. So also from a practical point of view, it is easier to combine the reference projects of HPC and UHPC in one chapter.

The main objectives of the study to the projects with UHPC is to know why UHPC is applied and what the results of the application of UHPC are. Interests are from a technical, but also from an economical point of view. After discussing the reference project, an overview of reasons to apply UHPC concrete in the reference projects is shown.

In the US is made an overview of applications of UPHC in bridges all over the world. In Figure A.2 is given where UHPC is applied in bridges. For example the majority of UHPC is used in joints. Also a lot of UHPC is applied to cast beams, for example U-shaped beams and Pi-shaped beams. Pi-shaped beams are specially developed for beams made of UHPC. This innovative beam will be explain in more detail in the discussion of reference project below.

It is quite logic that UHPC is applied for beams. Stronger concrete could result in longer or more slender beams. The reasons that a more than half of the application of UHPC in bridges is in the joints, are shortly (Perry, Scalzo, & Gary Weiss, 2007):

- Improved bridge deck performance through the reduction of joint size and complexity;
- Improved continuity and speed of construction;
- Elimination of field post-tensioning;
- Improved durability;
- lower maintenance;
- Extended usage life.

In other words, the bridge deck joint is no longer the weakest link (Ductal®, n.d.).

APPLICATION OF UHPC IN BRIDGES WORLDWIDE

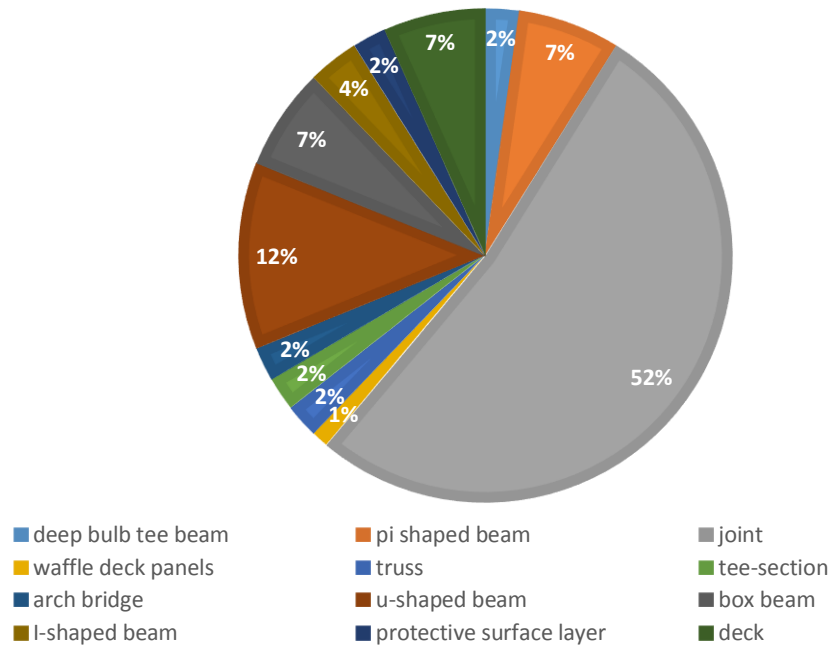


Figure A.2 – Application of UHPC in bridges worldwide. Data from (U.S. Department of Transportation, 2013)

A.2.1 Hodder Avenue Underpass: An Innovative Bridge Solution with Ultra-High Performance Fibre-Reinforced Concrete

The Hodder Avenue Underpass is a bridge construction over a Highway in Canada. Three important keywords to describe this bridge are quality, aesthetics and durability. The bridge has two spans of 33.5 m. The profile of the bridge is shown in Figure A.3. The superstructure consists of 16 precast prestressed high performance concrete (HPC) box girders connected by ultra-high performance fibre-reinforced concrete (UHPC) shear keys and no top slab.

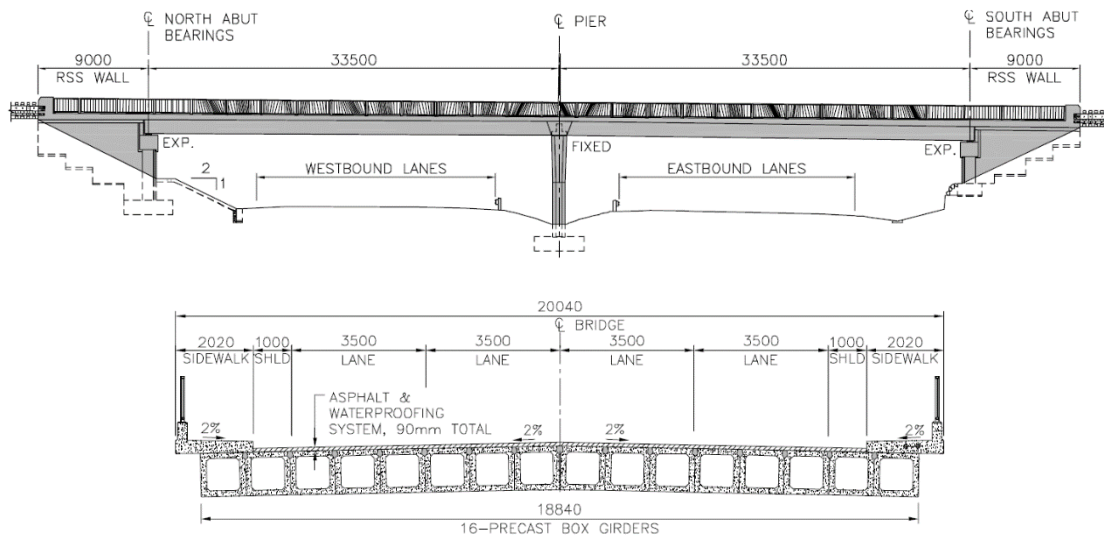


Figure A.3 – Profile of the Hodder Avenue Underpass and the profile of the bridge slab made of box girders

For the Hodder Avenue Underpass, all of its components except footings and columns were pre-fabricated. The pre-fabricated components include: a UHPC pier cap, UHPC pier column shells,

HPC box girders, sidewalks/parapet wall panels, abutment caps, ballast walls, slope paving panels and approach slabs.

Quality

By utilizing the modular construction approach, the project pushed many of the construction procedures off site and into the precast facility. The increased quality control in plants resulted in much improved quality and durability of the structure.

Aesthetic

- Slender: span-to-depth ratio of 29,1 where slab-on-girder system’s has a typical span-to-span ratio of 16 to 20
- Visual openness: Instead of a conventional pier design, which would look heavy and out of proportion with the slender girders, Hodder utilized an innovative UHPFRC pier cap that is embedded within the superstructure (Figure A.4)



Figure A.4 – Photos of pier in: (left) Hodder Avenue Underpass; and (right) a typical highway bridge over Highway 404 in Ontario, Canada

Durable

Pier columns: precast UHPFRC shells (Figure A.5) are filled with standard reinforced concrete in the field. The pier columns are frequently exposed to winter di-icing salt sprays. UHPFRC has a high durability against chloride ingress due to extremely low porosity.



Figure A.5 – Precast UHPFRC pier column shell

Source: (Li, Guo, Rajlic, & Murray, n.d.)

A.2.2 Kampung Ula Geroh Bridge

In January 2012 is the 25 metre long Kampung Ula Geroh Bridge opened after a year of construction. The bridge is made out of two precast UHPFRC T-girders with a height of 1.375 m and a width of the top flange of 1.5 m, casted together at side as shown in Figure A.6.

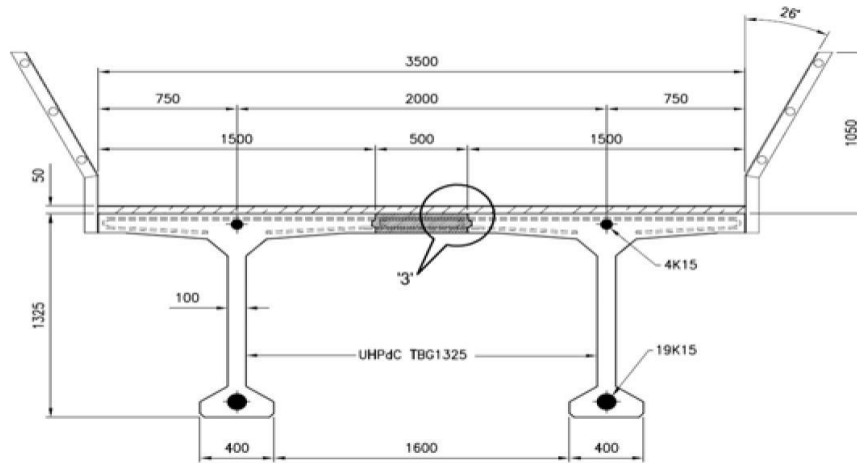


Figure A.6 – Cross sectional detail of the UHPFRC bridge at Kampung Ulu Geroh

The reason that this construction is chosen to cross the valley is mainly because of the conditions at side and partly because the requirements from the authority. The main reasons for this design are:

1. Poor existing access roads to the job site. This limits the maximum capacity of mobile crane to 20 tonnes and the maximum tray length to 8 metres.
2. The authority did not want a steel bridge to avoid maintenance.
3. A concrete centre pier was not allowed.

In the end, the UHPFRC T-beam is chosen because:

1. The weight of one beam is 25 tonnes only, such that two mobile crane can lift the beam
2. Remarkable durability, which is a requirement from the authority.
3. No shear reinforcement is needed, which is an additional advantage.

Source: (Voo, Nematollahi, Said, Gopal, & Yee, 2012)

A.2.3 Kampung Linsum Bridge

The Kampung Linsum Bridge is a 50 m long bridge crossing a river in Malaysia. An overview of this precast bridge is shown in Figure A.7. The bridge is made of single U-shaped girder with a height of 1.75 m and a maximum wide of 2.5 m, as shown in Figure A.8. As shown in the details the thickness of the flange varies over the length of the girder. This is done because of the prestressing cables in the flange. Conventional reinforcement is used at the anchorage zones against bursting, at the tendon deflector positions for lifting the bridge and at the top flanges where the connection with the reinforced concrete decks is required to resist the horizontal shear.



Figure A.7 – Overview of the Kampung Linsum Bridge

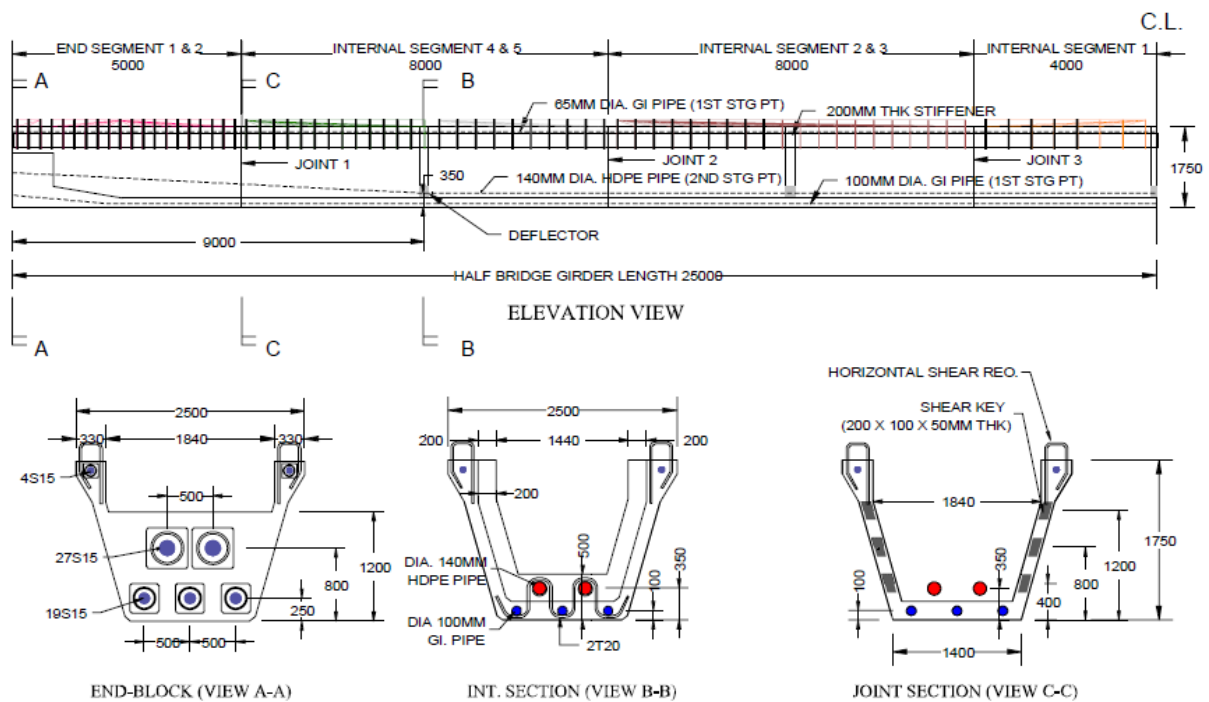


Figure A.8 – Details of the UHPFRC UBG1750 girder

Before the bridge is made, a comparison between a steel composite bridge and the UHPFRC composite bridge is made. The results of this comparison are shown in the graph of Figure A.9 the most important advantages of the concrete bridge over the steel bridge are:

- No piers in the waterway of the river
- Much lower maintenance
- More eco-friendly
- Better aesthetically
- Cheaper

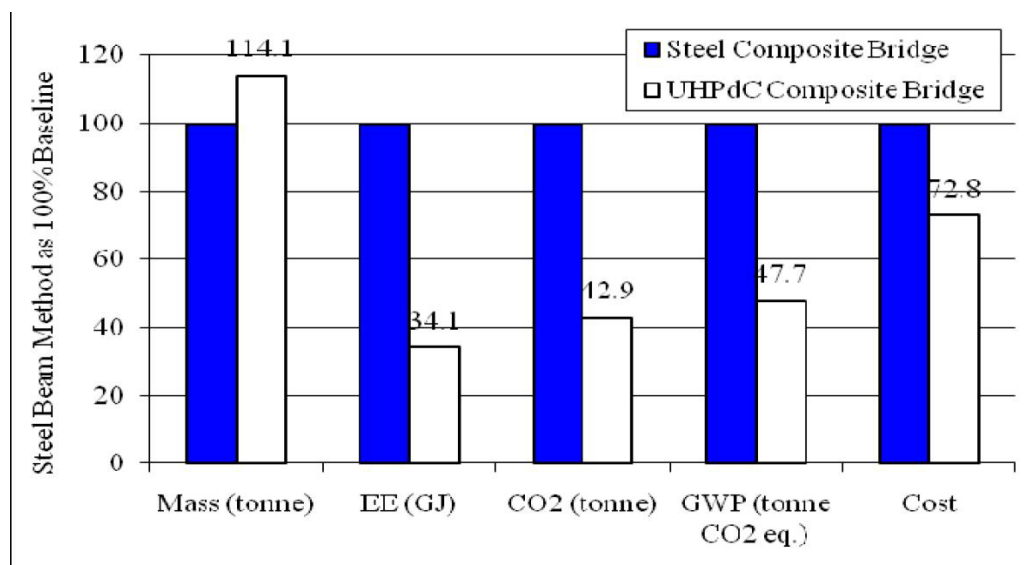


Figure A.9 – Comparison between the UHPFRC and steel composite bridge

Source: (Voo, Nematollahi, Said, Gopal, & Yee, 2012)

A.2.4 Cable-Stayed Footbridge with UHPC Segmental Deck in the Czech Republic

This cable-stayed footbridge is located in the town of Celakovice in the Czech Republic. It is the first bridge of in Czech made of UHPC. An overview of this bridge is shown in Figure A.10.

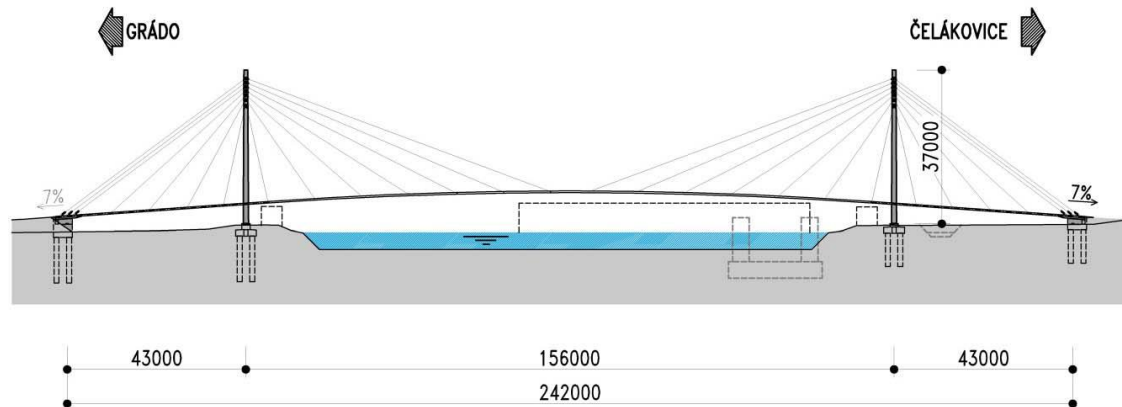


Figure A.10 – Overview of the cable-stayed Footbridge with UHPC Segmental Deck in the Czech Republic

In Figure A.11 is a cross section of the bridge deck shown. The deck is a composite structure consisting of two longitudinal side beams of steel profiles, steel cross beams placed by 2.5 m and a concrete slab. The steel fibre reinforcement concrete (C110/130) slab is designed from precast concrete elements, which are supported on the bottom flange of the side and cross beams.

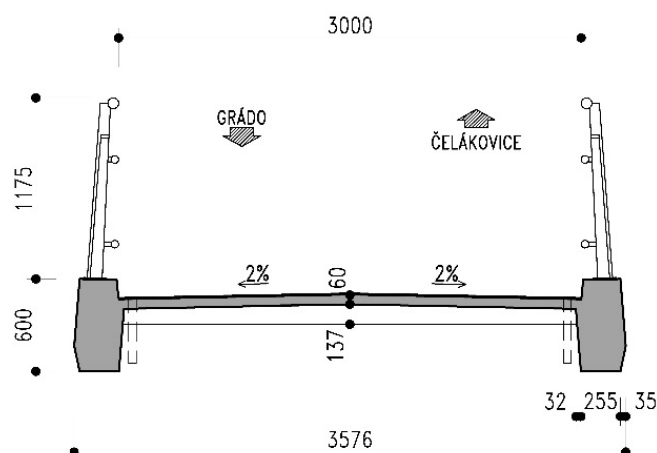


Figure A.11 – Cross section of the deck of the cable-stayed Footbridge

Because this footbridge was the first project where UHPC was applied, different test are done during execution. Because the slab is 60 mm thick only, shears resistance in the deck seems a problem. After some tests the load carrying capacity of the slab was proven to be much higher than the requirements described.

There are three main reasons to build the bridge with an UHPC Segmental deck:

1. Low maintenance
2. Reasonable life cycle costs
3. Favourable tender price

Source: (Milan, et al., n.d.)

A.2.5 Jakway Park Bridge, Buchanan County, Iowa USA

The Jakway Park Bridge is a 3 span bridge with the largest span of 15.5 m. The bridge is the first highway bridge in North America built with second generation UHPC pi-girders. These girders were created to optimize the UHPC mix by minimizing the cross section and taking advantage of the material properties for the bridge deck. The second generation pi-girder has the same basic cross sectional shape as the first generation beams. The exact dimensions of the beam are shown in Figure A.12. The modifications done in the design are:

- Increase deck thickness and width
- Increased web thickness
- Decreased web spacing
- Rounded re-entrant corners.

These modifications in the second generation pi-girders are done to:

- ease fabrication
- simplify construction
- add structural capacity

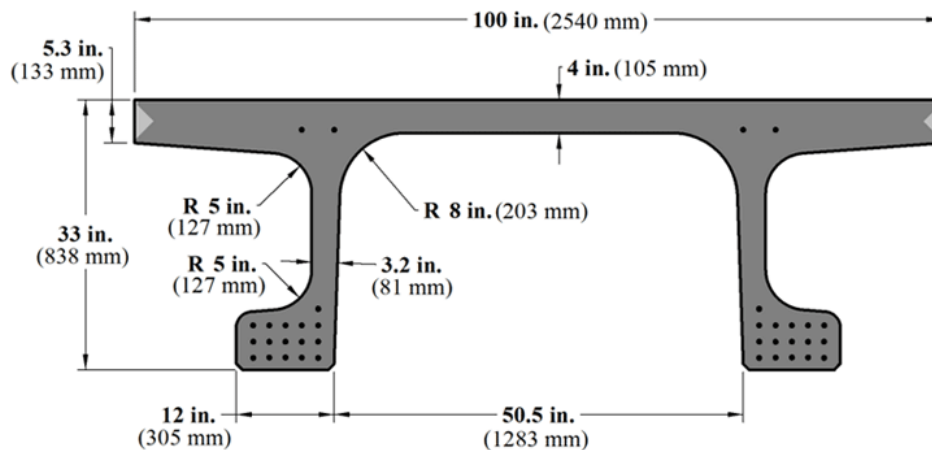


Figure A.12 – Cross section of the second generation pi-girder

The choice to utilize UHPC for the bridge is made on the negative and positive aspects of the UHPC material. These aspects are shown in the two columns below. Next to these material aspect, the learning goal for a girder made of UHPC of course is a positive aspect.

Negative aspects of UHPC Material:

- Material Expensive
- Labour and equipment intensive
 - o Mixing: ½ hr.
 - o Initial Set: 40 hrs.
 - o Curing: 48 hours at 195 degrees
- High shrinkage
- Concern fibre distribution
- Performance of cracked section
- Deck texture is an issue

Positive aspects of UHPC Material:

- Self-Consolidating
- High compressive strength (200 MPa)
- Low permeability
- Low creep post-cured
- High durability
- Fibres post-cracking strength

Sources: (Brain & P.E., 2009), (Aspire, 2010) and (Graybeal B. , 2009)

A.2.6 Jean Bouin Stadium, Paris, France: Focus on Ductal® UHPC Roof and Façade Panels

The undulating façade of the new Jean Bouin Stadium in Paris, France is clad with a unique Ductal® UHPC envelope that covers 23,000m². An impression of the stadium is shown on Figure A.13 The main reason to apply UHPC for the roof and the façade panels came from an architectural point of view. The UHPC made sure thin, lightweight envelope and waterproof panels could be made.



Figure A.13 – Impression of the Jean Bouin Stadium in Paris, France (Sadev, n.d.)

The remarkable envelope consists of three main areas:

- A perforated façade, with self-supporting lattice panels that permit the light to filter through to the interior;
- Transition panels between the roof and the façade, with a higher perforation rate and larger curvature;
- The roof, made from 1,600 panels with glass inserts.

A total of 18 moulds were required to produce the 3,600 UHPC panels. For a full year, the precaster (Bonna Sabla) cast thousands of panels at a rapid pace of more than 18 per day.

The thickness of the plates is 35 mm only which helps the directional dispersion of the fibres. The fibres needed to flow smoothly into the moulds and fully resist developing loads by having preferential orientation in the matrix. Several panels were tested by cutting small section samples of the UHPC out of each panel in order to prove that the casting process consistently produced correct fibre orientation and therefore viable precast elements for Bonna Sabla."

Another architectural requirement for this project was a waterproof roof system. When producing the roof panels, the glass pieces were first positioned into the moulds and then the UHPC material was cast around the glass. Waterproofness was guaranteed with a silicon joint placed around the glass before casting.

Source: (Ductal, n.d.), (Sadev, n.d.)

A.2.7 Shawnessy Light Rail Transit Station, Calgary, Canada

The station's twenty-four thin-shelled canopies, 5.1 m by 6 m and just 20 mm thick, supported on single columns as shown in Figure A.14. The choice to design this station with UHPC had the next reasons:

- Reduction of weight by applying a very strong material

- Design flexibility facilitated the architect's ability to create the attractive, off-white, curved canopies.
- Speed of construction
- Improved aesthetics
- Superior durability by:
 - Impermeability against corrosion
 - Abrasion and impact



Figure A.14 – Impression of the Shawnessy Light Rail Transit Station, Calgary, Canada (Shawnessy Lightrail station Galgary in vUHSB, n.d.)

Execution

By mixing the UHPC material a lot of heat can be generated by the kinetic energy from the mixing machine. This heat is undesirable and should be reduced to a minimum. During mixing the temperature should constantly be monitored to control the heat of the UHPC well. The heat in the concrete can be reduced by adding ice to the mix or put the components of the concrete gradually in the machine, such that less energy will generate more heat.

Next to the mixing procedure, the mould should be made very precisely. The thickness of the concrete components was designed to be 20 mm only. A deviation of for example 3 mm leads already in 20% more material than calculated.

Further the mould should be designed in such a way shrinkage in the mould can occur without additional stresses in the concrete. The orientation of the mould during casting and de-moulding the components are applied in such a way the components can shrink freely as much as possible.

After de-moulding the components are transported by truck, as illustrated in Figure A.15. The big advantage of casting the prefab construction is that the majority of the total shrinkage took place already before they are installed at the building side. At side the components were installed on columns. Those were lifted by crane. Here the reduction of the weight by using UHPC is favourable for the cost of the crane.



Figure A.15 – Precast UHPC elements transported to the building site

Source: (Perry & Zakariasen, 2004)

A.2.8 Wapello County Mars Hill Bridge (2006)

The Wapello County Mars Hill Bridge comprises three 110-ft-long precast concrete modified 45-in.-deep Iowa bulb-tee beams topped with a cast-in-place concrete bridge deck. The bridge resulted from a collaborative effort among several groups, including the Federal Highway Administration (FHWA), IDOT, Iowa State University (ISU), and Lafarge. Because this bridge is the first highway bridge in North America made of UHPC, a three years during exploration was done to the UHPC. Using the UHPC for the design gained impetus from the FHWA's innovative Bridge Research and Construction Program of 300,000 dollar for the use of UHPC for the design. After that it took only 9 months to build the bridge. An impression of the bridge is given in Figure A.16.



Figure A.16 – Impression of the Wapello County Mars Hill Bridge

Because of the strength of the UHPC, no shear reinforcement as needed. In Figure A.17 is the cross section of the bulb-tee beams shown. In the figure also the reinforcement and the prestressing cables are shown. The total costs to construct the bridge are 432,000 dollar.

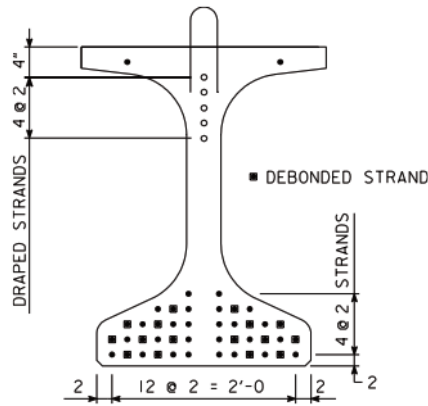


Figure A.17 – Cross section of the bulb-tee beams

As seen of the collaborative working on the project, it seems clear that the project is a part of a learning process to construct with UHPC. The other advantages to construct this bridge with UHPC are:

- Longer, thinner, more aesthetically pleasing beams
- Highly impermeable, which reduce the threat of corrosion within the structure.
- The speed the bridge was completed after testing. The beams were casted in June and July. In the following February (2006) the bridge was opened to traffic.

Source: (Endicott, 2007)

A.2.9 Sluis 0124, Amsterdam, The Netherlands

Sluis 0124 is the first sluice in the world with doors made of high strength concrete. An overview of the sluice, which is positioned in Amsterdam IJburg, is given in Figure A.18. Some facts of the project:

- The building and maintenance costs are both reduced (Europese prijs voor De Boer&De Groot, 2012)
- According to Europese prijs voor De Boer&De Groot (2012), the dimensions of the door are:
 - o Length of 6.50 m
 - o Height of 4.50 m
 - o Thickness of 0.10 m
- Sliding doors (Europese prijs voor De Boer&De Groot, 2012)
- Concrete class C90/105 (Haitsma , 2011)
- Cost are 3.5 million euros (De Boer & De Groot , n.d.)



Figure A.18 – Overview of the sluice with HPC sliding doors (Bouwinfonet , n.d.)

A.2.10 Summary of reasons to apply HPC or UHPC

In the graph of Figure A.19 are shown the main reasons to apply UHPC in the above mentioned project. In the graph is shown that two main reasons to apply UHPC are durability/maintenance and aesthetic. Both are due to the very dens matrix of UHPC. Due to the dens structure, designers has more freedom to do whatever they want to make the most beautiful structures.

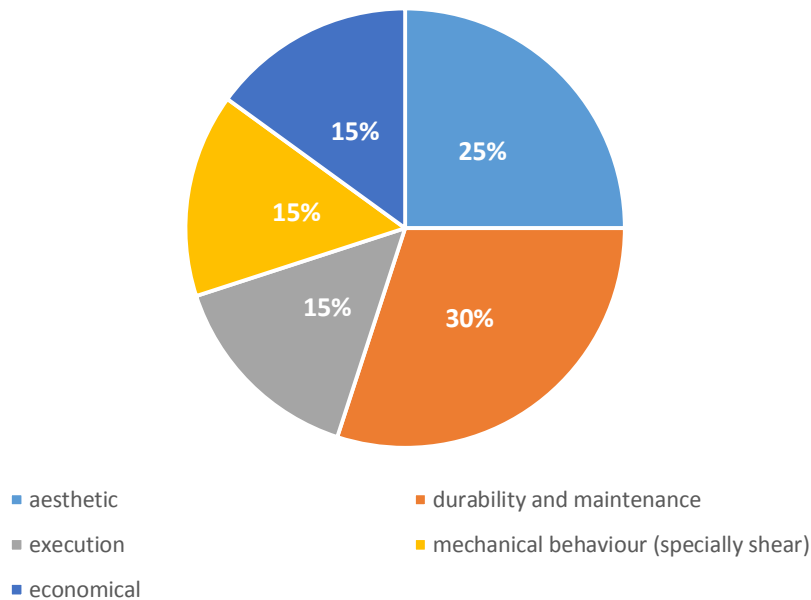


Figure A.19 – Overview of reasons to apply UHPC in practice for the above mentioned reference projects

A.3. Reference projects for SHCC

In this chapter are some projects described where SHCC is utilized. There is not a lot of information available about the projects where SHCC is applied, but the projects will at least indicate where SHCC can be interesting to apply. After analysing the reference project, an overview of reasons to apply SHCC in the reference projects is shown.

A.3.1 ECC in high-rise buildings to increase the earthquake resistance of the structure: Glorio Rappongi High Rise, Tokyo, Japan and the Nabeaure Tower, Yokohama, Japan

Recast ECC coupling beams connect the core walls on each floor and reportedly provide **high vibration damping** and **energy absorbing** during an earthquake. The new material enables structural engineers to achieve a more efficient building design and reduce construction cost (Li V. C., Bendable Composites: Ductile Concrete for Structures, 2006). In Figure A.20 is a schematisation of the Glorio Rappongi High Rise, Tokyo, Japan shown. In yellow the ECC coupling beams can be recognized. Similar structures include the 41-story Nabeaure Yokohama Tower.

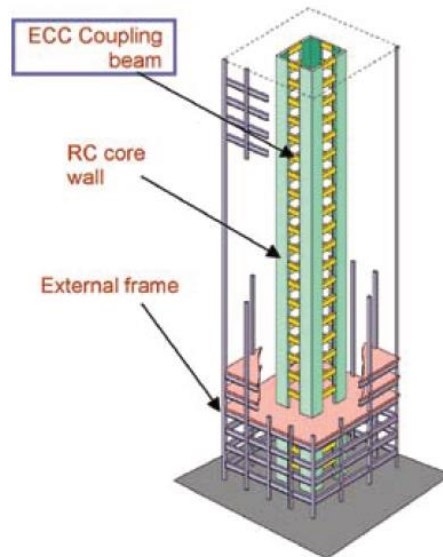


Figure A.20 – Schematisation of the Glorio Roppongi High Rise, Tokyo, Japan (Li, 2006)

The main reasons ECC is applied in these buildings are:

- High vibration damping
- Energy absorbing

Both characteristics reduce the damage to the buildings, which makes the material more durable compared with ordinary concrete. Next to this the buildings are safer.

A.3.2 Ellsworth Road Bridge over US-23

Ellsworth Road Bridge is repaired by HES-ECC, which is a High Early Strength – Engineering Cementitious Composite. The repair is step by step shown in Figure A.21 and step by step explained in more detail here. Construction of patch repair on the Ellsworth Road Bridge over US-23 began at 9am on Tuesday, November 28, 2006 with placement of traffic control devices. The MDOT repair personnel conducted partial depth concrete removal, sandblasted the patch area, replaced damaged reinforcement, and completed patch preparation. Before pouring the patch material, water fog was sprayed onto the concrete substrate to enhance repair bonding. HES-ECC mixing materials were pre-batched in the laboratory for easy field processing, and were transported to the repair site. A 7-cubic foot HES-ECC batch was mixed by the research personnel using a 12-cubic foot capacity concrete gas mixer provided by MDOT. The mixing time lasted around 30 minutes. The mixed HES-ECC exhibited desirable creamy viscosity, good fibre distribution and good flowability (Figure 9.11). Flowability test using a slump cone was conducted right after finishing the mixing. The 25.6" slump diameter indicated that the mixed HES-ECC had self-compacting property. The HES-ECC material was then poured into a wheelbarrow, transported to the patch area, and poured into the patch. The self-compacting property of HES-ECC allowed itself to easily flow into the corners of the patch area without any vibration. The surface of the HES-ECC patch was finished by hand using steel trowel.



Figure A.21 – Execution of HES-ECC and Thoroc 10-60 repair layer on the Ellsworth Road Bridge (Li, Lepech, & Li, 2005)

After execution, the repair of both HES-ECC and Thoroc 10-60 were observed for approximately three years. The conclusions in the end were:

- HES-ECC is a close-to-homogeneous, self-compacting material.
- HES-ECC was easy to pour
- HES-ECC shows a relative economic advantage compared with concrete and alternative field repairs.
- HES-ECC shows a better durability. After three years exposed to harsh environmental conditions of the Michigan winters (combination of restrained shrinkage, freezing and thawing, exposure to de-icing salts, temperature change, etc.) in addition to heavy traffic loads, the next observation to the repair patch were done to judge the durability of both cementitious materials:
 - o Maximum crack width HES-ECC and Thoroc 10-60 are respectively $100 \mu\text{m}$ and $1700 \mu\text{m}$.
 - o interfacial delamination width between the repair patch and existing concrete for HES-ECC and Thoroc 10-60 respectively $70 \mu\text{m}$ and $2200 \mu\text{m}$
 - o HES-ECC showed no disintegration
 - o HES-ECC showed no spalling or other deterioration

Sources: (Li, Lepech, & Li, Final Report On Field Demonstration of Durable Link Slabs for Jointless Bridge Decks Based on Strain-Hardening Cementitious Composites, 2005), (Li M. , 2009)

A.3.3 Grove Street Bridge Project, Michigan, US: ECC Link Slab in Bridge

Grove Street Bridge is the first infrastructure demonstration project of ECC material in the US. The ECC material is used to construct a durable joint between at the end of the bridge. The completed ECC link slab is shown in Figure A.22. The project was in cooperation with the Michigan Department of Transportation (MDOT), HNTB Engineering Consultants, Midwest Bridge Contractors, and Clawson Concrete Company. (ACE-MRL, n.d.)



Figure A.22 – Completed ECC Link Slab (Li, Lepech, & Li, 2005)

That the Grove Street Bridge needed an upgrade is perfectly shown in Figure A.23 and Figure A.24. Over time, deterioration of joint performance allowed water and de-icing chemicals to leak through the joint and over the substructure and ultimately resulted in severe damage to the bridge deck and substructure. (Michigan Technological University, 2007)



Figure A.23 – Bridge joint before reconstruction of the Grove Street Bridge



Figure A.24 – Substructure of the Grove Street Bridge before reconstruction

The reasons more expensive ECC material is chosen above ordinary joint are (Li V. C., Michigan's Experience with Ductile ECC for Bridge Decks, n.d.):

- The service life of concrete bridge decks will be longer
- Enhancing public mobility by reducing traffic interruption, because repairs are minimised.
- Sustainable by the long life time. The application of ECC leads to a reduction of 40% of carbon and energy footprints over the life-time of the bridge

From the above arguments to use the ECC material can be concluded that the main advantage of the ECC material in this project is the durable and sustainable character of the material.

A.3.4 Mihara Bridge, Hokkaido, Japan

The Mihara Bridge in Hokkaido, Japan, is a 1000m long composite ECC/steel bridge deck, with a middle span of 340m. An overview of the bridge is shown in Figure A.25. The bridge is opened for traffic in 2005. The deck is made out of a steel profile with a 38 mm thick layer of ECC placed on top of it. This design is chosen because of:

- High durable structure (expected service life of 100 years)
- 40% weight reduction. Due to the intrinsic crack control capacity of the ECC, a layer of only 35 mm ECC should be good enough to protect the underlying steel from penetration of moisture and chloride.
- 50% reduction in initial construction cost



Figure A.25 – Overview of The Mihara bridge, Hokkaido, Japan, made of a steel/ECC composite deck (Kunieda & Rokugo, 2006)

Sources: (Li V. C., Engineered Cementitious Composites (ECC) – Material, Structural, and Durability Performance, 2007) and (Kim Y. J., 2014)

A.3.5 Mitaka Dam near Hiroshima

The dam height of Mitaka Dam, a gravity concrete dam in Hiroshima Prefecture, was increased from approximately 33 m to 44 m by placing new concrete onto the existing dam body on the downstream side (Figure A.26). In 2003, 30 m³ of HPFRCC was sprayed on the upstream dam surface (area: 500 m²) with a thickness of 30 mm, to improve the shielding performance of the deteriorated existing concrete surface (Figure A.26). Anchors were driven at 1.5 m² intervals to ensure a strong bond between the substrate and HPFRCC.

Cracks, spalling and water leakage were concerns that prompted the use of ECC as a water-tight cover layer. This 20 mm layer was applied by spraying the ECC material directly onto approximately 600 m² of the upstream dam surface.



Figure A.26 – Overview of the dam and the spraying of the ECC

Source: (Kunieda & Rokugo, 2006)

A.3.6 Retaining wall in Japan

This retaining wall in Japan is one of first project where ECC is applied to repair a construction. The wall is shown in Figure A.27. On the left side of the figure, the wall is shown before the surface is repaired. At the right side the repaired wall is shown. The wall is approximately 18 m in width and 5 m in height.

The wall required an upgrade. In 1994 the wall was injected with epoxy resin and the coating because of damage due to ASR. When the surface repair also cracked, a layer of HPFRCC was sprayed on the surface. A shotcreting thickness of 50 to 70 mm was adopted to accommodate the reinforcement.

Observations after 7 months concludes there was no cracking yet. After 10 and 24 month after the repair, crack widths of 0.05 and 0.12 mm respectively were observed. On the other hand, cracking was visually observed on repair with normal repair mortar just one month after repair, with crack widths developing to 0.03, 0.2, and 0.3 mm at 3, 10, and 24 months after repair, respectively.



Figure A.27 – Surface repair of concrete retaining wall before and after repair (Kunieda & Rokugo, 2006)

The application of ECC for this wall is chosen because:

- Small cracking widths, which give
 - o A value from an aesthetic point of view
 - o A proper protection to the reinforcement in the existing wall

A.3.7 Summary of reasons to apply SHCC

In Figure A.28 is an overview given of the reasons of the above mentioned reference projects to apply SHCC in practice. The main reason to apply SHCC is durability. This is of course due to the unique cracking pattern of SHCC.

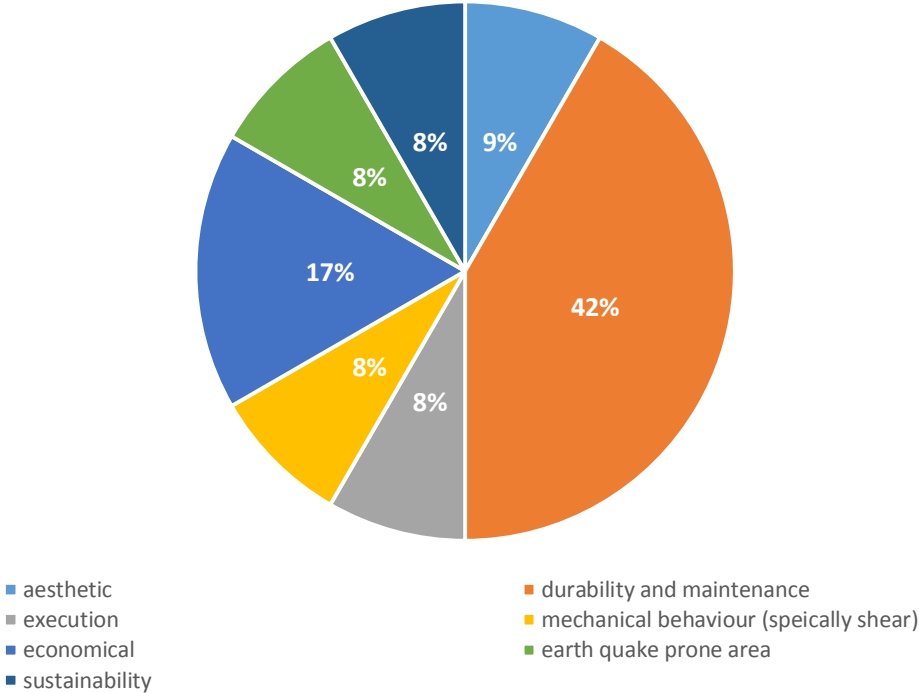


Figure A.28 – Overview of reasons to apply SHCC in practice for the above mentioned reference projects

A.4. Reference projects for Geopolymer Concrete

In this chapter are some reference projects described where GPC is applied. Only four reference projects are given, since GPC is not applied that much yet. The reference project of the water tanks is not a real project but more an experiment to the water tightness of GPC. Because this is an interesting application, the water tanks are included here as reference project.

A.4.1 Global Change Institute, multi-storey building, Australia, Brisbane

The new Global Change Institute building at the University of Queensland in Brisbane has 3 suspended floors of 40 MPa precast EFC beams. A total of 33 beams, each spanning 10.5 m and a width of 2.4 m make a large contribution to the building owner's goal for a building design to meet the world's highest sustainability standards. An impression of the building and of the beams is given in Figure A.29.



Figure A.29 – Left: impression of the Global Change Institute building. Right: precast EFC beam during execution (Glasby, Day, Kemp, & Aldred, *Earth Friendly Concrete – A sustainable option for tunnels requiring high durability*, 2013)

Sources: (Glasby, Day, Kemp, & Aldred, *Earth Friendly Concrete – A sustainable option for tunnels requiring high durability*, 2013) (Geopolymer Institute, 2013)

A.4.2 Water Tanks

Two water tanks (10 m diameter x 2.4 m high) were cast in March 2011 as part of an R&D study. The first water tank was constructed using a Grade 32 MPa concrete with a maximum aggregate size of 10 mm with blended cement consisting of 80% Portland cement and 20% fly ash. The second tank is constructed with a Grade 32 MPa EFC geopolymer concrete also with a 10 mm maximum aggregate. Figure A.30 shows the EFC tank on the right and crack width monitors used. Note the strong calcium deposits in the right hand side image typical of cement based concrete. (Glasby, Day, Kemp, & Aldred, *Earth Friendly Concrete – A sustainable option for tunnels requiring high durability*, 2013)



Figure A.30 – Two tanks made of Portland cement with fly ash and geopolymer concrete (EFC) (Glasby, Day, Kemp, & Aldred, *Earth Friendly Concrete – A sustainable option for tunnels requiring high durability*, 2013)

The objectives of the study were firstly to assess the water resistant properties of EFC and secondly to investigate the autogenous healing behaviour of this geopolymer concrete. Autogenous healing in Portland cement based concrete is primarily due to the deposition of calcium hydroxide. As there is no calcium hydroxide present in EFC, the performance of it in a water retaining application is of considerable interest. Nominal leaking through cracks in the EFC tank did heal relatively rapidly. Ahn and Kishi suggest that geomaterials may be able to autogeneously heal due to a gel swelling mechanism.

Source: (Glasby, Day, Kemp, & Aldred, Earth Friendly Concrete – A sustainable option for tunnels requiring high durability, 2013)

A.4.3 Geopolymer Aircraft Pavements at Brisbane West Wellcamp Airport (BWWA), Australia

The opening also marked a world first - the largest modern geopolymer concrete project containing absolutely no Portland cement. The main reason apply geopolymer concrete was becoming the first greenfield public airport in 48 years in Australia. A picture during execution is shown on Figure A.31.

Some facts in brief:

- First in the world with Wagners EFC – 6,600 tonnes less carbon than using traditional Portland cement concrete
- Runway 2.87km x 45m wide
- Turning node at the Northern end of the runway - 16,000 m² , 435 mm thick.
- Taxiway on the Western side of the runway - 32,000 m² , 435 mm thick



Figure A.31 – Execution of geopolymer concrete at Brisbane West Wellcamp Airport (Wagners and Brisbane West Wellcamp Airport, n.d.)

Source: (Wagners and Brisbane West Wellcamp Airport, n.d.)

A.4.4 Rocky Point Boat Ramp, Bundaberg, Australia

A boat ramp at Rocky Point, Winfield is the first application for Wagners new composite fibre reinforcing bar coupled with Wagners Earth Friendly Concrete (Wagners, n.d.)



Figure A.32 – Left: precast geopolymer concrete. Right: view of boat ramp (Aldred & Day, 2012)

Precast concrete boat plank units made from Grade 40 geopolymer concrete and reinforced with Glass Fibre Reinforced Polymer (GFRP) reinforcing bar were applied. The approach slab on ground to the ramp was made from site cast geopolymer and similarly reinforced with GFRP. The project was successfully completed during November - December 2011 as seen in Figure A.32. The precast ramp units were manufactured at Wagners precast facility in Toowoomba, while the site cast geopolymer for the approach slab was batched in Toowoomba, trucked to site with a 6.5 hour transit time and then activated with the chemical activators on site. A unique feature of this particular geopolymer is that the entire batch constituents can be mixed in a truck bowl and remain completely dormant until the activator chemicals are added.

The mixture has good durability properties. Coupled with V-Rod reinforcing bar which is made from glass fibre reinforced polymer. V-Rod does not corrode under any conditions and is a quarter of the weight of steel making it an ideal concrete reinforcement for highly corrosive marine applications.

Sources: (Aldred & Day, 2012) and (Wagners, n.d.)

A.4.5 Summary of reasons to apply GPC

As shown in the above mentioned project, the most important reasons to apply GPC are from a durability and sustainability point of view. GPC has very favourable characteristics to build a durable and sustainable construction.

A.5. Reference projects for Self-cleaning Concrete

In this chapter are some reference project given where self-cleaning concrete is applied. The best available source for these reference projects in the Italian company Italcementi. From economical reasons, this source will be quite positive about the projects where self-cleaning concrete is applied. Again, the reference projects do at least give an indication of projects where the application of self-cleaning concrete can be interesting. After discussing the reference project, an overview of reasons to apply self-cleaning concrete in the reference projects is shown.

A.5.1 Jean Bleuzen street, Vanves, France

Jean Bleuzen street is a “Canyon Street” in a North-South position with a good exposure to the sun and perpendicular to the main winds, with more than 13,000 cars per day.

The requalification project consisted in 300 m of TX ARIA® concrete overlay over a traditional concrete substrate, with sidewalks and curbs in paving stones made with TX ARIA® as well, for a total of 6,000 m² of depolluting surface. The concrete was fabricated by Italcementi. The execution of the road is shown on Figure A.33.

The immediate result was:

- Improved aesthetic landscape
- Noise reduction, thanks to a suitable concrete formulation and surface finishing
- Together with a pollution decrease of at least 20%



Figure A.33 - Execution of 300 m concrete overlay (Italcementi, 2009)

Source: (Italcementi, 2009)

A.5.2 Dives in Misericordia Church, Rome, Italy

The Dives in Misericordia Church has been consecrated in the Roman neighbourhoods of Tor Tre Teste, and realized by the American architect Richard Meier, winner of an international competition promoted by the Vicariate of Rome. An impression of the church is shown in Figure A.34.



Figure A.34 – Impression of the Dives in Misericordia Church - Rome, Italy (Jimwich, 2005)

In an area characterized by working-class buildings, lacking in focal points and areas dedicated to the community social relations, the church stands out with its high sails (the tallest one is 26m high) and its absolute white surfaces. In order to avoid the use of a steel framework covered with white panels - a not durable solution over time - the self-bearing sails have been subdivided into large, double curvature precast ashlar (blocks), weighing 12 tons each.

The self-cleaning nano concrete is applied to meet the aesthetic requirement of unparalleled and time-enduring white colour of the concrete. Monitoring results shows that the maintenance of primary colour of white concrete elements is confirmed, after more than 7 years of service life.

Source: (Italcementi, 2009)

A.5.3 La Cité de la Musique et des Beaux-Arts, Chambéry, France

La Cité de la Musique et des Beaux-Arts is located in a residential area. It is composed of two buildings which structure are made of precast elements with the function of load bearing exposed façade framework, as shown in Figure A.35. It is the city reference cultural centre in Chambéry.



Figure A.35 – Impression of La Cité de la Musique et des Beaux-Arts - Chambéry, France (Italcementi, 2009)

After approximately 5 years of monitoring, results of the colour in Chambéry are excellent. The values registered for the two buildings remain constant, even in different positions (West/North/East/South) of the façades.

Source: (Italcementi, 2009)

A.5.4 Hotel de Police, Bordeaux, France

Located downtown, the building is exposed to the action of the organic pollutants typical of these urban areas. Just to hinder these attacks to the building aesthetic quality, TX Active® cement is applied to manufacture the façades white, with smoothly finished precast concrete cladding panels. An impression of the building is shown in Figure A.36.

The double-layered panels containing white marble aggregates from Pirenei Mountains have been polished to a glossy finishing to enhance further the typical luminosity of TX products. In total, 750 panels, of which 700 are white in colour, cover a surface area of 5,400 m² of architectural precast concrete.



Figure A.36 – Impression of the Hotel de Police - Bordeaux, France (Italcementi, 2009)

Source: (Italcementi, 2009)

A.5.5 Summary of reasons to apply Self-cleaning concrete

There are not a lot of projects where self-cleaning nano concrete is applied yet. However, in Figure A.37 are the reasons to apply self-cleaning concrete in the above mentioned reference projects. From the figure, it seems clear that aesthetics is the main reason to apply nano titanium oxide in concrete. From the reference projects, cleaning of the environment seems to be an additional advantage only.

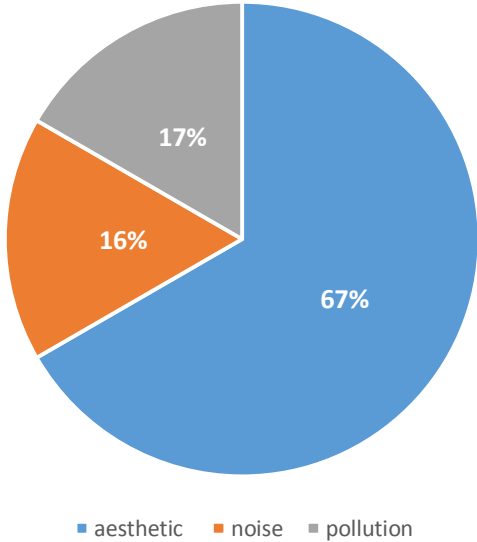


Figure A.37 – Overview of reasons to apply Self-cleaning nano concrete in practice for the above mentioned reference projects

Applications of Advanced Cementitious Materials in Infrastructure

Appendix 2: Field of Applications

Candidate

J. van Oosten
TU Delft and Heijmans

28-9-2015

Committee

Prof.dr.ir. D.A. Hordijk
Ir. A.D. Reitsema
Dr.ir. M. Ottelé
Dr.ir. C. van der Veen
Ir. L.J.M. Houben

TU Delft
TU Delft and Heijmans
TU Delft and Heijmans
TU Delft
TU Delft

Summary

This report is the second part of the research to the applications of Advanced Cementitious Material in infrastructure, to take up potential benefits. The objective of the total research is to make an overview of combinations of new concrete materials and constructions, which can be utilised to take up potential benefits. The total research is made up of three parts:

- Part 1 - Literature study
- Part 2 - Field of applications
- Part 3 - SHCC Joint

In this part of the thesis, the study to the field of applications, are made potential applications of ACMs in structures or parts of structures. Applications are made based on the knowledge from the part 1 of the thesis, the literature study. All applications are then judged as very potential, potential or not or nearly not potential, as shown in Table 1.

Table 1 – Applications of ACMs and structures divided in three categories of potential

Very potential	Potential	Not or nearly potential
HPC bridge deck	UHPC bridge deck	NSSFRC/HPSFRC cross beam
(U)HPC bridge girder	UHPC joint	NSSFRC/HPSFRC culvert
(U)HPC sluice door	(U)HPC cross beam	NSSFRC/HPSFRC aqueduct
UHPC deck of underpass	NSC and UHPC sluice door	UHPC tunnel elements
	UHPC embankment	(U)HPC sewage
	UHPC retaining wall	(U)HPC foundation slab
	UHPC aqueduct	UHPC and NSC sewage
	UHPC and NSC aqueduct	Steel and UHPC sluice door
SHCC bridge deck	SHCC barrier	SHCC aqueduct joint
SHCC for repair (deck,tunnel,...)	SHCC embankment	NSC and SHCC in culverts
SHCC bridge joint	SHCC joint in tunnel	NSC and SHCC in tunnel
	NSC with SHCC bridge girders	NSC and SHCC aqueduct
	Self-healing concrete aqueduct	
	GPC sluice door	GPC foundation slab
		GPC embankment
		GPC culvert
		GPC sewage
		GPC foundation piles
		Steel and GPC sluice door
	Self-sensing foundation piles	Self-cleaning noise barrier

The very potential applications are recommended to research in more detail, to judge if the applications should really be constructed in practice to pick up potential benefits. The SHCC bridge joint seems to be the most interesting application to spend the case study on. Reasons that the SHCC bridge joint is the most interesting applications are:

- Durability of a SHCC joint is expected to be relative high compared to a NSC joint, mainly because of the favourable cracking pattern and tensile strain hardening behaviour
- Relative low amount of SHCC, what reduces the costs
- Better road comfort
- Aesthetics

Guide line

In this part of the research, combinations between ACMs and structures are made based on the knowledge of Appendix 1: Literature study. The conclusions of this part of the research, the most potential applications, is the topic for the case study that is done in the third part of this research.

In chapter 2 Analysis the study to applications starts. This chapter starts with a short analysis problem from daily practice. Further in this chapter are given some researches to the application of ACMs that are done by others and projects where ACMs are already applied. Based on the analysis, some ideas for the application of ACMs are set up. The ideas are a kind of philosophy to make combinations of structures and ACMs.

In the chapter 3 Applications of ACMs in structures, are given potential applications of ACMs in structures. The chapter starts with an overview of applications. In the rest of the chapter, the applications are explained in more detail. In the conclusion at the end of this chapter the applications are judged on their potential. Also the best applications, where the case study is spent on, is given in this conclusion.

Table of Content

Summary	iii
Guide line	iv
Table of Content	v
1 General introduction	7
1.1 Problem definition	7
1.2 Research question	7
1.3 Objective	8
1.4 Methodology	8
2 Analysis	10
2.1 Problems from practice	10
2.2 Researched applications	11
2.3 Reference project	14
2.4 Design ideas	17
3 Applications of ACMs in structures	18
3.1 Overview	18
3.2 Foundations	21
3.3 Viaducts and bridges	21
3.4 Sluice	21
3.5 Embankment	24
3.6 Noise barrier	24
3.7 Tunnel, culverts and sewage	24
3.7.1 Bored circular tunnel	24
3.7.2 Square tunnels	25
3.7.3 Joint in tunnel	26
3.7.4 Retrofitting of tunnels	27
3.7.5 Culverts	27
3.7.6 Sewage	29
3.8 Underpass	29
3.9 Aqueduct	32
3.10 SHCC shotcrete	34
3.11 Self-sensing concrete	35
3.11.1 Increase of safety	35
3.11.2 Learn from constructions	35

3.12	Self-cleaning concrete	36
3.13	Conclusion.....	36
4	Conclusion	39
5	Recommendations	41
6	Bibliography.....	42
Appendix A:	Interview Marc Ottelé – Failure of concrete structures (May 1, 2015)	45

1 General introduction

Concrete is already used for centuries to build all kind of structures. In the Roman Empire cementitious materials are used already to construct. Some of those structures are nowadays still there. The last decades, material development have led to concrete that becomes stronger and stronger. One of the most important reasons is a reduced water binder ratio. This is schematically given in Figure 1. In the graph is shown that in 1950 the compressive strength of concrete was only 20 MPa with a w/c ratio of 0.65. Over the years the compressive strength increased with a decreasing water binder ratio. In the beginning of the 21st century, compressive strength of 350 MPa could already be reached. This much stronger concrete is well known as Ultra High Performance Concrete (UHPC). Nowadays research is still going on to make even stronger and better concrete materials.

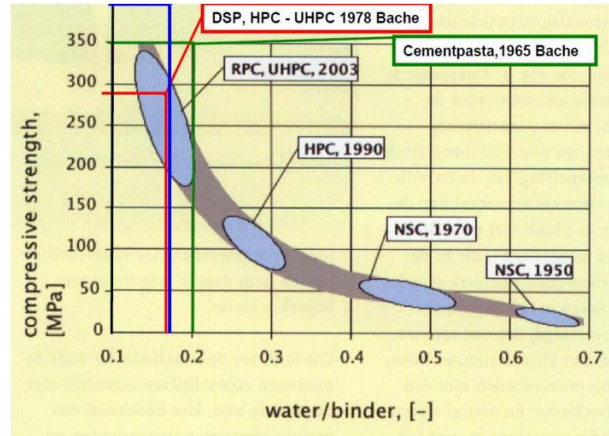


Figure 1 – Compressive strength of different concrete materials as a function of the water/binder ratio. Breugel and Schlangen (2014)

Besides concretes with high compressive strengths, other innovative concretes have been researched for the last years. These kinds of concretes have in comparison to ordinary concrete special properties. An example is the Strain Hardening Cementitious Composite (SHCC). This composite has a strain hardening effect which makes the material more ductile compared with normal strength concrete. (Naaman, 2008)

1.1 Problem definition

Although a lot of research is done to new concrete materials, ordinary normal strength concrete is still the most applied concrete in infrastructure. Not using these new concrete materials is undesirable for both the unexplored possibilities of enhancing infrastructure, as leaving the research input already delivered. New materials have different characteristics compared to normal concrete. This new characteristics can lead to new design opportunities. Designs can, depending on the characteristics of the concrete material, for example be made cheaper, more slender or more durable. Altogether, this could be defined as the problem that should be solved. The problem is defined as:

A lot of research at developing new concrete materials is done, however infrastructure potential benefits are lost since utilisation is lacking

1.2 Research question

From the problem definition the research question of this research could be formulated. The answer to this question should be the solution of the problem defined above. The research question is:

Which combinations of new concrete materials and constructions should be utilised to take up potential benefits?

1.3 Objective

The objective of this thesis is more or less to come up with some infrastructural constructions where new concrete materials can be utilised to increase the benefits of a project. The main aim of this research is provide in:

An overview of combinations of new concrete materials and constructions, which can be utilised to take up potential benefits

In the definition of the objective four keywords are explained in more detail to understand the objective better. The key words are:

- New concrete materials
- Constructions
- Utilise
- Potential benefits

In this thesis will be searched to as many applications as possible for new concrete materials in the infrastructure. The new concrete materials are only interesting if it could take up potential benefits for infrastructure.

'Advantageous for the constructions' is quite a broad concept, because materials can be beneficial in many ways. This is written consciously, because the benefits of the new concrete materials for constructions should still be explored. As soon as the benefits of the concrete materials are known, the benefits per material can be defined.

1.4 Methodology

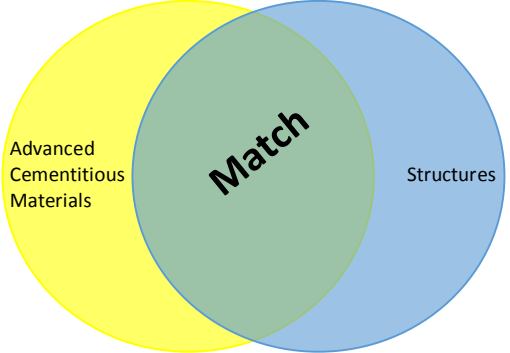
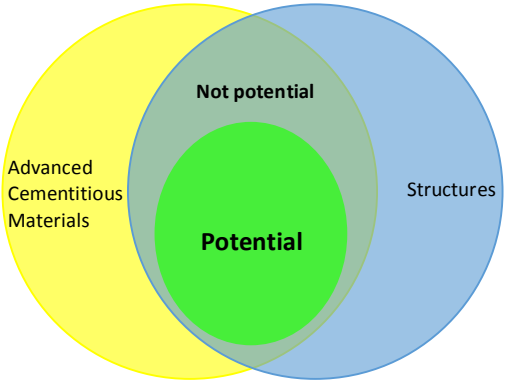
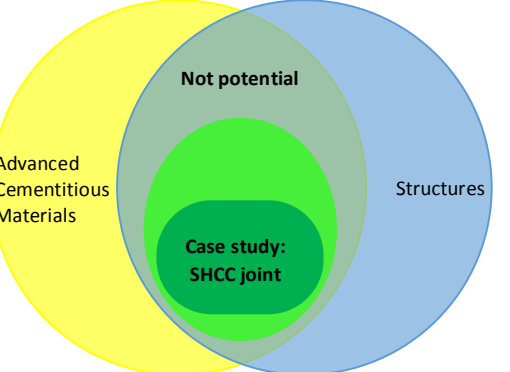
This research is set up as wide as possible. In the beginning of this study many new concrete materials and structures are analysed. Besides, researched applications and reference projects are analysed. After that a list of possible beneficial applications is made. This ends up in a big list of applications. During the research, this list becomes shorter by steps, such that in the end only the best combinations are left. The steps taken to shorten the list are shown in Table 2. Here the steps are explained briefly.

The first time that the list is shortened, is by the outcome of researched applications and reference projects. Some applications that are made in step 4 are probably already researched or even built. The results of these projects can strengthen or contradict some of the possible applications. If research from others is very negative about an application from the list, this application could be removed.

The second time that the list will be made shorter is when the potential of the combinations is judged. The potential applications are discussed with experts in the field of concrete structures. From the discussion, the best potential combination are chosen.

In the last step, one of the best potential combinations is researched in more detail in a case study. In the case study, literature is researched to make a list of points of attention of the SHCC link slab design. The critical issue of the design is researched in even more detail. In the end, some recommendations are given to improve the critical point of the design.

Table 2 – Methodology of research to Advanced Cementitious Materials by step-by-step plan

 <p>Figure 2 - The schematically exhibition of the idea of linking the new concrete materials with infrastructure</p>	<p>Step 1</p> <p>Step 2</p> <p>Step 3</p> <p>Step 4</p>	<p>Literature research</p> <ul style="list-style-type: none"> - Material properties - Infrastructure structures <p>Researched applications</p> <p>Researches about potential applications of new concrete materials in single constructions.</p> <p>Reference projects</p> <p>Already realised projects where new concrete materials are applied</p> <p>Linking the right concrete to the right structure</p> <ul style="list-style-type: none"> - Which concrete has the best properties to apply in certain structures - Which structures do not have benefits by applying new concrete materials? - Table the possible fields of applications
 <p>Figure 3 - The schematically exhibition of potential fields of applications</p>	<p>Step 5</p>	<p>Judging the success of the matches</p> <ul style="list-style-type: none"> - Judging the applications to separate the wheat from the chaff - Separation between potential and not-potential applications - Arrangement of the applications that are potential
 <p>Figure 4 - The schematically exhibition of the case study to SHCC link slab</p>	<p>Step 6</p> <p>Step 7</p>	<p>Case study: SHCC link slab</p> <ul style="list-style-type: none"> - Overview of point of attentions of the SHCC link slab design - Possibilities to improve the link slab design <p>Finish research</p> <ul style="list-style-type: none"> - Final conclusions and recommendations - Finish the definitive rapport and the presentation

2 Analysis

In this chapter is given the analysis to practical problems, researched applications, reference projects and some general design ideas. This analysis is the basic for the combinations of structures and ACMs in chapter 3 Applications of ACMs in structures.

The analysis to problems from practice is done to solve problems by the application of an ACM. For example if the crack width is a problem, an ACM with a small maximum crack width could be interesting. In the paragraphs to the researched applications and the reference projects are the structures mentioned that could directly be implemented in the structures of the scope of this research, as shown in Appendix 1: Literature study. The structures that can't be implemented directly in this research, are used for ideas to apply a certain ACM. In the last paragraph of this chapter, these and some other design ideas are mentioned for structures with ACMs in general.

2.1 Problems from practice

In this paragraph is done a short analysis to problem from practice. This is done with an interview with M. Ottelé and with an observation report of W. Rouwhorst. Problems that were mentioned are the complexity during execution, problems due to cracks in the concrete and problem with the reinforcement steel. These three problems are discussed in more detail below. After that a link with innovative cementitious materials is made.

First the complexity in projects is discussed in more detail. From an interview with Ottelé (2015), that can be found in A.1. Interview Marc Ottelé – Failure of concrete structures (May 1, 2015), and observations of Rouwhorst (2015) could be suggested that the application of complex ACMs results in many additional risks. This should be taken into consideration during the research. ACMs are mainly new materials, so the application of them, probably results in problems that are not foreseen in advance. Further, not any worker does have any experience with the new materials. If an ACM is applied a few times, more risks could be foreseen and workers have some experience by applying the material. The application of a new ACM the first time, is actually a kind of an investment of Heijmans. The first time the material is applied may cost money, but in the future, an ACM could probably bring more benefits than NSC.

Coming to the discussion of the second problem in practice, which are cracks. Because cracks have a strong relation with the reinforcement, both are discussed here together. Most failures of concrete structures are caused by cracks (Ottelé, 2015). Obviously, an ACM with a better crack behaviour could reduce the problems according to cracks. However, the origin of the cracks should be known before the problem can be solved. In principle, the reinforcement control the cracks. The reinforcement could fail if one of the next three faults is made:

1. Fault in the design
2. Fault during execution
3. Wrong material

All these faults can be caused by different reasons. Failure can be caused by failure in the process, for example bad communication between different parties as mentioned by Rouwhorst (2015). This kind of failure reasons is not in the scope of this research. Failure caused by the process will probably also happen if ACMs are applied.

The risk of failure in the design and execution stage is probably lower if the complexity decreases. The complexity could be reduced by reducing the amount of traditional reinforcement. The amount of

traditional reinforcement could for example be reduced if the design is changed, if concrete has a high tensile strength or if an alternative type of reinforcement is applied.

Here, the relation with the observation of Rouwhorst (2015) could be made. From his observations suggest that placing reinforcement cause risks in terms of physical work, failure during execution (steel was not fasten well), failure due to unforeseen loads during execution (for example the weight of the concrete hose) and failure due to unexperienced workers. By reducing the reinforcement or by substituting traditional reinforcement by fibres, some of these risks could be reduced. For example, the complexity decreases by applying less reinforcement, such that less experienced worker can do the job. In other words, the quality of the structure depends less on the experience of workers.

In Table 3 is made a relation between problems and potential solutions by ACMs. Because complexity is a broad and general problem, it is not included in the table. In the first column of the table are shown the other two problems; cracks and reinforcement. In the second column of the table are given the ACMs that have direct relations with the problems. All of the ACMs here contains fibres, such that the amount of traditional reinforcement could be reduced. In the third column of the table is explained shortly the relation between the problem and the ACM. In the last column are shown some reference project where a certain ACM is applied to avoid the problem mentioned in the first column. Not for every ACMs are reference projects found where ACMs are applied to control the cracks or to reduce the complexity of the reinforcement.

Table 3 – General problems of a concrete structure with ACMs that could be a potential solution

Problem	ACMs	Explanation	Reference project
Cracks (Ottélé, 2015)	NSSFRC	Favourable cracking pattern due to alternative reinforcement to replace or reduce the tradition reinforcement.	
	HPSFRC	Favourable cracking pattern due to alternative reinforcement to replace or reduce the tradition reinforcement.	
	UHPC	Favourable cracking pattern due to alternative reinforcement	
	SHCC	Exceptional favourable cracking pattern due to alternative reinforcement	
Reinforcement (Rouwhorst, 2015)	NSSFRC	An alternative way of reinforcement to replace or reduce the tradition reinforcement.	- Park Oceanographic, Valencia, Spain
	HPSFRC	An alternative way of reinforcement to replace or reduce the tradition reinforcement.	
	UHPC	An alternative way of reinforcement to replace or reduce the tradition reinforcement.	
	SHCC	An alternative way of reinforcement to replace the tradition reinforcement.	

2.2 Researched applications

In the last years quite some research to applications of innovative cementitious materials is done. Some of these researched applications could be helpful here to make useful combinations of ACMs

and innovative concrete. In this section is determined which applications could theoretically be implemented one on one in the structures from the scope of this research. From the applications that can not directly be implemented, design ideas can be taken.

First are discussed the applications that could theoretically be copied one on one. The applications that could in theory directly be implemented in the structures of the scope of this research are shown in Table 4, sort by the material. In the first column is called the material and in the second column are the applications shown that are researched for each material. In the last column are the qualitative conclusions from the researched applications.

Table 4 – Researched applications of UHPC and SHCC that could theoretically be implemented in the construction one on one

ACM	Application	Conclusion
UHPC	Retaining wall (López, Serna, & Camacho, n.d.)	<ul style="list-style-type: none"> - Reliable mechanical behaviour - Very ductile behaviour - Reduction of the final costs
	AASHTO Type II Girder (Graybeal B. , 2008)	<ul style="list-style-type: none"> - Larger flexural capacity - UHPC carries tensile load after cracking - The crack spacing in the tension flange of a UHPC I-girder is inversely proportional to the maximum tensile strain observed in said cracked region
SHCC	Bridge decks without joints (Michigan Department of Transportation’s Construction and Technology Division, 2005)	<ul style="list-style-type: none"> - Cost reduction - Reduction of CO₂ emission - Reduction of energy - Longer service life - Comfort during driving the bridge - Reduction bridge closings for routine maintenance
	Reinforced concrete beam strengthened with SHCC (flexural performance) (Kim, et al., 2014)	<ul style="list-style-type: none"> - Crack width of a beam can be controlled by applying the SHCC - The load-bearing capacity of beams can be improved by applying the SHCC and HSRS bars - A model for the nonlinear flexural analysis showed more significant strengthening effects of SHCC and in terms of load bearing capacity compared to behaviour the experiments
	Reinforced concrete beam strengthened with steel reinforced and unreinforced SHCC (Hussein, Kunieda, & Nakamura, 2012)	<ul style="list-style-type: none"> - The combination of the proposed steel reinforcement and UHP-SHCC, used to strengthen beam B-U- 2, was able to increase its load-carrying capacity to 100 kN, which is twice that of the control beam B-C. Moreover, it fulfilled the ductility criterion recommended by CEB-FIB (1990). - The role of the small amount of steel reinforcement is to reduce the stiffness degradation of the UHP-SHCC strengthening layer caused by cracking.

In Table 5 are mentioned application that can not directly be implemented in the constructions of the scope of this research. Again, in the first column are shown the materials and in the second column some applications for each ACM. In the third column are given the conclusions of the researches. With these conclusions, some ideas to apply a certain ACM can be made, as shown in the fourth column of Table 5.

Table 5 - General ideas of researched applications that could not be implemented directly on the constructions of the scope of the research

ACM	Application	Conclusion	Idea
UHPC	Large span shell structure (Maten, 2011)	<ul style="list-style-type: none"> - Material savings - Higher expected lifespan 	<ul style="list-style-type: none"> - Material savings - Higher expected lifespan
	Bolted joints (Camacho, Serna, & López, n.d.)	<ul style="list-style-type: none"> - Some verifying for the test method should be done. - Weakest failure: cleavage and net tension - Bearing failure was ductile 	<ul style="list-style-type: none"> - Ductility of UHPC
SHCC	Retrofitting unreinforced masonry walls with SHCC (Maalej, Lin, Nguyen, & Quek, 2010)	<ul style="list-style-type: none"> - Increase wall impact resistance - Preventing sudden and catastrophic failure - Contribute to damage mitigation in event of blast or explosion 	<ul style="list-style-type: none"> - High impact resistance - High ductility
	Corrosion resistant reinforced beams by preplacing the concrete surround the main flexural reinforcement by SHCC (Maalej, et al., 2012)	<ul style="list-style-type: none"> - Mitigation of aggressive substances, therefore, preventing reinforcement corrosion - In the extreme case when corrosion initiates, accelerated corrosion due to longitudinal cracks would be reduced (if not eliminated), and spalling and delamination problems would be prevented. 	<ul style="list-style-type: none"> - Reduced risk of corrosion of reinforcement - Crack pattern

2.3 Reference project

In practice, some innovative cementitious materials are applied already. Reference projects that are made abroad, could probably be constructed in The Netherlands as well. Besides, failed projects should be avoided to apply in The Netherlands or alternative designs with the same ACM should be made, to avoid the same mistakes. In the end, by analysing reference projects a lot of useful information could be known. The reference projects used here are discussed in more detail in Appendix 1: Literature study.

The reference project that can be copied one on one to the constructions that are in the scope of this research as shown in Table 6. In the fourth column of the table are the applications of the ACMs from the reference projects shown. In the fifth column is shown the reference project where the ACM is applied. All applications are sort by the construction parts where the ACM is applied, as shown in the third column. The construction parts are sort by the ACMs and the constructions as shown in the second and first column of the table.

In Table 7 are shown the reference projects that has no direct relations with the constructions from the scope of this research. However, in these reference projects is always a reason to apply an innovative concrete instead of NSC. From the reasons behind the application of ACMs can be determined a general idea to apply a certain ACM. In the second column of Table 7 are the reference projects shown that could not be applied one on one to the constructions of this research. The reference projects are sort by the ACMs shown in the first column. In the last column of the table are given the general ideas to apply a certain ACM.

Table 6 - Reference projects that could be copied one on one to the constructions in the scope of the research

Construction	ACM	Construction part	Application of ACM	Reference project	Advances	Disadvantages
Viaduct and girder bridge	HPC	Girder fully made of HPC	Girders fully made of HPC	Hodder Avenue Underpass ¹	- Slenderness - Quality	- Probably high costs ²
	UHPC	Girder/beam fully made of UHPC	Pier cap (cross-beam) fully made of UHPC	Hodder Avenue Underpass ¹	- Aesthetic value - Quality	- Probably high costs ²
			Precast T-beam fully made of UHPC	Kampung Ulu Geroh ³	- Reduced weight during execution - Remarkable durability - No shear reinforcement	
			Precast U-girder fully made of UHPC	Kampung Linsum Bridge ³	- Lower maintenance - Eco friendly* - Better aesthetics - Cheaper	
			Precast pi-girders fully made of UHPC	Jakway Park Bridge ⁴	- Optimize UHPC mixture by minimizing the cross-section due to pi-shape in cross-section - Self-consolidating - Low creep - High durability - Fibre post-cracking strength	- Expensive materil - Labour and equipment intensive - High shrinkage
			Iowa bulb-tee beams fully made of UHPC	Wapello County Mars Hill Bridge ⁵	- Longer, thinner and more aesthetically pleasing beams - Highly impermeable - High building speed	
	Column made of UHPC and NSC	Column shell of UHPC filled with 'standard reinforced concrete'	Hodder Avenue Underpass ¹	- High durability - No temporary formwork at side - Quality	- Extra step in the building process due to precast concrete	
	Joint	UHPC Joints for Precast Deck Panel Bridge Superstructures	CN Overhead Bridge at Rainy Lake, Ontario ⁶	- Reduced joint size - Reduced joint complexity - Improved continuity - Building speed - Service life - Maintenance - Durability	-	
	SHCC	Deck	Reparation of deck by HES-ECC	Ellsworth Road Bridge ⁷	- Close-to-homogeneous, self-compacting material. - Easy to pour - Relative economic advantage compared with concrete and alternative field repairs. - Better durability	
			Composite ECC/steel bridge deck	Mihara Bridge ⁸	- High durable structure - 40% weight reduction, due to unique cracking pattern of SHCC - 50% reduction in initial construction cost	
Joint		ECC Link Slab	Grove Street Bridge ⁹	- Longer service life: o Enhancing public mobility by reducing traffic interruption, because repairs are minimised. o Sustainable by the long life time.	- High investment costs	
Other bridges	HPC	Deck	Bridge slab fully made of HPC	Cable-stayed footbridge ¹⁰	- Low maintenance - Reasonable life cycle costs - Favourable tender price	
Retraining wall	SHCC	Retraining wall	Repair of wall	Retraining wall in Japan ¹¹	- Aesthetic (small crack width) - Durability (small crack width)	
Sluice	HPC	Sliding door	Sliding door fully made of HPC	Sluis 0124 ¹²	- Favourable building costs - Better durability	

* UHPC is mentioned as eco-friendly for the project Kampung Linsum Bridge. This could be doubt, since the sustainability of UHPC is relative bad as shown in the literature study. Of course reduction of material due to the high strength of UHPC could increase service life

¹ (Li, Guo, Rajlic, & Murray, n.d.)

² Assumption

³ (Voo, Nematollahi, Said, Gopal, & Yee, 2012)

⁴ (Brain & P.E., 2009), (Aspire, 2010), (Graybeal B., 2009)

⁵ (Endicott, 2007)

⁶ (Perry, Scalzo, & Weiss, 2007)

⁷ (Li, Lepech, & Li, Final Report On Field Demonstration of Durable Link Slabs for Jointless Bridge Decks Based on Strain-Hardening Cementitious Composites, 2005), (Li M., 2009)

⁸ (Li V. C., Engineered Cementitious Composites (ECC) – Material, Structural, and Durability Performance, 2007), (Kim Y. J., 2014)

⁹ (Li V. C., Michigan's Experience with Ductile ECC for Bridge Decks, n.d.), (Michigan Technological University, 2007), (ACE-MRL, n.d.)

¹⁰ (Milan, et al., n.d.)

¹¹ (Kunieda & Rokugo, 2006)

¹² (Europese prijs voor De Boer&De Groot, 2012), (Haitsma, 2011),

Table 7 - General ideas of reference projects that could not be implied directly on the constructions of the scope of the research

ACM	Reference project	General ideas
FRC	Park Oceanographic in Valencia, Spain ¹³	Reduction of the complexity of the reinforcement
UHPC	Jean Bouin Stadium, Paris, France ¹⁴	Aesthetic: thin, lightweight, waterproof
	Shawnessy Light Rail Transit Station, Calgary, Canada ¹⁵	Reduction of weight Aesthetic: curved structures Building speed Durability
SHCC	Glorio Rappongi High Rise, Tokyo, Japan and the Nabeaure Tower, Yokohama, Japan ¹⁶	High vibration damping Energy absorption of SHCC
	Mitaka Dam near Hiroshima ¹⁷	SHCC as shotcrete Upgrade by a layer of SHCC Water-tight (Cracks, spalling and water leakage)
GPC	Global Change Institute, multi-storey building, Australia, Brisbane ¹⁸	Sustainable building
	Geopolymer Aircraft Pavements at Brisbane West Wellcamp Airport (BWWA), Australia ¹⁹	Greenfield (sustainability)
	Rocky Point Boat Ramp, Bundaberg, Australia ²⁰	Completely dormant until activator are added Durability properties
Self-cleaning concrete	Jean Bleuzen street, Vanves, France ²¹	Aesthetics Decrease of pollution
	Dives in Misericordia Church, Rome, Italy ²¹	Aesthetic: white colour over time
	La Cité de la Musique et des Beaux-Arts, Chambéry, France ²¹	Aesthetic: white colour over time
	Hotel de Police, Bordeaux, France ²¹	Aesthetic: white colour

¹³ (NV Bekaert SA, 2008)

¹⁴ (Ductal, n.d.), (Sadev, n.d.)

¹⁵ (Perry & Zakariassen, 2004)

¹⁶ (Li V. C., Bendable Composites: Ductile Concrete for Structures, 2006)

¹⁷ (Kunieda & Rokugo, 2006)

¹⁸ (Glasby, Day, Kemp, & Aldred, 2013) (Geopolymer Institute, 2013)

¹⁹ (Wagners and Brisbane West Wellcamp Airport, n.d.)

²⁰ (Aldred & Day, 2012), (Wagners, n.d.)

²¹ (Italcementi, 2009)

2.4 Design ideas

Just before applications of ACMs in structures are given, in this paragraph some design ideas are given. A lot of the design ideas are from reference projects, which are shown above.

The design ideas are shown in Table 8. The ideas are divided by the three themes of this research; mechanics, durability, sustainability. Most of the ideas are based on costs. The ACMs are relative expensive compared to NSC, so a combination of NSC with an ACM is probably smarter to apply than a structure fully made of an ACM. ACMs for example could be applied at the critical spots only.

Table 8 - Design ideas for ACMs from different themes

Theme	Design idea
Mechanics	<ul style="list-style-type: none"> - Reduction of structure <i>height</i> by strong concrete - Reduction of the <i>self-weight</i> by strong concrete - Increase the <i>building speed</i> by a strong concrete (Ottelé, 2015) - Stiff concrete if <i>deformation</i> is the governing design parameter - Strong concrete at <i>highly loaded</i> parts - High strength fibre reinforced for structures with <i>special shapes</i>, to reduce the reinforcement complexity (aesthetic value)
Durability	<ul style="list-style-type: none"> - <i>Very durable</i> concrete at the outside of the concrete - Concrete with very small <i>cracks</i> at outside of the concrete - Concrete with small <i>cracks</i> if crack width is the governing design parameter - <i>Watertight</i> concrete by applying a dens concrete and/or a concrete with small cracks - Self-cleaning concrete for structures with a high <i>aesthetic value</i> (no degradation of aesthetic value due to the environment)
Sustainability	<ul style="list-style-type: none"> - <i>Minimize the amount of ACMs</i> with a low sustainability - Self-sensing on <i>critical parts</i> of a structure (safety and service life) - Self-sensing on elements that are <i>hard to monitor</i> with current methods (safety and service life)

3 Applications of ACMs in structures

In this chapter are given the applications of ACMs in structures. This chapter starts with an overview of the applications. For a complete overview, the researched applications and reference projects are also included. In the overview are also given the advantages of every applications.

After the overview, the applications that are not discussed in chapter 2.2 Researched applications or chapter 2.3 Reference project, are explained here in more detail. Three types of concrete that could be applied in almost every structure, SHCC (shotcrete) for repair, self-sensing concrete and self-cleaning concrete are mentioned separately. General reasons are given to apply one of these three cementitious materials for certain structures. Some applications that seem to be very promising are clarified some deeper already.

In this chapter is tried to make as many as possible useful combinations of structure and ACMs. However, there are probably more possible applications that are included in this chapter. Moreover, only applications with constructions that are in the scope of this research are mentioned. Probably, there are also interesting combinations of ACMs with structures that are not in the scope of this research. In the end, probably not all but at least a lot of interesting applications of advanced cementitious materials in structures are called in this chapter.

3.1 Overview

In Table 9 is given an overview of the applications of ACMs in structures. The applications are given per construction element, as shown in the second column of the table. In the first column are shown the constructions where the construction elements belongs to. Further, the table is vertically split up in three situations: new constructions fully made of one ACM, new constructions made of a combination of different materials (mainly an ACM and NSC) and existing constructions that could be repaired with an ACM. For the most situations are a few options given per construction element. The options mentioned in a column are discussed in the next column on the right.

Table 9 - Overview of potential applications of ACMs in structures

		New constructions										Existing constructions		
Construction	Construction element	Fully made of one ACM						Combination of different materials				Repair		
		Option 1	Discussion option 1	Option 2	Discussion option 2	Option 3	Discussion option 3	Option 4	Discussion option 4	Option 5	Discussion option 5	Option 6	Discussion option 6	
Foundations	Piles	GPC	- High durability	Self-sensing concrete	- Monitoring of piles to optimize next designs									
	Foundation slab	HPC/UHPC	- Smaller dimensions: o Weight reduction o Material reduction - Durability	GPC	- High durability									
Viaducts and bridges	Bridge girder/beam	HPC ²²	- Slenderness Quality	UHPC ^{22, 23}	- Weight reduction (execution, foundations, ...) - Longer span (reduction of columns, foundations, ...) - Durability - Slenderness - Building speed			NSC with SHCC at flexural tensile part ²³	- Crack width control - Load bearing capacity - Flexural strength			UHPC (replacement of the girder)	- Construction height - Construction weight	
	Bridge slab/deck	HPC ²²	- Low maintenance - Reasonable life cycle costs - Tender price	UHPC	- Weight reduction (execution, foundations, ...) - Durability - Shear strength - Slenderness - Building speed			SHCC and steel ²²	- High durability - 40% weight reduction, due to unique cracking pattern of SHCC - 50% reduction in initial construction cost			SHCC ²²	- Close-to-homogeneous, self-compacting material. - Easy to pour - Economic advantage	
	Joint	UHPC ²²	- Reduced joint size - Reduced joint complexity - Building speed - Service life: o Maintenance o Improved continuity	SHCC ^{22, 23}	- Cost reduction - Comfort during driving - Longer service life: o Reduction bridge closings for routine maintenance o Reduction of CO ₂ -emission									
	Pier cap/crossbeam	NSSFRC/HPSFRC	- Durability due to crack width - Faster execution for cast in situ (no reinforcement) - Higher shear capacity	HPC	- Slenderness - Quality	UHPC ²²	- Aesthetic availabilities - Quality						SHCC	- Close-to-homogeneous, self-compacting material. - Easy to pour - Economic advantage
	Barrier	SHCC	- Large energy absorption before failure - Large deflection											
	Column								UHPC and NSC ²⁴	- High durability - No formwork - Quality				
Sluice	Lock chamber							UHPC and NSC	- Durability, especially for sea locks					
	Door	HPC ²⁴	- Favourable building costs - Better durability	UHPC	- Very durable - Ultra high compressive strength - But, low tensile strength	GPC	- Durable ACM - But, low tensile strength	Steel and UHPC (or GPC)	- Very durable ACM - High compressive strength ACM	Combination of NSC and UHPC	- Very durable ACM - Relative cheap NSC - Sustainable NSC			

²² Reference project

²³ Researched application

²⁴ Reference project

								as UHPC)	- High tensile strength of steel		- But, Low tensile strength		
Embankment	Embankment elements	UHPC	- Mechanical behaviour Very ductile behaviour	SHCC	High impact energy to carry ship load	GPC	Very durable, especially in sea harbours						
Retaining wall	Retaining wall elements	UHPC ²⁵	- Mechanical behaviour - Very ductile behaviour - Reduction of the final costs									SHCC ²⁴ (repair)	- Aesthetic - Durability
Noise barrier	Noise barrier	Self-cleaning concrete	- Aesthetics										
Tunnel (rectangular)	Tunnel							NSC and SHCC	- Water tightness - Durability			SHCC shotcrete	- Durability - Water tightness
	Joints	SHCC	- Cost reduction - Longer service life: o Reduction tunnel closings for routine maintenance o Reduction of CO ₂ -emission										
Tunnel (circular)	Tunnel	UHPC	- Less elements to cast - Less transport to building pit - less transport on the building pit - Less elements to place										
	Joints	SHCC	- Cost reduction - Longer service life: o Reduction tunnel closings for routine maintenance o Reduction of CO ₂ -emission										
Culverts	Culverts	NSSFRC/ HPSFRC/ UHPC	- Crack width - Durability	GPC	- Durability Sustainability			Combina- tion of SHCC and NSC	- Crack width Durability				
	Joints		-										
Sewage	Sewage	HPC/ UHPC	- Durability	GPC	- Durability			UPHC and NSC	- Durability				
Underpass	Deck	UHPC	- Reduction length ramps (underpass principle) - Durability Low deflection (high stiffness)										
	Joints		-										
Aqueduct	Aqueduct	NSSFRC/ HPSFRC	- Durability - Water tightness - Underpass principle for HPSFRC	UHPC	- Underpass principle Durability - Water tightness	Self-healing concrete	- Water tightness - Durability	UHPC and NSC	- Durability - Water tightness - Reduction length ramps (depending on design)	SHCC and NSC	- Water tightness		
	Joints	SHCC	- Cost reduction - Longer service life: o Reduction tunnel closings for routine maintenance o Reduction of CO ₂ -emission										

²⁵ Researched application

3.2 Foundations

As shown in the Appendix 1: Literature study, foundations are exposed to quite tough environmental conditions. Further, the elements of a foundation are mainly loaded in compression. From these two conclusions could be advised to apply a durable concrete with a high compressive strength, like UHPC or HPC. However, these types of concrete are expensive compared to NSC. So the conditions should probably be extreme to make HPC or UHPC interesting to apply.

GPC is an option of a durable ACM with a compressive strength that is comparable to the compressive strength of NSC. Further, GPC is a very sustainable type of concrete. The costs of GPC are unknown at the moment. However, probably the costs of GPC is higher compared to the cost of NSC. So probably only in very bad environmental conditions, GPC could be beneficial to apply.

3.3 Viaducts and bridges

From reference projects can be concluded that viaducts and bridges can be applied in HPC and UHPC. In this paragraph, the application of ACMs for replacing of viaducts and bridges is discussed in detail.

In the next decades, probably a lot of old viaducts and bridges should be replaced by a new construction (Appendix 1: Literature study). In the new situation, it could for example be desirable to left out an intermediate support from a safety point of view. Then the span length is larger, so a stronger concrete should be applied. For certain span lengths, HPC or UHPC could be interesting to apply. This idea is shown in Figure 5. In the upper part of the figure is shown the situation with a NSC bridge and an intermediate support. In the lower part is shown the situation with and (U)HPC bridge and no intermediate support.

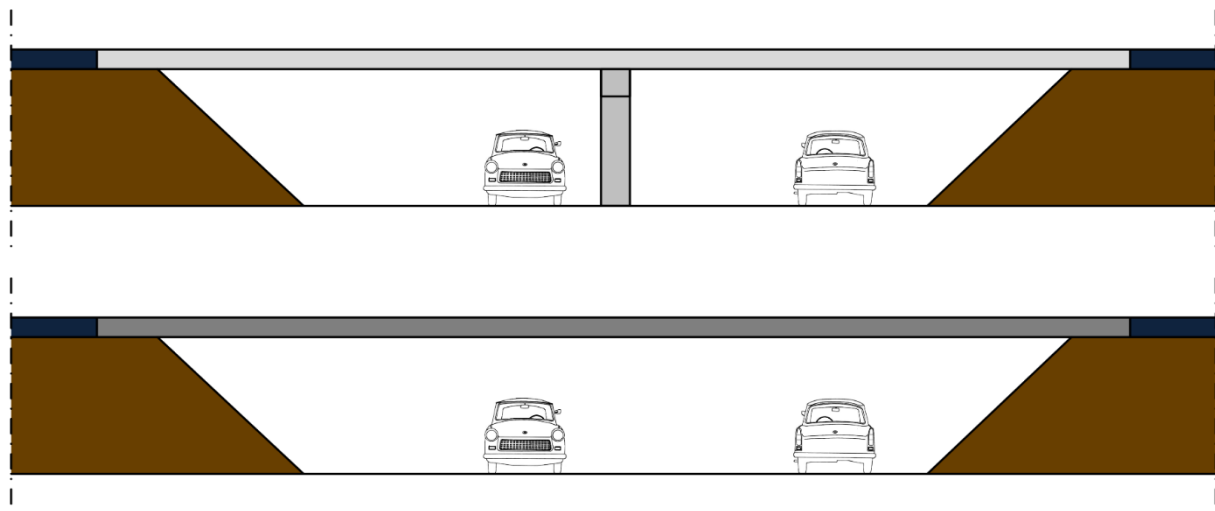


Figure 5 – Situation of a NSC bridge with an intermediate support and a (U)HPC bridge with no intermediate support

3.4 Sluice

According to engineers of Heijmans, durability, especially for sea locks, is a governing design parameter. Since steel corrodes faster in salt water, steel doors are not durable to apply.

However, a lot of sluices do have steel doors, because large peak tensions stresses are working in the doors. Concrete should be very strong, even in tension. It is obvious, concrete does not have a large tensile strength. Therefore, other designs may be made to avoid large tensile stresses in the door or a composite of a durable concrete combined with a material with a large tensile strength should be applied.

From a durable and mechanical point of view, the options to apply ACMs in a sluice doors are shown in Table 10. The first three options are door designs fully made of a durable ACM. All the combinations have the disadvantage of a low tensile strength. The design of HPC and UHPC has also the advantage of the high compressive strength.

Table 10 - Overview that could be applied ACMs in sluice doors with advantages and disadvantages

Door design	Advantages	Disadvantages
UHPC	Very durable Very high compressive strength	Low tensile strength
HPC	Durable High compressive strength	Low tensile strength
GPC	Durable	Low tensile strength 'normal' compression strength
Combination of steel and UHPC	Very durable ACM High compressive strength ACM High tensile strength of steel	Interface between steel and UHPC
Combination of NSC and UHPC	Very durable ACM Relative cheap NSC Sustainable NSC	Low tensile strength 'normal' compression strength Interface between steel and UHPC
Combination of steel and GPC	Durable ACM High tensile strength of steel	Low tensile strength of ACM 'normal' compression strength

In Table 10 are also given three combinations of an ACM with another ACM or steel. The combination of NSC and UHPC, as shown in Figure 6, is a NSC door with a layer of UHPC around it to increase the durability of the door. In the same philosophy, a steel door could be protected by a layer of UHPC or GPC to increase the durability. Now the tensile peak stresses can be carried by the steel and the ACM carries for the durability of the door.

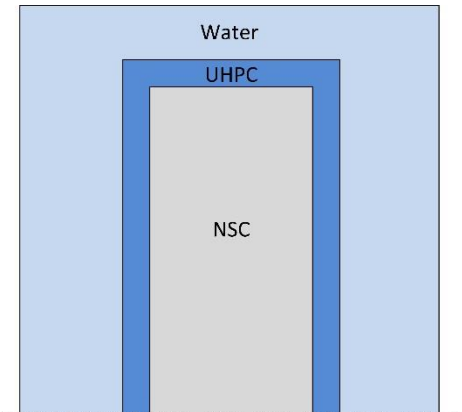


Figure 6 – Cross-section of a lock door made as a combination of NSC and UHPC

The lock itself could from a durability point of view also be made of HPC, UHPC or GPC. Because the strength of NSC is not really a problem, a layer of HPC or UHPC is probably enough to meet the durability requirements. The combination of NSC and UHPC in the lock is shown schematically on Figure 7.

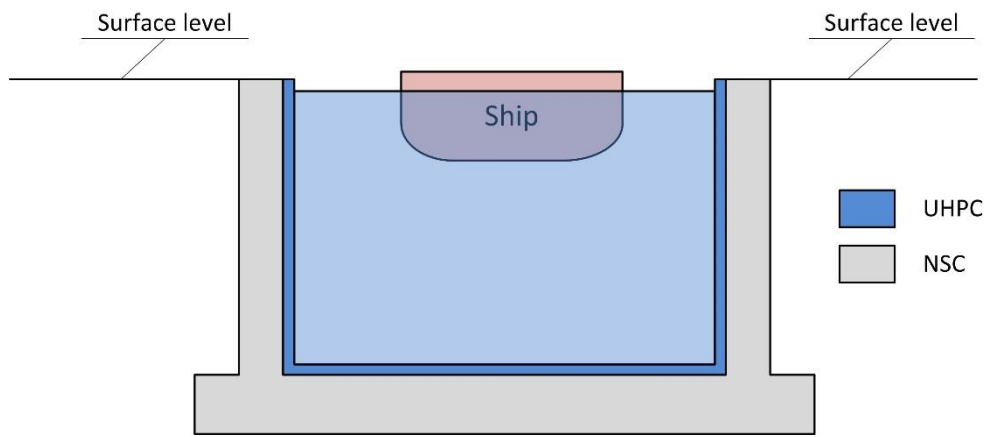


Figure 7 – Sluice made of a combination of NSC and UHPC

3.5 Embankment

Embankment structures are from a mechanical point of view quite similar to retaining walls. The only difference is that embankments are exposed to ground at one side and water on the other side, where retaining walls are also exposed to ground at one side and but air on the other side. Embankments could be exposed to fresh or salt water. In the case an embankment is exposed to salt water, the durability becomes an important issue. Durability types of concrete like UHPC and GPC could be interesting to apply then.

Taking into account a ship that crash the embankment, SHCC could be interesting to apply. Under tension, SHCC can deform far more than NSC before it fails. Maybe, protective structures and measurements against the impact of a crashing ship are not needed any more, if the embankment is made of SHCC.

3.6 Noise barrier

The noise barrier is a quite simple construction that should just absorb or reflect noise. In fact, it is not that interesting to apply advanced materials from a mechanical or durable point of view. However, from an aesthetic point of view, self-cleaning concrete could be interesting to apply in noise barriers. This is discussed in more detail in paragraph 3.12 Self-cleaning concrete.

3.7 Tunnel, culverts and sewage

In this chapter are given some designs of tunnels, culverts and sewage made with ACMs. These structures are discussed in the same chapter, because all are located under the surface. That means that the exposure classes and types of loads on these three structures have a lot of similarities. Potential designs with ACMs are probably also similar then.

In this chapter is first shown the idea of a bored circular tunnel made of UPHC. This application is especially interesting from an execution point of view. After that a square tunnel made of NSC and SHCC is discussed from reasons of durability and water tightness. At last, tunnel joints made of SHCC and retrofitting by SHCC is discussed. In fact, these applications for tunnels could also be applied in culverts and sewages. After the tunnel designs, some designs especially for culvert and sewage structures are given.

3.7.1 Bored circular tunnel

Before the applications of an ACM in a bored circular tunnel is explained, the execution steps from the fabrication until placing the concrete elements are briefly discussed. For a bored circular tunnel made of precast segment, the next steps from fabrication until placing the elements can be discerned.

1. Casting the elements in the fabric
2. Transport between the fabric and the building pit
3. Transport on the building pit to the tunnel
4. Placing the elements in the tunnel

These four steps are used to explain the advantages of a circular tunnel made of UHPC. By applying UHPC, the tunnel elements can be made more slender compared to NSC. There are three options for the element design now:

1. UHPC elements can be made lighter than NSC elements if the same dimensions are maintained, because the UHPC elements will be thinner
2. UHPC elements can be made longer than NSC elements if the same weight is maintained, because the UHPC elements will be thinner.

3. Optimal combination of the two above mentioned options.

A general advantage in all three options is that the outside diameter of the tunnel decreases, so less concrete is needed and less ground must be excavated. The advantage of the first option is that lighter material is needed to transport and place the lighter elements.

The second option, longer elements with the same weight, is schematically shown in Figure 8. The advantages of a tunnel made of UHPC according to option 2, longer and thinner elements with the same weight as NSC element, are:

- Less elements to cast in the fabric.
- Less elements to transport, what not only increases the transport, but also reduce the CO₂-emission.
- Less elements should be handled during transport, so the transport speed can increase
- Less elements are needed to make a ring of the tunnel, what also increase the building speed of a tunnel ring.

As a conclusion, by applying UHPC element instead of NSC elements, almost all steps will be done faster, so the tunnel could be realised in a shorter time.

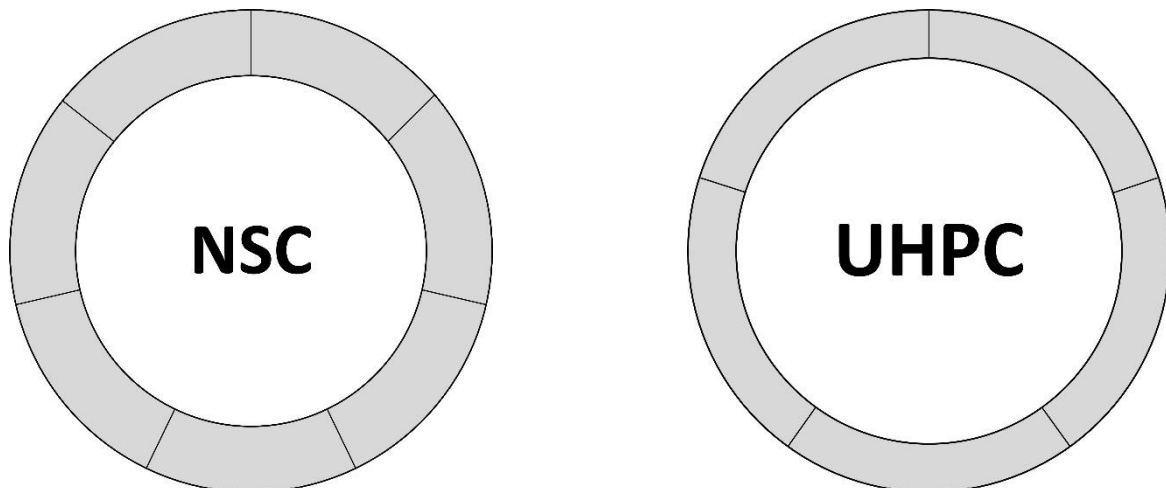


Figure 8 – Left: Tunnel made of NSC, right: Tunnel made of UHPC, where the elements are thinner and the number of elements is lower

3.7.2 Square tunnels

The application of HPC or UHPC in square tunnel segments has, else than more slender tunnels, not that much advantages. For a square tunnel, this advantage is probably smaller than the disadvantages HPC and UHPC brings in terms of costs and sustainability.

Analysing the deflection of a square tunnel, as shown in Figure 9, the application of SHCC at the tension zone could help to reduce the water permeability of a tunnel. SHCC can be effective at the tensile zone, because concrete under compression a low permeability already. The idea to apply SHCC is shown in Figure 10. SHCC is only applied at the tension zone of the concrete. SHCC at the outside of the walls will reduce the amount of water that comes in the tunnel from outside. The SHCC at the bottom and at the deck does not prevent water coming in the tunnel. Because concrete at the outside is in compression here, the concrete is already quite impermeable. However, here the SHCC does prevent

chlorides from de-icing salts ingress in the normal strength concrete. So here SHCC could protect the reinforcement steel.

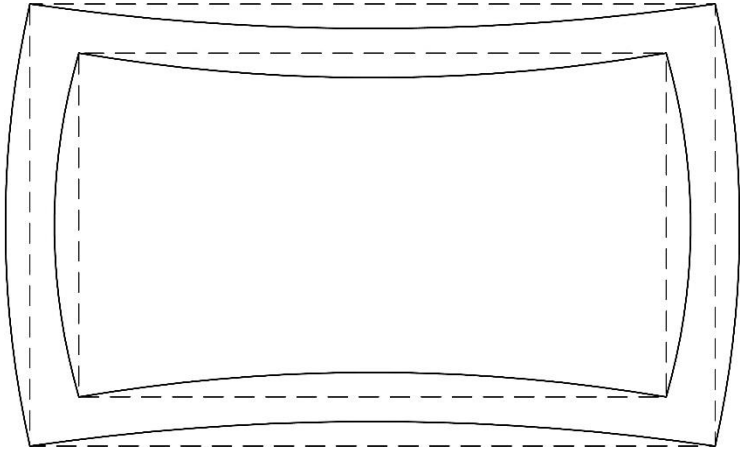


Figure 9 - Deflection of a square tunnel

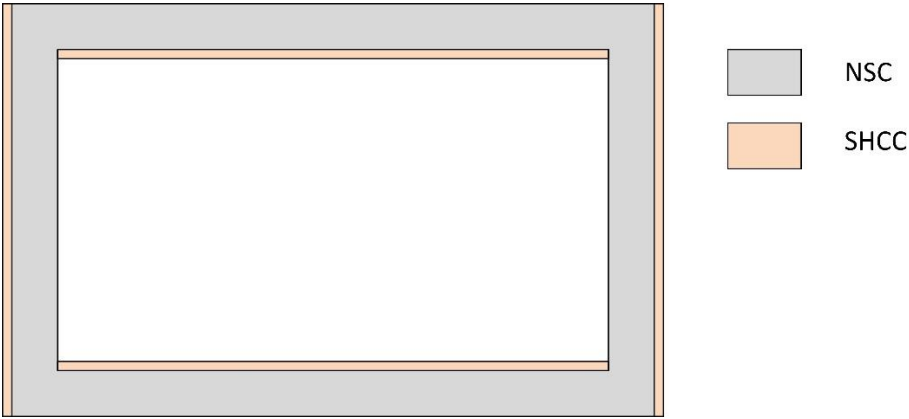


Figure 10 – Application of SHCC in a NSC tunnel to reduce the water permeability

3.7.3 Joint in tunnel

In the reference projects is shown that a bridge joint made of SHCC has potential benefits in term of durability of the joint. This benefits may also be interesting in concrete tunnels. The difference between both, the bridge and the tunnel, is the exposure class and deformation driven by temperature differences, since the tunnel is situated under the surface. The idea of the SHCC joint is shown in the cross-section of Figure 11.

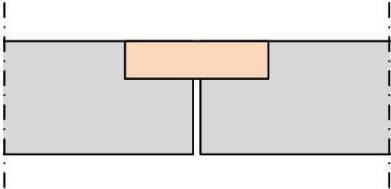


Figure 11 – Cross-section of the SHCC joint in a tunnel element

The biggest challenge of SHCC joints is probably the execution of the joint. It is assumed that the joint is casted in situ inside the tunnel, as shown in Figure 12. It is probably a big challenge to cast the SHCC joint at the vertical walls and the deck (upper part) of the tunnel.

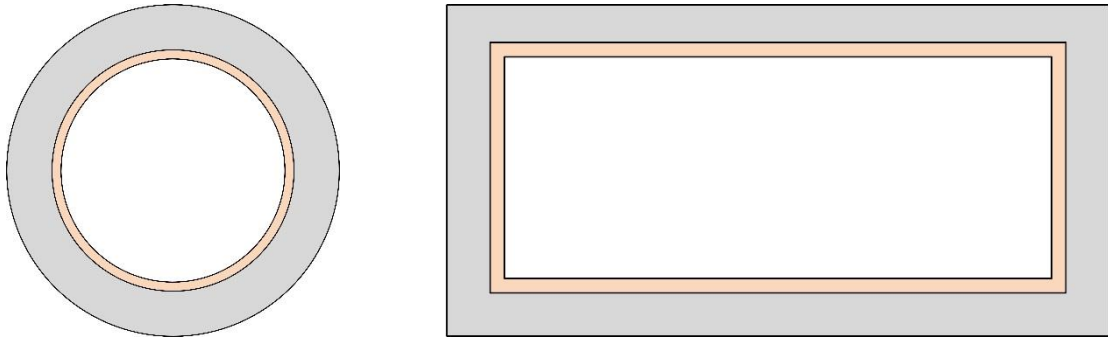


Figure 12 – Cross-section of the tunnel at the joint for circular (left) and rectangular (right) tunnels

To illustrate the challenge during execution, in Figure 13 are shown two tunnel elements and the formwork at the deck of the tunnel, where the joint should be casted. As shown in Figure 13, the fresh concrete should be supported under the concrete against gravity. However, since above the joint are situated the concrete elements, there is almost no space to cast the SHCC joint. Smart tricks should probably be taken to cast the joints. For example, SHCC shotcrete could be applied or a smart way to get the concrete in place due to some adjustments in the design.

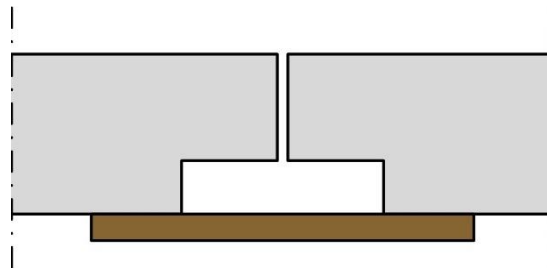


Figure 13 – Formwork under the deck between two tunnel elements to support the fresh SHCC for the joint

3.7.4 Retrofitting of tunnels

Retrofitting of tunnels could be done by SHCC shotcrete. The application of SHCC for retrofitting is not only applicable in tunnels, but also in constructions as underpasses and retaining walls. Therefore, retrofitting with SHCC shotcrete is explained in chapter 3.10 SHCC shotcrete in general.

An important issue for retrofitting of tunnels, is that retrofitting should be done from the inside. To put SHCC at the outside of the tunnel, ground should be removed first, what makes the job very expensive. Assuming tunnels are only retrofitted from inside, the possibilities and consequences for retrofitting by SHCC are:

- The tunnel could be strengthened by SHCC shotcrete, by increasing the structural thickness from inside.
- The durability of the tunnel could be increased against attack from inside the tunnel, for example attack by de-icing salts.
- The durability of the tunnel could not be increased against attacks from the outside of the tunnel, because the SHCC is assumed to be placed at the inside only.

3.7.5 Culverts

From a structural point of view, a culvert is quite similar a tunnel. However, the requirements, like water tightness, in a culvert of course differs from a tunnel. In a culvert, the water tightness is not a

big issue, since the water level in the culverts is mainly equal to the ground water level of the surrounding area. Therefore, concrete with a very low permeability is not that interesting.

Further, a culvert is not really known as a construction that should be very slender. Culverts are mainly positioned around the level of open water. Roads or other structures are mainly positioned on a higher level than the water level. So it could be estimated that the height of a culvert is in general not really an issue, so slender structures made of HPC or UHPC are not that interesting to apply.

However, four options to apply ACMs in culverts are worked out here. An overview of application of ACMs for culverts are given in Table 11.

Table 11 – Overview of applications of ACMs in culverts with advantages and disadvantages

Design	Advantages	Disadvantages
NSSFRC	- Durability due to crack width control by fibres	
HPSFRC	- Durability of HPC - Durability due to crack width control by fibres	
Fully UHPC	- Water tightness - Durability due to crack width control by fibres - Durability UHPC against salt water - Reduction or no shear reinforcement due to fibres	- Building costs - Sustainability
GPC	- Durability - Sustainability	- Building costs
Combination of SHCC and NSC	- Water tightness by crack width control	

From a durability point of view, a durable cementitious material could be an option for culverts that are exposed to salt water. Especially at the splash zones in the culverts, the durability can be an issue. In this situation, durable materials like UHPC, HPC and GPC could be smart to apply. However, from an economical and sustainable point of view, UHPC and HPC are not interesting to apply. More research should be done to conclude if the extra costs to make the culvert of HPC or UHPC and due to the low sustainability are lower than the benefits from the durability. GPC is, in contradiction to HPC and UHPC, more sustainable than NSC. The costs of GPC are not known yet, but probably GPC is quite expensive compared to NSC because it is a new type of concrete. The sustainable and durable benefits of GPC should be larger than the costs to make a culvert of GPC. More research should be done.

Similar as for tunnels, under the deck a layer of SHCC could be interesting to apply from a durability point of view. This is shown in Figure 14 schematically. In grey is the NSC construction. Because the culvert is most intensively loaded on its deck, cracks can be generated in the under part of the deck. Here SHCC could be interesting to protect the reinforcement steel. The same kind of effect could be achieved by applying NSSFRC or HPSFRC. The crack width of these ACMs is probably some larger, but the costs are, at least for NSSFRC lower compared to SHCC.

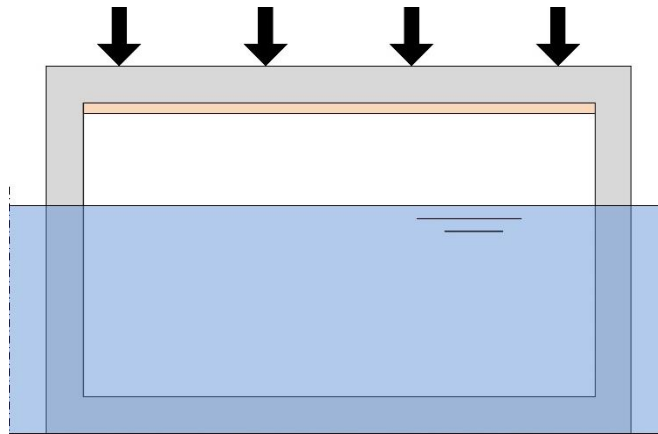


Figure 14 – Application of SHCC in a culvert to protect the deck against the environment

Concluding, in most cases NSC is probably the best cementitious material to construct culverts. For culverts exposed to extreme conditions, GPC is probably the most interesting material as an alternative for NSC. UHPC and HPC both have good durability characteristics, but the durable benefits are probably lower than the increase of the construction costs and the extra cost from sustainability.

3.7.6 Sewage

Sewages are exposed to very dirty water, exposure classes XC4 and XA3. So from a durability point of view, a very durable concrete material, like HPC, UHPC and GPC could be interesting to apply. Especially for UHPC, the sewage could be made as a combination of NSC with an ACM at the inside of the sewage to protect the NSC and to reduce the costs.

3.8 Underpass

In Figure 15 is a length cross-section shown of an underpass. An underpass could for example be situated under a railway or a road. In Figure 15 is schematically shown how the reduction of the deck thickness could result in a reduction of the length of the ramps. The height of the deck could be decreased by the application of a strong and stiff concrete like UHPC. In other words, the application of UHPC for the deck of the underpass, the deck thickness could be reduced. Due to the reduction of the deck thickness, the length of the ramps could be reduced as well. Let call this the 'underpass principle'.

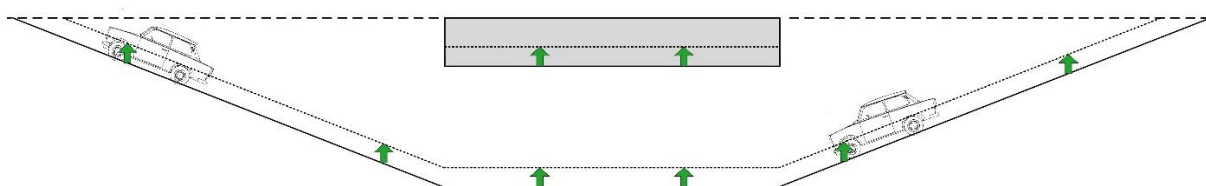


Figure 15 - The UHPC underpass principle

The reduction of the length of the ramps is equal to the reduction of the deck thickness, multiplied by the slope of the ramps. The slope of the ramps depends on the type of traffic, as shown in Table 12.

Table 12 – The reduction of the length of the ramps for different types of traffic

Type of traffic	Speed [km/h]	Slope [%]	Source	Shortening ramp per cm deck thickness reduction
Slow traffic (pedestrian and cyclist)	-	≤ 4	(Nederlands Normalisatie-instituut, 2001)	≥ 25 cm

Fast traffic	50	7	(Rijkswaterstaat Bouwdienst, 2005)	14 cm
	70	6	(Rijkswaterstaat Bouwdienst, 2005)	17 cm
	90 (highway)	4	(Rijkswaterstaat Bouwdienst, 2005)	25 cm
	90 (other than highway)	5	(Rijkswaterstaat Bouwdienst, 2005)	20 cm
	120	3	(Rijkswaterstaat Bouwdienst, 2005)	33 cm

Calculation example

The cost reduction can be illustrated by a small calculation. For the calculation, a NSC deck with a thickness of 1 meters and a width and length of 10 meters, as shown in Figure 16. As shown in the figure, it is assumed that a deck with the same length and width made of UHPC, should be 80 cm only. So compared with NSC, the thickness of the UHPC deck is reduced by 20 cm.

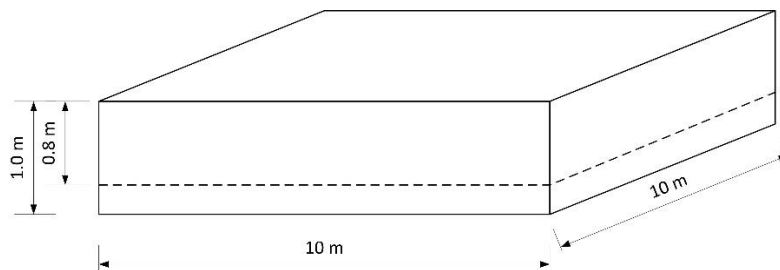


Figure 16 – Dimensions of the deck of the underpass made of NSC or UHPC

The dimensions of the deck are also shown in Table 13. In this table are also the dimensions of the ramps given, the amount of reinforcement steel and the costs of the materials.

Table 13 - Assumptions done for the dimensions and costs of an underpass

	Parameter			Unit
Deck	Length deck	l_{deck}	10	[m]
	Width deck	w_{deck}	10	[m]
	Thickness deck NSC	$t_{deck NSC}$	1.0	[m]
	Thickness deck UHPC	$t_{deck UHPC}$	0.8	[m]
	Volume deck NSC	$V_{deck NSC}$	100	[m ³]
	Volume deck UHPC	$V_{deck UHPC}$	80	[m ³]
Ramps	Wall thickness	t_{wall}	0.35	[m]
	Wall height	h_{wall}	3	[m]
	Bottom thickness	t_{bottom}	0.6	[m]
	Width of bottom	w_{bottom}	10	[m]
	Cross-sectional area walls and bottom	A_{ramp}	8.1	[m ²]
	Reinforcement steel	m_{steel}	150	[kg/m ³]
Costs	NSC	$€_{NSC}$	100	[euro/m ³]
	Steel reinforcement	$€_{steel}$	1	[euro/kg]
	UHPC	$€_{UHPC}$	500	[euro/m ³]

With the data from Table 13, the costs and the benefits, in terms of material costs only, of the applications of UHPC in the deck can be calculated. The calculations are shown here. The results for different slopes are shown in Figure 17. This figure shows that the UHPC deck for underpasses is interesting for roads that are designed for a maximum speed of 90 km/h or 120 km/h and for slow traffic roads.

However, the calculations that are done to make the graphs of Figure 17 are shown here. First the reduction of the length of the ramps should be calculated. The reduction of the length of the ramps at both sides of the underpass is calculated as:

$$\Delta l_{ramps} = 2 \cdot (t_{NSC\ deck} - t_{UHPC\ deck}) \cdot slope$$

The reduction of the amount of concrete and the amount of reinforcement steel due to the reduction of the length of the ramps is equal to:

$$\Delta concrete_{ramps} = \Delta l_{ramps} \cdot A_{ramp}$$

$$\Delta reinforcement\ steel_{ramps} = \Delta l_{ramps} \cdot A_{ramp} \cdot m_{steel}$$

The reduction of the costs of the ramps due to the reduction of building materials only is equal to:

$$\Delta \epsilon_{building\ materials} = \Delta concrete_{ramps} \cdot \epsilon_{NSC} + \Delta reinforcement\ steel_{ramps} \cdot \epsilon_{steel}$$

The difference between the extra costs of the deck made of UHPC and the costs of the ramps, is the total benefit of building materials only. The extra costs of the deck made of UHPC is calculated by the difference between the cost of the UHPC and NSC deck, as shown in the formulas below.

$$\epsilon_{deck\ NSC} = V_{deck\ NSC} (\epsilon_{NSC} + \epsilon_{steel} \cdot m_{steel}) = \text{€ } 25,000$$

$$\epsilon_{deck\ UHPC} = V_{deck\ UHPC} \cdot \epsilon_{UHPC} = \text{€ } 40,000$$

$$\Delta \epsilon_{deck} = \epsilon_{deck\ UHPC} - \epsilon_{deck\ NSC} = \text{€ } 15,000$$

Now the difference between the reduced costs of the building materials and the increased costs of the deck are the total benefits. These benefits are shown in Figure 17 for different slopes of the ramps. The blue lines are the benefits due to the reduction of materials in the ramps. The benefits are split up in a concrete and a steel part, as shown with the blue dotted lines. The black line represent the net benefits. For the net benefits, the extra costs of the deck are subtracted from the cost reduction of the ramps. From Figure 17 could be concluded that an UHPC deck is interesting to apply if steepness of the slope lower than 5.5%. In practice, this means that the UHPC deck of an underpasses is interesting for roads that are designed for a maximum speed of 90 km/h or 120 km/h and for roads that are made for slow traffic.

Note that in the calculations are only the building materials included. For a total analysis, also cost reductions of for example excavation, formwork and labour should be included. Further, the high impact on the environment to make one cubic UHPC should also be included in the total analysis.

Benefits of applying an UHPC deck as a function of the slope of the ramps

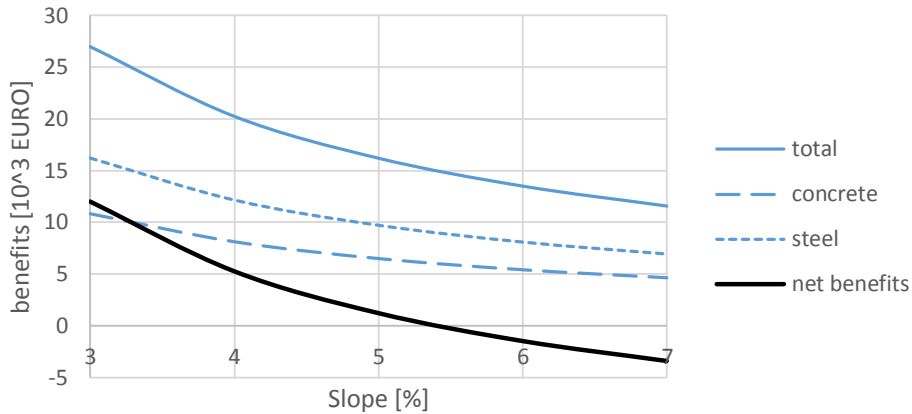


Figure 17 – Benefits of an underpass made with an UHPC deck relative to a NSC deck for different slopes

The costs of the UHPC is probably the most uncertain parameter in the above shown calculations. Therefore, the whole calculation is also done for an UHPC prices of 400, 600 and 700 euro/m³. The results of the different UHPC costs are shown in Figure 18. As shown in the figure, if the price of UHPC is around 650 euro/m³, it is not beneficial to apply an UHPC deck for any ramp steepness.

Benefits by applying an UHPC deck as a function of the slope of the ramps for different UHPC costs

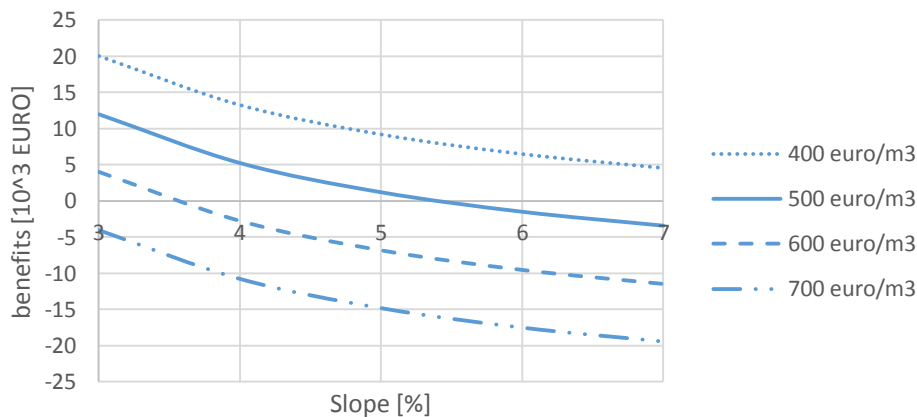


Figure 18 - Benefits of an underpass made with an UHPC deck relative to a NSC deck as a function of the ramp slopes for different unit prices of UHPC

3.9 Aqueduct

For an aqueduct, same as for an underpass the ‘underpass principle’ could be applied. This principle is explained in chapter 3.8 Underpass. At least the full deck should be made of UHPC have an effective working underpass principle. To reduce the costs, the walls could be made of a less expensive type of concrete.

From a durability point of view, an aqueduct of UHPC is favourable, especially if salt water is in the water road. Durable types of concrete to apply for aqueducts are; UHPC, HPC, Self-healing concrete, FRC and SHCC. These concrete types in general have a more favourable crack width compared to NSC,

what increases the durability of these materials. Some advantages per ACM are summed in Table 14. There are probably some more advantages or disadvantages. Probably the most important issues are mentioned. General disadvantages like higher material costs or lower sustainability are not explicit mentioned in the table.

Table 14 - Overview of applications of ACMs in aqueducts with advantages and disadvantages

Design	Advantages
NSSFRC	<ul style="list-style-type: none"> - Water tightness due to crack width control by fibres - Durability due to crack width control by fibres - Reduction or no shear reinforcement due to fibres
HPSFRC	<ul style="list-style-type: none"> - Underpass principle (chapter 3.8 Underpass) - Water tightness due to crack width control by fibres - Durability due to crack width control by fibres - Reduction or no shear reinforcement due to fibres
Fully UHPC	<ul style="list-style-type: none"> - Underpass principle (chapter 3.8 Underpass) - Water tightness - Durability due to crack width control by fibres - Durability of aqueduct against salt water or roads under (de-icing salts from roads) - Reduction or no shear reinforcement due to fibres
SHCC	<ul style="list-style-type: none"> - Water tightness by crack width control - Reduction or no shear reinforcement due to fibres
Self-healing concrete	<ul style="list-style-type: none"> - Water tightness - Durability
Combination of NSC walls and UHPC deck	<ul style="list-style-type: none"> - Underpass principle (chapter 3.8 Underpass) - Cost reduction due to NSC - Sustainability of NSC
Combination of NSC and UHPC walls and UHPC deck	<ul style="list-style-type: none"> - Underpass principle (chapter 3.8 Underpass) - Water tightness - Durability - Cost reduction due to NSC - Sustainability of NSC
Combination of SHCC and NSC	<ul style="list-style-type: none"> - Water tightness by crack width control

To reduce the costs, the expensive type of concrete could be applied as efficient as possible. In practice, this means that aqueduct could be designed as a combination of different types of concrete. The combinations of concretes are shown in the lower part of Table 14. The ideas of the combinations are schematically shown in cross-sections of Figure 19. On the left cross-section of Figure 19 is shown a full UHPC deck and NSC walls with a layer of UHPC at the inside of the walls. Here the underpass principle is valid. Further, the UHPC layer at the walls helps to increase the durability of the structure. At the right figure of Figure 19 is shown the variant where only a layer of UHPC is constructed at the inside of a NSC aqueduct. Here UHPC is only applied from a durability point of view.

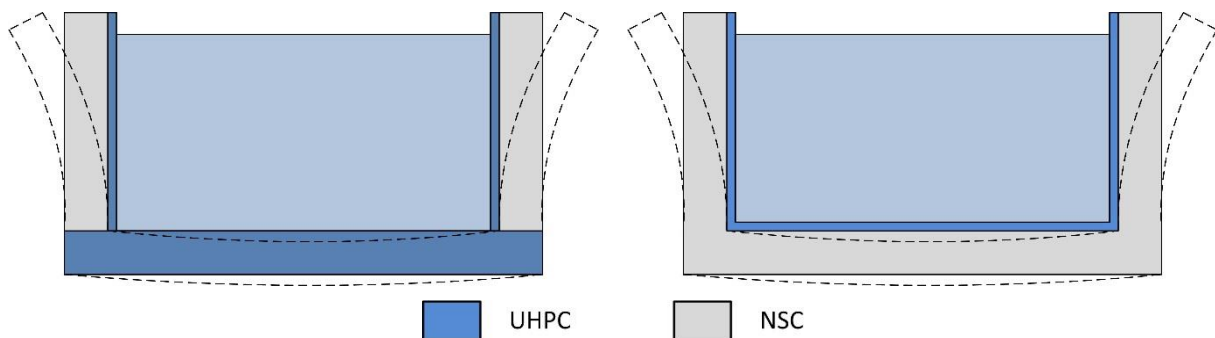


Figure 19 – Left: aqueduct made of an UHPC deck and NSC walls with a layer of UHPC. Right: NSC aqueduct with a layer of UHPC.

3.10 SHCC shotcrete

SHCC shotcrete could be a useful material to retrofit or repair a construction. As shown in chapter 2.3 Reference project, SHCC is already applied in practice to retrofit a dam.

Analysing the result from the literature study, it could be discussed shortly how effective SHCC will probably be to increase the strength. The stiffness of SHCC is significant lower than other types of concrete. SHCC has for example a stiffness of 18.5 GPa, where NSC has a stiffness of 33 GPa. So relatively, probably the most loads will still be carried by NSC.

Shotcrete is probably perfectly effective to increase the durability of concrete, because of the unique cracking pattern of it. However, by applying SHCC for durability reasons, the durability in fact only increase at the side the SHCC is applied. This sound a bit strange, but is explained in more detail with Figure 20. In the figure are shown two pictures of a wall made of NSC, which are retrofitted by SHCC shotcrete. On the both walls a bending moment is applied. At the left figure, SHCC can't prevent or at least can not cover cracks in NSC, so water can still penetrate in the cracked concrete. In the right figure, SHCC is place at the tensile side of the wall. Here, the SHCC does prevent water penetrating the concrete through cracks.

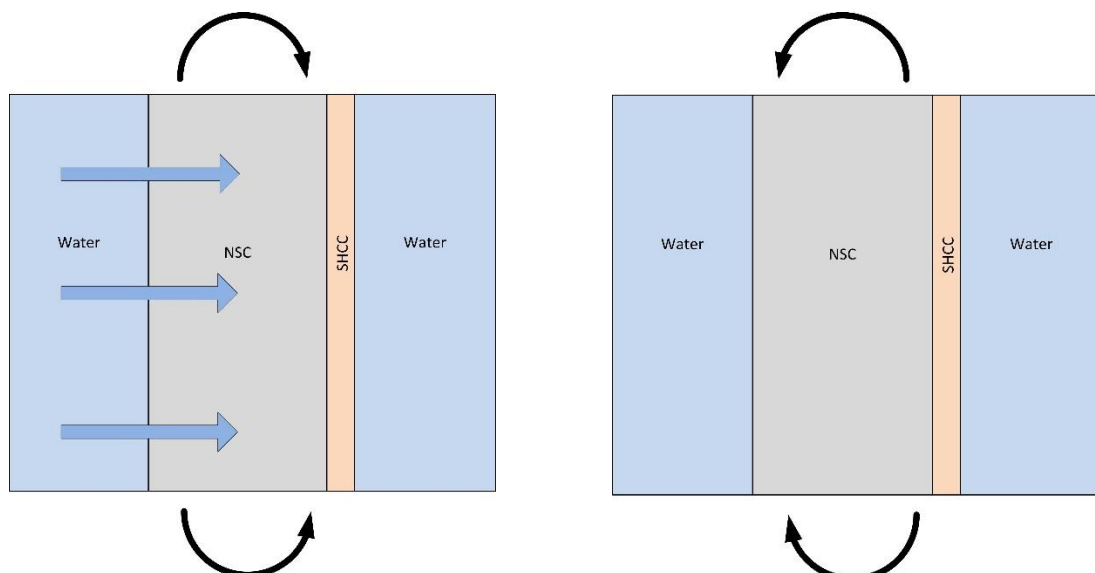


Figure 20 – Ineffective way of applying SHCC (left) and effective way of applying SHCC (right)

Good bonding between NSC and SHCC is an condition that should be met for SHCC shotcrete to be a good solution. In the Mitaka Dam (chapter 2.2 Researched applications) anchors were driven to ensure a good bonding between the SHCC and NSC. Something similar should probably be done to ensure the

bonding capacity between NSC and SHCC in other projects. More research should be done to the bonding capacity for specific applications of SHCC shotcrete.

3.11 Self-sensing concrete

The application of self-sensing concrete does not have direct influence on the mechanical, durable or sustainable characteristics of a concrete structure. In fact, self-sensing concrete is just a smart alternative of monitoring of the structure. Two main reasons to apply self-sensing concrete could be defined:

1. Increase safety
2. Learn from constructions

Both reasons to apply self-sensing concrete are explained in more detail in the next two paragraphs.

3.11.1 Increase of safety

The first reason to apply self-sensing concrete is to increase the safety of the structure. Reinforced concrete warns before it fails. The warning system is in fact the large deformation of the structure, before it fails. However, if concrete warns, it mostly can't serve properly any more. For safety reasons, the warning may be too late. Therefore, at critical parts of a structure it could be interesting to apply self-sensing concrete, such that the safety of a construction can almost be guaranteed. Further, structure parts that are hard to monitor visually, self-sensing concrete could be interesting, for example for foundation piles. At last, if a structure is monitored well, damage could probably be observed in an early stage. Mostly, the damage is relative small then, such that it could be repaired relative easy.

Some practical cases where self-sensing concrete could be interesting to apply to increase, the safety of a structure are shown below. The applications are divided in cases where self-sensing concrete is applied at critical parts and on parts that are hard to inspect visually.

Critical part of a construction	Nearly no visual inspection possible
Door of a sluice	Foundation piles
Long span bridge	Foundation slab
Crack width for water tight structures	Outside of a tunnel
	Embankment under water
	Side of a retaining wall what retains ground (in general in this part cracks are expected)
	Culvert

3.11.2 Learn from constructions

The second reason to apply self-sensing concrete is based on the old saying "Numbers tell the tale". In other words, a lot of knowledge could be gathered by monitoring structures. This knowledge could be used in future designs. In this way, constructions could be designed in smarter way. Measurements could be interesting for constructions where relative little knowledge is available for yet or for constructions that are applied often, such that it is interesting to optimize these designs further. Some practical examples to apply self-sensing concrete to learn are shown below.

Poorly known constructions	Much applied constructions
Foundation piles	Viaduct
Diaphragm walls	Underpass, especially under railroads

Innovative structures, such as link slabs made of SHCC or spans made of UHPC.

3.12 Self-cleaning concrete

In fact self-cleaning concrete can be applied in every construction that is in contact with the sun and rain. Probably the best reason to apply self-cleaning concrete is because of the aesthetic value of the structure. The effect of cleaning the environment is still a point of discussion. Constructions where self-cleaning concrete could be applied, so structures that are exposed to sun and rain, are:

- Viaduct and girder bridge
- Retaining wall
- Noise barrier
- Aqueduct (outside walls only)

In these constructions, self-cleaning concrete could be applied, but the question is still if it is smart to do from a practical point of view. Self-cleaning concrete is white, so probably reflects a lot of sun light. Noise barriers for example could be made of white self-cleaning concrete. However, the sun light that reflects on the barriers, makes it even more intense to drive a road where these white barriers are placed. This probably reduce the safety on the road. So from a point of aesthetics, white self-cleaning concrete can be very interesting, but from a functional point of view it could be better to apply the classic grey concrete.

3.13 Conclusion

As shown in this chapter, there are a lot of combinations of ACMs and structures possible. In Table 15 are shown again the applications of ACMs and structures. The applications are divided in three categories; Very potential, potential and not of nearly potential. In the first category, which is ‘very potential’, are the applications that seem to be very potential in theory. These structures seem to have a lot benefits, so the really should be applied in practice or at least additional research should be done to be able to apply them in practice.

The second category are the potential applications. These are the applications that are expected to be potential, but not that potential as the applications from the first category. Compared to the category ‘very potential’, the structures of the potential category are expected to have less secondary advantages or seem only be potential in certain conditions.

The last category is the category of applications that should be not be applied in practice, because these structures have no or nearly no benefits. These structures are expensive and no secondary advantages. However, there could of course be certain circumstances where these applications could be interesting to apply. However, taking into account the general picture, these applications should not be research in more detail.

Table 15 – Applications of ACMs and structures divided in three categories of potential

Very potential	Potential	Not or nearly potential
HPC bridge deck	UHPC bridge deck	NSSFRC/HPSFRC cross beam
(U)HPC bridge girder	UHPC joint	NSSFRC/HPSFRC culvert
(U)HPC sluice door	(U)HPC cross beam	NSSFRC/HPSFRC aqueduct
UHPC deck of underpass	NSC and UHPC sluice door	UHPC tunnel elements
	UHPC embankment	(U)HPC sewage
	UHPC retaining wall	(U)HPC foundation slab

	UHPC aqueduct	UHPC and NSC sewage
	UHPC and NSC aqueduct	Steel and UHPC sluice door
SHCC bridge deck	SHCC barrier	SHCC aqueduct joint
SHCC for repair (deck,tunnel,...)	SHCC embankment	NSC and SHCC in culverts
SHCC bridge joint	SHCC joint in tunnel	NSC and SHCC in tunnel
	NSC with SHCC bridge girders	NSC and SHCC aqueduct
	Self-healing concrete aqueduct	
	GPC sluice door	GPC foundation slab
		GPC embankment
		GPC culvert
		GPC sewage
		GPC foundation piles
		Steel and GPC sluice door
	Self-sensing foundation piles	Self-cleaning noise barrier

It is obvious that the applications for the case study is a structure which is very potential. The only three ACMs that are mentioned as very potential in combination with a structure are HPC, UHPC and SHCC, where HPC and UHPC of course have a lot of similarities. The applications of the first category can be split up into two other categories: slenderness optimisation and durability issues, as shown below. In the applications of the slenderness optimisation the benefits of the applications are caused by the slenderness of the structure. Research should be done to make the structure as slender as possible. Then the benefits of the idea can be estimated to judge the potential of the application more accurately.

In the second category, the durability is the main objective of the applications. The challenge here seem to be the mechanics. From a durability point of view, the ideas seem beneficial, but from a mechanical point of view, more research should be done before it could be constructed.

Slenderness optimisation	Durability issues
- HPC bridge deck	- SHCC bridge deck
- (U)HPC bridge girder	- SHCC repair
- UHPC deck of underpass	- SHCC joint in bridge
	- (U)HPC sluice door

In the end, the most interesting combination is research in more detail in the case study. From the very potential applications, the top 3 of applications seem to be the UHPC deck of underpass, UHPC bridge girder and SHCC joint. As shown in paragraph 3.8 Underpass, according to some simple calculations, the UHPC deck of the underpass seems to be beneficial already. More detailed calculations could result in even better results. Then the UHPC bridge girders could for example be beneficial in case of longer lengths or heavier loads, in some circumstances HPC or UHPC bridge girders seems needed to replace old bridges and viaducts, as mentioned in paragraph 3.3 Viaducts and bridges. At last, the SHCC joint in a bridge seems very interesting to apply according to the reference project in Michigan (Li V. C., Michigan's Experience with Ductile ECC for Bridge Decks, n.d.), (Michigan Technological University, 2007), (ACE-MRL, n.d.).

The option that is chosen for the case study is the bridge joint made of SHCC. The main advantage of this idea is the durability of the structure, what results in a lot of advantages. The reasons that this application is expected to be beneficial are:

- Durability of a SHCC joint is expected to be relative high compared to a NSC joint because:

- Favourable cracking pattern
- Strain hardening behaviour if it is in tension
- Prevent leakage water that could damage the substructure, for example the supports
- Prevent de-icing chemicals to go through the joint
- Protection of reinforcement
- Less maintenance what increase the service life
- Relative low amount of SHCC, what reduce the costs
- Better road comfort
- Aesthetics
- Interesting from an educational point of view

4 Conclusion

There are a lot of potential applications to apply Advance Cementitious Materials in structures in infrastructure. A lot of these applications are expected to be potential or even very potential. However, there are also a lot of structures that still smarter to be make of normal strength concrete. A list of potential, very potential and nearly or not potential applications is given in Table 16.

Table 16 – Applications of ACMs and structures divided in three categories of potential

Very potential	Potential	Not or nearly potential
HPC bridge deck	UHPC bridge deck	NSSFRC/HPSFRC cross beam
(U)HPC bridge girder	UHPC joint	NSSFRC/HPSFRC culvert
(U)HPC sluice door	(U)HPC cross beam	NSSFRC/HPSFRC aqueduct
UHPC deck of underpass	NSC and UHPC sluice door	UHPC tunnel elements
	UHPC embankment	(U)HPC sewage
	UHPC retaining wall	(U)HPC foundation slab
	UHPC aqueduct	UHPC and NSC sewage
	UHPC and NSC aqueduct	Steel and UHPC sluice door
SHCC bridge deck	SHCC barrier	SHCC aqueduct joint
SHCC for repair (deck,tunnel,...)	SHCC embankment	NSC and SHCC in culverts
SHCC bridge joint	SHCC joint in tunnel	NSC and SHCC in tunnel
	NSC with SHCC bridge girders	NSC and SHCC aqueduct
	Self-healing concrete aqueduct	
	GPC sluice door	GPC foundation slab
		GPC embankment
		GPC culvert
		GPC sewage
		GPC foundation piles
		Steel and GPC sluice door
	Self-sensing foundation piles	Self-cleaning noise barrier

The very potential applications from Table 16 are the combinations that are recommended to research in more detail. In general these applications could be divided over two categories: mechanics and durability. The applications that are in the category mechanics are primary interesting from a mechanical point of view. The structure for example can carry high loads or very slender. The durable applications are interesting from a durability point of view due to their material characteristics. A high durability can result is a lot of secondary benefits.

From the very potential applications, the top 3 of applications seems to be the UHPC girders, SHCC repair and SHCC joint. The application that is research in more detail in the thesis is the SHCC joint. SHCC has a few characteristics which are important for the advantages of the SHCC joint. These characteristics are:

- Reduced crack width
- Low tensile strength
- High tensile strain
- Low stiffness
- Relative high compressive strength compared to the tensile strength

If the characteristics of SHCC are used properly, a SHCC joint could an interesting connection to apply in bridge and viaduct. Based on the characteristics of SHCC, reasons that the SHCC joint could be interesting to apply in practice are:

- Deformation capacity
- Road comfort
- Protection of the substructure because leakage water can hardly penetrate through the link slab.
- Protection of the substructure because chemicals, for example from de-icing salts, can hardly diffuse through the link slab.
- Low stresses in the link slab if the link slab is exposed to imposed deformation (assuming only tensile stresses are generated in the design)
- Reinforcement is protection
- Probably less (or maybe even no) cost for maintenance required
- Increase service of the road because less maintenance is required
- Longer expected service life compared to most other types of connection

5 Recommendations

According to this research and the conclusions of this research, some recommendations are given here. Most of the recommendations are according to additional research that should be done. The recommendations are listed below.

- Application of ACMs in other structures, different from the structures in this research
- Additional research to the applications that are judged to be very potential
- The applications that are labelled as potential, are recommended to research in more detail if additional benefits are generated by utilising them in certain project. Additional benefits could for example be created in a project due to specific conditions, which create additional benefits to apply a certain ACM.
- It is recommended not include the applications that are judge as not or nearly potential in additional research.
- There are made more combinations of structures and ACMs of ACMs that are known better. It seems that per ACM there is a relation between the number of applications for an ACM and the knowledge that ACM. So if more knowledge of a certain ACM is known, maybe more applications with structure could be made. So after a few years from now, maybe more applications could be made with the same ACMs.
- Application of an ACM on higher level of detail, to research the application of ACMs in smaller part of the structure. Maybe more applications can be found then, because the structure is split up in more elements.

6 Bibliography

- ACE-MRL. (n.d.). *Durable Link Slab for Jointless Bridge Decks Based on Strain-Hardening Cementitious Composites Construction Timeline*. Retrieved from [www.umich.edu: http://www.umich.edu/~acemrl/NewFiles/projects/linkslab_timeline.html](http://www.umich.edu/~acemrl/NewFiles/projects/linkslab_timeline.html)
- Aldred, J., & Day, J. (2012). 37th Conference on Our World in Concrete & Structures . *Is geopolymer concrete a suitable alternative to traditional concrete?* , (p. 14). Singapore.
- Aspire. (2010). *FHWA, Iowa Optimize Pi Girder*. Retrieved from [www.aspirebridge.com: http://aspirebridge.com/magazine/2010Winter/jakway_win10.pdf](http://aspirebridge.com/magazine/2010Winter/jakway_win10.pdf)
- Brain, P., & P.E., K. (2009, April 1). Use of UHPC in Iowa Structural Design/Construction Quality Workshop. Ames, Iowa, USA.
- Camacho, E., Serna, P., & López, J. (n.d.). UHPFRC bolted joints: failure modes of a new simple connection system.
- Ductal. (n.d.). *Jean Bouin Stadium (France): Focus on Ductal® UHPC Roof and Façade Panels*. Retrieved from [ductal: http://www.ductal.com/wps/portal/ductal/3_6_1-Detail?WCM_GLOBAL_CONTEXT=/wps/wcm/connect/lib_ductal/Site_ductal/AllKeyProject/KeyProjectDuctal+Page_1385395657489/Content+KeyProjectDuctal](http://www.ductal.com/wps/portal/ductal/3_6_1-Detail?WCM_GLOBAL_CONTEXT=/wps/wcm/connect/lib_ductal/Site_ductal/AllKeyProject/KeyProjectDuctal+Page_1385395657489/Content+KeyProjectDuctal)
- Endicott, W. (2007). A whole new cast.
- Europese prijs voor De Boer&De Groot*. (2012, 11 14). Retrieved from "Workum.nl": <http://www.workum.nl/de/home/nieuws/1842>
- Geopolymer Institute. (2013, 12 10). *World's first public building with structural Geopolymer Concrete*. Retrieved from Geopolymer Institute - Promoting the Geopolymer science since 1979: <http://www.geopolymer.org/news/worlds-first-public-building-with-structural-geopolymer-concrete>
- Glasby, T., Day, J., Kemp, M., & Aldred, J. (2013). Earth Friendly Concrete – A sustainable option for tunnels requiring high durability. *Arabian Tunnelling Conference & Exhibition*, (p. 11). Dubai, United Arab Emirates.
- Graybeal, B. (2008). Flexural Behavior of an Ultrahigh-Performance. *Journal of bridge engineering*.
- Graybeal, B. (2009). Structural Behavior of a 2nd Generation UHPC Pi-Girder.
- Haitsma . (2011, 11 18). *Betonprijs 2011 voor innovatieve sluisdeuren van Haitsma Beton*. Retrieved from [haitsma beton: http://www.haitsma.nl/](http://www.haitsma.nl/)
- Hussein, M., Kunieda, M., & Nakamura, H. (2012). Strength and ductility of RC beams strengthened with steel-reinforced strain hardening cementitious composites. *Cement & Concrete Composites* 34, 1061-1066.
- Italcementi. (2009). *TX Active - The Photocatalytic Active Principle*.
- Kim, Y. J. (2014). *Advanced Composites in Bridge Construction and Repair*. Woodhead Publishing.
- Kim, Y. Y., Lee, B. Y., Bang, J.-W., Han, B.-C., Feo, L., & Cho, C.-G. (2014). Flexural performance of reinforced concrete beams strengthened with strain-hardening cementitious composite and high strength reinforcing steel bar. *Composites: Part B* 56, 512-519.

- Kunieda, M., & Rokugo, K. (2006). Recent Progress on HPFRCC in Japan: Required Performance and Applications. *Journal of Advanced Concrete Technology Vol. 4, No. 1*, 19-33.
- Li, M. (2009). *Multi-Scale Design for Durable Repair of Concrete Structures*. Michigan.
- Li, V. C. (2006). Bendable Composites: Ductile Concrete for Structures. *STRUCTURE magazine*, 45-48.
- Li, V. C. (2007). *Engineered Cementitious Composites (ECC) – Material, Structural, and Durability Performance*.
- Li, V. C. (n.d.). *Michigan's Experience with Ductile ECC for Bridge Decks*. Retrieved from www.concretebridgeviews.com: <http://www.concretebridgeviews.com/i77/Article2.php>
- Li, V. C., Lepech, M., & Li, M. (2005). *Final Report On Field Demonstration of Durable Link Slabs for Jointless Bridge Decks Based on Strain-Hardening Cementitious Composites*. Michigan Department of Transportation.
- Li, Y. E., Guo, L., Rajlic, B., & Murray, P. (n.d.). Hodder Avenue Underpass: An Innovative Bridge Solution with Ultra-High Performance Fibre-Reinforced Concrete.
- López, J., Serna, P., & Camacho, E. (n.d.). Structural design and previous tests for a retaining wall made with precast elements of UHPFRC.
- Maalej, M., Lin, V., Nguyen, M., & Quek, S. (2010). Engineered cementitious composites for effective strengthening of unreinforced masonry walls. *Engineering Structures* 32, 2432-2439.
- Maalej, M., Quek, S., Ahmed, S., Zhang, J., Lin, V., & Leong, K. (2012). Review of potential structural applications of hybrid fiber Engineered Cementitious Composites. *Construction and Building Materials - Volume 36*, 216-227.
- Maten, R. t. (2011). *Ultra High Performance Concrete in Large Span Shell Structures*. Rotterdam.
- Michigan Department of Transportation's Construction and Technology Division. (2005). Bridge Decks Going Jointless. *C&T Research Record*.
- Michigan Technological University. (2007, August). Bendable Concrete Provides Insight into Sustainable Material Development Process. *MDOT Office of Research and National Best Practice*, pp. 1-4.
- Milan, K., Vaclav, K., Jan, K., L., V. J., Robert, B., & Petr, K. (n.d.). Cable-Stayed Footbridge with UHPC Segmental Deck.
- Nederlands Normalisatie-instituut. (2001). *NEN 1814 (nl): toegankelijkheid van buitenruimten, gebouwen en woningen*.
- NV Bekaert SA. (2008). Park Oceanographic .
- Ottelé, M. (2015, May 1). Faalkosten. (J. v. Oosten, Interviewer)
- Perry, V. H., & Zakariasen, D. (2004, August). First Use of Ultra-High Performance Concrete for an Innovative Train Station Canopy. *Concrete Technology today Vol. 25, No.2*.
- Perry, V., Scalzo, P., & Weiss, G. (2007). Innovative Field Cast UHPC Joints for Precast Deck Panel Bridge Superstructures - CN Overhead Bridge at Rainy Lake, Ontario. *Concrete Bridge Conference*.

- Rijkswaterstaat Bouwdienst. (2005). Specifieke Aspecten TunnelOntwerp. Retrieved from http://www.rijkswaterstaat.nl/images/deel%202_tcm174-328961.pdf
- Rouwhorst, W. (2015). *Participerend observerend onderzoek Project SENS*. Rosmalen.
- Sadev. (n.d.). *Jean Bouin stadium get a new look!* Retrieved from SADEV architectural glass systems: <http://www.sadev.com/blog/le-stade-jean-bouin-fait-peau-neuve/?lang=en>
- Voo, Y. L., Nematollahi, B., Said, A. B., Gopal, B. A., & Yee, T. S. (2012). Application of Ultra High Performances Fiber Reinforced Concrete - The Malaysia perspective. *International Journal of Sustainable Construction Engineering & Technology, Vol 3, Issue 1*.
- Wagners and Brisbane West Wellcamp Airport. (n.d.). EFC Geopolymer Aircraft Pavements at Brisbane West Wellcamp Airport (BWWA).
- Wagners. (n.d.). *Rocky Point Boat Ramp*. Retrieved April 8, 2015, from wagners: <http://www.wagner.com.au/projects/rocky-point-boat-ramp/>

Appendix A: Interview Marc Ottelé – Failure of concrete structures (May 1, 2015)

In this appendix is given a summary of an interview with Marc Ottelé on May 1, 2015. The subject of the interview is failure of concrete structures in practice. The objective of the interview is to gather information about problems and failure mechanisms of concrete structures. These problems could be interesting input for the application of a certain ACM for certain structures.

Cracks

The most frequent failure in a concrete construction are cracks, with all the effects it gives. Cracks mostly result in:

- Leakage of the concrete
- Durability of the concrete decreases:
 - o More change on corrosion of reinforcement
 - o More change on chemical attack
 - o More change on frost damage, especially when de-icing salts are applied
- Aesthetics effect in term of colour differences, visible gravel pockets, visible cracks

The consequence of cracks could be injection of the concrete to repair the cracks. This costs a lot of money.

Complexity

Ottelé warns for the complexity of ACMs and the different characteristics of the ACMs during execution compared to NSC, what gives risks in terms of:

- **Execution method**; ACM should probably be executed in another way, what is probably a more complex way.
- **Production speed** is probably lower compared to the production speed of NSC. The capacity of concrete fabric is normally lower for complex concrete materials like the ACMs.
 - o As a result, the pouring front is longer bare. So the fresh concrete will probably has a worse connection with the cast concrete.
- Many ACMs contain more cement, so compared to NSC they become warmer during hydration. Measures during hardening should be taken to control this, else shrinkage could be critical.
- A low W/C-ratio normally results in more shrinkage. Some ACMs has a very low W/C ratio compared to NSC, so shrinkage could be an issue then.

Construction speed

In a lot of projects, the construction speed has become a critical issue. The construction speed can be that important, that the concrete should be on its 28 days strength after 2 days already. Mostly, this is not considered during the design phase. To increase the construction speed, more cement is added during execution to have the higher early strength. Adding more cement normally has negative effects on the durability of the concrete, which are not considered in the execution phase.

Marc suggest that durability problems in this kind of cases could be prevented by applying HPC. This types of concrete are specially made to have high strength, so also a high early strength, what will probably result in a more durable structure.

Concrete fabric

Not every fabric is certificated to make special kinds of concrete. Most fabrics are certificated to make concrete with a cubic compressive strength equal to or lower than 65 MPa. This could be factor that makes it even less attractive to apply ACMs.

Failure costs

It is hard to quantify failure costs of a concrete structure in term of money. The costs depend on the situation and the kind of failure. Fact is that costs to repair can be as high as the costs of the concrete itself and in some cases even higher. So for example, assuming a construction of 50 m^3 concrete with a concrete unit prices of 60 – 70 *euro/m³* in total costs about 3,000 – 3,500 *euros*. The repair cost for such project then can easily be more than 3,000 *euros*.

Applications of Advanced Cementitious Materials in Infrastructure

Appendix 3: SHCC Link Slab

Candidate

J. van Oosten
TU Delft and Heijmans

28-9-2015

Committee

Prof.dr.ir. D.A. Hordijk
Ir. A.D. Reitsema
Dr.ir. M. Ottelé
Dr.ir. C. van der Veen
Ir. L.J.M. Houben

TU Delft
TU Delft and Heijmans
TU Delft and Heijmans
TU Delft
TU Delft

Summary

This report is the third part of the research to the applications of Advanced Cementitious Materials (ACMs) in infrastructure, to take up potential benefits. The objective of the total research is to make an overview of combinations of new concrete materials and constructions, which can be utilised to take up potential benefits. The total research is made up of three parts:

- Part 1 - Literature study
- Part 2 - Fields of applications
- Part 3 - SHCC Link Slab

This appendix is done a case study to the SHCC Link Slab (SHCC Joint), which is expected to be an application of an ACM with a lot of potential. The main potential benefits that could be generated by utilising the SHCC link slab is an increased road comfort and creating a more durable connection with a certain horizontal deformation capacity. Due to durability, the service life could be expected to be increased, the maintenance could be expected to be reduced and the substructure is expected to be protected by the joint against water and chlorides.

In this research are included three SHCC link slab designs. The Thin SHCC Link Slab design is expected to be the most interesting one to apply in the Netherlands. The Thin SHCC Link Slab is a slab with a thickness of 75 mm only that links two concrete bridge spans together. The link slab is placed upon the concrete bridge decks, which are partly deepened, such that a flat surface is created. The link slab should be able to transfer vertical and horizontal loads. In the same time, the link slab should also be able to take care of imposed deformations.

From the analysis to these actions (vertical load, horizontal load and imposed deformations) follows a two points of attention from a structural point of view; execution of the debonding layer and vertical working load. The debonding layer has to do with the smoothness of the layer. If the layer could not be executed smooth enough, the joint can't deform horizontally in a proper way anymore. Vertical loads could cause vertical peak stresses at the end of the substructure, what causes spalling at the end of the concrete substructure. Due to spalling, the reinforcement in the concrete is not covered any more. Subsequently, failure of the reinforcement could be expected, what may result in failure of the total bridge structure.

Spalling can be prevented by reducing the peak stress or increasing the resistance. Three suggestions to reduce the risk of spalling are;

- **Chamfers at the end of the deck:** cheapest option to decrease the tensile stresses. However, the effectiveness is a point of discussion, because chamfers also increase the peak stress.
- **Prestressed anchored plate:** most effective option to increase the resistance against tensile stresses, but probably expensive in terms of labour and material costs.
- **Redistribution by stiff interlayer:** option with best additional advantage. It decreases the vertical peak stresses and could in potential create a properly working debonding layer easily. The debonding could be a governing problem to execute the link slab in practice.

The application of the SHCC link slab should be done by steps. Five pilot projects are recommended to work from the NSC flexible joint (buigslappe voeg) to the Thin SHCC Link slab. The five recommended pilot projects are given in Table 1. The structure, the advantage of the structure and the recommended research that seems needed before the pilot can be executed are given in the table. The pilot projects are explained in more detail in the recommendations of this appendix.

Table 1 – From Flexible joint to Thin SHCC Link Slab by steps

		Structure	Advantage	Research
Flexible Joint	Pilot 1	Flexible joint made of SHCC	No adhesive strip Practical learning goal SHCC	SHCC material
	Pilot 2	Flexible joint made of SHCC with GFRP reinforcement	Durable reinforcement Practical learning goal GFRP Lower stiffness of the joint	GFRP
	Pilot 3	Flexible joint made of SHCC with a reduced amount of reinforcement	Less reinforcement Lower stiffness of the joint	Influence of PVA fibres
Thin Link Slab	Pilot 4	Thin SHCC link slab with GFRP rebars (intermediate supports only)	Horizontal deformation capacity Lower stiffness of the joint	Peak stresses Debonding zone
	Pilot 5	Thin SHCC link slab with GFRP rebars (all supports)	Horizontal deformation capacity in all joints	Influence on the abutment

Guide line

This part of the research is spent on to the SHCC link slab. An overview of link slab designs that are experimentally researched can be found in chapter 2 Literature. One design of a NSC flexible joint and three designs of SHCC link slabs are given in this chapter. The chapter ends with an overview of the characteristics of all designs in paragraph 2.5 Overview.

Readers, who are interested in a detailed analysis of the Thin SHCC Link Slab design, which is expected to be a potential alternative joint, can find more information in chapter 3 Analysis of SHCC Link Slab. In this chapter the design of the Thin SHCC Link Slab is analysed in detail, for example the reaction of the link slab on actions like vertical load, horizontal load and imposed deformations.

As a first practical step to the Thin SHCC Link Slab is suggested to apply SHCC in a flexible joint first instead of NSC. This structure is described in chapter 4 SHCC Flexible Joint in a Concrete Bridge. In this chapter are described the advantages of this structures as a first step towards the Thin SHCC Link Slab.

In chapter 5 Options against the peak stresses are suggested five different design options to reduce the risk of spalling, such that the durability of the connection is increased. If spalling is not taking into consideration during the design stage, the concrete substructure is expected be damaged such that the reinforcement is not covered any more.

Table of content

Summary	iii
Guide line	v
Table of content	vi
1 General introduction	9
1.1 Joints issues.....	9
1.2 Alternative SHCC joint	10
1.3 SHCC joint and NSC joint.....	12
1.4 Research question	12
1.5 Objective	12
1.6 Boundary conditions.....	13
1.6.1 Interesting SHCC link slab design.....	13
1.6.2 Joint parameters.....	13
1.6.3 Homogenous material.....	14
1.6.4 Structural point of view.....	14
2 Literature	15
2.1 Flexible joint.....	15
2.1.1 Design.....	15
2.1.2 Load transfer system.....	16
2.1.3 Analysis to vertical loads on joint	17
2.1.4 Analysis to horizontal loads on joint	18
2.1.5 Analysis imposed deformations from spans	19
2.2 Deck Link Slab.....	22
2.2.1 Strain Hardening Cementitious Composite (SHCC)	22
2.2.2 Roofing paper	26
2.2.3 Design.....	26
2.2.4 Test results and conclusions.....	29
2.2.5 Load transfer system for working loads and imposed deformations	30
2.2.6 Monitoring of the Grove Street Bridge and SHCC Link Slab	49
2.3 Cast in place and precast thin link slabs	51
2.3.1 Material characteristics.....	52
2.3.2 Design.....	54
2.3.3 Test results	58
2.3.4 Conclusions.....	64
2.3.5 Load transfer system.....	65

2.4	Flexible Thin Link Slabs	78
2.4.1	Materials characteristics	78
2.4.2	Design.....	80
2.4.3	Test results	84
2.4.4	Conclusion	89
2.4.5	Load transfer system.....	90
2.5	Overview.....	94
3	Analysis of SHCC Link Slab	96
3.1	Joints types.....	96
3.2	Description of actions	97
3.3	In depth analysis on basic actions	98
3.3.1	Vertical load.....	98
3.3.2	Horizontal load	113
3.3.3	Vertical imposed deformation.....	125
3.3.4	Horizontal imposed deformation and imposed curvature.....	136
3.3.5	Evaluation and conclusion.....	147
4	SHCC Flexible Joint in a Concrete Bridge.....	149
5	Options against the peak stresses	151
5.1	Debonding layer in the active zone	152
5.2	Fibres	157
5.3	Chamfer	159
5.4	Locally reduced Young's modulus	161
5.5	Redistribution by stiff interlayer	166
5.6	Prestressed anchored plate	169
5.7	Overview.....	172
5.8	Evaluation and conclusion	173
6	Conclusion	174
7	Recommendations	176
7.1	Practical guidance.....	176
7.2	Additional research	178
7.2.1	Combination: horizontal imposed deformation and horizontal load	178
7.2.2	Vertical imposed deformation.....	178
7.2.3	Spalling of NSC substructure	178
7.2.4	Vertical peak stress in SHCC link slab.....	178
7.2.5	Variant to reduce the risk of spalling.....	179
7.2.6	Practical issues.....	180

8	Bibliography.....	182
	Appendix A: Deformation capacity of NSC flexible joint and thin SHCC link slab	184
	A.1. Imposed deformation due to temperature	184
	A.2. Deformation capacity of flexible joint	185
	A.3. Deformation capacity of SHCC link slab.....	185
	A.4. SHCC Link Slab behaviour in a bridge	187
	Appendix B: Load combinations.....	190
	Appendix C: Maximum span of the link slab.....	195

1 General introduction

There are a lot of different joints that serve for years already. In this thesis, research is done to joints made of SHCC, mainly called link slabs instead of joints. To apply SHCC link slabs, they should have (potential) advantages compared to the nowadays applied joints. In this chapter is shortly mentioned the potential of the SHCC link slabs. Based on the potential of the SHCC link slab, the research question and the objective of this case study is defined in this chapter also. At the end, some boundary conditions according to the objective are given.

1.1 Joints issues

Before the potential of the SHCC link slab idea is given, some issues of typical bridge joints are given. In short, practical issue of joint are:

- Expensive to install (Li, et al., 2003)
- Expensive to maintain (Li, et al., 2003), (Reyes & Robertson, 2011)
- Run-off water with aggressive chemicals (Lárusson, 2013), (Reyes & Robertson, 2011)
- Relatively short service life (Lárusson, 2013)

These issues are clarified a bit more here. The installation and maintenance of joints is expensive (Li, et al., 2003), (Reyes & Robertson, 2011). Also the service life of the joint is short (Lárusson, 2013). Of course the service life and maintenance have a strong correlations. A structure that has a short service life automatically requires a lot of maintenance. In Figure 1 is shown a joint that is at end of its service life. In the figure is clearly shown the damage of the joint and the road around the joint.



Figure 1 – Damage in pavement due to deterioration of expansive joints (Lárusson, 2013)

Of course, also the joints in the Dutch bridges are sensitive for damage and requires a lot of maintenance. In the B&O-kunstwerken program of the Netherlands (the Dutch management and maintenance program for civil structures), about 20 million euros per year are spent on joints (Voskuilen, Vliet, Booij, & Leendertz, n.d.).

The service life of a joint depends on the type of joint that is applied. A distinction can be made between hard and soft joints. Soft joints have a short service life, about three years. However, soft joints reduce the traffic noise very well. The policy of Rijkswaterstaat (manager of the Dutch national roads and one of the largest client of Heijmans) is to reduce traffic noise of the main network. Soft joint perfectly fit in the policy of Rijkswaterstaat. However, expensive maintenance and short service life could be expected (Rijkswaterstaat, n.d.).

Next to the costs and service life, run-off water can penetrate through joints. In this water could be dissolved aggressive chemicals, for example de-icing agents. Chemicals can damage the concrete significantly. But not only the concrete can be damaged by the chemicals, also the supports under the bridge can be attacked by run-off water and the aggressive chemicals that are in the water. An example damage of the supports cause by run-off water is shown in Figure 2 (Lárusson, 2013).



Figure 2 – Highly corroded steel in connection between girder and pier caps due to deterioration of expansive joints (Ho & Lukashenko, 2011)

1.2 Alternative SHCC joint

The SHCC link slab is an alternative joint construction where the above mentioned problems should be prevented. The aim of the SHCC link slab is that due to the characteristics of SHCC and the design geometry, a link slab can be constructed that creates a continuous road deck while it is still be able deform and to carry vertical and horizontal loads. The geometry of the link slab design in combination with the characteristics of SHCC, could make the link slab a very durable structure compared to most of the other commonly used link slabs. The main advantages of the SHCC link slab are shortly shown in the second column of Table 2. In the first column of the table are given the SHCC characteristics that have strong relations with these main advantages of the design.

Table 2 – Main advantages of the SHCC link slab design with relations to the SHCC characteristics

SHCC link slab characteristic	Advantages of the design
Continuous deck surface	Road comfort
Tensile strain hardening behaviour	Tensile strain capacity in order of a few percentages
Low tensile strength	No large stresses in the bridge if the link slab is exposed to imposed deformations that result in tensile stress in the link slab
Crack width control	Durability of the system: <ul style="list-style-type: none"> - If cracked; low coefficient of permeability (comparable to uncracked SHCC according to the literature study), so low amount of leakage water that can damage the substructure. - If cracked; low chloride diffusion coefficient (comparable to uncracked SHCC according to the literature study), so low diffusion of de-icing chemicals that can damage the substructure. - Longer service life - Lower maintenance - Higher service of the road - Well protection of reinforcement

The disadvantage of SHCC is the low sustainability of the material, mainly caused by the large amount of cement. However, it is expected that only a low amount of SHCC is needed to make a link slab, such that the influence on the environment is small in absolute values. Probably, the advantages could compensate the disadvantage in terms of sustainability.

In Figure 3 is shown a schematic example of the SHCC link slab between two concrete bridge spans. The figure clearly shows the idea of the SHCC link slab. The idea is that movements between the two concrete spans are carried by the cracking SHCC link slab, while vertical and horizontal loads must still be carried. The SHCC link slab should always be under tension, to minimise the stresses in the link slab.

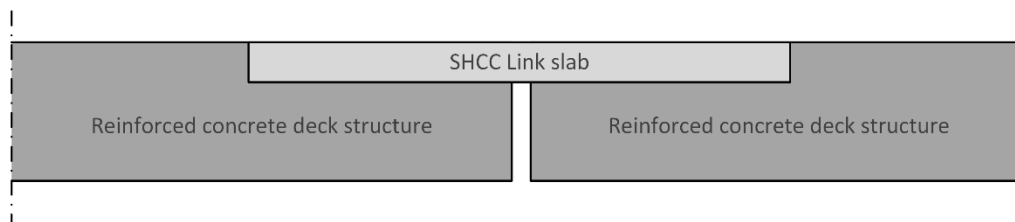


Figure 3 – Example of an SHCC link slab between two bridge spans

One job of the link slab is to take up horizontal deformations. SHCC has a deformation capacity in the order of a few percent. However, the tensile stress that is generated during the deformation is still low. That means that, assuming the link slab is quite thin, the force in the link slab is low too during deformations. Further, SHCC has a high tensile strain capacity. That means that the link slab could have, depending on the length, enough capacity to carry movement differences between two spans.

At last, the unique cracking pattern makes that the **water permeability** and **chloride diffusion** coefficient of cracked SHCC is almost the same as for uncracked SHCC. The unique cracking pattern does not only increase the durability of the SHCC, but also protects the reinforcement in the link slab properly. This could make the SHCC link slab to a very durable structure.

Now the design of Figure 3 is analysed in some more detail. Striking in the design is that the link slab is a closed joint. That means that the road can be made continuous, because there is no gap between the SHCC link slab and the concrete bridge. Further, in the link slab itself are no gaps either. The continuity does not only result in **road comfort**, but also prevent **leakage of water** with aggressive **chemical** to the supports. The continuous deck in combination with the unique crack width control, water can almost not penetrate through the link slab to the supports. In other words, the supports and substructure under the SHCC link slab is not damaged by leakage water and aggressive chemicals that are penetrating through the link slab.

The **service life** of SHCC link slab in practice should be research before conclusions could be made. The same is valid for the maintenance of the link slab. However, since the durability of SHCC is very high, a high service life could be expected. Further, because there is no gap, asphalt can be placed over the link slab. Then vehicles are not driving on the link slabs directly. That means that the link slab can't be damaged by vehicles that drive over the link slab directly. In other words, the service life could be expected to increase, the maintenance probably reduced, what both increases the service of the road.

Due to the high durability of the link slab, maintenance is expected to be reduced to a minimum. In theory, the maintenance may not even required. Assuming not maintenance is required, then there is according to the RTD 1007-2 no need to construct a corridor for maintenance (Rijkswaterstaat, 2013). This of course results in some more freedom in the design and lower costs.

1.3 SHCC joint and NSC joint

Joints that are made of normal strength concrete are applied for years already, as given in 2.1 Flexible joint. Because SHCC is a cementitious material as well, the comparison between the SHCC link slab and the NSC flexible joint is interesting to make. On forehand, the main differences between both material are expected to be:

- Deformation capacity
- Durability
- Reinforcement

Compared to the NSC joint the main advantage of the SHCC joint is probably the deformation capacity of the SHCC joint. The deformation capacity of the NSC joint is negligible small, while the SHCC joint has a significant horizontal deformation capacity in the order of 10-20 mm. Due to the deformation capacity of the SHCC joint, the undilated length could be made larger or in case of relative small dimensions, no additional finger joint is required at the end of the undilated length. This is explained further in the rest of the report, especially in Appendix A: Deformation capacity of NSC flexible joint and thin SHCC link slab.

Further, the durability of SHCC could be expected to be better than the durability of NSC, because of the reduced crack width in SHCC. Because tensile stresses are expected in the joint, cracks could also be expected. Because one of the characteristics of SHCC is the limited crack width, the durability of SHCC link slab is expected to remain stable.

To limit the crack width of NSC, a lot of reinforcement should be included. Here is also the third advantage to apply SHCC instead of NSC. In the NSC joint is required a lot of reinforcement, while in SHCC is placed a significant smaller amount of reinforcement. In the end, this will probably have a positive effect on the costs of the joint in terms of material costs and labour costs. However, SHCC itself is probably a lot more expensive compared to NSC, so in the end the costs to build an SHCC joint could still be higher than the costs to the NSC joint.

1.4 Research question

The total research until now consists of two parts; the literature study and the combination study. In the first study research is done to materials and construction. In the combination study are given ideas to apply ACMs in structures that were analysed in the literature study. In the combination study is mentioned the idea of a joint made of SHCC. Above are already mentioned the reasons that an SHCC joint is interesting to apply. The question is how SHCC should be applied in a joint to make a proper design. Therefore, the research question is:

How look the designs of SHCC joints?

1.5 Objective

As mentioned in the research question, SHCC seems an alternative material to construct a proper joints. There is done research to different types of SHCC joints and in practice, one of the joint designs is already applied in a bridge. Now it should be interesting to analyse the different researches and to find points of attention that should be researched in more detail such that the joint could be applied by Heijmans too. Research could for example be done theoretically or by experiments. Therefore the objective is:

An overview of points of attention of an interesting SHCC link slab design to apply in practice in the Netherlands

1.6 Boundary conditions

Some boundaries for the objective are set up for practical reasons. Here the boundary conditions of the case study are discussed. Every condition is explained in some detail. The included boundary conditions are:

- Interesting SHCC link slab design
- Joint parameters
- Homogenous material
- Structural point of view

1.6.1 Interesting SHCC link slab design

An interesting SHCC link slab design is still an undefined variable. The literature study should show the SHCC link slab designs that are researched already. From these designs, the most interesting design is taken into account in the rest of this research. Probably, the most interesting one is the design that is expected to be applied frequently by Heijmans or the design that has the most potential benefits. During the research, the most interesting SHCC link slab design is chosen.

1.6.2 Joint parameters

In this study the joint at a middle support is taken into consideration. The joint is situated in a multiple span bridge, as shown in shown Figure 4. Detail AA in Figure 4 is shown in Figure 5. In Figure 5 is also shown the deflection of the bridge girders. It is assumed that the deflection of the bridge girders are carried equally over both supports of the girder. So if the total strain in the girder is ε_{tot} , every support carries $\frac{1}{2}\varepsilon_{tot}$. Because the joint is situated between two supports, the strain in the joint is equal to the total strain of one girder, ε_{tot} .

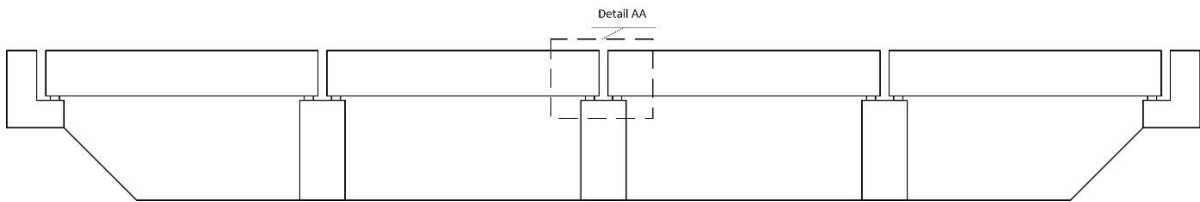


Figure 4 - Side view of multiple span bridge

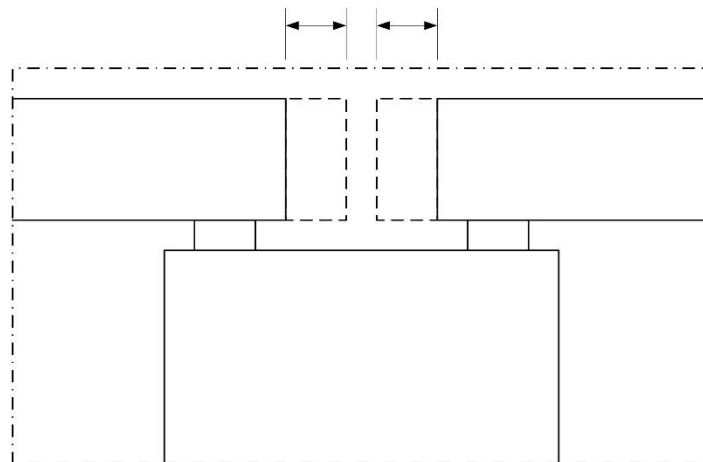


Figure 5 - Detail AA of Figure 4; elongation of the bridge beams at the middle support

1.6.3 Homogenous material

Concrete has certain deviations in its characteristics. This makes sense since materials from natural resources are used to make concrete. Further, the characteristics depend on the homogeneity of the mixture.

Suppose a bridge has two intermediate supports, both made of SHCC. The first joint is made of SHCC mixture 1 and the other joint is made of SHCC mixture 2. In theory, both materials are the same. However, in practice there are probably differences between both mixtures. If the tensile strength of both mixtures differs, as schematically shown in Figure 6, it could have consequences for the joints.

Suppose the SHCC 1 joint is cracked because the imposed deformation of the joint is around 0.5%. The stress in the joint will remain 3.5 MPa if the strain increases. That means that the joint at the other end of the beam will not crack, since this joint cracks at a tensile strength of 5.0 MPa. That means that all the deflections in the bridge are carried by the SHCC 1 joint. Depending on the deflections in the bridge, the SHCC 1 joint will probably fail, while the SHCC 2 joint is probably still uncracked.

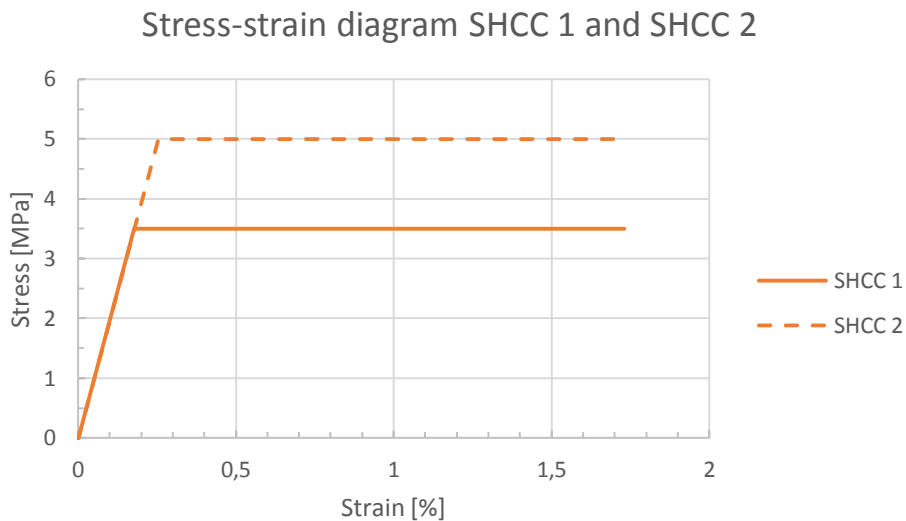


Figure 6 – Example of different tensile strength between two mixtures SHCC

However, in this research it is assumed that the stress-strain relations in all the mixtures is the same. So in theory, all joint cracks under the same imposed deformation.

1.6.4 Structural point of view

The overview of points of attention will be made from a structural point of view only. It is assumed that a proper design could only be made if all points of attention are known and solved. Other problems, like sustainability and costs are not included in the overview.

2 Literature

Before the point of attentions for the SHCC link slab design are analysed, first an analysis is done to the concrete flexible joint and some different types of SHCC link slabs. They are all discussed in this chapter. First the design of a concrete flexible joint is discussed. This joint type is applied successfully for decades already. After that, some SHCC link slab designs are analysed. Researches that are done by Li, et al. (2003), Reyes & Robertson (2011) and Lárusson (2013) are included in the analysis. Their research is mainly focused on the behaviour of the link slab that is exposed to horizontal imposed deformation. In this research, almost not attention is given to behaviour of the link slab exposed to vertical or horizontal loads.

With the exception of the flexible joint, the description of the different designs starts with the characteristics of the materials that are applied. After that, the design of the specific joint is analysed in detail. If some tests are described, the test results are analysed too. At last, the design and the test results together are used to determine the load transfer system of the joints.

2.1 Flexible joint

In this paragraph is described the idea of a standard flexible joint that is made of concrete according to Nosewicz & Jong (2009). The joint should take care of imposed deformations from the bridge girders. Further, the joint should be strong enough to carry the continuity of the road. In this paragraph, first the standard design is illustrated. After that, the imposed deformations and loads that work on the joint are analysed in more detail.

2.1.1 Design

There are made quite some alternative flexible joint designs. The idea of a flexible joint, what is more or less the same in every design, is shown on the cross sectional view in Figure 7. As shown in the figure, the joint is a relative thin concrete plate, which is fixed to the concrete beams. The concrete is cast on plywood, what can be considered as lost formwork. The plate is supported by polystyrene strips, to guarantee a certain free space between the joint and the substructure. Due to the free space under the joint, the joint can move freely.

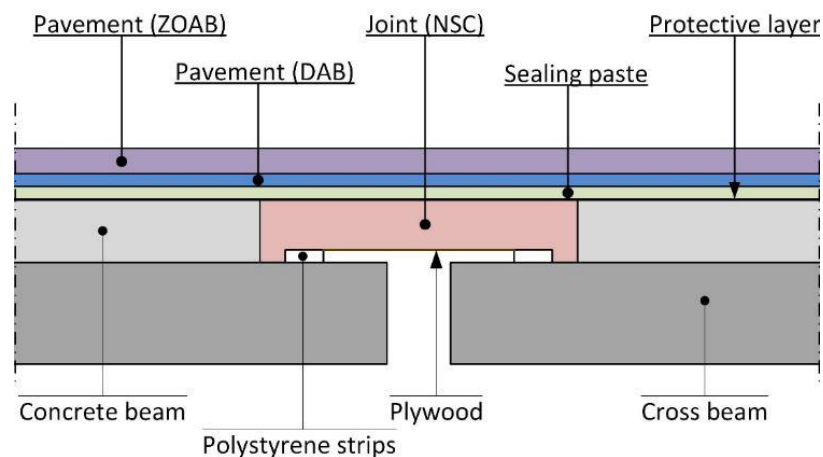


Figure 7 – Cross section of a flexible joint (NSC) according to Nosewicz & Jong (2009)

The flexible joint should carry imposed deformations and tensile loads, while crack width requirements should be met. In the same time, the joint should also transfer wheel loads to the substructure

(Nosewicz & Jong, 2009). Here, the free space under the joint becomes important to. The joint should be able to bend and deform. If there is no free space under the joint, the joint could not deform 'freely'.

The advantage of concrete flexible joints is that a continue deck can be created, without interruptions of joints that decrease drive comfort. The asphalt layer is just placed over the joint. This also increase the durability of the joint, because the joint is not directly load by wheel loads.

Nosewicz & Jong (2009) came up with a design of a 'standard flexible joint'. This standard joint is calculated with the computer program MathCad. The design of the joint is the same as the design shown in Figure 7. The dimensions of a standard flexible joint are given in Table 3.

Table 3 – Standard flexible joint according to (Nosewicz & Jong, 2009)

Joint dimensions	Box girder	Rail girder	Unit
Length of span	900	800	mm
Thickness	170	150	mm
Concrete in joint			
Concrete class	C35/45	C35/45	[-]
Joint reinforcement			
Total cross sectional area	2,827	2,610	mm ² /m
Bar diameter	12	12	mm
Centre-to-centre (up)	60	65	mm
Centre-to-centre (down)	120	130	mm

2.1.2 Load transfer system

In this paragraph is described the way vertical and horizontal loads are transferred to the substructure. This is done according to Nosewicz & Jong (2009) and the given design. The cross section of the design and the model of the flexible joint is given in Figure 8.

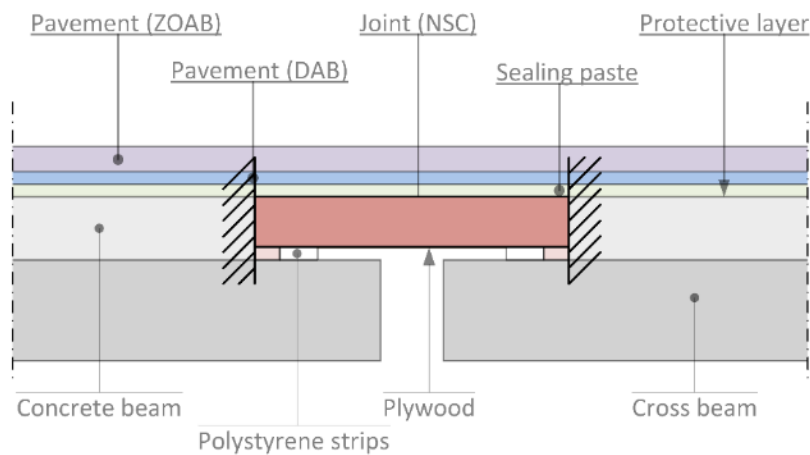


Figure 8 – Design of flexible joint according to Nosewicz & Jong (2009)

As shown in Figure 8, the concrete joint can be modelled as a beam that is clamped at both sides between the concrete bridge beams (Nosewicz & Jong, 2009). The supports are considered as fixed supports, because of the high amount of reinforcement to connect the joint to the concrete beam and the height of the structure.

It is assumed that polystyrene strips does not transfer any load from the joint to the cross beam. Looking to the stiffness of both materials, this seems a good estimation, because the stiffness of polystyrene ($E \approx 2,500 \text{ MPa}$) (WSV Kunststoffen BV, 2015) is significant lower compared to NSC ($E \approx 33,000 \text{ MPa}$). Further is assumed that both sealing paste and asphalt do not have any constructive capacity.

The dimensions of the joint are 900 mm long and 170 mm thick for box girders and 800 mm long and 150 mm thick for rail girders, as shown in Table 3. That means that the slenderness of both girders is $\frac{170}{900} \approx \frac{1}{5}$ and $\frac{150}{800} \approx \frac{1}{5}$ respectively, so the beam is relative thick. The thickness of the beams suggests that the beam is indeed strong enough to carry the vertical loads by bending moments and shear forces.

It is given that the link slab could be modelled as a beam that is clamped at both ends. For the vertical and horizontal stresses, this means that:

- Vertical forces are carried by bending moments and shear forces. As shown in Figure 8, the flexible joint is connected to the cross beam at both ends. It seems that this connection carries vertical stresses from the joint to the cross beam.
- Horizontal forces are carried by normal stresses. Probably compressive stresses are carried by the concrete and tensile stresses by the reinforcement steel and transferred to the concrete beams.

Nosewicz & Jong (2009) do not take into account horizontal stresses perpendicular. Horizontal stresses perpendicular to the drive direction, for example due to lateral displacement of vehicles, are assumed to be very small compared to the horizontal stresses parallel to the drive direction. From reasons of simplicity, horizontal stresses perpendicular to the drive direction are neglected here.

As a conclusion from the above analysis, the flexible joint could be modelled as a beam clamped at both ends. Horizontal and vertical loads are carried by normal stresses and bending moments and shear stresses respectively.

2.1.3 Analysis to vertical loads on joint

In this paragraph is shortly analysed the way vertical loads are carried by the joint. The vertical loads on the joint are assumed to be transferred to the substructure according to NEN-EN 1991-2 chapter 4.3.6 (2). This the load transfer system from the NEN-EN 1991-2 is shown in Figure 9. In the figure is shown the concentrated vertical wheel load (1). This load is distributed through the wear layer and the substructure under an angle of 45 degrees. Spreading of the load under 45 degrees is allowed to apply until the middle of the concrete substructure. To calculate the vertical load on the joint quantitatively, the model can be completed as shown in the rest of the NEN-EN 1991-2.

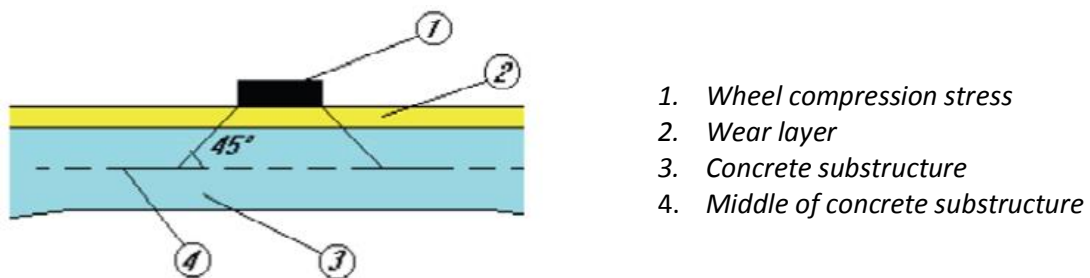


Figure 9 – Distributions of wheel load through wear layer and concrete substructure (Nederlands Normalisatie-instituut, 2003)

2.1.4 Analysis to horizontal loads on joint

In this paragraph is shown the way that horizontal load are carried by the bridge system if flexible joints are applied. In Figure 10 is shown a working horizontal loads on the span that is caused by braking loads. According to Nosewicz & Jong (2009), the bridge decks reacts like a plate. Therefore, in all supports work a certain reaction force to make horizontal equilibrium. If the braking vehicle is situated out of the middle of the bridge, a certain bending moment is generated, as shown in Figure 10. Assuming the length of the bridge span is larger than width, a reaction force perpendicular on the bridge axis is probably generated.

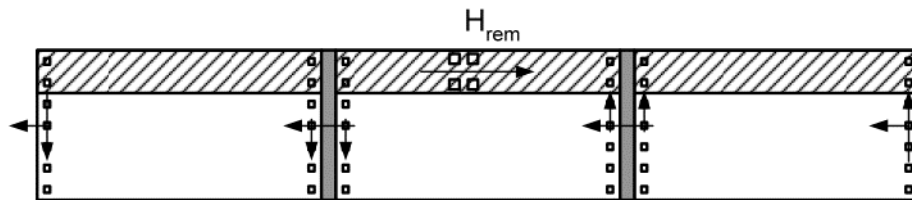


Figure 10 – Assumed distribution of brake load for a bridge with three spans (Nosewicz & Jong, 2009)

A more detailed calculation of the horizontal braking forces in the bridge is given by Nosewicz & Jong (2009). According to Nosewicz & Jong (2009) braking forces are equally distributed over all supports in the bridge, because the stiffness of the concrete in the flexible joint is an order higher than the stiffness of the support blocks. Then due to the link slabs, the horizontal stresses are distributed equally over all supports. The horizontal force that should be carried the link slabs depends on the number of spans and the magnitude of the braking forces, as shown in eq.(1). This equation is an expression to calculate the horizontal force in the joint that is caused by a certain braking force, R_d .

$$F_{joint} = R_d \left(1 - \frac{1}{n}\right) \quad \text{eq.(1)}$$

In Figure 11 and Figure 12 are shown two situations where a car brakes on the bridge. In the first case, Figure 11, a braking force causes tension in the link slabs. In the second case, Figure 12, a braking force causes a compressive stress in the left link slab and a tensile stress in the right link slab.



Figure 11 - Braking force on the bridge with reaction tensile stresses in the link slabs according to (Nosewicz & Jong, 2009)

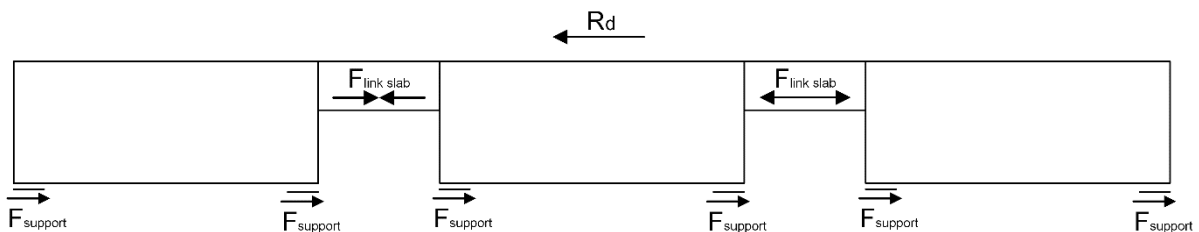


Figure 12 - Braking force on the bridge with reaction tensile and compressive stresses in the link slabs according to (Nosewicz & Jong, 2009)

The force in the link slab is larger if the number of spans is larger. Assume $n \rightarrow \infty$, then the force in the flexible joint is equal to R_d , according to eq.(1). Nosewicz & Jong (2009) describe that according to the VOSB the maximum value for R_d is equal to 300 kN for class 60. Assuming an effective width of 4 m (Nosewicz & Jong, 2009), the maximum force in the link slabs is equal to 75 kN/m.

2.1.5 Analysis imposed deformations from spans

Nosewicz & Jong (2009) also analysed the behaviour of the link slab if it is exposed by imposed deformations. In reality, imposed deformation could be caused by deformations in the spans. Three different imposed deformations are taken into consideration; curvature due to curvature in the span, curvature in the link slab due to vertical deformations of the supports and horizontal deformations due to shortening of the spans. The three types of imposed deformations are discussed in more detail in this paragraph.

2.1.5.1 Curvature

First the influence of imposed curvature is discussed in more detail. According to Nosewicz & Jong (2009), curvature of the span causes rotations of the ends of the link slab. Curvature in the spans is mainly generated by:

- Vertical deflections caused by permanent loads
- Vertical deflection caused by traffic load
- Temperature gradients

Curvature in the link slab could be modelled to calculate the link slab. The proposed model for the link slab that is exposed to imposed curvature, is explained in some more detail here. In Figure 13 is shown a span that is curved. Assuming that the ends of the link slabs are fixed to the ends of the span, both the end of the link slab and the end of the spans have the same rotation at the connection.

In Figure 13 is also given a horizontal deformation u_x . The consequences of this horizontal displacement is taken into consideration in paragraph 2.1.5.3 Horizontal displacement.



Figure 13 – Curved simply supported bridge span

In Figure 14 is shown the scheme of a flexible joint. The joint is curved on both sides by φ_1 and φ_2 . As shown in the figure, the rotations at the end of the link slab could be split up in two beams; one beam with a two even large rotations $\left(\frac{1}{2} \cdot (\varphi_1 + \varphi_2)\right)$ and one beam with two contra rotations $\left(\frac{1}{2} \cdot (\varphi_2 - \varphi_1)\right)$.

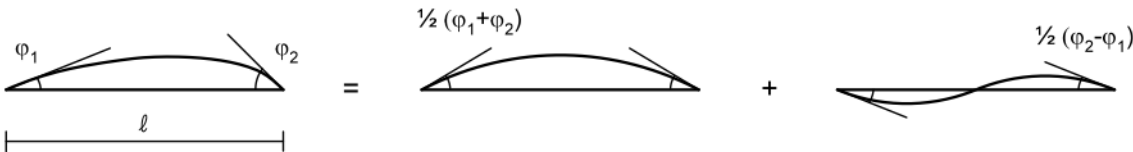


Figure 14 – Deformed link slab exposed to imposed curvature φ_1 and φ_2

The deflection of the beams, which are shown in Figure 14, can be modelled as a beam that is exposed to bending moments at the ends of the beam as shown in Figure 15. For two even curves at both ends of the link slab must work two even large bending moments, both in another direction (clockwise and anti-clockwise). A beam where both ends are curved in the opposite direction could be modelled as a beam that is exposed to two bending moments at both ends of the beam. Both bending moments work in the same direction as shown in the right picture of Figure 15.

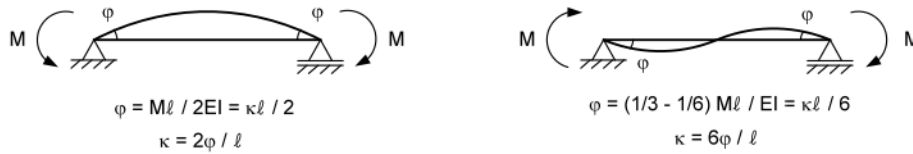


Figure 15 – Curvature in simply supported beam caused by bending moment

The curvature in the link slab could be expressed as a function of the working moment by applying some forget-me-nots. The bending moment can be expressed as a function of the curvature, $M = \kappa EI$. Then the curvature in the link slab at the ends of the joint ($\kappa_{\varphi_1}, \kappa_{\varphi_2}$) can be expressed as a function of the rotations at the end of the span (φ_1, φ_2), as shown in the equations below.

$$\kappa_{\varphi_1} = \frac{2 \cdot \left(\frac{1}{2} \cdot (\varphi_1 + \varphi_2)\right)}{L} - \frac{6 \cdot \left(\frac{1}{2} \cdot (\varphi_1 + \varphi_2)\right)}{L} = \frac{4 \cdot \varphi_1 - 2 \cdot \varphi_2}{L}$$

$$\kappa_{\varphi_2} = \frac{2 \cdot \left(\frac{1}{2} \cdot (\varphi_1 + \varphi_2)\right)}{L} + \frac{6 \cdot \left(\frac{1}{2} \cdot (\varphi_1 + \varphi_2)\right)}{L} = \frac{-2 \cdot \varphi_1 + 4 \cdot \varphi_2}{L}$$

If the bending moment is constant over the length of the beam, as shown in Figure 15 (left beam), the curvature over the length of the beam is also constant. Then in the middle of the beam the curvature is still $\frac{\varphi_1 + \varphi_2}{L}$.

For the right beam of Figure 15, the bending moment on the right is even large but in the other direction than the bending moment on the left, $M_{left} = -M_{right}$. If there are no other loads working on the link slab, then a linear distribution of the bending moment over the length of the beam could be expected. Then in the middle of the beam, the bending moment and also the curvature are equal to zero. Therefore, the curvature in the middle of the joint can be expressed as shown in eq.(2).

$$\kappa_{middle} = \frac{\varphi_1 + \varphi_2}{L} \quad \text{eq.(2)}$$

2.1.5.2 Vertical imposed deflection

In this paragraph is discussed the vertical imposed deflection, which is expected to work on the joint according to Nosewicz & Jong (2009). The vertical deflection is caused by deflections in the supporting blocks. Vertical deflections are mainly caused by:

- Dead load
- Traffic load

The idea of vertical displacement in supporting blocks is shown in Figure 16. In the left model of Figure 16 is schematically shown a joint that is exposed to a vertical deflection u_1 at the left support and u_2

at the right support. The model is split up in two other schemes; one with a constant vertical deflection over the length of the beam and one with a linear vertical deflection of the length of the beam, as shown in Figure 16.

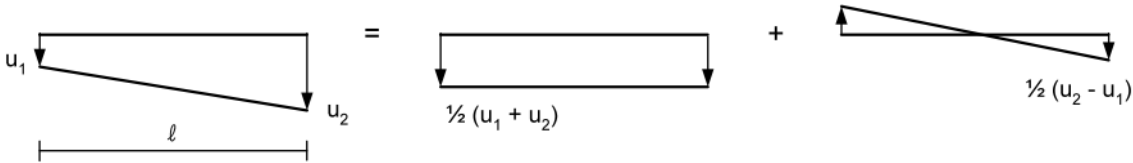


Figure 16 – Flexible joint that is exposed to imposed vertical deflections at the supports (Nosewicz & Jong, 2009)

In fact, if the vertical deflections at both supports is the same, then the vertical deflections at both ends of the joint is the same. In that case, no stresses that are caused by imposed vertical deformation are expected. However, stresses could be expected if both deflections differ.

In Figure 17 is shown a model of a flexible joint that is exposed to imposed vertical deformations at its supports. It is assumed that the imposed vertical deformations cause a vertical deflection difference, Δu , between both ends of the link slab. Further, the joint is modelled as a beam with two clamped supports at the ends. The right support is able to move vertically, to include the vertical imposed deformations. The clamped supports are assumed because:

- The joints are assumed to be fixed to the beams
- The vertical deflection is that small, that rotation in the span is assumed to be zero



Figure 17 – Joint that is exposed to imposed vertical deflection Δu

According to forget-me-nots, the curvature in the beam could be expressed as a function of the vertical imposed deformation, Δu , as shown in eq.(3).

$$\left. \begin{aligned} M &= \frac{6\Delta u \cdot EI}{L^2} \\ M &= \kappa EI \end{aligned} \right\} \kappa_{u1} = \kappa_{u2} = \frac{6\Delta u}{L^2} \quad \text{eq.(3)}$$

2.1.5.3 Horizontal displacement

In this paragraph is described the horizontal imposed deformation where the flexible joint could be exposed to. There are different reasons for horizontal deformations in a bridge or viaduct. Horizontal imposed deformations are mainly caused by shortening or elongation of the bridge deck, which could be caused by:

- Temperature reduction
- Shrinkage
- Preload
- Horizontal displacements as a result of curvature in the span (Figure 13)

Shortening in the bridge deck generates a reaction force in the supporting block. In Figure 18 are shown the horizontal reaction forces of the supporting blocks, that are caused by a constant shortening of

the bridge. In the figure are placed five columns where the supports are placed on at A until E. Upon every column are placed two supporting blocks. In the figure is only shown half of the total bridge. It is assumed that all supporting blocks have the same stiffness. Further, it is assumed that the middle of the bridge remains in place, because of symmetry in the bridge.

The load transfer system of the imposed horizontal deformation could be modelled according to the above mentioned assumptions. It is assumed that in the supports at the middle of the bridge (E) are not working any loads, because here is no imposed horizontal deformation. Then the reaction of the supporting blocks is zero as well. In the second supporting block at the left of the middle of the bridge (D_{right}), a certain horizontal reaction force is generated. Assuming the joint is very stiff, in the support block at the other side of the joint (D_{left}) is exposed to the same imposed deformations. So in this block is generated the same horizontal reaction force. In the next supporting block (C_{right}), is generated an imposed deformation, which is twice the imposed deformation that works on supporting block (D_{left}). Therefore, in block (C_{right}) a reaction force that is twice the reaction force in block (D_{left}) could be expected.

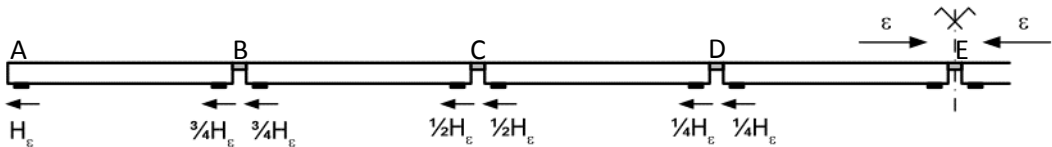


Figure 18 – Reaction forces in the supporting blocks caused by a constant shortening of the bridge

2.2 Deck Link Slab

In this chapter is discussed the deck link slab based on SHCC, that is described by Li, et al. (2003). The goal of the designed link slab is to provide a cost-effective solution, by developing a durable and maintenance-free SHCC link slab to create a jointless bridge decks. In de end, this SHCC joint acts similar to the NSC Flexible joint.

In this chapter, some SHCC characteristics and test results are discussed in more detail according to Li, et al. (2003). Only some interesting characteristics are given here. A general description of SHCC is given in Appendix 1: Literature study. After that, the design of Li, et al. (2003) is analysed. Next, the link slab design is discussed and some conclusions from the researach are presented. At last, some monitoring results of the link slab applied in Michigan, USA are given.

2.2.1 Strain Hardening Cementitious Composite (SHCC)

In this paragraph are given the characteristics of the SHCC that is applied in the link slab. The mixture that is applied in the link slab has a mean compressive strength of $f'_c = 60 MPa$ and a Young’s modulus of $E_c = 20 GPa$. First the mix design is shown. After that, some test results are presented to explain the tensile behaviour, shrinkage behaviour and the freeze thaw resistance of the material.

2.2.1.1 Mix design

The SHCC mix design that is researched is shown in Table 4. The ingredients are shown in the first row. In the second row are shown the amounts per ingredient. The proportions are given by weight. In the mixture is added a high amount of fly ash. The high amount of fly ash results in a mixture with a high flowability and low number of air voids.

Table 4 - SHCC mix proportions by weight (Li, et al., 2003)

Cement	Water	Sand	Fly Ash	SP	$V_{fibre}[\%]$
1.0	0.53	0.8	1.2	0.03	2.0

(SP: Superplasticizer)

2.2.1.2 Tensile behaviour

In this paragraph is given the tensile behaviour of the mixture that is described in the previous paragraph, chapter 2.2.1.1 Mix design. In this chapter are shown test results to describe the crack width behaviour, maximum tensile strain, tensile strength and the tensile strain capacity over time

In Figure 19 is shown the tensile stress and the crack width as a function of the strain of the researched SHCC mixture according to Li, et al. (2003). As shown in the figure, the maximum crack width is around 0.0022" ($\approx 0.05\text{ mm}$). In the figure are also shown the first cracking strength and the ultimate strength, which are equal to 580 psi ($\approx 4.0\text{ MPa}$) and 741 psi ($\approx 5.1\text{ MPa}$) respectively.

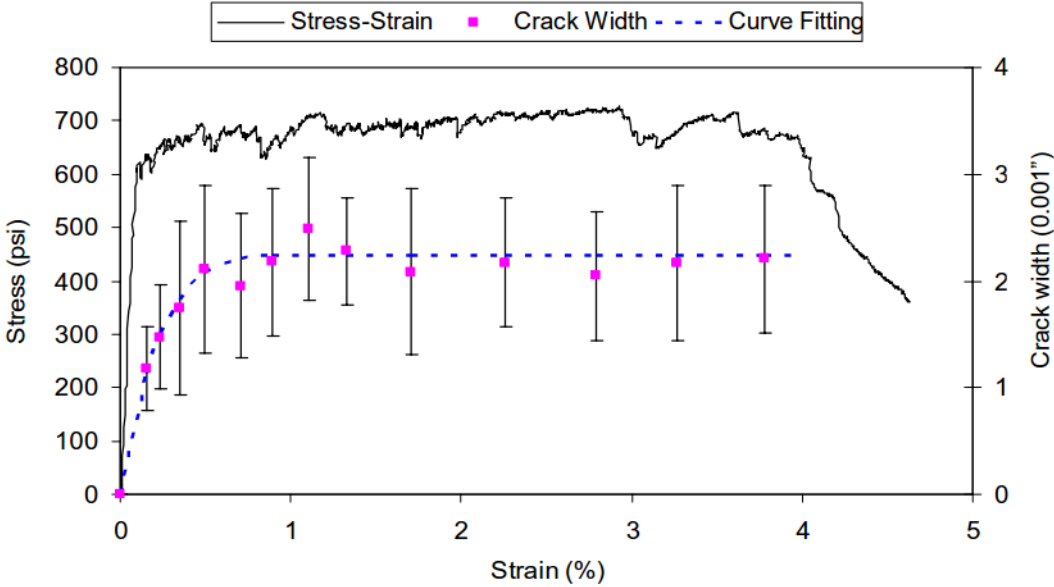


Figure 19 – Tensile stress and crack width as a function of the tensile strain of the reserached SHCC mixture (Li, et al., 2003)

One of the goals of Li, et al. (2003) is to create a durable link slab. Therefore , the SHCC should keep its tensile strain capacity over time. Test results of the strain capacity over time is shown in Figure 20. As shown in the figure, the tensile strain capacity of the researched SHCC decreases a lot in the first 28 days after casting. However, after 28 days, the strain capacity of the mixtures remains around 3.0%.

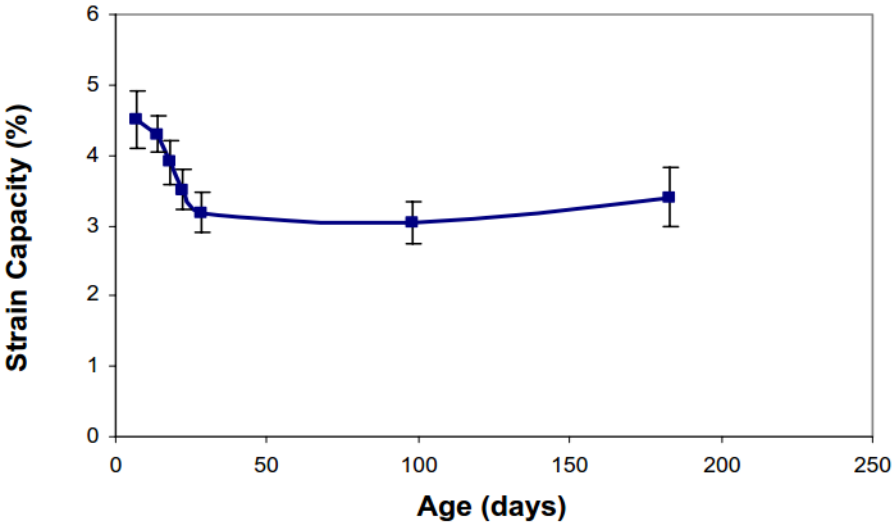


Figure 20 - Tensile strain capacity of SHCC over time

2.2.1.3 Shrinkage behaviour

In this paragraph is compared the shrinkage behaviour of SHCC compared to the shrinkage behaviour of concrete. To describe this behaviour, two different tests are done; tests to the free shrinkage and tests to the restrained shrinkage

Drying shrinkage of the SHCC mixture is found to be larger than for the concrete control specimen, as shown in Figure 21. This is mainly caused by the amount of cement and water, which is about twice as the amount of cement and water in the control concrete. However, outside the relative humidity is quite high. As shown in the graph of Figure 21, the total drying shrinkage difference between both, the control concrete and the SHCC is not that large yet.

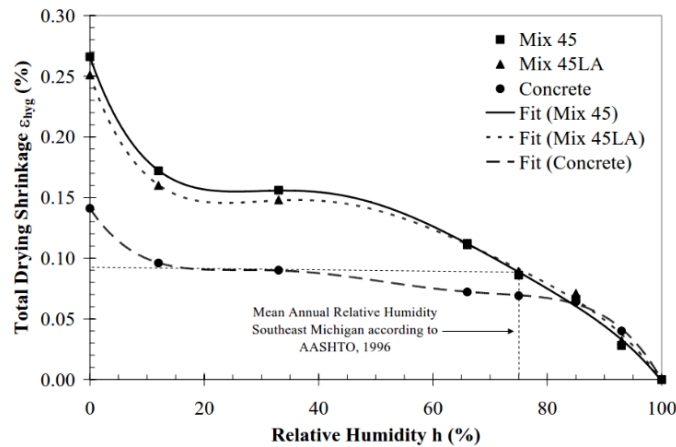


Figure 21 – Drying shrinkage of SHCC (mix 45 and mix 45LA) compared to concrete as a function of the relative humidity (Li, et al., 2003)

In Figure 22 is shown the crack width of a restrained shrinkage test as a function of the drying time. The graph shows that the crack width of SHCC (mix 45) due to restrained shrinkage is much smaller than for the control concrete, despite the drying shrinkage of SHCC is larger than for the control concrete as shown in the Figure 20 in the previous paragraph. This is caused by the cracking pattern. For the same test, in concrete only one crack arises, while in the SHCC ten cracks arise. Obviously, concrete with small cracks has a lower permeability than concrete with large cracks. So small cracks are favourable for the durability of the link slab. Combining the results of Figure 22 with the knowledge of the literature study the water permeability of cracked SHCC could be expected equal to the water permeability of uncracked SHCC, because of the very small crack width ($w_{crack} < 0.002mm$).

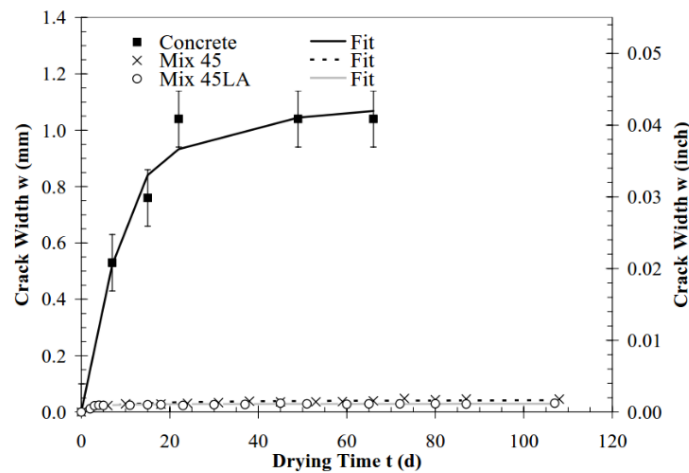


Figure 22 – Average crack width as a function of the drying time in restrained drying shrinkage test (Li, et al., 2003)

2.2.1.4 Freeze-thaw resistance

The link slab that is designed by Li, et al. (2003) should be placed in Michigan, USA. Because of the climate in Michigan and the durability requirements, the link slab should have a certain freeze-thaw resistance. Therefore, some tests were done to the freeze-thaw behaviour of the researched SHCC mixtures. The results of the test are presented in this paragraph.

Before the test results are presented, the mix designs of the NSC and SHCC are given. The mixtures that are included in this part of the research are shown in Table 5. Compared to the reference concrete, the SHCC mixtures (M34, M45 and M45 LA) have finer aggregate particles. Further, M45 and M45 LA has smaller aggregate particles than M34, bus less cement. The difference between M45 and M45 LA is the amount of alkali in the cement, what is in M45 LA lower than in M45.

Table 5 - SHCC and reference concrete mix designs according to Li, et al. (2003)

Mix no.	Cement	Gravel	Sand	Fly Ash	Water	Superplasticizer	Methyl Cellulose	PVA Fibre
M34	813	0	813	89	346	16	1	26
M45	561	0	449	673	327	14	0	26
M45 LA	*561*	0	449	673	327	14	0	26
Concrete	432	864	864	0	192	4	0	0

* low alkali cement

Dynamic modulus

In Figure 23 is shown the influence of the number of freeze-thaw cycles on the dynamic modulus of the materials that are given in Table 5. In the left diagram (a) are shown the absolute test results from the tests. In the right diagram (b) are given the relative values of the dynamic modulus. As clearly shown in both diagrams, the dynamic modulus of regular concrete is very sensitive for the number of freeze-thaw cycles compared to the SHCC mixtures. The dynamic moduli of both M34 and M45 are not influenced by the number of freeze-thaw cycles. The dynamic modulus of M45 LA is increased during the early portion of freeze-thaw exposure. Probably this is caused by the slightly different hydration rate of the low alkali content cement of M45 LA compared to the other mixtures. After approximately 120 cycles, the dynamic modulus of M45 LA is similar to the dynamic modulus of M45.

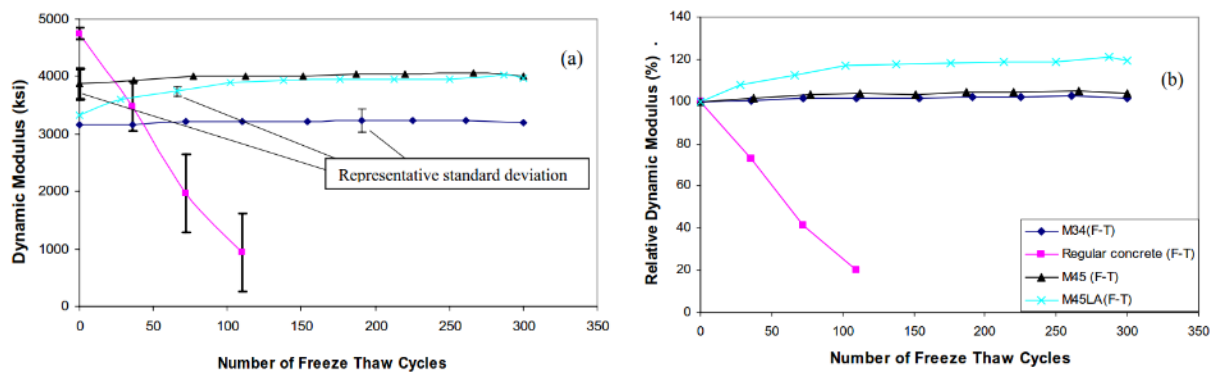


Figure 23 – Dynamic Modulus (absolute and relative) as a function of the number of freeze-thaw cycles (Li, et al., 2003)

Mass

Compared to regular concrete samples, the SHCC samples show less mass loss after the freeze-thaw tests. The average mass loss of the SHCC specimens after 300 cycles is about 0.9%. For the regular concrete, the average lost after 110 cycles is already 2.0% (Li, et al., 2003).

Tensile strain

The SHCC specimens retain much of their initial tensile ductility after the freeze-thaw experiments. After 300 cycles in 14 weeks, the SHCC specimens have an average ultimate strain capacity over 2.0%. This is close to the specimens of the same age that were not subjected to the freeze-thaw cycles, which have an average ultimate strain capacity of 2.5-3.0%

Compressive strength

The compressive strength of the SHCC specimens is reduced significantly after the freeze-thaw tests. The compressive strength of M45 and M45 LA is decreased 24% and 38% respectively, compared to the specimens that were hydrated in fog room curing conditions. Li, et al. (2003) mentioned two reasons for the reduction of the compressive strength, which are:

1. The specimens for compressive test failed primarily at the ends of the specimen. This may be the reason for the premature failure and low compressive strength.
2. Different maturity of the specimens that are hydrated in freeze-thaw conditions and fog room conditions.

2.2.1.5 Summary of characteristics

All test results are analysed above, so a summary of the characteristics of the SHCC applied by Li, et al. (2003) for the link slab is given here. In short, the main characteristics of the research SHCC mixtures are:

- High tensile strain compared to regular concrete
- Small crack width compared to regular concrete
- Larger total drying shrinkage compared to regular concrete
- Small crack width under restrained drying shrinkage compared to regular concrete
- Dynamic modulus of SHCC seems independent of the number of freeze-thaw cycles.
- Only minor loss of weight after 300 freeze-thaw cycles
- Only minor loss of tensile strain after 300 freeze-thaw cycles
- Significant reduction of compressive strength after 300 freeze-thaw cycles

2.2.2 Roofing paper

Li, et al. (2003) applied roofing paper in the active zone of the link slab to create a debonding zone. Probably, roofing paper has the right characteristics to make a debonding layer. However, no characteristics of the applied roofing paper is given by Li, et al. (2003). In literature, no mean characteristics of roofing paper are found. Therefore, no characteristics of roofing paper could be given here.

2.2.3 Design

In this chapter are discussed the designs that are suggested by Li, et al. (2003). First, some general modification on the link slab to improve the interface between the link slab and the deck are given. After that, the designs of the link slabs are described in detail.

2.2.3.1 Improvement of the interface

In this paragraph, the improvements of the interface that are suggested by Li, et al. (2003) are discussed. The improvement of the interface between the link slab and the NSC deck is a main point of attention in the research. To strengthen the interface, some design modification are done Li, et al.

(2003). Their design is compared to the conventional method to make a concrete link slab. In order to strengthen the interface, the next modification are suggested:

- Continuous longitudinal reinforcement through the interface
- Installing shear studs
- Additional concrete surface preparation

The proposed SHCC link slab design that includes interface zones, which is suggested by Li, et al. (2003), is shown in Figure 24. In the figure are shown two link slab. The upper design is an example of a concrete link slab with a debond zone, a lap splice and new reinforcement bars in the link slab. In the lower design is shown the link slab of SHCC. Compared to the upper design, a transition zone is made at the ends of the link slab. Shear studs are applied in the transition zone to connect the link slab to the steel girders. Because of the transition zone, the SHCC link slab design is a bit longer compared to the concrete link slab. The idea of the transition zone is that the stresses at the interface between the link slab and the deck are reduced and the strength of the interface is increased.

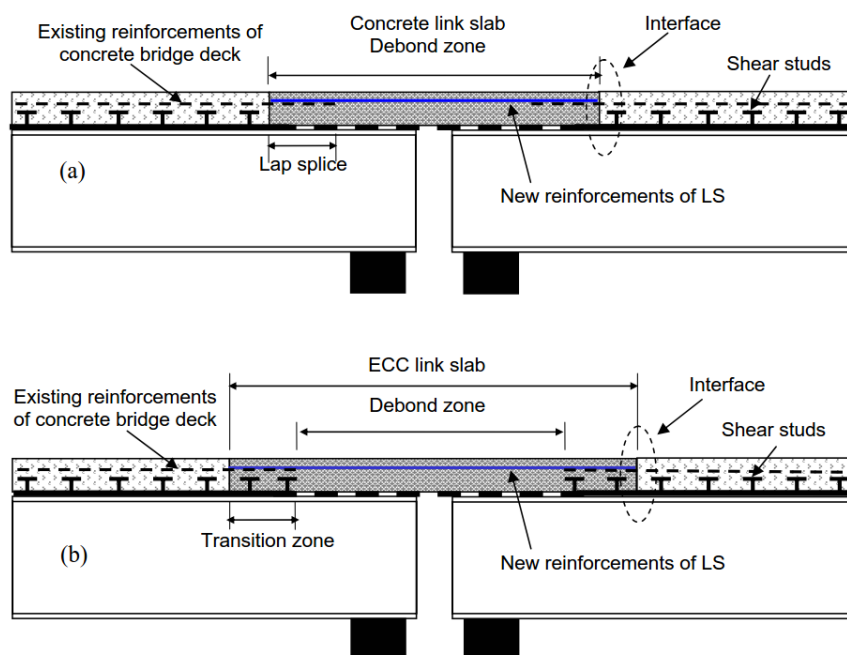


Figure 24 – Comparison between the interface of the conventional method (a) and the improved method (b) (Li, et al., 2003)

Before the new link slab design was casted, some experiments have been done by Li, et al. (2003) to:

- Determine the length of reinforcement in SHCC, by pull-out tests
- Determined the load capacity of a shear stud connection in SHCC, by a push-out tests

According to these tests, the optimum reinforcement length and number of shear studs could be chosen to create a well working transition zone. The results of the tests are shortly shown in Table 6. In the first column of this table are given the parameters that are researched. In the second column is given the tests that are done to research these parameters. In the last column are given the test results.

Table 6 – Experiments on the improved SHCC link slab design (Li, et al., 2003)

Unknown	Experiment	Results
Reinforcement length in SHCC	Pull-out test	<ul style="list-style-type: none"> - Reinforcement that is embedded in SHCC has comparable bond properties compared to reinforcement that is embedded in concrete, in terms of the peak load - With SHCC material as the surrounding matrix, there is no major difference between the pull-out behaviour of bare and epoxy-coated reinforcement. - Adoption of the AASHTO code is expected to be conservative for the design of reinforcement splicing in SHCC
Shear capacity of stud connection	Push-out test	<ul style="list-style-type: none"> - Failure modes are switched from brittle matrix failure in concrete specimens to ductile steel yielding in SHCC specimens. This results in a higher ductility of SHCC specimens at higher loads - With the exception of one specimen, SHCC specimens failed due to yielding and large deformation of the studs.

Interesting is the comparison between the load capacity of the tests and the load capacity that are calculated according to the AASHTO codes. The average peak load of the shear studs in SHCC according to the tests is 20-25% higher than the average peak load according to the codes. The difference between the codes and the tests is mainly due to the fact that the compressive strength is a main contributing factor in the AASHTO code, but the compressive strength is not relevant for failure of SHCC specimens.

2.2.3.2 Link slabs

After testing the shear capacity of the studs and the optimum reinforcement length in SHCC, two SHCC link slab designs have been made by Li, et al. (2003). The designs of the SHCC link slabs are discussed in the chapter. The cross section of these designs are schematically shown in Figure 25. The first link slab (Figure 25 (a)) is a reference link slab made of NSC. The debonded zone of the reference NSC link slab is created by roofing paper.

In the link slabs of the other two designs (Figure 25 (b) and Figure 25 (c)) is applied SHCC. In these designs is also applied roofing paper to create a debonded zone. The difference between the two SHCC designs are the reinforcement ratio and diameter of the rebars. In the bottom design (Figure 25 (c)), the new reinforcement bars in the link slab have a smaller diameter compared to the other SHCC link slab design (Figure 25 (b)).

Based on research of Caner & Zia (1998), the length of the debonding zone of the link slab is recommended to be equal to 5% of each girder span in order to reduce the stiffness of the link slab. The debond length of the test joints is about 1.27 m (50"). That means that the length of the span is about 24.1 m $\left(= \frac{1.27}{5} \cdot 95\right)$.

The dimensions of the design, which is shown in Figure 25, are given in inch. The exact dimensions in SI-units are given in Table 7. The three different link slabs are subjected to different tests. More details of the tests can be found in Li, et al. (2003). The conclusions from the tests are given in the next paragraph.

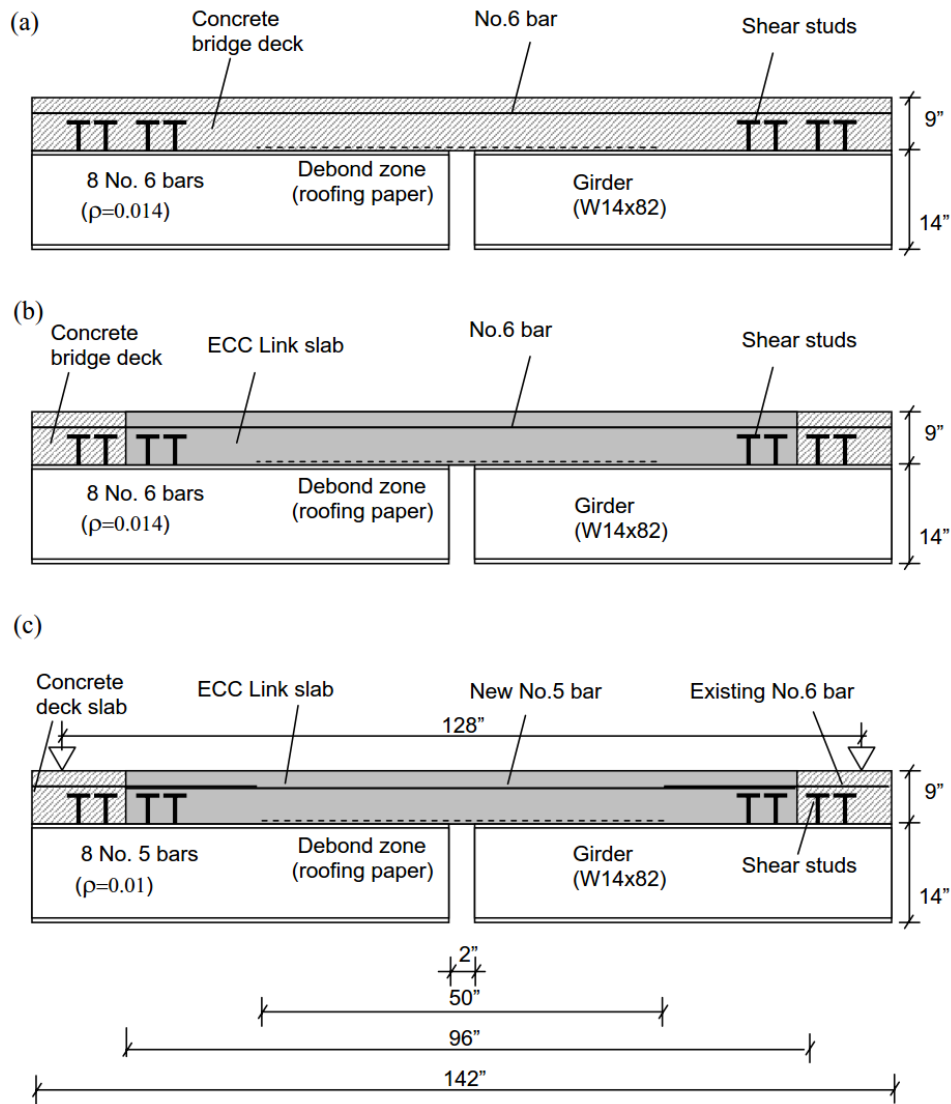


Figure 25 – Geometry of three link slab designs (Li, et al., 2003)

Table 7 – Dimensions of the link slabs from Figure 25 calculated to SI-units

Bar	Diameter [mm]	Area [mm ²]
No. 5 bars	15.875	200
No. 6 bars	19.05	284
Dimension	Length [inch]	Length [mm]
Gap between girders	2	25.4
Thickness concrete deck / link slab	9	228.6
Height girder	14	355.6
Length debonded zone	50	1,270.0
Length link slab	96	2,438.4
Total length	142	3,606.8

2.2.4 Test results and conclusions

In this paragraph are given the most important results and conclusions from the tests on the SHCC link slab designs that are shown in Figure 25 in the previous paragraph. All observations and conclusions are described here shortly according to Li, et al. (2003).

1. SHCC material shows a strain-hardening behaviour with tensile strain capacity of 3-5% accompanied by multiple cracking with crack widths smaller than 0.10 mm.
2. Monotonic test results revealed the compatible deformation mode of the SHCC link slab. Due to the high tensile ductility of SHCC, the matrix can deform compatibly with the reinforcement steel. Therefore, yielding of the reinforcement steel was delayed compared to the concrete matrix. Because the stress in the reinforcement is lower, less reinforcement is needed. A lower amount of reinforcement result in a lower stiffness of the link slab.
3. The cyclic tests that have been performed on three link slabs revealed that the stiffness of the three specimens remained unchanged during cyclic testing. However, the crack widths of the concrete link slab (0.025"=0.635 mm) at 100,000 loading cycles were substantially larger than those of the SHCC link slabs (< 0.002"=0.051 mm), by one order of magnitude (Figure 26). This suggests a better durability of the SHCC link slabs.

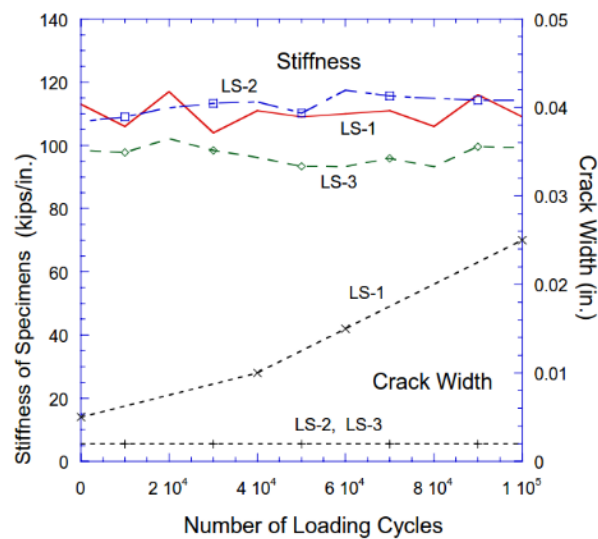


Figure 26 – Stiffness and crack width of link slabs as a function of the number of loading cycles

4. There was observed no cracking at the interface between the SHCC link slab and the concrete deck slab during cyclic testing, while cracking formed over the debonded section. This is caused by the addition of the passive section in the interface zone between SHCC and NSC.
5. Due to the low structural stiffness of the SHCC link slab, the link slab acts more like a hinge rather than a continuous element
6. Fatigue cracking resistance of SHCC link slabs, in terms of crack width, is independent of the reinforcement ratio because of the inherent multiple cracking and tight crack width control of SHCC.

2.2.5 Load transfer system for working loads and imposed deformations

In this paragraph are discussed the load transfer systems and models for the link slab, which is exposed to different actions. Schemes of the link slabs are made to determine the reaction of the link slab if it is exposed to vertical loads, horizontal loads, imposed curvature, vertical imposed deformation or horizontal imposed deformation. The transfer systems are modelled according to Li, et al. (2003) as much as possible.

Before the load transfer systems are discussed, first some material characteristics and in potential weak spots in the design are given here. In Table 8 are shown the material characteristics of the SHCC link slab according to Li, et al. (2003). The characteristics are just given to have a better feeling of the

SHCC that is applied in the link slabs. The construction of different link slabs is split in two phases, east and west. The data of Table 8 is based on the material that is applied in the west phase.

The bold printed values in Table 8 are according to Li, et al. (2003). The other values are derived from the bold values. The calculations of these values are given here shortly. The characteristic compressive and tensile stresses are calculated by the mean values and the standard deviations. This is shown in the formula of eq.(4).

$$f_k = f_m - 1.645 \cdot \sigma \quad \text{eq.(4)}$$

The values for the standard deviations of the compressive and tensile strength are given by Li, et al. (2003). The characteristic values of compressive and tensile strength are given in eq.(5) and eq.(6) respectively.

$$f_{ck} = f_{cm} - 1.645 \cdot \sigma \quad \text{eq.(5)}$$

$$f_{ck} = 53 - 1.645 \cdot 4.4 = 45 \text{ MPa}$$

$$f_{tyk} = f_{tym} - 1.645 \cdot \sigma \quad \text{eq.(6)}$$

$$f_{tyk} = 4.4 - 1.645 \cdot 0.26 = 4.0 \text{ MPa}$$

Table 8 – Assumed material characteristics of SHCC according to (Li, Lepech, & Li, Final Report On Field Demonstration of Durable Link Slabs for Jointless Bridge Decks Based on Strain-Hardening Cementitious Composites, 2005)

Characteristics	Symbol	Unit	
Average cylinder compressive strength	f_{cm}	[MPa]	53
Characteristic cylinder compressive strength*	f_{ck}	[MPa]	45
Design value cylinder compressive strength [@]	f_{cd}	[MPa]	29.4
Mean tensile yield strength	f_{tym}	[MPa]	4.4
Characteristic tensile yield strength [#]	f_{tyk}	[MPa]	4.0
Design tensile yield strength [@]	f_{tyd}	[MPa]	2.7
Mean tensile strain capacity		[%]	2.2
Elastic strain [§]	ε_t	[%]	0.1

* eq.(5);

@ $0.85 \cdot \frac{\text{characteristic value}}{\gamma_c}$, where $\gamma_c = 1.3$ (Japan Society of Civil Engineers, 2008);

eq.(6);

§ $\varepsilon_t = \frac{f_{tyk}}{E_c \cdot \gamma_c}$ (Japan Society of Civil Engineers, 2008)

It could be expected that cracks are generated in the link slab due to tensile stresses, for example caused by imposed deformation. Cracks normally arise at the weakest spots, at interface zones or the heaviest loaded zone. The link slab could be divided in a few zones if cracks are expected whether or not. The zones are given schematically in Figure 27. As shown in Figure 27, the zones the link slab could be separated in:

- A. **Active zone;** in this zone is expected the majority of cracks if tensile stresses are generated in the link slab. Tensile stresses could be generated if imposed curvature works on the link slab. The tensile stresses are probably the highest in the active zone, because the cross sectional area of the link slab is relative small and there is no collaboration with the substructure because of the deboning layer.
- B. **Interface between the active and the passive zone;** possible peak stresses could be generated here because of change in the geometry of the design.
- C. **The zone between the first dowels and the interface of the active zone and the passive zone;** the maximum tensile stresses in this zone could be expected to be as high as in the active zone, A, assuming that stresses are only transferred to the steel girders by shear studs. However, maybe in realty in zone C work shears stresses between SHCC and the steel girders what decreases the stress in zone C of the link slab.
- D. **Peak stresses in zone around the dowels;** especially the around the first row of dowels. Peak stresses could be expected here because the cross sectional area of the concrete here is reduced due to the shear studs.
- E. **Interface zone between the link slab and the NSC deck slab;** this interface can be expected as a weak spot because the connection between both materials is only carried by reinforcement bars. The tensile capacity of the connection that is carried by reinforcement only could be expected relative small compared to the other zones of the link slab.

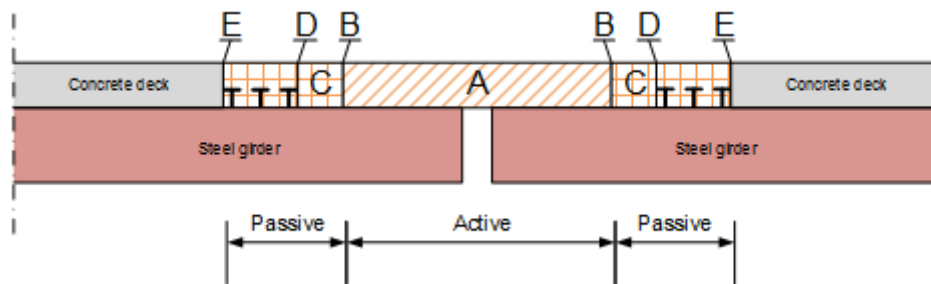


Figure 27 – Zones in the link slab design of Li, et al. (2003)

2.2.5.1 Vertical working loads

As mentioned paragraph, the thickness of the link slab is equal to 230 mm (9"). That means that the link slab has probably a certain load transfer capacity. Taking a closer look to the design in the cross sectional direction, the link slab should have some load transfer capacity to transfer the load in cross direction to the substructure of steel girders. The cross section view of the construction is shown in Figure 28.

According to Figure 28, it could be concluded that the SHCC joint work also as a deck slab to transfer the loads. The joint is supported by steel girders. Vertical loads on the link slab should be transferred to the steel girders, partly directly and partly by bending moments and shear stresses.

In Figure 28 is also given a detail of the cross section of the girders. According to the shape of the cross section could be concluded that the bending moment capacity in this direction could be neglected. So it is assumed that the girders can only work as a vertical support in this direction.

Table 9 – Dimensions of Figure 28 in SI-units

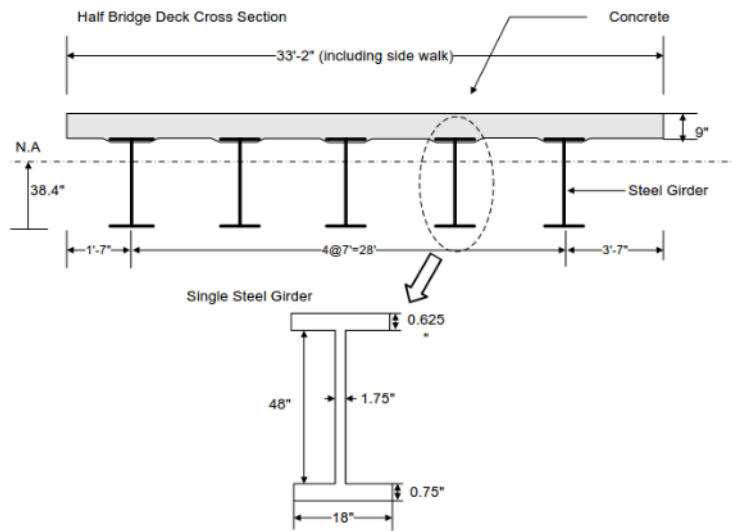


Figure 28 – Cross section of the bridge deck (Li, et al., 2003)

	Imperial Standard System [ft-in]	International System of Units [mm]
Total structure	33'-2"	10,109
	28'	8,534
	7'	2,134
	3'-7"	1,092
	38.4"	976
	1'-7"	483
	9"	229
Steel girder	0.625"	16
	48"	1219
	1.75"	44
	0.75"	19
	18"	457

According to the above mentioned analysis, the cross section of the link slab could be modelled as a beam on simple supports, as shown in Figure 29. As shown in the model, it is assumed that the moment capacity of the supports in the cross direction of the bridge could be neglected, such that the beams can be models as simple supports. The load of a wheel should be transferred to the supports through shear stresses and bending moments in the deck.

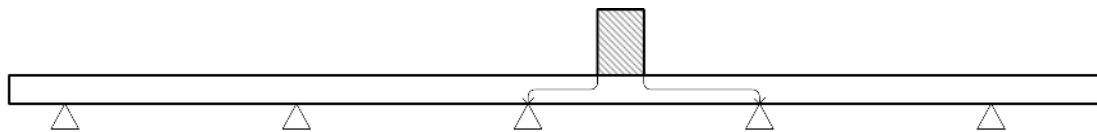


Figure 29 – Schematisation of the cross section of the bridge shown on Figure 28, with a wheel load

2.2.5.2 Horizontal working loads and imposed horizontal deformations

In this paragraph is come to a loading scheme to describe how horizontal loads working on the link slab are transferred to the substructure and how the link slab react on horizontal imposed deformations. The reaction of the link slab on both, horizontal loads and imposed horizontal deformations are not described by Li, et al. (2003). However, from the design could be argued the reaction of the link slab on both actions.

Horizontal imposed deformation

Analysing the design, the SHCC link slab has in fact no horizontal deformation capacity. If the SHCC is imposed to shortening (compression), it could deform in the order of a few per mille only. So shortening of the link slab could be neglected. Next to that, SHCC is not allowed to elongate. In the link slab is steel reinforcement included. Based on earlier research, Li, et al. (2003) limited the stress in steel reinforcement to 40% of the yield stress. The calculations below show that the deformation capacity in the link slab could be neglected.

Calculations are done to the maximum elongation in the link slab. In Figure 30 is shown the end of the link slab with extending steel reinforcement. This is the reinforcement that connect the link slab to the concrete deck. It is assumed that in the vertical plane, the SHCC Deck Slab and the NSC deck are

connected by reinforcement only. So here, the highest stress could be expected in the reinforcement. Further, the influence of the shear studs is neglected from reasons of simplicity.

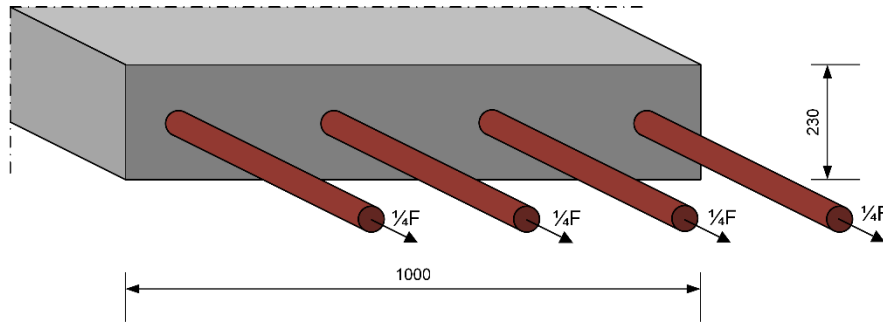


Figure 30 – End of the link slab with extending reinforcement

The maximum stress in the steel is $\sigma_{s,max} = 0.4f_y$ (Li, et al., 2003). This maximum stress is probably chosen in order to prevent fatigue failure of the reinforcement. The applied reinforcement steel has a yield strength of $f_y = 414 \text{ MPa}$ (Li, et al., 2003). The amount of reinforcement the NSC deck is $\rho_{NSC \text{ deck}} = 1.4\%$. The amounts of reinforcement in the two different SHCC designs of Li, et al. (2003) are; $\rho_1 = 1.4\%$ and $\rho_2 = 1.0\%$. It is assumed that Young's modulus of reinforcement steel is equal to $E_s = 20 \cdot 10^5 \text{ MPa}$. Then for $\rho = 1.4\%$ the maximum force that the reinforcement can introduce in the link slab per metre width is equal to:

$$F_{max} = A_s \cdot \sigma_{s,max} = \rho \cdot A_c \cdot 0.4 \cdot f_y =$$

$$F_{max} = 0.014 \cdot 230 \cdot 1000 \cdot 0.4 \cdot 414 = 533 \text{ kN}$$

The maximum force that is calculated above, is introduced in the link slab by the reinforcement steel. In the link slab, the maximum forces is carried by the SHCC and the reinforcement. Assuming the SHCC and steel work together and are in the elastic stage, the maximum elongation and deformation capacity in the link slab could be calculated as:

$$\varepsilon_{link \text{ slab},max} = \frac{F_{max}}{(EA)_{link \text{ slab}}} = \frac{F_{max}}{E_s \cdot A_s + E_c \cdot A_c}$$

$$\varepsilon_{link \text{ slab},max} = \frac{533 \cdot 10^3}{20 \cdot 10^5 \cdot 0.014 \cdot 230 \cdot 1000 + 20 \cdot 10^3 \cdot 230 \cdot 1000} = 4.83 \cdot 10^{-5} = 0.05\%$$

$$\Delta u_{max} = 4.83 \cdot 10^{-5} \cdot 1270 = 6.13 \cdot 10^{-2} \text{ mm}$$

The maximum strain is smaller than both, the maximum elastic strain of steel and SHCC. So the calculation method seems ok. This deformation capacity seems negligible. For a reduced amount of reinforcement in the SHCC Deck Slab, $\rho_2 = 0.01$, the maximum elongation and the deformation capacity of the link slab is equal to:

$$\varepsilon_{link \text{ slab},max} = 5.80 \cdot 10^{-5}$$

$$\Delta u = 7.36 \cdot 10^{-2} \text{ mm}$$

The elongation and deformation is a bit larger now, but could still be neglected. Reducing the steel reinforcement in the link slab further until zero, then the total force could only be carried by the SHCC cross section. The stress that works over the cross section in that case is equal to:

$$\sigma_{SHCC} = \frac{F_{max}}{A_c} = \frac{533 \cdot 10^3}{230 \cdot 1000} = 2.3 \text{ MPa}$$

The characteristic tensile strength of the mixture is used in order to check if the SHCC will crack. There are no safety factors applied for the load yet. However, as shown in the unity check below, the capacity of the strength is almost twice the maximum expected tensile load.

$$\frac{\sigma_{SHCC}}{f_{tyk}} = \frac{2.3}{4.4} = 0.53$$

Because the stress in the link slab probably stays under the cracking strength of SHCC, the strain in the link slab is expected to be smaller than 0.1%. That means that even if no steel is applied in the link slab, the maximum strain is only equal to $0.1\% \cdot 1270 = 1.27 \text{ mm}$. This horizontal deformation capacity seems negligible.

From the above mentioned calculations, it seems that the link slab has enough capacity to take care of horizontal stresses. SHCC then reacts elastically. Let assume that in the case that also an imposed curvature works, SHCC still has enough deformation capacity to rotate. Then for what reason reinforcement in the longitudinal direction is added to the link slab?

The basic of the design of the SHCC Deck Slab is a NSC Deck Slab. This NSC joint type should have a certain rotation capacity, to take care of imposed rotations. Therefore, reinforcement should be added to the tensile zone. The same amount of reinforcement is applied in the first design of the SHCC Deck Slab.

However, in order to investigate the influence of the reinforcement steel on fatigue, also slabs with a lower reinforcement ratio were researched. Tests show that the reinforcement ratio has no influence on the fatigue behaviour of the link slab if SHCC is used (Li, et al., 2003).

In the end, it seems that no longitudinal reinforcement is required in the link slab anymore. SHCC seems to be strong enough to take care of horizontal loads. Further, test shows that reinforcement has no influence on the fatigue behaviour of the link slab. However, in practice, reinforcement is applied. A reason for this could be that fibres can be every in the link slab in every direction. To reduce the risk on large cracks in the tensile zone where fibres could possibly be orientated in an inefficient way or that fibre are not even presented, reinforcement is applied. Another reason could be that longitudinal reinforcement has the main function to be practical reinforcement for the reinforcement in the transverse direction. In the transverse direction could be generated bending moments, what may result in a minimum amount of reinforcement in this direction.

Horizontal load

The SHCC link slab should have a certain horizontal strength in order to carry horizontal load caused by traffic or imposed deformations. The passive zone of the link slab is connected to the steel girders by shear studs. So horizontal stresses in the passive zone of the link slab could be transferred to the steel girders easily.

Between the active zone and the steel girders is created a debonding layer. The layer makes sure that there can't be generated horizontal friction forces between both in the cracking zone and the steel beams. Therefore, the active part of the link slab should be capable to transfer horizontal loads to the passive zone of the link slab by normal stresses. Normal stresses could result in compressive and tensile stresses in the link slab.

To explain the load transfer in the active part of the link slab, the active part could be modelled as shown in Figure 31. It could be expected that if a load F works in the middle of the beam, in both supports work a force of $0.5F$ in order to create horizontal equilibrium. Here it is assumed that the

tensile stress and compressive stress in the material are even. In practice, the compressive strength of SHCC is larger than the tensile strength. Therefore, for certain values of F , a high compressive strength in the link slab could be expected what result in a low reaction force the left support and high reaction force in the right support.

In reality, there will be a certain reaction force in the left support, because there is reinforcement steel in the slab. This reinforcement steel will also carry a part of the horizontal load. The exact distribution of forces should be researched in more detail.

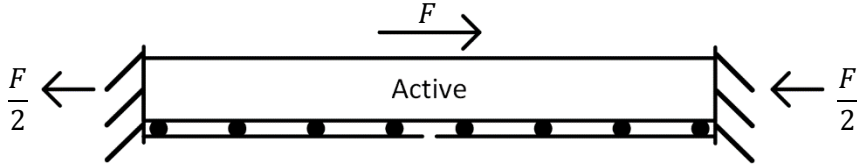


Figure 31 – Model for horizontal loads working on the active part of the link slab

A short calculation to judge the horizontal load capacity of the link slab is given here. As described earlier, the thickness of the link slab is equal to the thickness of the concrete slab, which both are equal to 229 mm (9"). As mentioned in chapter 2.1.3 Analysis to vertical loads on joint, the maximum force in the link slabs is equal to 75 kN/m if a distribution width of 4 m is assumed (Nosewicz & Jong, 2009). Then the maximum stress in the link slab is equal to $\frac{75 \cdot 10^3}{0.229 \cdot 10^6} = 0.33 \text{ MPa}$. This is significant lower than the tensile and compressive capacity of SHCC, which are $f_{tyd} = 3.0 \text{ MPa}$ and $f_{cd} = 32 \text{ MPa}$ respectively.

2.2.5.3 Imposed curvature

At last option, SHCC joints are exposed to imposed curvature from the bridge girders. In this paragraph is clarified the reaction of the joint according to imposed curvature in detail. First the joint design under imposed deformation is analysed theoretically. After that, some tests of Li, et al. (2003) are given. The theory then is validated to the experimental results. In case of imposed rotations in longitudinal direction, again cracks are expected at the weakest zone, at interface zones or the heaviest loaded zone, as mentioned before (Figure 27).

In Figure 32 is shown the situation where the link slab is exposed to an imposed deformation. The composite structure of the steel girders with concrete deck are curved, what result in imposed curvature to the SHCC link slab. The curvature in the beams is assumed to be relative low compared to the curvature in the link slab. Therefore, the composite girders are assumed to remain straight.

As mentioned earlier, the passive zones are assumed as clamped supports again. All together makes that the link slab will probably deform as shown in Figure 32. In the detail of Figure 32 are shown the working stresses in the link slab if it is deformed. In fact the imposed curvature is partly restrained by the link slab. Therefore, due to the link slab stresses are generated as a consequence of the imposed deformation. Because the link slab is curved and stretched, a bending moment and normal stress work in the link slab. Because the steel girder remains straight, probably a vertical peak stress is generated at the end of the girder. For vertical equilibrium, the same force should work at the end of the active zone of the link slab.

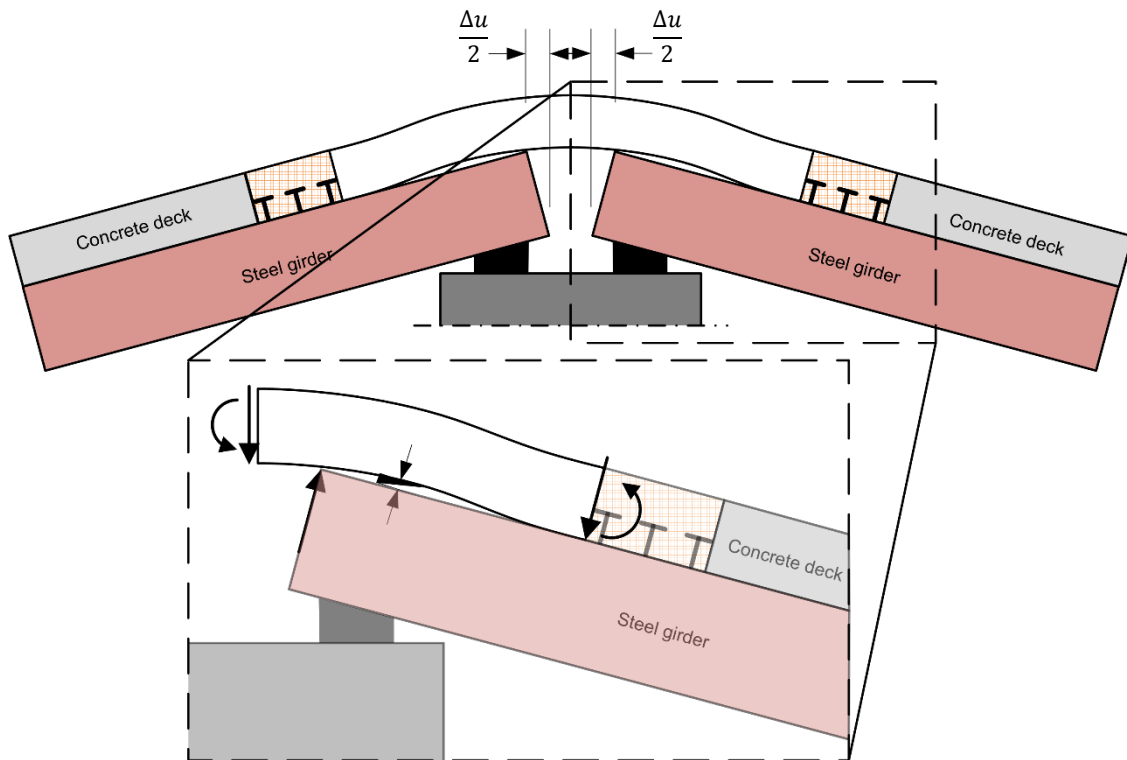


Figure 32 – Expected deformation of the link slab exposed to an imposed curvature from the steel girders

Theoretical model

Now a model of the link slab is made to determine the deformation that could be expected and to check the above mentioned hypotheses for the deformation. First the link slab is assumed to be a beam exposed to imposed deformation only. In Figure 32 is shown that a connection between the steel girder and the link slab is assumed at the end of the steel girder. From the model, the deflection of the link slab due to imposed curvature and the deflection of the steel girder is calculated to judge if there is indeed a connection between both at the end of the steel girder.

In fact, due to the curvature of the steel bridge, also a horizontal displacement Δu is generated. This horizontal displacement is restrained by the link slab, so normal stresses are generated in the link slab. These normal stresses can result in through cracks in the link slab. This phenomena is important to describe the crack pattern of the link slab. However, the mechanism behind is relative simple. Therefore, in the first steps the horizontal deformation due to curvature of the steel girders is not taken into account in the model.

If only an imposed curvature works on the link slab, the link slab could be modelled as a simple supported beam exposed to a constant bending moment over the length of the beam. A constant bending moment is assumed, because it is assumed that the imposed curvature in the beam is equally carried by the active part of the link slab. Therefore, two bending moments are applied on both supports, as schematically shown in Figure 33.

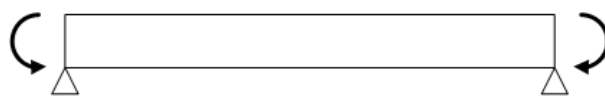


Figure 33 – Simply supported beam exposed to a constant bending moment

The vertical deflection of a simply supported beam exposed to a constant bending moment, as shown in Figure 33, can be described by a forget-me-not formula. The vertical deflection of a simply supported beam exposed to a bending moment at one of the supports, is a linear function of the bending moment, the stiffness and the length and a third order function of the place in the beam. This is shown in eq. (7), where the whole forget-me-not is given.

$$f = \frac{M}{6EI} \left(3x^2 - \frac{x^3}{l} - 2lx \right) \tag{eq.(7)}$$

The shape of the link slab that is modelled as a simple supported beam with a bending moment on the left or right support is shown in Figure 34 with the dotted blue and dotted orange line respectively. Adding both lines, results in the total deflection of the link slab exposed with a bending moment on the left and the right which are both even big. The summation of both are given by the black line that represents the deflection of the model from Figure 33.

The passive zone of the link slab is assumed to be fixed to the steel beams, as mentioned already. That means that the steel girder and the link slab has the same rotation at the place of the passive zone. So if the steel girders could move freely, they will deform like the yellow lines of Figure 34. The yellow lines have the same steepness as the black line has at the supports ($x = 0$ and $x = L = 3500$ mm).

As shown in Figure 34, the steel girders are situated above the link slab. In other words, if the steel girders could move freely, they deflect more than the link slab. However, in reality the steel girders are situated under the link slab. That means that there should be constant between the girder and link slab so there should be a reaction force between both the steel girders and the link slab.

Note: in reality the steel girders are curved a bit. However, the curve in the steel girders will only make the effect of the reaction force between the link slab and the steel girder bigger. Moreover, the curve in the steel girders could probably be neglected relative to the curvature in the link slab.

Deflection of steel girders and link slab due to imposed rotation of the steel girders

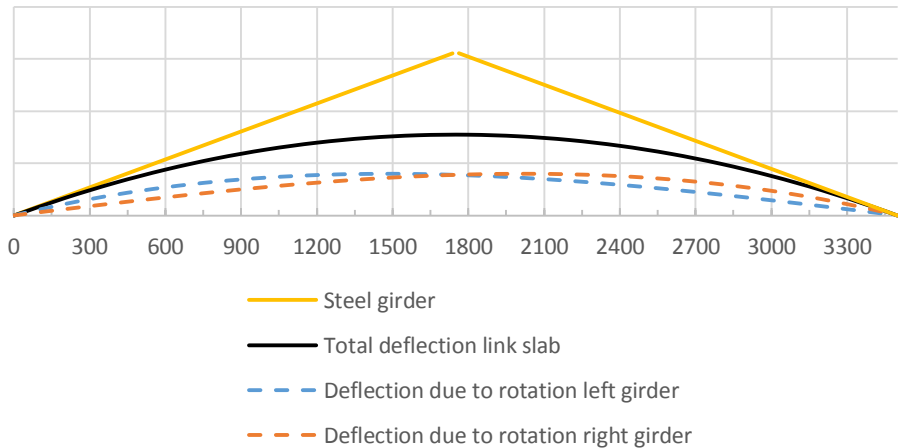


Figure 34 - Deflection of steel girders and link slab due to imposed rotation of the steel girders

Now, the imposed horizontal deformation caused by curvature of the steel girders can be added to the model easily. In fact, the model remains exactly the same, only normal stresses that are caused by the imposed deformation are added. There could be expected three possible effects of the additional normal stress. Even more cracks are generated due to the higher stress or wider cracks could be expected. Further, because of the tensile stress caused by the imposed deformation, the tensile zone will increase and the compressive zone will decrease. Assuming concrete under tension cracks, deeper cracks could be expected.

To make the model more quantitative, a few equations could be set up. Equations that should be valid for the total model are:

- At the ends of the active part of the link slab works a bending moment, shear load and normal load.
- The interaction between the link slab and the steel girder in the middle could be modelled as an upwards point load working on the link slab.
- The bending moment causes a curvature and vertical deflection over the length of the link slab
- The normal load only results in horizontal deflection.
- The point load in the middle causes a curvature and vertical deflection over the length of the link slab
- For the model, the vertical deflection at the middle of the link slab should be equal to the vertical deflection at the end of the steel girders:

$$(u_{ver}(F) + u_{ver}(M))_{link\ slab\ middle} = \theta_{steel\ girder} \cdot \frac{L_{link\ slab\ active\ section}}{2} \quad eq.(8)$$

- For the model, the rotation at the end of the link slab should be equal to the rotation of the steel girder:

$$(\theta(F) + \theta(M))_{link\ slab\ ends} = \theta_{steel\ girder} \quad eq.(9)$$

The total vertical deflection and the curvature in the link slab is shown in Figure 35. In the left part of the figure is shown the curvature and deformation caused by the point load F. In the right part, the same is done for a beam exposed to a constant bending moment. In the figure are defined the deflection and curvatures of eq.(8) and eq.(9).

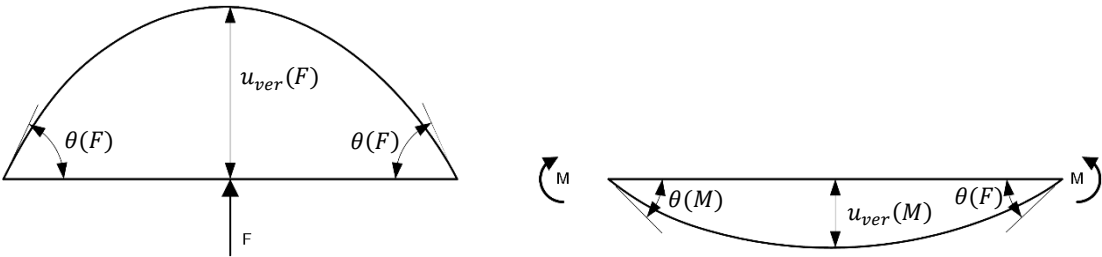


Figure 35 – Deformation of the link slab caused by point load F (left) and bending moments M (right)

Conclusion

From the above analysis, the place of three points of the link slab are known. These points are the ends of the active link slab and the middle of the link slab. These and some other conclusions from the above mentioned analysis are:

- The curvature at the ends of the link slab should be equal to the curvature to the curvature of the steel girders
- At the middle of the link slab/the ends of the steel girders; the underside of the link slab should be on the same height as the upside of the steel girder
- There should be a force from the steel girders that works the SHCC link slab upwards, because of geometry
- At the ends of the steel girders, a certain bending moment and shear force work
- Space could be created between the link slab and the steel girder due to the curvature of the SHCC link slab, while the steel girder remains straight

So it could be concluded that the link slab will probably deform as shown in Figure 32. At last, due to the deflection of the link slab, there could be some space between the link slab and the steel girder in the zone between the end of the steel girder and the beginning of the active zone. This is also shown in Figure 32.

2.2.5.4 Vertical imposed deflection

To analyse the reaction of the link slab according to vertical imposed deflection, the link slab is split up in two parts; the steel girders and the SHCC link slab. Both are only analysed over the active length of the link slab construction.

First the steel girders are analysed. In Figure 36 are shown two steel girders. One of the supports is settled down, as clearly shown in the detail. As shown in the figure, the steel beam can deform freely. Therefore no stresses are expected in the structure, or at least in theory. Further is assumed that the vertical settlement is very small compared to the length of the steel girder, such that the rotation in the steel girder can be assumed. In other words, the steel girder is assumed to remain horizontally. In fact, due to imposed vertical deformation, the steel girder simply moves in the vertical direction only, if the settlements are relative small compared to the length of the steel girder.

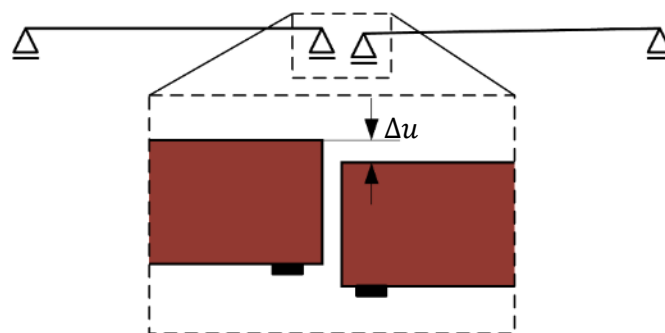


Figure 36 – Deflection of steel beams due to settlement in the supports

As second is analysed the SHCC link slab. As mentioned earlier, the passive part of the link slab is assumed to be fixed to the steel girder. So if the steel girder moves vertically, the passive part of the link slab will also move vertically. Neglecting the steel girders under the active section of the link slab for a while, the active part of the link slab could be modelled as a beam fixed on both sides as shown in Figure 37. In the same figure is also shown how the active section of the link slab deforms according to the scheme. According to the scheme could be concluded that the beam can't deform freely. Since

the beam has a certain stiffness, the bending moments and shear stresses are expected in the link slab according to forget-me-nots as shown in Figure 37.

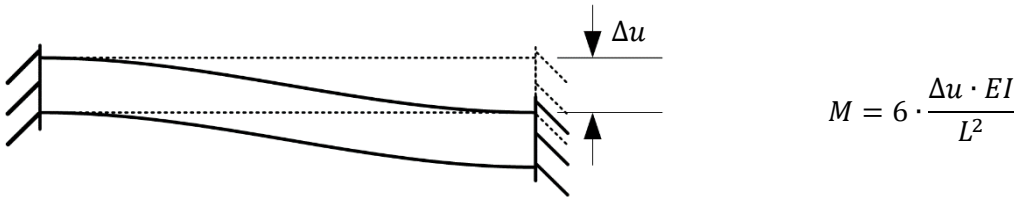


Figure 37 – Deflection of the link slab due to imposed vertical deformation

At last, the total model can be formed by combining both models of the steel girders and the SHCC link slab, as shown in Figure 38. Figure 38 shows that the SHCC link slab will deform under the steel girder, while in practice this is impossible. In practice, the steel girder pushes up the SHCC link slab or/and the SHCC link slab pushes down the steel girder.

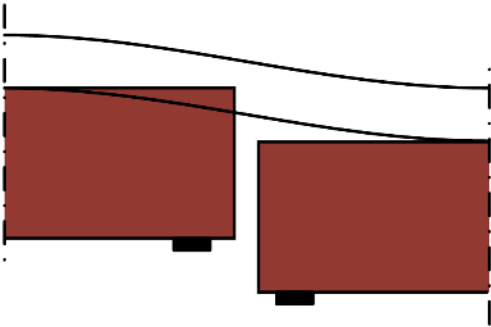


Figure 38 – Deflections of steel girder and SHCC link slab in one figure

The imposed deformation is introduced by one of the support under the steel girder. The support under the other girder remains in place, such that there is a certain different settlement between both supports. Both supports now are assume to remain in place after the settlement. To describe the deflection in the steel girder and the link slab, the stiffness and the moment of inertia of both is calculated as shown below.

The stiffness and the moment of inertia of the steel girder are:

$$\left. \begin{aligned} E_{steel} &= 200 \text{ GPa} \\ I_{steel \text{ girder}} &= 3.67 \cdot 10^8 \text{ mm}^4 \end{aligned} \right\} (EI)_{steel \text{ girder}} = 7.34 \cdot 10^{13} \text{ N/mm} \quad \text{eq.(10)}$$

The steel girder are situated every 2.1 m (7'). The stiffness and moment of inertia of the SHCC link slab over a width of 2.1 m is equal to:

$$\left. \begin{aligned} E_{SHCC} &= 20 \text{ GPa} \\ I_{SHCC} &= \frac{1}{12} \cdot 2.1 \cdot 10^3 \cdot 229^3 = 2.12 \cdot 10^9 \text{ mm}^4 \end{aligned} \right\} (EI)_{SHCC} = 4.25 \cdot 10^{13} \text{ N/mm} \quad \text{eq.(11)}$$

The flexural rigidity (EI) of the steel girder is almost twice the flexural rigidity as for the SHCC link slab. Compared to the steel girder and the link slab, the flexural rigidity of the composition of the concrete

deck slab and steel girder is assumed to be infinite. The flexural rigidity of the structure is shown in Figure 39.

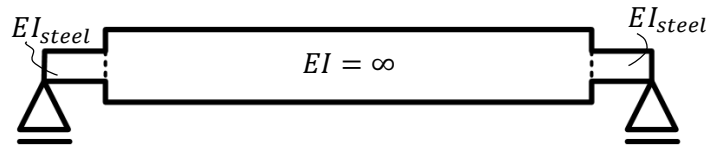


Figure 39 – Flexural rigidity of the span

From the geometry of Figure 39 could be concluded that the composite of steel and concrete does not deform or curve. So only the active section of the SHCC link slab and the ends of the steel girder can deform and curve.

The system of the link slab, the composite beam and the steel girder only are shown separately in Figure 40. The model of the active part of the link slab in Figure 40 is exactly the same as shown in Figure 37. The only difference is that the supports are replaced by bending moments and shear forces, which gives exactly the same deformation of the link slab. There should be bending moment and vertical equilibrium between the SHCC link slab, the composite of steel and concrete and the ends of the steel girders. That means that the bending moment and shear force in the composite beam is equal to the bending moment and shear forces in the link slab. The composite beam should also make equilibrium with the steel beam. That means that also in the steel beam works the same bending moment and shear force. This is schematically shown in Figure 40.

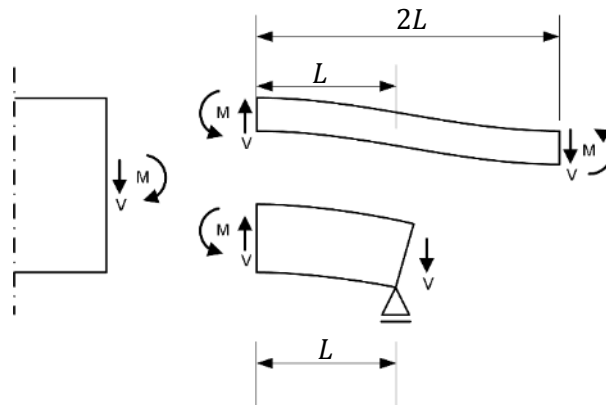


Figure 40 – Moment and shear force equilibrium between SHCC link slab, composite beam and steel beam

Note: for total equilibrium, at the other side of the composite beam should work the same bending moment and shear force. This is not shown in Figure 40.

For both, the steel girder and the SHCC link slab, the deformation could be determined. The deformation in the steel beam can be determined by eq.(12). The flexural stiffness of the link slab is half of the flexural stiffness of as shown in eq.(10) and eq.(11). The deformation in the steel part now can be expressed as a function of the flexural stiffness of SHCC, as shown in eq.(13).

$$\Delta u_{steel} = \frac{1}{3} \cdot \frac{M \cdot L^2}{(EI)_{steel}} \quad \text{eq.(12)}$$

$$\left. \begin{aligned} \Delta u_{steel} &= \frac{1}{3} \cdot \frac{M \cdot L^2}{(EI)_{steel}} \\ (EI)_{SHCC} &= \frac{1}{2} \cdot (EI)_{steel} \end{aligned} \right\} \Delta u_{steel} = \frac{1}{6} \cdot \frac{M \cdot L^2}{(EI)_{SHCC}} \quad \text{eq.(13)}$$

The deformation in the SHCC link slab over the total length ($2L$), can be determined according to the expression of Figure 37. The deformation of half of the link slab is expressed in eq.(14). Then the bending moment in the can be expressed as a function of the deformation in the link slab as shown in eq.(15).

$$\Delta u_{SHCC} = \frac{M \cdot (2L)^2}{6(EI)_{SHCC}} \rightarrow \frac{1}{2} \Delta u_{SHCC} = \frac{4}{12} \cdot \frac{M \cdot L^2}{(EI)_{SHCC}} = \frac{1}{3} \cdot \frac{M \cdot L^2}{(EI)_{SHCC}} \quad \text{eq.(14)}$$

$$\Delta u_{SHCC} = \frac{M \cdot (2L)^2}{6(EI)_{SHCC}} \rightarrow M = \frac{\Delta u_{SHCC} \cdot 6 \cdot (EI)_{SHCC}}{4L^2} \quad \text{eq.(15)}$$

The bending moment working in the SHCC link slab should be equal to the bending moment working in the steel beam. Eq.(13) and eq.(15) could be combined to eq.(16). As shown in the eq.(16), the expected deformation in the steel is a quarter of the deformation in the link slab.

$$\Delta u_{steel} = \frac{1}{6} \cdot \frac{M \cdot L^2}{(EI)_{SHCC}} = \frac{1}{6} \cdot \frac{\left(\frac{\Delta u_{SHCC} \cdot 6 \cdot (EI)_{SHCC}}{4L^2} \right) \cdot L^2}{(EI)_{SHCC}} = \frac{1}{4} \cdot \Delta u_{SHCC} \quad \text{eq.(16)}$$

At the connection between the link slab and the steel beam, the deformation in both the steel beam and the SHCC link slab is the same. According to eq.(16), the deformation at the steel girder is about a quarter of the deformation at the middle of the link slab. So the deflection of the steel girder due to the bending moment from the link slab is equal to a quarter of the deflection of the link slab. That means that there is steel an interaction between the steel and the link slab what cause additional stresses. The deflection in the connection could be expected as shown in Figure 41. As shown in Figure 41, a certain gap vertical between the link slab and the steel girder could be expected. To determine the real deflection of the connection, a more complex model should be used.

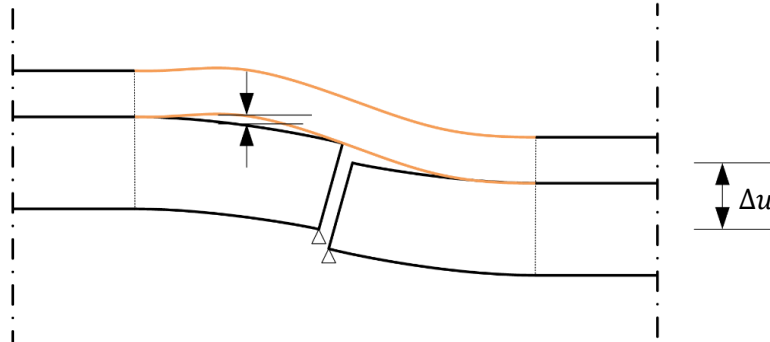


Figure 41 – Expected deflection of the Deck Link Slab exposed to a vertical deformation Δu

2.2.5.5 Experiments imposed curvature

In this paragraph, experiments according to imposed curvature that are done by Li, et al. (2003) are discussed. According to the tests the reaction of the link slab to impose curvature is described. The test results are analysed and compared with the exceptions from the model explained earlier in this paragraph. In Figure 42 is shown the test setup of the link slab that is exposed to an imposed curvature from the steel girders. During the test, the link slab first was exposed to monotonic pre-loading and then to cyclic loading.

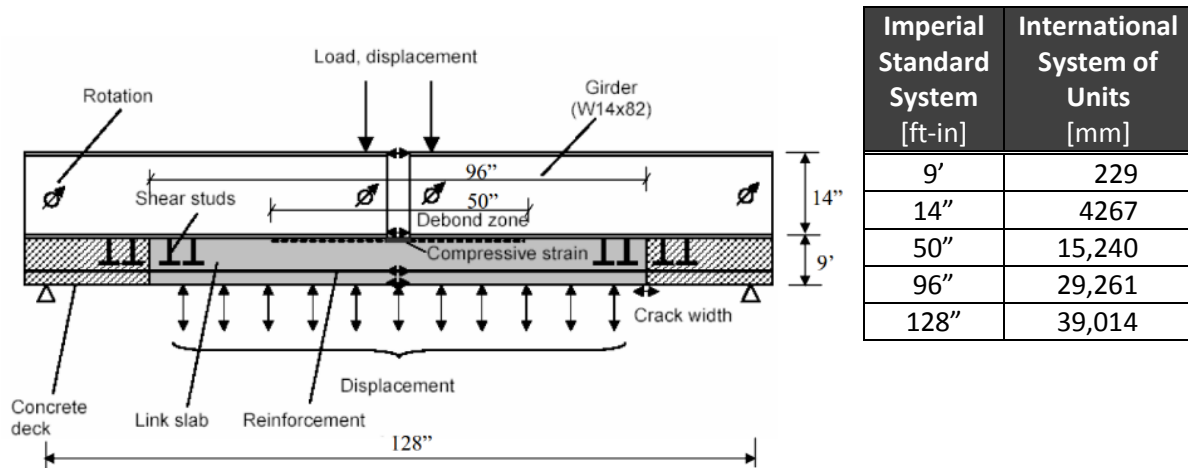


Figure 42 – Test setup of the link slab exposed to imposed curvature (Li, et al., 2003)

From the tests could made some conclusions according to the failure and cracking behaviour of the link slab exposed under imposed curvature. According to Li, et al. (2003), the next conclusions are made:

- There are micro cracks in debond zone Figure 43
- There are no cracks in the interface zone between NSC deck slab and SHCC link slab
- There are only a few cracks in the composite zone between the shear studs and the active zone

In the end, it could be concluded that the debonded zone probably prevents cracks at the interface zone between NSC and SHCC and in the bonded zone. Only in the interface zone between the active and the passive zone are still a few cracks in the passive zone. Therefore, the assumption that the link slab at the interface with the NSC remains in place in the model seems a good one.

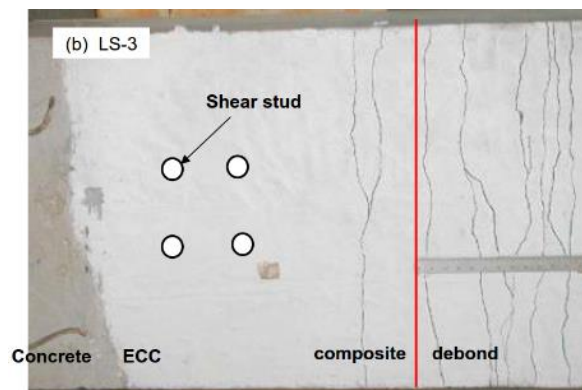


Figure 43 – Visual inspection of the link slab after testing (Li, et al., 2003)

The above mentioned conclusions are actually all the same as in the model. The only differences are that according to the model, the peak stress at the end of the steel girder was expected what is not mentioned in the test results of Li, et al. (2003) and no cracks were expected in the passive zone.

Maybe the rotation of the steel girders was too small to have large peak stresses between steel and SHCC at the end of the girder. There maybe was a peak stress, but not big enough to damage the link slab. Another reason could be that the priority of the research of Li, et al. (2003) was the interface zone, more than the contact zone between the steel girder and the link slab at the end of the girder. To be sure about the expected peak stress, maybe some more research should be done.

In Figure 43 are shown cracks in the passive zone, different from the model. The model is probably not exactly right. The question is how the cracks at the end of the passive zone can arise.

To clarify the cracks and the place of the crack in the passive zone, a more detailed analysis is done to the stresses working in the link slab, especially in the passive zone of the link slab. In fact, an analysis is done to the reason that there are no cracks in SHCC near the shear studs and to the reason that there are cracks in the passive zone near the interface with the active zone.

A slab exposed to an imposed curvature is, over the height of the cross section, partly loaded in tension and partly in compression. At the tension side, cracks are generated. As mentioned in paragraph 2.2.5.2 Horizontal working loads and imposed horizontal deformations already, in theory the tensile stresses from the link slab are transferred to the steel girders by the shear studs.

Assuming that stresses in the link slab is only transferred to the steel girders through shear studs, cracks could be expected near the shear studs. Here the loads that are caused by the imposed curvature are the same as in the active zone. However, the cross sectional area is reduced a bit due to the area of the shear studs, so peak stresses are expected. This is schematically shown in Figure 44, where a top view of a part of the link slab is given with the steel girders and shear studs in the detail of the figure is shown how the stresses goes around the shear studs, so a peak stress could be expected near the shear studs (Figure 43). However, test results show that there are no cracks near the shear studs. In other words, there should be another mechanism working in the passive zone, to explain the place where cracks are formed.

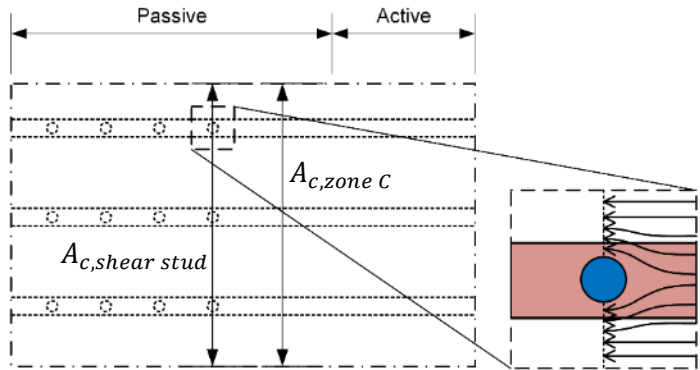


Figure 44 – Top view of SHCC link slab with detail of stress paths

The concrete material in the whole link slab is everywhere the same. Assuming as mentioned above the tensile stresses are only carried by the shear studs, peak stresses and cracks could be expected around the shear studs. However, the test results of Figure 43 show that cracks are near the interface and not near the shear studs. There could be two reasons for this:

- Friction between the SHCC and the steel girder, such that the peak stress near the studs is smaller than the cracking strength of SHCC
- Influence of longitudinal reinforcement in the passive zone, such that the crack strength increases due to composite working

Of course both reasons can work on the same moment. Then the crack pattern is caused by a combination of both, the friction between SHCC and steel and the longitudinal reinforcement.

Reinforcement is mainly effective if the concrete is cracked already. However, if there are no cracks in the concrete, there is still a certain composite working between the reinforcement and the concrete. A reinforcement bar needs a certain anchor length before it works properly. The reinforcement bar starts at the interface between the passive and active zone of the link slab. Because of the anchor length, it could be the case that the passive part of the link slab has enough tensile strength capacity at a certain distance from the interface between the active and passive zone.

Another explanation of the formation of cracks near the interface between the active and passive zone in Figure 43 is the friction between the SHCC and the steel girder in combination with the characteristics of SHCC. First the idea of friction is explained. Then the combination with SHCC is made to come to the total clarification.

The idea of friction between SHCC and steel is schematically shown in Figure 45. In the figure is shown the link slab exposed to imposed deformations (same as Figure 43), the schematic link slab design and the exposed tensile stresses in the link slab. In the diagram of the exposed tensile stresses are two lines. The red line represents the cracking strength of SHCC. Because cracks are caused by imposed deformations and the tensile strength capacity of SHCC remains constant if it cracks according to the tensile stress-strain relation (Japan Society of Civil Engineers, 2008), the actual stress in the active zone is in theory equal to the cracking strength of SHCC. The black line represents the exposed tensile strength that actually works in link slab. Both lines are qualitative graphs.

It is assumed that in zone A, the active zone, is not friction between the link slab and the steel girder. The tensile stress in zone A therefore remains constant. The zone with the shear studs, it is assumed that there is high friction between the link slab and the steel girder. Therefore, the tensile stresses in the link slab caused by the imposed curvature decrease significantly, while the generated bending moment of the whole cross section (SHCC link slab and steel girder) is the same as the moment generated by the imposed curvature in the link slab. Now the question is how big the tensile stresses in the interface zone, zone C, are.

Assuming there is a certain friction between the steel girders and the SHCC link slab in zone C, the graph of the actual working tensile stress could be drawn qualitatively as shown in Figure 45. In fact, in zone C there is a certain cooperation between the link slab and the steel girders. The friction here is probably smaller than in the zone with shear studs, but larger than zero. Since there is a cooperation between the steel and the concrete, the tensile stresses in the SHCC could be smaller than the cracking strength while the bending moment from the curved link slab could be resisted. So in theory, the actual working stress could be drawn as shown in the graph of Figure 45. In theory, the actual stresses in zone C are under the cracking strength of SHCC, so cracks are still not expected.

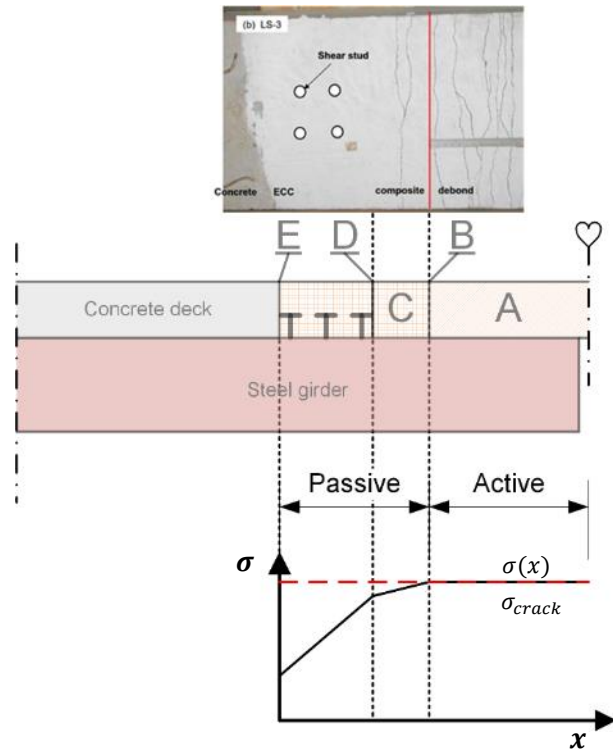


Figure 45 – Theoretical working stresses and tensile cracking capacity of the link slab structure

However, in reality, the SHCC characteristics differs a bit from the applied models. The tensile cracking strength of the SHCC is larger for higher tensile strains, as mention in paragraph 2.2.1.2 Tensile behaviour. In other words, SHCC has a certain strain hardening behaviour. Further, SHCC is an inhomogeneous material, so the tensile cracking strength is not the same everywhere. Both could explain why there are still some cracks at the end of zone C (near the active zone).

The first idea, strain hardening behaviour of SHCC, is schematically shown in Figure 46. The tensile strain in the active part of the link slab caused by imposed curvature is $\epsilon_{imposed}$. According to the recommendations of Japan Society of Civil Engineers (2008), the stress in the active part of the link slab is equal to σ_{crack} . Taking into consideration the strain hardening of the material, the tensile stress caused by an imposed deformation, $\epsilon_{imposed}$, is equal to $\sigma_{active,real}$. Assuming the strain hardening behaviour, $\sigma_{active,real} > \sigma_{crack}$.

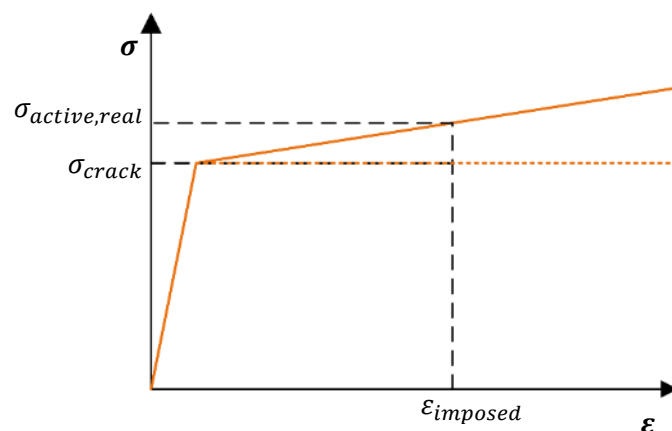


Figure 46 - Tensile stress-strain relations for SHCC with and without strain hardening behaviour

The stresses in the beginning of the passive zone (near the interface with the active zone) are more or less the same as is the active zone. The stresses reduce over the distance from this interface, due to the friction between the link slab and the steel girder. So the actual stress in the link slab can become lower than the cracking strength at a certain distance from the active zone. This is schematically show in Figure 47. As shown in the figure, until a certain distance from the interface between the passive and active zone, the actual stress is larger than the cracking strength of SHCC. This could be the reason that only a few crack are deform in zone C.

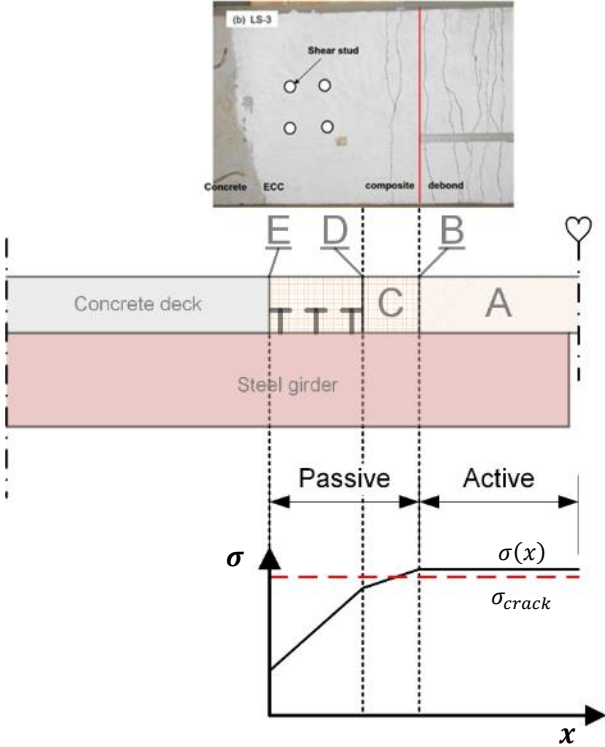


Figure 47 – Theoretical working stresses and tensile cracking capacity of the link slab structure, assuming SHCC has a strain hardening behaviour and that the imposed tensile strain in the link slab is higher than the cracking strain

Another explanation for the cracks in the passive zone is the inhomogeneous character of SHCC. Assuming the link slab behaviour of Figure 45, cracks in the passive zone near the interface with the active zone could be there because the SHCC at this part is some weak due to the inhomogeneity of the material. However, the chance that the weak spot in the SHCC is exactly near the interface zone in the passive zone of the link slab is probably low. So this explanation is in practice probably unlikely to occur.

Experimental conclusions and evaluation

The main conclusion from the experiments with the link slab is that there are a few cracks, so some movement, in the passive zone. However, in the model is estimated that the passive zone could be modelled as a clamped support. Since in the passive zone are a few cracks only, probably the assumption that the passive zone is clamed gives probably still realistic results.

In paragraph 2.2.5.3 Imposed curvature, is analysed that there could be a certain peak stress between the link slab and the steel girders caused by imposed curvature. However, in the tests is not paid any attention to this mechanism. Probably the curvature is that small that no significant load is generated or the phenomena is simply not taken into consideration during the tests.

Further, in the model of paragraph 2.2.5.3 Imposed curvature is assumed a certain bending moment that creates a compressive stress at the end of the active zone of the link slab. However, cracks were observed at the surface of the passive and active zone, so tensile stresses are generated here. So the expectation of the model of paragraph 2.2.5.3 Imposed curvature are against the test results. Probably the model does not describe the reality properly.

The interesting to analyse are the reasons that the model does not describe the situation from the test properly. Two reasons for this could be there; the tensile stress due to elongation has been underrated and compressive stress due to rotation has been overrated in the model. Elongation is not taken into account in the model or at least not in a proper way. Further, compressive stress that is expected according to the model at the surface of the link slab at the end of the active zone is probably a bit overrated.

Taking a closer look to the generation of tensile stresses, the geometry of the test setup should be analysed. The link slab is placed at the outside of the structure where the elongation due to rotation is the largest. So a relative small curvature results in a large elongation of the link slab. However, in the model this elongation is not even taken into account. According to the test result, this tensile stress is probably relative large compared to the tensile strength of the link slab.

Then the compressive stress in the link slab is probably overrated. The overestimation could be explained by the assumed flexural stiffness of the link slab and the connection between the passive zone and the substructure. However, no results of the stiffness and the connection are mentioned in the test results, so only some guesses could be done. The flexural stiffness of the link slab is probably that small, that the imposed deformation of the link slab is in such a way that no significant compressive stresses can be generated at the end of the active section. Further, maybe the connection between the passive zone and the substructure is worse than estimated, such that the passive section could curve a bit such that even less compressive stresses could be generated due to imposed deformation.

2.2.5.6 Conclusion

In the end, it seems that the SHCC Deck Slab that is designed by Li, et al. (2003) works more or less the same as the Flexible joint that is applied in the Netherlands a lot. In short:

- The link slab is able to carry vertical loads by bending moments and shear forces in the link slab.
- The active part of the link slab seems able to carry horizontal loads by normal tensile and compressive stresses in the link slab.
- The passive part of the link slab is connected to the steel girders, so can transfer horizontal loads by the studs to the steel girders.
- The link slab has a negligible horizontal deformation capacity due to the limited stress in the steel reinforcement.
- The link slab has a certain rotation capacity

2.2.6 Monitoring of the Grove Street Bridge and SHCC Link Slab

The SHCC link slab in the Grove Street Bridge is monitored periodically until 27 months after the bridge was opened for traffic. The monitoring is reported by Li, Yang, & Li (2008). In this paragraph, the results of the monitoring are shown briefly.

14 months after opening

According to Li, Yang, & Li (2008), the observations done 14 months after opening of the bridge are:

- The deterioration of the concrete surface was found to be much severer than that of the SHCC surface
- The SHCC link slab and the slab remained in a very good shape pretty much similar to the condition when the bridge was just completed.
- The crack width of the early age cracking was found to remain approximately 0.15 mm to 0.025 mm .

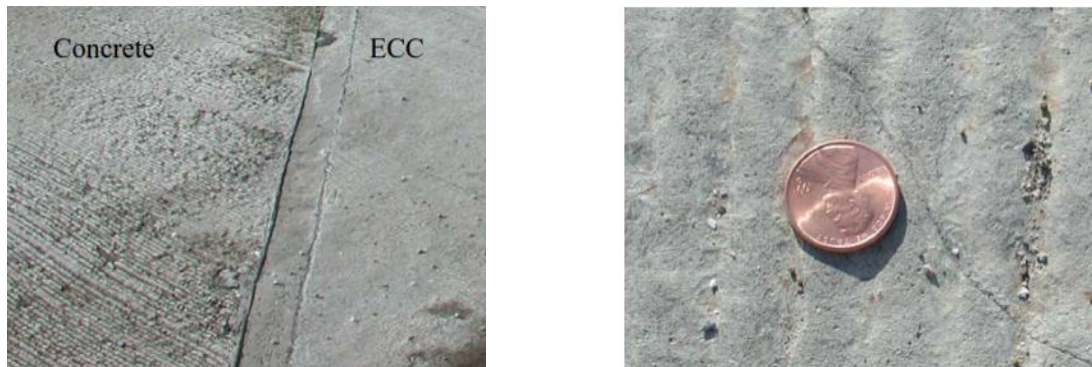


Figure 48 – Left: deterioration of concrete and SHCC surface, right: crack due to early age cracking (14 months) (Li, Yang, & Li, Field Demonstration of Durable Link Slabs for Jointless Bridge Decks Based on Strain-Hardening Cementitious Composites – Phase 3: Shrinkage Control, 2008)

21 months after opening

Here the observations after 21 months after the opening of the bridge are given. According to Li, Yang, & Li (2008), the observations done 21 months after opening of the bridge are:

- Crack width of early age crack within the SHCC link slab maintains approximately 0.15 mm to 0.025 mm (Figure 49)
- Cracking and spalling was observed in the adjacent concrete deck. The crack width is about half inch
- Severe cracking (dark colour area) was found in the sharp corner of the skewed concrete deck (Figure 49)



Figure 49 - Left: crack due to early age cracking, right: severe cracking at sharp corner of skewed concrete deck (21months) (Li, Yang, & Li, Field Demonstration of Durable Link Slabs for Jointless Bridge Decks Based on Strain-Hardening Cementitious Composites – Phase 3: Shrinkage Control, 2008)

24 months after opening

In this paragraph are shown the observations 24 months after opening. According to Li, Yang, & Li (2008), the observations done 24 months after opening of the bridge are:

- Crack width of early age crack within the SHCC link slab maintains approximately 0.15 mm to 0.025 mm (Figure 50)
- The crack width did not increase and in some cases cracks sealed with blackish colour material perhaps calcite mixed with dirt from traffic (Figure 50)



Figure 50 - Crack due to early age cracking (24 months) (Li, Yang, & Li, *Field Demonstration of Durable Link Slabs for Jointless Bridge Decks Based on Strain-Hardening Cementitious Composites – Phase 3: Shrinkage Control*, 2008)

27 months after opening

In this paragraph, the last mentioned observations are discussed. This observations are done 27 months after opening. According to Li, Yang, & Li (2008), the observations done 27 months after opening of the bridge are:

- The link slab has now been exposed to three winters of Michigan weather and the crack width remains unchanged.



Figure 51 - Crack due to early age cracking (27 months) (Li, Yang, & Li, *Field Demonstration of Durable Link Slabs for Jointless Bridge Decks Based on Strain-Hardening Cementitious Composites – Phase 3: Shrinkage Control*, 2008)

2.3 Cast in place and precast thin link slabs

In this chapter is discussed the research to link slabs for jointless bridge decks that has been done by Reyes & Robertson (2011). The aim of this chapter is to understand the design and the functioning of the link slab. To do so, first the characteristics of the SHCC mixture is explained in detail. After that three different link slab designs are shown. Then these designs are discussed according to

experimental data of Reyes & Robertson (2011). At last some general conclusions of the research are given.

2.3.1 Material characteristics

In this paragraph are described the characteristics of the materials that are applied in the design to the thin link slabs. First the mix design of SHCC is given. Then the main characteristics of Glass Fibre Reinforced Polymer (GFRP) bars, that are applied in the design are given. At last, some general information about plexiglass is given.

2.3.1.1 Strain Hardening Cementitious Composite (SHCC)

In this paragraph is discussed the SHCC that is applied in the research of Reyes & Robertson (2011). First the mixture is given in more detail. After that, the characteristics of SHCC are discussed a bit.

The applied mix design is given in Table 10. In the first column are shown the material that are in the mixture. In the second column are shown the amounts of materials, which are expressed as percentage by weight. As shown in the table, Portland cement, silica sand, fly ash and water are the main ingredients. In the report of Reyes & Robertson (2011) is not given any information about the production method of the SHCC, except the type of mixer that is used. Also no information of the characteristics of the applied SHCC mixture is given.

Table 10 – SHCC mixture percentage by weight (Reyes & Robertson, 2011)

Portland Cement	Water	#90 Silica Sand	Fly Ash	Polycarboxylic Ether (Admixture)	Methyl Cellulose (Admixture)	Polyethylene fibres
27.80%	15.00%	22.25%	33.33%	0.36%	0.03%	1.23%

Neglecting the fibres, the percentages of materials in the SHCC mixture by weight according to Reyes & Robertson (2011) are almost the same as for the SHCC mixture of Li, et al. (2003). The SHCC mixture of Li, et al. (2003), is shown in Table 11. Because the mixture of Reyes & Robertson (2011) is almost the same as the mixture of Li, et al. (2003) and the fact that no SHCC characteristics are given by Reyes & Robertson (2011), it is estimated that both mixtures have the same characteristics.

Table 11 – SHCC mixture percentage by weight neglecting fibres according to Li, et al. (2003)

Cement	Water	Sand	Fly Ash	SP
28%	15%	22%	34%	1%

2.3.1.2 Glass Fibre Reinforced Polymer (GFRP) reinforcement

Glass Fibre Reinforced Polymer (GFRP) Bars are used as longitudinal and transverse reinforcement in the SHCC link slab designs. According to Reyes & Robertson (2011), reasons to apply GFRP bars instead of steel reinforcement are:

- GFRP bars do not corrode
- GFRP bars have similar or greater tensile strength compared to reinforcement steel
- GFRP bars have a lower modulus of elasticity compared to steel rebars

2.3.1.3 Plexiglass

In this chapter is given a general overview of the characteristics of Plexiglas. Reyes & Robertson (2011) did not describe the characteristics of plexiglass which are applied to create a debonding layer. Therefore, the general characteristics of plexiglass that are given in this paragraph are assumed to be valid for the plexiglass that is applied by Reyes & Robertson (2011) as well.

The scientific name of plexiglass is polymethylmethacrylate (PMMA). In Table 12 is shown a general overview of the characteristics of plexiglass. As mentioned already, it is assumed that the applied plexiglass has similar characteristics as the characteristics that are given in Table 12.

The most important characteristics of plexiglass that are shown in Table 12 are highlighted green. These characteristics are discussed in some more detail here.

- As shown in Table 12, the tensile strength of plexiglass (70 MPa) is much higher compared to the tensile strength of the applied SHCC mixture (≈ 4.5 MPa). So if tensile stresses are generated by friction between SHCC and plexiglass, because of wrong functioning of the deboning layer, probably plexiglass remains intact while SHCC could fail.
- The plexiglass keeps its elastic tensile strength until 5% strain, what is the cracking strain of plexiglass. The cracking strain capacity of plexiglass is much higher than for NSC. So if NSC expand, the plexiglass is exposed to imposed deformation from the NSC. Then the NSC will fail before the plexiglass will fail.
- The Young's modulus of plexiglass is about 1.5 times the Young's modulus of SHCC. Young's modulus of plexiglass is comparable to the Young's modulus of NSC. So if a certain imposed deformation works on the concrete and plexiglass, in both materials work the same stress.
- The operation temperature of plexiglass is between -20°C and 80°C , what is probably within the limits of the minimum and maximum temperature where the bridge should serve in.
- The friction coefficient of plexiglass is about half of the friction coefficient of dry steel, what seems quite low. If the friction coefficient is lower, the debonding layer will serve better.

Table 12 – General overview of characteristics of plexiglass (polymethylmethacrylate)

Characteristic	Unit		Source
Specific weight	$[\text{g}/\text{cm}^3]$	1.19	(ThyssenKrupp Stokvis Plastics BV) (WSV Kunststoffen BV, 2015) (Proga plastics B.V., 2015)
Tensile strength	$[\text{MPa}]$	70	(WSV Kunststoffen BV, 2015) (Proga plastics B.V., 2015)
Cracking strain	$[\%]$	5	(ThyssenKrupp Stokvis Plastics BV) (Proga plastics B.V., 2015)
Young's modulus	$[\text{MPa}]$	3200 - 3300	(ThyssenKrupp Stokvis Plastics BV) (WSV Kunststoffen BV, 2015) (Proga plastics B.V., 2015)
Impact strength	$[\text{kJ}/\text{m}^2]$	10	(ThyssenKrupp Stokvis Plastics BV) (WSV Kunststoffen BV, 2015)
Notched impact strength	$[\text{kJ}/\text{m}^2]$	1.5-2	(ThyssenKrupp Stokvis Plastics BV) (Proga plastics B.V., 2015)
Indentation hardness	$[\text{MPa}]$	185-190	(ThyssenKrupp Stokvis Plastics BV) (Proga plastics B.V., 2015)
Maximum Operating Temperature	$[\text{°C}]$	80	(ThyssenKrupp Stokvis Plastics BV) (WSV Kunststoffen BV, 2015) (Proga plastics B.V., 2015)
Minimum Operating Temperature	$[\text{°C}]$	-20	(ThyssenKrupp Stokvis Plastics BV) (WSV Kunststoffen BV, 2015)
Linear expansion coefficient	$[\text{mm}/\text{m}/\text{°C}]$	0.07	(ThyssenKrupp Stokvis Plastics BV) (WSV Kunststoffen BV, 2015) (Proga plastics B.V., 2015)
Moisture absorption	$[\%]$	0.3	(ThyssenKrupp Stokvis Plastics BV) (Proga plastics B.V., 2015)

Friction coefficient relative to dry steel	[-]	0.55	(Proga plastics B.V., 2015)
--	-----	------	-----------------------------

2.3.2 Design

In this paragraph are discussed the link slab designs that are made and tested by Reyes & Robertson (2011). Reyes & Robertson (2011) made three different designs. The three designs are analysed and described in this paragraph, in order to understand load transfer system of the link slab. For every design is made one specimen, so in total, three specimens were made which were all tested. The three specimens are:

1. Cast-in-place SHCC link slab
2. Precast SHCC link slab that is dowelled horizontally and vertically
3. Precast SHCC link slab that is dowelled vertically only

In Figure 52 is schematically shown the general design of the specimen, which is supported on a concrete deck. The concrete deck is supported by steel beams. As shown on the design, every specimen has a 1 foot (0.31 m) bonded and a 6 feet (1.83 m) debonded section. The idea is that cracks develop in the deboned zone only. In the figure are also shown GFRP rebars that extend from the link slab to create a connection with the reinforced normal strength concrete.

As mentioned, Glass Fibre Reinforced Polymer (GFRP) is applied as reinforcement material instead of reinforcement steel. The most important reasons that GFRP bars are applied in the design according to Reyes & Robertson (2011) are:

- GFRP is non-corrosive, what increases the durability of the reinforcement compared the steel rebars.
- GFRP has an equal to or greater than the tensile strength of structural steel.
- GFRP can be used in most of the same applications as steel.
- GFRP has a much lower modulus of elasticity than steel. This means that a lower tensile force is needed to deform the bars such that the micro cracks are able to develop. For the application of jointless bridge decks, because higher elongations are expected, the unbonded length of the link slab must have an adequate length to reduce the strain in the concrete to remain within the elastic region of the GFRP bars.

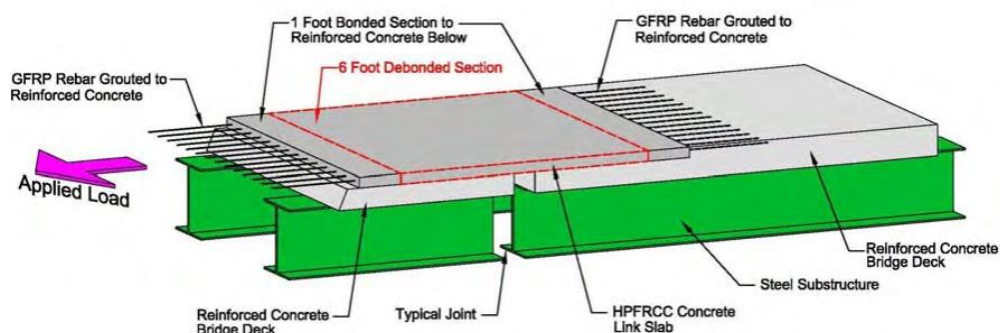


Figure 52 – Specimen frame diagram

2.3.2.1 Specimen 1

The first specimen is a cast-in-place link slab. One advantage of using a cast-in-place link slab is that the GFRP bars of the link slab are well bonded to the reinforced concrete and hooked bars can be used in the bonded section. An impression of the first specimen is shown in Figure 53. In the figure are shown the existing concrete deck and the reinforcement of the link slab.



Figure 53 – Impression of the cast in place SHCC link slab, specimen 1

The details of the reinforcement configuration are shown in the schematically top view on Figure 54. Unfortunately, in the figure the transverse reinforcement is not shown. More details of the reinforcement can be found in Table 13. As given in the table the reinforcement in the transverse direction is the same as the reinforcement in the longitudinal direction. In Table 13 are shown also the width and the thickness of the specimen.

To create a bonded section, the bond strength between the NSC and the SHCC should be as high as possible. Therefore the NSC at the bonded section is roughened, before the link slab is installed. Further steel anchor hooks are placed in the bonded zone for an even better connection between the link slab and the NSC. The advantage of the cast-in-place link slab is the good bonding between SHCC and the hooked bars.

Between the link slab and the reinforced concrete in the debonded section is placed a layer of plexiglass. This should ensure a smooth surface, such that the link slab can move freely in horizontal direction if it is exposed to horizontal stresses or horizontal imposed deformations.

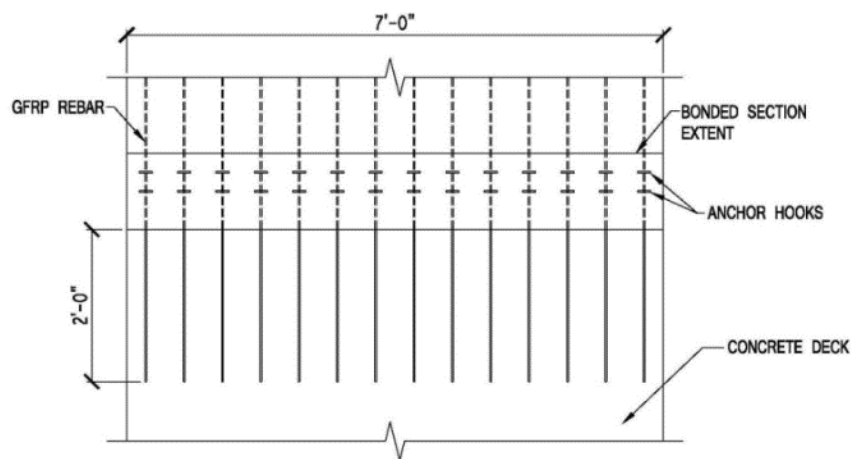


Figure 54 - Top view of specimen 1 with GFRP rebars and steel anchor hooks

Table 13 – Dimensions link slab and reinforcement of specimen 1

Dimensions	US size	Dutch size [mm]
Width link slab	7'-6"	2,290
Thickness link slab	3"	76
<i>Longitudinal and transverse reinforcement</i>		
Longitudinal length GFRP bars extending the formwork	2'-0"	610
GFRP bars	#3	9.5 (diameter)
Centre-to-centre	6"	152
Steel anchor hooks	#3	9.5 (diameter)

2.3.2.2 Specimen 2

The second specimen is, unlike specimen 1, a precast link slab. This variant is more appropriate for reconstructions and renovations rather than new constructions, because SHCC has a long setting and curing time. An impression of the precast slab is shown in Figure 55. In this figure is shown the reinforcement and formwork during casting the concrete in the fabric.



Figure 55 – Impression of the precast link slab, specimen 2

An overview of the positions of the reinforcement rebars and the dowels are shown in the top view of Figure 56. In the figure is also shown the extended longitudinal reinforcement. The longitudinal reinforcement is grouted into the reinforced concrete deck if the precast slab is placed in its final position. The dimensions of the link slab, the reinforcement bars and the dowels are shown in Table 14.

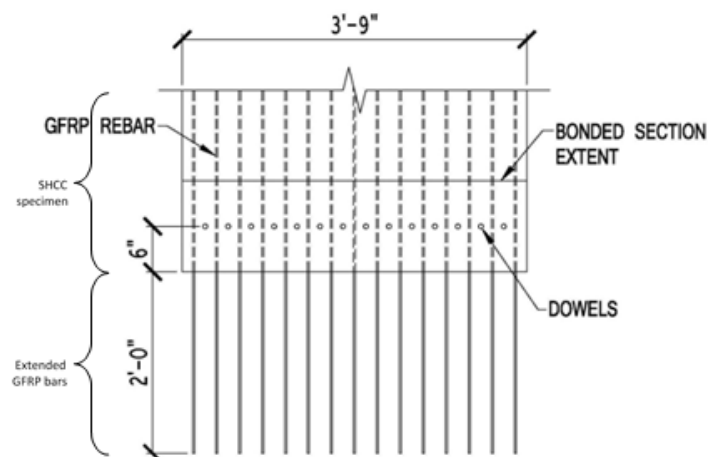


Figure 56 – Top view of specimen 2 with GFRP rebars, anchor and steel dowels

Table 14 - Dimensions link slab, reinforcement and dowels of specimen 2

Dimensions	US size	Dutch size [mm]
Width link slab	3'-9"	1,143
Thickness link slab	3"	76
<i>Longitudinal GFRP reinforcement</i>		
Length GFRP bars extending the formwork	2'-0"	610
GFRP bar diameter (longitudinal direction)	#2	6.4
Centre-to-centre (longitudinal direction)	3"	76
<i>Transverse GFRP reinforcement</i>		
GFRP bar diameter (transverse direction)	#2	6.4
Centre-to-centre (transverse direction)	6"	152
<i>Steel Dowels</i>		
Length dowels	6"	152
Dowels diameter	#4	12.4
Centre-to-centre dowels	3"	76

Specialty in specimen 2 is that it is precracked before it is installed. Cracks are generated by a constant bending moment that is applied on the slab as shown in Figure 57 (four point bending load). Micro cracks, that are generated by precracking, allow some compressive strain capacity during service life. The precracking is done in the middle 6'-0" ($\approx 1.8\text{ m}$), which is the unbonded section of the link slab. The average stain in the specimen due to precracking is equal to $\varepsilon_{precrack,II} = 0.107\%$. In theory, the link slab could be compressed 0.107% without generating any stresses in the slab. However, in practice the concrete particles will probably not move back to its original positions. Compressive stresses will probably be generated from a compressive strains lower than 0.107%.

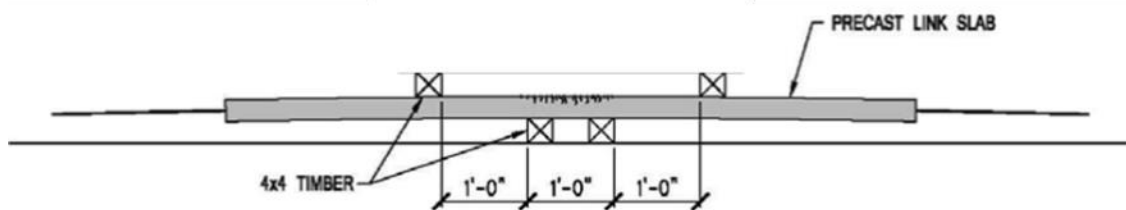


Figure 57 – Precracking setup for specimen 2

The bonding between the SHCC and the concrete at the bonded section is generated by dowels and longitudinal GFRP bars, as shown in Figure 56. In total there are placed fourteen steel dowels in a row in transverse direction. The dowels have a length of 6" ($\approx 152\text{ mm}$) and are embedded about 3" ($\approx 76\text{ mm}$) into the reinforced concrete. The longitudinal GFRP bars are horizontally doweled 2'-0" ($\approx 610\text{ mm}$) into the reinforced concrete. At last, the reinforcement concrete is roughened and bonded by grout to increase the bond strength even more.

2.3.2.3 Specimen 3

The last link slab variant that is designed and analysed in the research of Reyes & Robertson (2011) is also a precast link slab. As shown in Table 15, the design of specimen 3 is almost the same as specimen 2. The difference between both specimens is the design of the bonding section. In specimen 3, the reinforcement in the link slab stops at the end of the link slab, while in specimen 2 the reinforcement in the link slab ends in the reinforced concrete deck. To make a proper debonded zone, in specimen 3 are applied more dowels than in specimen 2 (21 instead of 14), as shown in the top view on Figure 58. Also the positions of the dowels are different in this design compared to the design of specimen 2. At last, specimen 3 is constructed in the same way as specimen 2.

Table 15 – Dimensions link slab, reinforcement and dowels of specimen 3

Dimensions	US size	Dutch size [mm]
Width link slab	3'-9"	1,143
Thickness link slab	3"	76
<i>Longitudinal reinforcement</i>		
GFRP bar diameter (longitudinal direction)	#2	6.4
Centre-to-centre (longitudinal direction)	3"	76
<i>Transverse reinforcement</i>		
GFRP bar diameter (transverse direction)	#2	6.4
Centre-to-centre (transverse direction)	6"	152
<i>Dowels</i>		
Length dowels	6"	152
Dowels diameter	#4	12.4

Further, specimen 3 is precracked in the same way as specimen 2. However, the average strain due to precracking in specimen 3 is higher than in specimen 2. The strain in specimen 3 due to precracking is equal to $\varepsilon_{precrack,III} = 0.171\%$, while in the strain in specimen 2 was $\varepsilon_{precrack,II} = 0.107\%$.

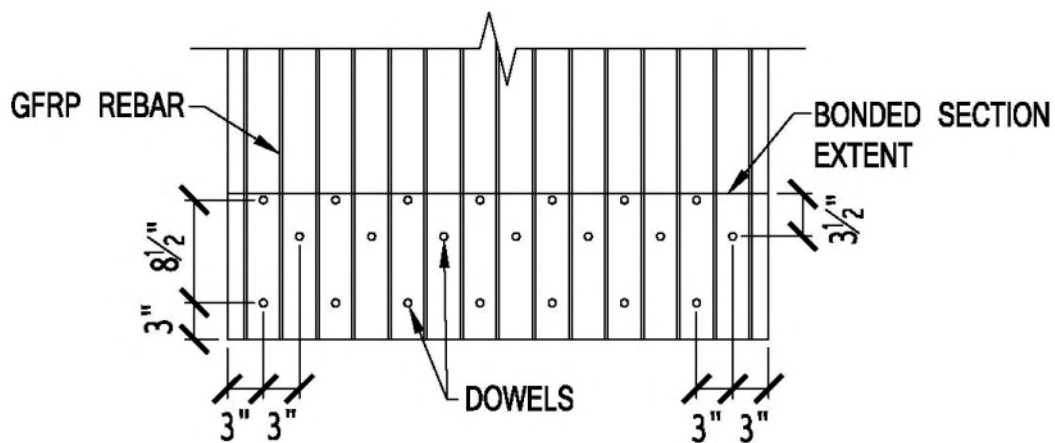


Figure 58 – Top view of specimen 2 with GFRP rebar and dowels

2.3.3 Test results

The specimens that are described above are tested by an imposed horizontal deformation test. The test and the test results per specimen are described in this paragraph. For every specimen is shortly described the experiment. In the rest of the paragraph are described the advantages, disadvantages and failure modes of the design.

The test setup that is used by Reyes & Robertson (2011) is schematically shown in Figure 59. In the figure is shown an overview and a side view of the test setup. The imposed deformation is generated by moving the steel girders with an actuator load as shown in the side view.

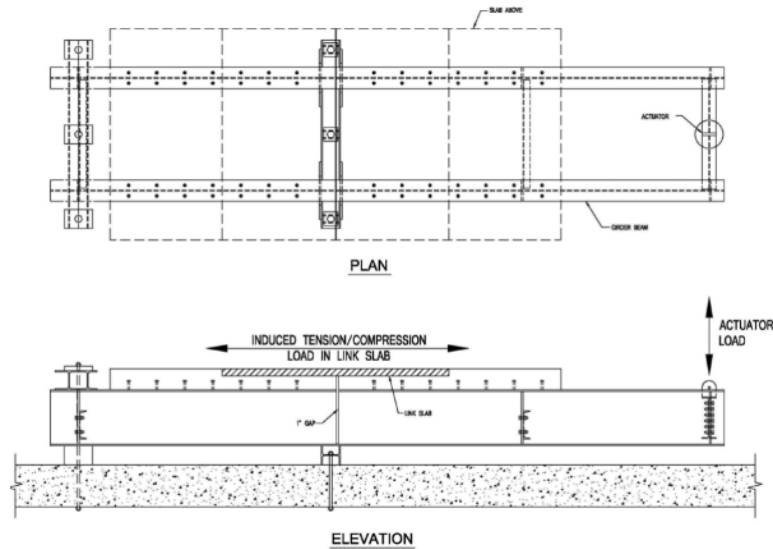


Figure 59 – Test setup to imposed the link slab to imposed horizontal deformation

Reyes & Robertson (2011) determined that in the perfect situation, the link slab act as follows if it is exposed to imposed horizontal deformations:

- The gap displacement and unbonded displacement should be about equal meaning the unbonded section is acting elastically
- The link slab remains elastic over numerous cycles
- The link slab retains its compressive capacity
- Tensile failure occurs well beyond the actual loads expected
- Micro cracks remain uniform over the entire debonded section and does not localize.

2.3.3.1 Specimen 1

In this paragraph are described the tests that are done on specimen 1 and the results of the tests. The loads that work on the specimen during the tests are displacement controlled. The loads are applied alternatively static or cyclic as shown in Figure 60.

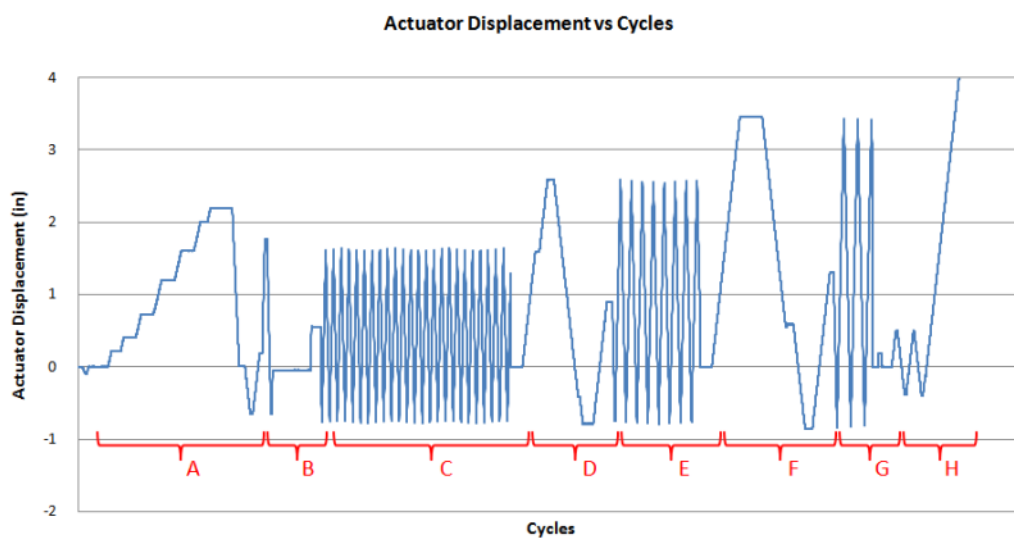


Figure 60 – Displacement of the links slab as a function of the cycles, specimen 1 (Reyes & Robertson, 2011)

The displacement during the test is increased by steps. In every phase is applied a certain maximum tensile strain on the link slab. The maximum strain during the test in different phases of the test are shown in Table 16. The maximum tensile strain until failure is unknown.

Table 16 – Type of load and maximum tensile strain per load phase, defined in Figure 60 (Reyes & Robertson, 2011)

Phase	Loading type	Maximum tensile strain
A.	Load	0.5%
B.	First cycle	0.5%
C.	Cycles	0.5%
D.	Load	0.6%
E.	Cycles	0.6%
F.	Load	0.85%
G.	Cycles	0.85%
H.	Max Compression and Load to Failure	

During the test are done observations on the link slab. According to the observations, some advantages and disadvantages of the specimen 1 are given, as shown below.

Advantages according to Reyes & Robertson (2011):

- Link slab was very well bonded to the reinforced concrete deck.
- Majority of the micro cracks developed exclusively within the unbonded section.
- Up to 0.6% tensile strain, almost all strain is taken up by micro cracks within the unbonded section.

Disadvantage according to Reyes & Robertson (2011):

- At tensile strains greater than 0.6% either the crack at the transition point has opened up, the bonded section has begun to undergo elongation as well or a combination of both of these.
- Link slab movement and elongation was no limited to unbonded section.
- In a cast-in-place link slab, micro cracks must be developed after installation. In practical applications, service loads may or may not be large enough to develop the micro cracks that are needed in the link slab to have an effective working link slab.
- Low compressive strain capacity of the link slab because precracking is not possible. This is due to the polyethylene fibres
- If micro cracks develop during tensioning the SHCC link slab, the material never fully return to their original place if the slab is under compression load again. Theoretically, this could create a compressive stresses.

Also the failure of the link slab is observed during the test. The failure mechanism is schematically shown in Figure 61 in four steps. Some conclusions about the failure of specimen 1, according to Reyes & Robertson (2011), are:

- Localisation of one crack propagating to the entire cross section near the transition point between the unbonded and bonded section.
- It was observed that the GFRP bars have not enough capacity to carry the entire load after failure of the SHCC link slab, so the GFRP rebars failed soon after.

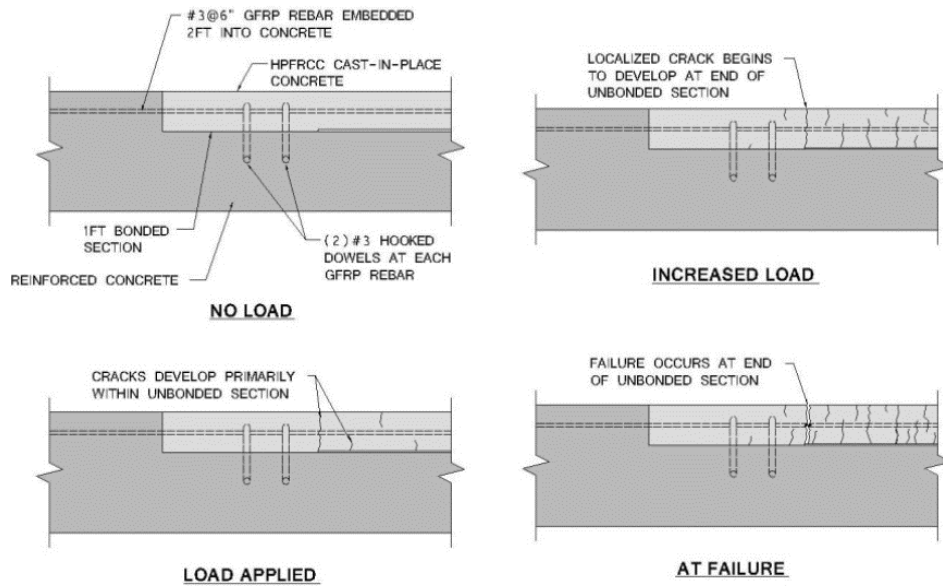


Figure 61 – Failure of specimen 1 during testing step by step (Reyes & Robertson, 2011)

2.3.3.2 Specimen 2

In this paragraph are shown the test results on specimen 2, according to Reyes & Robertson (2011). The specimens are loaded by a displacement controlled test. The displacement in the specimen is shown in the graph of Figure 62.

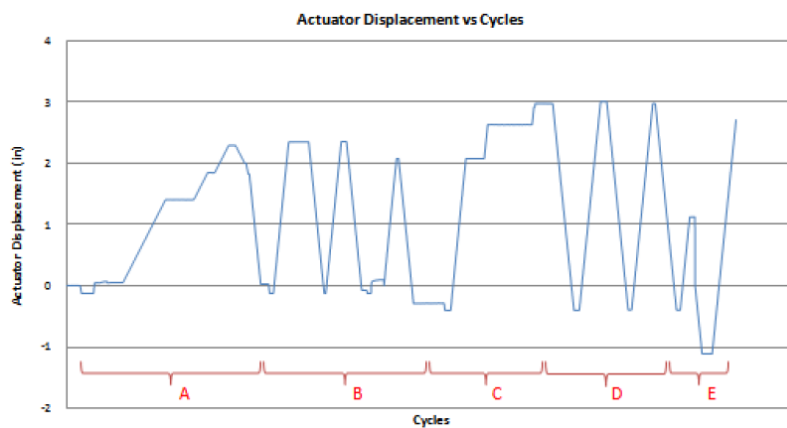


Figure 62 – Displacement of the links slab as a function of the cycles, specimen 2 (Reyes & Robertson, 2011)

As shown in Figure 62, the maximum displacement during the test is increased stepwise. The maximum deformation in different stages of the test could be expressed as the maximum strain during the test. These maximum strain values are given in Table 17. As shown in the table, the maximum strain at failure of the specimen is not known.

Table 17 – Type of load and maximum tensile strain per load phase, defined in Figure 62 (Reyes & Robertson, 2011)

Phase	Loading type	Maximum tensile strain
A.	Load	0.55%
B.	Cycles	0.55%
C.	Load	0.8%
D.	Cycles	0.8%
E.	Load to Failure	

Specimen 2 is observed during the tests. According to the observations, advantages and disadvantages of the design of specimen 2 are given below according to Reyes & Robertson (2011).

Advantages according to Reyes & Robertson (2011):

- The link slab is precracked, so the link slab has some capacity to shorten when a compressive force is applied without generating large compressive stresses in the link slab.
- The doweled GFRP bars were resisting tensile loads.

Disadvantages according to Reyes & Robertson (2011):

- Cracks developed outside the unbonded section
- In practical applications, a precast link slab is more suitable for retrofits because of the long setting and curing times of SHCC.
- Anchoring method of the bonded section, which was the failure mechanism as discussed in more detail at the end of this paragraph.
- The maximum tensile strain was limited to 0.6% as a consequence of the higher compressive strain capacity and anchoring of the link slab.

At last, from the observations is also determined the failure mode of specimen 2. Figure 63 is schematically shown the failure mechanism step by step. Conclusions according to the failure mechanism according to Reyes & Robertson (2011) are written below.

- Uplifting of the bonded section is probably because:
 - o The grout below the bonded section was not effective;
 - o The vertical steel dowels had some capacity to deflect before they could resist load;
 - o The grout was not bonded well to the horizontal GFRP bars.
- Localized cracking was observed at the transition point between the unbonded and bonded section.
- The slab failed during cycling load that causes a tensile strain in the link slab of 0.5%, when the GFRP bars reached their shear capacity limit.

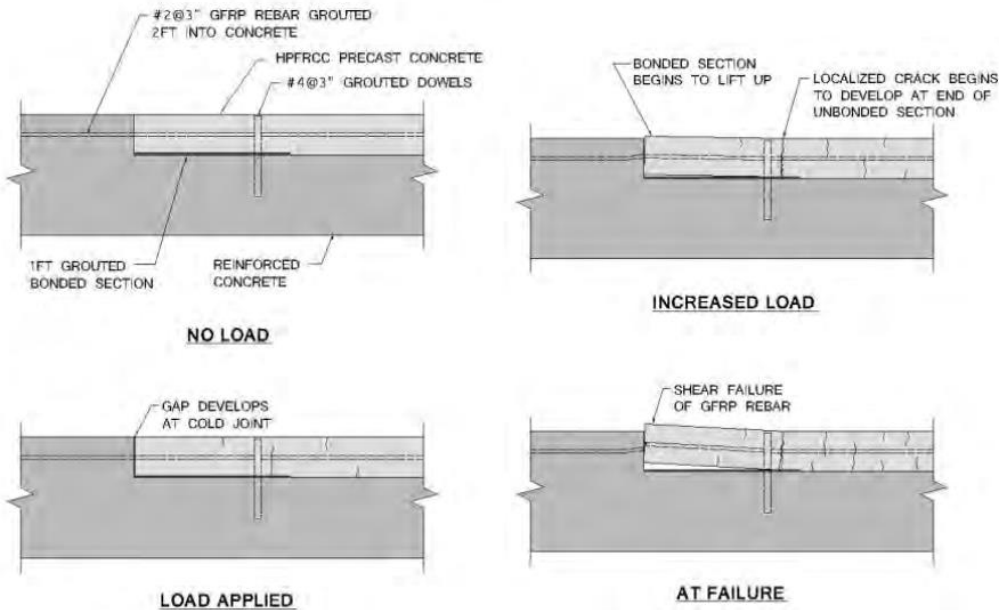


Figure 63 – Failure of specimen 2 during testing step by step (Reyes & Robertson, 2011)

2.3.3.3 Specimen 3

In this paragraph are analysed the test result of specimen 3. The applied displacements that are applied during the displacement controlled test are shown in the graph of Figure 64.

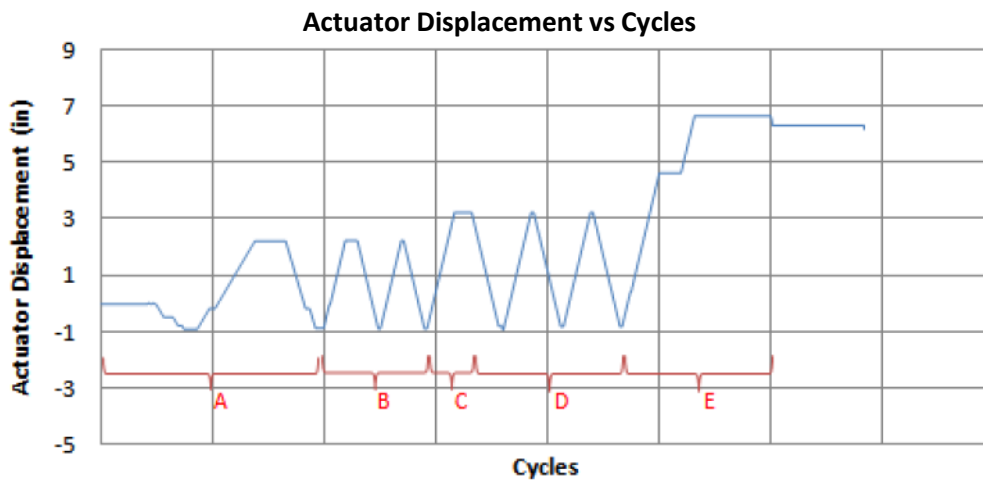


Figure 64 – Displacement of the links slab as a function of the cycles, specimen 3 (Reyes & Robertson, 2011)

Again, the displacement is increased step by step during the test. The displacements of the graph of Figure 64 can be calculated to strain. The maximum tensile strains per loading phase are shown in Table 18.

Table 18 – Type of load and maximum tensile strain per load phase, defined in Figure 64 (Reyes & Robertson, 2011)

Phase	Loading type	Maximum tensile strain
A.	Load	0.55%
B.	Cycles	0.55%
C.	Load	0.85%
D.	Cycles	0.85%
E.	Load to Failure	

In specimen 3 is tried to make an improved version of specimen 2. The test results therefore are given relative to the test result of specimen 2. According to the test results, the design of specimen 3 turned out to be worse than specimen 2, so only some disadvantages of specimen 3 are given here.

Disadvantages of specimen 3 relative to specimen 2 according to Reyes & Robertson (2011):

- The maximum compressive strain was limited to approximately 0.14%.
- The maximum tensile strain was limited to approximately 0.45% only, probably due to the increased number of dowels and the place of the dowels.

At last, the failure mechanism is discussed here. The failure mode is schematically shown in Figure 65. According to failure mechanism, it could be concluded that:

- The link slab failed at the cold joint between the SHCC and the reinforced concrete. As shown in Figure 65, the entire link slab lifted up if to large horizontal deformations are applied.

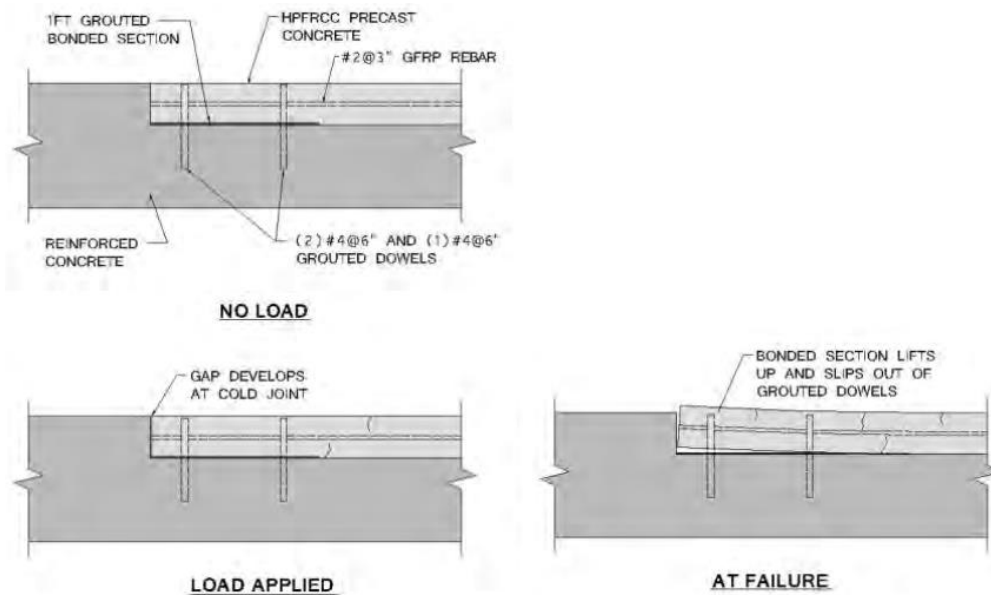


Figure 65 – Failure of specimen 3 during testing step by step (Reyes & Robertson, 2011)

2.3.4 Conclusions

From the analysis to the link slabs that are exposed to imposed horizontal deformation as described above could be made some general conclusions. The most important conclusions according to Reyes & Robertson (2011) are:

- Advantage of **cast-in-place link slab** is providing good continuity between the ends of the link slab and the concrete or bridge deck.
- Disadvantage of **cast-in-place link slab** is the limitation of permanent strain in the link slab. This link slab is not very effective to take up elongation of the spans.
- **Cast-in-place link slab** may not be practical, because SHCC requires a long setting and curing time to reach its optimal strength.
- To minimize crack localization of the **precracked link slabs**, physical bending of the link slab may be more effective than inducing an internal moment as done in the experiments of specimens #2 and #3.
- **Precracking** of the link slab gave an adequate compressive strain capacity to the link slab
- If the specimen were **precracked and anchored** properly, higher tensile strain capacities could be attained.
- **Precast slabs** has the advantage of precracking
- **Precast slabs** have a limited bond strength between the link slab and the existing concrete deck. The following bonding methods may be considered:
 - a. Vertical dowels can be installed under an angle such that the slab is essentially pulled downward during tension loads.
 - b. A combination of vertical dowels and horizontal GFRP bars could be more effective than either acting alone.
- In all 3 specimens, **localized cracking** was a problem. Increasing the thickness of the SHCC link slab may be a solution.
- **Water or rain run-off** may seep through the cracked link slab and get trapped below the link slab causing the unbonded section to be susceptible to deterioration and traffic induced damage.

2.3.5 Load transfer system

In this paragraph, the load transfer system is determined. This transfer system is based on the analysed of the previous paragraphs. The link slab is assumed to be exposed to vertical and horizontal loads and imposed curvature, horizontal deformation and vertical deformation. For every action, the reaction of the link slab design is determined. For the thin link slab, it is assumed that imposed curvature and horizontal imposed deformation both have the same effect on the link slab.

As mentioned already, Reyes & Robertson (2011) considered three different link slabs. An overview of the dimensions of the different link slab designs are shown in Table 19. There are some differences between the different specimens. However, taking into account the thickness, length of the bonded and unbonded zone, the span and the reinforcement ratios, it could be concluded that all link slabs have the same load transfer system.

Table 19 – Dimension of link slab specimen 1, 2 and 3 (Reyes & Robertson, 2011)

Dimensions	Unit	Specimen 1	Specimen 2	Specimen 3
Width link slab	mm	2,290	1,143	1,143
Thickness link slab	mm	76	76	76
Total length	mm	2,440	2,440	2,440
Length unbonded zone	mm	1,830	1,830	1,830
Length bonded zone	mm	305	305	305
Span	mm	25	25	25
Longitudinal reinforcement				
Length GFRP bars extending the formwork	mm	610	610	0
GFRP bar diameter	mm	9.5	6.4	6.4
Centre-to-centre	mm	152	76	76
Reinforcement ratio	%	0.61	0.55	0.55
Transverse reinforcement				
GFRP bar diameter	mm	9.5	6.4	6.4
Centre-to-centre	mm	152	152	152
Reinforcement ratio	%	0.61	0.27	0.27
Dowels				
Length	mm	Anchor hooks	152	152
Diameter	mm	9.5	12.4	12.4

According to the data of Table 19, a general picture of the three specimens in made, as shown in Figure 66. In the figure are given also some general dimensions like the length of the link slabs. As an exception, the length of the reinforcement bars that are placed in the reinforced concrete bridge decks (610 mm) is not valid for the design of specimen 3.

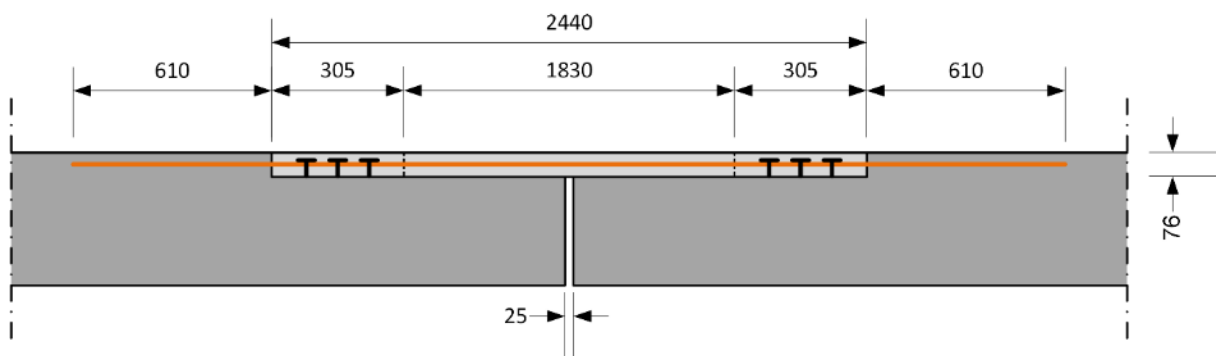


Figure 66 – General lay out of link slab design according to Reyes & Robertson (2011) (length in mm)

2.3.5.1 Vertical loads

In this paragraph is discussed the way that vertical loads are carried by the link slab. In fact, vertical loads could work upwards and downwards. In this paragraph, only vertical downwards working load are taken into account, because main downward loads work on the link slab. However, upwards working stresses could be expected, for example because of curvature in the bridge spans. This is only shortly taken into account in paragraph 2.3.5.3 Scheme.

According to the data of Table 19 and the design lay out of the specimens, some remarks according the load transfer system could be made:

- The link slab is thin, so probably wheel loads can't be carried by shear forces and bending moments in the link slab
- The reinforcement ratio is low ($\approx 0.6\%$) so the bending moment capacity is probably low too
- The link slab is equally supported by the reinforced concrete bridge deck
- The span between the reinforced concrete bridge decks is 25 mm only, at least in the test setups (Reyes & Robertson, 2011)

From these remarks could be concluded that vertical load on the link slab is transferred directly to the reinforced concrete bridge deck. The link slab is assumed to have no, or at least a negligible low, capacity to transfer loads by bending moments and shear stresses to the bonded zones, because the link slabs are very slender ($\approx 75/1830 = 1/24$) and have a low GFRP reinforcement ratio. Moreover, the link slabs are supported equally by the concrete bridge deck in horizontal plane. In the tests, the gap between both concrete bridge decks is 25 mm only. The link slab has a thickness of 75 mm, so assuming that compressive stresses are transferred to the substructure under an angle of 45 degrees, compressive stresses can be transferred directly to the substructure if the gap is 25 mm only.

In both Figure 67 and Figure 68 is schematically shown a wheel load that is transferred through the link slab to the concrete bridge deck. In Figure 67 is shown the wheel load and the structure from a side view. In Figure 68 is shown a cross section of the wheel load and the structure. In both figures is shown that the load is transferred through the link slab under an angle of 45 degrees, what is according to the NEN-EN 1991-2 chapter 4.3.6 (2) (Nederlands Normalisatie-instituut, 2003).

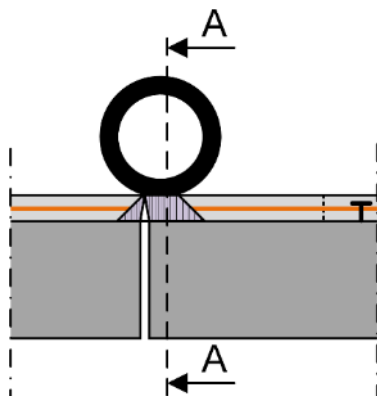


Figure 67 – Vertical wheel load transferred through link slab to the concrete bridge deck

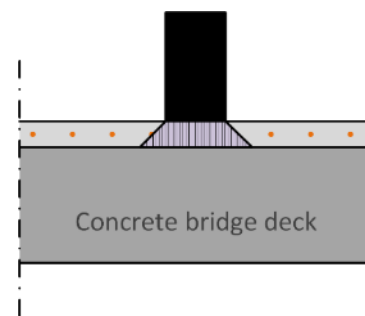


Figure 68 – Cross section AA of Figure 67, vertical wheel load transferred through link slab to the concrete bridge deck

Taking a closer look to the vertical stresses near the gap between the concrete bridge decks, vertical peak stresses could be expected between the link slab and the concrete bridge deck. The expected distribution of vertical loads in the longitudinal way is shown in Figure 69. In the figure are shown three pictures; one overview at the left and two details. In the first detail (middle) is shown the vertical stress

distribution qualitatively with the expected peak stress. In the other detail (right) is shown the expected directions of the stresses near the gap.

As shown in the first detail of Figure 69 (middle), there is a gap between the concrete decks what probably results in vertical peak stresses at the end of the deck. The stress distribution in the link slab itself will probably have parabolic directions near the gap as shown on the first detail (middle) of Figure 69. So more stresses must be supported at the end of the substructure, so a certain peak stresses could be expected here.

In the second detail (right) of Figure 69 are shown the expected directions of the stresses that are caused by the vertical wheel load that is situated above the gap. The stresses above the gap should deflect to the substructure. Because of the deflection of stresses, the stresses get a certain horizontal component. This horizontal component could cause a certain tensile stress in the link slab, as shown in the detail of Figure 69 with the blue arrow.

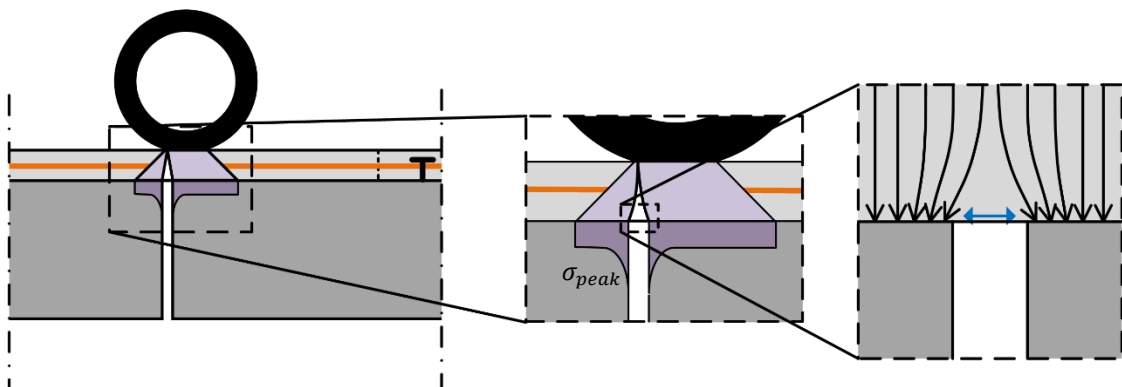


Figure 69 – Vertical peak stress between the link slab and the concrete bridge deck caused by wheel load

Now the influence of the peak stresses and the horizontal tensile component on the link slab and the substructure could be discussed. Some variable where both stresses probably depends on are:

- *The gap between the concrete girders:* a larger gap probably results in higher stresses, because more stresses should be carried by the ends of the concrete decks.
- *The thickness of the link slab:* if the link slab is thick, the vertical load is distributed over a larger area what decrease the stress (assuming that the loads are spread over 45 degrees).
- *Thickness of the asphalt layer upon the link slab:* same is valid as for the thickness of the link slab. If the thickness of the link slab is higher, the peak stress will be lower.
- *Stiffness of the concrete bridge deck:* if the stiffness is very high, more higher stresses are carried, such that the peak stress becomes higher.

2.3.5.2 Horizontal loads

In this paragraph is discussed the reaction of the link slab on horizontal loads. Before conclusions according to the horizontal load transfer are made, some remarks from the design should be mentioned.

- Due to the plexiglass between the concrete deck and the link slab at the unbonded zone, it is assumed that there is no horizontal friction in this zone, or at least the horizontal friction could be neglected.
- There is horizontal friction between the link slab and the concrete bridge deck at the bonded zone, because of shear studs, rough NSC area and grout between NSC and SHCC. This

horizontal connection is responsible to transfer horizontal loads from the link slab to the substructure.

- Horizontal loads that work on active zone of the link slab should be transferred to the passive zones by normal compressive and tensile stresses in the link slab.
- The reinforcement and the fibres together should take care of horizontal normal tensile stresses in the link slab.
- Because the reinforcement of the link slab is anchored in the concrete deck, it is assumed that the reinforcement is able to transfer tensile stresses from the link slab to the deck slab.

The connection between the link slab and the concrete bridge deck that is designed by Reyes & Robertson (2011) is quite similar to the connection between the link slab and the steel girders that is designed by Li, et al. (2003). Probably, in both designs the horizontal stresses that work on the link slabs are transferred to the substructure in a similar way.

As mentioned in the assumptions that are listed above, in the link slab work normal stresses because of horizontal external loads. In the bonded zones, the normal stresses are transferred to the concrete bridge deck. Normal stresses could be transferred to the substructure by the horizontal or vertical connection between the link slab and the substructure.

The first way to transfer the normal stresses is by the horizontal shear connection (roughened NSC, grouted connection and shear studs) between the deck and the bonded zone of the link slab. The second way to transfer the normal stresses is by compressive or tensile stresses in the vertical connection between the link slab and the substructure at the ends of the link slab. In the vertical connection, tensile stresses could be transferred by the reinforcement and compressive stresses by the concrete itself.

The vertical connection between the NSC deck and the SHCC link slab could be expected to be a weak spot in the design. Therefore, the normal stresses in this connection should be reduced to a certain minimum by the horizontal connection between the deck and link slab. So a part of the normal stresses should be transfer to the substructure by the horizontal connection, such that the risk of failure of the vertical connection is reduced to a certain minimum. This is schematically shown in Figure 70. As shown in the figure, the stress in the passive zone decreases over the length because of the horizontal connection between the link slab and the substructure. The residual stress at the end of the SHCC link slab should be carried by the vertical connection.

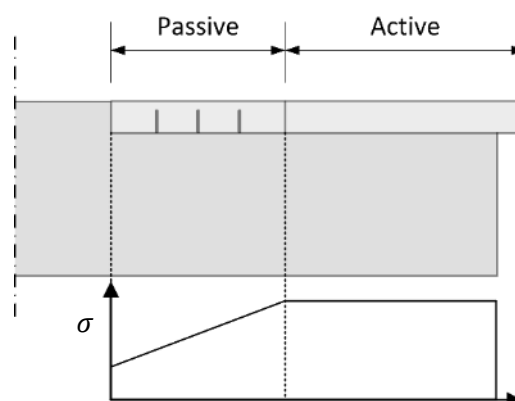


Figure 70 – Schematic stress distribution of normal stresses over the link slab

In chapter 2.1.3 Analysis to vertical loads on joint is mentioned that the bridge spans together with the link slabs act like one slab to carry horizontal loads. In these designs, the active zone of the link slab is 76 mm only, while the height of the link slab design from chapter 2.1.1 Design is 150-170 mm.

Therefore, it should be analysed if the 76 mm thick SHCC link slab has enough capacity to carry horizontal loads and could be estimated to be one slab together with the bridge spans.

Two situations should be analysed to determine the horizontal strength of the link slab, as shown in Figure 71. In this figure are shown three spans that are connected by two SHCC link slabs. On the middle span a horizontal force R_d works, for example caused by a braking vehicle. As shown in the figure, in both link slabs are generated compressive and tensile stresses. Both situations should be analysed to determine the horizontal strength of the link slabs.

First the situation that the horizontal stresses in the active link slab are transferred to the passive zone by compression stresses is analysed. The maximum horizontal load capacity per metre width is calculated as shown in eq.(17).

$$H_{Rd} = 76 \cdot 30 = 2280 \text{ kN/m} \tag{eq.(17)}$$

If the horizontal stresses in the active zone should be carried by tensile stresses, then the horizontal capacity in the active zone is equal to 205 kN/m only, as shown in eq.(18). Because the tensile strength of SHCC is smaller than the compressive strength of SHCC, the tensile strength is governing.

$$H_{Rd} = 76 \cdot 2.7 = 205 \text{ kN/m} \tag{eq.(18)}$$

As mentioned in chapter 2.1.3 Analysis to vertical loads on joint, the maximum force in the link slabs is equal to 75 kN/m assuming a distribution width of 4 m (Nosewicz & Jong, 2009). The tensile (205 kN/m) and compressive (2280 kN/m) capacity of the link slab are both higher than 75 kN/m. So the SHCC link slab and the spans work probably together to carry horizontal loads.

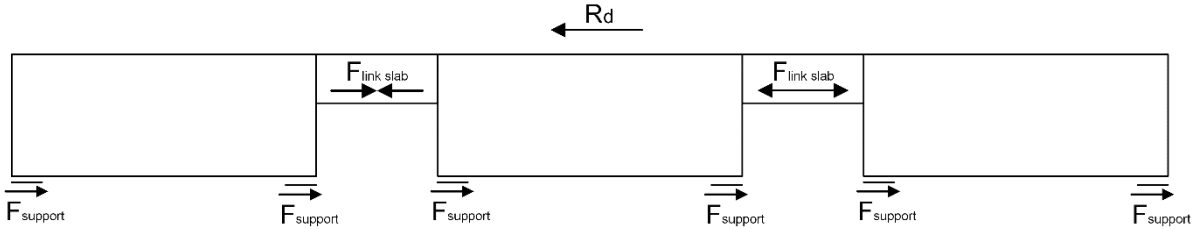


Figure 71 - Braking force on the bridge with reaction tensile and compressive stresses in the link slabs according to (Nosewicz & Jong, 2009)

2.3.5.3 Scheme

In this paragraph is suggested a scheme that fits with the design and load transfer system that are analysed above. From the above mentioned analysis, the precast link slab can be modelled as a beam with a certain supporting system. Some assumptions that are done to make the model:

- The passive part of the link slab is assumed to be connected to the substructure, such that it remains in place all the time. In other words, it is assumed that the horizontal connection with the substructure (roughened NSC, grouted connection and shear studs) and the vertical connection (longitudinal reinforcement) together make sure that the passive part is assumed to be connected tight to the substructure.
- The passive and active part of the link slab is poured in one. Therefore the connection between the active and passive part is assumed to be tight.
- Between the active section and the substructure is no horizontal friction.

- Vertical compressive stresses that work on the active part can be transferred to the substructure by compressive stresses in the link slab.
- The active part can't carry vertical upwards tensile stresses from the deck

It can be doubted if vertical upward loads work on the link slab. However, if the link slab is exposed to an imposed curvature or a bending moment, which are discussed in the next paragraphs, the link slab could lift up, at least partly. In that case, the active part of the link slab has no capacity to carry any vertical tensile loads between the substructure and the link slab.

In fact, two different schemes of the link slab should be made. The first scheme is for the situation where upward vertical loads and/or horizontal loads work. Because of the debonding layer, the vertical upward loads can't be carried by the connection between the active part and the substructure. Therefore, vertical upward loads should be transferred to the passive sections by bending moments and shear forces. However, the bending moment and shear capacity of the link slab is low.

The other scheme is for the situation where downward vertical loads and/or horizontal loads work. In this situation the vertical load can be carried by the horizontal connection between the active section and the substructure. This results in compressive stresses between the link slab and the substructure.

Both situations, vertical upward and downward load, are shown in Figure 72. At the upper part of the figure is shown the total link slab that is split in two parts; on the left is shown the situation that the link slab is exposed to vertical compression and on the right to tension. For both situations, compressive and tensile loads, are also made scheme on the left and the right side of the figure respectively.

As shown in Figure 72, the passive part of the link slab is modelled as a clamped support. The passive zones are the connection between the active zone and the substructure. This part of the link slab should not crack or move. However, in practice the passive zone probably moves a bit. However, as a first estimation movements in the passive zone are neglected, or at least are neglected relative to the movements in the active zone.

The active part is supported over equally over the whole horizontal plane (with exception of the space between the two concrete deck structures). This plane can only carry compressive stresses, as shown in Figure 72.

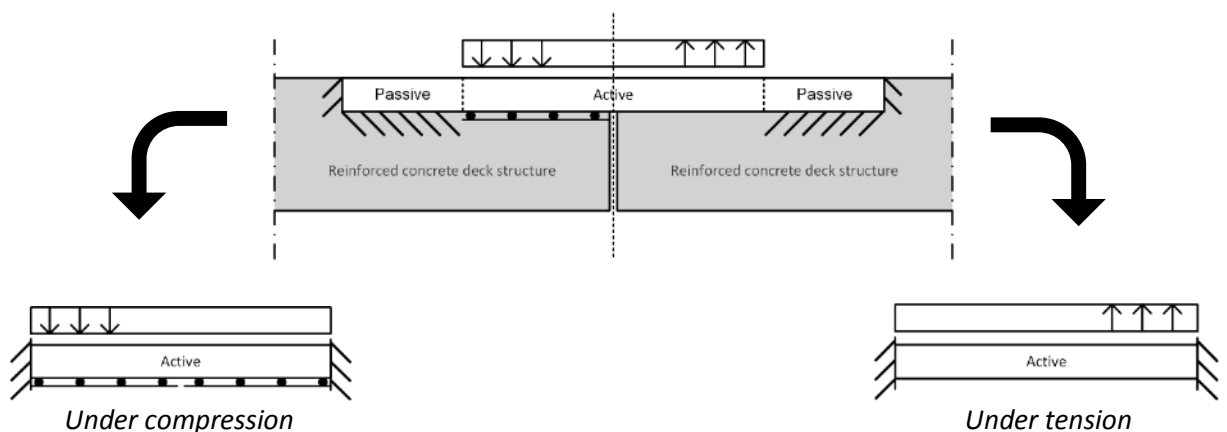
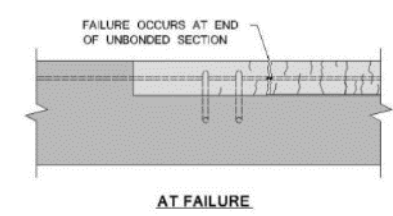
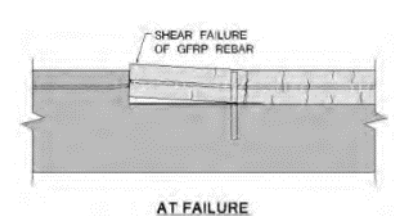
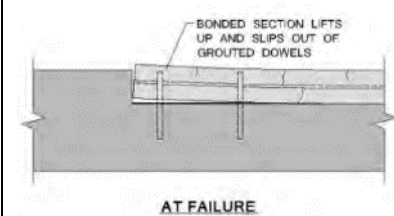
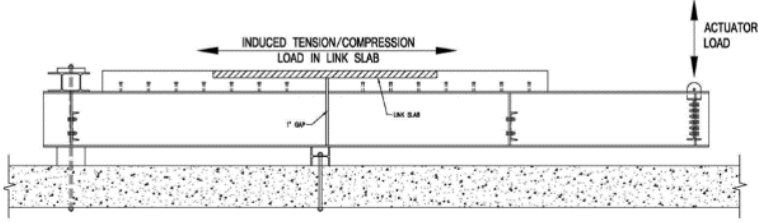


Figure 72 – Schematisation of the total link slab under compression and under tensions and the schemes of the active part of the link slab under compression (left) and under tension (right)

2.3.5.4 Imposed curvature according to tests

Reyes & Robertson (2011) tested the three different specimens. The test results are discussed already in chapter 2.3.3 Test results. In this chapter the discussed the reasons of failure and are made relations with the scheme that is suggested in paragraph 2.3.5.3 Scheme. In Table 20 is given an overview of the failure modes of the three different specimens. In the table is also shown the test setup again.

Table 20 – Overview of failure modes of specimen 1, 2 and 3 exposed to induced tensions/compression load in the link slab (Reyes & Robertson, 2011)

Specimen 1	Specimen 2	Specimen 3
		
Through crack at end unbonded section	Shear failure GFRP rebar at the end of link slab Localized cracking at end of unbonded section	The end of link slabs slips out of the dowels
		

To interpret the test results properly, the test setup is discussed in some more detail first. In the picture of the test setup (Table 20) is given that the link slab is exposed to tension and compression only. According to the geometry of the setup and the thickness of the link slab, it is probably a good assumption that only normal stresses work. The bending moment due to the imposed curvature can probably be neglected.

However, taking a closer look, there could be some bending moment in the link slab, because there is expected a small imposed curvature in the link slab. In Figure 73 is shown the test setup. The setup is exposed to a large vertical deflection at the end of the steel girder. Because of the supporting system, the right part of the test setup rotates as shown in Figure 73. As a consequence of the rotation, a certain curvature could be expected in the link slab. This curvature is restrained by the link slab, so a certain bending moment in the link slab could be expected.

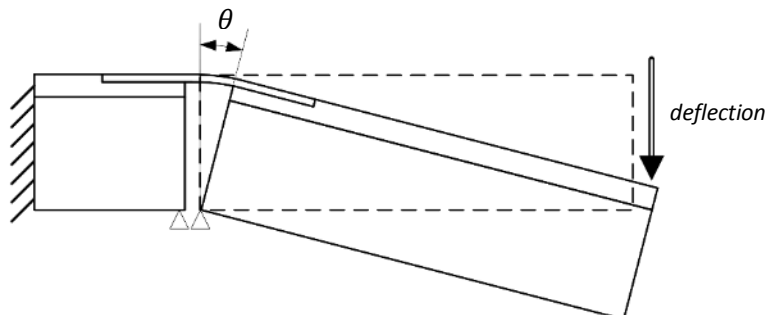


Figure 73 – Curvature in the link slab during tests

Concluded, for small rotations, the curvature and thus the bending moment could probably be neglected. Therefore, as a first estimation, the curvature in the link slab is neglected. It is assumed that rotation in the substructure results only in tensile and compressive stresses in the link slab. Naturally, imposed horizontal deformations also result in tensile and compressive stress in the link slab only. So the test results are assumed to be valid for imposed curvature as well as for imposed horizontal deformation. However, if the test results can't be explained by tensile and compressive stresses only, maybe a certain bending moment should be taken into account to explain the test results properly.

The test results of specimen 1, 2 and 3 are discussed in detail in this chapter. From practical reasons, the analysis start with specimen 2, followed by specimen 3 and at last is specimen 1 is discussed in detail.

Specimen 2

In Figure 74 is shown the failure of specimen 2 again. As shown in the figure, the passive part of the link slab is curved clock wise a bit. There should work a certain bending moment to rotate the passive part of the link slab. This is analysed in more detail in the rest of the paragraph.

Note: Figure 74 implies that the dowels are placed in the passive zone, next to the interface between the active and passive part of the link slab. However, in reality the dowels are places in the middle of the passive zone. This is shown in Figure 56 of paragraph 2.3.2.2 Specimen 2, where the exact place of the dowels is given in a schematic top view.

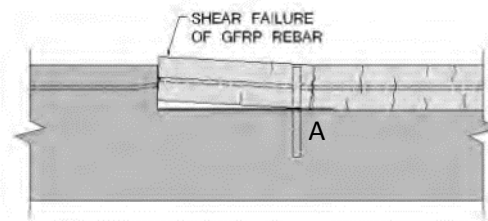


Figure 74 – Failure of specimen 2

If the link slab is not failed yet, various loads probably work on the link slab. Horizontal and vertical stresses could be expected at the passive part of the link slab as shown in Figure 75 and Figure 76. In fact, an imposed horizontal deformation causes stresses in the active zone. These stresses should be carried by the passive zone of the link slab, because both are connected. Horizontal and vertical stresses working on the link slab are discussed in more detail.

In Figure 75 are shown the expected horizontal stresses if the link slab is exposed to imposed horizontal deformation. As shown in Figure 75, at the right side are expected horizontal stresses from the active part of the link slab. These stresses work because the passive section is assumed to be fully connected to the active zone and fully restraint. At the left side of the link slab is expected a reaction tensile stress in the reinforcement. In the horizontal connection are expected friction stresses. The direction of the friction stresses is expected to be in the opposite direction of the stresses from the active section, as shown in Figure 75. At last, the shear studs cause a horizontal reaction stresses, as shown in the figure. It is assumed that the studs are stronger than SHCC, such that a constant horizontal stress is generated over the height of the studs, as shown in the Figure 75.

In the passive part of the link slab, which is shown in Figure 75 should be bending moment equilibrium. Taking into account the test result of the link slab, the passive part of the link slab rotates around the point A, as shown in Figure 74 and Figure 75. Assuming horizontal equilibrium in the passive section,

the resultant horizontal force creates a bending moment around point A in clock wise direction, as shown in Figure 75.

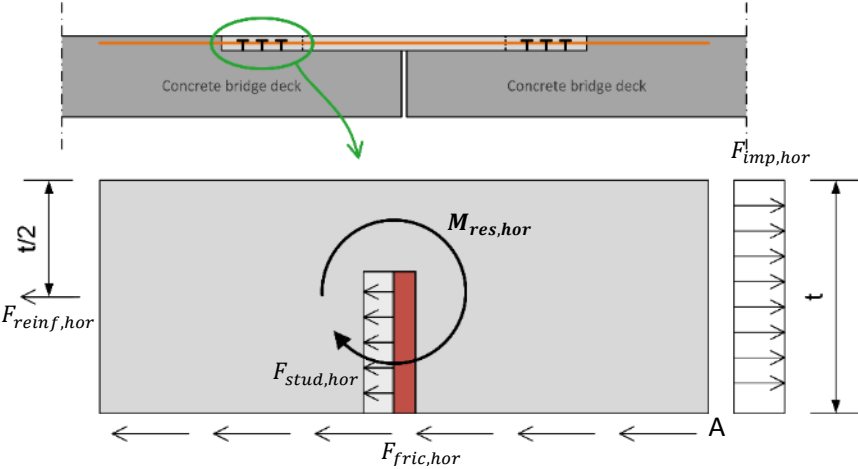


Figure 75 – Bending moment caused by horizontal imposed deformation and reaction forces

To have bending moment equilibrium in the passive section, an opposite bending moment should be generated in the passive zone. To generate an opposite bending moment, the vertical stresses should work in the passive section, as shown in Figure 76.

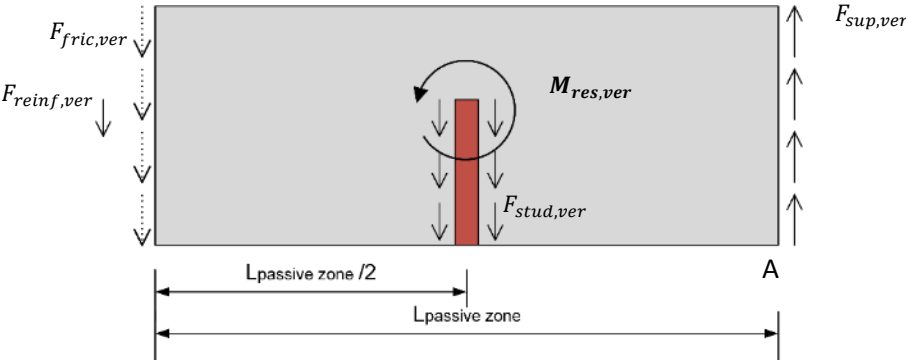


Figure 76 – Bending moment caused by vertical reaction forces

To generate an opposite bending moment around point A, the vertical stresses in the longitudinal reinforcement, $F_{reinf,ver}$, and the dowels, $F_{stud,ver}$, should work downwards. From vertical equilibrium, also an upwards working loads should work. This load could be generated by the connection with the active zone of the link slab and the support from the concrete deck, $F_{sup,ver}$.

In theory, there could work a vertical frictions stress in the vertical connection between the link slab and the concrete deck. However, in the test results is shown that the as soon as the horizontal imposed deformation is applied, a gap in the vertical connection between the concrete deck and the link slab develops. That implies that the vertical friction stress between the SHCC link slab and the concrete deck, $F_{reinf,ver}$, could probably be neglected.

Taking into consideration all stresses from Figure 75 and Figure 76 and the test results from Figure 74, it could be concluded that the bending moment that is generated by horizontal stresses is larger than the bending moment that is generated by the vertical stresses. Probably, this is mainly because of the small downwards stresses. Because of the gap in the vertical connection, the vertical friction between the reinforced concrete and the link slab is probably negligible. Further, the vertical friction between

the shear studs and SHCC is probably quite small too. Assuming the shear studs are meant to generate a horizontal shear connection, it could be expected that the vertical friction is relative small.

Because the vertical upwards stress at the right side of the passive zone of the link slab (interface between the active and passive zone of the link slab and the support from the substructure) is the only point that is able to stay in place. Therefore, the passive part of the link slab can be expected to rotate around this point. In this way the test results could be clarified.

Specimen 3

In Figure 77 is schematically shown the failure of specimen 3. Same as for specimen 2, the bonded section lifts up at the end of the link slab. The design difference with specimen 2 is that the longitudinal reinforcement is not connected to the concrete deck. Instead of the reinforcement, an extra row of dowels is placed at the end of the link slab. Further, the same mechanism could be expected to occur as in specimen 2.

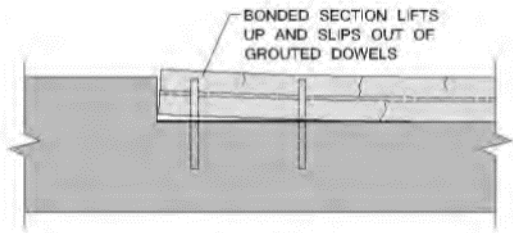


Figure 77 – Failure of specimen 3

Specimen 1

The failure mode of specimen 1 is significant different from the failure mode of specimens 2 and 3. In specimen 1 the passive zone remains in place during the test, while the passive zone of specimens 2 and 3 rotate (Reyes & Robertson, 2011). Probably the reaction opposite bending moment that is generated by the vertical reaction stresses is large enough to keep the passive part of the link slab in place.

In specimen 1 is generated a through crack at the interface between the active and passive zone, as shown in Figure 78. A through crack is normally the result of tensile stresses in the cross section. Reyes & Robertson (2011) exposed the specimen under a tensile test, so a through crack could be expected. However, the question is why the crack is generated at the end of the unbonded zone and not somewhere in the middle of the undonded zone.

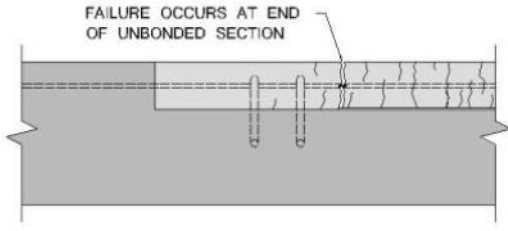


Figure 78 – Failure of specimen 1

However, fist is clarified that the failure crack is not expected in the bonded section in any case. On Figure 70 in paragraph 2.3.5.2 Horizontal loads is shown that the tensile stresses are expected to decrease over the length of the passive zone. Therefore, the failure crack is not expected in this zone.

To clarify the place of the through crack, the place of the anchors should be analysed more precisely. In Figure 79 is shown a picture of the anchor hooks. The picture is taken when the SHCC link slab was poured. In the picture is clearly shown the smooth unbonded and the rough bonded sections. The picture shows that the first row of anchor hooks is actually placed at the interface between the bonded and unbonded section, different from Figure 78.



Figure 79 - Anchor hooks placed on the bonded section

The failure crack is generated and the end of the unbonded section (Figure 78) and the first row of anchor hooks is placed at the interface between the bonded and unbonded sections (Figure 79). Probably there is a relation between the failure and the place of the anchors.

A possible reason that specimen 1 fails around the anchor hooks is the peak stresses that could be expected around the anchor hooks as shows in Figure 80. In the detail of Figure 80 are shown the tensile stresses that have to be transferred through the concrete cross sections between the steel anchors. Because of the anchors, the total cross sectional area of concrete that should transfer the total horizontal load becomes smaller. That means that the horizontal stress becomes larger. This larger tensile stress could be the reason of failure at this point of the link slab.

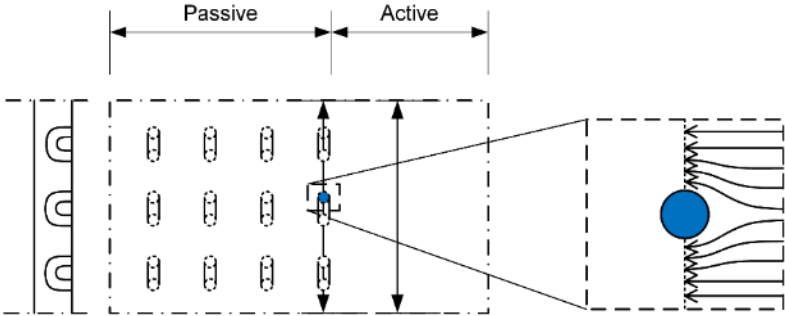


Figure 80 – Stress distribution at the anchor hooks of specimen 1

The failure mechanism that shown in Figure 80 is also mentioned in the analysis of the test results of Li, et al. (2003). However, in the case of the design of Li, et al. (2003), the shear studs where placed at a certain distance from the interface between the passive and active zone. The tensile stresses around the shear studs were reduced due to the horizontal friction between the link slab and the reinforced concrete in the passive zone. In the case of specimen 1 of Reyes & Robertson (2011), there is no distance between the end active zone and the first anchors. That means that the tensile stress at the anchor hooks are not reduced by the horizontal friction between the passive part of the link slab and the reinforced concrete. So in this case, the high tensile stress is transferred through a reduced cross sectional concrete area, what could result in peak stresses and a through crack.

Conclusion

All specimens that are exposed to the test, the passive zone of the link slab failed. It could be concluded that for the designs of Reyes & Robertson (2011), the passive sections, or at least the connections between the passive sections with other sections, are the weak spots of the link slab. Some general conclusions from the tests are:

- Imposed horizontal deformation can cause a bending moment in the passive section of the link slab (specimen 2 and 3)
- Dowels seem to have limited vertical slip capacity (specimen 2 and 3)
- Anchor hooks near the interface between the passive and active zone seem to induce horizontal peak stresses in the link slab (specimen 1)
- Combination of grout bonded section, vertical steel dowels and grouted horizontal GFRP bars is not able to prevent a vertical gap between the reinforced concrete and the end of the link slab (specimen 2) (Reyes & Robertson, 2011)
- Vertical steel dowels have some capacity to deflect before a resisting load is generated (specimen 2) (Reyes & Robertson, 2011)

The above mentioned conclusions are mainly about the passive zone of the link slab. Evaluating the scheme made in paragraph 2.3.5.3 Scheme, the supporting system of the link slab should probably be modified a bit. To evaluate the scheme, the scheme of paragraph 2.3.5.3 Scheme is shown on Figure 81 again.

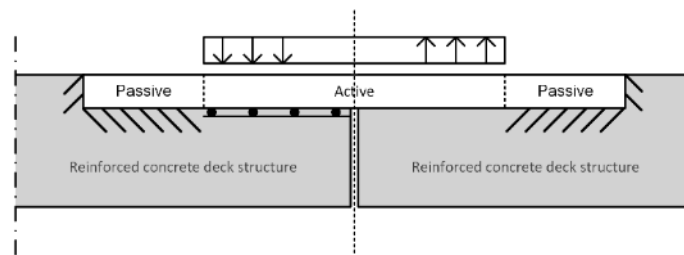


Figure 81 – Scheme of the link slabs designed by Reyes & Robertson (2011)

As shown in Figure 81, the passive zone is assumed to be connected to the reinforced concrete like a clamped support. However, in two of the three tests, there was a certain movement in the passive section of the link slab, what in the end results in failure of the slab. In the case of specimen 2 and 3, the vertical connection between the link slab and the concrete deck fails. Further, the horizontal connection needed some horizontal deformation before it could generate horizontal stresses.

Probably, in a better model the horizontal connection should be modelled by springs instead of a clamping support is, because springs also require a certain movement before they can carry loads. However, a system with springs is a relative complex model compared to the model of Figure 81. Probably only with the help of a computer, the addition of springs in the model is interesting to apply. A model with springs probably shows better results than the model of Figure 81.

2.3.5.5 Vertical imposed deflection

The analysis to the reaction of the link slab on vertical imposed deflection for the link slab design of Reyes & Robertson (2011) is done in the same way as for the designs of Li, et al. (2003). The method is to split the link slab into two parts; the concrete substructure and the SHCC link slab. Both are only analysed over the active length of the link slab construction.

First the concrete substructure is analysed. In Figure 82 are shown two concrete substructures without a link slab. The right support is settled down, as shown in the detail for the figure. As shown in the figure, the concrete substructure is able to deform freely. Therefore no stresses are expected in the substructure. Further it is assumed that the vertical settlement is very small compared to the length of the substructure, such that the rotation in the substructure caused by settlement of the support can be neglected. In other words, the substructure is assumed to remain horizontally. In fact, due to imposed vertical deformation, the substructure moves in the vertical direction only, assuming that the settlements are relative small compared to the length of the substructure.

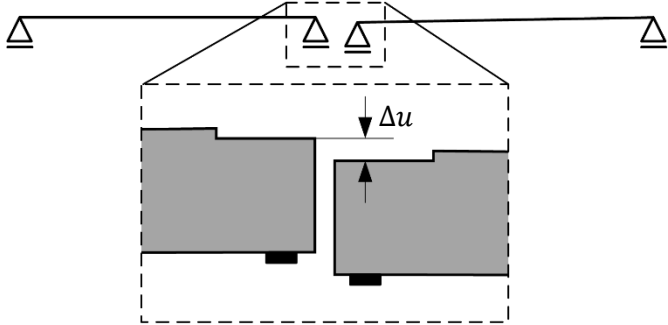


Figure 82 – Deflection of substructure due to settlement in the supports

As second is analysed the SHCC link slab. As mentioned earlier, the passive part of the link slab is assumed to be fixed to the substructure. So if the substructure moves vertically, the passive part of the link slab will also move vertically. Neglecting the support of the substructure under the active section of the link slab for a while, the active part of the link slab could be modelled as a beam fixed on both sides as shown in Figure 83. In the same figure is also shown how the active section of the link slab deforms according to the scheme. According to the scheme could be concluded that the beam can't deform freely. Since the beam has a certain stiffness, the bending moments and shear stresses are expected in the link slab according to forget-me-not as shown in Figure 83.

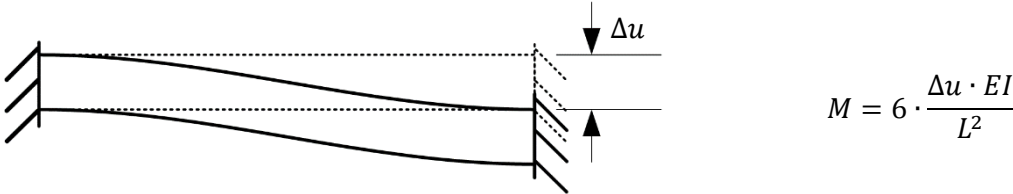


Figure 83 – Deflection of the link slab due to imposed vertical deformation

At last, the total model can be formed by combining both models of the substructure and the SHCC link slab, as shown in Figure 84. Figure 84 shows that the SHCC link slab will deform under the substructure, while in practice this is impossible. In reality, the substructure pushes against the SHCC link slab.

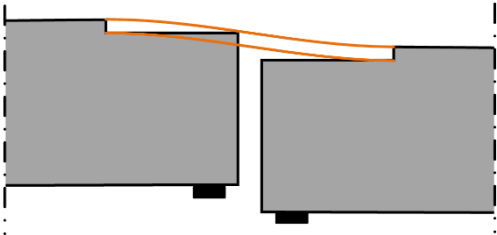


Figure 84 – Deflections of substructure and SHCC link slab in one figure

The SHCC link slab is assumed to be relative flexible compared to the concrete substructure. The SHCC link slab is relative thin; 76 mm thick link slab, while the substructure is assumed to be about 200-1000 mm thick. Further can the SHCC link slab be assumed to be cracked, so the Young's modulus of SHCC is assumed to be much lower compared to NSC. To illustrate this, according to the rule $E_{crack} = E_{cm}/3$ from Eurocode 2, the Young's modulus of cracks SHCC is about 6.7 GPa, while the young's modulus of NSC is about 33 GPa. In the end, it could be concluded that the concrete substructure remains more or less in its original shape and the SHCC link slab probably deflects as shown in Figure 85.

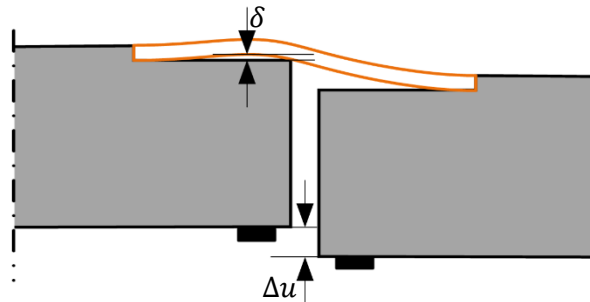


Figure 85 – Expected deflection of the SHCC link slab due to imposed vertical deformation Δu

At both connections of the active part of the link slab with the substructure is assumed that the link slab can be modelled as a fixed support. Further is assumed that the link slab is pushed up by the concrete substructure at the edge of the substructure. Due these assumptions, there is generated a certain δ between the link slab and the substructure and a point load between the substructure and the link slab at the edge of the substructure. Assuming the imposed vertical deformation due to settlement is just a few millimetre, δ is probably very small.

Another interesting thing to mention shortly is the vertical imposed deformation in combination with a vertical wheel load. At the moment, the link slab is assumed to have no moment and shear capacity, as mentioned in paragraph 2.3.5.1 Vertical loads. So if a vertical wheel load work on the part of the link slab that is not supported by the substructure, failure in the link slab could be expected. Taking the situation of Figure 85 where a wheel load works on, then the link slab will probably fail due to the wheel load.

2.4 Flexible Thin Link Slabs

In this chapter is analysed the research of Lárusson (2013) to flexible link slabs using SHCC in combination with GFRP reinforcement. Same as in the previous paragraphs, the analysis starts with the characteristics of the materials that are applied. After that the design is analysed in detail. At last some test results are discussed also. In the end, a load transfer system for different actions that work on the link slab is suggested.

2.4.1 Materials characteristics

In this chapter are described some characteristics of the SHCC mixture. Because SHCC is already analysed in detail in Appendix 1: Literature study, only the mix design of SHCC is given here. Also the characteristics of the GFRP reinforcement and the debonding layer are described in some more detail.

2.4.1.1 Strain Hardening Cementitious Composite

The mix design that is applied in the link slab designed by Lárusson (2013), is shown in Table 21. As shown in the table, a lot of cement and fly ash and 2 V% fibres are applied in the mixture, what is typical for SHCC. Further in this specific mixture quartz powder and a viscosity agent are added.

Table 21 – SHCC mixture for flexible link slab using Ductile Fiber Reinforced Concrete (Lárusson, 2013)

Cement [kg/m ³]	Water [l/m ³]	Sand (< 0.18mm) [kg/m ³]	Fly Ash [kg/m ³]	Quartz powder [kg/m ³]	Super plasticizer [kg/m ³]	Viscosity agent [g/m ³]	PVA fibres [kg/m ³]
430	320	150	860	150	4.3	480	26 (= 2 V%)

PVA fibres: length = 8 mm, diameter = 40 μm

Some characteristics of the mix design, which is shown in Table 21, are given in Table 22. As shown in the table, the Young's modulus is relative small compared to NSC with the same strength.

Table 22 – Characteristics of the SHCC mixture shown defined in Table 21 (Lárusson, 2013)

Characteristics	Unit	
Average compressive strength	[MPa]	66
Tensile cracking strength	[MPa]	3.0-3.6
Ultimate tensile strength	[MPa]	4.1-5.2
Young's Modulus	[GPa]	20

2.4.1.2 Glass Fibre Reinforced Polymer (GFRP) reinforcement

In this paragraph are given some characteristics of the GFRP reinforcement. Before the characteristics of the GFRP reinforcement are given, first is described the desired characteristics of the reinforcement in the link slab. Lárusson (2013) defines three main features for the reinforcement in the link slab:

1. Relatively soft axial load-deformation response, so a low elastic modulus
2. A relatively large linear-elastic strain capacity, for a reduced permanent deformations
3. A high corrosion resistance, to minimise the link slab thickness

In Figure 86 is given the stress-strain diagram of five different reinforcement materials. As shown in the figure, AFRP and GFRP both have the lowest elastic stiffness and a relatively large linear-elastic capacity, what are both of the features that are defined by Lárusson (2013). However, because AFRP rebars are significantly more expensive and less available, GFRP is chosen for the link slab design. Further, GFRP has a high corrosion resistance.

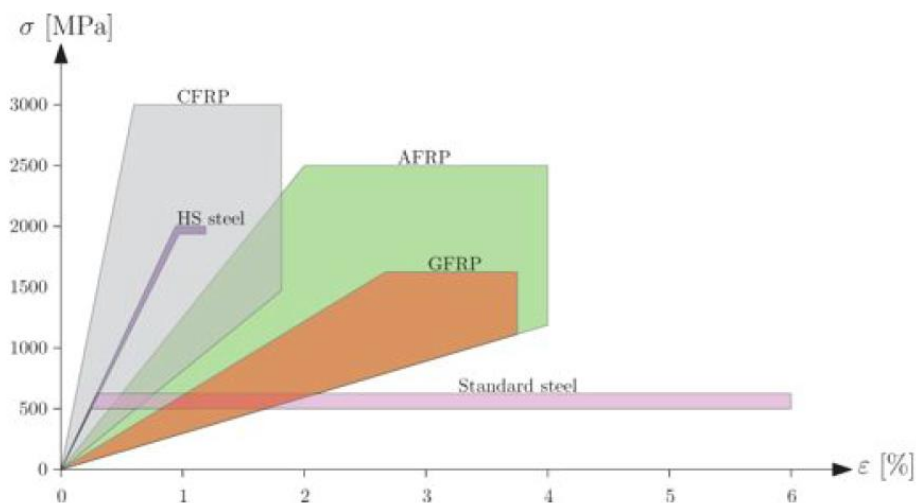


Figure 86 – Approximate stress-strain response ranges of various reinforcement types according to Model code 2010, (Lárusson, 2013)

The GFRP rebars that are chosen in the design of Lárusson (2013) have the next characteristics:

- Bar diameter of 6 mm
- Elastic modulus of 46 GPa
- Linear tensile strain capacity of 2.5%

The stress-strain relations of the GFRP rebars, which are applied in the research of Lárusson (2013), are given in Figure 87. In three of the four designs are applied the GFRP1 rebars. In one design are applied GFRP2 rebars. As a reference, the stress-strain relation of a steel rebar is also included in the figure.

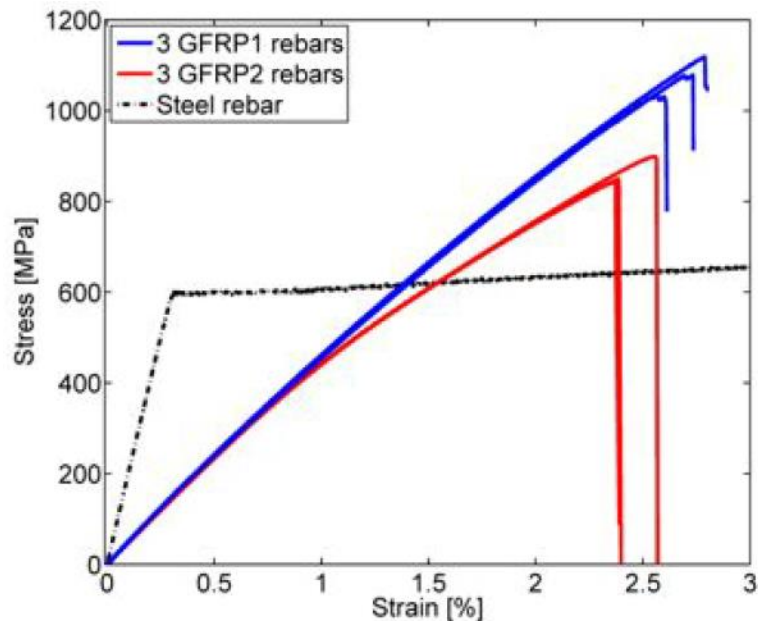


Figure 87 – Stress-strain relations for GFRP1, GFRP2 and steel rebars (Lárusson, 2013)

2.4.1.3 Roofing paper and plastic sheeting

The debonding zone of the designs of Lárusson (2013) is made by roofing paper and plastic sheeting. However, no characteristics for roofing paper and plastic sheeting are given. As mentioned already in chapter 2.2.2 Roofing paper the mean characteristics are not found in literature.

It is also impossible to approach the characteristics of the plastic sheeting. Plastics have a wide range of characteristics. Therefore, it does not make sense make assumptions for the characteristics, because possibly the real characteristics of the plastic sheeting differs a lot from the assumed characteristics.

2.4.2 Design

In this chapter is given the design of the proposed link slab. The aim of the design is to implement a slender link slab design concept with a relatively low stiffness (Lárusson, 2013). Four different designs are made by Lárusson (2013), which all have more or less the same dimensions. The difference between the designs is in the reinforcement and the execution method. After the analysis of the designs, the ideas behind design choices are explained. In the end, some information about the execution of the link slab is given shortly, where a distinction is made between prefabricated and cast in situ link slabs.

A side view of the design is given in Figure 88 (Lárusson, 2013). In the figure is shown a concrete bridge deck that is supported by a substructure. Over the gap between both deck ends is made the SHCC link slab. The GFRP rebars and grout connect the link slab and the bridge deck to each other. Further is

shown the debonding layer in the middle of the link slab. The debonded part of the slab should deflect to take care of movements of the bridge deck. A layer of roofing paper and plastic sheeting between the link slab and the concrete substructure should result in a debonding layer between both.

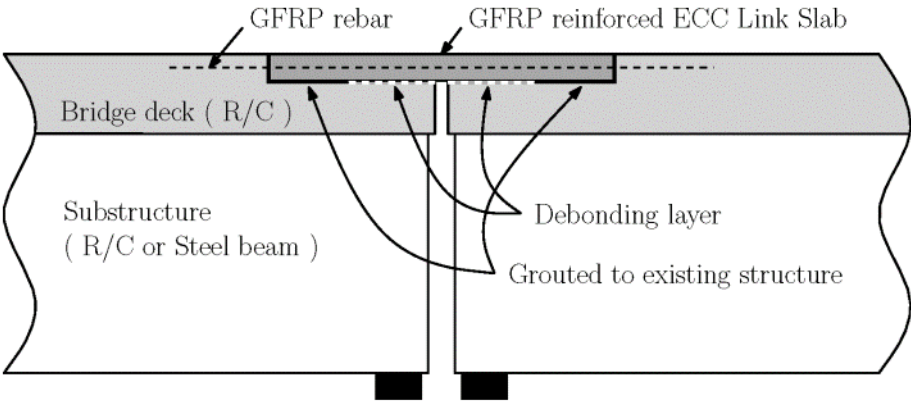


Figure 88 – Proposed GFRP reinforced SHCC link slab concept by Lárusson (2013)

The general dimensions of the link slab are shown in Table 23. These dimensions are equal for all test specimens. In the table are also shown the active and passive length. These are the lengths of the debonded and bonded parts of the link slab.

Table 23 - General dimensions for all test link slab specimens according to Lárusson (2013)

Dimension	Unit	
Length	mm	2,000
Width	mm	1,000
Thickness	mm	75
Active length	mm	1,000
Passive length	mm	500

The dimensions given in Table 23 are shown in the top and side view of Figure 89. As shown in the figure, in the passive (bonded) part (cross section CC) is placed almost twice of the amount of reinforcement that is placed in the active (unbonded) part of the link slab (cross section BB).

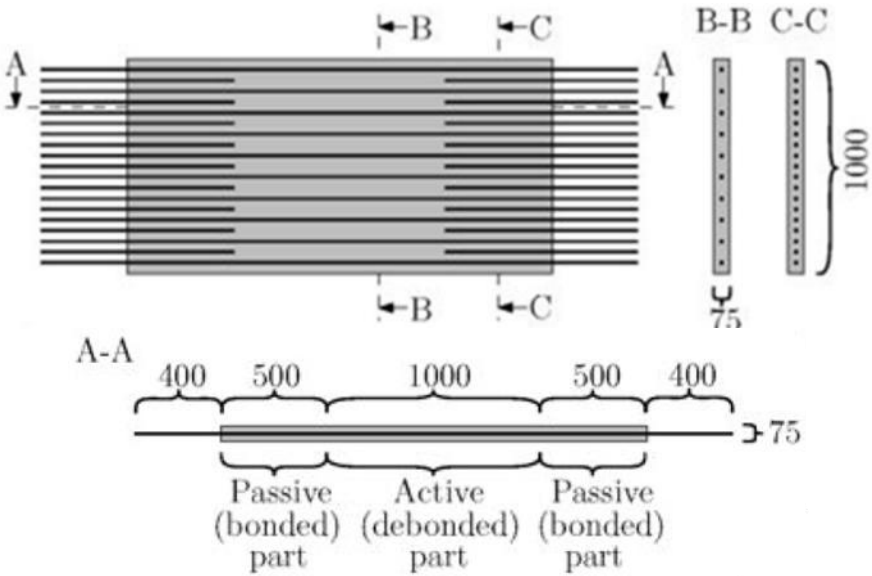


Figure 89 – Top view and side view of the link slabs (Lárusson, 2013)

The details of the four link slabs are given in top view on Figure 90 and in Table 24. The length of the active and passive parts of the link slabs is in all slabs the same. The variables that have been changed during the experiments are the number of bars, the bar diameter, the extending length of the GFRP bars in combination with the casting method. Because link slab 3 is a cast in place design, the extending bars are made shorter.

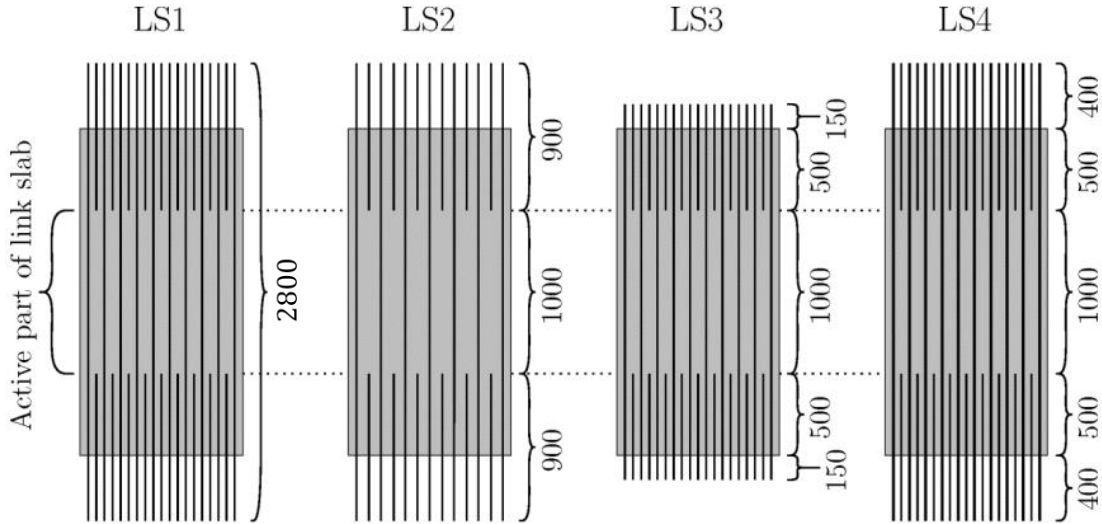


Figure 90 - Top view of the reinforcement design of the four link slabs (Lárusson, 2013)

Table 24 - Reinforcement characteristics of the link slabs that are shown in Figure 90 (Lárusson, 2013)

Variables	Unit	Link slab 1	Link slab 2	Link slab 3	Link slab 4
Number of primary bars per metre width	[-]	10	7	10	10
Bar diameter	[mm]	6.3	6.3	6.3	6.9
Reinforcement ratio	[%]	0.42	0.30	0.42	0.50
Extending GFRP	[mm]	400	400	150	400
Casting method	[-]	Prefabricated	Prefabricated	Cast in place	Prefabricated
GFRP type	[-]	GFRP 1	GFRP 1	GFRP 1	GFRP 2

Lárusson (2013) described some reasons to research these four designs. These reasons are:

- Due to the unique cracking pattern of SHCC, limited crack width and crack spacing will develop in the active part of the link slab. This unique characteristic makes that cracked SHCC keep its strength if it is cracked and of course keeps its durability characteristics.
- The relative low stiffness of the GFRP reinforcement compared to steel results in a low stiffness of the composite element. Compared to steel reinforcement, relative low stresses are generated if the link slab deforms.
- Low reinforcement ratio to accommodate deformations without significant moment- or axial resistance.
- Due to the high corrosion resistance of GFRP, a corrosion resistant design is made.
- The low reinforcement ratio in the active part and the choice of GFRP results in small moment and axial resistance if deformations between spans must be accommodated.
- Small diameters of the rebars are chosen to maximize the rebar circumference while a relative low reinforcement ratios is maintained and to effect the crack width and crack spacing in a positive way (smaller rebar diameters results in smaller crack widths).

- Different reinforcement ratios are chosen for the active and passive parts, such that the expected deformations are carried by the softer active middle part of the link slab.
- Due to the strain compatibility between GFRP reinforcement and SHCC, the composite response results in low degradation of rebar-matrix interface which improves durability if the slab is loaded statically and cyclically.
- A debonding layer of roofing paper and plastic sheeting is made under the active part of the link slab to debond this part of the slab from the concrete deck. In this way, deformations could be carried by the middle part easier.
- Transverse ribs patterns were provided in the passive (bonded) parts to increase the effectiveness of the transition zone.
- Shear studs are not considered a viable option to connect the prefabricated link slab to the bridge deck or girders within the length of the prefabricated element due to practical issues.

Prefabricated link slabs

Three of the four link slab design of Lárusson (2013) are prefabricated. The execution of the prefabricated link slabs for the tests is shown in Figure 91 and Figure 92. In Figure 91 is given an overview of the test setup with reinforcement before any concrete is casted.

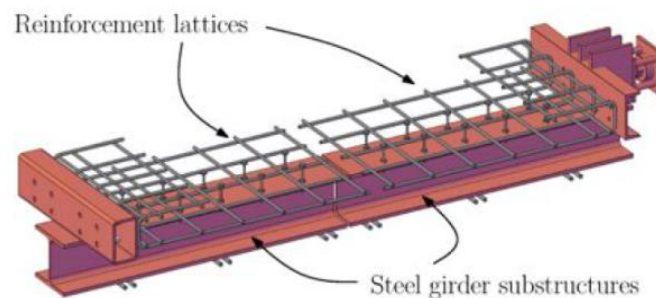


Figure 91 – Reinforcement lattices of a bridge deck installed on the top of a steel beam substructure

In Figure 92 are given the steps that should be taken to construct the link slab in the concrete deck with the setup that is shown in Figure 91. The first step is to place the prefabricated link slab between the two adjacent reinforcement lattices of the bridge deck. As soon as the elements are aligned, self-consolidating concrete is poured to complete the connection between the bridge deck, the link slab and the girders.

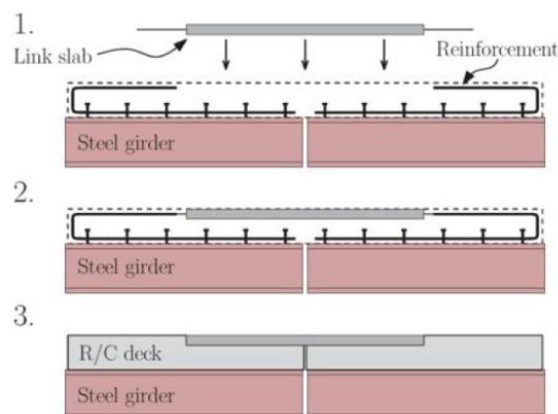


Figure 92 – Execution overview to install the prefabricated link slab; placement of the prefabricated link slab and self-consolidating concrete pouring

Cast in place

One of the link slab is casted in place. In Figure 93 is shown the reinforcement and the debonding layer of the link slab, just before the concrete is casted. In the figure is also shown the formwork and the reinforcement that is grouted in the concrete deck.

The cast in place method could be interesting to apply to construct SHCC link slabs in existing structures. Two meters concrete bridge deck must be removed. Then the debonding layer must be placed. After that 150 mm deep holes must be drilled in the concrete deck. In the holes must be placed the reinforcement. Grout in the holes must carry the connection between the reinforcement bars and the bridge deck. At last, the formwork must be placed and the SHCC link slab can be casted in place.

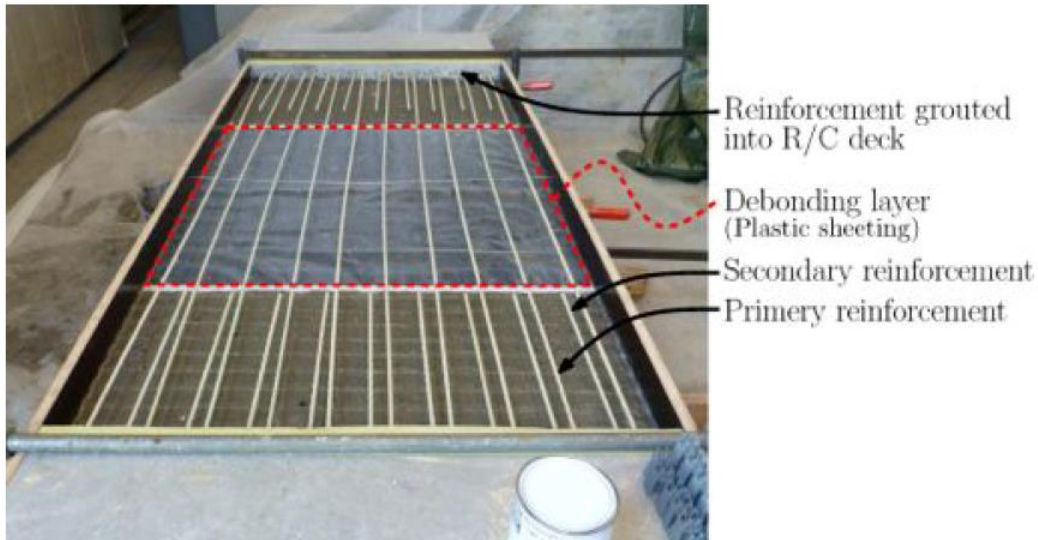


Figure 93 – Formwork, GFRP reinforcement grouted in the concrete deck and the debonding layer at the active part

2.4.3 Test results

Lárusson (2013) did some different tests on the link slabs, which are discussed in this chapter. From the test follows the influence of the variations between the different link slab designs. The specimens are tested by:

- Static loading
- Cyclic loading
- Interface between the rebar and the SHCC
- Crack width

In all tests carried by Lárusson (2013), the maximum strain is 1.0%. This strain value is based on the rotation and the temperature difference in the spans. Lárusson (2013) shows by a simple design example that a strain capacity of 1.0% should be large enough. For the calculations a few assumptions are done by Lárusson (2013):

- Shrinkage is neglected because a prefabricated link slab is assumed
- Maximum vertical deflection of the spans is equal to $u_{max} = L/800$
- The beams are simply supported
- The height of the beams is equal to $h = 550 \text{ mm}$
- The active length of the link slab is equal to $L_{ls} = 1000 \text{ mm}$
- The maximum temperature differences is equal to $\Delta T = 50^\circ\text{C}$
- The length of the link slab is 5% of the length of the span, $L_{ls} = 0.05L_{sp} \rightarrow L_{sp} = \frac{1000}{0.05} = 20 \text{ m}$

According to the above mentioned assumptions, first the maximum strain in the link slab due to rotation in the span can be calculated. The maximum rotation in the span is expressed in eq.(19).

$$\theta_{max} = \theta_{deflection} \cdot \frac{u_{max}}{u_{deflection}} = \frac{1}{24} \frac{qL^3}{EI} \cdot \frac{\frac{800}{5} \frac{qL^4}{EI}}{\frac{384}{EI}} = \frac{1}{250} = 0.004 \text{ rad} \quad \text{eq.(19)}$$

Now the maximum strain in the link slab can be calculated according to eq.(20).

$$\Delta\varepsilon_{\theta} = \frac{2(\theta_{max} \cdot h)}{L_{ls}} = \frac{0.008 \cdot 550}{1000} = 0.44\% \quad \text{eq.(20)}$$

The maximum horizontal strain difference in the link slab due to temperature differences in the bridge deck could be calculated by eq.(21).

$$\Delta\varepsilon_T = \frac{\alpha_T \cdot \Delta T \cdot L_{sp}}{L_{ls}} = \frac{1.2 \cdot 10^{-5} \cdot 50 \cdot L_{sp}}{2 \cdot (0.05 \cdot L_{sp})} = 0.6\% \quad \text{eq.(21)}$$

Now the total expected strain is the summation of both, the strain due to rotation and the strain due to temperature differences. The total strain is expressed in eq.(22).

$$\Delta\varepsilon_{tot} = \Delta\varepsilon_{\theta} + \Delta\varepsilon_T = 0.4\% + 0.6\% = 1.0\% \quad \text{eq.(22)}$$

As a conclusion, in the test, the specimens are deflected until the link slab elongates by 1.0%. This target tensile strain is defined because this is approximately equal to the sum of the rotation induced strain due to vertical deflection of the span and the volume change due to temperature differences. The deformations due to shrinkage are not considered, since prefabricated elements are proposed. The test results are analysed in the next paragraphs.

2.4.3.1 Static loading

In this paragraph are presented the results of the static loading tests. For every link slab is given the:

- Elastic tensile strength
- Tensile stress if the elongation of the deck is 1%
- Deformation of the link slab at 1% elongation
- Permanent deformation after deloading.

For every link slab, these test results are also given in stress-strain diagrams. In the diagrams is also given the strain-strain relation of the GFRP rebars. The difference between these relations is an indication of the compatibility between concrete and reinforcement. This is discussed in more detail in chapter 2.4.3.3 Interface rebar-SHCC.

Link slab 1

- *Elastic tensile strength* = 230 kN
- *Tensile strength* _{$\varepsilon=1.0\%$} = 380 kN
- *Deformation* _{$\varepsilon=1.0\%$} = 10 mm
- *Permanent deformation* \approx 0.4%

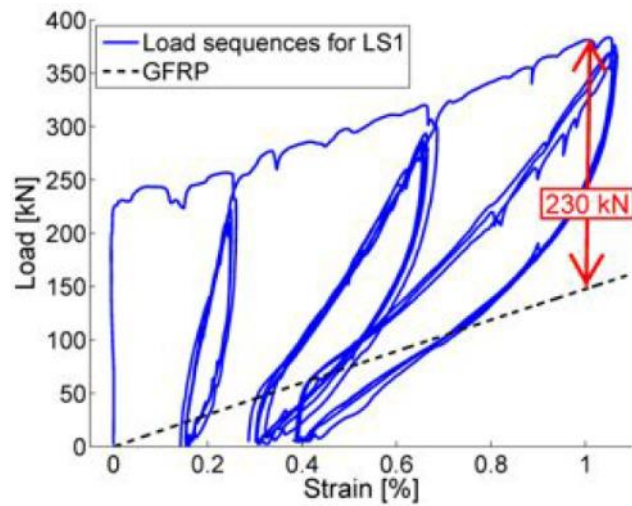


Figure 94 - Static loads as a function of the strain for LS1 (Lárusson, 2013)

Link slab 2

- Elastic tensile strength = 180 kN
- Tensile strength $_{\varepsilon=1.0\%}$ is unknown due to technical difficulties with test setup
- Deformation $_{\varepsilon=1.0\%}$ is unknown due to technical difficulties with test setup
- Permanent deformation $\approx 0.5\%$

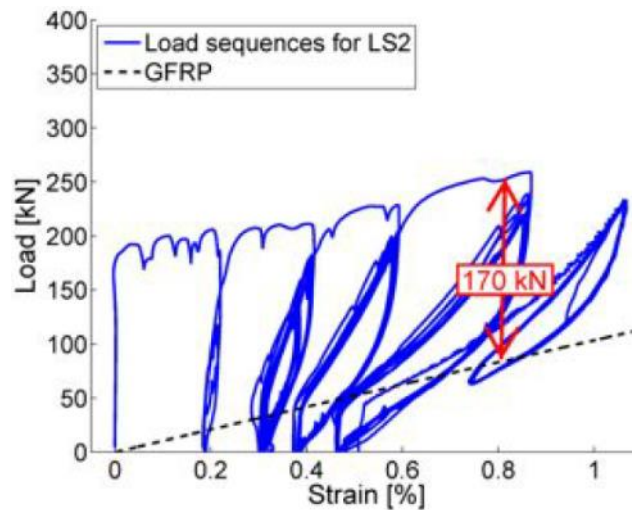


Figure 95 - Static loads as a function of the strain for LS2 (Lárusson, 2013)

Link slab 3

- Elastic tensile strength = 175 kN
- Tensile strength $_{\varepsilon=1.0\%}$ = 375 kN
- Deformation $_{\varepsilon=1.0\%}$ = 10 mm
- Permanent deformation $\approx 0.4\%$

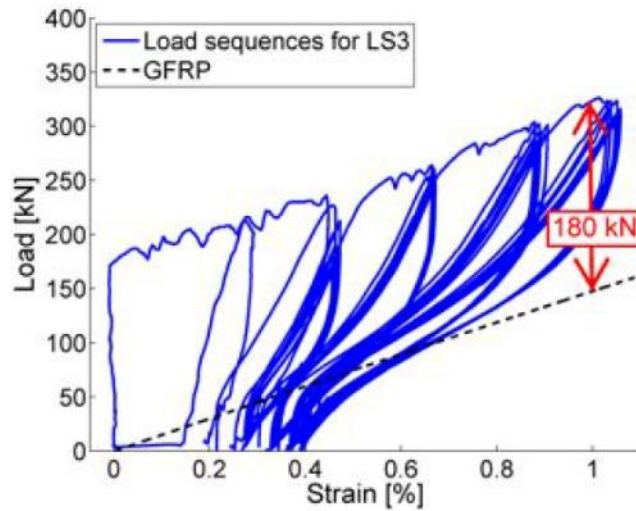


Figure 96 - Static loads as a function of the strain for LS3 (Lárusson, 2013)

Link slab 4

- Elastic tensile strength = 200 kN
- Tensile strength $_{\varepsilon=1.0\%}$ = 300 kN
- Deformation $_{\varepsilon=1.0\%}$ is unknown
- Permanent deformation $\approx 0.5\%$

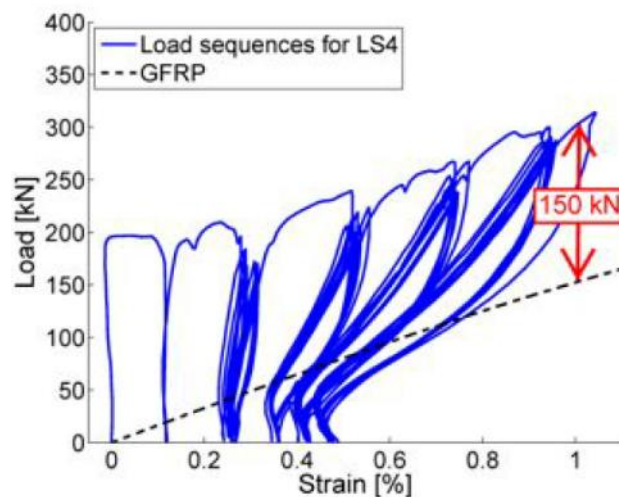


Figure 97 - Static loads as a function of the strain for LS4 (Lárusson, 2013)

2.4.3.2 Cyclic loading

To make some conclusions for the fatigue behaviour of the link slabs, cyclic loading tests are done. The result for LS 1 and LS 2 are shown below. The test results of the cyclic loading of LS3 and LS4 are not given. The experiments were discontinued shortly after they were initialized due to failure of the load transfer zone and rupture of the rebars respectively.

In Figure 98 and Figure 99 are shown the results of the cyclic test for LS1 and LS2 respectively. For LS1, only 300 load cycles are performed, because of a malfunction during the experiment. However, Figure 98 shows that after 300 cycles, there is no significant degradation of the link slab. This implies that the composition of GFRP reinforcement and SHCC is well suited for the tensile fatigue in terms of maintaining structural integrity of the link slab (Lárusson, 2013).

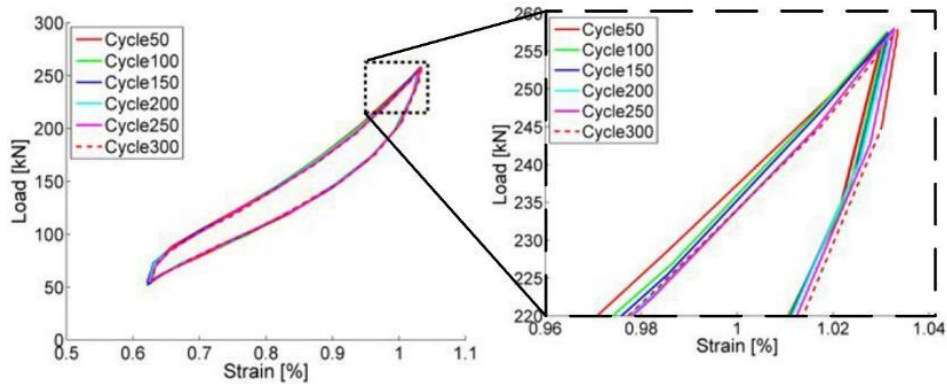


Figure 98 – Load as a function of the strain for cycling test of LS 1 (Lárusson, 2013)

The load response of LS2 is decreased a bit from the 100th to the 1000th cycle, as shown in Figure 99. This result indicates a diminishing composite interaction. This is undesirable in terms of maintaining structural integrity.

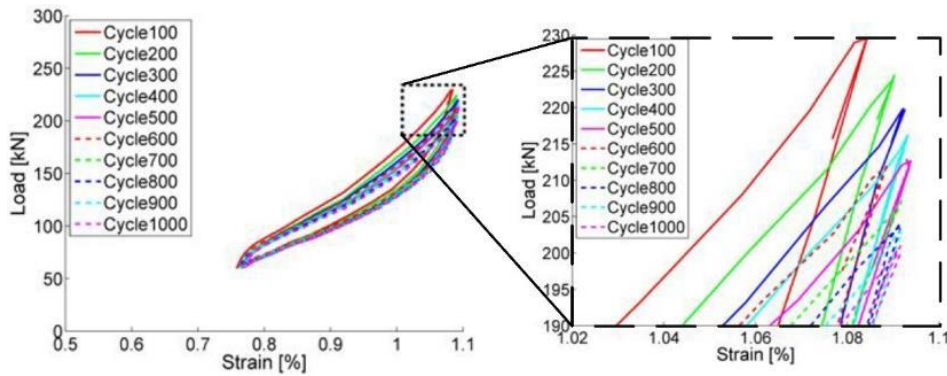


Figure 99 - Load as a function of the strain for cycling test of LS 2 (Lárusson, 2013)

2.4.3.3 Interface rebar-SHCC

To make a prediction of the long term behaviour of the link slabs, the interface between the rebar and the SHCC is an important issue. The differences between the stiffness of the link slab and its GFRP rebar gives an indication of the interaction between the concrete and the reinforcement. In Figure 100, the difference between the link slab response and the bare GFRP response, suggests that the interface between the rebar and the surrounding SHCC matrix is intact and effectively transferring stresses between both the matrix and the rebar.

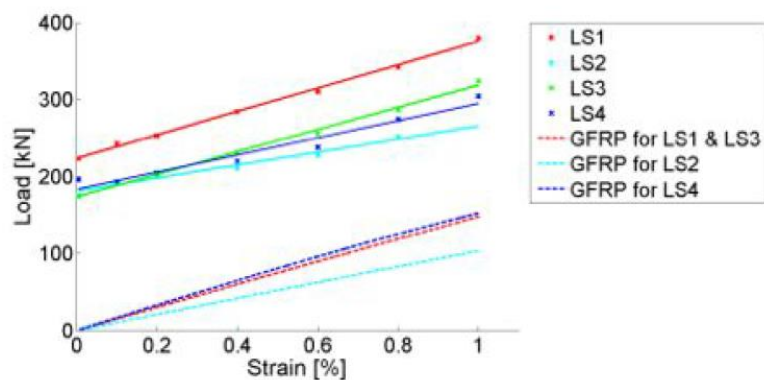


Figure 100 – Comparison between the stiffness of the composite link slab and the GFRP reinforcement for all link slab design in a force strain diagram (Lárusson, 2013)

2.4.3.4 Crack width

Since the crack width is a very important parameter for the durability of the link slab, test are done to determine the crack width of the different link slabs. In Figure 101, the crack width in the link slabs are given as a function of the elongation of the link slab. In the graphs is also given the limit value for the crack width according to the AASHTO. Further is given the crack width where the water permeability is smaller than 10^{-10} m/s, which is about 0.1 mm.

From the graphs of Figure 101 could be concluded that LS1 has the smallest crack width. Even if LS1 is elongated 1%, the crack width is still under the limit of AASHTO. The crack width in LS2 is the largest compared to the other link slabs.

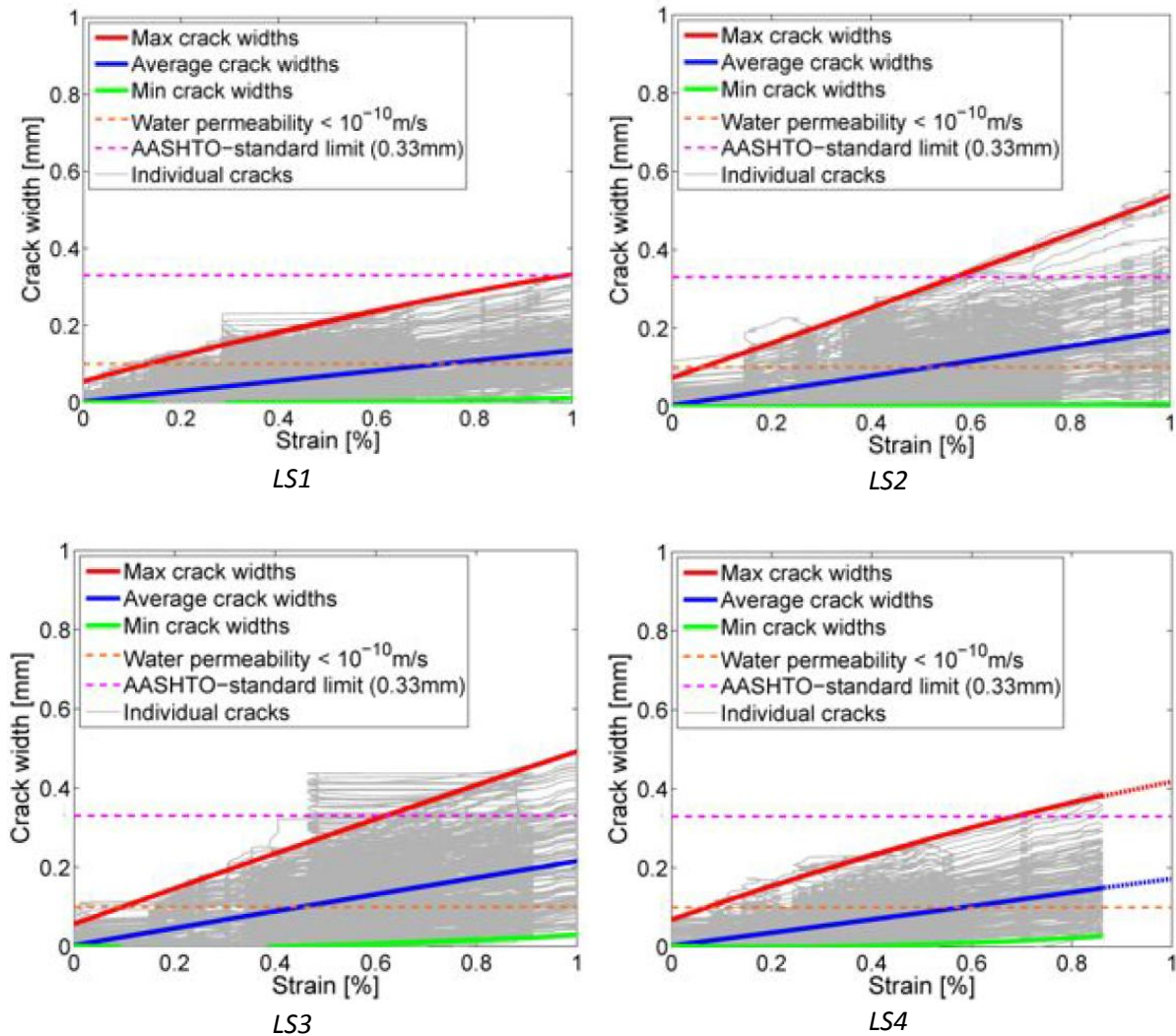


Figure 101 – The crack width as a function of the strain for all four link slabs (Lárusson, 2013)

2.4.4 Conclusion

According to the test results from above the best link slab design could be chosen. The link slab with the best overall performance is LS1, because of its sustained composite load-deformation response and the crack width and crack spacing measurements (Lárusson, 2013). Both results suggest a high durability of the link slab, so an increased service life could be expected compared to other joint types.

In short, the reasons why the other link slabs are not chosen as the best design are mentioned here. Tests on LS2 resulted in deterioration of the composite interaction during cyclic loading and produced

excessive crack widths when compared to LS1 (Lárusson, 2013), what suggest that LS2 is less durable compared to LS1.

The difference between LS3 and LS1 is most evident in the dissimilarity of the first crack composite stresses of LS1 (3.1 MPa) and LS3 (2.3 MPa) and the subsequent tensile stiffening effect of SHCC. It is noted the failure mode of LS3, where the rebars ends were embedded into the R/C deck could have been avoided with proper anchorage length (Lárusson, 2013).

In LS4 is applied less stiff GFRP2 reinforcement. This results in deterioration of the composite responds and failure of the link slab where the rebars ruptured. As a conclusion, GRFP2 reinforcement is not recommended in the link slab design (Lárusson, 2013).

2.4.5 Load transfer system

According to the knowledge of this chapter, the load transfer system for different actions could be determined. The actions that are taken into account are vertical and horizontal loads and imposed horizontal deformation, where imposed curvature is included, and vertical imposed deformation.

Lárusson (2013) has included four different link slab designs. The most important dimensions of the link slab designs are given in Table 25. As shown in the table, the total, active and passive length and the thickness of the link slab is the same for all designs. The reinforcement in the link slabs is different in all designs. Variable parameters for the reinforcement are the number of bars, the diameter, the reinforcement ratio, the length of the extending GFRP bars and the type of GFRP. However, the difference between the different link slabs is that small, that it is assumed that the loads in all designs is transferred to the substructure in the same way.

Table 25 – Dimension of link slab 1, 2, 3 and 4 (Lárusson, 2013)

	Variables	Unit	Link slab 1	Link slab 2	Link slab 3	Link slab 4
Link slab	Total length link slab	[mm]	2,000	2,000	2,000	2,000
	Length active part	[mm]	1,000	1,000	1,000	1,000
	Length passive part	[mm]	500	500	500	500
	Thickness link slab	[mm]	75	75	75	75
Reinforcement	Number of primary bars per metre width	[-]	10	7	10	10
	GFRP bar diameter	[mm]	6.3	6.3	6.3	6.9
	Reinforcement ratio	[%]	0.42	0.30	0.42	0.50
	Length extending GFRP	[mm]	400	400	150	400
	GFRP type	[-]	GFRP 1	GFRP 1	GFRP 1	GFRP 2

With the date of Table 25 is made a general cross section of the link slab as shown in Figure 102. The figure is valid for all link slabs. Only the length of the extending GFRP bars of link slab 3 differs. For LS3, this length is 150 mm, while in the figure is given that the extending length is 400 mm.

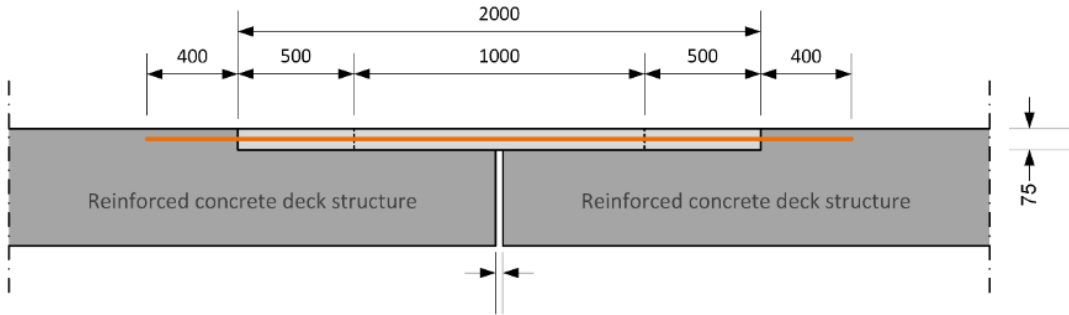


Figure 102 – Lay out of link slab design according to Lárusson (2013) (length in mm)

The design of the link slabs of Lárússon (2013) is quite similar to the design of the link slab of Reyes & Robertson (2011). To illustrate the similarities between both designs, the mean dimensions of the link slabs of Reyes & Robertson (2011) and Lárússon (2013) are given in Table 26. According to Table 26 could be assumed that the link slabs both take care of loads in the same.

Table 26 – Mean dimensions of link slab designs of Reyes & Robertson (2011) and Lárússon (2013)

Variables	Unit	Reyes & Robertson (2011)	Lárússon (2013)
Total length link slab	[mm]	2,440	2,000
Length active part	[mm]	1,830	1,000
Length passive part	[mm]	305	500
Thickness link slab	[mm]	76	75
GFRP bar diameter	[mm]	6	6
Reinforcement ratio	[%]	0.6	0.4
Length extending GFRP	[mm]	610	400

2.4.5.1 Vertical loads

In this paragraph is discussed the vertical load distribution in the link slab. According to the data of Table 25 and the design lay out of the specimens, some remarks according the load transfer system could be made:

- The link slab is too thin to make a large span and carry vertical loads
- The reinforcement ratio is low ($\approx 0.4\%$) so the bending moment capacity is probably low too
- The link slab is equally supported by the reinforced concrete deck structure

Given these remarks, it could be concluded that the vertical loads will be transferred the same as for the designs of Reyes & Robertson (2011). Therefore, the way vertical loads are transferred to the substructure are not discussed here. Details of the way vertical loads are carried by the structure are shown in chapter 2.3.5 Load transfer system.

2.4.5.2 Horizontal loads

In this paragraph is discussed the way horizontal loads are probably carried by the link slab. According to the data from Table 25 and Figure 102 some remarks are mentioned here.

- Due to the debonded layer between the concrete deck and the link slab at the unbonded zone, it is assumed that there is no horizontal friction in this zone.
- Due to the grouted connection between the link slab and the concrete bridge structure, there is horizontal friction between the link slab and the concrete structure at the bonded zone.
- If the link slab is not exposed to imposed tensile strain, SHCC could transfer horizontal loads by normal compressive stress
- The reinforcement and the fibres together are able to transfer horizontal loads through normal tensile stresses.
- Because the reinforcement of the link slab is anchored in the concrete deck, it is assumed that the reinforcement is able to transfer tensile stresses from the link slab to the deck slab.

From the above mentioned remarks could be concluded that the horizontal stresses are probably carried the same as in the designs of Reyes & Robertson (2011). The only difference is that the friction at the horizontal plane between the link slab and the concrete structure at the passive zone is carried by grout instead of shear studs. However, the idea is the same, only the execution method is different. Explanation of the way horizontal loads are transferred from the link slab to the reinforced concrete is given in chapter 2.3.5 Load transfer system.

2.4.5.3 Imposed horizontal deformation according to test results and imposed horizontal deformation
 The reaction of the link slab according to imposed horizontal deformation is discussed here according to test result from Lárusson (2013). Same as for the link slab design of Reyes & Robertson (2011), it is assumed that imposed curvature results in an imposed horizontal deformation in the link slab. The test results are shown in paragraph 2.4.3 Test results. It is assumed that the imposed horizontal deformations are carried in a similar way as horizontal loads.

The test setup that is applied to determine the imposed horizontal deformation capacity of the SHCC link slab is shown in Figure 103. As shown in the figure, the test setup is supported in a ways, such that the concrete deck structure and the SHCC link slab are both exposed to horizontal imposed deformation only.

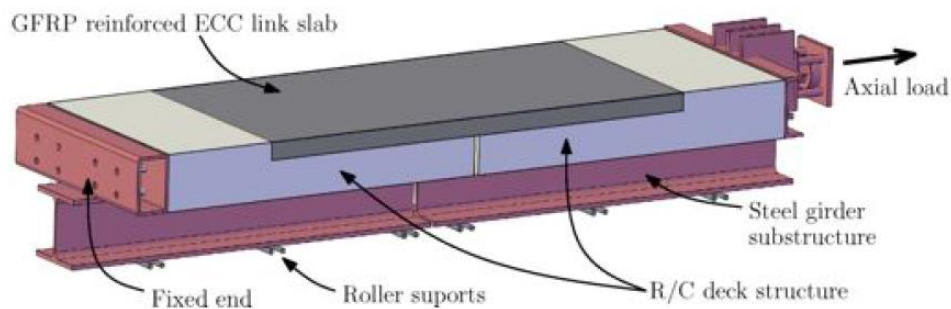


Figure 103 – Overview of the test setup to test the link slab on imposed horizontal deformation

Table 27 – Reinforcement of link slab 1, 2, 3 and 4 (Lárusson, 2013)

	Variables	Unit	Link slab 1	Link slab 2	Link slab 3	Link slab 4
Reinforcement	Number of primary bars per metre width	[-]	10	7	10	10
	GFRP bar diameter	[mm]	6.3	6.3	6.3	6.9
	Reinforcement ratio	[%]	0.42	0.30	0.42	0.50
	Length extending GFRP	[mm]	400	400	150	400
	GFRP type	[-]	GFRP 1	GFRP 1	GFRP 1	GFRP 2

Lárusson (2013) concluded that link slab 1 has the best overall performance, based on sustained composite load-deformation response and the crack width and crack spacing measurements from paragraph 2.4.3 Test results. The other link slab designs all have one reinforcement variable that differs from the design of link slab 1, as shown in Table 27. The variables per link slab that differs from link slab 1 are coloured yellow. Lárusson (2013) concluded that:

- **LS2:** fewer rebars in the active cross section, resulted in deterioration of the composite interaction during cyclic loading and produced excessive crack widths when compared to LS1.
- **LS3:** difference in material properties of SHCC as a result of the casting procedures, cast in place (LS3) vs. prefabricated (LS1). The difference is most evident in the dissimilarity of the first crack composite stresses of LS1 (3.1 MPa) and LS3 (2.3 MPa) as well as the subsequent tensile contribution of SHCC.
- **LS4:** for GFRP2 rebars gradual deterioration of the composite response was observed with increased tensile straining.

In Figure 104 is shown the displacement of the total link slab and the active part of the link slab for different deformations. As shown in the figure, the displacement of the total link slab is exactly the same as the displacement in the active part of the link slab only for displacement of until 3 mm. For

the higher displacement values in the graph of Figure 104, there is also some displacement in the passive sections. However, for total displacement of 11 mm, the displacement in the active part is still about 90% of the total displacement. According to the tests, Lárusson (2013) concludes that the deformations were subsequently distributed evenly throughout active middle part while the passive parts did not deform.

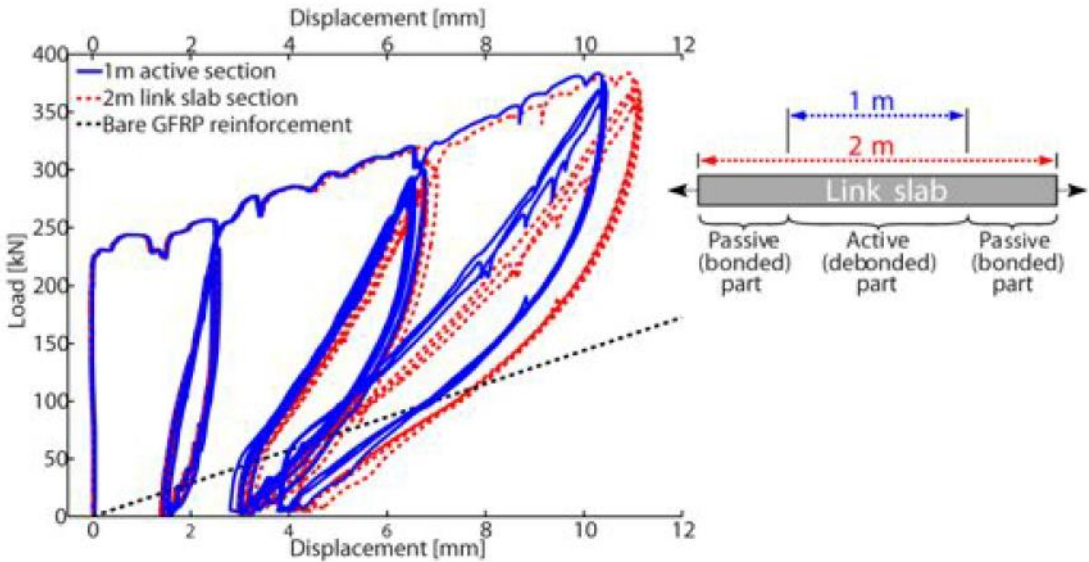


Figure 104 - Displacement of the total link slab and the active part of the link slab as a function of the displacement

Conclusion and evaluation

According to tests, Lárusson (2013) concludes that the passive part did not deform, so the assumption that the passive part could be modelled as a clamped support seems ok. Further could be concluded that there is a certain optimum amount of reinforcement to construct a link slab with the lowest crack width. Also the type of reinforcement has an influence on the crack width due to the composite response with the concrete. At last, there is a difference between the crack strength of cast in place and prefabricated link slabs. Prefabricated link slabs shows higher tensile strength compared to cast in situ link slabs, probably caused by the different casting procedures.

2.4.5.4 Vertical imposed deflection

The reaction of the link slab on vertical imposed deflection is assumed to be the same as for the link slab design of Reyes & Robertson (2011). The system behind both designs are more or less the same. Looking to the design, both designs probably have the same shape. There will probably be some difference in the exact shape caused by, for example, difference in length. The way vertical imposed deformations are carried are explained in detail in chapter 2.3.5.5 Vertical imposed.

2.5 Overview

In this paragraph is given an overview of the link slabs that are discussed in this chapter. In Table 28 is shown an overview of the characteristics of the four different types of link slabs. Table 28 is horizontally split up in four parts. In the upper parts are given the material that are applied in the design, like the type of concrete and reinforcement. In the second horizontal part are given the main properties of the link slab design. Here are called for example the dimensions of the link slab and the reinforcement. In the third horizontal part are given the characteristics of the applied concrete in some more detail. Characteristics like the compressive strength and the tensile strain are mentioned here. In the last horizontal part of the table are mentioned the vertical and horizontal load transfer systems. The systems are described and a model of the system is given.

In Figure 105 are given some definitions of dimensioned that are given in Table 28. With green, orange and blue are highlighted the vertical connection, the horizontal connection and the debonding layer. Further are shown the definitions of total length that could be split up in the passive and active lengths. At last, the thickness of the link slab is defined.

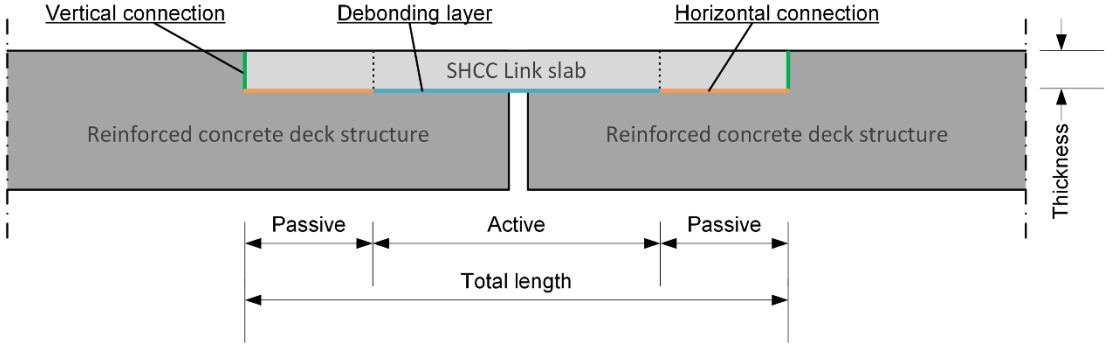
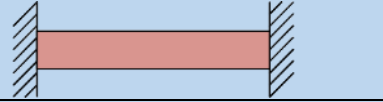
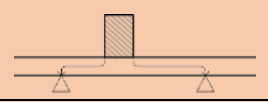
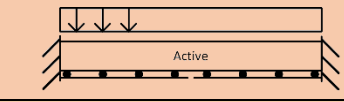
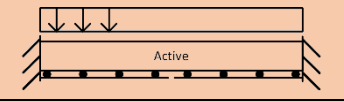
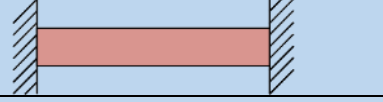
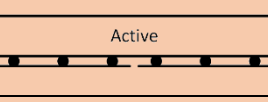
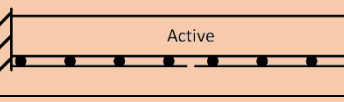
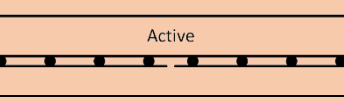
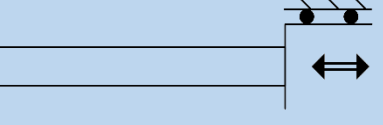
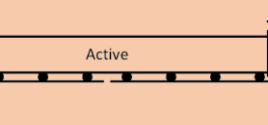
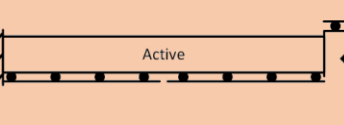
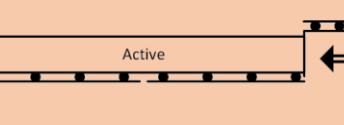


Figure 105 – Definition of dimensions in the link slab that are mentioned in Table 28

Table 28 – Overview of main characteristics of four different joints/link slabs made of NSC and SHCC

			Flexible joint	Deck link slab	Thin link slab	Flexible thin link slab
			Nosewicz & Jong (2009)	Li, et al. (2003)	J. Reyes and I.N. Robertson (2011)	Lárusson (2013)
Materials	Concrete type	[–]	NSC	SHCC	SHCC	SHCC
	Reinforcement	[–]	Steel	Steel	Glass Fibre Reinforced Polymer	Glass Fibre Reinforced Polymer
	Type of fibre	[–]	No fibres	PVA	Polyethylene	PVA
	Amount of fibres	[–]	No fibres	2.0 V%	1.23 M%	2.0 V%
Link slab design	Total length	[m]	0.8	2.4	2.4	2.0
	Length debond zone	[m]	0.8	1.3	1.8	1.0
	Length bonded zone	[m]	-	$2 \cdot 0.58 = 1.17$	$2 \cdot 0.30 = 0.6$	$2 \cdot 0.5 = 1.0$
	Thickness	[mm]	150	229	76	75
	Volume concrete	[m ³ /m]	0.1	0.5	0.18	0.15
	Reinforcement ratio ρ (debond zone)	[%]	2.3	1.4 or 1.0	0.6	0.30 – 0.50
	Bar diameter	[mm]	12	15.8 or 19	6.4 or 9.5	6.3 or 6.9
	Casting method	[–]	Cast in situ	Cast in situ	Prefab or cast in situ	Prefab or cast in situ
	Debonding layer	[–]	No connection (air)	Roofing paper	Plexiglass	Roofing paper and plastic sheeting
	Horizontal connection (passive zone)	[–]	Cold connection	Steel shear studs	Roughened NSC Steel anchor hooks or steel dowels Grouted	Grouted
Vertical connection (passive zone)	[–]	Steel reinforcement	Steel reinforcement	GFRP reinforcement (spec. 1+2) Cold joint (spec. 3)	Grouted GFRP reinforcement	
Concrete characteristics	Mean cylinder compressive strength	[MPa]	Unknown	60	Assumed similar to Li, et al. (2003)	66
	Tensile cracking strength	[MPa]	Unknown	4.0	Assumed similar to Li, et al. (2003)	3.0-3.6
	Ultimate tensile strength	[MPa]	Unknown	5.1	Assumed similar to Li, et al. (2003)	4.1-5.2
	Young's modulus	[GPa]	Unknown	20	Assumed similar to Li, et al. (2003)	20
	Tensile strain capacity	[%]	Unknown	3-3.5%	Assumed similar to Li, et al. (2003)	<i>Tested until 1.0% only</i>
Load transfer system	Transfer vertical loads	[–]	Bending moments and shear stresses	Direct to substructure with normal stresses and due to bending moments and shear stresses	Direct to substructure with normal stresses	Direct to substructure with normal stresses
	Model vertical loads	[–]				
	Transfer horizontal loads	[–]	Normal stresses carried by concrete and reinforcement steel	Normal stresses that are transferred to the substructures through shear studs in the passive zone	Normal stresses that are mainly transferred to the substructures through shear studs in the passive zone	Normal stresses that are mainly transferred to the substructures through grouted connection in the horizontal plane in the passive zone
	Model horizontal loads	[–]				
	Model horizontal imposed deformation	[–]				

3 Analysis of SHCC Link Slab

In this chapter, the SHCC link slab is analysed in more detail. With the knowledge from the previous chapter and the knowledge of the actions that work on the link slab, the reaction of the link slab on different actions is analysed. It should be a lot of work to do this analysis for all joints that are mentioned in the previous chapter. Therefore, the analysis is only done for SHCC link slab that has the most change to be applied in the next decades in Dutch bridges and viaducts.

3.1 Joints types

From the research that is done in chapter 2 Literature, the different joints could be divided into three types of joints. The division could be done by the way the stresses are transferred to the substructure. In the bullets bellow, a short description of the three types is given. Per type is also given the model of the link slab and the way vertical and horizontal loads are carried by the joint.

1. **Flexible joint:** concrete joint working as a beam clamped at two sides (Nosewicz & Jong, 2009)
 - Modelled as beam clamped at two sides
 - Vertical loads transferred through moments and shear
 - Horizontal loads transferred through normal strength
 - Rotation capacity
 - No horizontal deformation capacity
2. **Deck Link Slab:** SHCC joint working as a slab supported by steel girders (Li, et al., (2003))
 - Modelled as a deck slab supported by line supports
 - Vertical loads transferred through moments and shear to steel girders
 - Horizontal loads transferred through normal strength
 - Rotation capacity
 - No horizontal deformation capacity
3. **Thin Link Slab:** SHCC link slab supported by the concrete deck (Reyes & Robertson, (2011) and Lárusson, (2013))
 - Modelled as a deck slab that is equally supported by the substructure deck
 - Vertical loads directly transferred to the concrete deck by normal stresses
 - Horizontal loads transferred through normal strength
 - Rotation capacity
 - Horizontal deformation capacity

The flexible joint of course will not be analysed in a high level of detail, because this joint is applied for decades already. It should probably be more interesting to research a joint type that is not applied often in practice.

Together with Heijmans it is decided to research the Thin SHCC Link Slab, which is supported by a concrete deck, in more detail in the rest of the report. In the Netherlands, the deck of bridge or viaducts is mainly made of concrete. Therefore, it is expected that the Deck Link slab, which is supported by steel beams, will not or nearly be applied in the Netherlands in the next decades. Furthermore, the Thin Link Slab has some advantages compared to the Deck Link Slab, which are:

1. Horizontal deformation capacity (Reyes & Robertson, 2011), (Lárusson, 2013)
2. Lower stress required for deformations in the SHCC link slab (Reyes & Robertson, 2011)
3. Lower stiffness and tight crack width due to the application of GFRP bars instead of steel bars (Reyes & Robertson, 2011), (Lárusson, 2013)

Ad. 1. Both, SHCC and GFRP do have a certain deformation capacity. The deformation capacity of SHCC is caused by cracks in the material in the strain hardening phase. The maximum tensile strain of SHCC is in the order of 3-5%, while cracks remain below 0.1 mm (Li, et al., 2003). The strain capacity of GFRP is about 2.5%. GFRP deforms elastically, with a Young's modulus of 46 GPa.

Ad. 2. SHCC has a certain tensile strength, which remains more or less constant during plastic tensile deformation. So to deform the link slab, a certain stress is required. Obviously, a thick slab is able to carry higher loads before it fails compared to a thin slab.

The FHWA recommends a minimum reinforcement ratio of $\rho = 0.015$ and a clear cover of 2.5 inch ($\approx 64 \text{ mm}$) to control the crack width in the concrete link slab. That means that in total the minimum thickness of the link slab should be about 5 inch (130 mm). This recommendation is taken into account by Li, et al. (2003), who designed a 230 mm thick link slab.

However, in practical application, the load that is required to crack a 5 inch thick SHCC link slab may not occur (Reyes & Robertson, 2011). Therefore, in practice a slender link slab is interesting to develop because then only small horizontal forces are required to deform the link slab.

Furthermore, Lárusson (2013) implies that the cover thickness is significantly reduced in reinforced SHCC members. Normally, the cover thickness and the rebar diameter have a lot influence on the crack width. However, because of the fibre bridging and limited crack widths in SHCC, the effect of the cover thickness is significantly reduced. Therefore, the SHCC link slab could be made very slender while its crack width is still limited. The reinforcement layout of the link slab could still be optimised in terms of crack width limitations by applying more rebars with smaller diameters rather than fewer rebars with larger diameters (Lárusson, 2013).

Ad. 3. The combination of SHCC with GFRP rebars shows a better compatibility than SHCC with steel reinforcement (Lárusson, 2013). According to experimental results from Lárusson (2013) it could be concluded that the combination of ductile SHCC with GFRP are shown to be compatible resulting in a good composite interaction and strain compatibility during short term and long term loading. In practice, this results in a relatively low composite stiffness, conserved structural integrity and tight crack widths, which are highly desirable for the link slab design.

Next to the strain compatibility of the SHCC and the GFRP, other advantages of the GFRP is the large linear elastic strain capacity and the low elastic modulus. Due to the large elastic strain, the permanent deformation in the link slab is reduced. In combination with a low elastic modulus, the stresses in the bars during elastic deformation of the bars remain relative low. So if stresses are generated due to imposed deformations, these stresses are relative low if the deformation is still in the elastic zone.

3.2 Description of actions

Before the analysis to the SHCC link slab is done, the actions that are expected to work on the link slab are shortly mentioned. The actions that work on the link slab are determined according to Nosewicz & Jong (2009). It is assumed that the actions that work in case of a flexible joint, that is described by Nosewicz & Jong (2009), are the same as in the case of the thin SHCC link slab.

Nosewicz & Jong (2009) describe that on the link slab work horizontal and vertical loads. Horizontal loads included brake and acceleration loads and reaction loads of the support blocks of the girders. The vertical load working on the link slab are the wheel loads only. Self-weight of the slab and the weight of the asphalt is neglected relative to the wheel loads.

Next to the loads, according to Nosewicz & Jong (2009) a bridge deck is exposed to permanent loads, traffic loads, shrinkage, creep and temperature differences what cause imposed deformations in the link slab. All imposed deformations can be expressed as strains and curvatures.

In short, the actions working on the link slab are:

1. Working loads
 - a. Horizontal brake and acceleration loads
 - b. Vertical wheel loads
2. Imposed deformations from the spans
 - a. Rotation of the bridge girders
 - b. Horizontal deformation of the bridge girders

3.3 In depth analysis on basic actions

In this chapter are five basic action analysed in detail. These actions include the most important loads and imposed deformations that are expected to work on the link slab. Loads are mainly caused by external loads, like vehicles, or come from the bridge span. Imposed deformations in the link slab are caused by movements of the bridge or movement in the link slab itself. All the basic actions are discussed in detail in this paragraph. The five actions are:

1. Vertical load
2. Horizontal load
3. Imposed vertical deformation
4. Imposed horizontal deformation
5. Imposed curvature

The goal of this in depth analysis is a better insight of the link slab under certain load of imposed deformation and to know the issues of the construction as to the influences on the capacity to resist one of the five basic actions.

3.3.1 Vertical load

The first action is the vertical load working on the link slab. The situation where the link slab is loaded by a vertical load only is already mentioned in 2.3.5.1 Vertical loads. Here a more detail analysis is given. There are a few interesting positions of vertical loads for the analysis. An overview of positions of the vertical loads is given in Figure 106. In the figure are shown three different place:

- A. Vertical load above the passive zone
 1. No dowels in the passive zone
 2. Dowels in the passive zone
- B. Vertical load above the active zone, else than above the gap
- C. Vertical load above the gap of the active zone

In Figure 106 is shown that the vertical load above the passive zone is divided into two cases, A_1 and A_2 . The reason therefore is the way the horizontal friction in the passive zone is generated. In the case of A_1 , in the passive zone are applied dowels to increase the friction. In case A_2 , no dowel are applied. In this case, the horizontal friction is carried by grout between the NSC and the link slab and roughening of the surface. In both cases, the load is carried a bit differently.

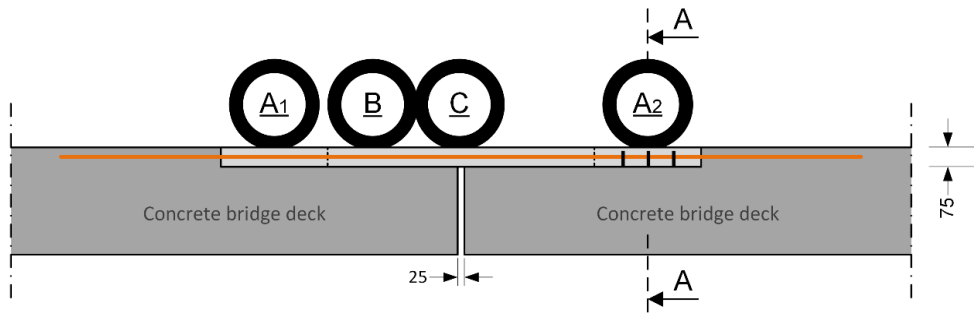


Figure 106 – Places of interest of vertical loads

In Figure 107 is shown cross section AA of Figure 106. In the figure is roughly shown the way vertical loads are transferred to the concrete bridge deck. In the other cases, A_1 , B and C, the vertical loads in the over the cross section are carried the same way. In detail, there are some differences. These differences are clarified in more detail further in this chapter.

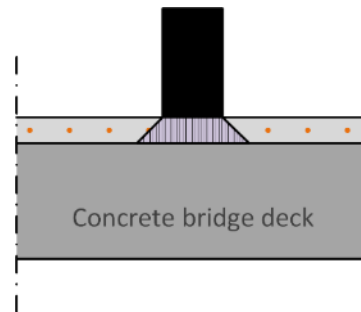


Figure 107 – Cross section AA of Figure 106, vertical wheel load transferred through link slab to the concrete bridge deck

3.3.1.1 Case A_1 and A_2

In Figure 108 is given again the overview of the different places of interest to place a wheel load. In the figure is shown where the cross section for wheel load A_1 are taken. For wheel load A_1 are taken two cross section. The first cross section (cross section I) is taken just at the left side of the wheel load. The second cross section (cross section II) is taken over the vertical boundary between the link slab and the concrete bridge deck, the horizontal boundary between the link slab and the concrete bridge deck until a certain distance from the vertical interface between the link slab and the concrete bridge deck, where the boundary of the cross section of going up again. Both cross section are discussed in more detail in the paragraph.

Note: The stresses in the paragraph are analysed in one direction only, as shown in Figure 108. However, in realty stresses go in two directions. It is assumed that the stresses in the cross direction are carried the same way as in the analysed direction. Therefore, the cross direction is analysed here.

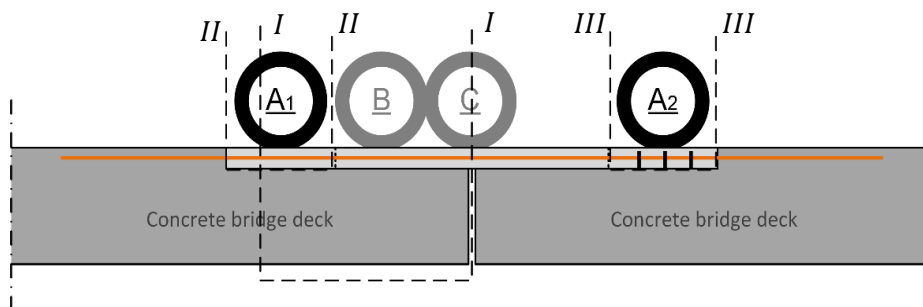


Figure 108 – Overview of cross sections to analyse case A_1 and A_2

In Figure 109 are shown the loads that work in the cross section. The support should make vertical equilibrium with the wheel load. Because of eccentricity, both loads make a bending moment in the section. Horizontal tensile and compressive stresses in the concrete and the reinforcement should make bending moment equilibrium with the vertical loads. The horizontal working loads should also be in equilibrium.

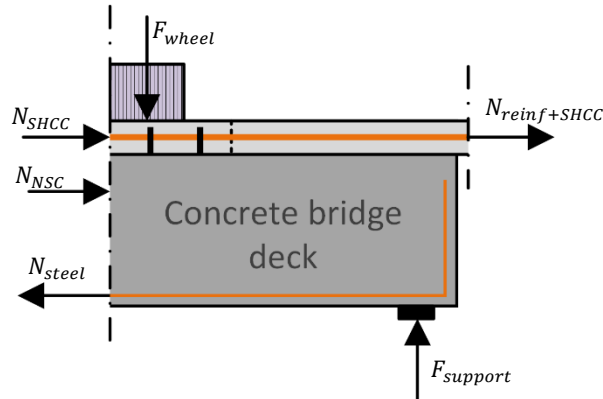


Figure 109 – Cross section II of Figure 108: Wheel load, reaction load in support and reaction forces over the cross section

In Figure 110 is shown cross section II of Figure 108. In the figure are shown the wheel stress and the reaction stresses caused by the distribution of the wheel load. As mentioned before, according to the NEN-EN 1991-2 chapter 4.3.6 (2) (Nederlands Normalisatie-instituut, 2003), the wheel load is distributed over the height of the link slab under an angle of 45 degrees. This has two effects on the way the vertical wheel load is carried:

1. The length where the load is carried over is larger at the bottom of the link slab, what reduce the reaction stress ($\sigma_{support} < \sigma_{wheel}$).
2. Horizontal stresses are generated, so there should be generated a horizontal reaction stress as well. The reaction stress can be generated by concrete around or by horizontal shear stresses should make horizontal equilibrium with the distributed wheel load ($\tau_{support}$).

Ad 1. As shown in Figure 110, the length the vertical wheel stress works over is smaller than the length where the vertical support stress works over. The support stress is carried by the concrete substructure where the link slab is supported on. The length the support stress works over is equal to the length the wheel stress works over with the addition of two times the thickness of the link slab. Since the length where the supporting stress works over is larger than the stress the wheel load works over, the supporting stress is smaller than the wheel stress to have vertical equilibrium.

Ad 2. In Figure 110 is shown by arrows how the wheel stress is probably distributed over the thickness of the link slab. If the link slab is uncracked, what is the intention of the passive zone, the horizontal stresses are probably carried by compressive stresses of the concrete around the place the horizontal stresses work. In the worst case scenario, the concrete around can not carry the horizontal stresses by compressive stresses, for example if the SHCC is fully cracked.

If the concrete around can not carry the horizontal stresses by compressive strength, shear stresses at the horizontal interface between the link slab and the concrete deck as shown in Figure 110. At the bottom of the link slab, the stress in the link slab has a certain horizontal and vertical component. It is assumed that the vertical component of the stress is equal over the width of the link slab. The horizontal component of the stress depends on the place the stress works. Right under the middle of the wheel load, the horizontal component will be equal to zero. At the ends of the distribution width,

the horizontal component will be the largest. In between, a linear relation between the horizontal stress and the place in the link slab is expected as shown with the blue line in Figure 110.

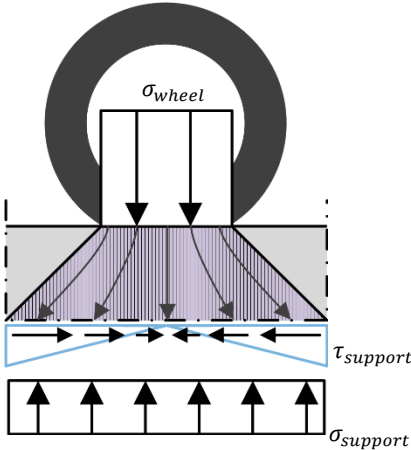


Figure 110 – Cross section II of Figure 108: wheel stress and reaction stresses in case A₁ (no dowels)

In Figure 111 is show cross section III of Figure 108. The figure is the same as cross section II, which is shown in Figure 110, with the addition of a dowel. The function of the dowel is to carry horizontal shear forces, so the dowel could care to take up a part of the horizontal component of the wheel stresses. The horizontal stresses that are carried by the dowel, do not have to be carried by the shear plane between the link slab and the substructure. In other words, due to the addition of the shear force in the dowel, the shear stress ($\tau_{support}$) is reduced.

The situation of a dowel is shown in Figure 111. In the figure is shown that:

1. Horizontal equilibrium is shown in eq.(23)

$$\tau_{support(left\ side)} \cdot L \cdot b = \tau_{support(right\ side)} \cdot L \cdot b + F_{dowel} \tag{eq.(23)}$$

2. Vertical equilibrium is still carried by the wheel load and the support load as shown in eq.(24)

$$F_{wheel} = F_{support} \tag{eq.(24)}$$

Ad. 1. It is assumed that the dowel carries a part of the total wheel stress. It is assumed that the dowel is ineffective to carry vertical loads, so the vertical stresses that are carried by the dowels are neglected. So in the end, it is assumed the dowel carried horizontal stresses only.

It is assumed that the dowel has a certain area of influence shown by the dotted arrows in the purple part of the link slab. due to the stresses carried by the dowel, the friction between the link slab and the substructure is assumed to be reduced over the area where the dowel has influence on. The shear stress, $\tau_{support}$, is reduced as shown by the blue line. The area of the green plane is equal to the force of the dowel, F_{dowel} .

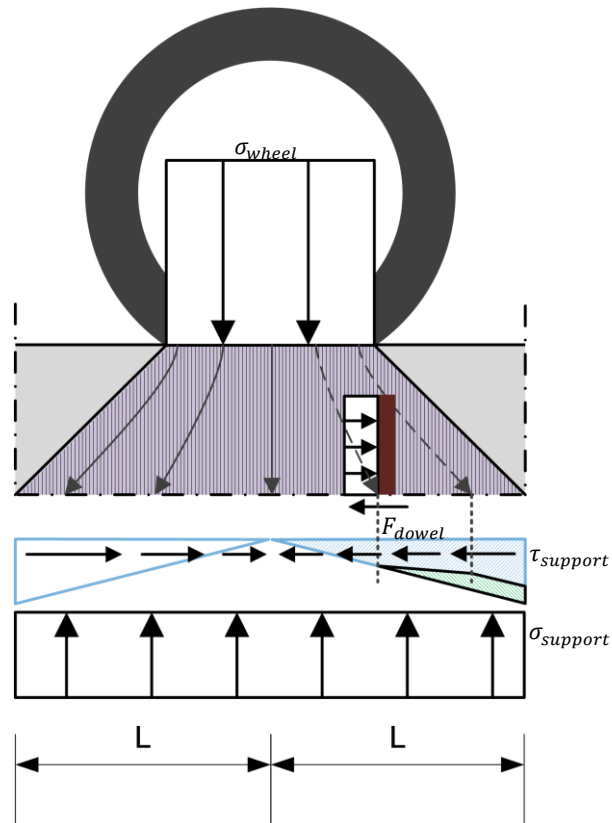


Figure 111 – Cross section III of Figure 108: wheel stress and reaction stresses in case A₂ (addition of dowel)

Dowel has a limited influence on the horizontal shear capacity, what is schematically shown in Figure 112 and Figure 113. In Figure 112 are shown two dowel, 1 and 2. Dowel 1 is place under the wheel load and dowel two is place next to the wheel load. As shown in figure, due to the angel oaf 45 degrees, dowel 2 carries horizontal loads only partly, while dowel 1 is fully effective in transferring horizontal loads. it could be concluded that dowel 1 is far more effective compared to dowel 2. In the cross direction, exactly the same thing happens.

Dowel are normally placed in rows, as shown in the top view of Figure 113. In the figure are shown three rows of dowels, purple, green and orange. The green row of dowels of course is the most effective because, especially the middle green one, because in this row the dowels can carry the most horizontal stresses (same idea as in Figure 112). In the same way, the purple row is less effective. The orange row has almost no effect.

Between the rows of dowels is a certain distance. In theory, the distance could be that large, that no any dowel is in the influence area of the horizontal stresses. In that case, all the horizontal stresses from the link slab should be transferred to the substructure by friction between the link slab and the substructure only. If dowels are applied, the effectiveness of the dowels for this loading system should be taken into account.

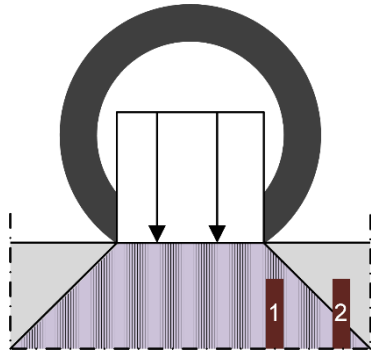


Figure 112 – Effectiveness of dowels in the side view of the link slab loaded by a wheel load

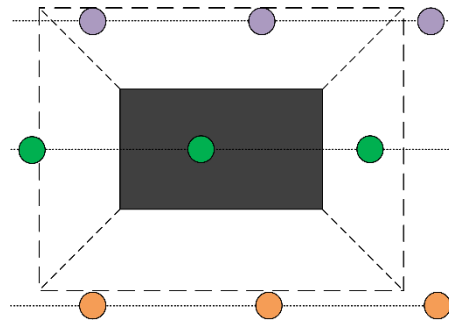


Figure 113 – Top view of link slab exposed to vertical wheel load; effectiveness of a row of dowels depending on the place

From the above mentioned analysis could be concluded that stresses are generated in the horizontal and vertical direction. Vertically, stresses are transferred through the link slab to the substructure. Horizontally, stresses are transferred from the link slab to the substructure by dowel and/or friction in the horizontal plan. The friction in the horizontal plane is mainly increased by roughening and/or grouting the surface.

Now the variables that have influence on the capacity to carry stresses in both the vertical and horizontal direction, are show below.

Vertical direction	Horizontal direction
<ul style="list-style-type: none"> - Compressive strength NSC - Compressive strength SHCC - Thickness of the link slab, what has influence on the reduction of the stress due to spreading of stresses 	<ul style="list-style-type: none"> - Dowel design: <ul style="list-style-type: none"> ○ Number of dowels per row ○ Distance between rows of dowels ○ Shear strength of dowels ○ Height of the dowels ○ Thickness of the dowels - Shear capacity of the grout between the link slab and the substructure - Shear capacity of the roughened surfaced between link slab and substructure - Tensile strength of NSC - Thickness of the link slab, what has influence on the reduction of the stress due to spreading of stresses

3.3.1.2 Case B

Case B is if the active part of the link slab, else than around the gap, is exposed to a vertical load. In Figure 114 is shown the cross section that is used to analyse the forces that work in the link slab in case B.

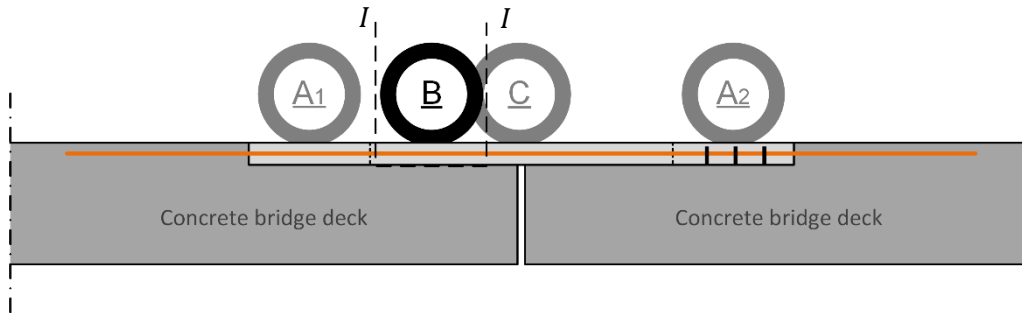


Figure 114 – Overview of cross sections to analyse case B

In Figure 115 is shown the only cross section that is shown in Figure 114. In the figure is shown a part of the active part of the link slab. In the figure are given the stresses that are expected in the active section if it is loaded by a wheel load.

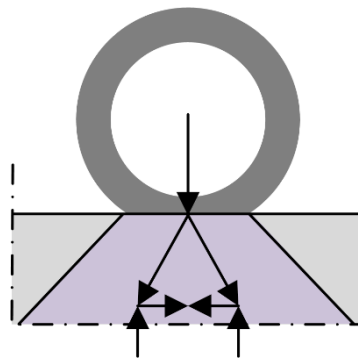


Figure 115 – Truss and tie model for horizontal equilibrium in the link slab loaded by a wheel load

The stresses shown in Figure 116 are wheel load, reaction stresses in the link slab and support stress from the substructure. For stability in the structure vertical, horizontal and bending moment equilibrium equations should be satisfied. Because of symmetry in the figure, it is assumed that bending moment equilibrium is met everywhere. The other equilibrium equations and specialties are:

1. Vertical equilibrium is still carried by the wheel load and the support load:

$$F_{wheel} = F_{support} \quad \text{eq.(25)}$$

2. Due to the debonding layer, there is no friction between the link slab and the substructure in the horizontal plane

$$\tau = 0 \quad \text{eq.(26)}$$

3. Internal horizontal equilibrium due to reaction compressive stresses of the concrete around the wheel load and, especially if the link slab is fully cracked, tensile stresses in the reinforcement and fibres

Ad 1. Again, vertical equilibrium should be made between the wheel load and the reaction forces of the substructure the link slab is supported on. This is already discussed in detail in paragraph 3.3.1.1 Case **A₁** and **A₂**, so it will not be discussed here again in detail.

Ad 2. Different from case A, in case B can no friction between the link slab and the concrete substructure be generated, because of the debonding layer. Therefore, horizontal equilibrium should

be made by compressive stresses of the concrete around or tensile stresses generated by fibres or reinforcement rebars.

In the case of failure of de debonding layer, there will be friction between the link slab and the substructure. That means that a part of the horizontal stresses then can be carried by the friction between the link slab and the substructure. In the case of only a vertical wheel load, no problems seems to occur.

Ad 3. As mentioned already, horizontal equilibrium could be generated in two ways. The first way is horizontal equilibrium by horizontal compressive stresses from the concrete around, as already mentioned in case A. The second way to carry horizontal stresses is by tensile stresses in the concrete. These tensile stresses should be generated in the reinforcement and the fibres.

Which of the two mechanism works to make horizontal equilibrium probably depends on the conditions. If the link slab is fully cracked, because the link slab is exposed to imposed horizontal deformation, tensile stresses are generated faster compared to compressive stresses. For example, if the link is elongated by 0.5%, the link slab should in theory shorten again by 0.5% before any compressive stress can be generated. Also the tensile capacity of the SHCC is a point of discussion if extra tensile stresses should be generated, in case the horizontal stresses should be carried by tensile stresses of the SHCC and reinforcement. This point of discussion is discussed in more detail in .

In Figure 116 is shown how horizontal equilibrium could be made by tensile stresses in the fibres and reinforcement in the case that the concrete around is not able to take care for the horizontal stresses. In the figure is shown how the reinforcement (orange) and the fibres (blue) are able to make equilibrium with the tensile stresses that are generated due to the distribution of the stresses. In the detail of Figure 116 is shown how tensile stresses are carried by fibres. In blue the fibres are shown.

The horizontal tensile stresses could be expected larger at the bottom and near the end of the influence zone. At the combination of both, around the spot D in Figure 116, the stresses could be expected the highest. The distribution of the tensile stresses is discussed in more detail in paragraph 3.3.1.3 Case C.

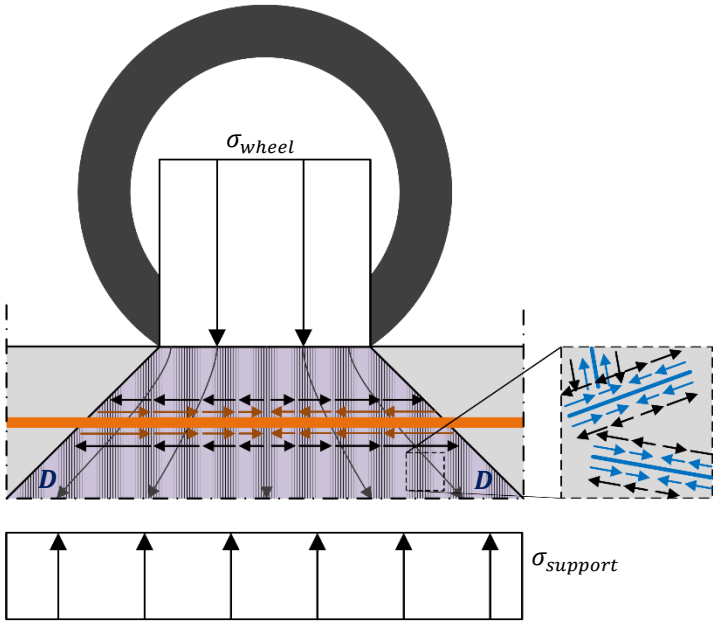


Figure 116 – Cross section I of Figure 114: wheel stress and reaction stresses in case B

In the analysis above is shown that vertical and horizontal stresses are generated due to a vertical load working on the active part of the link slab. Vertical stresses from the wheel are transferred through the link slab to the substructure where a certain support stress is generated to make vertical equilibrium. Horizontal stresses can't be transferred to the substructure by friction as at the passive zone, because of the debonding layer. Horizontal stresses should be carried internally by tensile stresses in the reinforcement and the fibres.

The horizontal and vertical stress capacity of the link slab depends on a few variables. Below are shown the most important variables that influence the horizontal and vertical stress capacity.

Vertical direction	Horizontal direction
<ul style="list-style-type: none"> - Compressive strength NSC - Compressive strength SHCC - Thickness of the link slab, what has influence on the reduction of the stress due to spreading of stresses 	<ul style="list-style-type: none"> - Reinforcement and fibres: <ul style="list-style-type: none"> o Reinforcement ratio o Fibre percentage o Material characteristics like; tensile strength, Young's modulus o Dimensions o Composite working (for example pull-out strength) o Distribution of fibres - Friction of debonding layer

3.3.1.3 Case C

In this paragraph is discussed the analysis to the active part of the link slab positioned above the gap that is between the two concrete bridge decks. This situation is shown in Figure 117 with wheel C. in the figure are also shown two cross sections and one detail. The cross sections and detail are used to describe the next situations:

- I* - Stresses working in the active section above the gap
- II* - Horizontal stresses working above the gap
- Detail A - Concrete that spalls off, due to vertical peak stress

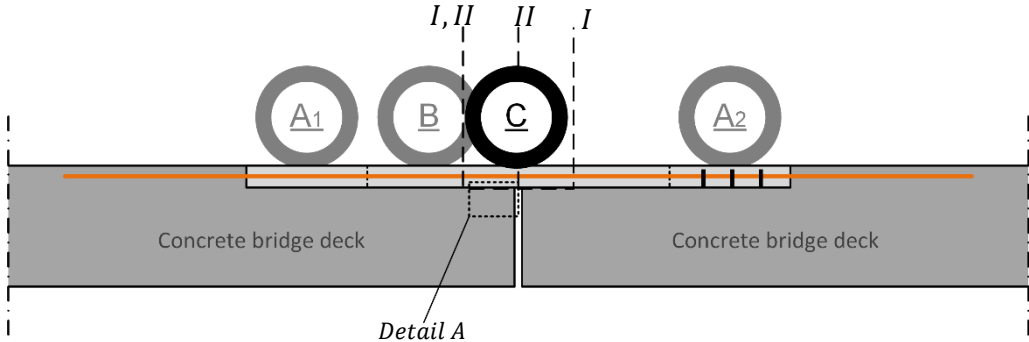


Figure 117 – Overview of cross sections and detail A to analyse case C

Stresses working in the active section above the gap

In Figure 118 is shown cross section I of Figure 117. In Figure 118 are shown the stresses from the wheel load and the reaction stresses to carry the wheel load. A lot of activities that happens in the link

slab in case C are more or less the same as in case B. Some additional specialties happens due to the gap between the concrete bridge decks. Interesting issues of Figure 118 are:

1. Vertical equilibrium is carried by the wheel load and the support load:

$$F_{wheel} = F_{support} \tag{eq.(27)}$$

2. Redirecting of vertical stresses, due to the gap between the concrete bridge decks. This results in vertical peak stresses at the end of the concrete bridge decks.
3. Due to the debonding layer, there is no friction between the link slab and the substructure in the horizontal plane:

$$\tau = 0 \tag{eq.(28)}$$

4. Internal horizontal equilibrium due to tensile stresses in the reinforcement and fibres

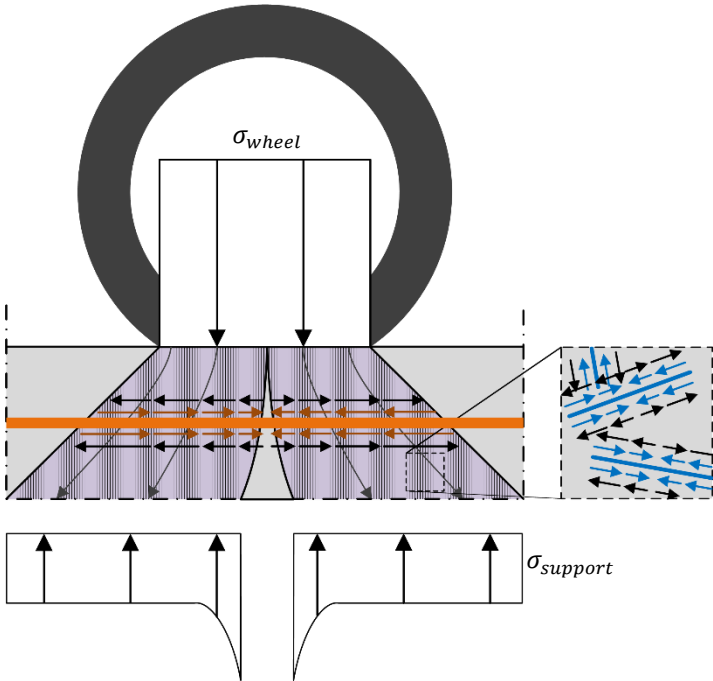


Figure 118 – Cross section I of Figure 117: wheel stress and reaction stresses in case C

Ad 1. Vertical equilibrium works the same as in the other cases described before. Here the vertical equilibrium is not discussed in detail. More details could be found in paragraph 3.3.1.1 Case **A₁** and **A₂**.

Ad 2. Normally, stresses are distributed in the shortest or easiest way. In the case of vertical stresses of Figure 118, this means that vertical stresses are distributed downwards directly. Under the wheel is a gap between the two parts of the substructure. The gap can not carry vertical loads, so vertical loads should be redirected around the gap, as shown in Figure 118. The shortest way of stresses in the middle of the wheel are to the end of one of the concrete bridge decks. Compared to case B, due to the addition of stresses that in case B are carried by supports at the place of the gap, peak stresses are generated at the end of the concrete decks. The detail A (Figure 119) are the peak compressive stresses discussed in more detail.

Ad 4. Horizontal stresses in case C are assumed to be carried in the same way as in case B. However, it is interesting to analyse the horizontal equilibrium around the gap in some more detail. The horizontal

stresses in the concrete above the gap should completely be carried by horizontal tensile stresses in the fibres and the reinforcement. The way rebars and fibres works is already discussed in detail in paragraph 3.3.1.2 Case B. Tensile stresses in the reinforcement and the fibres above the gap are discussed in more detail in this chapter according to cross section II (Figure 124).

Spalling of NSC at the end of the substructure

In Figure 119 is shown the detail A of Figure 117. In Figure 119 is shown the vertical stress distribution working on the substructure, including the peak stress near the end of the concrete deck. In the structure are drawn circles to indicate the concrete aggregates schematically. Further is shown the reinforcement steel by the brown lines.

In Figure 119 are also shown two details. In the upper detail are shown concrete aggregates that are in compression. In the detail is shown how compressive stresses are generated between the particles. However, at the end of the concrete deck, the last particle (right) can not make equilibrium by compressive stresses only. Therefore, tensile stresses should be generated, as shown with the red arrow. Cement should generate tensile stresses between the particles, such that horizontal equilibrium could be generated.

Tensile stresses of concrete relative low compared to the compressive strength. At the end of the concrete substructure, a peak compressive stress is working. Because of the peak compressive stress in the substructure, also large tensile stresses could expected. However, the tensile stress of concrete is relative low, so failure in tension could be expected. That means that aggregate could be expected to spall off. Due to spalling, the reinforcement is not protected any more, such that the change of failure of the reinforcement steel is significant increased.

It is assumed that in the substructure is placed steel reinforcement. In the bottom detail is shown the way reinforcement could carry the horizontal tensile stresses in the concrete to make horizontal equilibrium again. The particles can compress to the reinforcement, what generate tensile stress in the reinforcement. Reinforcement, mainly made of steel, can easily generate tensile stresses. In this area, no spalling of concrete is expected, provided that the steel and concrete works together properly. However, if concrete spalls off and the reinforcement corrode, such that it can not carry the tensile stresses anymore, even more concrete will spall off.

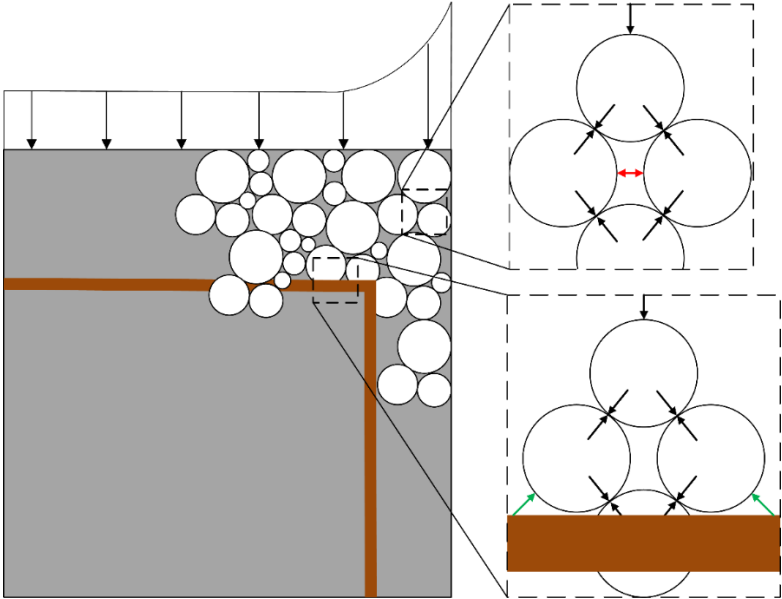


Figure 119 – Detail A of Figure 117: compressive stress at the end of the concrete substructure due to a vertical wheel load

Now the question is, where does the concrete spall off and where can it serve? It is clear that around the reinforcement no spalling is expected because horizontal equilibrium could be made with the reinforcement steel. Here it is assumed that the steel and concrete work together properly. So spalling could be expected somewhere between the reinforcement and the concrete surface. Assuming spalling is under 45 degrees, spalling can be assumed at the right side of the blue line shown in Figure 120.

Now let assume that only the end of the substructure is exposed to a compressive stress that is too large to be carried by the concrete. This is schematically shown in Figure 120. In the detail of the figure are shown the some aggregate particles the end of the substructure that is exposed to a vertical compressive load from above.

Now let assume that only the blue particles are carried by the highest peak stress, as shown in Figure 120. This peak stress causes tensile stresses shown by the red arrows. The dotted line in Figure 120 shows qualitatively the maximum compressive stress, such that spalling is not expected to occur. At the end of the substructure, where the tensile stress generated by the peak compressive stress is higher than the tensile strength, the tensile connection between the aggregate particles will fail. Neglecting possible generation of shear stresses, a line of failure could be drawn, as done with the red line in Figure 120. Then the blue collared particles will crumble off.

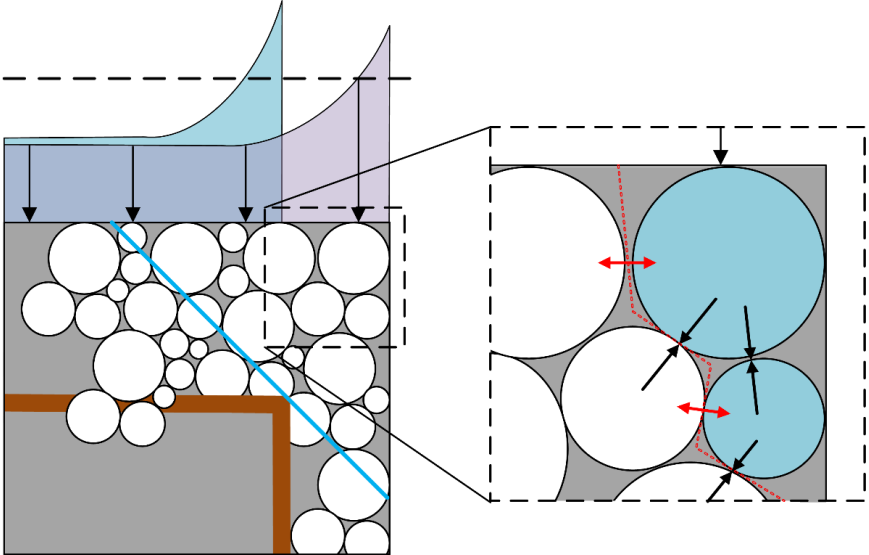


Figure 120 – Concrete spalls off at the end of the concrete bridge deck due to the point load caused by imposed vertical deformation

As soon as a part of the substructure is crumbled off, the compressive stresses are redistributed over the substructure. The crumbled part can not be used to carry compressive stresses anymore, so the area the wheel load is carried over is increased. Or in other words, the gap is increased. Larger stresses are expected now, as drawn with the blue stress distribution of Figure 120. Since higher stresses work on the substructure, spalling of the concrete is expected again. No spalling can be expected to happen until the blue line, where the reinforcement becomes active to prevent the spalling mechanism.

Peak stress on SHCC link slab

The peak stress working on the link slab of course also works on the SHCC link slab. In Figure 121 are shown two pictures of the link slab exposed to peak stress modelled as a point load. On the left picture is shown that tensile stresses are generated, according to the tie and strut model. On the right figure are shown the fibres and rebar that are placed in the link slab. Both, the fibres and rebar can carry the

tensile stresses. Because the fibres are situated everywhere over the height of the link slab, tensile stress can be generated everywhere over the height of the link slab. That means that at the point the point load is introduced, horizontal equilibrium can already be made. However, as shown at the right figure of Figure 121, the resultant tensile force in the link slab could be expected to work in the middle of the link slab, because fibres could be assumed to be distributed equally over the height of the link slab and the rebar is placed in the middle of the link slab.

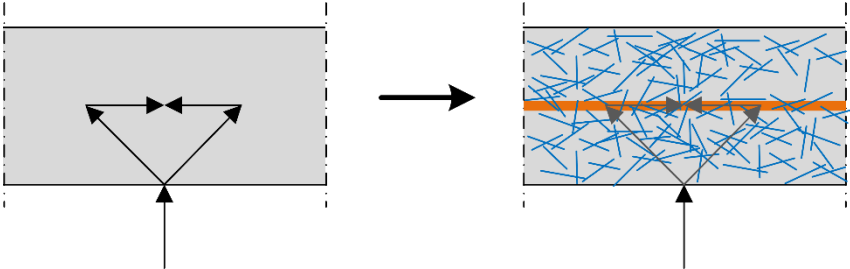


Figure 121 – Left: tensile stresses in the link slab caused by a point load, right: rebar and fibres carry tensile stresses

Depending on the strength and the amount of fibres, no damage could be expected on the link slab. Besides, in contrast to the end of the substructure, the link slab is surrounded by SHCC. Assuming the link slab is not cracked yet, the surrounding SHCC can generate compressive stresses to make horizontal equilibrium. So in the end, the horizontal stresses can be generated by a combination of compressive stresses caused by the surrounding SHCC and tensile stresses in the fibres and rebars.

Horizontal stresses above the gap

Before the horizontal tensile stresses in the link slab are discussed in detail, first is roughly shown the reason that tensile stresses could be expected at all. This reason is explained according to Figure 122. In this figure is shown a truss and tie model for the distribution of the wheel load. The wheel load in this case is modelled as two point loads instead of a distributed load. Wheel load is assumed to be spread over 45 degrees. Together with that fact that even more stresses should be distributed horizontally due to the gap, the point loads will be in the link slab under a certain angle as shown in Figure 122. The substructure can only generate vertical stresses, because of the debonding layer. So two vertical point loads could be modelled. To make equilibrium in the point the compressive loads meet, horizontal tensile loads should be induced. In fact more or less the same mechanism takes place in case B (paragraph 3.3.1.2 Case B). However, due to the gap, the horizontal tensile stresses are expected higher compared to case B. Therefore, the distribution of tensile stresses is discussed in this paragraph is more detail.

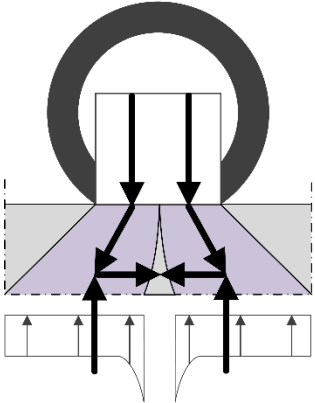


Figure 122 – Truss and tie model for horizontal wheel load above the gap of the substructure

In Figure 124 is shown cross section II of Figure 117. The section is cut half of the wheel, to describe the tensile stresses in more detail. Tensile stresses are carried by reinforcement and fibres. The tensile resistance of the reinforcement bars could be modelled as a point load. The fibres are a lot smaller than the reinforcement and divided over the thickness of the link slab. The tensile stress in the fibres could be expected to vary over the height of the link slab as shown in Figure 124. Considering the link slab as a homogenous material, it could be expected that the stresses have the largest horizontal component at the lower part of the link slab. At the part of the link slab, probably the largest part of the stresses will be redirected to the supporting deck. Further, according to the truss and tie model, the resultant tensile force could be expected at the lower part of the link slab also.

In Figure 123 is shown a model on aggregate level to imply the mechanism of the fibres. In the figure, the link slab is modelled as a very thin SHCC link slab made of three layers of aggregate. The layers are perfectly positioned and are all even large. In reality, this is not the case, but the idea behind the model is the same. The model is assumed to be half of the total model, because of symmetry.

In the model of Figure 123 are applied vertical external load exactly on the middle of the particles. The two vertical loads are the wheel load and the support load, which are together in vertical equilibrium. Under the blue particle is situated the gap. That means that no vertical stresses can be carried by the blue particle of the model. The grey particles are able to carry compressive stresses. The green particles are no loads. Because of vertical equilibrium, no vertical stresses can be generated in the green particles.

In the grey particles, vertical stresses should be distributed, because the grey particles are exposed to vertical stresses at the top (wheel load) and the bottom (concrete bridge deck). The vertical stresses are distributed under an angle, because of the particle distribution. Because of the angle, a horizontal component is generated if vertical stresses are distributed. To make horizontal equilibrium, tensile stresses should work between the particles. The expected tensile stresses according to the model are drawn by yellow arrows. The horizontal stresses between the particles should partly be carried by the fibres and partly by the reinforcement.

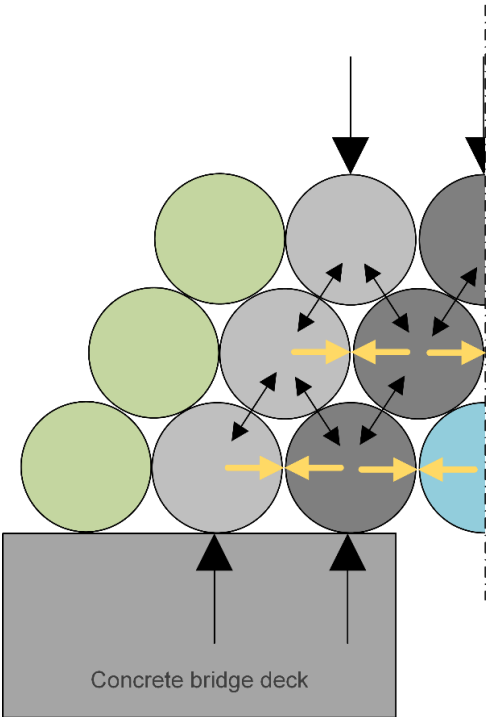


Figure 123 – Stresses through aggregate particles caused by vertical wheel load and support reaction

In Figure 124 is shown cross section II of Figure 117. In the cross section is shown half of the wheel load and the support reaction of one of the substructures. In the figure are shown the force in the reinforcement and the stresses from the fibres again. The stresses are shown on a larger scale no compared to Figure 123. From the figure could be concluded that:

1. Horizontal equilibrium should be made with the vertical wheel stress and the vertical reaction stress from the substructure
2. Because of symmetry over the vertical axis in the figure, horizontal tensile stresses make intern equilibrium. In this figure, the stress of the reinforcement and the fibres should make equilibrium with the total horizontal stress caused by the distribution of the vertical wheel load.
3. There should be moment equilibrium by adding the moment caused by the vertical loads and the moment caused by the horizontal tensile loads caused by the reinforcement and the fibres. Taking moment equilibrium around the end of the reinforcement, equilibrium should be made as shown in eq.(29).

$$F_{wheel} \cdot a + F_{fibres} \cdot b - F_{support} \cdot c = 0 \tag{eq.(29)}$$

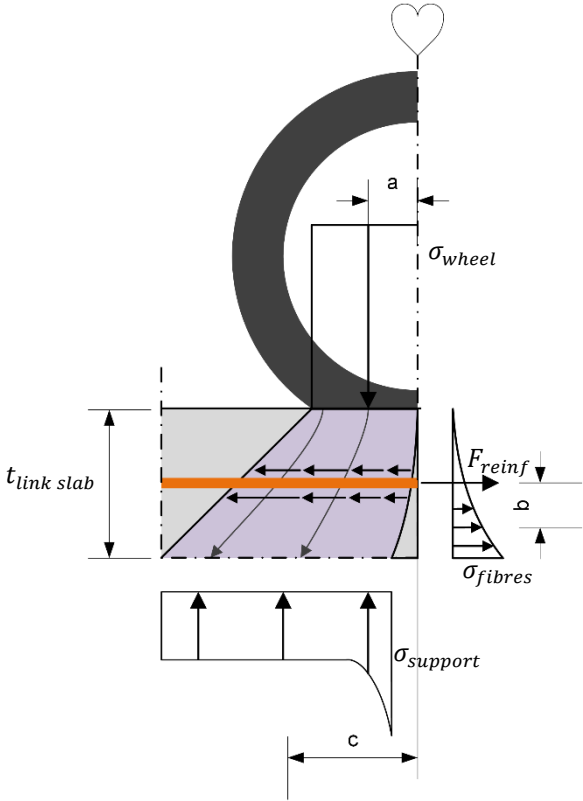


Figure 124 – Cross section II of Figure 117: wheel stress and reaction stresses in case C

Ad 2. At the top of the structure, where the wheel load is just introduced, there are no horizontal stresses yet. At the bottom, horizontal stresses could be expected the largest, because here the most stresses are redirected to flow around the gap. Therefore, the horizontal stresses could be expected the largest at the bottom of the link slab. Between the top and the bottom of the link slab, a parabolic shape could be expected for the flow of the stresses. Therefore also a parabolic shape could be expected for the horizontal stresses over the thickness of the link slab. In the end, the tensile stresses, that should make equilibrium with the horizontal stresses from the load, are also expected to have a parabolic shape.

The resistance against spalling off depends of course on the tensile strength of NSC, according to the mechanism behind. Also the reinforcement design has a certain influence on the resistance, because reinforcement can take up tensile stresses that cause spalling. At the place the reinforcement has no or nearly influence to increase the spalling resistance, fibres could be added. This is especially interesting near the surface of the substructure.

The other variables that influence spalling of the concrete called above, has influence of the quantity of the peak stress. The stiffness of the concrete and SHCC, the moment of inertia of the link slab and the substructure, the thickness of the link slab and the length of the gap all have a certain influence on the quantity of spalling. All these variable are shortly clarified here.

It is obvious that the length of the gap has influence on spalling. A larger gap results in higher compressive peak stresses, so a higher change on spalling. The stiffness and the moment of inertia of the link slab and substructure probably also influence the quantity of the peak stress. A structure with a high stiffness and a high moment of inertia carries a lot of stresses. Then the peak stress depends on the stiffness of SHCC and NSC and the moment of inertia of the link slab and the substructure. At last has the thickness of the link slab influence on the peak stress. In short, in a thick link slab, the compressive stresses are low because the stress can be distributed over a larger area. This is mentioned in previous sections already. Obviously, a lower peak stress reduces spalling.

Same as in case A and B, in the above analysis are shown horizontal and vertical stresses that are generated if a vertical wheel load is applied. The variables that influence the capacity to carry horizontal and vertical stresses are shown below.

Vertical direction	Horizontal direction	Spalling
<ul style="list-style-type: none"> - Compressive strength NSC - Compressive strength SHCC - Thickness of the link slab, what has influence on the reduction of the stress due to spreading of stresses 	<ul style="list-style-type: none"> - Friction of debonding layer - Reinforcement and fibres: <ul style="list-style-type: none"> o Reinforcement ratio o Fibre percentage o Material characteristics like; tensile strength, Young's modulus o Dimensions o Composite working (for example pull-out strength) o Distribution of fibres 	<ul style="list-style-type: none"> - Tensile strength of NSC - Reinforcement design - Addition of fibres - Stiffness of NSC and SHCC - Moment of inertia of link slab and substructure - Length of the gap - Thickness of the link slab what has influence on the reduction of the stress due to spreading of stresses

3.3.2 Horizontal load

The second action that is described in the chapter is the horizontal load that works on the link slab. In Figure 125 is shown the situation where the link slab is exposed to a horizontal load. The load per metre width in this case is equal the horizontal stress multiplied by the thickness of the concrete bridge deck, $\sigma_{hor} \cdot t_{NSC}$. In Figure 125 are tensile stresses assumed.

However, in the link slab could also work compressive stresses. Probably, compressive stress in the link slab is not the governing loading scheme for the design of the link slab, since the compressive strength of concrete is relative large compared to the tensile strength. Assuming the tensile stress is governing in all sections of Figure 125, only the tensile situation is analysed in detail. To complete the analysis,

for every section is shortly mentioned what happens if the link slab is exposed to compressive stress instead of tensile stress.

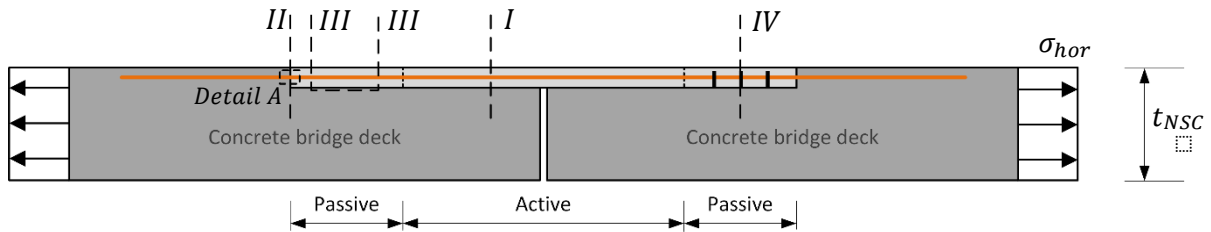


Figure 125 - Overview of cross sections to analyse the link slab under horizontal load

In Figure 125 are shown four interesting cross sections if the link slab is exposed to horizontal stresses. These cross sections are:

- I - Horizontal stresses in the active zone
- Detail A - Vertical interface between NSC and SHCC (passive zone)
- II - Vertical interface between NSC and SHCC (passive zone)
- III - Horizontal interface between NSC and SHCC (passive zone)
- IV - Horizontal interface between NSC and SHCC with dowels (passive zone)

3.3.2.1 Horizontal stresses in the active zone

In this paragraph is analysed how horizontal stresses are carried by the active part of the SHCC link slab. In Figure 126 are shown the reaction stresses caused by the horizontal tensile load working as shown in Figure 125. In the cross section, only horizontal equilibrium should be made. As shown in Figure 125:

1. Horizontal equilibrium is carried by tensile stresses in the reinforcement and the fibres. Assuming a constant stress of fibres over the height of the link slab, the horizontal equilibrium could be written as shown in eq.(30).

$$\sigma_{hor} \cdot t_{NSC} = \sigma_{fibres} \cdot t_{link\ slab} + F_{reinf} \quad \text{eq.(30)}$$

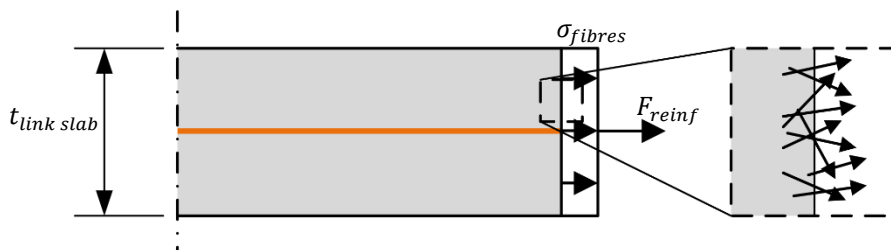


Figure 126 – Cross section I of Figure 125: reaction stresses caused by horizontal load

From tensile strength of the Figure 126 could be concluded that the tensile strength of the cross section depends on the strength capacity of the fibres and the reinforcement. The tensile stress of the SHCC is assumed to be carried by the fibres, so in fact the tensile strength of the fibres (Figure 126) is the tensile strength of SHCC as a composite material. Of course the composite work between the fibres and SHCC and the reinforcement and SHCC is important too.

In the detail of Figure 126 are shown the fibres over the height of the link slab. As shown in the detail, the fibres are randomly distributed. It is assumed that only tensile stresses can be generated in the fibres. That means that the direction of the fibre determines the direction of the force that is generated

in the fibre. Only the horizontal component of the fibres contributes to the tensile capacity in the horizontal direction.

If the cross section of Figure 126 is in compression, a distributed compressive stress is expected of the thickness of the link slab. The load capacity of the link slab then depends on the thickness of the link slab and the concrete compressive strength.

From the analysis from above again a list of variables that influence the horizontal strength of the active part of the link slab could be made.

Tensile stress	Compressive stress
<ul style="list-style-type: none"> - Thickness of the link slab - Distribution of fibres - Reinforcement and fibres: <ul style="list-style-type: none"> o Reinforcement ratio o Fibre percentage o Material characteristics like; tensile strength, Young’s modulus o Dimensions o Composite working (for example pull-out strength) 	<ul style="list-style-type: none"> - Compressive strength SHCC - Thickness of the link slab

3.3.2.2 Vertical interface between NSC and SHCC (passive zone)

In the paragraph is analysed the vertical interface between the NSC deck and the passive part of the SHCC link slab. The reaction of the interface is analysed in two situations; the link slab exposed to horizontal tensile stress and horizontal compressive stress.

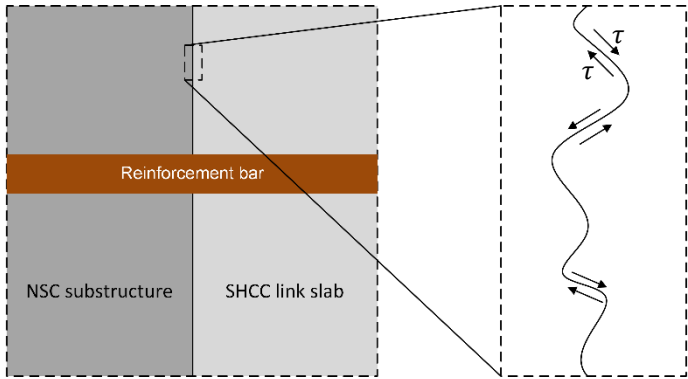


Figure 127 – Detail A of Figure 125: reaction stresses at the vertical interface between SHCC and NSC caused by horizontal load

In Figure 127 is shown a detail of the vertical interface at the end of the link slab. At the interface, SHCC and NSC meet each other. It is assumed that fibres are only in SHCC, so that fibre are not able to transfer tensile stresses between SHCC and NSC, so between the end of the link slab and the end of the concrete deck. Probably there will be a connection between both types of concrete due to cement particles that connects both type of concrete. However, this connection is probably weaker than the tensile strength of concrete itself. So the tensile stresses that could be transferred through the connection between both concretes could probably better be neglected. In fact, only the

reinforcement connects both NSC and SHCC in the vertical interface. As shown in the figure, this is the only construction part that is in both types of concrete. So all tensile stresses should go through the reinforcement bars.

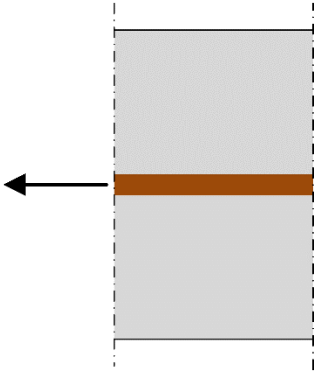


Figure 128 – Cross section II of Figure 125: horizontal force in bar to connect the SHCC link slab to the NSC substructure

As soon as the reinforcement fails, there is no connection between NSC and SHCC any more in the vertical interface. To keep the connection, the reinforcement should be chosen such that it won't fail during life time. If the connection fails, a gap between the end of the link slab and the end of the deck can be expected, what probably has negative effects on the durability of the structure.

If the link slab is in compression, the compressive stresses could be expected in the horizontal interface. In the connection, horizontal compressive stresses could probably be distributed from the link slab to the substructure and the other way around. So in this case, the connection does not only depend on the tensile strength of the reinforcement.

From the analysis from above again a list of variables that influence the horizontal strength of the active part of the link slab could be made.

Tensile stress	Compressive stress
<ul style="list-style-type: none"> - Reinforcement: <ul style="list-style-type: none"> o Reinforcement ratio o Material characteristics like; tensile strength, Young's modulus o Dimensions of reinforcement bars o Composite working (for example pull-out strength) 	<ul style="list-style-type: none"> - Compressive strength SHCC - Compressive strength NSC - Thickness of the link slab

3.3.2.3 Horizontal interface between NSC and SHCC (passive zone)

Here, the horizontal interface between the NSC deck and the SHCC link slab in the passive zone is analysed. In this paragraph, it is assumed that there are placed no dowels in the horizontal interface. As mentioned in paragraph 3.3.2.1 Horizontal stresses in the active zone, in the active part the horizontal stresses caused by fibres and the reinforcement steel is called the horizontal force H. Assuming the reinforcement bar is place in the middle of the link slab and the fibres are equally distributed over the height of the link slab, the horizontal force H works at the middle of the cross section of the link slab, as shown in Figure 129. As shown in the figure, fibres, reinforcement and the horizontal shear connection with the substructure should make horizontal equilibrium everywhere in the passive part of the link slab. From Figure 129 could be conclude that:

1. Horizontal equilibrium should be made by the reinforcement bars, fibres and the horizontal shear connection, as shown in eq.(31).

$$F_t = F_{reinf} + \tau_{hor} \cdot L_{active} \quad \text{eq.(31)}$$

2. A bending moment from the active part of the link slab and vertical stresses working on the active link slab are expected to be generated to make moment equilibrium. The equation of the bending moment equilibrium around point B is given in eq.(32).

$$(\tau_{ver} \cdot t_{link\ slab} + F_{reinf,ver}) \cdot L_{active} - \tau_{hor} \cdot \frac{1}{2} \cdot t_{link\ slab} \cdot L_{active} + M_{SHCC} = 0 \quad \text{eq.(32)}$$

3. The vertical equilibrium should be made with the vertical friction at the interface, shear stress at the active part of the link slab and a supporting force near the active section of the link slab:

$$(\tau_{ver} - \tau_{SHCC}) \cdot t_{link\ slab} - F_{sup} + F_{reinf,ver} = 0 \quad \text{eq.(33)}$$

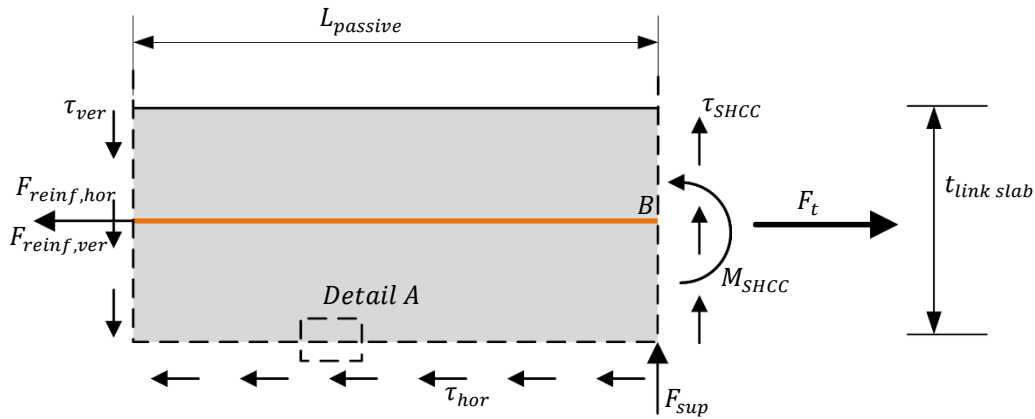


Figure 129 – Detail of Figure 125: stresses working on the passive zone of the link slab due to horizontal load

The horizontal stresses in the passive part of the link slab are assumed to work in a similar way as in the active zone. In reality, the tensile stresses in the passive zone probably works a bit different from the tensile stresses in the active zone, because the tensile stresses are partly transferred to the substructure by horizontal friction. The due to the horizontal friction, the horizontal stress distribution, carried by fibres, may not be exactly linear any more. However, for reasons of simplicity, the horizontal stress distribution in the passive part of the link slab is assumed to be linear.

Ad. 1. The horizontal force in the reinforcement at the interface, F_{reinf} , is already discussed in the previous paragraph. In Figure 130 is shown detail A of Figure 129. In the figure is shown the roughen surface of the link slab and the substructure that generates friction if there is some difference between the movement of the link slab and the substructure.

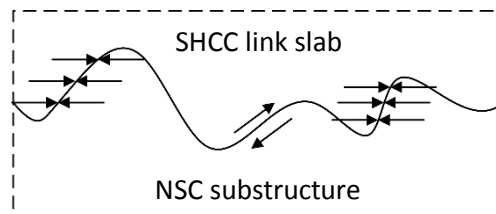


Figure 130 – Detail A of Figure 129: friction between the SHCC link slab and the NSC substructure

Ad. 2. The horizontal forces generates a certain bending moment in the clockwise direction. If the passive part of the link slab rotates clock wise, certain reaction forces are generated. According to the same philosophy as discussed in chapter 2.3.5.4 Imposed curvature according to tests, reaction forces are expected. Assuming the passive section rotates, the next reactions are expected:

- τ_{ver} , because of vertical friction at the interface
- $F_{reinf,ver}$, because of shear strength in the reinforcement
- M_{SHCC} , because the passive and active zone are together one element

Ad. 3. As mentions in point 2, at the vertical interface vertical friction between the link slab and the concrete substructure and vertical shear force of the reinforcement is expected. Additional vertical stresses should work to have vertical equilibrium in the passive part of the link slab. A counter shear stress could be expected in the interface between the active and the passive part of the link slab, τ_{SHCC} . Further, a vertical point load could be expected from the substructure at the end of the link slab, F_{sup} . Both, the shear stress and the point are shown in Figure 129.

Taking into account test results from Reyes & Robertson (2011), which are shown in chapter 2.3.5.4 Imposed curvature according to tests, the expected stresses caused by horizontal stress are in line with the test results to imposed horizontal deformation. This could be expected on forehand, because horizontal imposed deformation also results in horizontal stresses. Probably, horizontal stresses in both cases are distributed in the same way.

Because of vertical equilibrium, the vertical shear stress, τ_{SHCC} , should also be carried by the active part of the link slab. At the bottom of the active zone tensile stresses should work to make vertical equilibrium. However, due to the debonding layer, the no tensile stresses can be generated in the horizontal interface between the link slab and the substructure. This is schematically shown in Figure 131. On both sides of the passive link slab of Figure 131 work a shear stress SHCC. Vertical equilibrium should be there, but no reaction stress can be generated in the passive section. The only other connection between the link slab and the substructure is at the horizontal interface between the link slab and the substructure. A tensile stress, σ_{sup} , should be generated. However, because of the debonding layer, it is assumed that no tensile stresses are generated between the passive part of the link slab and the substructure. For vertical equilibrium, both shear stresses, τ_{SHCC} , should be even large so zero.

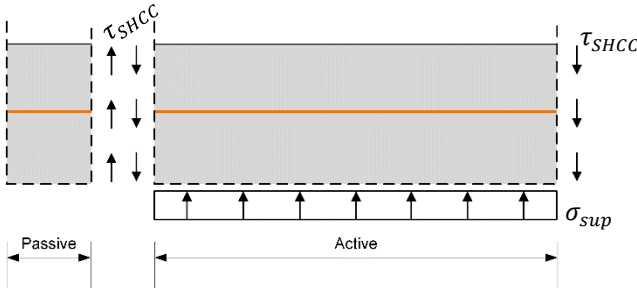


Figure 131 – Vertical stresses working on the passive part of the link slab in case of horizontal tensile load

In Figure 132 are shown the bending moments from the active part of the link slab that should also work on the passive section. In theory, a beam exposed to two bending moments make bending moment equilibrium, what is the case in Figure 132. However, due the substructure under the link slab, the active part of the link slab can't bend downwards due to the working bending moment. Due to deflections in the active part of the link slab caused by the bending moment, M_{SHCC} , a vertical stress (σ_{sup}) in the horizontal interface between the link slab and the substructure should be generated

against the vertical deflection. For vertical equilibrium, the resultant forces of this stress should be equal to the resultant shear forces at both end of the link slab. These shear stresses also works on the passive zone of the link slab, as shown in Figure 132. Here the shear stress working on the passive section is in the same direction as in Figure 129.

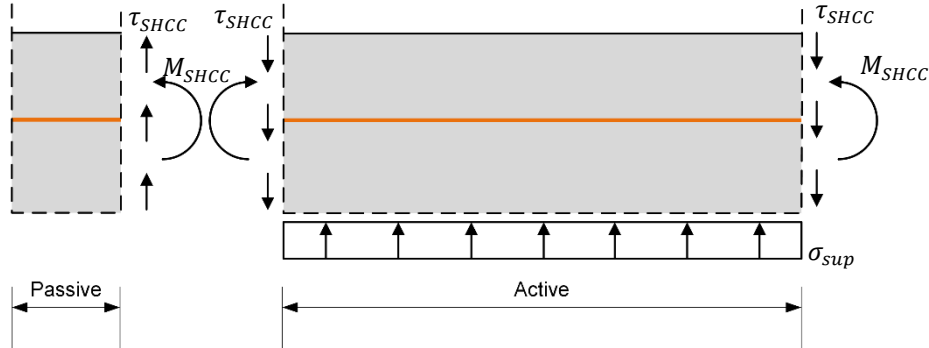


Figure 132 – Bending moments working on the passive part of the link slab in case of horizontal tensile load

Because the vertical deflection is restrained by the substructure, the bending moments should make moment equilibrium with the vertical stresses caused by the restrained vertical deflection. In Figure 132 the vertical support stress, σ_{sup} , is assumed to be constant over the length of the link slab. However, in reality, the vertical support stress may not constant at all.

Both sides of the active section are exposed to two bending moments working in the opposite direction and two shear forces working downwards. Assuming that the active part is clamped between the two passive section, a point load or a distributed load should work upwards to make vertical equilibrium.

The rotation that is caused by bending moment and distributed load both can be expressed as shown in eq.(34) and eq.(35).

$$\theta_m = \frac{ML}{2EI} \quad \text{eq.(34)}$$

$$\theta_q = \frac{QL^2}{24EI} \quad \text{eq.(35)}$$

The bending moment pushes the link slab down. However, due to the substructure, the link slab should stay in place. The rotation caused by the distributed force should be equal to the rotation caused by the bending moment, as shown in eq.(36)

$$\theta_m = \theta_q$$

$$\frac{ML}{2EI} = \frac{QL^2}{24EI} \quad \text{eq.(36)}$$

$$Q = \frac{12M}{L}$$

Now the deflection in the middle of the beam can be expressed as a function of the bending moment, as shown in eq.(37). Comparing the deflection that is caused by the distributed force (eq.(37)) with the deflection of the bending moment (eq.(38)), the deflection caused by the distributed force is larger than the deflection caused by bending moments. The difference between both is shown in eq.(39). In reality, this is impossible, because the substructure can't push the link slab up, but can only prevent that it bends downwards. So in reality, not a distributed constant load is working, but a distributed load that is not constant over the length of the link slab, such that the rotation at the ends of the active part is zero and the deflection in the rest of the active section is zero as well.

$$u_{max,q} = \frac{5}{384} \frac{\frac{12M}{L} L^3}{EI} = \frac{5}{32} \frac{ML^2}{EI} \quad \text{eq.(37)}$$

$$u_{max,m} = \frac{4}{32} \frac{ML^2}{EI} \quad \text{eq.(38)}$$

$$\Delta u_{max} = \frac{1}{32} \frac{ML^2}{EI} \quad \text{eq.(39)}$$

If the situation is in compression instead of tension, more or less the same mechanism works, but in the opposite direction. The expected stresses, forces and bending moments on the passive part of the link slab in the case that the link slab is under compression is shown in Figure 133. The idea behind is the same as in the case that the link slab is under tension. The equilibrium equations for the passive part the link slab exposed to compressive stresses as shown in Figure 133 are:

1. Horizontal equilibrium could be made between compressive stresses in the interface zone and the active part of the link slab. However, because the link slab is not infinite stiff, shortening of the passive part of the link slab is expected if compressive stresses are working. Because of the shortening, friction stresses are generated in the horizontal plane between the active part of the link slab and substructure (τ_{hor}). Compared to the compressive stresses, the friction stress is compared relative small.

$$\sigma_{c,NSC} \cdot t_{link\ slab} + \tau_{hor} \cdot L_{active} = \sigma_{c,SHCC} \cdot t_{link\ slab} \quad \text{eq.(40)}$$

2. The horizontal stresses working on the results in a certain bending moment, working on the active part of the link slab. Vertical stresses and bending moments should make equilibrium, like in the case of tension. Bending moment equilibrium around point B:

$$\left(\tau_{ver} \cdot t_{link\ slab} + F_{reinf,ver} + F_{sup} \right) \cdot L_{active} - \tau_{hor} \cdot \frac{1}{2} \cdot t_{link\ slab} \cdot L_{active} + M_{SHCC} = 0 \quad \text{eq.(41)}$$

3. The vertical equilibrium should be made with the vertical friction at the interface, shear stress at the active part of the link slab and a supporting force near the active section of the link slab:

$$\tau_{ver} \cdot t_{link\ slab} + F_{sup} + F_{reinf,ver} = 0 \quad \text{eq.(42)}$$

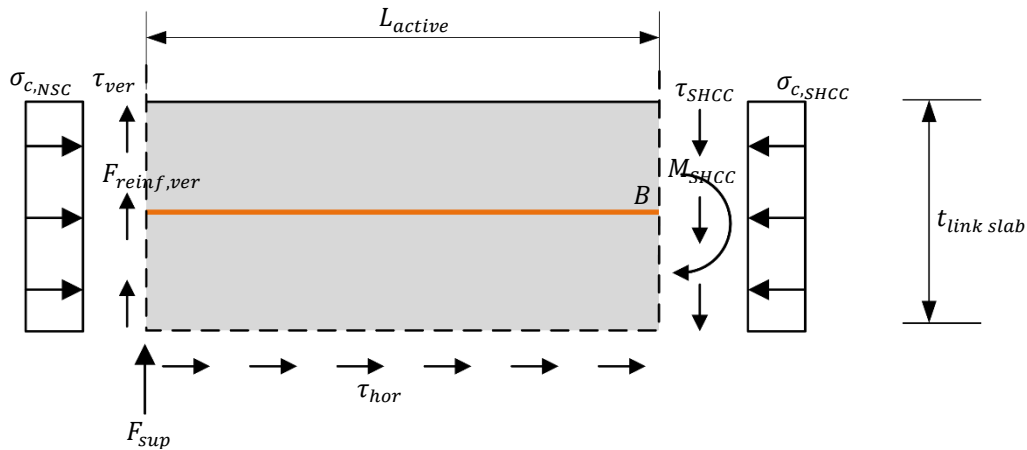


Figure 133 – Stresses working on the passive part of the link slab due to horizontal compressive load

In Figure 134 are shown the vertical stresses that work on the active part of the link slab, due to vertical stresses at the interface with the passive zone. As shown in the figure, in the horizontal plane should work a certain tensile stress to make vertical equilibrium. However, since there is a debonding layer at this horizontal plane, not tensile stresses could be carried by the plane. In other words, no vertical equilibrium is possible, assuming that no permanent vertical load works above the link slab. That means that the shear stress τ_{SHCC} can not be generated. As a result, no vertical stresses can be generated in the passive part of the link slab at all, what means that no counter bending moment can be generated against the bending moment caused by the horizontal stresses.

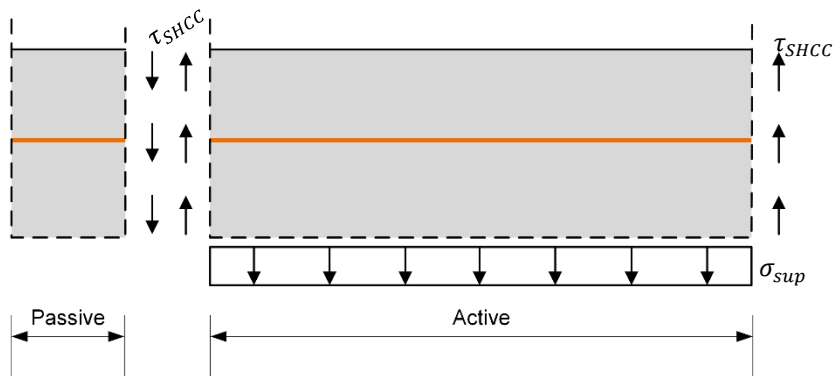


Figure 134 – Vertical stresses working on the passive part of the link slab in case of horizontal tensile load

Also the bending moment, M_{SHCC} , can not be carried by the vertical stresses, because the stresses can only work in the direction that is shown in Figure 132. However, if on the other side of the active link slab works a similar bending moment, what could theoretically be expected if only a horizontal load is working, bending moment equilibrium in the active part of the link slab could be made.

At last, the horizontal stresses could be analysed in more. The shear stress at the bottom of the link slab could cause that the count compressive stress is not constant over the thickness of the link slab any more. Due to the shear stresses in the horizontal interface, the compressive stresses could have a pattern as shown in Figure 135. In the figure is shown that due to the different shape of the diagram of the left compressive stress, a certain bending moment is generated by the left compressive stresses. Depending on the shape of the compressive stress diagram and the magnitude of both, the compressive stress and the horizontal shear stress, bending moment equilibrium could be made.

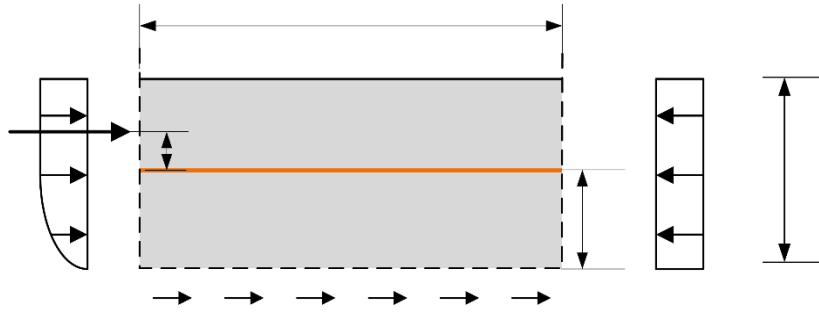


Figure 135 – In depth analysis of horizontal stresses caused by horizontal load on the link slab

So as a conclusion for the link slab under compressive stresses, could be mentioned that the vertical stresses caused by the horizontal loads, can not be carried. Therefore, no vertical stresses can work to make bending moment equilibrium. Assuming that the shape of the compressive stresses is not constant any more, the horizontal stresses could make bending moment equilibrium.

From the analysis from above again a list of variables that influence the horizontal strength of the active part of the link slab could be made.

Tensile stress	Compressive stress
- Thickness of the link slab	- Compressive strength SHCC
- Length of the passive part of the link slab	- Compressive strength NSC
- Distribution of fibres	- Thickness of the link slab
- Reinforcement and fibres:	- Length of the active part of the link slab
o Reinforcement ratio	- Shear capacity SHCC
o Fibre percentage	- Shear capacity interface NSC/SHCC
o Material characteristics like; tensile strength, Young's modulus	- Shear capacity steel reinforcement
o Dimensions	
o Composite working (for example pull-out strength)	
- Shear capacity SHCC	
- Shear capacity interface NSC/SHCC	
- Shear capacity steel reinforcement	

3.3.2.4 Horizontal interface between NSC and SHCC with dowels (passive zone)

Here the horizontal interface between the NSC deck and the SHCC link slab is analysed again. However, in this paragraph it is assumed that the connection between the deck and the link slab is also carried by dowels. The passive zone of the link slab with dowel react almost the same as the passive zone of a link slab without dowels or studs. The main difference is that a lot of shear stress is carried by the dowels or studs, instead of only friction at the horizontal plane between the SHCC and NSC. In Figure 136 are shown the horizontal stress and the vertical friction between the link slab and the dowel. The equilibrium equations in the detail B of Figure 125 are:

1. Horizontal equilibrium in Figure 136 is expressed in eq.(43).

$$\sigma_{t,SHCC} \cdot t_{link\ slab} = F_{reinf} + \#_{dowels} \cdot H_{dowel} + \tau_{hor} \cdot L_{active} \quad \text{eq.(43)}$$

2. Bending moment is taken about point B, shown in Figure 136. The bending moment equilibrium is shown in eq.(44)

$$\begin{aligned} (\tau_{ver} \cdot t_{link\ slab} + F_{reinf,ver}) \cdot L_{active} - \#_{dowels} \cdot (H_{dowel} + V_{dowel}) - \tau_{hor} \\ \cdot \frac{1}{2} \cdot t_{link\ slab} \cdot L_{active} + M_{SHCC} = 0 \end{aligned} \quad \text{eq.(44)}$$

3. At last, vertical equilibrium is taken in Figure 136. This equilibrium is shown in eq.(45).

$$(\tau_{ver} - \tau_{SHCC}) \cdot t_{link\ slab} - F_{sup} + F_{reinf,ver} + V_{dowels} = 0 \quad \text{eq.(45)}$$

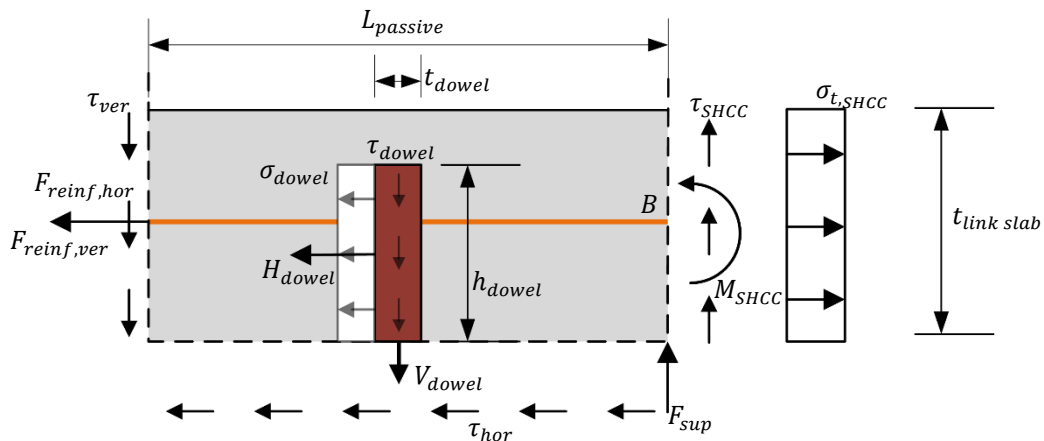


Figure 136 – Stresses working on the passive part of the link slab that included dowels, due to horizontal compressive load

Ad. 1. Stark & Stark (2009) describe two ways dowels fails; crushing of the concrete or failure of the steel dowel. Both failure modes are shown in Figure 137. The failure mode with the lowest capacity is the governing one. Both failure modes have its own failure strength, as shown in the formulas of Figure 137. From the formulas the variables for the capacity of the dowels can be determined. If the steel dowel fails, the steel strength and the diameter of the dowel determine the shear capacity. If the concrete fails, the diameter, concrete strength, concrete modulus of elasticity and the length of the dowel (α).

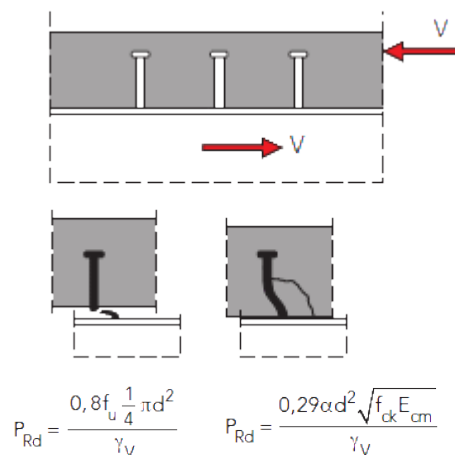


Figure 137 – Failure modes of steel dowel in concrete slab (Stark & Stark, 2009)

Ad. 3. The vertical friction of the dowels and shear studs is probably very small compared to the horizontal shear capacity. The friction between the dowels and the concrete is probably quite small, especially if the dowel is smooth. The shape of the dowel also influence the vertical strength of the dowel. This idea is schematically shown in Figure 138, where two different shapes of dowels are shown. As shown in the figure, a dowel like the left one is expected to have more vertical strength capacity than the right one.

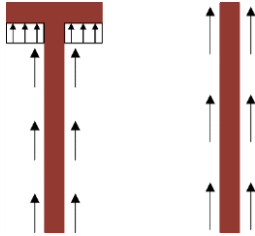


Figure 138 – Vertical strength of two different shaped dowels

Under vertical stress, the dowel itself can fail or the concrete. However, probably the friction between the dowel and SHCC is too small to get failure in the dowel or the concrete. If there is a vertical part above the dowel, as at the left dowel of Figure 138, the change of failure is larger, because larger stresses can be expected in this kind of dowels.

The way the shear stress, τ_{SHCC} , and the bending moment at the vertical interface between the passive and active sections, are assumed to work the same as if no dowels are applied. In Figure 132 of the previous paragraph is already shown how the shear stress and bending moment in the active zone make vertical and bending moment equilibrium.

In Figure 139 is shown the passive part of the link slab with dowels in case of horizontal compressive loads working on the link slab. Same as for the link slab without dowels, the shear stress at the interface between the passive and active part of the link slab can not be carried by the active part of the link slab, as explained in the paragraph 3.3.2.3 Horizontal interface between NSC and SHCC (passive zone) already. Since the shear stress, τ_{SHCC} , is equal to zero, the shear stress around the dowels, τ_{dowel} , should be carry the downward vertical stresses to make vertical equilibrium with the shear stress, τ_{ver} , the support point load, F_{sup} , reinforcement shear force, $F_{reinf,hor}$, at the vertical interface with the NSC. However, the shear stress around the dowel, τ_{dowel} , is expected to be small as mentioned before. Therefore, to make bending moment equilibrium, the shape of the concrete stress with the interface should change as, same as for the passive zone without dowel as shown in paragraph 3.3.2.3 Horizontal interface between NSC and SHCC (passive zone).

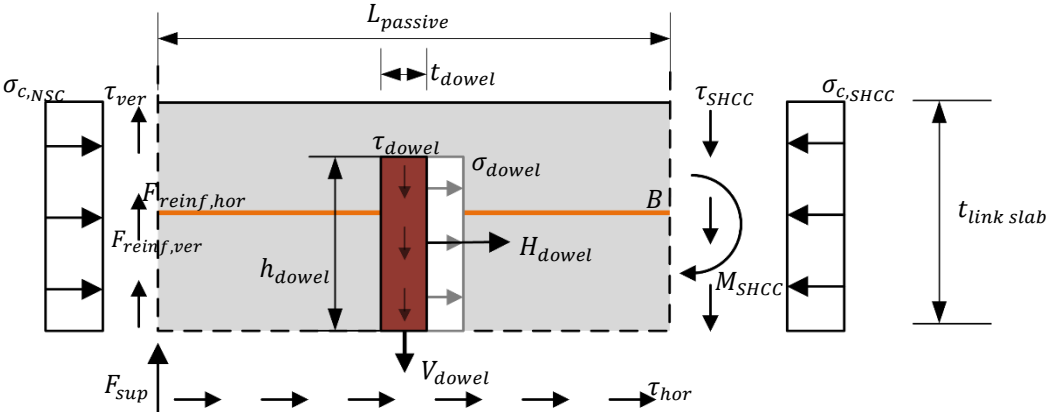


Figure 139 – Stresses working on the passive part of the link slab with dowels due to horizontal compressive loads

In chapter 2.3.5.4 Imposed curvature according to tests, the reaction of the thin SHCC link slab that is exposed to imposed curvature according to tests is discussed. In the chapter is written that imposed curvature of the bridge lead to imposed horizontal deformation in the link slab. Comparing the stresses working in the case of horizontal load with the case of imposed curvature/imposed horizontal deformation, the same stresses seems to work.

In fact, it is quite logic that the same kind of stresses work in the case of imposed horizontal deformation and horizontal load. Imposed horizontal deformation gives horizontal stresses in the structure, because the deformation is restrained in the link slab. The stresses that are generated in the link slab, because of imposed deformation, also results in stresses between the link slab and the substructure. The stresses between the link slab and the substructure are carried by similar mechanisms as stresses that are generated by horizontal loads.

From the analysis from above again a list of variables that influence the horizontal strength of the passive part of the link slab could be made. However, only the variables for the studs are called here. The other variables are already called in the previous paragraph.

Failure of steel	Failure of concrete
- Steel strength	- Diameter
- Diameter of dowel	- Concrete strength
- Friction between steel and SHCC, in case of vertical stresses	- Concrete modulus of elasticity
	- Length of dowel
	- Friction between steel and SHCC, in case of vertical stresses

3.3.3 Vertical imposed deformation

The third basic action, the vertical imposed deformation of the thin link slab, is already partly discussed in chapter 2.3.5.5 Vertical imposed . In this chapter, the discussion is in some more detail, such that all the factors that influence the vertical imposed deformation could be known. In Figure 140 is shown the situation that one of the bridge spans is deflected down, for example because of settlement in one of the supports. In the figure are given three cross sections and two details, to analyse the link slab properly. The cross sections and details are used to describe:

- I* - Stresses working over the cross section in the active zone
- II* - Stresses working in passive section without dowels
- III* - Stresses working in passive section with dowels
- Detail A - Overview of loads working on the active part of the link slab
- Detail B - Stresses working at the end of the concrete bridge deck

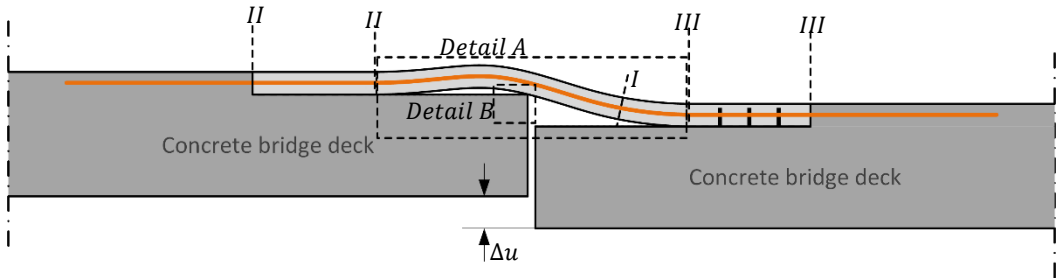


Figure 140 – Overview of cross sections and details to analyse the link slab exposed to vertical imposed deformation

3.3.3.1 Loads working on the active zone of the link slab

In this paragraph are discussed the loads that work on the active section of the link slab. The description is done with detail A of Figure 140. This detail is shown in Figure 141. As shown in the figure, the link slab is made to a model. The model is used to describe the deformation of the link slab in a proper way.

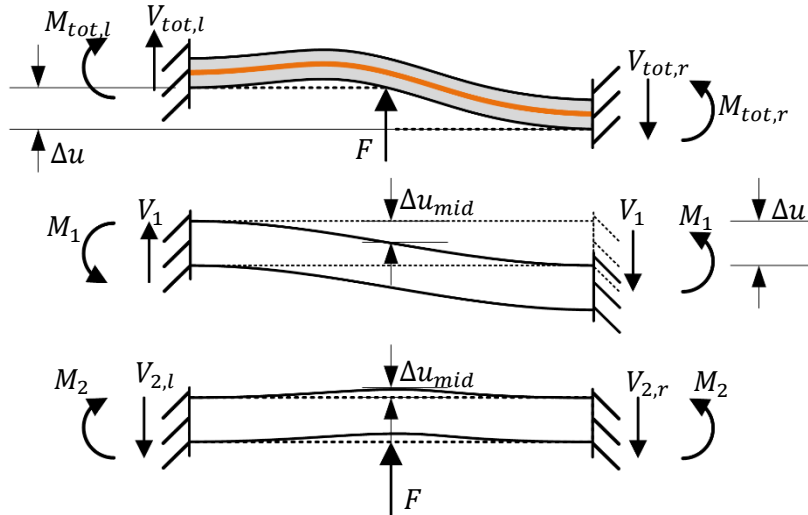


Figure 141 – Detail A of Figure 140: modelling of active part of thin link slab exposed to imposed vertical deformation

In Figure 141 is shown the model of the active part of the thin link slab. In the figure are shown three link slabs. In the upper link slab is shown the expected total deflection of the thin link slab exposed to a imposed vertical deformation, Δu . The link slab is split up in two models, as shown in lower two link slabs of Figure 141.

In the first model, middle link slab of Figure 141, is shown the vertical settlement in the link slab. Due to the vertical settlement, shear forces and bending moments work on both supports. In the second model, the point load working on the link slab is modelled. The point load should be large enough to keep the link slab in place at the middle of the link slab, what is required from the geometrical boundary conditions. In other words, the deflection in the middle of the link slab caused by the point load should be even large as the deflection in the middle of the link slab caused by the imposed vertical deformation at the support. In a shorter way;

$$\Delta u_{middle}(\text{imposed vertical deformation}) = \Delta u_{middle}(\text{point load})$$

Both vertical displacements in the middle of the link slab caused by imposed vertical deformation and the point load can be expressed as a function of the bending moment and the point load respectively.

$$\Delta u_{middle}(\text{imposed vertical deformation}) = \Delta u_{middle}(\text{point load})$$

$$\frac{M_1 L^2}{12EI} = \frac{FL^3}{192EI} \quad \text{eq.(46)}$$

$$M_1 = \frac{FL}{16}$$

From forget-me-nots:

$$M_{2,l} = M_{2,r} = \frac{FL}{8} = M_2 \quad \text{eq.(47)}$$

From the bending moment lines per model combined with the expression of the bending moments and the lengths, the shear forces are:

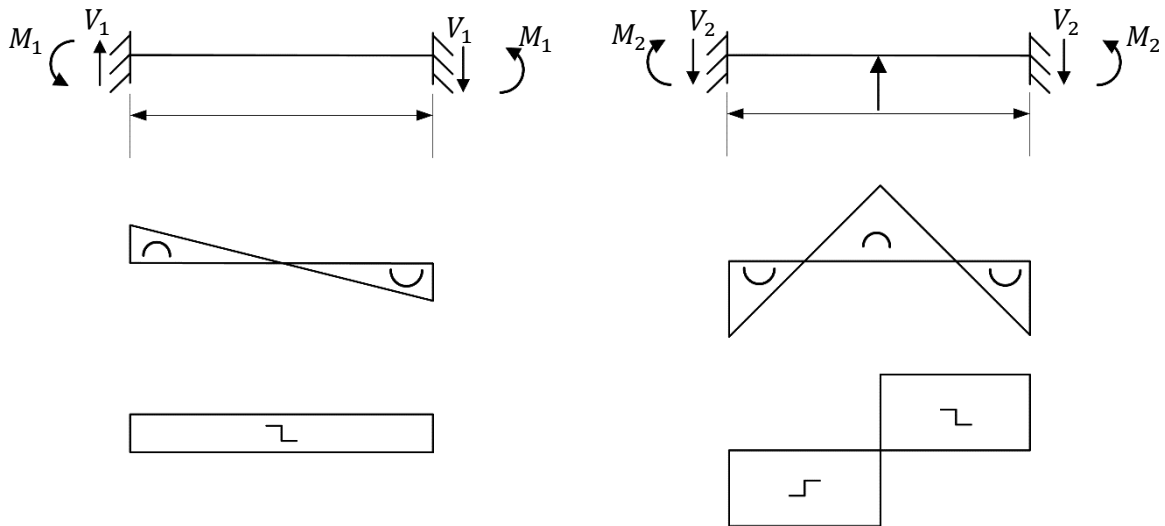


Figure 142 – Bending moment and shear force lines for link slab model of Figure 141

$$V_{1,l} = V_{1,r} = M_1 \cdot \frac{L}{2} = \frac{F}{8} = V_1 \quad \text{eq.(48)}$$

$$V_{2,l} = V_{2,r} = \frac{2FL}{8} \cdot \frac{2}{L} = \frac{F}{2} = V_2$$

The total working shear forces and bending moments are:

$$V_{tot,l} = V_{1,l} + V_{2,l} \quad \text{eq.(49)}$$

$$V_{tot,l} = \frac{F}{8} - \frac{F}{2} = -\frac{3}{8}F$$

$$V_{tot,r} = V_{1,r} + V_{2,r} \quad \text{eq.(50)}$$

$$V_{tot,r} = \frac{F}{8} + \frac{F}{2} = \frac{5}{8}F$$

$$M_{tot,l} = M_{1,l} + M_{2,l} \quad \text{eq.(51)}$$

$$M_{tot,l} = -\frac{FL}{16} + \frac{FL}{8} = \frac{FL}{16}$$

$$M_{tot,r} = M_{1,r} + M_{2,r} \quad \text{eq.(52)}$$

$$M_{tot,r} = \frac{FL}{16} + \frac{FL}{8} = \frac{3}{16}FL$$

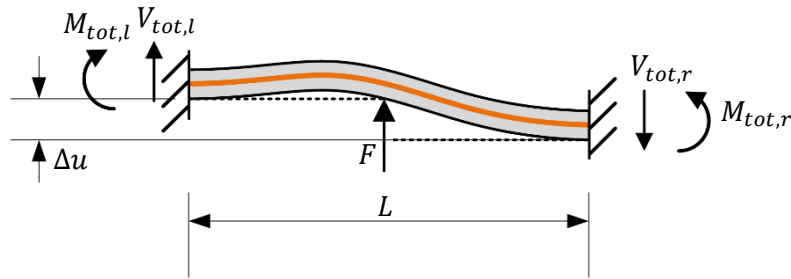


Figure 143 – Point load, shear forces and bending moment working on active part of the link slab due to imposed vertical deformation Δu

Check on moment equilibrium and vertical equilibrium

$$M_{tot,l} - M_{tot,r} + V_{tot,l} \cdot L + F \cdot \frac{L}{2} = 0 \quad \text{eq.(53)}$$

$$\frac{FL}{16} - \frac{3}{16}FL + -\frac{3}{8}F \cdot L + F \cdot \frac{L}{2} = 0 \rightarrow OK$$

$$V_{tot,l} + F - V_{tot,r} = 0 \quad \text{eq.(54)}$$

$$-\frac{3}{8}F + F - \frac{5}{8}F = 0 \rightarrow OK$$

The variables that influence on the shear and bending moment capacity are discussed in the next paragraph, 3.3.3.2 Stresses working over the cross section in the active zone. In that paragraph the reaction stresses over the cross section of the active part of the link slab are analysed in more detail.

3.3.3.2 Stresses working over the cross section in the active zone

Imposed vertical deformations could cause internal stresses. The link slab should have a certain strength to carry these internal stresses. However, the quantity of the stresses also depends on some

design variable of the link slab. In this paragraph, first the strength capacity of the link slab is determined and after that the quantity of the stresses caused by imposed vertical deformation are discussed. In the end, all variables are list together.

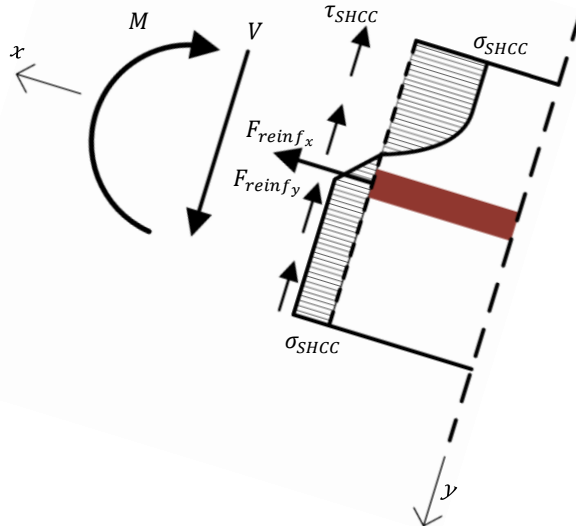


Figure 144 – Cross section I of Figure 140: stresses working over the thickness of the link slab

In Figure 144 is shown cross section I of Figure 140. Over the height of the cross section are shown the stresses that are expected. From the analysis of paragraph 3.3.3.1 Loads working on the active zone of the link slab are determined the working shear force, V , and bending moment, M . Over the cross section are expected friction and compressive and tensile stresses to make equilibrium with the working loads.

The stresses over the cross section are explained here in some more detail according to Japan Society of Civil Engineers (2008). In these Japanese recommendations are given formulas to determine the shear strength, compressive strength and tensile strength over the cross section of the SHCC link slab. The calculation of these three strengths are already shown in Appendix 1: Literature study. According to the formulas and the geometry of Figure 144, the variables that influence the strengths can be determined, as shown in Table 29.

Table 29 – Overview of variables that influence the shear, compressive or tensile strength of the SHCC link slab

Strength	Composite part	Variable
Shear strength	SHCC shear capacity without shear reinforcement and excluding reinforcing fibres.	Concrete compressive strength
		Effective width
		Effective depth
		Cross sectional area of tension reinforcement
	Shear capacity of reinforcing fibres	Tensile yield strength of SHCC
		Effective width
Compressive strength	SHCC capacity	Concrete compressive strength
		SHCC compressive cross sectional area
	Longitudinal reinforcement steel capacity	Steel yield compressive strength
		Steel cross sectional area

Tensile strength	SHCC tensile capacity with fibres	Tensile strength
		SHCC tensile cross sectional area
	Longitudinal reinforcement	Steel tensile yield strength
	steel	Steel cross sectional area

Next to the variables called in Table 29, for the bending moment capacity internal level arms between tensile and compressive resultant forces have a lot of influence on the total bending moment capacity. The internal level arms depends next to the already mentioned variable of Table 29, also on the height of the cross section, the geometry of the cross section and the distribution of fibres and reinforcement.

Before all variables are listed, the variables that influence the quantity of the internal stresses caused by a certain imposed vertical deformation are analysed. In paragraph 2.1.5.2 Vertical is given the bending moment caused by a certain vertical imposed deformation, Δu , as shown in eq.(55)

$$M(\Delta u) = \frac{6 \cdot \Delta u \cdot EI}{L^2} \quad \text{eq.(55)}$$

In the previous paragraph, 3.3.3.1 Loads working on the active zone of the link slab, is shown the relation between the bending moment caused by imposed vertical deformation and the point load F in order to hold the link slab in place at the middle of the link slab.

$$M_1 = \frac{FL}{16} \quad \text{eq.(56)}$$

Combining eq.(55) and eq.(56), the working load can be expressed as a function of the deformation, as shown in eq.(57).

$$F(\Delta u) = \frac{96 \cdot \Delta u \cdot EI}{L^3} \quad \text{eq.(57)}$$

The bending moment and shear force in the link slab have both a linear relation with the point load F, as shown in paragraph 3.3.3.1 Loads working on the active zone of the link slab. So to hold the shear force and bending moment as low as possible, the point load F should also be as small as possible. To reduce the point load F, the Young's modulus and the moment of inertia should be low and the length of the link slab should be large. Assuming a rectangular cross section of the link slab, the moment of inertia depends on the height of the link slab as shown in eq.(58).

$$I = \frac{1}{12} h^3 [mm^4/m] \quad \text{eq.(58)}$$

Above, the shear strength, moment capacity of the link slab and the magnitude of internal stresses are analysed. Here the variables that influence the capacities and stresses are listed.

Shear strength	Moment capacity	Magnitude of internal stresses
- SHCC compressive strength	- Concrete compressive strength	- Vertical settlement (Δu)
- Effective width		- Young's modulus SHCC
- Effective depth		- Height link slab

<ul style="list-style-type: none"> - Cross sectional area of tension reinforcement - Tensile yield strength of SHCC - Internal level arm 	<ul style="list-style-type: none"> - SHCC compressive cross sectional area - Steel yield compressive strength - Steel cross sectional area - SHCC tensile strength - SHCC tensile cross sectional area - Steel tensile yield strength - Link slab thickness - Place of fibres and reinforcement 	<ul style="list-style-type: none"> - Length active part of link slab
---	---	---

3.3.3.3 Stresses working at the end of the concrete bridge deck

In this paragraph is analysed the end of the concrete bridge deck. A point load is expected here, taking into account the expected deformation of the link slab. Due to the point load, spalling off of the concrete could be expected, what is analysed in more detail in this paragraph.

In Figure 145 is shown the end of the concrete bridge deck where at the end of the deck are shown four point loads, F_1 until F_4 . According to the expected deformation due to imposed vertical deformation as shown in Figure 140, a point load could be expected at the end of the bridge deck. In Figure 145, this point load is shown by F_1 . If the part under the load F_1 is spalling off, the point load working on the bridge deck is expected at F_2 . If this part of the concrete also spalling off the, the point load can be expected at F_3 and then F_4 . Assuming spalling in concrete is under 45 degrees, spalling stops if the point load is at F_5 , assuming the reinforcement is able to carry the tensile stresses properly.

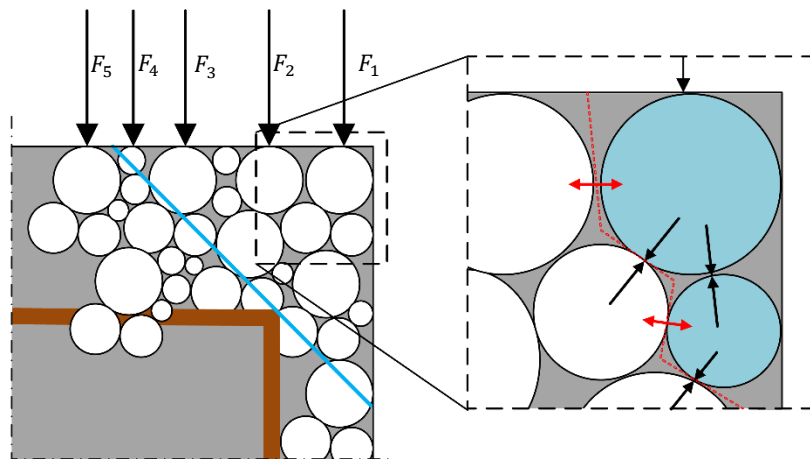


Figure 145 – Spalling of concrete at the end of the concrete bridge deck due to the point load caused by imposed vertical deformation

In Figure 146 is shown the influence of the horizontal shift of the point load. In the figure is given the expected deformation in the upper link slab. The two bottom link slabs are models for imposed vertical deformation and a point load.

In the model of the imposed vertical deformation, middle link slab of Figure 146, is shown that the vertical deformation (Δu_4) that should be carried by the point load F is smaller compared to Δu_{mid} . Due the smaller deformation that should be carried, the point load could also expected to be smaller.

However, the point load F is shifted to the left support. Going into extremes, assuming the point load is placed very close to the support, a very large point load is needed to have a certain displacement. So it could be expected that the shift of F also results in an increase of the load to have a certain vertical displacement.

Combining the fact that the vertical displacement at the end of the girder due to vertical imposed deformation Δu is smaller and the fact that the point load is shifted, so the point load should probably be larger for a certain displacement can result in a higher or a smaller point load.

Taking into account the total deflection of Figure 146 (upper model) the link slab seems to be bended a bit less. Assuming the same level or restraint in combination with the assumption that the link slab is deformed less, reduced internal and external stresses could be expected. Then the point load F could also be expected to be lower. However, it is hard to quantify if the point load is lower whether or not.

Assuming the point load indeed decrease if it shift from the middle, spalling of concrete may stop before the addition of the reinforcement is really noticed (so left from F_5 of Figure 145). In that case the tensile strength of the concrete is larger than the tensile stress that is caused by the point load.

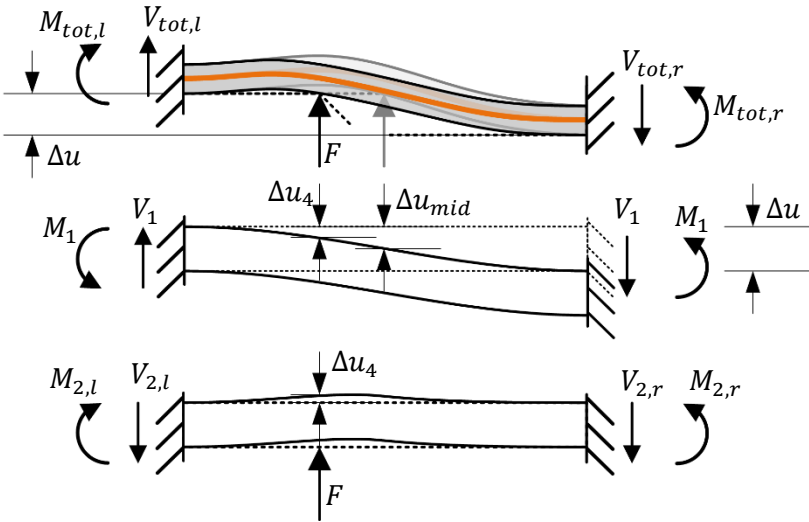


Figure 146 – Modelling of active part of thin link slab exposed to imposed vertical deformation taking into account shifting of the point load

Note: the point load is assumed to work vertically. However, in reality the point load probably also has a horizontal component, because in reality the point load is probably under a certain angle. In the link slab are bending moments and shear forces working. Shear forces work parallel to the cross section. Since the link slab is expected to be under a certain angle, the reaction force at the end of the substructure could be expected to be under a certain angle as well to make equilibrium. The point load, F , working under a certain angle is schematically shown in Figure 147. Due to the horizontal component of the point load, horizontal equilibrium could be generated. The horizontal component of the point load, F , together with the tensile stress carried by the concrete, σ_t , should make horizontal equilibrium with the horizontal components of the compressive stresses, σ_c . However, in the discussion is only the vertical component discussed. This makes the story easier and the horizontal component is probably very small compared to the vertical component.

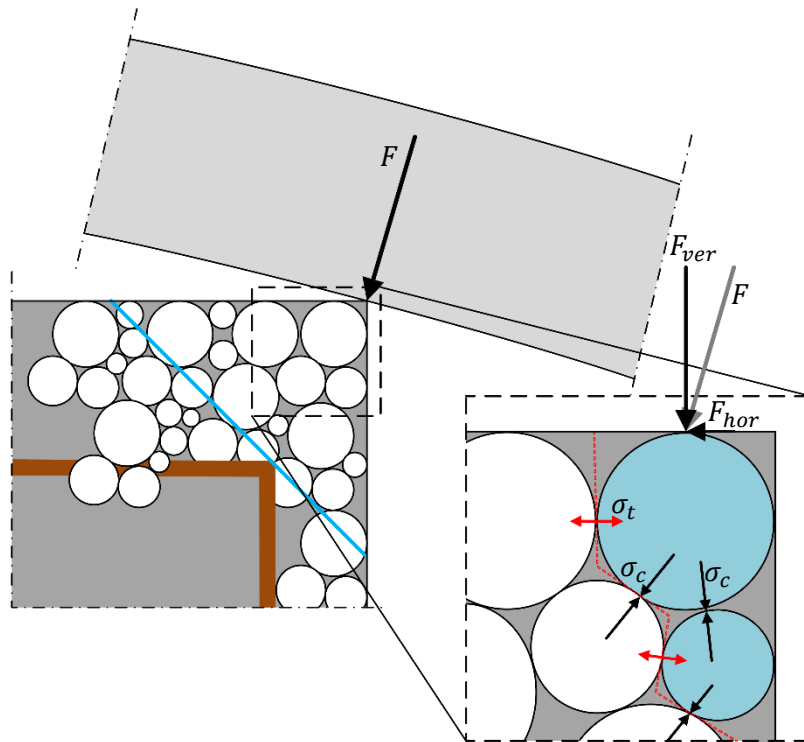


Figure 147 – Spalling of concrete at the end of the concrete bridge deck due to the point load caused by imposed vertical deformation. Point load in actual expected direction

At last, the variables that influence spalling of the substructure can be determined. In fact, to prevent spalling, the concrete should have a certain resistance against spalling or the point load should be that small that spalling does not occur. Both the concrete resistance against spalling and the point load that causes spalling are already discussed in paragraph 3.3.1.3 Case C and 3.3.3.2 Stresses working over the cross section in the active zone respectively. The influence factors are given again below.

Spalling resistance	Point load that causes spalling stresses
- Tensile strength of NSC	- Vertical settlement (Δu)
- Reinforcement design	- Young's modulus SHCC
- Addition of fibres	- Height link slab
-	- Length active part of link slab

3.3.3.4 Stresses working in passive section without dowels

Due to imposed vertical deformation, stresses in the passive section are expected to distribute stresses from the active section to the concrete substructure. In this paragraph are discussed the stresses that are expected in the passive section if no dowel are applied.

From the active section, a bending moment and a shear force are expected to work over the cross section of the passive zone of the link slab. This is schematically shown in Figure 148 with M_{act} and V_{act} that both represent the bending moment and the shear force from the active section respectively. In the figure are also shown the reaction stresses that are expected. The stresses are determined according to equilibrium equations. The three equilibrium equations are shown under Figure 148 and explained in detail below.

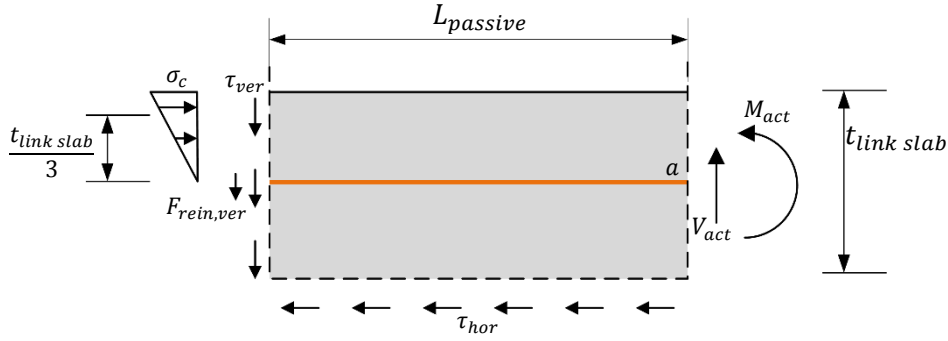


Figure 148 – Cross section II of Figure 140: stresses working on the passive zone of the link slab due to horizontal load

$$1. \quad \sum V = 0 \rightarrow V_{act} = \tau_{ver} \cdot t_{link\ slab} + F_{rein,ver} \quad \text{eq.(59)}$$

$$2. \quad \sum M|_a = 0 \rightarrow M_{act} + (\tau_{ver} \cdot t_{link\ slab} + F_{rein,ver}) \cdot L_{passive} = \frac{1}{2} \cdot \sigma_c \cdot \frac{t_{link\ slab}}{6} + \tau_{hor} \cdot L_{passive} \cdot \frac{t_{link\ slab}}{2} \quad \text{eq.(60)}$$

$$3. \quad \sum H = 0 \rightarrow \tau_{hor} \cdot L_{passive} + F_{rein,hor} = \frac{1}{2} \cdot \sigma_c \cdot \frac{t_{link\ slab}}{2} \quad \text{eq.(61)}$$

Ad 1. As shown in the previous paragraphs, in the active part of the link slab works a shear force, V_{act} . Because the passive part of the link slab and the active part are one piece, the shear force at the begin of the passive section will be the same as the shear force at the end of the active part of the link slab. Vertical equilibrium can only be achieved with the vertical component of the reinforcement and the shear stress at the vertical interface with the NSC. It is assumed that the vertical component of the friction between at the horizontal interface between the link slab and the substructure can be neglected. The tensile strength of concrete is neglectable small and potential shear stresses in the vertical direction can be neglected as well.

Ad 2. Also shown in the previous paragraphs, in the active part of the link slab works a bending moment. The vertical forces generates a bending moment working in the same direction as the bending moment from the active section. Horizontal stresses should be generated to make bending moment equilibrium. A compressive stress at the vertical interface with NSC and shear stresses at the horizontal interface with the NSC should be able to make moment equilibrium. It is assumed that the compressive stress is elastically and works over halve of the thickness of the link slab. If the compressive stress becomes partly plastic, the internal level arm will reduce. The reduction is limited to $\frac{t_{link\ slab}}{2} - 0.38 \cdot t_{link\ slab} = 0.12 \cdot t_{link\ slab}$. It could be noted that the smaller level arm results in smaller bending moments. The horizontal friction between the link slab and the substructure in the horizontal interface has a limited value. This limit depends among other things, on the way the connection is made. For example, grout in the connection increases the horizontal friction.

Ad 3. From reasons of horizontal equilibrium the that is force generated in the compressive stress at the vertical interface should be equal to the force generated in the horizontal interface due to shear stresses and the tensile force in the reinforcement.

The stress that works at the horizontal interface is carried by friction. At the end of the surface, an upwards pointing shear force is expected. Friction stresses only work if there is a certain movement. The upwards pointing shear force could lift up the link slab, depending on the magnitude of the shear forces. As soon as the link slab is lifted a bit, the horizontal friction decreases.

In the above analysis, a few variables that influence the amount vertical imposed deformation that can be carried by the passive zone of the link slab, if no dowels are applied. The influence factors are show below.

Vertical working stresses	Horizontal working stresses
- Thickness of the link slab	- Compressive strength SHCC
- Reinforcement (shear capacity):	- Compressive strength NSC
o Reinforcement ratio	- Thickness of the link slab
o Material characteristics like; tensile strength, Young's modulus	- Length of the passive part of the link slab
o Dimensions	- Friction at horizontal interface NSC/SHCC
o Composite working (for example pull-out strength)	- Tensile strength steel reinforcement
- Shear capacity SHCC	
- Friction at vertical interface NSC/SHCC	

3.3.3.5 Stresses working in passive section with dowels

In this paragraph are, same as in the previous paragraph, discussed the stresses that are generated in the passive zone due to stresses in the active part of the link slab caused by imposed vertical deformation. The difference with the previous paragraph is that in this paragraph are dowels included in the passive section. These dowels have a certain influence of the stress distribution in the link slab.

The situation of a passive section with dowels exposed to a bending moment and shear force is shown in Figure 149. In the figure are shown more or less the same stresses as in the previous paragraph, Figure 148, but with the addition of stresses generated by the dowels.

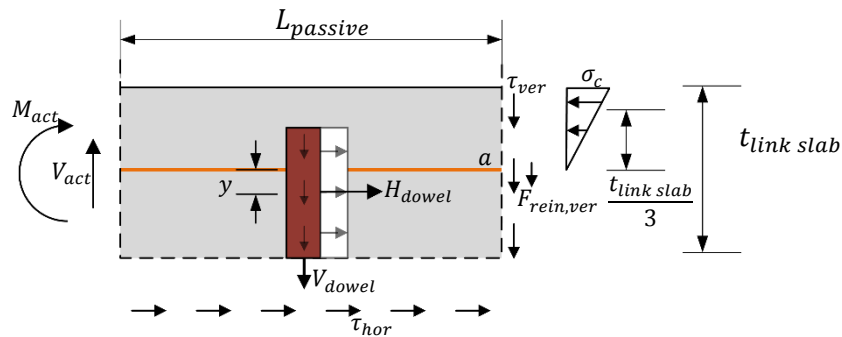


Figure 149 – Cross section III of Figure 140: stresses working on the passive zone of the link slab with dowels due to horizontal load

$$1. \quad \sum V = 0 \rightarrow V_{act} = V_{dowel} + \tau_{ver} \cdot t_{link\ slab} + F_{rein,ver} \quad \text{eq.(62)}$$

$$2. \quad \sum M|_a = 0 \rightarrow M_{act} + (\tau_{ver} \cdot t_{link\ slab} + F_{rein,ver}) \cdot L_{passive} + \#_{dowel} \cdot V_{dowel} \cdot \frac{L_{passive}}{2} = \#_{dowel} \cdot H_{dowel} \cdot y + \frac{1}{2} \cdot \sigma_c \cdot \frac{t_{link\ slab}}{6} + \tau_{hor} \cdot L_{passive} \cdot \frac{t_{link\ slab}}{2} \quad \text{eq.(63)}$$

$$3. \quad \sum H = 0 \rightarrow \tau_{hor} \cdot L_{passive} + \#_{dowel} \cdot H_{dowel} + F_{rein,hor} = \frac{1}{2} \cdot \sigma_c \cdot \frac{t_{link\ slab}}{2} \quad \text{eq.(64)}$$

Ad 1. In Figure 149 the same vertical forces work as in Figure 148. The working vertical forces are already discussed in 3.3.3.4 Stresses working in passive section without dowels. The vertical stress in the dowels are expected to be relative small.

Ad 2. For the bending moment equilibrium the bending moment generated by the horizontal component of the dowels work the opposite direction of the bending moment generated by the vertical component. The horizontal force of the dowels are expected to be larger than the vertical forces of the dowels. On the other hand, the level arm of for the horizontal forces is probably significant smaller than the level arm of the vertical forces. Depending on the design, the bending moment of the vertical component of the dowels is larger or smaller than the horizontal component of the dowels. Probably in most designs, the horizontal component is that large that the bending moment capacity caused by the horizontal component of the dowels.

Ad 3. In the horizontal equilibrium equation, the horizontal component of the dowels is included. In the previous paragraph is already discussed that the maximum of both the horizontal shear force and the horizontal compressive force is governing for the maximum working horizontal force. The addition of the dowels increase the limited horizontal force that works against the concrete compressive force in the vertical interface with the NSC. If the shear forces in the horizontal interface is governing, the addition of dowels can increase the compressive strength of the compressive strength in the vertical interface, what can increase the bending moment capacity in the passive section of the link slab.

Note that in reality, the stresses around the upper part of the dowel probably work in the opposite direction as shown in Figure 149. Having a bending moment over the cross section and assuming the normal stress could be neglected, in the upper half of the link slab compressive stresses are expected and in the bottom half tensile stresses. That means that the direction of stresses in the dowels that are in the upper half of the link slab are expected to be in opposite direction as stresses in the dowels that are in the lower half of the link slab.

3.3.4 Horizontal imposed deformation and imposed curvature

Horizontal imposed deformation and imposed curvature in the link slab are discussed together in this paragraph. Based on test result from chapter 2.3.5.4 Imposed curvature according to tests, it is assumed that the imposed curvature results in a horizontal imposed deformation in the link slab. Therefore, it seems to be allowed to discuss both basic action as one mechanism.

In Figure 150 is shown the situation that the link slab is exposed to imposed horizontal deformation. The concrete substructure can shorten or elongate the link slab, what is in Figure 150 shown by Δu_2 and Δu_1 respectively. The shortening and elongation is discussed in more detail under Figure 150.

In Figure 150 are also show some cross section that are analysed in more detail in the chapter. Four cross section are taken, to describe the stresses in the active part of the link slab. A short description of the cross section is shortly given here:

- I* - Stresses working over the cross section in the active zone
- II* - Stresses working in debonding layer of the active zone
- III* - Stresses working in passive section without dowels
- IV* - Stresses working in passive section with dowels
- V* - Stress distribution around the dowels

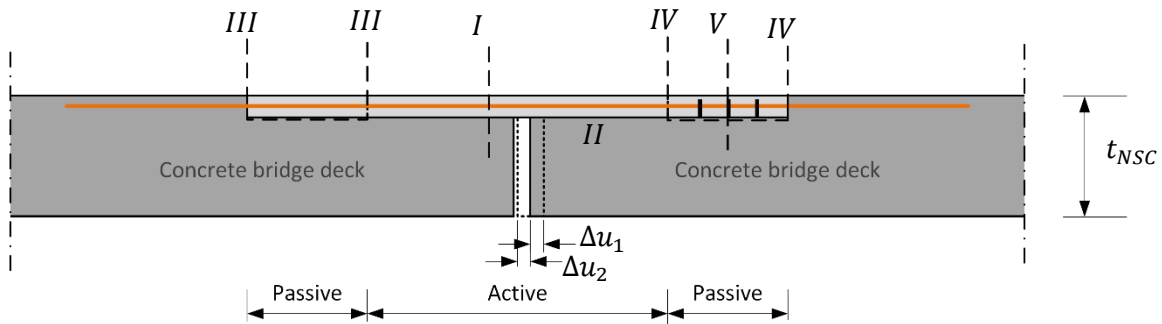


Figure 150 – Overview of cross sections to analyse the link slab exposed to horizontal imposed deformation

Horizontal imposed deformation starts with horizontal deformation of the concrete bridge deck. The bridge decks can move away from each other, Δu_1 , or move to each other, Δu_2 . Without the link slab, the concrete bridge decks are able to move from each other without generating any stresses. The passive parts of the link slabs are assumed to be connected to the concrete bridge, such that both are exposed to the same horizontal movement. The active part of the link slab connect both passive parts. Because the active part has a certain stiffness, so stresses are generated if the active section is exposed to a certain imposed deformation. The stresses that are generated in the active section, should be transferred to the substructure through the passive part of the link slab, to make horizontal equilibrium.

3.3.4.1 Stresses working over the cross section in the active zone

It is assumed that the active zone of the link slab is exposed to an elongation (Δu_2) or shortening (Δu_1). The elongation or shortening is assumed to be carried equally over the whole length of the active section. According to eq.(65), a certain stress in the link slab is expected in the linear elastic zone.

$$\left. \begin{array}{l} \varepsilon = \frac{\Delta u}{l_{act}} \\ \sigma = E \cdot \varepsilon \end{array} \right\} \rightarrow \sigma = E \cdot \frac{\Delta u}{l_{act}} \quad \text{eq.(65)}$$

As shown in eq.(65), the stress caused by a certain imposed deformation, Δu , depends on the stiffness and the length of the active part of the link slab.

In Figure 151 and Figure 152 are shown the stress strain relation for SHCC in compression and tension respectively. The strength of the SHCC mixture applied by Li, Lepech, & Li (2005), is similar to the SHCC mixture reserached in Appendix 1: Literature study. According to Appendix 1: Literature study, the parameters that are shown in Figure 151 and Figure 152 are determined. These parameters are shown in Table 30.

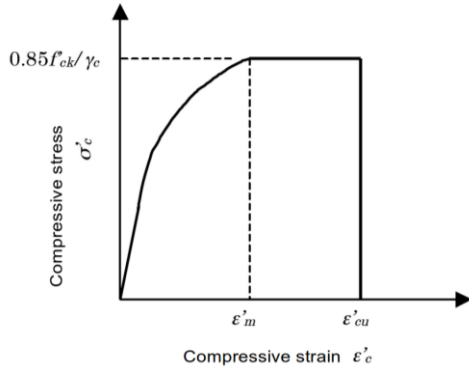


Figure 151 – Typical compressive stress strain diagram of SHCC according to Japan Society of Civil Engineers (2008)

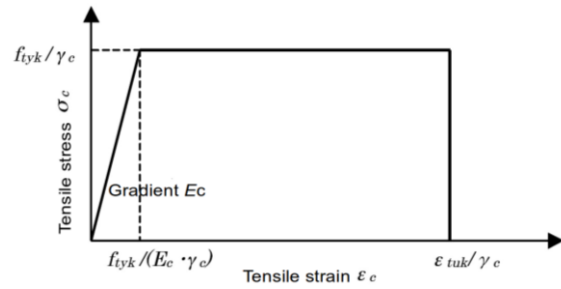


Figure 152 – Typical tensile stress strain diagram of SHCC according to Japan Society of Civil Engineers (2008)

Table 30 – Compressive and tensile characteristics of SHCC according to the literature study and the rules of Japan Society of Civil Engineers (2008)

	Material characteristics	Symbol / formula		Unit
Compressive diagram (Figure 151)	Characteristic compressive strength	f_{ck}	41	MPa
	Material safety factor	γ_c	1.3	[-]
	Design compressive strength	$0.85 \cdot \frac{f_{ck}}{\gamma_c}$	26.8	MPa
	Maximum compressive strain	ϵ'_{cu}	0.3	%
Tensile diagram (Figure 152)	Characteristic tensile strength	f_{ctk}	4.4	MPa
	Design tensile strength	$\frac{f_{ctk}}{\gamma_c}$	3.4	MPa
	Young's Modulus	E_c	18.5	GPa
	Linear tensile strain	$\frac{f_{ctk}}{E_c \cdot \gamma_c}$	0.17	‰
	Ultimate characteristic tensile strain	ϵ_{tuk}	1.73	%
	Ultimate tensile strain	$\frac{\epsilon_{tuk}}{\gamma_c}$	1.33	%

In Figure 153 and Table 31 is given information about the reinforcement steel according to according to Nederlands Normalisatie-instituut (2011). In the table is assumed that the reinforcement steel B500 is used. In Figure 153 is shown the tensile stress strain relation of reinforcement steel according to Eurocode 2 (Nederlands Normalisatie-instituut, 2011). In Table 31 are given values for the steel characteristics to draw the stress strain relation of Figure 153.

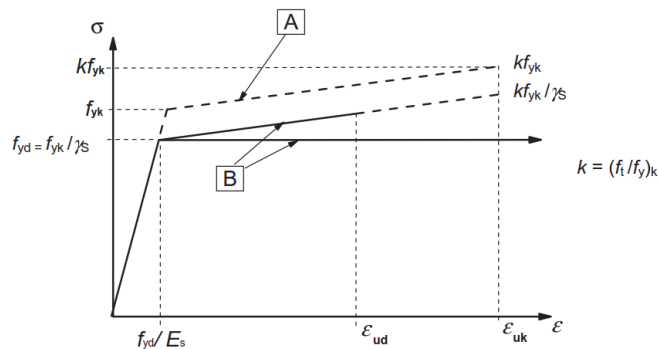


Figure 153 – Stress-strain diagram for reinforcement steel in a schematically way (A) and for calculations (B) (Nederlands Normalisatie-instituut, 2011)

Table 31 – Reinforcement steel characteristics of B500 according to Nederlands Normalisatie-instituut (2011)

	Material characteristics	Symbol		Unit
Tensile diagram (Figure 153)	Characteristic tensile strength	f_{yk}	500	MPa
	Partial factor reinforcement steel	γ_s	1.15	[-]
	Design tensile strength	f_{yd}	435	MPa
	Young's Modulus	E_s	200	GPa
		$\frac{f_{yd}}{E_c}$	0.2	%
	Ultimate characteristic tensile strain	ϵ_{tuk}	2.5-7.5*	%
	Ultimate design tensile strain	ϵ_{tud}	2.3-6.8	%

* depending on the reinforcement class (A, B or C) (Nederlands Normalisatie-instituut, 2011)

At last material characteristics are given the characteristics of GFRP rebars. The characteristics of GFRP are mentioned in chapter 2.3.1.2 Glass Fibre Reinforced Polymer (GFRP) reinforcement. GFRP bars react linear elastic. In Table 32 are shown some material characteristics of the GFRP rebars.

Table 32 – Characteristics of GFRP rebar (Lárusson, 2013)

	Material characteristics	Symbol		Unit
	Young's Modulus	E_s	46	GPa
	Ultimate linear tensile strain	ϵ_{tu}	2.5	%

In Figure 154 is shown cross section I of Figure 150 in the case it is exposed to imposed deformation Δu_1 . This deformation causes a shortening in the link slab. The direction of the deformation is positive (pointing away from the surface) so a positive value for the stress, so a tensile stress, can be expected according to eq.(66).

$$\sigma = E \cdot \frac{\Delta u_1}{l_{act}} \quad \text{eq.(66)}$$

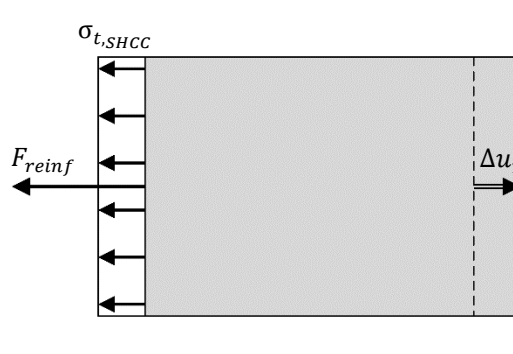


Figure 154 – Cross section I of Figure 150 : stresses over the cross section of the active zone of the link slab exposed imposed deformation Δu_1

Assume that the imposed elongation of the active part of the link slab is equal to a strain of 0.5%. According to the stress strain relation of SHCC, steel and GFRP, the stresses in the composite of SHCC with reinforcement steel and SHCC with GFRP can be determined. This is schematically shown in Figure 155, where the stress strain relations of SHCC and reinforcement steel are given. Both graphs are not in scale regarding to the tensile stress in the material. The strain in the elastic and plastic zone and at failure are in scale.

As shown in in Figure 155, if the link slab is exposed to 0.5% elongation, the maximum tensile stress in both, the SHCC and steel, are reached at least in theory. In practice, both steel and SHCC have probably

a certain hardening behaviour. However, this is not taken into consideration here. As mentioned before, for SHCC it is not allowed to take into consideration a hardening behaviour according to Japan Society of Civil Engineers (2008). According to Eurocode 2, a certain hardening could be taken into account for all three reinforcement classes. The hardening is different for every class. From reasons of simplify, the hardening behaviour is neglected here. Besides, according to Eurocode 2, it is allowed to neglect the hardening behaviour.

Tensile stress-strain relation of SHCC and reinforcement steel

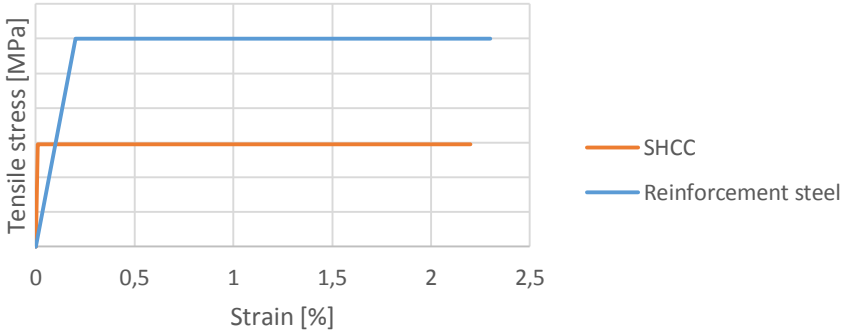


Figure 155 – Tensile stress-strain relation of SHCC and reinforcement steel

In Figure 156 is shown the tensile stress-strain relation of SHCC and GFRP. As shown in the diagram, GFRP has an elastic behaviour until 2.5%. Depending on the amount of GFRP reinforcement, the maximum tensile stress works by a strain of 2.3% (maximum tensile strength of SHCC) or 2,5% (maximum tensile strength of GFRP, where the SHCC is failed)

Tensile stress-strain relation of SHCC and GFRP

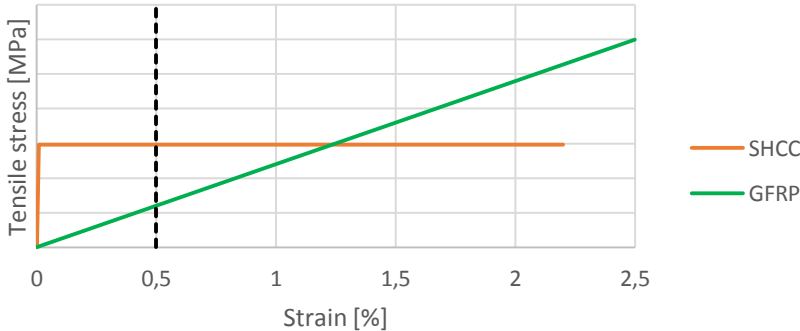


Figure 156 – Tensile stress-strain relation of SHCC and GFRP

The Young’s modulus of reinforcement steel is a lot larger than the Young’s modulus of GFRP. Further, steel has a plastic behaviour, while GFRP is elastic until failure. In Figure 157 are used the characteristics of B500 reinforcement steel and GFRP what is applied by Lárusson (2013). For B500 is assumed no hardening behaviour is the plastic zone. The GFRP is fully linear elastic. As shown in the diagram, if the strain is smaller than 0.95%, the tensile stress in GFRP is lower than the tensile stress in steel. However, if the strain is larger than 0.95%, the tensile stress in steel is smaller than the tensile stress in GFRP. In the compression with some other types of steel or GFRP, this turning point could be

at some different strain values. At least, it is clear that GFRP rebars results in lower tensile stresses if the strain is relative small and that reinforcement steel results in lower tensile stresses is the strain is relative large.

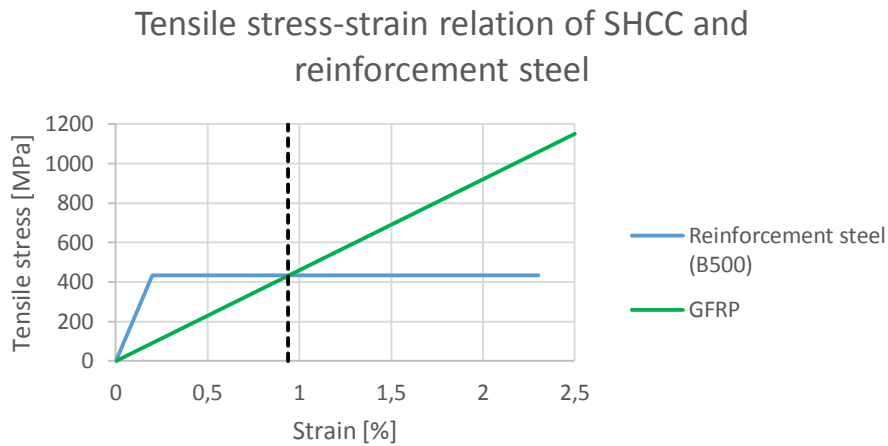


Figure 157 – tensile stress-strain comparison between reinforcement steel and GFRP

From the analysis above could be concluded that the tensile strength in the active part of the link slab depends on:

- Geometry of the link slab
- SHCC characteristics
- Reinforcement characteristics
 - o Steel
 - o GFRP

Working force Magnitude	Strength capacity		
	SHCC	Steel	GFRP
- Horizontal imposed deformation	- Tensile strength	- Tensile yield strength	- Tensile strength
- Length active section	- Young's modulus	- Young's Modulus	- Young's modulus
- Young's modulus	- Plastic behaviour	- Plastic behaviour	- Elastic behaviour
- Thickness of link slab			

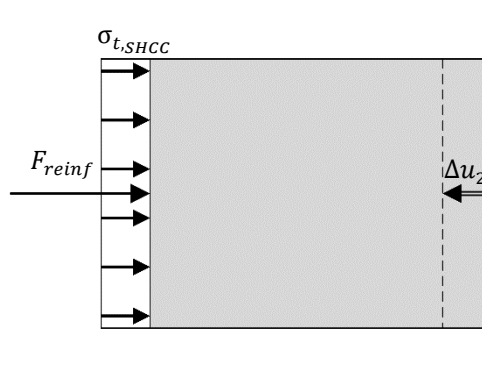


Figure 158 – Cross section I of Figure 150 : stresses over the cross section of the active zone of the link slab exposed imposed deformation Δu_2

In Figure 158 is shown cross section I of Figure 150 in the case it is exposed to imposed deformation Δu_2 , what causes a shortening in the link slab. The direction of the deformation is negative (pointing to the surface) so a negative value of the stress, so a compressive stress, can be expected according to eq.(67).

$$\sigma = E \cdot \frac{\Delta u_2}{l_{act}} \tag{eq.(67)}$$

In Figure 151 is shown the relation between compressive stress and the strain of SHCC. The compressive stress of SHCC is relative large compared to the tensile stress. Also in the reinforcement are compressive stresses expected. The total compressive stress over the cross section is the sum of both, the SHCC compressive stress and the compressive stress in the reinforcement.

In the active zone of the link slab the ration between the cross sectional area of the reinforcement over the cross sectional area of the concrete is about 0.30% to 0.60%, as shown in the overview of chapter 2.5 Overview. Therefore, the compressive component of the reinforcement is neglected compared to the compressive stress of SHCC.

If the link slab is in compressive, because in imposed deformation, compressive stresses will be carried by the SHCC itself. Because reinforcement nearly influences the capacity of the link slab in this case, a lower number of variable could influence capacity to resist horizontal deformation. The variables that have a certain influence are shown below.

Working force	Strength capacity
Magnitude	SHCC
- Horizontal imposed deformation	- Compressive strength
- Length active section	- Young's modulus
- Young's modulus	- Plastic behaviour
- Thickness of link slab	

3.3.4.2 Stresses working in debonding layer of the active zone

As mentioned before, there should be a debonding zone in the active section. This debonding zone is mostly created by a debonding layer of plexiglass or roofing paper. In theory, there are no problem in the debonding layer. However, in the debonding layer, it is assumed that no shear stresses are working. In this paragraph is analysed the debonding layer in more detail, in order to make conclusions about the shear stresses in the debonding zone in practice.

In Figure 159 is shown a part of an SHCC link slab. In the detail Figure 159 is shown the debonding connection between SHCC and NSC. In blue is shown the thin debonding layer that is installed on the concrete deck. As shown in the detail, the surface of SHCC and concrete are both expected to be not perfectly smooth. The smoothness of both material is limited, because of imperfection during execution. Further, concrete is made of particle (sand, cement and ect.), so to have a very smooth surface, the diameter of the particle should run to infinite small to fill all the imperfections in the surface. In other word, a perfectly smooth surface is impossible to make.

Now the effect of imperfections in the surface, is that shear stresses between the SHCC and the concrete could be generated, even if a deboning material is in between them. The quantity of the shear

stresses depend on the size of the imperfections of the surface. If the stresses are limited to a minimum, no problems are expected. However, if the shear stresses are too big, they will probably have a negative influence on functioning of the active zone. For example, a certain negative influence on the crack width in the active zone could be expected if too large shear stresses are generated between SHCC and concrete.

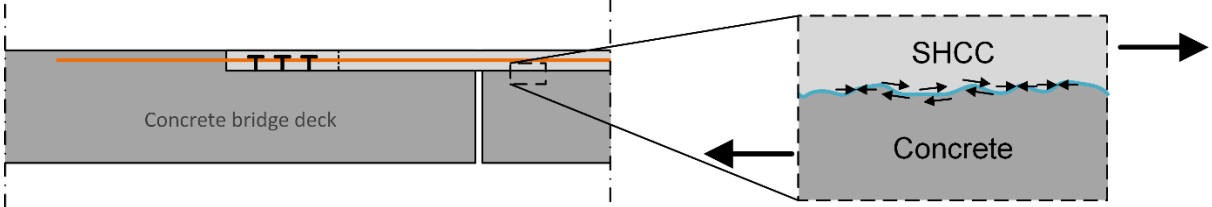


Figure 159 – Detail of the connection between the SHCC link slab and the concrete substructure

Going in some more practical details, the question is; what are the consequences of the expected problem from Figure 159 in practice. In fact, the only consequence is that both, the concrete surface and the SHCC surface should have a certain smoothness. The execution method is analysed in some more detail here in order to analyse the smoothness of the SHCC and concrete layer.

3.3.4.3 Stresses working in passive section without dowels

Imposed horizontal deformation generates stresses in the active zone as explained in the previous paragraph. So the passive section is exposed to tensile or compressive stresses from the active zone of the link slab, depending on the direction of the deformation. In the case of horizontal load, which is discussed in chapter 3.3.2 Horizontal load, the active zone is also exposed to a horizontal stresses. It could be expected that the passive section carries the horizontal stress from the active zone in both cases in a similar way. Therefore, the same similar stresses in the passive section could be expected for both cases.

In Figure 160 are shown the stresses and forces that are expected in the link slab if a tensile stress is generated in the active part of the link slab due to imposed horizontal deformation. As shown in the figure, the working stresses are exactly the same as for the link slab that is exposed to horizontal load, as shown in chapter 3.3.2.3 Horizontal interface between NSC and SHCC (passive zone), Figure 129. The only difference here is that the tensile stresses in Figure 160 are caused by imposed deformation instead of tensile loads. However, it is assumed that the horizontal stresses in both cases are also carried the same in the passive part of the link slab. The stress distribution is explained in detail in chapter 3.3.2.3 Horizontal interface between NSC and SHCC (passive zone).

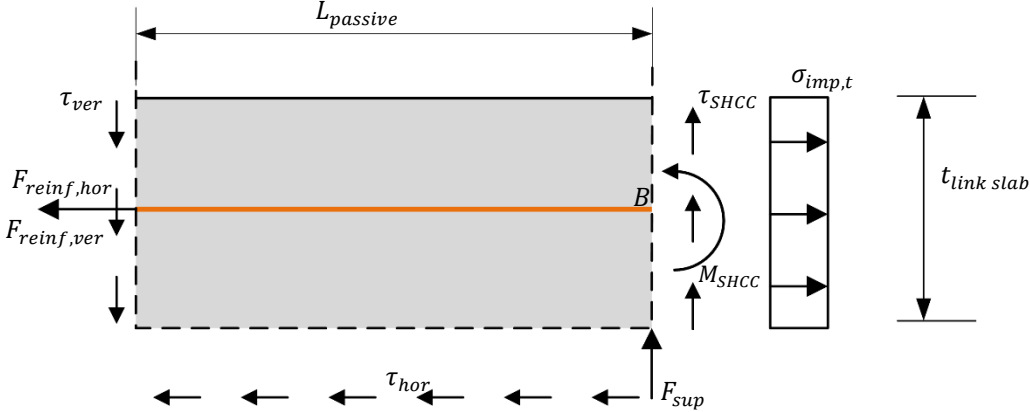


Figure 160 – Stresses working on passive part of the link slab caused by imposed tensile stresses from the active section

In Figure 161 is shown the passive part of the link slab without dowels in the case of imposed compressive stress in the link slab. The imposed compressive stress is caused by imposed shortening of the active part of the link slab. The working stresses in the link slab of Figure 161 are exactly the same as in the case of horizontal loads, as shown in paragraph 3.3.2.3 Horizontal interface between NSC and SHCC (passive zone) Figure 133. The equilibrium equations and the distribution of shear stress τ_{SHCC} , are discussed it that paragraph already.

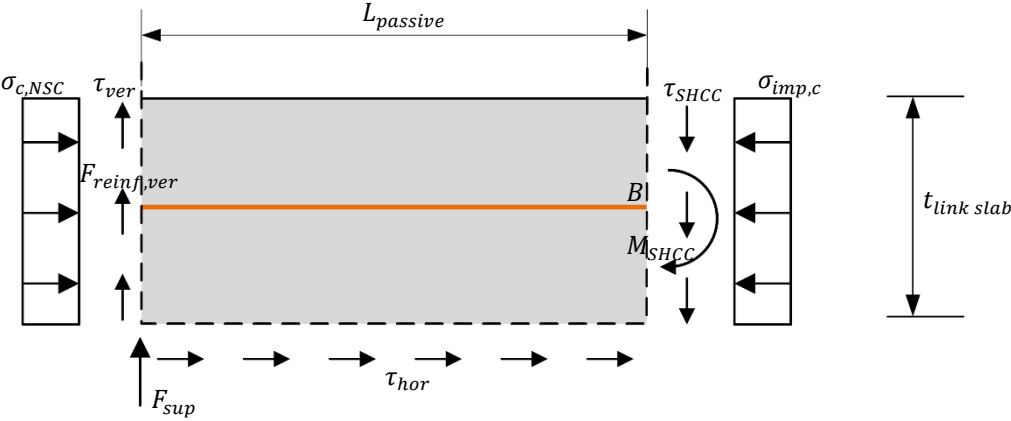


Figure 161 – Stresses working on passive part of the link slab caused by imposed tensile stresses from the active section

From the above shown analysis, could be concluded that the weak points during the described mechanism are the same in the case of horizontal loads. The variables that influence the strength in case of horizontal loads, are described in chapter 3.3.2.3 Horizontal interface between NSC and SHCC (passive zone). It is assumed that the same variables also influence the strength in case of imposed horizontal deformation.

3.3.4.4 Stresses working in passive section with dowels

In the case that dowels are included in the passive section of the link slab, the stress distribution of a link slab exposed to imposed horizontal deformation is probably the same as for the link slab exposed to horizontal load. In Figure 162 are shown the stresses in the passive part of the link slab where dowels are place in the passive zone. In Figure 162 is assumed that the passive part of the link slab is exposed to tensile stresses from the active zone. The stresses that work in the figure are exactly the same as in case of a horizontal tensile stress, as shown in chapter 3.3.2.4 Horizontal interface between NSC and SHCC with dowels (passive zone), Figure 136. Only the tensile stress in Figure 162 has a different name; $\sigma_{imp,t}$. Equilibrium and stresses are already discussed in detail in chapter 3.3.2.4 Horizontal interface between NSC and SHCC with dowels (passive zone).

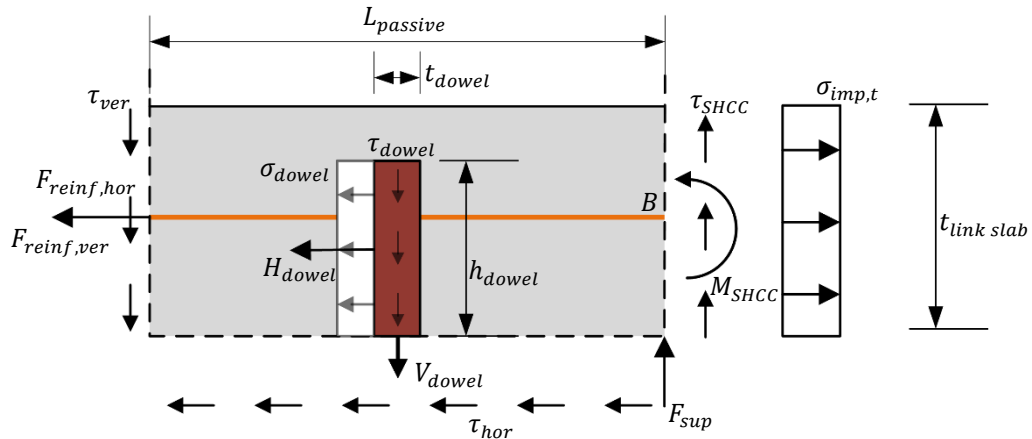


Figure 162 – Stresses working on passive part of the link slab including dowel, caused by imposed tensile stresses from the active section

in Figure 163 is shown the passive part of the link slab with dowels again, but in this case, the link slab is exposed to imposed compressive stresses from the active part of the link slab. The stresses that work due to the compressive stress from the active section, are exactly the same in case of compressive loads. The equilibrium equations and some more detail of the stresses are given in chapter 3.3.2.4 Horizontal interface between NSC and SHCC with dowels (passive zone), where the passive section exposed to horizontal loads is discussed. It is assumed that this discussion is also valid for the link slab exposed to compressive stresses caused by imposed deformations.

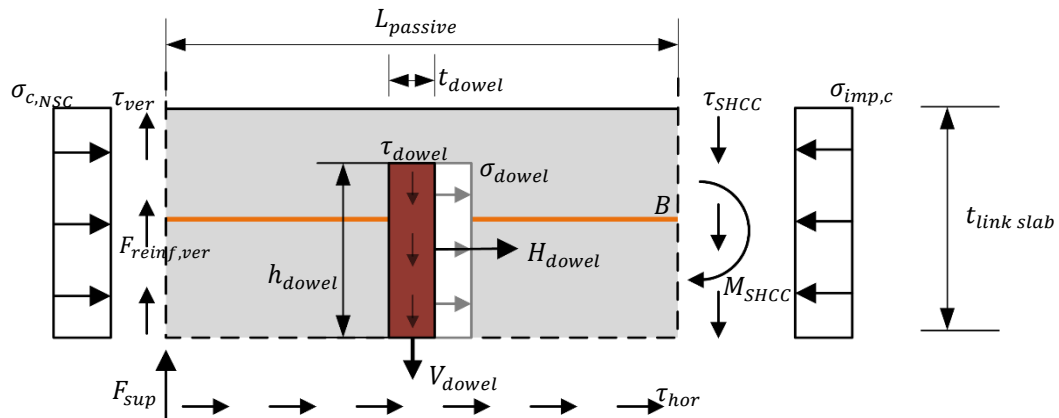


Figure 163 – Stresses working on passive part of the link slab including dowel, caused by imposed compressive stresses from the active section

Again, the analysis from above is that same as in the case of horizontal load instead of horizontal imposed deformation. The analysis to variables that influence if horizontal loads work, is already described in chapter 3.3.2.4 Horizontal interface between NSC and SHCC with dowels (passive zone). It is assumed that in case of horizontal imposed deformation, the same variables influence the strength capacity as for direct horizontal loads.

3.3.4.5 Stress distribution around the dowels

The dowels can only generate compressive stresses between SHCC and the steel dowel. That means that the stresses around the dowels are expected to occur as shown Figure 164.

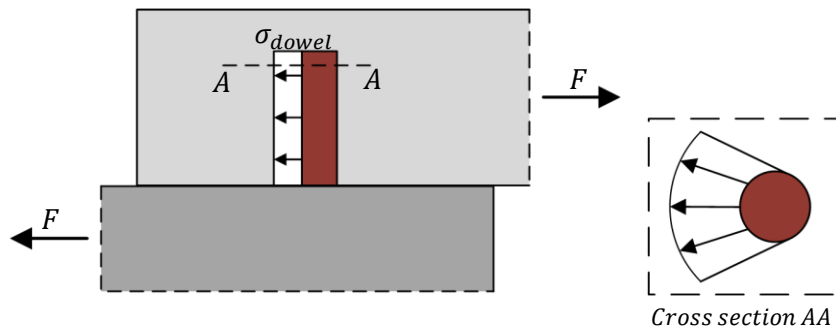


Figure 164 – Stresses between SHCC link slab and the steel dowel in case of tension forces F working on the link slab and the substructure

In Figure 165 are shown dowels in different ways. At the left, a side view and an overview of the dowels in the link slab are shown. At the right side, two details of the same place in the link slab are shown. According to the details, the stress distribution around the dowels can be described.

The analysis of stresses around the dowels starts with detail A. In the detail is shown that the stresses that are distributed around the dowels, come closer to each other on the cross section of the row of dowels. This means that the stress becomes higher (same force over a smaller area). Especially near to the dowels, higher stresses are expected, because there the most stresses are distributed over a relative small area. As shown in detail A of Figure 165, peak stresses are expected near the dowels.

Because of the peak stresses and higher mean stress, the area between the dowels may form a weak part of the link slab. If the active part of the link slab is horizontally loaded until its upper limit, the horizontal stress at the end of the passive part is also assumed to be at the upper limit. If the first row of dowels is placed at the end of the passive part near the active part, stresses between the dowels could be higher than the cracking strength. If the dowels are placed further away from the interface with the active zone, the horizontal stresses are reduced already, such the cracking stress is not reached.

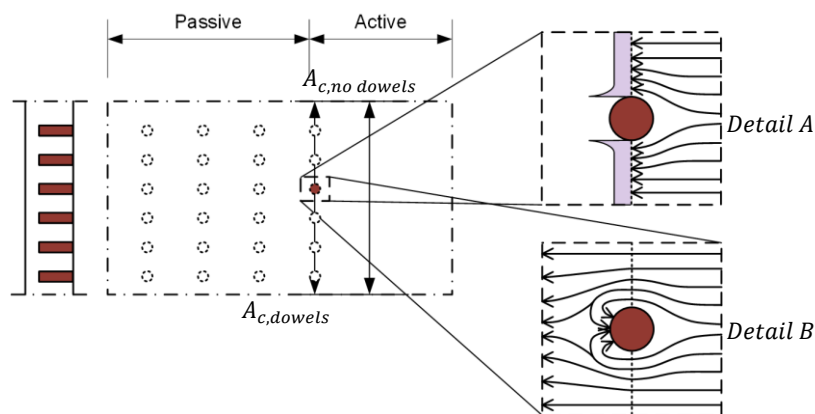


Figure 165 – Overview of dowels (side view and overview) and two details of the stress paths around the dowels

In detail B of Figure 165 is shown the way stresses are expected to walk after the dowel. Because the dowels are only able to carry compressive stresses, the tensile stress in the link slab should go around the dowels as shown in detail B.

3.3.4.6 Horizontal deformation capacity

Because horizontal imposed deformations are expected, it is interesting to know the horizontal deformation capacity of the SHCC link slab. This is done in detail in Appendix A: Deformation capacity of NSC flexible joint and Thin SHCC link slab. In this appendix, the deformation capacity of the Thin SHCC link slab is compared to the deformation capacity of the NSC flexible joint. The results of the calculations are given in this paragraph shortly.

From the calculations of Appendix A could be concluded that the SHCC link slab has deformation capacity in the order of 10-20 mm, while the deformation capacity of the NSC flexible joint is negligible small. The deformation capacity of the link slab is a large advantage of the SHCC link slab compared to the NSC flexible joint. In practice there are two ways to take up the benefits of the horizontal deformation capacity of the SHCC link slab:

- **Application of link slabs only;** because the joints have a certain horizontal deformation capacity, no additional finger joint is required at the end of the undilated length.
- **Longer undilated length;** because the SHCC link slabs have a certain horizontal deformation capacity, more spans can be applied before an alternative joint, for example a finger joint, is needed. So a longer undilated length could be made compared to the undilated lengths if NSC flexible joints are applied.

3.3.5 Evaluation and conclusion

In this chapter are analysed five basic actions that could work on the link slab. There are two direct loads and three imposed deformations, where the imposed horizontal deformation has the same effect on the link slab as the imposed curvature. In fact, the way horizontal loads are carried by the link slab is more or less in the same way as the way that the horizontal stresses caused by imposed horizontal deformation are carried by the link slab. In fact, three groups could be made according to the stress distribution:

1. Vertical load
2. Horizontal load/ imposed horizontal deformation/imposed curvature
3. Vertical imposed deformation

From a practical point of view, vertical loads and horizontal loads or imposed deformation will probably always be generated in the link slab caused by traffic, temperature differences or another reason. It is quite hard, maybe even impossible to reduce these two kinds of stress. Therefore, the link slab should be designed to carry these stresses.

However, vertical imposed deformations could be limited, such that this mechanism can nearly damage the link slab or the substructure. In practice, the beams of two different spans are mainly supported on the same cross-beam, as shown in Figure 166. In this figure is schematically shown how two beams are supported on the same cross-beam and connected to each other with an SHCC link slab. Assuming that the height of the beams remain constant and the cross-beam does not rotate, or at least has limited rotations, the beams can only have a different deformation caused by the support blocks. For example, the support blocks can have different Young's moduli through time, such that the vertical deformation of both beams differs.

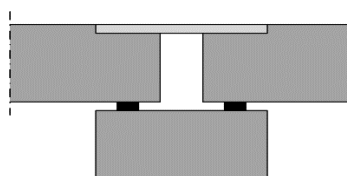


Figure 166 – Two bridge beams supported on cross-beam

So taking into account practice, only two groups should be taken into account:

1. Vertical load
2. Horizontal load/ imposed horizontal deformation/imposed curvature

Taking into consideration the issues shown in the analysis above, the peak stress near the end of the beam due to vertical load on the link slab is probably the most critical point in the design. Compared with the vertical load, the horizontal strength is relative easy to increase. In the analysis is already explained how the thickness of the link slab, the reinforcement and fibres influence the horizontal strength. The reduction of the vertical peak load or the increase of the resistance against the peak load are both a lot more complex to achieve. Therefore, the peak stress near the end of the substructure is assumed to be the main problem in the link slab design.

In the horizontal direction, the combination of horizontal load and imposed horizontal deformation or imposed curvature that in fact also results in imposed horizontal deformation, is an interesting load combination to analyse in more detail. However, this combination is not used in the rest of this research. Therefore, a short analysis to this load combination is given in Appendix B: Load combinations. Further, the large advantage of the SHCC link slab in the horizontal direction is the deformation capacity. This is a large advantage of the SHCC link slab compared to the NSC flexible joint. The comparison between the deformation capacity of the SHCC link slab and NSC flexible joint are given in Appendix A: Deformation capacity of NSC flexible joint and thin SHCC link slab.

The peak stress works on both, the SHCC link slab and the concrete deck. It is assumed that the SHCC link slab is can resist the peak stress better than the concrete deck, because:

- In the link slab are a lot of fibres and rebars that are able to generate tensile stresses to make horizontal equilibrium.
- The point of the peak stress is completely surrounded by SHCC, such that compressive stresses can be generated to make horizontal equilibrium.

4 SHCC Flexible Joint in a Concrete Bridge

In chapter 3 Analysis of SHCC Link Slab is done a detailed analysis to the thin SHCC link slab. From the analysis is concluded that the vertical peak stress at the end of the bridge girder and the execution of the unbonded layer both seem points of attention. These points should be researched in some more detail before the design of the Thin SHCC Link Slab could be applied in practice.

Maybe, a flexible joint that is made of SHCC instead of NSC is an interesting first and relative easy step towards the application of SHCC in practice in the Netherlands. Until now, SHCC in the Netherlands is only used in the lab. To have some practical experience with SHCC, it may be interesting to apply in a structure that is applied successfully in practice for a long time already. The flexible joint seems a useful structure to get some experience with SHCC in practice. In fact, an SHCC Flexible joint is combining the idea of the SHCC Deck Slab that is constructed in Michigan, USA, with the commonly applied NSC Flexible Joint.

Next to practical experience, the SHCC Flexible Joint may have some additional interesting advantages compared to the NSC Flexible Joint. The SHCC Deck Slab in Michigan, USA, has some advantages compared to a concrete deck slab (Li, et al., 2003). So maybe an SHCC Flexible Joint also has some advantages compared to the NSC Flexible joint. Therefore, in this paragraph are shortly analysed the expected advantages of an SHCC Flexible Joint compared to the NSC Flexible joint.

Before the idea of SHCC in a flexible joint is analysed, first the common situation with a NSC flexible joint is shown. In Figure 167 is shown a common situation of a precast concrete inverted T-girder with a cast in situ concrete deck to make a bridge construction (Consolis Spanbeton, n.d.). The bridge spans are connected by a flexible joint, which is made of normal strength concrete as discussed in chapter 2.1 Flexible joint. The flexible joint is shown in the left picture of Figure 167, schematised as a block. As shown in the figure, the flexible joint creates a small bridge between both bridge spans. The joint is explained in more detail in chapter 2.1 Flexible joint. In practice, this joint has:

- Vertical and horizontal load capacity
- Rotation capacity
- No horizontal deformation capacity

Because the NSC Flexible joint has no horizontal deformation capacity, this joint should be combined with an expansion joint, for example a finger joint. In Appendix C: Maximum span of the link slab, this is explained in some more detail.

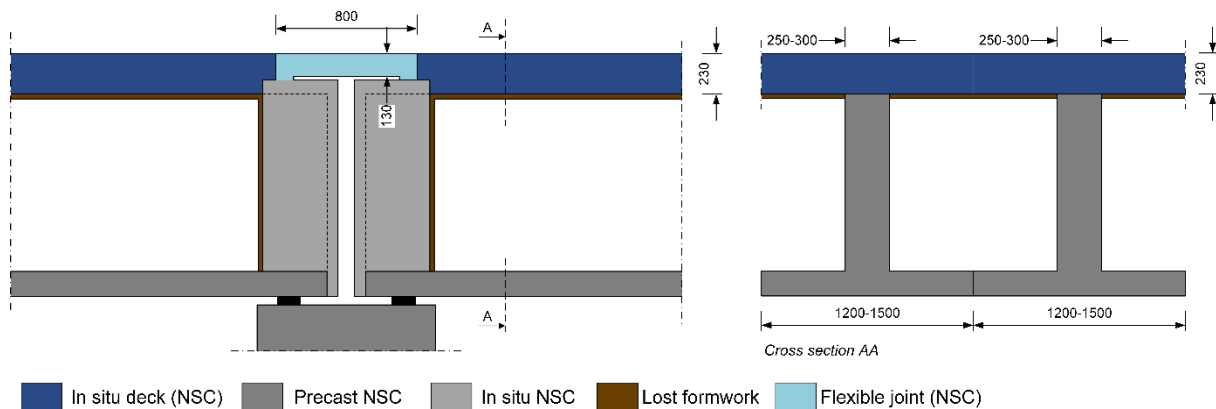


Figure 167 – Precast NSC inverted T-girder with in situ NSC deck and flexible joint according to (Consolis Spanbeton, n.d.)

Now, let analyse the flexible joint if it is constructed with SHCC. The main objective of the SHCC Flexible Joint is to apply SHCC in practice. Further, there are some additional advantage of the SHCC Flexible Joint, mainly based on the results of Li, et al. (2003). These advantages are described here in some detail.

First of all, SHCC has a limited crack width. In chapter 2.2 Deck Link Slab is already mentioned that the crack width of the SHCC link slab of Li, et al. (2003) is limited to 0.05 mm. This limited crack width is under monotonic tests and cyclic tests the same. In practice, this means that the crack width remains limited if a lot of cars drive over the link slab. That means that water and chlorides can hardly penetrated into the link slab. This makes the link slab a durable structure. Further, the adhesive strip could be left out because of the durability of the link slab.

If the flexible joint is made of SHCC instead of NSC, probably less reinforcement is required in the joint. There are two reason for this. The first reason has to do with the high tensile ductility of SHCC. The second reason has to do with decoupling of the dependency of the crack width and the amount of reinforcement. Both are clarified is some more detail here.

First, SHCC has a high tensile ductility compared to NSC. That means that the SHCC material is able to deform more compatibly with the reinforcement bars compared to NSC. As a result, yielding of the reinforcement steel was delayed in the SHCC matrix compared to the NSC matrix. Because the stress is lower, a smaller amount of reinforcement steel is needed. In practice, this results in a more flexible joint.

As second, cycling test shows that the amount of reinforcement does not influence the crack width of the link slab. The crack width of the link slab only depends on the SHCC itself. In the case of a NSC link slab, the crack width increases if the link slab is exposed to more load cycles. To reduce the crack width, more reinforcement should be added. However, the crack width control of the link slab is now decoupled from the reinforcement ratio. Therefore, less reinforcement could be applied in the link slab.

Less reinforcement in the link slab does not only result in lower costs, but also reduces the stiffness of the link slab. That means that the link slab act more like a hinge. So lower stresses are needed to bend the link slab.

In the end, is could be concluded that there are a few advantages of constructing the flexible joint with SHCC. The main goal of course is to have some practical experience with SHCC at take the first step to the Thin SHCC Link Slab. All the advantages in short are:

- Practical experience with SHCC
- Lower amount of reinforcement compared to the NSC Flexible Joint because of:
 - o The high tensile ductility of SHCC
 - o In SHCC, the crack width is independent of the reinforcement ratio.
- No adhesive strip
- Lower stiffness of the link slab compared to the NSC Flexible joint, such that the joint act more like a hinge.
- The crack width under cycling load is limited

5 Options against the peak stresses

In chapter 3 Analysis of SHCC Link Slab is analysed that the vertical peak stress at the end of the substructure could be considered as the main problem of the link slab design, from a structure point of view. Because of these issues, in chapter 4 SHCC Flexible Joint in a Concrete Bridge is proposed the application of an SHCC Flexible Joint as a first step to the Thin SHCC Link Slab. The application of this structure results in some experience with SHCC in practice, to reduce the risks of the application of the Thin SHCC Link Slab. Further, there are some additional advantages compared to the NSC Flexible Joint.

However, because in the end the Thin SHCC Link Slab seems to be interesting to apply, some options are given in this chapter according to the issued due to vertical peak stresses. Due to the peak stress, concrete probably spalls off, what is undesirable for the durability of the structure. To solve this problem, in this paragraph are given some possibilities to deal with the peak stress and the risk of spalling.

In this paragraph is estimated that spalling is indeed a problem and options to solve it are presented. However, before the options to reduce the risk on spalling are further researched, spalling itself should be research is more detail. Here, spalling is assumed to be a mechanism that causes failure of the substructure. However, maybe in reality, the vertical peak stresses cause small tensile stresses only. Maybe, in reality the tensile stresses are smaller than the tensile strength of concrete. In that case, there is no problem, so the options do not have to be researched at all. So to determine if spalling will be a governing problem, experiments should be done. In the experiments, the link slab should be loaded by vertical forces. Because the link slab is expected to be loaded by fatigue loads during life time, in the experiments the link slab should also be loaded by fatigue loads.

The working vertical peak stress that causes spalling of the concrete does have a certain relation with the debonding layer, because the vertical peak stresses work upon de debonding layer. In practice, problems could be expected in the debonding layer as mentioned in chapter 3.3.4.2 Stresses working in debonding layer of the active zone. Therefore, in the variants that should reduce the risk of spalling, the debonding layer between the link slab and the substructure is also taken into account. Maybe certain options could also reduce the shear stress in the debonding layer, which is caused by the limited smoothness of the surface of concrete. Another advantages could be that a certain smoothness of the surface could made easier in certain variants.

In Figure 168 are shown five design options to reduce the vertical peak stress or to increase the resistance against spalling. The five designs can shortly be described as:

1. **Fibres:** adding fibres in the concrete of the substructure at the part where spalling is expected.
2. **Chamfer:** by adding a chamfer, the peak force is divided over a larger area, what reduce the stresses
3. **Locally reduced Young's modulus:** reduction of the Young's modulus should result in lower stresses in the area where the Young's modulus is reduced.
4. **Redistribution by stiff interlayer:** this plate should redistribute the vertical stresses, such that the peak stresses are reduced.
5. **Prestressed anchored plate:** this plate should carry the horizontal tensile stresses at the end of the concrete substructure that causes spalling.

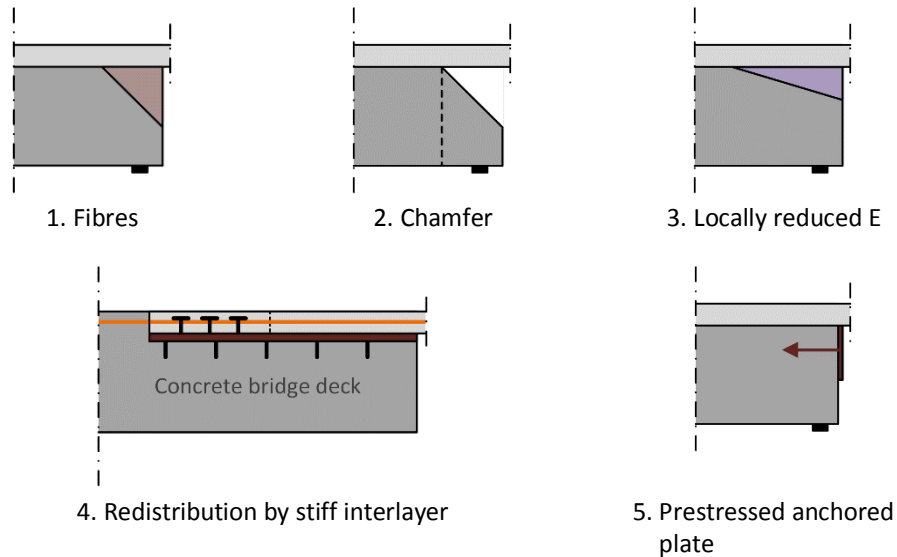


Figure 168 – Overview of options to prevent spalling

In this chapter, the five designs of Figure 168 are described and analysed in detail. The main advantages and disadvantages per option are described. Further is given additional recommended research.

Note: at the sides of the deck, also peak stresses are expected. In Figure 169 is shown that peak stresses also cause spalling at the sides of the bridge. In the side view of the bridge is shown how the peak stresses are expected to be generated. This peak stresses work over the whole width of the bridge as shown in detail AA. Detail AA is a cross section in the top view. As highlighted by red circle, due to the peak stresses, spalling at the sides could be expected. However, the peak stress at the sides of the deck is not taken into account in the analysis of the options.

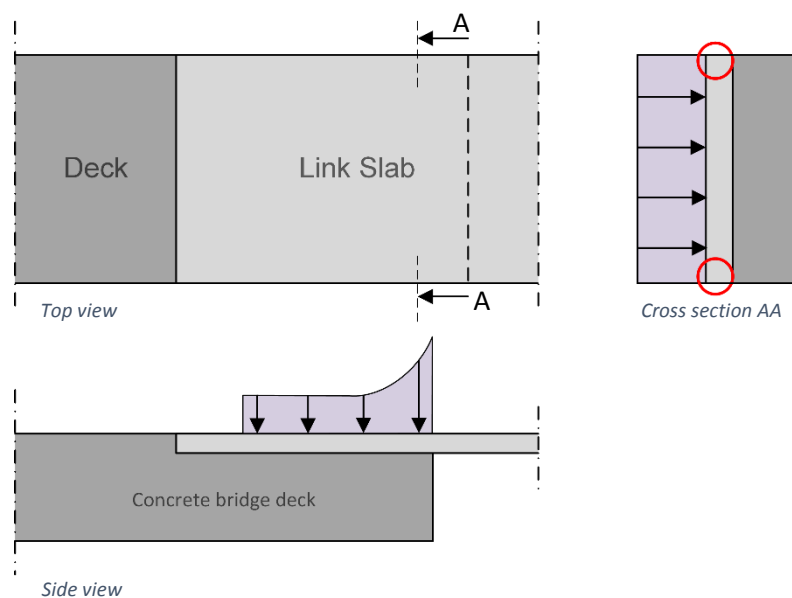


Figure 169 – Peak stresses causing spalling at the sides of the bridge

5.1 Debonding layer in the active zone

As mentioned in the literature study of chapter 2 Literature, in the active zone of the link slab should be a debonding layer. The function of this layer is to prevent shear stresses between the link slab and

the substructure during horizontal deformation. This makes that the active zone can take up imposed deformation properly.

In the link slab designs that are analysed in chapter 2 Literature, three different material are applied to make the debonding layer:

1. Roofing paper (Li, et al., 2003)
2. Plexiglass (Reyes & Robertson, 2011)
3. Roofing paper in combination with a plastic sheeting (Lárusson, 2013)

Based on the information that is given chapter 2 Literature, it is assumed that these materials to make the debonding layer works the same. It is assumed that a thin layer is made on the substructure that has nearly shear stresses with the SHCC layer. Probably, this thin layer works in the same way as the material teflon does. The application of teflon in the Netherlands is more commonly used than roofing paper, plexiglass or a combination of roofing paper with a plastic sheeting. Therefore, from now on teflon is assumed as material in the debonding layer.

In table are shown some characteristics of teflon. To compare teflon with plexiglass, also the characteristics of plexiglass are given. Compared to plexiglass, the cracking strain of teflon is a lot higher, while the tensile strain is lower. Further, Young's modulus of teflon is even lower than Young's modulus of plexiglass. The temperature limits teflon is able to function are a lot larger compared to plexiglass, what could be an advantage in extreme conditions. At last, the friction coefficient of teflon is a lot smaller compared to plexiglass.

Table 33 – Overview of mean characteristics of teflon compared to plexiglass

Characteristic	Unit	Plexiglass	Teflon	Source
Specific weight	[g/cm ³]	1.19	2.2	(WSV kunststoffen BV, n.d.) (PTFE, n.d.) (Proga plastics B.V., n.d.)
Tensile strength	[MPa]	70	16-28	(WSV kunststoffen BV, n.d.) (PTFE, n.d.) (Proga plastics B.V., n.d.)
Cracking strain	[%]	5	>50	(WSV kunststoffen BV, n.d.) (PTFE, n.d.) (Proga plastics B.V., n.d.)
Young's modulus	[MPa]	3200 - 3300	500-700	(WSV kunststoffen BV, n.d.) (Proga plastics B.V., n.d.)
Maximum Operating Temperature	[°C]	80	240-260	(WSV kunststoffen BV, n.d.) (PTFE, n.d.) (Proga plastics B.V., n.d.)
Minimum Operating Temperature	[°C]	-20	-200	(WSV kunststoffen BV, n.d.) (PTFE, n.d.) (Proga plastics B.V., n.d.)
Linear expansion coefficient	[mm/m/°C]	0.07	0.12-0.18	(WSV kunststoffen BV, n.d.) (PTFE, n.d.) (Proga plastics B.V., n.d.)
Moisture absorption	[%]	0.3	0.01	(WSV kunststoffen BV, n.d.)
Friction coefficient relative to dry steel	[-]	0.55	0.08-0.10	(PTFE, n.d.) (Proga plastics B.V., n.d.)

In most of the options that are shown in Figure 168, there is a direct connection between the SHCC link slab and the NSC substructure. It is estimated that between the SHCC and the concrete is a thin debonding layer, for example made of teflon. In some options, the debonding layer could be made better in another way. This is mentioned in the next paragraphs.

In Figure 170 is shown the connection between SHCC and NSC. In blue is shown the teflon debonding layer that is installed on the concrete deck. The teflon itself creates a debonding layer. However, if the surface of the concrete and the SHCC are not smooth, stresses could still be expected as shown with the small arrows. This should be taken into account during execution.

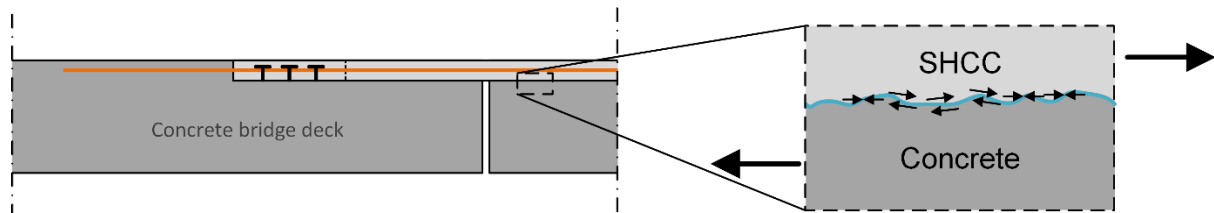


Figure 170 – Detail of the connection between the SHCC link slab and the concrete substructure

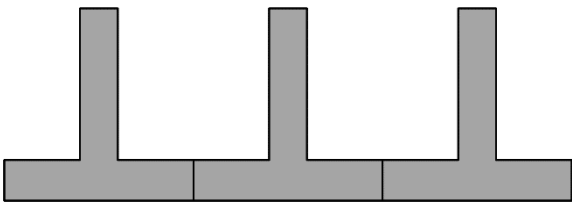
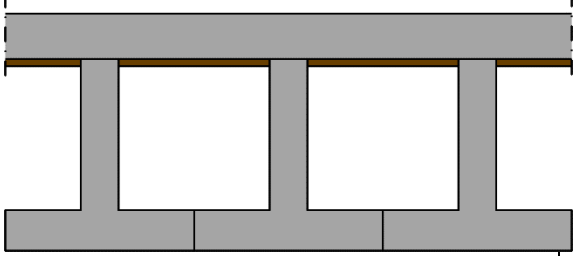
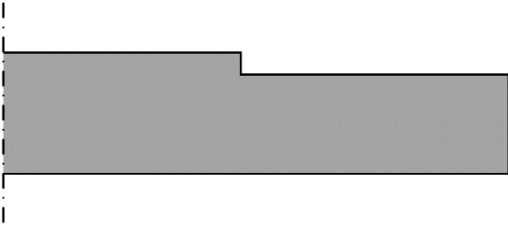
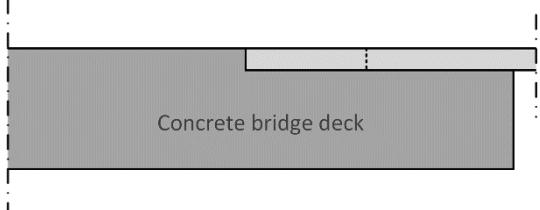
Going in some more practical details, the question is; what are the consequences of the expected problem from Figure 170 in practice. In fact, the only consequence is that both, the concrete surface and the SHCC surface should have a certain smoothness. The execution method is analysed in some more detail here in order to analyse the smoothness of the SHCC and concrete layer.

The estimated execution method to make a bridge with an SHCC link slab is shown in Table 34. As shown in the table, it is assumed that prefabricated concrete girders are applied. If the girders are placed, the concrete deck is assumed to be placed in situ. Here two options are there. In option A, the deck is cast in situ as done normally. If the deck is casted, place must be made for the link slab. This can for example be done by mill the concrete off. The surface of the place where the link slab should be placed must be finished, such that the surface is smooth enough. The other option, option B, is that the place where the link slab must be placed, formwork can be placed. However, this option is probably hard to execute.

At last step, the teflon layer and the link slab must be placed. The link slab can be cast in situ or can be prefabricated. The advantage of cast in place method, is that the surface that is placed on the teflon layer follows the surface of the deck. So if the deck is smooth enough, the link slab surface is probably smooth enough as well. The other method is a precast link slab that is placed at side. The disadvantage here is that the surface of the link slab is not the same as the surface of the deck. That means that the change on local peak stresses can be expected to be larger.

Taking into consideration the debonding layer only, probably the best method is to place concrete girders. Cast the deck as shown in option A. Then mill and finish the concrete deck, such that the link slab can be placed. At last the SHCC link slab must be cast in situ. This method is estimated for all given options of Figure 168. If debonding layer design or the casting method differ for a given option, the alternative method is described in the paragraph where the options are described in detail.

Table 34 – Overview of estimated execution method to construct a bridge with an SHCC link slab

Prefab girders		
	Cast in situ deck option A	Cast in situ deck option B
Cast in situ deck		
Place for link slab		
	Cast in situ link slab	Prefab link slab
Placing link slab		

An alternative method to create a debonding zone is to apply a thicker layer of a material with a low Young's modulus. The advantage of this method is that no strict requirements are needed for the smoothness of the SHCC and NSC surfaces to function properly. However, there are some disadvantages for this option too.

In Figure 171 is shown the idea a layer of a material with a low stiffness as an alternative for a teflon layer. In the upper picture of the figure is shown the link slab if it is undeformed. In the lower picture, the link slab is shown in its deformed situation. The soft material is in the deformed situation expected to deform as shown in the lower picture of the figure. To have a certain horizontal deformation capacity in the soft layer, the layer must have a certain thickness. Assuming that the material can deform until 45 degrees, then the layer should be about 10 mm thick to have a link slab with a deformation capacity of 20 mm.

At the interface with the passive zone, no deformation is expected in the soft material. At the middle of the link slab, the largest deformation is expected. Between both, a constant deformation in the link slab is assumed, what result in a linear increasing shear stress between the soft material and the link slab from the interface until the middle of the link slab. So in case of a soft material, the shear stress distribution is expected to be linear, while in the case of teflon, a constant shear stress distribution is expected. Assuming the same deformation in the link slab, the peak stress in the middle of the link slab in case of a soft material is expected to be twice the shear stress in the link slab if teflon is applied.

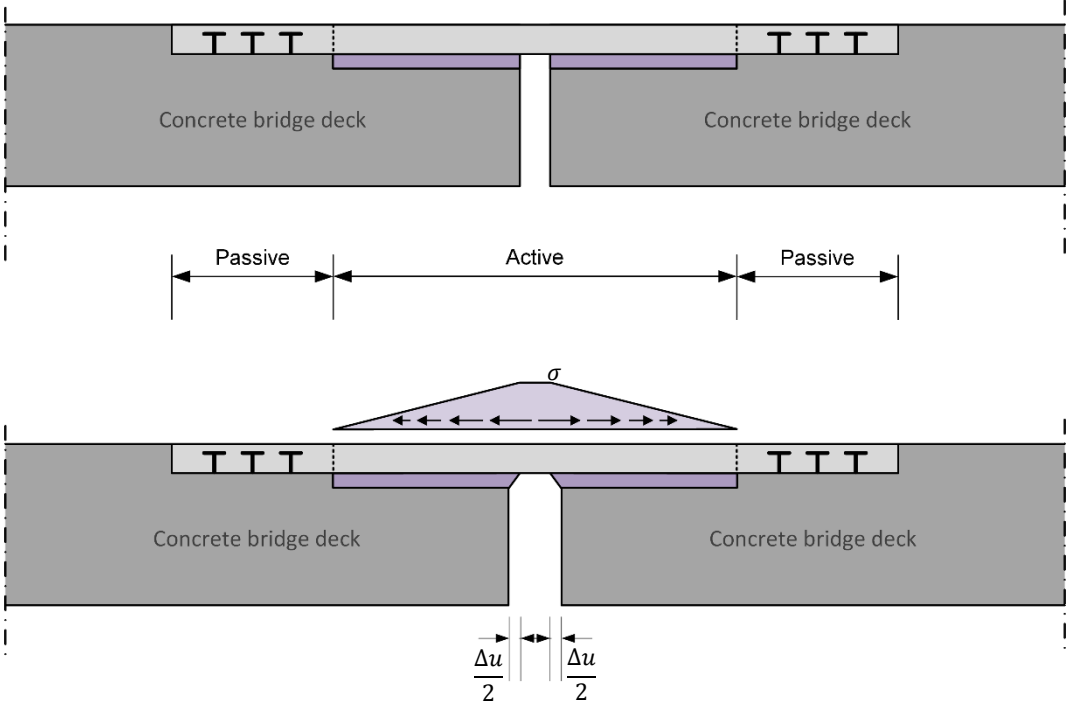


Figure 171 – Material with a low Young’s modulus to create a debonding layer in the active part of the link slab

Another disadvantage is that an additional vertical peak stress is generated at the interface between the active and passive section of the link slab. In the interface, the link slab goes from the passive zone to the active zone, what makes the interface a point of attention already. The stiffness jump in the supporting deck does it not make a better situation.

The stiffness difference could partly be solved by changing the stiffness over a certain length, as shown in Figure 172. In the figure is shown that the ‘stiffness jump’ is change into a zone where the stiffness changes linearly over a certain length. It could be expected that the peak stresses are reduced due to this zone. An additional advantage is that in this zone not only the vertical stiffness, but also the horizontal stiffness varies over the length of the zone. That means that the shear stresses are also expected to vary linearly over the length of the zone. A less abrupt change of horizontal shear stresses could result in a stronger interface zone.

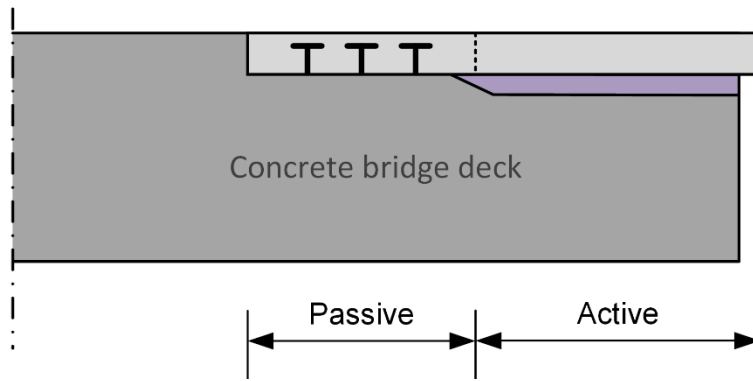


Figure 172 – Linear stiffness change over the length at the interface zone between the passive and active section

The disadvantage, or at least a point of attention to be researched in more detail, is the vertical support of the soft layer. The layer of soft material probably deforms a lot if it is loaded vertically. Probably a deformation in the order of a few millimetres could be expected, if the link slab is loaded by a vehicle. If the deformation is constant over a certain length, the link slab lowers a few millimetres too, probably without any problems. However, a wheel load works locally. If the link slab, which is supported by spring, is locally loaded, a certain curvature could be expected in the link slab. This can result in additional compressive and tensile stresses in the link slab or even additional cracks in the link slab if the tensile stress becomes too large.

In short, the large disadvantage of applying teflon are the requirements according to the smoothness of the surface of NSC and SHCC. Further, there seems to be no negative issues to create a debonding layer with teflon. However, if the requirements can't be met, an alternative design to create a debonding layer should be made, for example with a material with a low stiffness. Compared to teflon, the soft material has a few additional advantages and disadvantages, which are shortly listed below.

Advantages	Disadvantages
If interface zone is applied, the horizontal shear stress at the interface changes less abrupt No requirements for smooth surfaces	Linear stress distribution results in higher peak stress in the middle of the link slab Additional vertical peak stress at interface between the passive and active zone Soft vertical support

5.2 Fibres

Adding fibres to the concrete deck is in theory a very simple solution to increase the resistance against spalling. As shown in the analysis to vertical stresses, chapter 3.3.1 Vertical load, concrete spall off because of tensile stresses that are generated at the end of the concrete deck. By adding fibres to the concrete, the tensile strength increases. This idea is schematically shown in Figure 173. In the figure is shown the edge of the concrete deck, where spalling is expected. The green line is the line where spalling probably occurs. In the detail of the figure is shown that fibres that have the right direction can bridge the crack. Research should be done to judge if the fibres are strong enough to resist the high tensile stresses at the end of the link slab.

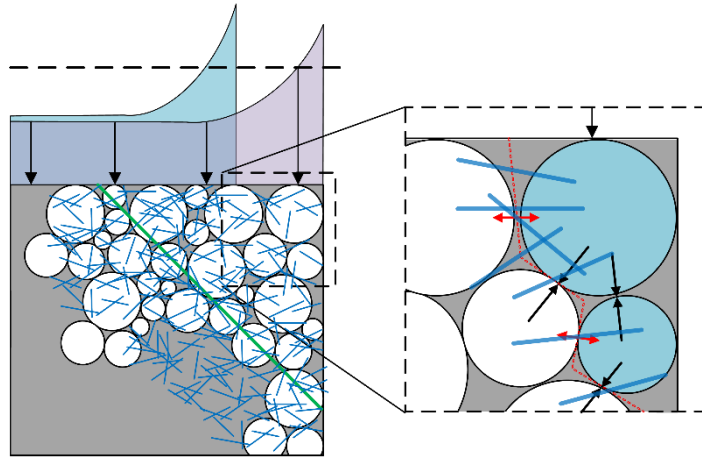


Figure 173 – Fibres in the corner of the concrete deck to resist spalling

The disadvantage of fibres is the direction they work. Fibres are randomly distributed, while spalling is only in the direction parallel to the driving direction. Only at the corners of the substructure, spalling could be expected in the direction perpendicular to the driving direction. However, from reason of simplicity, this is not taken into consideration here.

However, in theory it is possible that all the fibres at a certain location in the substructure are situated in the wrong direction. In that case, the concrete will spall off. The change that all fibres are pointing in the wrong direction is very small. However, that change that only a few fibres are point the right direction is already larger. If only a few fibres are point the right direction, the change that the concrete spalls off is still large. In other words, because of the random distribution of fibres, the change of failure of the concrete due to spalling could still too large.

Next to the direction, the distribution of the fibres could also be critical. In the worst case, there are places in the substructure where no fibres are situated, while there should be fibres to resist spalling. Then the concrete spalls off because of the 'wrong' distribution of the fibres.

To solve problems according to the fibre distribution and the direction of the fibres, more fibres could be added. If there are more fibres in the structure, the change that there are everywhere enough fibres working in the right direction to resist spalling becomes larger. However, there is a limited number of fibres that could be added to the concrete mixture. If too much fibres are added, the fibres are probably not effective any more. More research should be done, to have the optimum amount of fibres that to resist spalling.

At last, the idea of adding fibres locally only is probably hard to execute. The concrete substructure is probably cast in layers, independent of the casting method; cast is situ or precast. Therefore, it should be possible to make a layer of fibre reinforced concrete. However, it is desired that the fibres are only at the corner of the substructure, as shown in the cross section of Figure 168. An alternative casting method should be applied to have fibres in the desired place only.

Overview and addition research

Below, the advantages and disadvantages of the option with fibres are listed. It could be concluded that applying fibres to increase the resistance of spalling could be effective, at least in theory and has low material costs. However, there are uncertainties in the fibres distribution and the direction of the fibres. Further for this option should the execution method be adjust a bit.

Advantages	Disadvantages
Low material costs	Fibre direction Fibre distribution Execution Discussion of capacity of fibres

However, additional research should be done before this option could be applied in practice. Some recommended further research is:

- Execution method to place fibres locally
- The increase of the resistance of the substructure against spalling, so the effectiveness of the option
- Fibre distribution, fibre directions and an optimum number of fibres for different types and lengths of fibres. This part of further research of course has strong relations with the effectiveness of the option.

5.3 Chamfer

The second design option to prevent spalling is the application of the chamfer at the end of the deck. The idea behind the chamfer is shifting the peak stress, such that the high stress can be spread by compressive stresses. This is schematically shown in the grain model of the cross section of Figure 174. Because the peak stress is now spread over a larger area, the stresses are expected to be smaller, such that spalling is not expected any more.

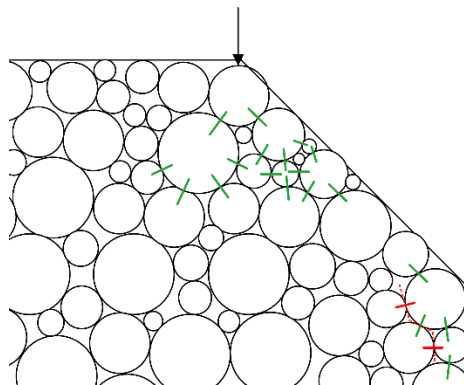


Figure 174 – Grain model at the end of the deck for a deck where a chamfer is applied

The big advantage of applying a chamfer is that the chamfer is relative easy to make while no additional materials are needed in the design. In practice, only a small modification of the formwork should be made to construct the chamfer. So from executorial and material point of view, the chamfer is interesting to apply.

There are also some disadvantages of this solution. First of all, the application of the chamfer results in an increase of the peak stress. In fact, due to the application of chamfers, the span of the link slab increases. According to the analysis given in chapter 3.3.1.3 Case C, the vertical peak stress working on the substructure increase by an increase of the gap length.

The larger peak stress in the substructure should not be the problem, because the resistance against spalling should be larger. In other words, the larger peak stress just have influence the effectiveness of the solution. However, in the link slab itself, the peak stress increases in this option, while the resistance of the link slab against peak stresses remain the same. More research should be done to the capacity of the link slab to resist this peak stresses.

Further, the length of the chamfer itself is limited due to the strength of the link slab. If the chamfer is chosen larger, the span of the link slab becomes larger, such that the bending moment and shear capacity of the link slab becomes critical. In Appendix C: Maximum span of the link slab is done a calculation to the maximum span of the link slab, assuming a thickness of 75 mm. From the calculations done in the appendix follows that the maximum span of the SHCC link slab is about 620 mm or 675 mm for a reinforcement ratio of 0.3% and 0.6% respectively. From here, calculations are done with the lowest length of the gap, 620 mm. The length of the chamfer depends on the length of the gap, as shown in eq.(68).

$$L_{chamfer} = \frac{(L_{span_{max}} - L_{gap})}{2} \quad \text{eq.(68)}$$

In the chapter 5.7 of the RTD 1007-2 (Rijkswaterstaat, 2013) is given that the minimum length of the gap is required to be 100 mm for maintenance and inspections. In that case, the maximum length of the chamfer is equal to $L_{chamfer} = \frac{(620-100)}{2} = 260 \text{ mm}$, which is not that much. Assuming the link slab is that durable that no maintenance or inspection is required during service life, then the length of the chamfer could be increased a bit. Assuming the length of the gap is 50 mm only, the length of the chamfer could already be equal to 285 mm.

Now it should be evaluated if this chamfer is large enough to avoid large risks on spalling. However, a deeper analysis should be done to evaluate the effect of the chamfer. If the chamfer should be larger to reduce the peak stress even further, there are a few options:

- More accurate calculation: better scheme, better description of working stress distribution.
- Increase thickness of the link slab
- Increase the reinforcement ratio
- Stiffer reinforcement
- Applying a stronger type of SHCC
- Thicker layer of asphalt

The calculations can be made more accurate easily by using an infinite element model. However, scheme and the working stress distribution can also be improved in the analytical calculations. The actual working vertical distributed load is almost half of the stress distributed that is assumed in the calculation. By adapt the stress distribution, the length of the chamfer can probably be increased significantly already.

The design of the link slab could of course be adapted also in order to increase the length of the gap and the chamfer. Obviously, by increasing the thickness of the link slab, the reinforcement ratio and by applying stronger or stiffer reinforcement and/or concrete, the bending moment resistance of the link slab increases. However, by changing the design, probably the behaviour of the link slab under imposed horizontal deformation also changes. For example, by increasing the thickness, the stresses in the link slab become higher under imposed deformation. Further, it could be expected that the crack behaviour of the material changes.

At last, the thickness of the layer of asphalt could be increased. If the thickness is increase, the stress can be distributed over a larger area, such that the stress in the link slab decreases. For now, the thickness of the layer is assumed to be 120 mm, such that the calculation is valid for most roads. However, for a specific road, an increased thickness could be chosen.

The effectiveness of the chamfer against spalling could be determined as the reduction of the tensile stresses due to the distribution in the substructure as a function of the increase of the peak stresses. So to judge the effectiveness of the chamfer theoretically, the reduction of the tensile stresses in the concrete and the increase of the working peak stresses should be determined theoretically. Determining the working peak stresses is probably quite hard. Therefore, an alternative method is to determine the effectiveness experimentally.

Overview and additional research

Here the advantages and disadvantages of the option of chamfers are listed, as shown below. It could be concluded that applying chamfers at the end of the substructure is an easy and cheap way to increase the resistance against spalling. However, if this option is chosen, of course further research should be done. Some optimisation according the calculation method are already mentioned in this paragraph.

Advantages	Disadvantages
Lower material costs Easy to execute	Increase of peak stress Discussion of effectiveness of the reduction of the tensile stresses Limitation of the length of the chamfer Determining the effectiveness

From the analysis could be concluded that additional research is necessary before the chamfers are applied in practice. Interesting things to invest in more detail are:

- The increase of the peak stress caused by the increase of the length of the gap, in order to check if the resistance of the SHCC link slab is high enough
- The reduction of the stress in the substructure that causes spalling
- More detailed research on the maximum length of the gap

5.4 Locally reduced Young’s modulus

The third option is to reduce the Young’s modulus locally. The idea is to reduce the Young’s modulus near the end of the bridge beams to reduce the peak stress. Normally, the stiffest materials carries the most stresses. So by reducing the stiffness at the end of the beam, the working peak stresses should be reduced. This idea is based on Hooke’s law. The construction of the locally reduced Young’s modulus option is schematically shown in Figure 175. In the figure is shown the link slab place on the concrete deck. In purple is shown an alternative material with a lower young’s modulus. The alternative material (purple) could for example be a harsh. The thickness of this layer has a liner relation with the vertical stiffness. So by varying the thickness of the softer layer, the stiffness of the supporting substructure can be varied.

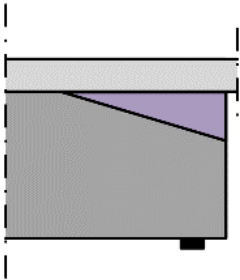


Figure 175 – Locally reduced Young’s modulus by applying a softer material

It is hard to make conclusions of the reduction of the peak stress analytically. To determine the reduction of the peak stress, it is probably better to do an analysis with a finite element method or to do experiments to the reduction of the peak stress if the Young’s modulus is locally reduced.

Simplified example

However, to imply the idea of locally reducing the Young’s modulus, a simplified situation is analysed. In this situation, it is assumed that the link slab moves evenly vertically downward. Further it is assumed that the link slab remains straight. For reasons of simplicity, the reduced young’s modulus is modelled as strips with different reduced moduli of elasticity. The whole model is shown in Figure 176. The moduli of elasticity of the strips differs from 10 to 30 GPa. It is assumed that over the length of the substructure, an equal vertical deformation Δu works.

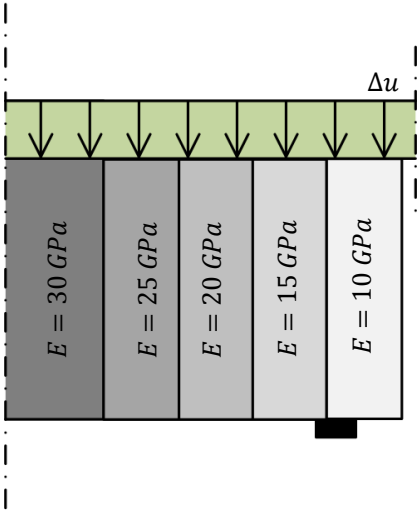


Figure 176 – Model of the end of the substructure with strips of different moduli of elasticity

Under the assumption that every strip has the same vertical deformation, Δu , the stresses can be calculated according to Hooke’s law as shown in eq.(69). In the equation, the strain is can be written as the deformation over the height of the structure, such that Hooke’s law can be rewritten as shown in eq.(69).

$$\left. \begin{aligned} \sigma &= E \cdot \varepsilon \\ \varepsilon &= \frac{\Delta u}{h} \end{aligned} \right\} \rightarrow \sigma = E \cdot \frac{\Delta u}{h} \quad \text{eq.(69)}$$

Assuming all strips are shortened 1.0‰, assumed a constant deflection and a constant height, $\left(\frac{\Delta u}{h} = 1.0\text{‰}\right)$, the stresses in the strips can be calculated. The results from the calculation are shown in Table 35. As shown in the table, in the strips that have the lowest Young’s modulus, the stress is the lowest. The results of this example illustrate the idea behind the reduction of the Young’s modulus in order to reduce local peak stresses.

Table 35 – Stresses in strips with different moduli of elasticity

Young’s modulus [GPa]	Stress [MPa]
10	10
15	15
20	20
25	25
30	30

The results of Table 35 are schematically shown in Figure 177. In the graph of Figure 177 is clearly shown the linear distribution of stresses over the length of the substructure.

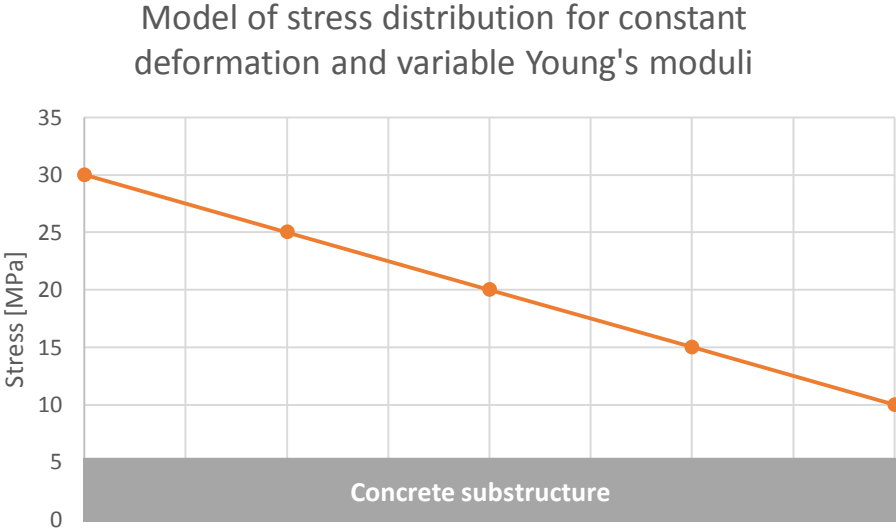


Figure 177 – Stress distribution over the length of the substructure by applying a constant deformation and variable Young’s moduli in the model as shown in Figure 176

Distribution of vertical stresses

Now this idea could also be implemented in the problem of the peak stress near the end of the substructure. In the example above is shown that if the stiffness of the substructure is variable, the stress is also variable, assuming a certain deformation. If the stiffness of the substructure is everywhere the same, large stresses could be expected near the end of the substructure. If the stiffness of the substructure near the end of the substructure is reduced, the large stresses could be expected to be smaller compared with the situation where the substructure has a constant stiffness. The idea behind is that stiff parts carry the most stress.

The expected stresses working in the substructure in the case of a constant Young’s modulus or a variable Young’s modulus are schematically shown in the graph of Figure 178. As shown in the graph, in case of the variable stiffness, the peak stress is expected to be a lower. To make vertical equilibrium with the wheel load, the area under both graphs shown in Figure 178 should both be equal to the vertical working wheel load.

Based on the calculations of Appendix C: Maximum span of the link slab, it is assumed that the link slab is strong enough to be locally supported by a reduced stiff supporting system. In the Appendix is determined the maximum span of the link slab. In this case, the span is still supported, but the stiffness of the supporting system varies.

Expected stress distribution for constant and variable Young's modulus

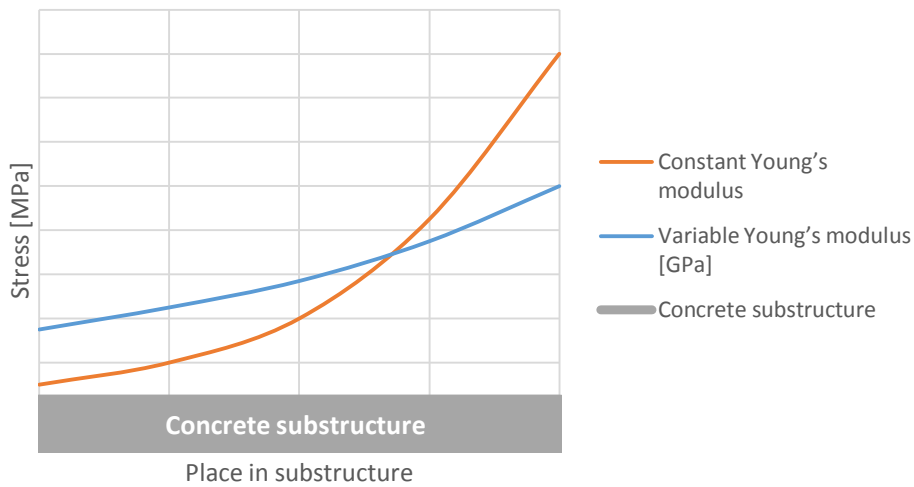


Figure 178 – Expected stress distribution for constant and variable Young's modulus over the place of the concrete substructure

However, it could be concluded that it is quite complex to determine the influence of the stiffness on the stress in the substructure. Probably, a finite element method should be applied to make proper theoretical conclusions. Another way to invest the influence of the stiffness of the substructure is experimentally.

Analysis

Here the locally reduced Young's modulus variant is analysed in some more detail. In this analysis, an interesting thing to take into account is the combination with the debonding layer. The analysis is done according to Figure 179. In this figure is shown the option combined with a debonding layer that is made of teflon. In the figure are given three different zones; zone A, point B and zone C. All three zones are described here shortly.

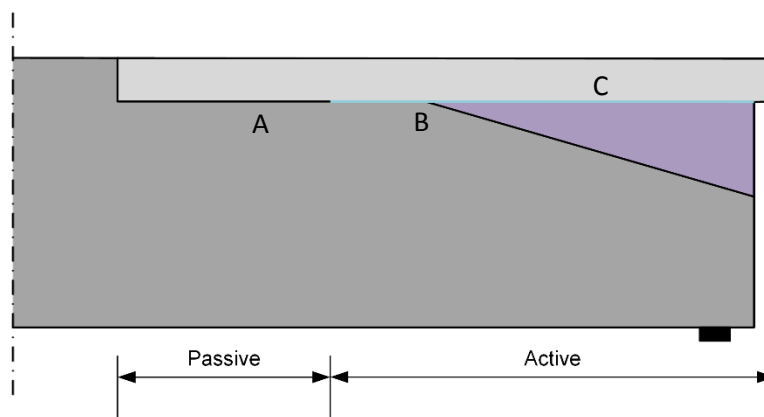


Figure 179 – Variable Young's modulus at the end of the substructure assuming Teflon for the debonding layer

Zone A is in fact the situation that is described in chapter 5.1 Debonding layer in the active zone; a teflon layer between the SHCC link slab and the NSC substructure. According to the debonding layer, no specialties are expected in this zone different from the description given in chapter 5.1 Debonding layer in the active zone.

Point B is the point where the stiffness of the supporting system becomes about 33 GPa again, what is about the stiffness of the normal strength concrete. At this point, the stiffness changes from linearly increasing value to a constant value. Because of this change, peak stresses could be expected. However, the peak stresses probably remains quite small, because in theory, there is no jump in stiffness, but a kink in the vertical stiffness over the length only. Additional research should show if peak stresses are expected here.

In zone C the teflon is placed upon softer material. Normally, teflon is placed between stiff layers. It could be the case that if teflon is placed on softer material, problems arise. Problems could then for example be generated if the softer material deforms. However, in paragraph 5.1 Debonding layer in the active zone, Table 33 is given that the cracking strain of teflon is very high (>50%) and Young's modulus is very low (around 600 MPa). Probably, the soft material has a lower strain capacity and a higher modulus of elasticity. Therefore no failure of teflon is expected on forehand.

Teflon should take care of the debonding layer, so the friction should remain low. Therefore, maybe some research should be done to the effect of deformation on the friction coefficient or the connection between the soft material and teflon. However, on forehand, based on the material characteristics of Table 33, no significant trouble according to the debonding layer made of teflon on the soft material is expected.

Further, because the reduced stiffness, the link slab itself should have a certain strength to be able to distribute the vertical stresses over a larger area. It is assumed that the deformation capacity in the local reduced stiffness area is significant larger than the deformation capacity of the SHCC link slab. The means that the SHCC link slab should have a certain strength to distributed the peak stresses over a larger area. If the strength of the link slab is not high enough, the link slab will fail because it is not supported well.

Failure in the link slab probably depends on the length where the softer material is applied and the thickness of the layer. If the length where the material is applied over is larger, the link slab should have a larger strength because vertical peak stresses should be transferred over a larger zone. Also if the thickness of the layer is larger, the peak stresses should be distributed over a larger area, because if the thickness is larger the stiffness is locally lower so the link slab is supported less.

Additional research

Because too little knowledge is available at the moment, no conclusion about advantages and disadvantages are made at the end of this paragraph. If the idea work, the main advantages is that peak stresses are not generated or at least reduced to a certain minimum. So the option of locally reducing the Young's modulus seems promising, but more research should be done to the working and effectiveness of the idea. Some additional research that is recommended is:

- Reduction of the peak stress
- Optimum length of the soft material
- Optimal stiffness reduction
- Optimal distribution of the stiffness over the length (for example linear or exponential distribution)
- Peak stresses at the end of the soft material (point B)
- Behaviour of teflon according to friction if it is deformed

Probably the best first step to take in further research is to insert this variant in a computer model. In a finite element program, the locally reduced stiffness can be modified easily, such that the influence

of varying the stiffness according to the maximum working stress could be determined relative easily. Another interesting variable to take into account in the influence of the length where the stiffness is reduced over. It could be expected that the strength of the link slab itself becomes the governing factor if the stiffness is reduced over a large length. Further, at the end of the locally reduced stiffness area, the effect of the change from linear varying stiffness to constant stiffness should be analysed according to the model. This change could result in local peak stresses.

Additional research according to the debonding layer that is made with teflon, could probably done the best experimentally. Probably, problems that could arise are too complex to analyse by a computer model. However, if there are proper computer models to analyse the working of the teflon layer until a certain detail, of course this computer model is recommended first.

5.5 Redistribution by stiff interlayer

The idea of a stiff interlayer between the link slab and the substructure is redistribution of stresses, such that the peak stress that works on the substructure is reduced. The mechanism can be explain the best with Figure 180 and Figure 181. In Figure 180 is assumed that the stiffness of the plate is infinite while the stiffness of the link slab and the substructure is equal to zero. The vertical peak stress is the figure modelled as a point load F . If the plate is loaded by F , the plate will turn around its centre of gravity, as shown in Figure 180.

However, in reality the link slab and the concrete substructure both have a certain stiffness, what is taken into account in Figure 181. Due to the stiffness of the link slab, a certain reaction force R could be expected, which keeps the plate under the link slab. Assuming the stiffness of the substructure is zero, the plate moves as shown in Figure 181. However, because the substructure does have a certain stiffness, a distributed reaction force is expected as shown in Figure 181. According to Hooke's law, the distributed reaction force is expected to be linear. That means that the original peak stress, which is also shown in Figure 181 by the dotted line, is reduced a lot due to redistribution.

The horizontal plate should be connected tight to the substructure, such that it remains in place if it is exposed to a horizontal deformation or stress. Probably the simplest option to create a horizontal connection is to put dowels in the concrete where the plate is connected on.

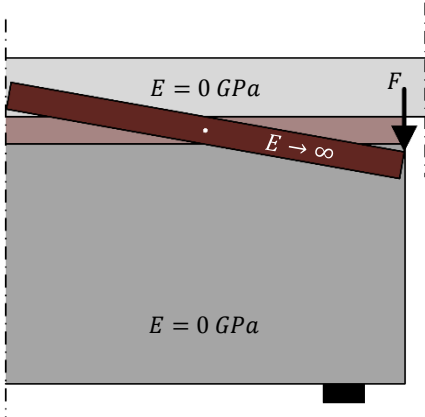


Figure 180 – Displacement of the horizontal plate due to vertical load assuming no stiffness of concrete and SHCC

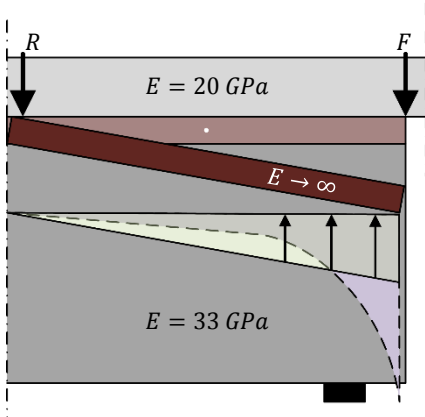


Figure 181 – Displacement of the horizontal plate and the stress distribution due to vertical load

Analysing the above described mechanism, there are some issues according to the functioning of the design. The analysis to issues is described in this paragraph. In short, the main points in the design that are included in this analysis are:

- Peak stress in SHCC link slab
- Peak stress at the end of the interlayer
- Execution methods

First of all, the peak stress in the substructure is expected to be reduced by the application of a stiff horizontal plate. However, the peak stress that works in the link slab is expected to be increased because of the stiff plate. This is schematically shown in Figure 182. As shown in the figure, if a stiff interlayer is applied, the peak stress at the end of the substructure is expected to be higher compared to the situation without a stiff interlayer. The area under both graph, which is the total working force, should of course be equal.

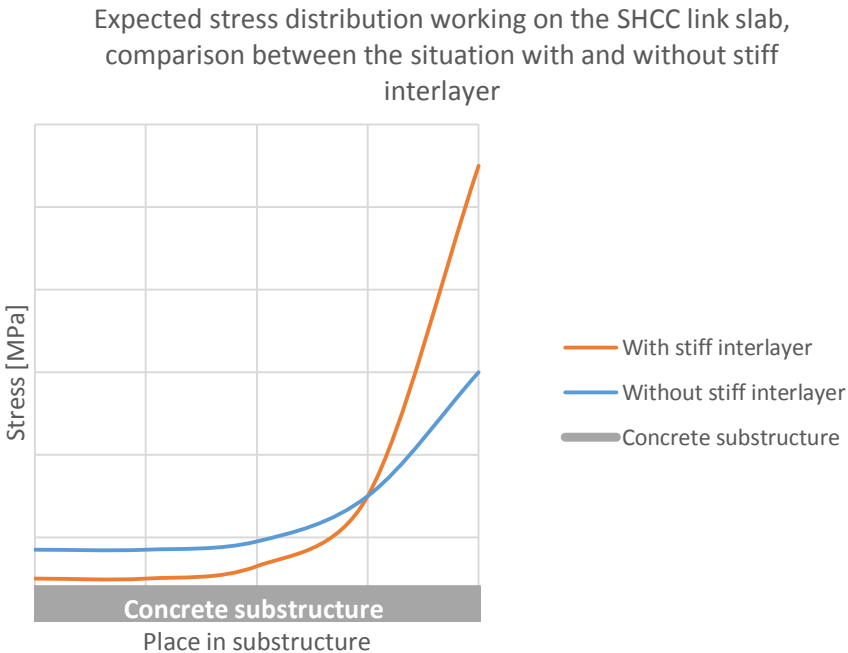


Figure 182 – Excepted vertical peak stresses in the situation with and without stiff interlayer

Second disadvantage of this option is the expected peak stress at the other end of the stiff plate. Here is a jump in vertical stiffness because the stiff interlayer ends. Additional research should be done to this stresses. If at the end of the interlayer are generated to large peak stresses, an alternative option should be chosen or the design should be modified in a way that there are not generated governing peak stresses, or at least that possible peak stresses does not have negative influences.

Another issue of this solution is in the execution limitations, what is also mentioned in the case to SHCC and concrete only in chapter 5.1 Debonding layer in the active zone. The smoothness of the surface of the SHCC link slab, the concrete deck and probably also the stiff plate are limited. Because of the limited smoothness, small peak stresses could be expected. This idea is shown in the detail of Figure 183. In the figure is shown a cross section of the option with the stiff horizontal plate. The concrete and SHCC layers are shown to be quite rough. Between these layers, the stiff plate is situated. The Teflon layer is placed between the stiff plate and the SHCC. The stiff plate is expected to be perfectly smooth, just for reasons of simplicity. Due to the roughness in the layers, local peak stresses are

expected to be generated. In practice, the stiff plate is probably not perfectly smooth as well, what even increase local peak stresses. This could also increase the shear stresses in the unbonded zone, what is undesirable.



Figure 183 – Smoothness of different layers, assuming the stiff plate is perfectly smooth

Peak stresses between the concrete and the stiff plate, could be decreased by placing the stiff plate on the concrete deck during casting the concrete deck. The stiff plate then works as a formwork, such that the concrete is poured against the stiff plate everywhere under the plate. The same can be done for the SHCC, by casting it in situ upon the stiff plate. Peak stresses than are reduced to a minimum.

However, taking a closer look to the connection between the SHCC link slab and the stiff plate in the debonded zone, still trouble could be expected. This is schematically shown in Figure 184. In the figure are again shown a layer of SHCC, the stiff plate and a layer of concrete. Both, the concrete layer and the SHCC layer are casted against the stiff plate. So the roughness of the surface of both layers are the same as the surface as the horizontal plate. As shown in Figure 184, if a horizontal deformation Δu works on the structure, stresses can be expected between the SHCC layer and the stiff plate if both are not perfectly smooth. Then the active section of the link slab can't deform without shear stresses, such that the link slab does not function properly anymore. As a conclusion, the connection between the SHCC and the stiff plate should be perfectly smooth or at least should have a certain minimum smoothness to reduce the shear stresses.

On the other side, it is maybe easy to make a smooth surface on the stiff plate. Assuming the SHCC link slab is casted upon the stiff plate, the shear stresses could be expected to be reduced to a minimum. In other words, to have a properly working debonding zone, it would maybe be interesting to apply a stiff material, where the surface could be made very smooth.

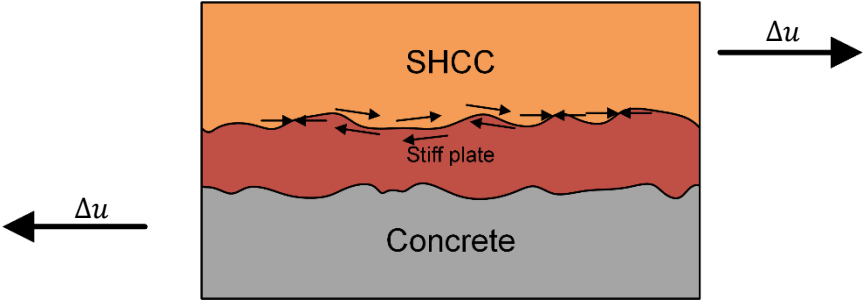


Figure 184 – Working shear stresses between the SHCC link slab and the stiff plate

Overview and additional research

At last part of this paragraph, an overview of the advantages and disadvantages is given and is some additional research recommended. An overview of the advantages and disadvantages is given bellow.

Advantages	Disadvantages
Within the execution limits, easy to execute Depending on the material, maybe easier to meet the smoothness requirements of the plate	Peak stress at the other side of the plate Plate should be very to infinite stiff Smoothness of the plate Possible increase of peak stresses working on the link slab

In the end, the stiff interlayer seems easy to execute, if practical deviations are in the required limits. So for example the practical smoothness of the plate should be better than the required smoothness from theory. Another disadvantages is the peak stress that is generated at the other side of the plate. For a practical solution, it is recommended to invest the:

- The reduction of the peak stress at the end of the structure, so the effectiveness of this option
- The effect on generating peak stresses at the other side of the stiff plate
- The stiffness of the plate to be effective (in practice, stiffness can be infinite)
- Connection between the steel and the upper and lower concrete layer
- Generation of peak stresses due to limited smoothness of the layers

5.6 Prestressed anchored plate

In this paragraph is discussed the idea of the prestressed anchored plate. The design and the load distribution is explained in some more detail. The paragraph ends with an overview of the advantages and disadvantages of this option and some recommended additional research before this variant could be applied in practice.

The idea behind a prestressed anchored plate at the end of the deck is to increase the resistance against spalling by a counter load. There should be generated a compressive stress between the concrete and the plate, such that there could be made horizontal equilibrium without tensile stresses in the concrete. This is schematically shown in Figure 185.

In Figure 185 is shown the place the prestressed anchored plate should be situated. In the detail of Figure 185 are shown the stresses that are generated by the vertical plate. In fact the plate only needs to work over the distance where spalling is a risk. The plate should be connected to the concrete by an prestressed anchor. In the anchors, tensile forces should work, such that the steel plate pushes against the concrete deck.

In the detail of Figure 185 is shown the idea of the prestressed anchor plate is some more detail. Green arrows shows the compressive stresses that are generated due to the plate that pushes against the particles of the concrete substructure. Because of this compressive stress, the tensile stresses between the particles (red arrows) are not needed to make horizontal equilibrium. These tensile stresses are exactly the stresses that causes failure by spalling. So if the tensile stresses do not have to be generated, spalling is avoided.

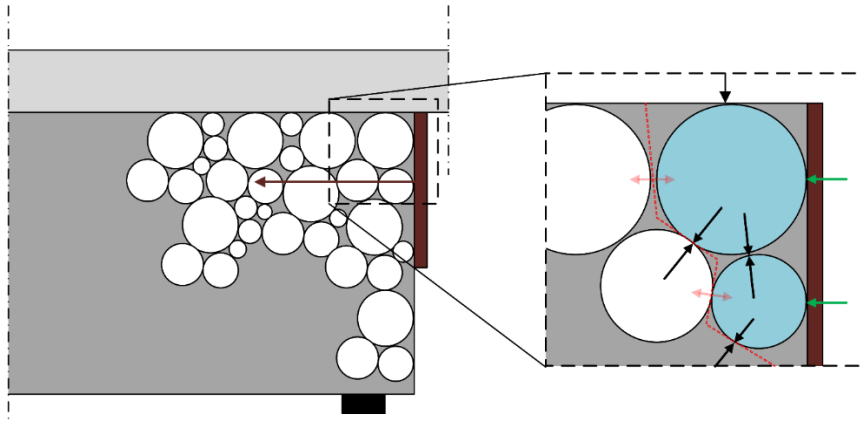


Figure 185 – Prestressed anchored plate at the end of the deck to increase the resistance against spalling

For an effective result, it is necessary that the vertical plate and the anchor both have a certain stiffness. The tensile strain of concrete is in general around 0.1‰. So around 0.1‰, the concrete cracks. To prevent spalling the compressive stress from the vertical plate should already be high enough.

Further, if the concrete shortens, the stresses in the steel reduces. This problem is shown in the detail of Figure 186. In the detail of the figure is shown the plate that is placed against the concrete deck. The concrete is exposed to a deformation Δu for example due to shrinkage of the concrete. If the anchors are not prestressed, due to the deformation of the concrete the vertical plate does not push against the concrete any more.

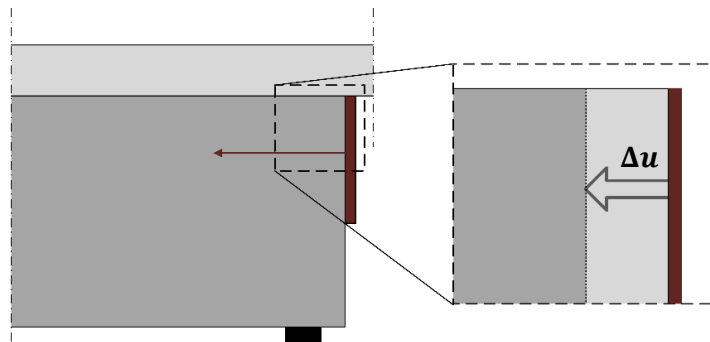


Figure 186 – Shortening of the concrete substructure

In fact, the two above mentioned phenomena both can be carried by the application of prestressed anchors. So these are mainly the cause that prestressed anchors are chosen in this option. Due to prestressed anchors, there works a certain compressive stress from the plate on the concrete substructure constantly. If the concrete for example shortens, the stress in the anchors of course reduce a bit. The design should be made in such a way that there is always working a certain stress in the anchors to reduce the risk on spalling to a certain minimum.

To execute the design of Figure 185 in practice, regular execution methods could be applied. Prestressed anchors are placed in concrete for years. Connecting a plate to the anchors also does not seem to be a tough job to do. So all together, the execution seems not complicated. However, the execution process probably takes some time.

The plate should be constructed in a way that it does not carry vertical stresses from the link slab, to prevent peak stresses. This can be explained according to Figure 187. In the figure is shown the option with the prestressed anchored plate, exposed to a vertical wheel load. The plate is assumed to be

infinite stiff. According to Hooke’s law, a very high peak stress working on the vertical plate can be expected, assuming the connection between the plate and the substructure is tight. To prevent the peak stress, the plate should be able to move freely in the vertical plane. This could be achieved by adjust the connection between the concrete and the plate.

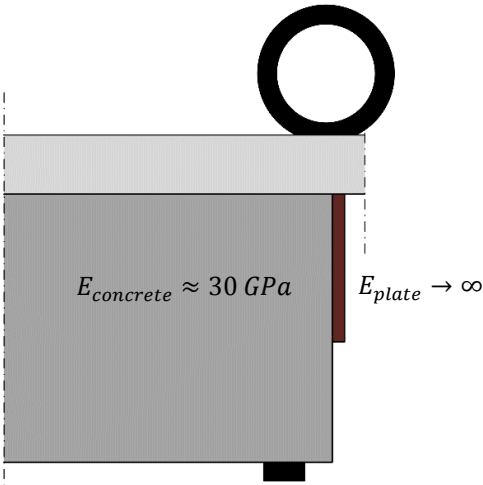


Figure 187 – Vertical wheel load working on the link slab in the case a prestressed anchored plate is applied

An advantage of the vertical placed plate is that it is at the outside of the concrete. That means that the plate could be replaced during the service life of the bridge. The only thing then is that the bridge should be spared for traffic, because if the plate is replaced, the deck is temporary not able to resist spalling. Of course the anchor in the concrete deck can’t be replaced that easy.

The stiff plate should probably be made of steel to have a cheap and easy solution. Because the steel is placed at the outside of the deck, the change on corrosion is very big. To ensure a certain service life, the steel plate should be protected against corrosion, what unfortunately increase the costs. Further, since corrosion is became an issue, the steel plate should be able to be inspected according to the RTD 1007-2, chapter 5.7. That means that a corridor should be made, what probably increases the costs.

Overview and additional research

Below are listed the advantages and disadvantages that are called in the analysis above. Because of the stiffness of the materials and the expected deformation of concrete during service life, this option seems not that promising to apply in practice.

Advantages	Disadvantages
Relative easy to replace the plate itself compared to the other solutions Regular execution methods Probably very effective	Expensive due to prestressed anchors Effectiveness of the system if the concrete shortens Longer execution time due to extra steps

However, before the option is labelled as a bad option, additional research should be done. Research should mainly done to:

- The influence of shrinkage on the effectiveness of this option
- The influence of the stiffness of materials on the effectiveness of this option
- The effect of prestressing steel

5.7 Overview

In Table 36 is given an overview of options that are described and analysed in this chapter. In the table is given the philosophy behind the option to reduce the risk of spalling. In the third and fourth column are given the advantages and disadvantages per variant. In the last column are given some recommendations according to additional research per design option. Since due to a lack of knowledge, no conclusions could be made for the local reduced Young's modulus option, no advantages and disadvantages are given for this variant.

Table 36 – Overview of variants to resist or decrease spalling of the concrete caused by vertical load

Variant	Philosophy	Advantages	Disadvantages	Additional recommended research
Fibres	Increase resistance against spalling	- Low material costs	- Fibre direction - Fibre distribution - Execution - Discussion of capacity of fibres	- Execution method - Resistance against spalling - Fibre distribution - Fibre directions - Optimum number of fibres
Chamfers	Increase resistance against spalling	- Lower material costs - Easy to execute	- Increase of peak stress in the link slab - Discussion of effectiveness of the reduction of the tensile stresses - Limitation of the chamfer - Determining the effectiveness	- Increase of the peak stress - Reduction of spalling - Maximum length of the gap
Locally reduced Young's modulus	Decrease the peak stress			- Reduction of the peak stress - Maximum length of the soft material - Optimal stiffness reduction - Optimal stiffness over the length - Peak stresses at the end of the soft material - Friction behaviour of deformed teflon
Redistribution by stiff interlayer	Decrease the peak stress	- Within the execution limits, easy to execute - Depending on the material, maybe easier to create a smooth surface	- Peak stress at the other side of the plate - Plate should be very to infinite stiff - Smoothness of the plate	- The reduction of the peak stress - Peak stresses at the other side of the stiff plate - The stiffness of the plate - Connection between steel and concrete/SHCC - Smoothness of the layers
Prestressed anchored plate	Increase resistance against spalling	- Relative easy to replace the plate itself for maintenance - Regular execution methods	- Application of anchors - Effectiveness of the system if the concrete shortens	- Influence of shrinkage - Influence of the stiffness of materials - The effect of prestressing steel

5.8 Evaluation and conclusion

Based on the overview in Table 36 in the previous paragraph, the optimised can be evaluated and some conclusions can be made. Before conclusions are made according to the best option, the options are evaluated here shortly.

- The fibre variant has low material costs, but uncertainties caused by the fibre distribution and direction of the fibre can still result in local spalling.
- The chamfer variant is easy to make, but had its limits in terms of the length of the chamfer because of the gap that is created by the chamfers. Further, the effectiveness of the chamfer is a point of discussion.
- Locally reduced Young's modulus variant seems interesting to increase the peak stress, but more research should be done to judge the effectiveness of this option.
- The success of the redistribution by stiff interlayer depends probably a lot on the limitation of the smoothness of the surface of the stiff material. If the material can be made smooth easily, a properly working debonding layer could be created easily. However, the effectiveness of the redistribution of the peak stresses, which mainly depends on the stiffness of the plate, should be researched in more detail.
- If the anchors are not prestressed, the effectiveness of the prestressed anchored plate is a point of discussion. Probably, this option is a lot more effective if the anchors are prestressed

Based on the evaluation and the overview, it could now be concluded that:

- The **cheapest option** is the chamfer variant, because only the form work should be modified a bit.
- The **most effective option** is probably the prestressed anchored plate.
- The option with the **most additional advantages** is the redistribution by stiff interlayer, provided that the surface can be made very smooth easily.

These three options are probably the most interesting to research in some more detail.

Recommended research per option is given in the last column of Table 36.

6 Conclusion

This conclusions consist of two parts. First some general conclusions are given for the SHCC Link Slab, with a small distinction between the Deck Slab and the Link Slab design in the active zone. After that, some conclusions are made for the Thin SHCC Link Slab design, which seems an interesting alternative joint to apply in the Netherlands in practice.

General conclusions for the SHCC Link Slab

- The general design of an SHCC Link Slab is shown in Figure 188. The link slab, which is poured in one, consists of an active part in the middle and two passive parts at both ends.

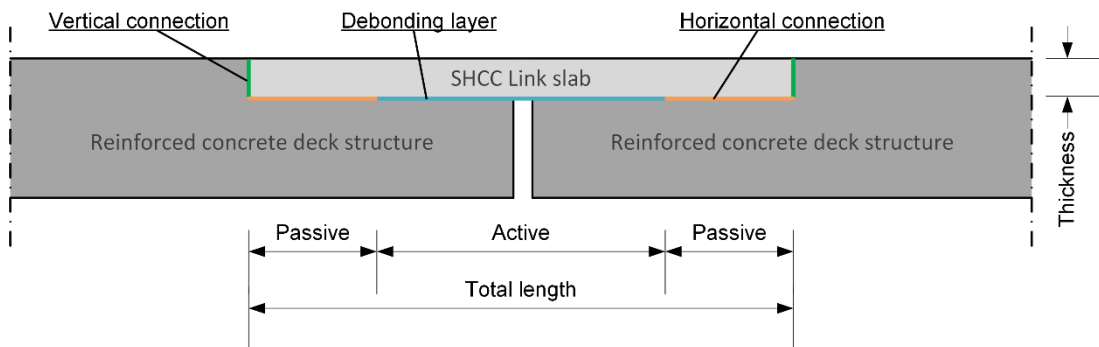


Figure 188 – Schematisation of the design of the Thin SHCC Link Slab

- The total SHCC link slab creates a continuous connection between two bridge decks, which should take care of horizontal loads and vertical loads.
- The passive zone should, next to carry vertical and horizontal loads, take care of the connection between the active zone and the concrete deck
 - o No cracks should be generated here and a proper vertical connection and horizontal connection should be made by for example, reinforcement, studs and grout.
- The functions of the active zone, next to carry vertical and horizontal loads, depends on the design. Two link slab types are analysed in this research:
 - o SHCC Deck Slab reinforced with steel (SHCC Deck Slab), which is successfully applied on steel girders in Michigan, USA (Li, et al., 2003):
 - The active part has rotation capacity to take care of imposed rotations
 - The active part has no horizontal deformation capacity (shorten or elongate)
 - The debonding layer in the active zone should guarantee that the active section can move freely
 - o Thin SHCC Link Slab reinforced by GFRP (Thin SHCC Link Slab), which tis only research on its deformation capacity at the moment (Reyes & Robertson, 2011), (Lárusson, 2013):
 - The active part has rotation capacity to take care of imposed rotations
 - The active part has a horizontal deformation capacity, preferably at a low stress, to take up imposed horizontal deformation.
 - The debonding layer in the active zone should guarantee that the active section can move freely

Thin SHCC Link Slab

- In future practice, the Thin SHCC Link Slab, which is described by Reyes & Robertson (2011) and Lárusson (2013), seems the most interesting link slab to apply in the Netherlands.
- Point of attention is the vertical stress that causes a peak stress at the end of the substructure, what results in a high risk on spalling.

- The execution of the debonding zone is a point of attention to create a properly working debonding zone, but is only partly taken into consideration.
- The cheapest way to reduce the risk on spalling is the application of chamfers at the end of the deck. However, the effectiveness is a point of discussion, because chamfers also increase the peak stress.
- Probably the most effective way is a prestressed anchored plate at the end of the deck that is connected to prestressed anchors. However, this is probably a very expensive option.
- The most additional advantages is the redistribution by stiff interlayer, depending on the material, a properly working debonding layer could be easier to create.

7 Recommendations

In this chapter are given some recommendations according to the research that is presented in this report. The recommendations have two parts. In the first part is give a practice guidance. In this part is given a guidance of steps that are recommended to take to apply the SHCC link slab in practice. The guidance contains six steps. In every step, a pilot should be executed until the last step what is the pilot of a thin SHCC link slab.

After the practical guidance, some recommendations are given according to the additional research. These recommendations are in terms of the Thin SHCC Link Slab. These are based on results and assumptions during the analysis of the Thin SHCC Link Slab.

In fact the second part of these recommendations gives addition research that should be done if the Thin SHCC Link Slab is applied without any experience of the material. To reduce risks and to start execution of SHCC at short notice, it is recommended to follow the practical guidance that is given in the first part of these recommendations.

7.1 Practical guidance

In this report are done analyses to different types of SHCC link slabs to create an innovative joint. From the analysis, the Thin SHCC Link Slab seems to be the best design to create an SHCC joint. From this research, there are two options to construct the Thin SHCC Link Slab in practice. Both options are shown in Figure 189. At the left of the figure is today's practice, where common joint designs are applied. At the right is future practice, where it seems interesting to apply the Thin SHCC link slab.

There are two ways to apply the Thin SHCC Link Slab in the future. The first one is to research the Thin SHCC link slab until it seems ready to apply in practice. This cost a lot of money for research, bring a lot of risks with it, but is the fastest method if the Thin SHCC Link Slab is applied successfully.

The second method to apply the Thin SHCC Link Slab in the next years is to do some pilot projects. In every pilot project are some minor changes, until the last project where the Thin SHCC Link Slab is executed. This method also cost a lot of money, but the risks are very limited and the method takes some more time.

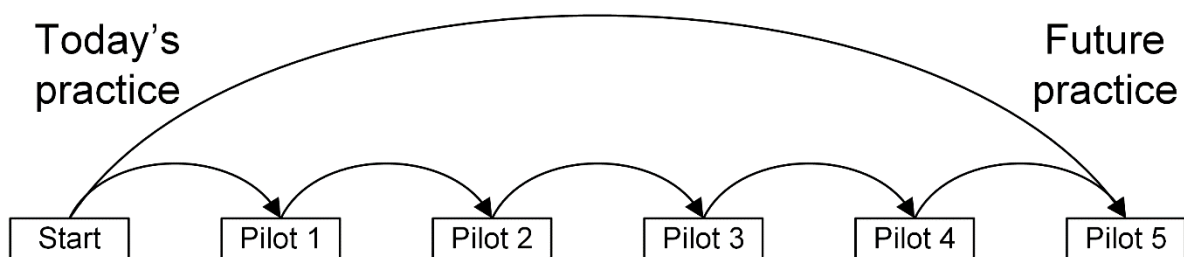


Figure 189 – Two methods to change today's practice to the future practice

Here five pilots are suggested that should be made to execute the Thin SHCC Link Slab in the future practice. An overview of the five pilots is given in Table 37. The five pilots are divided over two categories; flexible joints and Thin SHCC Link Slab. In the table are given the structures that are made in the five pilot projects. Further are given the advantages of the pilot by the application of the structure. The advantages are mainly given compared to the previous pilot and for pilot 1 compared to the NSC flexible joint. In the last column is shortly given the research that should be done before the pilot could be executed. Under Table 37 the pilots are described in some more detail. In the

description are not given much technical details. These could be find in the rest of the report where all joints are explained in detail.

Table 37 – From NSC Flexible Joint to Thin SHCC Link Slab by steps

		Structure	Advantage	Research
Flexible Joint	Pilot 1	Flexible joint made of SHCC	No adhesive strip Practical learning goal SHCC	SHCC material
	Pilot 2	Flexible joint made of SHCC with GFRP reinforcement	Durable reinforcement Practical learning goal GFRP Lower stiffness of the joint	GFRP
	Pilot 3	Flexible joint made of SHCC with a reduced amount of reinforcement	Less reinforcement Lower stiffness of the joint	Influence of PVA fibres
Thin Link Slab	Pilot 4	Thin SHCC link slab with GFRP rebars (intermediate supports only)	Horizontal deformation capacity Lower stiffness of the joint	Peak stresses Debonding zone
	Pilot 5	Thin SHCC link slab with GFRP rebars (all supports)	Horizontal deformation capacity in all joints	Influence on the abutment

To apply the Thin SHCC Link Slab in the future, the first step could be taken tomorrow. The first three pilot project still functions as a flexible joint. As a first pilot project it is recommended to make a ‘classic’ flexible joint of SHCC instead of NSC. The main goal is to get some practical experiments with the execution of SHCC. Further, as a small modification of the flexible joint design, the adhesive strip could be left out. The crack width of SHCC is in general smaller than 0.1 mm (Li, Engineered Cementitious Composites (ECC) – Material, Structural, and Durability Performance, 2007). So crack width of the SHCC flexible joint remain smaller than 0.2mm, what is probably the required maximum crack width if the adhesive strip is not applied. Before the pilot could be done, some research should be done to the right SHCC mixture to apply.

The next step is to apply a flexible joint with GFRP reinforcement instead of steel reinforcement. The main goal here is to get some experience with GFRP reinforcement and to research the behaviour of it. Besides, by applying GRFP, the reinforcement in the link slab is very durable.

As a third pilot, a part of the reinforcement could be left out. Because of the PVA fibres that are added to the mixture, less reinforcement bars should be required. According to this pilot, the influence of PVA fibres should be known better. The advantage of this pilot is that less reinforcement is required what reduce the cost and that the behaviours of a joint with less reinforcement could be monitored.

The fourth and the fifth pilot should be the Thin SHCC Link Slab. From reasons of simplicity, the Thin SHCC Link Slab should first be applied in at intermediate supports only. The large advantage of this link slabs of course is the horizontal deformation capacity.

If the Thin SHCC Link Slab is applied successfully above the intermediate supports, the last step is to apply the Thin SHCC Link Slab also at the abutments. Then the Thin SHCC Link Slab is applied everywhere in the bridge. Before the last pilot is executed, some research to the influence of the Thin SHCC Link Slab on the abutment is recommended.

7.2 Additional research

In this part of the recommendations are given recommendations according to the SHCC Link Slab. The given recommendations are mainly based on results and assumptions during the analysis of the Thin SHCC Link Slab. Probably some of these recommendations should also be done if the plan of Table 37 is carried. Interesting additional research seems to be:

- Combination of horizontal imposed deformation and horizontal load
- Vertical imposed deformation
- Spalling of NSC substructure
- Vertical peak stress in SHCC link slab
- Variants to reduce the risk of spalling
- Execution issues

7.2.1 Combination: horizontal imposed deformation and horizontal load

An interesting issue to research in more detail is the reaction of the SHCC link slab if it is under imposed deformation and then exposed to a horizontal load. In theory, the link slab has no capacity to take care of horizontal tensile stresses if the imposed deformation has caused cracks already. Furthermore, the link should probably deform quite a lot if it is elongated due to imposed deformation and then exposed to a compressive force. Both situations are analysed in more detail in Appendix B: Load combinations.

7.2.2 Vertical imposed deformation

In this research is assumed that the vertical imposed deformation could be neglected, because two spans that are connected by a link slab are normally placed upon the same cross beam. However, both beams are of course placed upon separate support blocks. There could be some difference in the vertical stiffness of the support blocks due to imperfections during execution. These difference could be strengthened by the conditions the blocks are exposed to, although two support blocks placed on the same cross beam seems to be exposed to more or less the same conditions. If research implies that the difference of vertical deformation between two support blocks is too large to take up by the link slab, maybe some research should be done to decrease the difference of vertical deformation between the support blocks. In other words, to be sure, the maximum allowed vertical imposed deformation the link slab should be determined, as well as the expected imposed vertical deformation from the support blocks.

7.2.3 Spalling of NSC substructure

The risk on spalling at the end of the concrete deck, caused vertical working peak stresses on the link slab, seems to be the main point of attention for the design of the link slab. However, this estimation should be research is more detail, before research to reduce the risk on spalling should be done. Maybe in reality, the vertical peak stresses cause small tensile stresses only. Then, in reality the tensile stresses could be smaller than the tensile strength of concrete. In that case, there is no problem, so the options do not have to be researched at all. So to determine if spalling will be a governing problem, experiments should be done. In the experiments, the link slab should be loaded by vertical forces. Because the link slab is expected to be loaded by fatigue loads during life time, in the experiments the link slab should also be loaded by fatigue loads.

7.2.4 Vertical peak stress in SHCC link slab

Subsequently, if spalling of the concrete substructure is proven experimentally to be a problem, research should be done to the influence of the peak stress on the SHCC link slab. In this report, it is assumed that the SHCC link slab is able to resist the peak stress. But in t reality, failure could also be

expected in the link slab. In the end, it is recommended to do some research to the behaviour of the SHCC link slab that is loaded by vertical peak stresses, to check if the assumption is correct.

7.2.5 Variant to reduce the risk of spalling

In this report are given some option to reduce the risk of spalling at the edge of the substructure. The effectiveness of these options should be research in more detail. The three recommended options to take into consideration during further research are:

1. Chamfers, because of the low costs
2. Prestressed anchored plate, because of the high effectiveness
3. Redistribution by stiff interlayer, because of potential additional benefits for the debonding layer

These three options should be researched in more detail. Some recommendation per interesting option are given below.

1. Chamfer

In short, before the chamfers are chosen to apply in practice, research is recommended to:

- Effectiveness
- Maximum length of the chamfer

Both subjects are explained in more detail here. The first issue that should be researched for the chamfer is the effectiveness of the chamfer. If the length of the chamfer is chosen larger, the peak stresses can be distributed over a larger area. So if the chamfer is chosen larger, the peak stresses at the place where spalling is a risk, are reduced more. So in the end the risk on spalling is reduced more if the length of the chamfer is chosen larger.

However, if the chamfer is chosen larger, the span of the SHCC link slab is larger, such that peak stress could be expected to be larger until a certain maximum. The influence of the length of the chamfer on the reduction of spalling and the increase of the peak stress should be researched in some more detail.

At last, the length of the chamfer is limited because the span of the link slab is limited. The maximum span of the link slab should be determined in more detail in order to determine the maximum length of the chamfer. If the maximum length of the chamfer is known, the maximum effect of the chamfer could be determined.

2. Prestressed anchored plate

In short, recommended research for the this option should be done to:

- Effect of the stiffness of the material on the reduction of spalling
- Costs
- Material

For this option, the most important issues to invest to the choice of a material. Before the material can be chosen, the effect of the stiffness of a material on the effectiveness of this option should be researched. Probably steel is the cheapest and easiest executed material to use. However, maybe a very stiff plastic is also a good alternative to apply. Besides, plastic is in general more durable than steel, what is an issue since the plate is not protected by a concrete cover.

3. Redistribution by stiff interlayer

In short, for the redistribution by stiff interlayer is recommended to research:

- The consequences of the limited smoothness of SHCC and concrete on the functioning of the active zone
- The smoothness of the materials that are interesting to use for the plate
- The effect of the vertical peak stress that is expected at the other side of the plate
- Effect of the stiffness of a certain material on the effectiveness of this option

If the limited smoothness of the surface of SHCC and NSC does not hinder the functioning to the active section, the other options are probably more interesting to apply. However, if the limited smoothness of the SHCC and NSC is indeed a problem, the surface of the plate should still be able to be made very smooth easily to be successful. If the effect on the debonding layer is really positive, this option has a high chance to be successive.

Further, at the other end of the plate, an additional peak stress is expected to be created. The effect of this peak stress should also be researched in more detail. Also the effect of the stiffness of a certain material on the effectiveness of this option should be determined.

If the effectiveness of this option according to the reduction of the peak stress is low, but the influence on the debonding layer is positive, maybe the combination with one of the other options could be interesting to research. For example, it could be the case that the risk on spalling is not reduced enough if fibres or a redistribution by stiff interlayer is applied, but if both are combined, the risk is maybe reduced to a certain desirable minimum.

7.2.6 Practical issues

Execution issues are brought under attention in this research only a little, while execution could have a large influence on the success of the SHCC link slab. However, in this research is chosen to invest the constructive point of attentions only. Additional research to execution issues is highly recommended. Next to that, some other additional research is recommended in term of optimize the design. Here a few point of attention according to the SHCC link slab are mentioned shortly for additional recommended research:

1. Tensile stresses in the link slab only
2. Inhomogeneity of SHCC
3. Stresses working in the transverse direction of the link slab
4. Increase of the strain in SHCC
5. Optimum way to make vertical and horizontal connections at the boundaries of the passive zone with the concrete deck
6. Optimum length of the passive zone to reduce the amount of SHCC, while there is a proper connection between the active zone and the substructure
7. Optimum thickness of the link slab
8. The required smoothness of the SHCC and NSC surface in order to have a properly working debonding layer, assuming a thin layer is made of a material like teflon.
9. Debonding layer made of a relative thick layer of soft material, if the thin debonding layer is not possible due to execution issues

Some of the points that are made above are quite obvious to research further. This point are not discussed any further here. The point that are not that obvious or that should be explained in some more detail, are discussed below.

Ad. 1. The tensile stress of SHCC is very low compared to the compressive stress of SHCC ($f_t \approx \frac{1}{10} f_c$). That means that tensile stresses will not influence the bridge spans that much. Further, high compressive stresses could be generated under low strains. While, if the link slab is in tension, the material has a high deformation capacity and low stresses. It is desirable that the link slab can take care of imposed horizontal deformation without generating too high forces.

To prevent high compressive forces, it is desirable to construct the link slab in such a way, that it is under tension during service life. All variables that influence the deformation of the link slab and the deck, are also the variables that determine if the link slab is in tension or compression during life time. For example, if the bridge spans are very long during execution of the link slab, for example because the outdoor temperature is very high, the change on compressive stresses during life time, or at least the time that the link slab is under compression is reduced.

In other words, to reduce the risk of compressive stresses due to imposed horizontal deformations, during execution the link slab and the bridge deck both should be at its largest. Variables that reduce the risk of compressive stress during service life are:

- Outdoor temperature, the higher the temperature, the lower the risk of compression
- Shrinkage of concrete, what reduce the risk of compression
- Precracking of the link slab, what reduce the risk of compressive stresses
- Load working on the spans in combination with creep of concrete, what reduce the risk of compression

Ad. 2. The issues according to the homogeneity of SHCC are already mentioned in the boundary conditions of this research. In short, SHCC is an inhomogeneous material. In case of multiple spans and SHCC link slabs, at least in theory, it could be the case that some link slabs are deformed to its maximum already, while some other link slab are not even cracked if the link slabs are exposed to the same imposed deformation.

Ad. 4. The link slab could be even more effective if the strain capacity of SHCC is increased. It could be imagined that the crack distribution, the number of crack and the width of the crack do influence the strain capacity of SHCC. Further, according to Tai (2015), the size of the structure influence the strain capacity of the structure. So maybe it is interesting to invest what the influence of the thickness of the link slab is on the strain capacity of the link slab.

Ad. 7. The optimum thickness of the link slab is the optimum between the forces that are generated by imposed deformations and the load that the link slab should resist. Forces that are generated by imposed deformation are desired to be as small as possible. However, vertical and horizontal loads should be resisted by the link slab as well. Further, as mentioned at the effectiveness of the link slab, a lower thickness may result in a higher strain capacity.

8 Bibliography

- WSV Kunststoffen BV. (2015). *PMMA – Acrylaat – Perspex – Plexiglas*. Retrieved from WSV Kunststoffen BV: <http://wsvkunststoffen.nl/pmma-acrylaat/>
- Caner, A., & Zia, P. (1998). *Behavior and Design of Link Slab for Jointless Bridge Decks*.
- Consolis Spanbeton. (n.d.). *Railbalkoplossingen ZIP & ZIPXL*. Retrieved from Spanbeton: http://www.spanbeton.nl/content/files/Files/Kennisportaal/Railbalk/ZIPZIPXL_A4_projectbladen_v6.pdf
- Ho, E., & Lukashenko, J. (2011). *Link Slab Deck Joints*.
- Japan Society of Civil Engineers. (2008). *Recommendations for Design and Construction of High Performance Fiber Reinforced Cement Composites with Multiple Fine Cracks (HPFRCC)*.
- Lárusson, L. H. (2013). *Development of Flexible Link Slabs using Ductile Fiber Reinforced Concrete*. Lyngby.
- Li, V. C. (2007). *Engineered Cementitious Composites (ECC) – Material, Structural, and Durability Performance*.
- Li, V. C., Fischer, G., Kim, Y., Lepech, M., Qian, S., Weimann, M., & Wang, S. (2003). *Durable Link Slabs for Jointless Bridge Decks Based on Strain-Hardening Cementitious Composites*.
- Li, V. C., Lepech, M., & Li, M. (2005). *Final Report On Field Demonstration of Durable Link Slabs for Jointless Bridge Decks Based on Strain-Hardening Cementitious Composites*. Michigan Department of Transportation.
- Li, V. C., Yang, E.-H., & Li, M. (2008). *Field Demonstration of Durable Link Slabs for Jointless Bridge Decks Based on Strain-Hardening Cementitious Composites – Phase 3: Shrinkage Control*.
- Nederlands Normalisatie-instituut. (2003). *NEN-EN 1991-2 (en): Eurocode 1: Actions on structures - Part 2: Traffic loads on bridges*.
- Nederlands Normalisatie-instituut. (2011). *NEN-EN 1990+A1+A1/C2/NB*.
- Nederlands Normalisatie-instituut. (2011). *NEN-EN 1991-2+C1:2011/NB:2011 - Nationale bijlage bij NEN-EN 1991-2: Eurocode 1: Belastingen op constructies, Deel 2: Verkeersbelasting op bruggen*.
- Nederlands Normalisatie-instituut. (2011). *NEN-EN 1992-1-1+C2*. Delft.
- Normalisatie-instituut, N. (2014). *NEN-EN 1993-1-1:2006+A1:2014 Algemene regels en regels voor gebouwen*.
- Nosewicz, H., & Jong, P. d. (2009). *Buigslappe voegen. Cement 2000/2, 78-82*.
- Proga plastics B.V. (2015). *PMMA Eigenschappen*. Retrieved from Proga plastics: <http://www.proga.nl/page/PMMA-Eigenschappen.htm>
- Proga plastics B.V. (n.d.). *PTFE Eigenschappen*. Retrieved from Proga Plastics: <http://www.proga.nl/page/PTFE-Eigenschappen.htm>
- PTFE*. (n.d.). Retrieved from Electrisol kunststoffen : <http://www.electrisol.nl/html/materialen/ptfe.html>

- Reyes, J., & Robertson, I. (2011). *Precast link slabs for jointless bridge decks*.
- Rijkswaterstaat. (2013). *RTD 1007-2: Eisen voor voegovergangen*.
- Rijkswaterstaat. (2014). *RTD 1007-2: Eisen voor voegovergangen*.
- Rijkswaterstaat. (n.d.). *Stille en duurzame voegovergangen: minder geluids- en verkeershinder*. Retrieved from Rijkswaterstaat: http://www.rijkswaterstaat.nl/zakelijk/innovatie/doorstroming_door_innovatie/lopende_projects/projecten/stille_en_duurzame_voegovergangen.aspx
- Spanbeton, C. (n.d.). *Kokerbalkoplossingen SKK & PIQ*. Retrieved from Spanbeton: http://www.spanbeton.nl/content/files/Files/Kennisportaal/Kokerbalk/SKK-PIQ_A4_projectbladen_v7_1.pdf
- Stark, J., & Stark, . (2009). *staal-beton, deel 2 liggers*.
- Tai, R. (2015). *Upscaling of Strain-Hardening Cementitious Composites: The effect of upscaling element size on the composite performance*.
- ThyssenKrupp Stokvis Plastics BV. (n.d.). *PMMA (Polymethylmethacrylaat)* . Retrieved from ThyssenKrupp Stokvis Plastics : www.thyssenkrupp-stokvisplastics.nl/download/2425/
- Voskuilen, J., Vliet, W. v., Booij, N., & Leendertz, H. (n.d.). *Stille en duurzame voegovergangen: noodzaak!* Retrieved from Rijkswaterstaat: <http://rijkswaterstaat.nl/rws/corporate/Wegen%20naar%20de%20toekomst/Minder%20hinder/Tijdelijke%20bruggen/tijdelijke%20bruggen-%20stille%20en%20duurzame%20voegovergangen%20noodzaak.pdf>
- Welleman, J. (n.d.). *thema: is bezwijken het bereiken van de vloeigrens?* Retrieved from http://icozct.tudelft.nl/TUD_CT/CT3109/collegestof/plasticiteitsleer/files/les1-2.pdf
- WSV Kunststoffen BV. (2015). *PS – Polystyreen*. Retrieved from WSV KUNSTSTOFFEN BV: <http://wsvkunststoffen.nl/polystyreen/>
- WSV kunststoffen BV. (n.d.). *PTFE – Teflon*. Retrieved from WSV kunststoffen BV: <http://wsvkunststoffen.nl/teflon-polytetrafluoretheen/>

Appendix A: Deformation capacity of NSC flexible joint and thin SHCC link slab

In this chapter is researched the deformation capacity of the NSC flexible joint and the thin SHCC link slab in more detail. Knowing the deformation capacity of both joint systems, the undilated length is determined for different span lengths. In the conclusion is mentioned the structural scheme that should be made if SHCC link slabs are applied.

A.1. Imposed deformation due to temperature

In this paragraph, the deformation of the spans that are caused by temperature differences are analysed. A certain temperature results in a certain strain. Depending on the length of the span, the strain results in a certain deformation. Here three different span lengths are analysed:

1. *Span length* = 15 m
2. *Span length* = 30 m
3. *Span length* = 50 m

Taking into account temperature only, the elongation or shortening in the link slab can be determined. In the RTD 1007-2 are described requirements for joints (Rijkswaterstaat, 2014). According to the RTD 1007-2 (5.1.2), the temperature difference should be calculated as shown in eq.(70)

$$\Delta T_{n,ej} = T_{e,max,ej} - T_{e,min,ej} \quad \text{eq.(70)}$$

$$\Delta T_{n,ej} = +35 - (-20) = 55^{\circ}\text{C}$$

The linear coefficient of thermal dilation of concrete is equal to 10^{-5} (Rijkswaterstaat, 2014). The maximum imposed strain from the span can be calculated according to eq.(71).

$$\varepsilon_{\Delta T} = \alpha_c \cdot \Delta T = 10^{-5} \cdot 55 = 0.55\text{‰} \quad \text{eq.(71)}$$

1. $\Delta L_{span} = \varepsilon_{\Delta T} \cdot L = 0.55\text{‰} \cdot 15 = 8.25 \text{ mm}$ per span
2. $\Delta L_{span} = \varepsilon_{\Delta T} \cdot L = 0.55\text{‰} \cdot 30 = 16.5 \text{ mm}$ per span
3. $\Delta L_{span} = \varepsilon_{\Delta T} \cdot L = 0.55\text{‰} \cdot 50 = 27.5 \text{ mm}$ per span

In deformation in the spans can cause elongation or shortening in the link slab. If the spans shorten, the link slabs expand under imposed deformation and the other way around, as the spans expand, the link slabs shorten by imposed deformations. In the calculations here, it is assumed that all the deformations results in elongation of the SHCC link slab, such that only tensile stresses can be generated in the link slab. If compressive stresses should be generated, the stresses probably becomes too large until the structure fails.

A.2. Deformation capacity of flexible joint

Based on (Nosewicz & Jong, 2009) the deformation capacity of the flexible joint is determined. The characteristics that determine the deformation capacity of the flexible joint are shown in Table A 1.

Table A 1 – Characteristics about the cracking behaviour of the standard flexible joint

Characteristic	Source
$w_{max} = 0.40 \text{ mm}$	(NEN-EN 1992-1-1, Tabel 7.1N (exposure class X0) (Nederlands Normalisatie-instituut, 2011))
$s_{r,max} = 224 \text{ mm}$	(Nosewicz & Jong, 2009)
$length = 800 \text{ mm}$	(Nosewicz & Jong, 2009)

Knowing the length of the flexible joint and the space between the cracks, the mean number of cracks in the link slab can be determined, as shown in eq.(81). In reality of course, 3.5 cracks can't be generated. The mean deformation capacity of the length is then equal to the mean number of cracks multiplied by the maximum allowed length of the cracks, as shown in eq.(82).

$$\text{Mean number of cracks per joint} = \frac{800}{224} = 3.5 \quad \text{eq.(72)}$$

$$\text{Mean deformation capacity per joint} = 3.5 \cdot 0.40 = 1.43 \text{ mm} = 1.75\text{‰} \quad \text{eq.(73)}$$

For different span lengths, the net deflection over the undilated length can be determined, as shown below. As shown in the results, the net length differences are negative, so a joint at the end of the undeleted length is required to take care of the expected deformations.

1. $\Delta L_{flex \text{ joint}} = 1.43 \cdot (10 - 1) = 12.9 \text{ mm}$
 $\Delta L_{net} = \Delta L_{flex \text{ joint}} - \Delta L_{tot} = 12.9 - 82.5 = -70 \text{ mm}$
2. $\Delta L_{flex \text{ joint}} = 1.43 \cdot (5 - 1) = 5.7 \text{ mm}$
 $\Delta L_{net} = \Delta L_{flex \text{ joint}} - \Delta L_{tot} = 5.7 - 82.5 = -77 \text{ mm}$
3. $\Delta L_{flex \text{ joint}} = 1.43 \cdot (3 - 1) = 2.9 \text{ mm}$
 $\Delta L_{net} = \Delta L_{flex \text{ joint}} - \Delta L_{tot} = 2.9 - 82.5 = -80 \text{ mm}$

So, depending on the number of spans, the net deformation capacity of the flexible joints over a 150 m undilated bridge are 3 to 13 mm for 10 to 3 spans. That means that the other 70 to 80 mm should be taken up with joints at the abutment. Here only the deformations are caused by temperature difference.

A.3. Deformation capacity of SHCC link slab

The calculation that are done in A.2 Deformation capacity of flexible joint, can be done for the SHCC link slab. If the deformation capacity of both joint is calculated, both can be compared to each other in terms of horizontal deformation capacity.

To determine the deformation capacity of an SHCC link slab, some assumption are done. These assumptions has mainly to do with the design of the link slab. The assumption are:

- The active length of the link slab is assumed to be equal to $L_{active} = 1.5 \text{ m}$, based on:
 - o Lárusson (2013), $L_{active} = 1.8 \text{ m}$
 - o Reyes & Robertson (2011) $L_{active} = 1.0 \text{ m}$

- The maximum strain in the active part of the link slab is assumed to be equal to 1.0%, what seems a conservative assumption, based on the maximum given tensile strain in chapter 2.2.1.2 Tensile behaviour.

Based on both above mentioned assumptions, the total deformation capacity of the SHCC link slab is expressed in eq.(83)

$$\text{total deformation capacity per link slab} = 1.0\% \cdot 1.5 = 15 \text{ mm} \quad \text{eq.(74)}$$

Now the net deformation of the undilated length can be determined for different span lengths, as shown in the expressions below. If the length of the link slab is chosen 15 m, the deformation capacity of all the link slabs together is 52.5 mm higher than required. In the other two cases, length span of 30 and 50m, a joint is required at the end of the undilated length to take care of the net length difference that are shown below.

1. $\Delta L_{link\ slab} = 15 \cdot (10 - 1) = 135 \text{ mm}$
 $\Delta L_{net} = \Delta L_{link\ slab} - \Delta L_{tot} = 135 - 82.5 = 52.5 \text{ mm}$
2. $\Delta L_{link\ slab} = 15 \cdot (5 - 1) = 60 \text{ mm}$
 $\Delta L_{net} = \Delta L_{link\ slab} - \Delta L_{tot} = 60 - 82.5 = -22.5 \text{ mm}$
3. $\Delta L_{link\ slab} = 15 \cdot (3 - 1) = 30 \text{ mm}$
 $\Delta L_{net} = \Delta L_{link\ slab} - \Delta L_{tot} = 30 - 82.5 = -52.5 \text{ mm}$

Depending on the number of spans, the net deformation capacity of all the link slabs together is 135 to 30 mm. That means that if 10 spans are applied, the link slabs has 52.5 mm deformation capacity that is not even used. In the other two cases, the remaining 22.5 to 52.5 mm should be carried by a joint at the end or/and beginning of the undilated length.

The calculation of the net horizontal deformation of the SHCC link slab is also shown in the graph of Figure A 1. In the graph are the deformation capacity of the link slab, the expected deformation of the total undilated length and the differences of both given as a function of the span length. As shown in the graph, for spans smaller than 27 m, the deformation capacity of the link slabs is larger than the expected horizontal deformation.

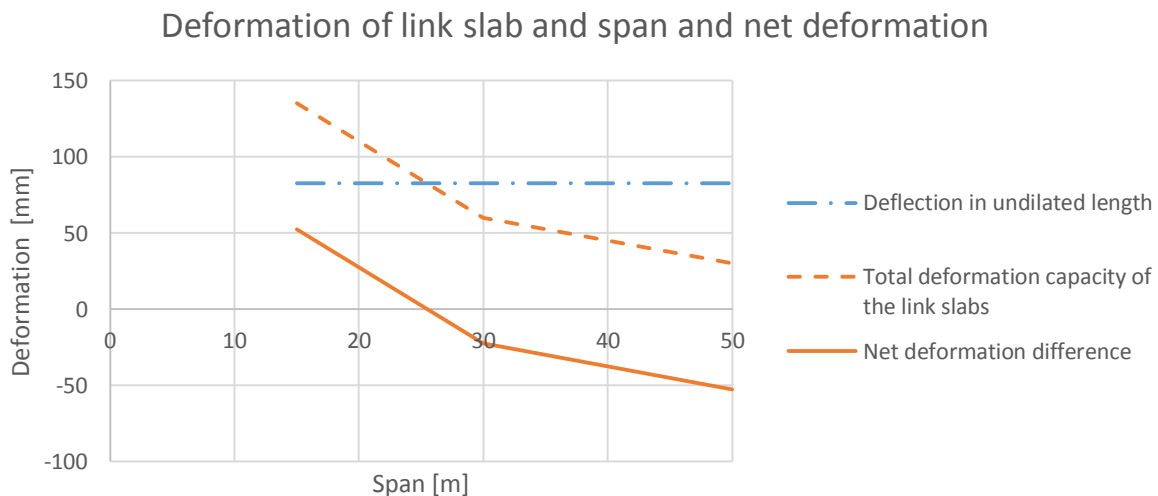


Figure A 1 – Net link slab deformation as a function of the span length in case of SHCC link slabs for an undilated length of 150 m

It should be mentioned that the link slab length of 1.5 m may be relative large compared to Lárusson (2013). However, the maximum strain of 1.0% is relative small compared to the maximum strain that could be expected to be around 2.2%, as mentioned in Table 8 of chapter 2.2.5 Load transfer system for working loads and imposed deformations. The influence of the chosen maximum strain in the links slabs is shown in the diagram of Figure A 2. As shown in the diagram, the maximum length of the spans where link slab can carry all the deformation by themselves is in theory about 33 m for a maximum assumed strain of 1.5% in the link slabs.

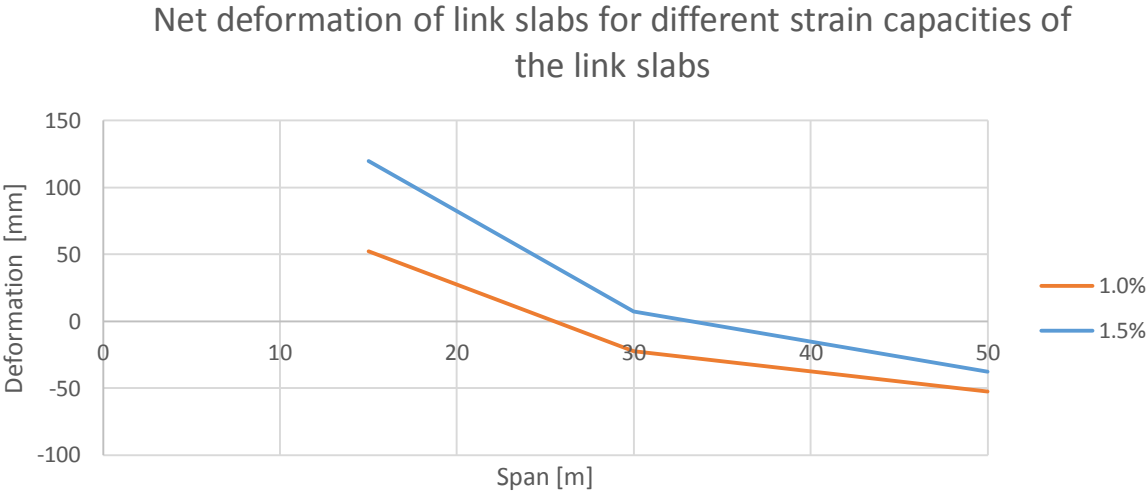


Figure A 2 – Net deformation of the link slabs for different strain capacities of the link slabs over an undilated length of 150 m

A.4. SHCC Link Slab behaviour in a bridge

From the above calculations could at least be concluded that the deformation capacity of the link slab is significant larger compared to the flexible joint. In the three cases that are analysed, give the next results:

- The deformation capacity of the flexible joints in the undilated length is 4-17 % of the total horizontal deformation in the undilated length from 15 to 50 m. therefore the deformation capacity of the flexible joint is neglected.
- The horizontal deformation capacity of the link slab is 40 to 180 % of the total deformation over the undilated lengths from 50 to 15 m respectively.

Now the horizontal deformation capacity of the link slabs and the flexible joints are analysed in a practical structure. In Figure A 3 are schematically shown three bridge structures. All structures are shortly discussed here in order to have a proper structure scheme in case of SHCC link slabs.

In structure A is shown a three span bridge with two NSC flexible joints at the intermediate supports. The left support is horizontally fixed. All other supports can move freely in the horizontal direction. The NSC flexible joints are assumed to have no horizontal deformation capacity. Therefore all horizontal deformations in the structure must be carried by the joint at the right end of the structure. Here could for example be constructed a finger joint.

In structure B of Figure A 3 is shown the same three span bridge as in structure A, but the NSC flexible joints are replaced by SHCC link slabs. It is assumed that in the bridge is a certain horizontal deformation, which should be carried by the SHCC joints and the finger joint. But, the SHCC joints has

a certain stiffness while the stiffness of the finger joints is zero. That means that probably all horizontal deformations are still be carried by the finger joint. In that case, the horizontal deformation capacity of the SHCC link slabs is nearly utilised.

To utilise the horizontal deformation capacity of the SHCC link slab, both end supports should be fixed, as shown in structure C of Figure A 3. If the structure deforms, stresses could be generated such that the SHCC link slab cracks and deforms. That means that the SHCC link slab should only be applied without free moving joints.

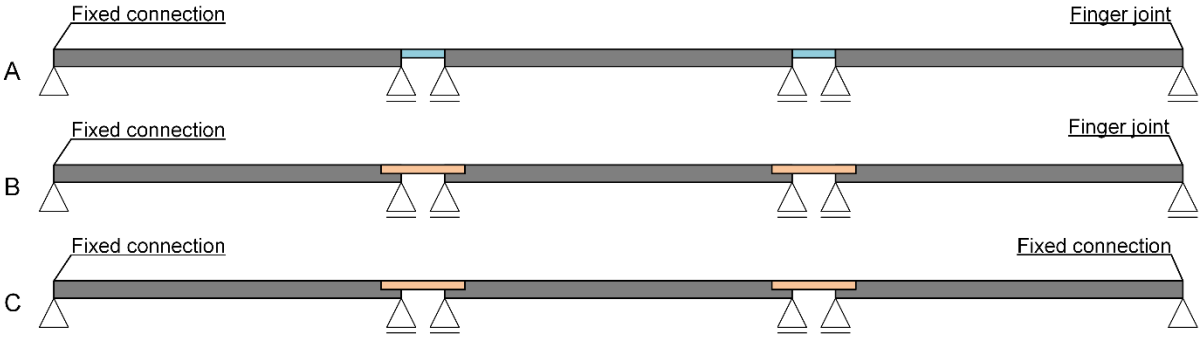


Figure A 3 – Mechanical scheme of a three span bridge with NSC flexible joint and SHCC link slab

If only SHCC link slabs can be applied in a structure, the maximum span length is limited. This limitation depends on the expected horizontal deformation in the span per meter length, the length of the active zone and the maximum strain in the SHCC. Obviously, if the horizontal deformation in the spans is small and the length of the active zone and the maximum strain of SHCC are large, then the maximum length of the span can also be chosen large. In Table A 2 are shown some maximum span lengths for different values of the horizontal deformation in the span and the horizontal deformation capacity of the link slab. In practice, normally a horizontal deformation of 1.0 mm/m is assumed. In the table is also given the maximum span length for 0.5 and 1.5 mm/m deformation in the span. The maximum span length for different horizontal deformations in the spans and different maximum strain in the SHCC link slab are also shown in the graph of Figure 190.

Table A 2 – Maximum span length as a function of the horizontal deformation in the spans an the horizontal deformation capacity of the link slab

Horizontal deformation [mm/m]	Length of the active zone [m]	Maximum strain SHCC [%]	Horizontal deformation capacity link slab [mm]	Maximum span length [m]
0.5	1.5	1.0	15.0	30
	1.5	1.5	22.5	45
	1.5	2.0	30.0	60
1.0	1.5	1.0	15.0	15
	1.5	1.5	22.5	22.5
	1.5	2.0	30.0	30
1.5	1.5	1.0	15.0	10
	1.5	1.5	22.5	15
	1.5	2.0	30.0	20

Maximum span length for different horizontal deformations in the span and different maximum strains in the SHCC Link Slab

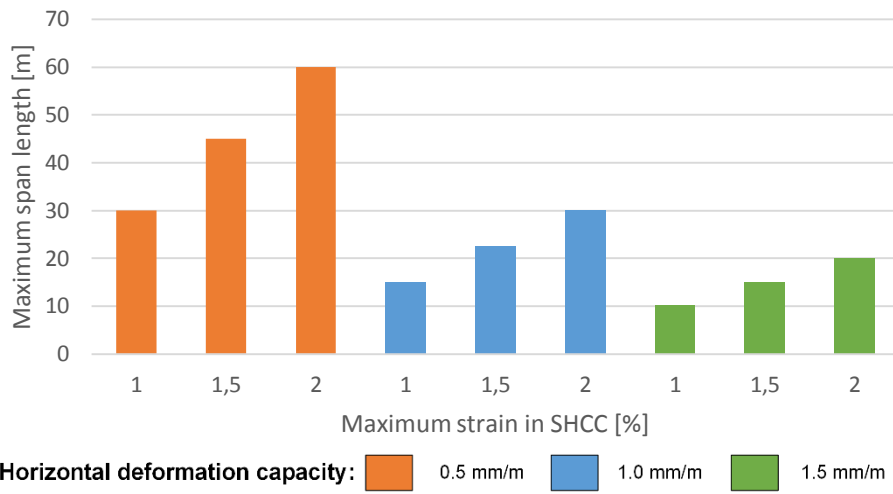


Figure 190 – Maximum span length for different horizontal deformations in the span and different maximum strains in the SHCC Link Slab

Appendix B: Load combinations

During service life of the link slab, different actions can work at the same time. For example, the link slab can be exposed to an imposed horizontal deformation and at the same time loaded by a vertical wheel load. Nosewicz & Jong (2009) describe three different load combinations to check. The first check is on the strength of the joint in ULS. The second check is the fatigue behaviour of the joint also in ULS. The last check is the crack width of the joint in SLS. These checks are not considered in this research. However, the reaction of the link slab caused by a combination of actions could be interesting to analyse.

In evaluation of action in chapter 3.3.5 Evaluation and conclusion is concluded that the main action working on the link slab are:

1. Vertical load
2. Horizontal load/ imposed horizontal deformation/imposed curvature

For the research, the vertical load is considered to be the governing action working on the link slab. however, the combination of the horizontal load and imposed horizontal deformation or imposed curvature that also results in imposed horizontal deformation, seems to be an interesting combination to analyse in more detail.

According to Nosewicz & Jong (2009) braking forces are equally distributed over all supports in the bridge. Therefore it is assumed that the stiffness of the concrete joint is an order higher than the stiffness of the support blocks. It is assumed that this is also valid in this case. The stiffness of SHCC ($\approx 20 \text{ GPa}$) is smaller than the stiffness of NSC ($\approx 33 \text{ GPa}$). However, the stiffness of SHCC is probably still an order higher than the stiffness of NSC.

Because the stiffness of the link slab is an order higher than the stiffness of the supports, the link slabs distribute the stresses equally over all supports. The stresses that goes through the link slabs depends on the number of spans and the magnitude of the braking forces. The maximum stress through the link slab can be calculated according to eq.(75)

$$F_{link\ slab} = R_d \left(1 - \frac{1}{n}\right) \quad \text{eq.(75)}$$

The horizontal stresses are distributed over all supports because of the stiffness of the concrete and the link slabs. In fact, the bridge deck and the link slabs together act like a slab. Therefore, the place where a vehicle brakes, so the place the load is introduced, does not influence the way the horizontal

loads are carried by the support blocks. In other words, a braking vehicle above the link slab has the same influence as a vehicle braking above the bridge girders.

In Figure B 1 are shown two situations that can occur in the link slab due to a braking vehicle on the bridge. The link slab situated at the left, the braking force causes compression in the link slabs. In the right link slab on Figure B 1, the braking force causes tension in the link slab.

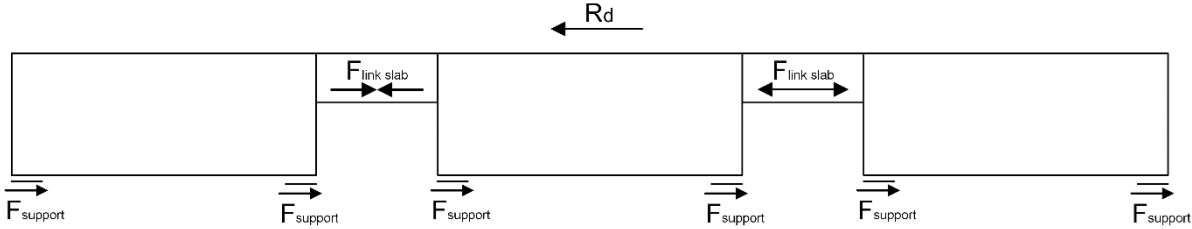


Figure B 1 – Braking force on the bridge with reaction tensile and compressive stresses in the link slabs according to (Nosewicz & Jong, 2009)

The maximum force in the link slab is for a maximum amount of spans. Assume $n \rightarrow \infty$, then the force in the link slab is equal to R_d . Nosewicz & Jong (2009) describe that according to the VOSB the maximum value for R_d is equal to 300 kN for class 60. Assuming an effective width of 4 m (Nosewicz & Jong, 2009), the maximum force in the link slabs is equal to 75 kN/m

It is interesting how the link slabs behave if it is exposed to an imposed horizontal deformation and a horizontal brake force. The link slab is assumed to be cracked. In other words, the link slab is assumed to be elongated by an imposed horizontal deformation. According to the above shown analysis, the horizontal load can cause additional tension or compression in the link slab. Both situations are analysed in detail here.

The other way around, a link slab that is exposed to a horizontal load and then to an imposed elongation, is not taken into consideration. There reason therefore is because in practice, this situation will probably never happen. A braking forces is a variable load that can change quite fast. Compared to the horizontal load, the horizontal imposed deformation (creep, temperature change, shrinkage) is a relative slow process. In fact, relative to the braking load, the imposed deformation almost act like permanent loads. So in practice, the link slab will be exposed to imposed deformation. That situation is then exposed to a braking vehicle.

First the situation of a link slab that is exposed to imposed horizontal elongation, such that cracks are generated and a horizontal tensile load is described. According to Japan Society of Civil Engineers (2008) the tensile-strain relation in ULS and SLS should be used as shown in Figure B 2. From reasons of simplicity, the mixture of Li, Lepech, & Li, Final Report On Field Demonstration of Durable Link Slabs for Jointless Bridge Decks Based on Strain-Hardening Cementitious Composites (2005) is taken as a reference mixture. As mentioned earlier, Reyes & Robertson (2011) and Lárusson (2013) both applied the same and a similar mixture respectively. As shown in graph of Figure B 2, the strain capacity is about 2.2%, with a maximum tensile design strength of 3.0 MPa. The maximum elastic tensile strain is calculated as 0.01%, as shown in Table 8 in chapter 2.2.5 Load transfer system for working loads and imposed deformations.

Now let assume the situation that the link slab is exposed to an imposed elongation and a tensile stress. Let assume the link slab is deflect until a tensile strain 0.5% due to imposed deformation, as shown with the star in the graph of Figure B 2. The material is in the plastic zone and has reached the tensile capacity of 3.0 MPa. According to Figure B 2 the tensile strength can not be higher than 3.0 MPa. So if

the tensile strain is in the plastic zone, in theory the SHCC has no capacity to carry additional horizontal tensile stresses. In fact, according to Figure B 2 if the tensile strain is above 0.01% SHCC has in theory no tensile capacity to carry brake forces.

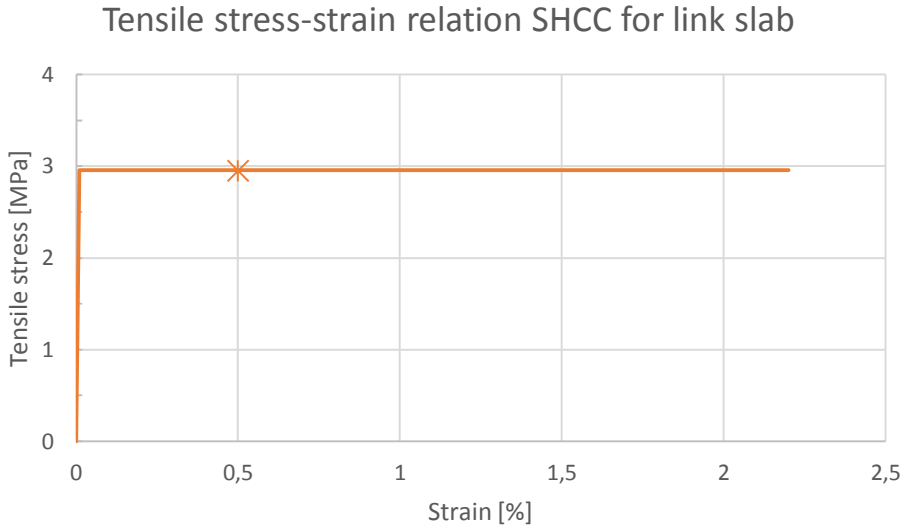


Figure B 2 – Tensile stress-strain diagram for SHCC according to Li, Lepech, & Li, Final Report On Field Demonstration of Durable Link Slabs for Jointless Bridge Decks Based on Strain-Hardening Cementitious Composites (2005) and Japan Society of Civil Engineers (2008)

However, in practice SHCC, at least the SHCC mixture of Li, Lepech, & Li, Final Report On Field Demonstration of Durable Link Slabs for Jointless Bridge Decks Based on Strain-Hardening Cementitious Composites (2005), does have a strain hardening behaviour in tension, as shown in Figure B 3. That means that in reality the link slab does have a certain capacity to carry additional horizontal stresses. Only the question is; is the increased strength due to the strain hardening behaviour large enough to carry the additional horizontal stresses in combination with the imposed elongation?

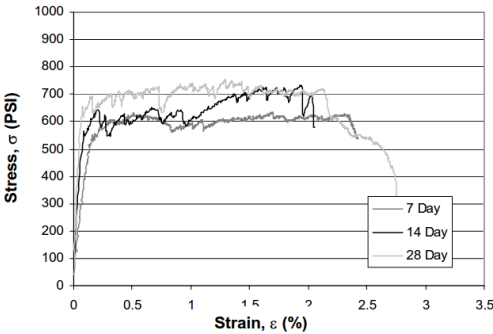


Figure B 3 – Stress strain diagram for SHCC link slab Li, Lepech, & Li, Final Report On Field Demonstration of Durable Link Slabs for Jointless Bridge Decks Based on Strain-Hardening Cementitious Composites (2005)

As mentioned before, the horizontal load of a braking vehicle is assumed to be 75 kN/m. For a link slab of 75 mm (smallest type analysed here) the concrete stress due to the braking vehicle is equal to:

$$additional\ stress = \frac{load_{brake}}{thickness_{link\ slab}} = \frac{75}{75} = 1.0\ MPa = 145\ PSI$$

For the situation where the imposed strain is equal to 0.5%, the SHCC link slab does not seem to have enough additional tensile capacity (145 PSI) to carry the load of a braking vehicle, taking into consideration the graph of Figure B 3.

Assuming the situation of 0.5% imposed elongation again, the SHCC link slab does seem to have enough additional tensile capacity to carry the load of a braking vehicle, taking into consideration the graph of Figure B 3.

As second, the situation where the cracked, elongated by 0.5%, link slab is exposed to a compressive stress caused by a braking vehicle. The maximum characteristic compressive strength of SHCC is assumed to be 45 N/mm². The maximum additional stress is about 1 MPa as calculated above. So the compressive strength of the SHCC link slab is high enough. However, before the compressive strength can be generated, the link slab should first shorten by 0.5% before compressive stresses could even be generated in the link slab. The issue is that quite some deformation is required before the link slab has a compressive capacity. Neglecting the elongation needed to generate 1 MPa compressive strength, the shortening of the link slab to generate the compressive strength is equal to the elongation of 0.5% in this particular case. If the elongation of the link slab due to temperature for example is larger, the deformation before a compressive stress can be generated is even larger than 0.5%.

Zooming back to a structural level, there are three options according to the reaction of the link slabs in the structure:

1. All link slabs are under tension
2. All link slabs are under compression
3. Combinations of link slabs under tension and compression

Now these three situations are analysed in the structure with the knowledge from above.

In Figure B 4 is shown the first situation; all link slabs under tension. As discussed above, according to the Japanese recommendations (Figure B 2) the link slabs have no capacity to carry additional horizontal tensile loads. That means that, as shown in Figure B 4, the horizontal loads caused by braking vehicles can not be distributed over all support any more. So if for instance, a vehicle brakes on span number 1, as shown in Figure B 4, in theory only the supports under span number 1 are able to make equilibrium with the horizontal braking forces.

In practice, an SHCC mixture mostly have a strain hardening behaviour. So in practice, from a certain minimum link slab thickness, the link slab is able to carry horizontal loads. In that case, the horizontal braking load can be distributed over all support in the link slab.



Figure B 4 – Bridge structure; all link slabs under tension

In Figure B 5 is shown the second practical situation that is analysed. In this situation all link slabs in the bridge are exposed to compressive stress. Again the link slabs are assumed to be cracked and elongated by 0.5%. To transfer compressive stresses through the link slab, the cracks must be closed. It is assumed that the active part of the link slab is equal to 1.0 m and the strain in the slab is equal to

0.5%. That means that the span that is exposed to a braking vehicle, span 3 is in the case of Figure B 5, should move 5 cm horizontally before the compressive stresses can be transferred to the second span. So to transfer horizontal loads from span 3 to span 2 by compression, the supports must be able to carry this large movement. Depending on the type of supports, the supports are probably already activated by the horizontal movement to carry all horizontal load by the supports. During the design, the supports therefore should be strong enough to carry the horizontal load from the braking vehicle or the supports should have enough horizontal deformation capacity, such that loads are transferred to the other spans. To transfer the stresses to the span 1, span 3 should even move 10 cm horizontally, what is even less likely to occur. So it is assumed that only span 2 could be able to carry horizontal loads.

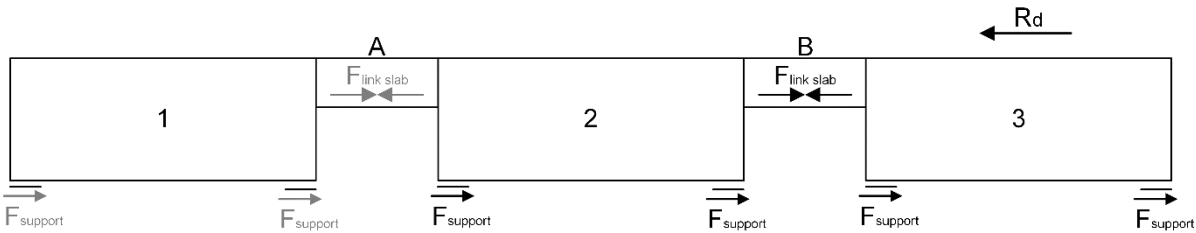


Figure B 5 – Bridge structure; all link slabs under compression

In Figure B 6 is shown the third situation. This situation is a three span bridge where one link slab is exposed to compressive stress (A) and one link slab is exposed to tensile stress (B), because a vehicle brakes on span 2. Both link slabs are again assumed to be crack and elongate by 0.5%. As mentioned in the first situation, link slab B is assumed to have no capacity to transfer horizontal tensile stresses, because of the 0.5% elongation of the link slab. If the supports are able to move vertically enough, compressive stresses can be generated in link slab A, such that a part of the stresses of the horizontal load can be carried by the supports of span 1. The question is if the supports have enough horizontal movement capacity.

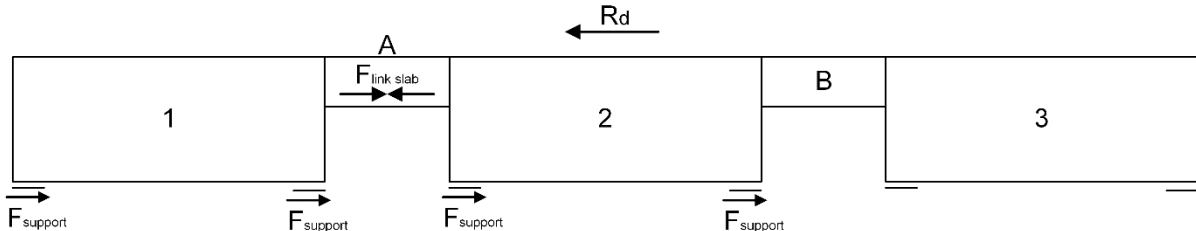


Figure B 6 – Bridge structure; link slabs under compression (A) and under tension (B)

Appendix C: Maximum span of the link slab

In this appendix is shown the calculation for the maximum span to the link slab, in order to determine the maximum length of the chamfer at the end of the substructure. Assuming a chamfer under 45 degrees, the length of the chamfer has a linear relation with the maximum span of the link slab. A chamfer could be interesting to apply as an option of decrease the resistance against spalling at the end of the substructure.

Before the calculation is done, first some assumptions are made. Then the maximum span of the link slab is determined according to the bending moment resistance of the link slab. At last, the shear strength of the link slab is checked.

Assumptions for the calculation

General:

- Calculations are done per metre width
- ε'_{cu} , the maximum compressive strain, is assumed to be generated at the outer fibre of the compressive zone of the link slab
- Pure bending is assumed, so all the strain are generated by bending moments only
- It is assumed that the shape of the compressive zone remains the same
- For reasons of simplicity, only on wheel load is taken into account
- For reasons of simplicity, the wheel load is assumed to work over the whole length of the link slab

Design:

- The thickness of the link slab is assumed to be equal to 75 mm, according to Reyes & Robertson (2011) and Lárusson (2013)
- The minimum reinforcement ratios in the active part of the link slab is 0.3% based on:
 - o Reyes & Robertson (2011), reinforcement ratio $\rho = 0.6\%$
 - o Lárusson (2013), reinforcement ratio $\rho_{1,3} = 0.42\%$; $\rho_2 = 0.30\%$; $\rho_4 = 0.50\%$
- The maximum reinforcement ratios in the active part of the link slab is 0.6% based on:
 - o Reyes & Robertson (2011), reinforcement ratio $\rho = 0.6\%$
 - o Lárusson (2013), reinforcement ratio $\rho_{1,3} = 0.42\%$; $\rho_2 = 0.30\%$; $\rho_4 = 0.50\%$
- The length of the active part of the link slab is assumed to be 1.5 m

Material characteristics:

- The bending moment resistance of the cross section is calculated according to Japan Society of Civil Engineers (2008)
- The characteristic of GFRP are given in chapter
- The SHCC characteristics are according to Li, et al. (2003), which are given in chapter 2.2.5 Load transfer system for working loads and imposed deformations
- $\varepsilon'_m = \varepsilon'_{cu}$ because no appropriate test data is available (Japan Society of Civil Engineers, 2008 (3.3.2))
- It is assumed that according to the Appendix 1: Literature study SHCC fails in compression if the compressive strain is larger than the limit, $\varepsilon'_{cu} = 0.3$.

Calculation

In Figure C 1 is shown the cross section of the SHCC link slab with the horizontal forces working on the cross section. The forces that works in the cross section are the SHCC compressive force (N_{cuc}), the

tensile reinforcement force (N_{su}) and the SHCC tensile force (N_{cut}). These forces can be expressed as shown in eq.(76), eq.(77) and eq.(78).

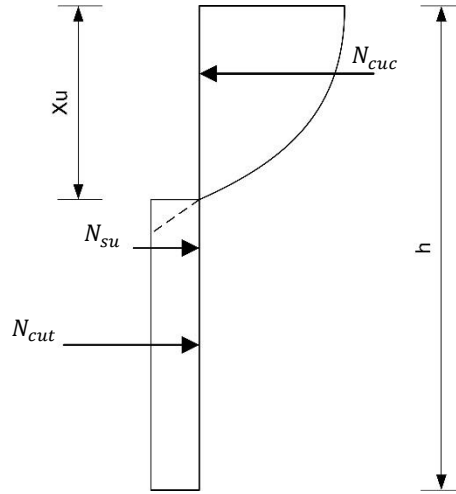


Figure C 1 – Resultant forces working over the cross section of the link slab

$$N_{cuc} = \frac{2}{3} \cdot X_u \cdot f_{cd} \cdot b = \frac{2}{3} \cdot X_u \cdot 29.4 \cdot 1000 = 19,600X_u \quad \text{eq.(76)}$$

$$N_{cut} = f_{ctd} \cdot b \cdot (h - X_u) = 2.7 \cdot 1000 \cdot (75 - X_u) = 202,500 - 2,700X_u \quad \text{eq.(77)}$$

$$N_{su} = A_s \cdot f_s = A_c \cdot \rho \cdot E_s \cdot \varepsilon_s = 75,000 \cdot \rho \cdot 46 \cdot 10^3 \cdot \varepsilon_s = 3,450 \cdot 10^6 \cdot \rho \cdot \varepsilon_s \quad \text{eq.(78)}$$

Over the cross section of Figure B 6 should be horizontal equilibrium, as shown in eq.(79). In eq.(79) are three unknowns, so the equations can't be solved. The reinforcement ratio is chosen 0.3% and 0.6%, because these are the outer limits of reinforcement ratios applied in literature. Therefore, different values for the reinforcement strain are chosen, such that the height of the compressive zone can be determined.

$$N_{cuc} = N_{cut} + N_{su} \quad \text{eq.(79)}$$

$$19,600X_u = 202,500 - 2,700X_u + 3,450 \cdot 10^6 \cdot \rho \cdot \varepsilon_s$$

Here the calculation is clarified further for $\varepsilon_s = 1.0\%$ and $\rho = 0.3\%$. For, $\varepsilon_s = 1.0\%$ and $\rho = 0.3\%$, eq.(79) can be used to calculate the height of the compressive zone, as shown in eq.(80).

$$19,600X_u = 202,500 - 2,700X_u + 3,450 \cdot 10^6 \cdot 0.3\% \cdot 1.0\% \quad \text{eq.(80)}$$

$$X_u = 13.7 \text{ mm}$$

The resultant forces working in the compressive zone, the tensile zone and the reinforcement for $\varepsilon_s = 1.0\%$ and $\rho = 0.3\%$ can now be calculated as shown in eq.(81), eq.(82) and eq.(83) respectively.

$$N_{cuc} = 269 \text{ kN} \quad \text{eq.(81)}$$

$$N_{cut} = 165 \text{ kN} \quad \text{eq.(82)}$$

$$N_{su} = 104 \text{ kN} \quad \text{eq.(83)}$$

The resultant forces are shown in Figure C 2. In the figure are also given the distances from the bottom of the link slab to the resultant forces of the SHCC compressive stress, the SHCC tensile stress and the GFRP tensile stress. Clarification of these distances:

- $D_{cuc} = h - \frac{2}{5}X_u = 75 - \frac{2}{5} \cdot 12.2 = 70 \text{ mm}$, where $\frac{2}{5}X_u$ is approximately the point of gravity for a parabolic shape.
- $D_{su} = \frac{h}{2} = 38 \text{ mm}$
- $D_{cut} = \frac{h-X_u}{2} = 31 \text{ mm}$

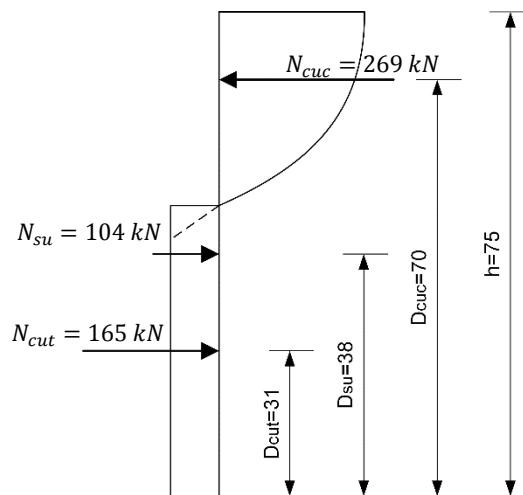


Figure C 2 – Stresses working over the cross section of the link slab

In Figure C 2 are given all data to calculate the resistant bending moment of the cross section. Taking bending moment equilibrium at the bottom of the link slab, the resistant bending moment of the cross section for $\varepsilon_s = 1.0\%$ and $\rho = 0.3\%$ is calculated as shown in eq.(84)

$$\sum M = 0 \rightarrow M_{Rd} = 269 \cdot 70 - 104 \cdot 38 - 165 \cdot 31 = 9.7 \text{ kNm} \quad \text{eq.(84)}$$

Note: For the calculation of the SHCC tensile force is assumed a rectangular shape of the stress, as shown in Figure C 2. However, in reality the upper part of the stress does not make a right angle. In reality the stress profile at the upper part will be under a certain angle as shown with the dotted line in Figure C 2. For reasons of simplicity, a rectangular shaped profile for tensile stresses is assumed

From the resistance bending moment, the maximum length of the span can be determined. Therefore, first the design bending moment should be determined. To calculate the design bending moment the wheel load should be determined, which can be inserted in the forget-me-not formula. In Figure C 3 is shown the governing pattern of wheel loads for the flexible link slab that is described by Nosewicz & Jong (2009). Because the active part of the link slab is assumed to be smaller than 1.6 m, the pattern of Figure C 3 is assumed to be governing for the link slab too. The length of the wheel load is 300 mm. The thickness of the link slab is 75 mm. The asphalt layer is assumed to be 120 mm thick. Then the load in the middle of the link slab is distributed over $300 + 75 + 2 \cdot 120 = 615 \text{ mm}$. The distributed load per metre width than is calculated in eq.(85).

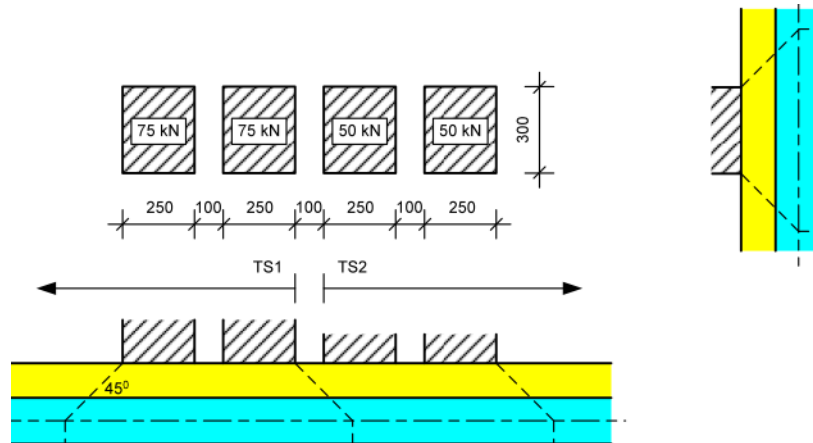


Figure C 3 – Distribution of wheel loads (Nosewicz & Jong, 2009)

$$Q_{ULS} = 1.5 \cdot \frac{F_{wheel}}{L_{wheel} + t_{link\ slab} + 2 \cdot t_{asphalt}} = 1.5 \cdot \frac{75}{0.615} = 183 \text{ kN/m} \quad \text{eq.(85)}$$

Knowing the distributed load in the ULS and taking the working bending moment equal to the resistant bending moment of the link slab, the maximum length of the gap for $\rho = 0.3\%$ and $\varepsilon_s = 1.0\%$ is equal to 510 mm as shown in eq.(86).

$$M_{Ed} = \frac{1}{8} \cdot Q_{ULS} \cdot l^2$$

eq.(86)

$$l = \sqrt{\frac{9.7 \cdot 10^6 \cdot 8}{183}} = 652 \text{ mm}$$

The forget-me-not formula applied is quite conservative. The formula is meant for a simple supported beam. However, in reality, the link slab will not really act like a simply supported beam. The connection between the active and the passive sections of the link slab could probably be modelled the best as a spring. The simple supported beam is in fact a bit conservative. Further, it is assumed that the wheel load works over the whole gap, which is 652 mm long. In reality, the length the wheel load is distributed over is 375 mm only.

Length of the gap as function of the strain in the active section of the link slab

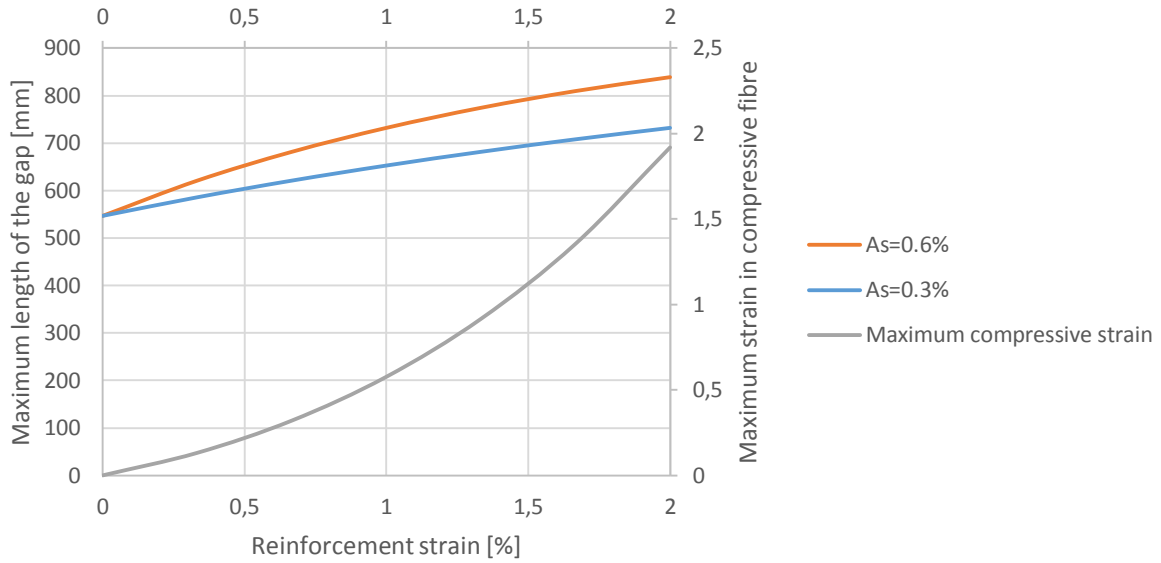


Figure C 4 – Length of the gap as function of the strain in the reinforcement of the link slab for $\rho = 0.6\%$ and $\rho = 0.3\%$

In the graph of Figure C 4 is also given a line of the maximum compressive strain in the outer fibre as a function of the strain in the rebars. The graph of the maximum compressive strain is calculated according to the Figure C 5. In the figure is shown the strain over the height of the cross section of the SHCC link slab. A linear behaviour is assumed. According to eq.(87), the compressive strain in the outer fibre can be calculated. In eq.(88) is shown the calculation for $\epsilon_s = 1.0\%$

$$\epsilon_c = \frac{X_u \cdot \epsilon_s}{\frac{h}{2} - X_u} \quad \text{eq.(87)}$$

$$\epsilon_c = \frac{13.7 \cdot 1.0\%}{\frac{75}{2} - 13.7} = 0.58\% \quad \text{eq.(88)}$$

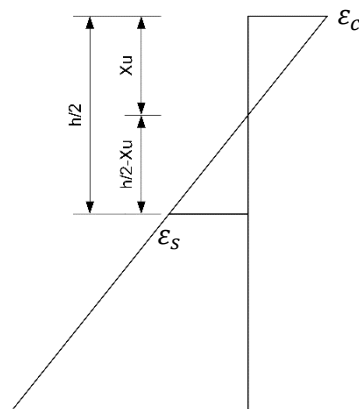


Figure C 5 – Strain over the height of the SHCC link slab

As mentioned, the maximum compressive strain of SHCC is equal to 0.3%. In Figure C 6 are shown the graphs of the maximum length as a function of the reinforcement strain again and the strain in the compressive fibres as a function of the strain in the reinforcement. As shown in Figure C 6, the strain in the rebars is about 0.64%. The maximum length of the gaps if the strain in the reinforcement is 0.64% is 620 mm and 675 mm for a reinforcement ratio of 0.3% and 0.6% respectively.

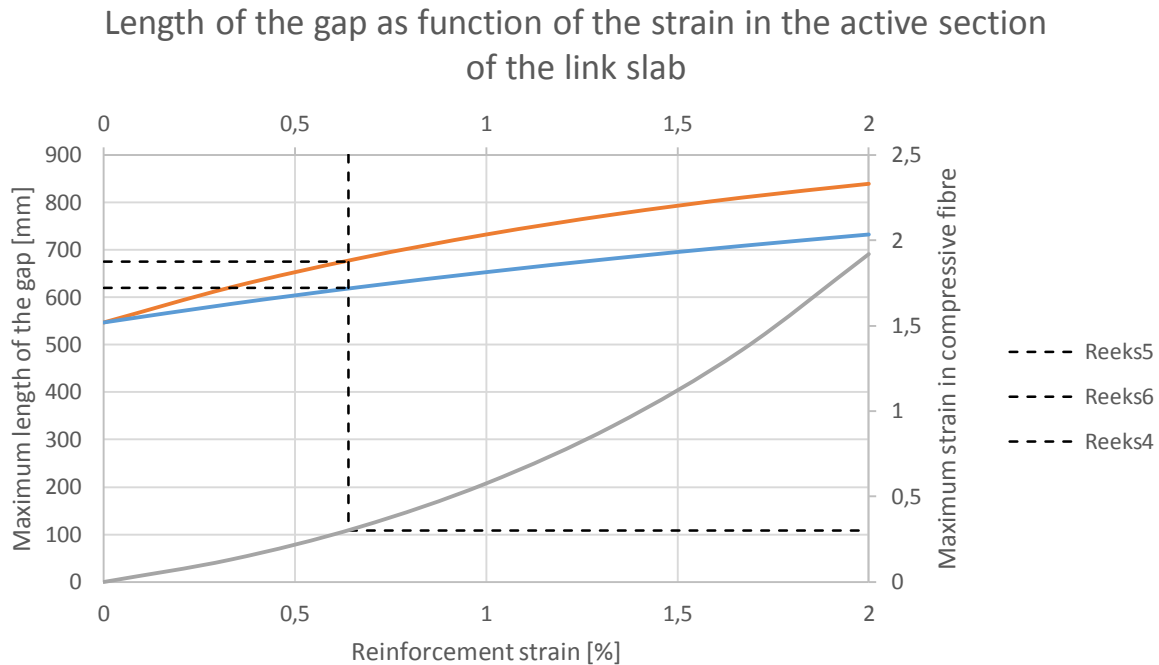


Figure C 6 – Maximum length of the gap for $\rho = 0.6\%$ and $\rho = 0.3\%$

Check on shear strength

The calculation above for the maximum width of the gap is based on the bending moment capacity of the link slab. Here, the link slab is also checked on the shear capacity. The shear working on the link slab is determined assuming a distributed load over the whole length of the link slab, as shown in eq.(89) what is a conservative assumption. The maximum length of the gap is assumed, what is 675 mm for a reinforcement ratio of 0.6%.

$$V_{Ed} = \frac{1}{2} \cdot l \cdot Q_{ULS} = \frac{1}{2} \cdot 0.675 \cdot 300 = 101 \text{ kN} \quad \text{eq.(89)}$$

In eq.(90) is shown the shear strength of the link slab, taking into consideration the contribution of the fibres only. As shown in the unity check in eq.(91), the shear force capacity of the fibres is already high enough to carry the maximum working shear force in the link slab.

$$V_{Rd} = V_{fd} = \frac{f_{vd}}{\tan\beta_u} \cdot b_w \cdot \frac{0.9 \cdot \frac{h}{1.15}}{\gamma_b} = \frac{2.7}{\tan 45} \cdot 1000 \cdot \frac{0.9 \cdot \frac{75}{1.15}}{1.3} = 122 \text{ kN} \quad \text{eq.(90)}$$

$$\frac{V_{Ed}}{V_{Rd}} = \frac{101}{122} = 0.83 \quad \text{eq.(91)}$$